frontiers | Research Topics

Case reports in hematological malignancies 2022

Edited by
Arpad Szallasi, Ahmad Antar and Osamu Imataki

Published in
Frontiers in Oncology

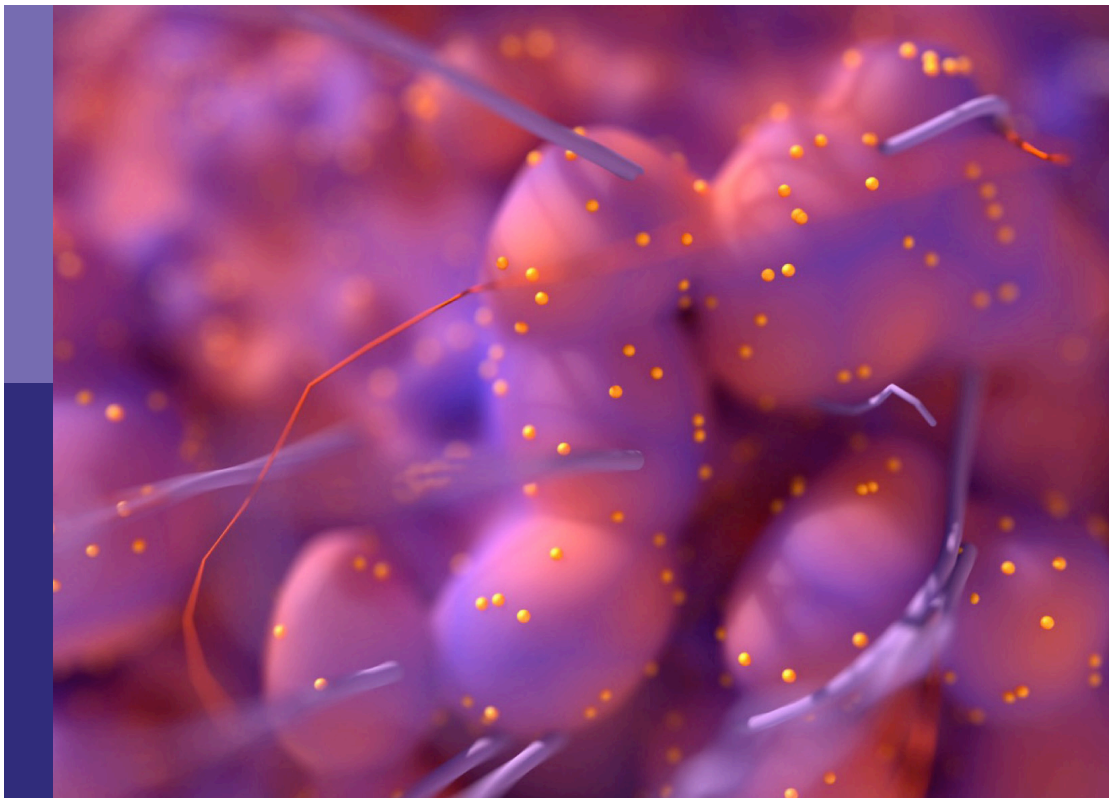

ISSN 1664-8714
ISBN 978-2-8325-3408-3
DOI 10.3389/978-2-8325-3408-3

About Frontiers

Frontiers is more than just an open access publisher of scholarly articles: it is a pioneering approach to the world of academia, radically improving the way scholarly research is managed. The grand vision of Frontiers is a world where all people have an equal opportunity to seek, share and generate knowledge. Frontiers provides immediate and permanent online open access to all its publications, but this alone is not enough to realize our grand goals.

Frontiers journal series

The Frontiers journal series is a multi-tier and interdisciplinary set of open-access, online journals, promising a paradigm shift from the current review, selection and dissemination processes in academic publishing. All Frontiers journals are driven by researchers for researchers; therefore, they constitute a service to the scholarly community. At the same time, the *Frontiers journal series* operates on a revolutionary invention, the tiered publishing system, initially addressing specific communities of scholars, and gradually climbing up to broader public understanding, thus serving the interests of the lay society, too.

Dedication to quality

Each Frontiers article is a landmark of the highest quality, thanks to genuinely collaborative interactions between authors and review editors, who include some of the world's best academicians. Research must be certified by peers before entering a stream of knowledge that may eventually reach the public - and shape society; therefore, Frontiers only applies the most rigorous and unbiased reviews. Frontiers revolutionizes research publishing by freely delivering the most outstanding research, evaluated with no bias from both the academic and social point of view. By applying the most advanced information technologies, Frontiers is catapulting scholarly publishing into a new generation.

What are Frontiers Research Topics?

Frontiers Research Topics are very popular trademarks of the *Frontiers journals series*: they are collections of at least ten articles, all centered on a particular subject. With their unique mix of varied contributions from Original Research to Review Articles, Frontiers Research Topics unify the most influential researchers, the latest key findings and historical advances in a hot research area.

Find out more on how to host your own Frontiers Research Topic or contribute to one as an author by contacting the Frontiers editorial office: frontiersin.org/about/contact

Case reports in hematological malignancies: 2022

Topic editors

Arpad Szallasi — Semmelweis University, Hungary

Ahmad Antar — Almoosa Specialist Hospital, Saudi Arabia

Osamu Imataki — Kagawa University, Japan

Citation

Szallasi, A., Antar, A., Imataki, O., eds. (2023). *Case reports in hematological malignancies: 2022*. Lausanne: Frontiers Media SA.

doi: 10.3389/978-2-8325-3408-3

Table of contents

frontiers | Frontiers in Oncology

TYPE Editorial
PUBLISHED 21 August 2023
DOI 10.3389/fonc.2023.1272547

OPEN ACCESS

EDITED AND REVIEWED BY
Alessandro Isidori,
AORMN Hospital, Italy

*CORRESPONDENCE
Ahmad Antar
a.antar@almoosahospital.com.sa

RECEIVED 04 August 2023
ACCEPTED 08 August 2023
PUBLISHED 21 August 2023

CITATION
Antar A, Szallasi A and Imataki O (2023) Editorial: Case reports in hematological malignancies: 2022.
Front. Oncol. 13:1272547.
doi: 10.3389/fonc.2023.1272547

Editorial: Case reports in hematological malignancies: 2022

Ahmad Antar[1]*, Arpad Szallasi[2] and Osamu Imataki[3]

[1]Department of Hematology-Oncology, Almoosa Specialist Hospital, Al-Ahsa, Saudi Arabia, [2]Faculty of Medicine, Semmelweis University, Budapest, Hungary, [3]Faculty of Medicine, Kagawa University, Kita-gun, Japan

KEYWORDS

hematological malignances, leukemia, lymphoma, multiple myeloma, myeloproliferative neoplasms, bone marrow transplantation (BMT), CAR (chimeric antigen receptor) T cells, case reports

Editorial on the Research Topic
Case reports in hematological malignancies: 2022

Hematological malignancies are tumors of the hematopoietic and lymphoid tissues, referring to a group of cancers that affect the blood, lymph nodes, and bone marrow. They include leukemias, myelodysplastic syndrome (MDS), myeloproliferative neoplasms (MPNs), lymphomas, plasma cell neoplasms, and other rare bone marrow diseases like histiocytic or dendritic cell tumors. The most recent World Health Organization (WHO) classification of hematolymphoid tumors (5th edition) was released in August 2022 (1).

The aim of this Research Topic entitled "*Case reports in hematological malignancies*" was to collect articles that highlight rare cases with typical features, frequent cases with atypical features, or cases with a convincing clinical response to new off-label use therapy. Such cases may provide valuable insights into the pathomechanism of the disease. They can also serve as a basis for creating hypotheses for future research. A total of seventy-three manuscripts were submitted, of which thirty-three have been accepted for publication: a 45% acceptance rate.

Eleven of the accepted manuscripts are cases of acute leukemia. Long et al. reported a case of acute myeloid leukemia (AML) treated with a lower dose of venetoclax (100 mg once daily) with the combination of grapefruit juice (a strong CYP3A4 inhibitor, 200 ml 3 times daily), and azacitidine 75 mg/m2 on days 1–7 of each 28-day cycle (2, 3). The patient achieved complete remission (CR) with the venetoclax Cmax within the effective concentration range at 7 and 14 days of treatment and maintained remission with manageable side effects. This case highlights the importance of drug-food interaction combinations in reducing the dose and cost of venetoclax, especially in low to middle-income countries. A case of concurrent Langerhans cell histiocytosis (LCH) and AML which shared driver mutations in an 84-year-old female patient was reported by Kazama et al. The diagnosis was based on biopsy where LCH was primarily identified in the skin, lymph nodes, and bone marrow, while AML was predominantly present in the bone marrow and peripheral blood. Only a few numbers of cases of LCH and AML diagnosis at the same time have been reported, the majority of which included generalized LCH, and monocytic leukemia, and was associated with dismal prognosis (4, 5). In summary, this

case is in favor of classifying LCH and other forms of histiocytosis as myeloid/myeloproliferative malignancies.

Two cases of invasive fungal infection in AML patients were reported. Tabak et al. described a case of AML with lungs and sinuses mucormycosis at diagnosis and who had a loss of function mutation in the *TNFRSF13B* gene. This mutation increases the likelihood of developing immunodeficiency syndromes since it has been demonstrated to impair B-cell differentiation and homeostasis (6). These data highlight the importance of next-generation sequencing for the prognosis and treatment of AML. The other case was a patient with myeloid sarcoma in her right breast who, while receiving the first consolidation course of chemotherapy, acquired a severe fungal infection caused by Saprochaete clavata. The patient was refractory to maximum antifungal therapy and the treatment was successful only when granulocyte transfusion therapy was initiated. In this case, Pasqualone et al. suggest the addition of granulocyte transfusions as adjunctive therapy for patients with profound and long-lasting neutropenia and severe fungal infections resistant to broad-spectrum antimicrobial treatment (7).

Interestingly, three cases of atypical acute promyelocytic leukemia (APL) were presented in this Research Topic. Zhao, J. et al. reported a case of AML with Retinoic acid receptor gamma gene rearrangement which resembled classical APL in clinical features, morphology, and immunophenotype but did not carry the diagnostic PML-RARA fusion gene (8). This APL-like case showed resistance to all-trans retinoic acid (ATRA) and Arsenic trioxide but responded well to homoharringtonine and cytarabine. The second case reported by Chen, L. et al. was a variant APL with BCOR-RARA instead of PML-RARA fusion gene. The patient was successfully treated by ATRA plus standard chemotherapy followed by allogeneic hematopoietic stem cell transplantation (allo-HSCT) and ATRA maintenance and maintained molecular remission. Variant APL cases have a high risk of relapse which warrants accurate identification and optimal aggressive therapy (9). The third case reported by Chen, X. et al. was an APL-like case in a 3-year-old child caused by torque teno mini virus (TTMV) fragment integration into the RARA locus which suggests that TTMV: RARA is a recurrent cause of APL missing PML: RARA. Only two similar APL-like cases caused by TTMV integration were reported in the literature (10, 11). This case highlights the identification of more TTMV: RARA positive APL-like cases considering the widespread prevalence of TTMV in the general population.

Two reports of stem-cell transplantation in AML patients were included in this Research Topic. Zheng et al. reported the first 2 cases in the literature of successful haploidentical allo-HSCT in AML patients from donors having mild alpha(a)-thalassemia. Follow-up on these 2 patients showed a full donor chimerism, no development of chronic GVHD, and both experienced conversion to donors' thalassemia type with mild microcytic anemia and maintaining Hb levels between 10 to 12 g/dL without transfusion.

Wang, Y. et al. reported a case of Gastrointestinal-GVHD in an AML young female after allo-HSCT that was complicated by small bowel obstruction. The patient experienced prolonged bloody diarrhea after stopping cyclosporine and the gradual reduction in steroids. Imaging showed intestinal stricture 10 months after the transplant. She was treated successfully with surgical resection of the small intestinal stenotic loop after the failure of appropriate immunosuppressive therapies.

The last two case reports in the acute leukemia set were two cases of acute lymphoblastic leukemia (ALL). Ni et al. reported a case of Donor-derived leukemia (DDL) in a patient who was initially diagnosed with B-cell ALL, for which she received induction chemotherapy then she received salvage chemotherapy after relapse. Last she underwent umbilical cord blood transplantation (UCBT) after the first relapse and achieved CR2.

Unfortunately, the patient had a disease relapse again after UCBT. Interestingly, the result of chimerism still showed complete donor chimerism which is consistent with DDL. DDL is an uncommon but serious complication after transplant (12). DDL after UCBT is usually resistant to chemotherapy and the prognosis is very dismal (13). The patient was resistant to chemotherapy, however, she received anti-CD19 chimeric antigen receptor T-cell (CAR-T) cell therapy and achieved CR with negative minimal residual disease (MRD). Then she received preemptive interferon-a treatment after the rise of MRD levels and maintained CR for 41 months. Interferon-a enhances the graft-versus-leukemia effect and is used as an adjuvant or maintenance therapy after transplant to eliminate MRD and lower the risk of leukemia recurrence (14). This study offers a novel therapeutic strategy for DDL.

The second case reported by Wang, R. et al. was a child with B-cell ALL carrying the rare mutation TP53 c.C275T. This mutation is very rare and is associated with poor prognosis (15). The patient showed resistance to most conventional chemotherapy regimens. *In vitro*, drug sensitivity tests have shown that bortezomib had a very strong susceptibility to the patient's leukemic cells. Therefore, the patient was then treated with bortezomib in combination with vindesine, fludarabine, and cytarabine. She achieved MRD-negative CR after one course of therapy and continued recurrence-free after a 9-month. According to this report, bortezomib in combination with chemotherapy may be an effective therapy for ALL patients carrying TP53 c.C275T mutation.

Cases of chronic leukemias are well represented in this Research Topic. Ramdohr et al. reported 2 patients with atypical chronic myeloid leukemia (CML) carrying the BCR: ABL1 e6a2 fusion transcript. Most CML patients are diagnosed with the e13a2 or e14a2 BCR: ABL1 fusion transcripts. However, there is a growing number of CML cases with atypical clinical presentations that are associated with other transcripts, such as e19a2, e8a2, e13a3, e14a3, e1a3, and e6a2. These transcripts have been described in 1% of CML patients and their clinical significance is yet to be determined (16–18). For example, the atypical e6a2 BCR: ABL1 transcript seems to portend poor prognosis as it is associated with an aggressive phenotype and early transformation into acute leukemia (19). The reported 2 patients expressing the atypical e6a2 BCR: ABL1 fusion transcript were treated effectively with the 2nd generation tyrosine kinase inhibitor, nilotinib. The second article on CML was reported by Pasquale et al. The patient developed severe pleural effusion secondary to nilotinib therapy and was managed with steroids and permanent withdrawal of the medication. Pleural effusion is a well-known toxicity related to dasatinib, which has been linked to either

the expansion of cytotoxic T and NK cells or the activation of additional kinases (20). But it's extremely rare during nilotinib therapy, especially in first-line settings.

Bi et al. described the first case of the coexistence of primary pulmonary lymphoma and opportunistic pneumonia in a patient with CML on imatinib therapy. Primary pulmonary lymphoma is a rare neoplasm and has very nonspecific clinical features that can overlap with infection and often cause delay or neglect in diagnosis (21). This patient continued to have lung disease progression even after optimal antimicrobial coverage. The lymphoma was then diagnosed by CT-guided biopsy, and he received chemotherapy and is still alive at the date of report writing.

Vermeersch et al. reported a case series (n=5) of chronic neutrophilic leukemia (CNL) associated with monoclonal gammopathy. They analyzed the genetic characteristics of these cases using cytogenetic and molecular studies. CNL is a rare type of BCR: ABL1 negative MPN, defined by persistent mature neutrophilia and hypercellular bone marrow (22). CSF3R mutation is found in up to 80% of CNLs. CNL is associated with plasma cell neoplasms in approximately 32% of cases, wherein CSF3R mutation tends to be less frequent (23, 24). In this series, 3 patients have shown a predominant lambda light chain expression. Four patients progressed into plasma cell myeloma. All patients received treatment for the associated malignancies such as AML and multiple myeloma (MM), and among these two patients underwent allo-HSCT.

Two manuscripts reported cases of chronic lymphocytic leukemia (CLL). The first one by Valvano et al. described a very rare association of CLL with hairy cell leukemia (HCL) with the challenges in diagnosis using multicolor flow cytometry and PCR (25). The patient was initially treated with cladribine and rituximab. The other report by Ballotta et al. described 2 cases of CLL with post-COVID-19 condition. Both patients had persistent SARS-CoV-2 infection without seroconversion for 7-8 months. The patients were effectively treated with monoclonal antibodies casirivimab/imdevimab infusion. This data highlights the effectiveness of monoclonal antibodies in immunocompromised patients with persistent SARS-CoV-2 infection (26).

The topic of lymphomas with rare presentation has been covered in 10 articles. Among them, 3 reports presented the unusual association of lymphoma with other neoplasms. A case of concurrent diffuse large B-cell lymphoma (DLBCL), rectal adenocarcinoma, and hepatocellular carcinoma was reported by Qiu et al. He was successfully treated with six cycles R-GEMOX followed by six cycles R-CHOP to achieve CR for DLBCL. During this course of therapy, the patient received a PD-1 inhibitor (Sintilimab) as a treatment for HCC and, ultimately, he ended up with curative intent right hemihepatectomy and Dixon surgery. The second case reported by Bhakta et al. described an elderly man with untreated prostate cancer who presented with left thigh pain and eventually developed a pathologic fracture. After fixation surgery, the pathology came out as DLBCL. Staging by PET scan FDG revealed no evidence of disease outside the thigh. The patient was then diagnosed with primary bone lymphoma (PBL) and was treated with chemotherapy R-mini-CHOP protocol. PBL represents less than 5% of all primary bone malignancies and less than 1% of all lymphomas (27). Pathologic fracture is an unusual complication of PBL (28). The authors highlight the importance of suspecting PBL in patients with pathologic fractures. The third case was reported by Accorsi Buttini et al. who described the development of high-risk MDS following CAR T-cell therapy in a patient with relapsed refractory DLBCL. Prolonged pancytopenia after CAR T-cell therapy is most likely related to active inflammation milieu together with the impact of previous cytoreductive chemotherapy (29). Bone marrow biopsy showed deletion of chromosome 7 and acquisition of RUNX1 mutation. The authors concluded that the development of MDS could be related to previous chemotherapy, however, impairment of immunosurveillance related to either lymphodepletion or CAR T-cell infusion could play a role too. Two case reports of lymphoma with unusual site involvement were described in this Research Topic. Johnson et al. reported a case of classic HCL with CNS involvement at relapse. The patient was initially treated with cladribine, pentostatin, and rituximab with long-lasting response till he developed CNS disease. Most classic HCL harboring BRAF V600E mutation offers a targeted therapy for the pretreated population (30). This patient achieved CR of relapsed HCL with CNS involvement after treatment with a BRAF inhibitor (Vemurafenib). Yang et al. reported a case of relapsed/refractory DLBCL with cardiac involvement. The patient developed cardiac metastasis after 12 months of treatment by conventional first-line chemotherapy and anti-CD19 CAR T cell immunotherapy. Secondary cardiac lymphoma is a rare disease and is associated with a high mortality rate (31). The patient was then treated with salvage chemotherapy, followed by CAR-NK cell immunotherapy and allo-HSCT. Unfortunately, he died of severe pneumonia. This report highlights the significance of early diagnosis and timely treatment to improve the prognosis of secondary cardiac lymphoma.

Two articles on Burkitt Lymphoma (BL) and CAR T-cell therapy have been presented in this Research Topic. Ye et al. reported a 61-year-old patient with high-risk relapsed-refractory BL who was treated successfully by salvage auto-HSCT followed by CAR T-cell consolidation therapy. The authors highlight the safety and feasibility of CAR T-cell therapy for older high-risk BL patients. The patient is still in CR after 4 years of treatment. The second case, by Wang, Y.-L. et al., is a young patient who developed cognitive impairment after CAR T-cell salvage therapy for BL. Neurotoxicity, including cognitive impairment, is a well-known adverse event of CAR-T cell infusion and is associated with a poor outcome (32). The main mechanism of neurotoxicity is neuroinflammation secondary to cytokine release syndrome and effector cell-associated neurotoxicity syndrome (33). Currently, CAR-T therapy-related cognitive impairment has no effective treatment. Sodium oligomannate is an effective treatment for cognitive deficits in mild-to-moderate Alzheimer's dementia through inhibition of neuroinflammation (34). The patient was treated with sodium oligomannate with rivastigmine and had significant improvement in cognitive function.

Sun et al. reported a case of lymphoma-associated hemophagocytic lymphohistiocytosis complicated by acute necrotizing encephalopathy. This complication is related to

cytokine storm. Brain insult secondary to this disease is not uncommon, however, the association with acute necrotizing encephalopathy is rarely reported (35). The patient was successfully treated with chemotherapy, immunoglobulin, and early initiation of steroids.

One case of lymphoma with pathologic challenges was reported by Zhang et al. The patient was diagnosed with AITL, or Angioimmunoblastic T-cell lymphoma. AITL is always presented with immense follicular dendritic cell meshwork (36). In this case, the proliferation of spindle cells was so profuse that was easily misdiagnosed as follicular dendritic cells sarcoma. Immunochemical and molecular examinations were consistent with AITL.

The last article about lymphoma was reported by Xing et al. The patient was diagnosed with double expression (MYC and BCL2) DLBCL with mutations of ATM and CD58 genes. She received 4 cycles of R-CHOP plus zanubrutinib and achieved only a partial response. An *in-vitro* high-throughput drug screening using a panel of 117 compounds was applied and showed sensitivity to single-agent bortezomib, thalidomide, and gemcitabine, and to the combination of bortezomib, thalidomide, and dexamethasone (VTD). The patient achieved CR after 2 cycles of VTD followed by 2 cycles of VTD-gemcitabine.

Moving to plasma cell neoplasm case reports, Bonometti et al. reported a case of small bowel obstruction secondary to plasma cell myeloma (PCM). GI involvement by PCM is extremely rare (37). The patient presented with abdominal pain and signs of small bowel obstruction by CT scan abdomen, for which he underwent urgent ileal resection. Histopathology revealed PCM. Subsequent investigations found serum monoclonal gammopathy, osteolytic bony lesions, and clonal bone marrow plasma cell infiltrate. He was treated with myeloma protocol. The authors emphasize the importance of prompt diagnosis and management of rare GI presentation of PCM. Another case of rare extramedullary disease of myeloma was reported by Li et al. They presented a patient with isolated CNS relapse 7 years after being treated for myeloma by induction therapy followed by auto-HSCT. CNS involvement is very rare, it occurs in only about 1% of patients (38). Isolated CNS relapse is even rarer with only a few case reports, these patients have a very poor prognosis (39). The patient was treated successfully with high-dose methotrexate and lenalidomide. Otsuka-Kamakura et al. reported a case of plasmablastic neoplasm with multinucleated giant cells that were difficult to distinguish from plasmablastic lymphoma or PCM of plasmablastic type. Both multinucleated giant cells and mononuclear cells had the same profile, according to IHC and FISH analyses. The authors concluded that the multinucleated giant cells were compatible with cancer stem cells.

The last three published articles in this Research Topic presented rare hematological diseases. Yoshida et al. reported a case of Rosai-Dorfman disease (RDD) with simultaneous multiple extranodal lesions in the skin, heart, liver, and pelvis. The patient has no cervical lymphadenopathy. She was successfully treated with steroids. RDD is a non-Langerhans cell histiocytosis characterized by fever and bilateral cervical lymphadenopathy. It's commonly presented with extranodal site lesions in the skin, bones, head and neck, kidneys, and CNS (40). The simultaneous cardiac and pelvis involvement has not been reported. This case highlights the atypical distribution of uncommon extranodal lesions of RDD and the need to avoid delays in diagnosis and treatment. Xu et al. reported three cases of TEMPI syndrome. TEMPI syndrome is a novel and ultra-rare disease characterized by Monoclonal gammopathy, Erythrocytosis, Telangiectasis, Perinephric fluids collection, and Intrapulmonary shunting (41). Only 29 cases were reported worldwide (42). The patients showed various responses to Myeloma-directed therapy. The response to therapy was assessed by measuring hemoglobin, erythropoietin, and M protein levels throughout the course of treatment. Zhao, L. et al. reported 2 cases of HLH, the first one was secondary to NK T-cell lymphoma and the second one was associated with missense variants in the perforin 1 gene. Both cases responded rapidly to ruxolitinib plus dexamethasone protocol without obvious adverse effects. The primary first-line treatment for HLH is chemotherapy-containing regimens. However, some patients are resistant to treatment or unfit for intensive chemotherapy (43, 44). This report highlights the importance of ruxolitinib plus dexamethasone as a potential treatment for HLH.

In summary, the thirty-three articles published on this Research Topic provide clinical practitioners and researchers valuable insights into diagnosing and treating diseases with unusual presentation and open the door for future research.

Author contributions

AA: Writing – original draft, Writing – review & editing. AS: Writing – review & editing. OI: Writing – review & editing.

Conflict of interest

The authors declare that the research was conducted in the absence of any commercial or financial relationships that could be construed as a potential conflict of interest.

The authors declared that they were an editorial board member of Frontiers, at the time of submission. This had no impact on the peer review process and the final decision

Publisher's note

References

1. Khoury JD, Solary E, Abla O, Akkari Y, Alaggio R, Apperley JF, et al. The 5th edition of the World Health Organization classification of haematolymphoid tumours: myeloid and histiocytic/dendritic neoplasms. *Leukemia* (2022) 36(7):1703–19. doi: 10.1038/s41375-022-01613-1

2. Megias-Vericat JE, Solana-Altabella A, Ballesta-Lopez O, Martinez-Cuadron D, Montesinos P. Drug-drug interactions of newly approved small molecule inhibitors for acute myeloid leukemia. *Ann Hematol* (2020) 99(9):1989–2007. doi: 10.1007/s00277-020-04186-0

3. Dolton MJ, Roufogalis BD, McLachlan AJ. Fruit juices as perpetrators of drug interactions: The role of organic anion-transporting polypeptides. *Clin Pharmacol Ther* (2012) 92(5):622–30. doi: 10.1038/clpt.2012.159

4. Egeler RM, Neglia JP, Puccetti DM, Brennan CA, Nesbit ME. Association of langerhans cell histiocytosis with Malignant neoplasms. *Cancer* (1993) 71(3):865–73. doi: 10.1002/1097-0142(19930201)71:3<865::AID-CNCR2820710334>3.0.CO;2-0

5. Egeler RM, Neglia JP, Aricó M, Favara BE, Heitger A, Nesbit ME, et al. The relation of langerhans cell histiocytosis to acute leukemia, lymphomas, and other solid tumors. the LCH-Malignancy study group of the histiocyte society. *Hematol Oncol Clin North Am* (1998) 12(2):369–78. doi: 10.1016/s0889-8588(05)70516-5

6. Salzer U, Chapel HM, Webster AD, Pan-Hammarstrom Q, Schmitt-Graeff A, Schlesier M, et al. Mutations in Tnfrsf13b encoding taci are associated with common variable immunodeficiency in humans. *Nat Genet* (2005) 37(8):820–8. doi: 10.1038/ng1600

7. Mousset S, Hermann S, Klein SA, Bialleck H, Duchscherer M, Bomke B, et al. Prophylactic and interventional granulocyte transfusions in patients with haematological Malignancies and life-threatening infections during neutropenia. *Ann Hematol* (2005) 84:734–41. doi: 10.1007/s00277-005-1055-z

8. Zhang X, Sun J, Yu W, Jin J. Current views on the genetic landscape and management of variant acute promyelocytic leukemia. *biomark Res* (2021) 9(1):33. doi: 10.1186/s40364-021-00284-x

9. Geoffroy MC, de The H. Classic and variants APLs, as viewed from a therapy response. *Cancers (Basel)* (2020) 12(4):967. doi: 10.3390/cancers12040967

10. Astolfi A, Masetti R, Indio V, Bertuccio SN, Messelodi D, Rampelli S, et al. Torque teno mini virus as a cause of childhood acute promyelocytic leukemia lacking PML/RARA fusion. *Blood* (2021) 138(18):1773–7. doi: 10.1182/blood.2021011677

11. Rau RE. A viral cause of APL. *Blood* (2021) 138(18):1653–5. doi: 10.1182/blood.2021013630

12. Engel N, Rovo A, Badoglio M, Labopin M, Basak GW, Beguin Y, et al. European Experience and risk factor analysis of donor cell-derived leukaemias/MDS following haematopoietic cell transplantation. *Leukemia* (2019) 33(2):508–17. doi: 10.1038/s41375-018-0218-6

13. Shiozaki H, Yoshinaga K, Kondo T, Imai Y, Shiseki M, Mori N, et al. Donor cell-derived leukemia after cord blood transplantation and a review of the literature: Differences between cord blood and BM as the transplant source. *Bone Marrow Transplant* (2014) 49(1):102–9. doi: 10.1038/bmt.2013.127

14. Shen MZ, Zhang XH, Xu LP, Wang Y, Yan CH, Chen H, et al. Preemptive interferon-a therapy could protect against relapse and improve survival of acute myeloid leukemia patients after allogeneic hematopoietic stem cell transplantation: Long-term results of two registry studies. *Front Immunol* (2022) 13:757002. doi: 10.3389/fimmu.2022.757002

15. Petitjean A, Mathe E, Kato S, Ishioka C, Tavtigian S, Hainaut P, et al. Impact of mutant p53 functional properties on TP53 mutation patterns and tumor phenotype: lessons from recent developments in the IARC TP53 database. *Hum Mutat* (2007) 28 (6):622–9. doi: 10.1002/humu.20495

16. Shtivelman E, Lifshitz B, Gale RP, Canaani E. Fused transcript of abl and bcr genes in chronic myelogenous leukaemia. *Nature* (1985) 315(6020):550–4. doi: 10.1038/315550a0

17. Hochhaus A, Reiter A, Skladny H, Melo JV, Sick C, Berger U, et al. A novel BCR-ABL fusion gene (e6a2) in a patient with Philadelphia chromosome-negative chronic myelogenous leukemia. *Blood* (1996) 88(6):2236–40. doi: 10.1182/blood.V88.6.2236

18. Branford S, Rudzki Z, Hughes TP. A novel BCR-ABL transcript (e8a2) with the insertion of an inverted sequence of ABL intron 1b in a patient with Philadelphia-positive chronic myeloid leukaemia. *Br J Haematol* (2000) 109(3):635–7. doi: 10.1046/j.1365-2141.2000.02042.x

19. Schultheis B, Wang L, Clark RE, Melo JV. BCR-ABL with an e6a2 fusion in a CML patient diagnosed in blast crisis. *Leukemia* (2003) 17(10):2054–5. doi: 10.1038/sj.leu.2403079

20. Quintas-Cardama A, Kantarjian H, O'brien S, Borthakur G, Bruzzi J, Munden R, et al. Pleural effusion in patients with chronic myelogenous leukemia treated with dasatinib after imatinib failure. *J Clin Oncol* (2007) 25:3908–14. doi: 10.1200/JCO.2007.12.0329

21. Yu JY, Ma TG, Li YL, Ma L, Gao R, Liu J. An 11 years delayed diagnosis of primary pulmonary diffuse large b cell lymphoma. *Chin Med J (Engl)* (2019) 132:2000–1. doi: 10.1097/CM9.0000000000000378

22. Szuber N, Elliott M, Tefferi A. Chronic neutrophilic leukemia: 2022 update on diagnosis, genomic landscape, prognosis, and management. *Am J Hematol* (2022) 97:491–505. doi: 10.1002/ajh.26481

23. Maxson JE, Tyner JW. Genomics of chronic neutrophilic leukemia. *Blood* (2017) 129:715–22. doi: 10.1182/blood-2016-10-695981

24. Pardanani A, Lasho TL, Laborde RR, Elliott M, Hanson CA, Knudson RA, et al. CSF3R T618I is a highly prevalent and specific mutation in chronic neutrophilic leukemia. *Leukemia* (2013) 27:1870–3. doi: 10.1038/leu.2013.122

25. Giné E, Bosch F, Villamor N, Rozman M, Colomer D, López-Guillermo A, et al. Simultaneous diagnosis of hairy cell leukemia and chronic lymphocytic leukemia/small lymphocytic lymphoma: A frequent association? *Leukemia* (2002) 16(8):1454–9. doi: 10.1038/sj.leu.2402553

26. Rabascall CX, Lou BX, Navetta-Modrov B, Hahn SS. Effective use of monoclonal antibodies for treatment of persistent COVID-19 infection in a patient on rituximab. *BMJ Case Rep* (2021) 14(8):e243469. doi: 10.1136/bcr-2021-243469

27. Bindal P, Desai A, Delasos L, Mulay S, Vredenburgh J. Primary bone lymphoma: A case series and review of literature. *Case Rep Hematol* (2020) 2020:4254803. doi: 10.1155/2020/4254803

28. Messina C, Christie D, Zucca E, Gospodarowicz M, Ferreri AJ. Primary and secondary bone lymphomas. *Cancer Treat Rev* (2015) 41(3):235–46. doi: 10.1016/j.ctrv.2015.02.001

29. Cordeiro A, Bezerra ED, Hirayama AV, Hill JA, Wu QV, Voutsinas J, et al. Late events after treatment with CD19-tar- geted chimeric antigen receptor modified T cells. *Biol Blood Marrow Transplant* (2020) 26(1):26–33. doi: 10.1016/j.bbmt.2019.08.003

30. Tiacci E, Trifonov V, Schiavoni G, Holmes A, Kern W, Martelli MP, et al. BRAF mutations in hairy-cell leukemia. *N Engl J Med* (2011) 364(24):2305–15. doi: 10.1056/NEJMoa1014209

31. Jeudy J, Burke AP, Frazier AA. Cardiac lymphoma. *Radiol Clin North Am* (2016) 54(4):689–710. doi: 10.1016/j.rcl.2016.03.006

32. Lee EQ. Neurologic complications of cancer therapies. *Curr Neurol Neurosci Rep* (2021) 21:66. doi: 10.1007/s11910-021-01151-w

33. Brudno JN, Kochenderfer JN. Recent advances in CAR T-cell toxicity: Mechanisms, manifestations and management. *Blood Rev* (2019) 34:45–55. doi: 10.1016/j.blre.2018.11.002

34. Xiao S, Chan P, Wang T, Hong Z, Wang S, Kuang W, et al. A 36-week multicenter, randomized, double-blind, placebo-controlled, parallel-group, phase 3 clinical trial of sodium oligOmannate for mild-to-moderate alzheimer's dementia. *Alzheimer's Res Ther* (2021) 13:62. doi: 10.1186/s13195-021-00795-7

35. Bassuk AG, Burrowes DM, McRae W. Acute necrotizing encephalopathy of childhood with radiographic progression over 10 hours. *Neurology* (2003) 60(9):1552–3. doi: 10.1212/01.WNL.0000058757.52327.17

36. Moskowitz AJ. Practical treatment approach for angioimmunoblastic T-cell lymphoma. *J Oncol Pract* (2019) 15(3):137–43. doi: 10.1200/JOP.18.00511

37. Talamo G, Cavallo F, Zangari M, Barlogie B, Lee CK, Pineda-Roman M, et al. Clinical and biological features of multiple myeloma involving the gastrointestinal system. *Haematologica* (2006) 91(7):964–7. doi: 10.3324/%x

38. Jurczyszyn A, Grzasko N, Gozzetti A, Czepiel J, Cerase A, Hungria V, et al. Central nervous system involvement by multiple myeloma: A multi-institutional retrospective study of 172 patients in daily clinical practice. *Am J Hematol* (2016) 91:575–80. doi: 10.1002/ajh.24351

39. Chen CI, Masih-Khan E, Jiang H, Rabea A, Cserti-Gazdewich C, Jimenez-Zepeda VH, et al. Central nervous system involvement with multiple myeloma: Long term survival can be achieved with radiation, intrathecal chemotherapy, and immunomodulatory agents. *Br J Haematol* (2013) 162:483–8. doi: 10.1111/bjh.12414

40. Goyal G, Ravindran A, Young JR, Shah MV, Bennani NN, Patnaik MM, et al. Clinicopathological features, treatment approaches, and outcomes in rosai-dorfman disease. *Haematologica* (2020) 105:348–57. doi: 10.3324/haematol.2019.219626

41. Sykes DB, Schroyens W, O'Connell C. The TEMPI syndrome–a novel multisystem disease. *N Engl J Med* (2011) 365(5):475–7. doi: 10.1056/NEJMc1106670

42. Kubik T, Minoo P. TEMPI syndrome associated with IgM monoclonal gammopathy. *Blood* (2022) 139(8):1254. doi: 10.1182/blood.2021014393

43. Trottestam H, Horne A, Aricó M, Egeler RM, Filipovich AH, Gadner H, et al. Chemoimmunotherapy for hemophagocytic lymphohistiocytosis: Long-term results of the HLH - 94 treatment protocol. *Blood* (2011) 17:4577–84. doi: 10.1182/blood-2011-06-356261

44. Bergsten E, Horne A, Aricó M, Astigarraga I, Egeler RM, Filipovich AH, et al. Confirmed efficacy of etoposide and dexamethasone in HLH treatment: Long - term results of the cooperative HLH - 2004 study. *Blood* (2017) 25:2728–38. doi: 10.1182/blood-2017-06-788349

frontiers | Frontiers in Oncology

TYPE Case Report
PUBLISHED 03 August 2022
DOI 10.3389/fonc.2022.949647

OPEN ACCESS

EDITED BY
Luca Arcaini,
University of Pavia, Italy

REVIEWED BY
David Brian Sykes,
Massachusetts General Hospital and Harvard Medical School, United States
Breno Moreno De Gusmão,
Beneficência Portuguesa de São Paulo, Brazil

*CORRESPONDENCE
Daobin Zhou
zhoudaobinoffice@163.com
Wei Zhang
vv1223@vip.sina.com

SPECIALTY SECTION
This article was submitted to Hematologic Malignancies, a section of the journal Frontiers in Oncology

RECEIVED 21 May 2022
ACCEPTED 14 July 2022
PUBLISHED 03 August 2022

CITATION
Xu Z-F, Ruan J, Chang L, Wu S, Lin J, Wang W, Cao XX, Zhang L, Li J, Zhou D and Zhang W (2022) Case Report: TEMPI syndrome: Report of three cases and treatment follow-up. *Front. Oncol.* 12:949647. doi: 10.3389/fonc.2022.949647

Case Report: TEMPI syndrome: Report of three cases and treatment follow-up

Zhuo-Fan Xu[1,2], Jing Ruan[1], Long Chang[1], Sijin Wu[1], Jinkai Lin[1], Wei Wang[1], XinXin Cao[1], Lu Zhang[1], Jian Li[1], Daobin Zhou[1]* and Wei Zhang[1]*

[1]Department of Hematology, Peking Union Medical College Hospital, Beijing, China, [2]School of Medicine, Tsinghua University, Beijing, China

The TEMPI syndrome is a novel and rare disease with five distinct clinical features: Telangiectasis, Erythrocytosis, Monoclonal gammopathy, Perinephric fluids collection, and Intrapulmonary shunting. Here, we report three cases of TEMPI syndrome and their treatment response. The three patients were presented to our department with polycythemia, abdominal distension, and dyspnea. On admission, all patients manifested telangiectasis, erythrocytosis, monoclonal gammopathy, and intrapulmonary shunting. Patient 1 and 2 manifested perinephric fluids collection. In addition, all patients had skin pigmentation, patient 1 and 2 had polyserosal effusion, two symptoms that had not been associated with TEMPI syndrome before. The three patients showed various response to plasma cell-directed therapy. We demonstrated their treatment response by measuring erythropoietin, hemoglobin, and M protein levels throughout therapy. This report suggested that TEMPI syndrome is a rare yet treatable disease. The diagnosis and treatment of it remain challenging.

KEYWORDS

TEMPI syndrome, monoclonal gammopathy, erythrocytosis, plasma cell disorder, case report

Introduction

The TEMPI syndrome is a rare disorder characterized by Telangiectasis, Erythrocytosis, Monoclonal gammopathy, Perinephric fluids collection, and Intrapulmonary shunting. First described by Sykes et al. in 2011 (1), there are only 29 cases reported worldwide (1–11). Herein, we report three new cases of TEMPI syndrome diagnosed in our department. We presented comprehensive clinical evaluations and relevant history of the patients and highlighted the possible association between skin pigmentation and TEMPI syndrome. Two of the patients showed favorable long-term treatment response. We demonstrated their response by monitoring the biochemical markers throughout therapies.

Case presentation

Patient 1

A 60 years old male with a five–year history of polycythemia was presented to our department in 2020. For the past five years, his polycythemia had been presumed to be due to polycythemia vera (PV). He was treated with hydroxyurea and phlebotomy, to which he reported moderate response and frequent recurrence. In 2019, he tested positive for IgA-κ and was suspected of multiple myeloma. The patient came to our department for further evaluations.

On admission, he had an oxygen saturation (SpO2) of 94%. Physical exams showed telangiectasis on his face, chest, and back. Skin pigmentation was found on his face and lips. His blood tests demonstrated polycythemia (RBC 7.13×10^{12}/L, HGB 151g/L). Laboratory findings included increased EPO level (676.16 mIU/mL) and monoclonal gammopathy (M protein 5.10g/L, IgA-κ(+)). Additionally, increased IL-6, IL-8, and TNFα levels were detected. A bone marrow biopsy showed 1.5% of plasma cells. Enhanced computed tomography (CT) revealed moderate amount of perinephric fluid and small amount of abdominal and pelvic fluid. Doppler bubble test indicated intrapulmonary shunt, while the result of lung perfusion scintigraphy (LPS) with Tc-99m MAA was unremarkable. (Table 1)

Meeting all major criteria (telangiectasis, elevated EPO and erythrocytosis, monoclonal gammopathy) and minor criteria (perinephric fluid, intrapulmonary shunting) (12), the diagnosis of TEMPI syndrome was established. The patient was initiated on plasma cell-directed therapy with bortezomib and dexamethasone (Bd). After two courses of Bd, he developed peripheral neuropathy (grade I), with no obvious decrease in EPO level. Ixazomib and dexamethasone (Id) were then prescribed. After one course of Id, there was a significant decrease in EPO and HGB levels. However, the patient reported itchiness and general discomfort. Ixazomib was discontinued, and therapy of lenalidomide and dexamethasone

TABLE 1 Characteristics of patients with TEMPI syndrome.

Characteristic	Patient 1	Patient 2	Patient 3
Demographic			
Age (yr)	60	57	57
Gender	Male	Male	Female
First presentation	Polycythemia	Abdominal bloating	Dyspnea
TEMPI syndrome			
Telangiectasias	Face, chest, back	Chest, back	Neck, chest
Erythrocytosis and EPO			
RBC ($\times10^{12}$/L)	7.13	7.32	4.73
HGB (g/L)	151	175	181
HCT (%)	52.3	61.6	55.9
EPO (mIU/mL)	676.16	>741.00	209.77
Monoclonal gammopathy			
M protein (%)	6.90%	12.00%	35.40%
M protein (g/L)	5.1	9.6	NR
Type	IgA-κ	IgG-κ	IgG-λ
Light chain	sFLC-λ↑	sFLC-κ↑	sFLC-λ↑
κ/λ	0.528	2.059	0.483
Perinephric fluid	+	+	–
Intrapulmonary shunting			
SpO2	94%	93%	89%
Bubble test	+	+	+
LPS	–	Lung telangiectasis	–
Shunting fraction	–	21.10%	10.40%
Others			
Venous thrombosis	–	–	–
Serous effusion	Abdominal, pelvic	Chest, abdominal, pelvic	–
Inflammation markers	IL-6↑, IL-8↑,TNFα↑	–	TNFα↑
Bone marrow plasma cells	1.50%	2.50%	10.50%
Skin pigmentation	+	+	+

(Rd) was initiated. After two courses of Rd, he demonstrated satisfactory response: The telangiectasis on his face and chest improved substantially; EPO fell within the normal range; M protein was tested negative; Perinephric fluids were decreased. (Figure 1)

Patient 2

A 57 years old male with a seven-year history of skin pigmentation and a three-year history of abdominal distension was presented to our department in 2020. The patient developed facial pigmentation and lips cyanosis in 2013. He was hospitalized for diarrhea, abdominal distension, and fatigue in 2017. His laboratory and endoscopy examinations were unremarkable except for elevation of RBC and HGB levels. The patient was treated with supportive medicine for diarrhea and hydroxyurea for suspicious PV. During treatment, his diarrhea improved, his HGB level decreased, while his abdominal distension and fatigue remained. In 2018, the patient started to suffer recurrent upper respiratory infection and dyspnea. His CT images suggested chest and abdominal fluids collection. In 2020, he experienced progressive abdominal distension and came to our department for further examination.

On admission, he had a SpO2 of 93%. His physical exams showed whole-body skin pigmentation, white nails, and telangiectasis on the chest, back, and oral mucosa. He was positive for abdominal distension signs and shifting dullness. Lab tests revealed elevated HGB (175g/L) and EPO levels (>741.00mIU/mL), and monoclonal gammopathy (M protein 9.60g/L, IgG-κ(+)). Bone marrow biopsy showed 2.5% plasma cells. Enhanced CT revealed extensive perinephric, abdominal, and pelvic fluids. (Figure 2) Ascites puncture aspirated 800mL transudate ascites with normal cell counts and protein level. Arterial blood gas (ABG) test indicated right-to-left shunting (pO2 60mmHg, pO2(A-a)e 54.3mmHg, FShumte 31.9%). Doppler bubble test showed intrapulmonary shunting. LPS demonstrated pulmonary telangiectasis. First-pass LPS confirmed intrapulmonary shunting (shunt fraction 21.1%). (Table 1)

The diagnosis of TEMPI syndrome was established for all major and minor criteria were fulfilled. After four courses of Rd, the patient demonstrated mixed response. While his dyspnea and abdominal distension improved and EPO level dropped, his HGB and M protein levels remained high, and his perinephric fluids collection increased. He was then given bortezomib, cyclophosphamide, and dexamethasone (BCD) for further treatment. After three courses of BCD, the patient experienced dizziness, dyspnea, and aggravated abdominal distension. He went through ascites drainage and discontinued BCD therapy for 1 month. Lab tests showed increased EPO, HGB, and M protein levels. The patient then started melphalan, dexamethasone, and thalidomide (MDT) therapy. He responded well to MDT. After seven courses, the telangiectasis on his chest became less prominent, and his EPO and M protein

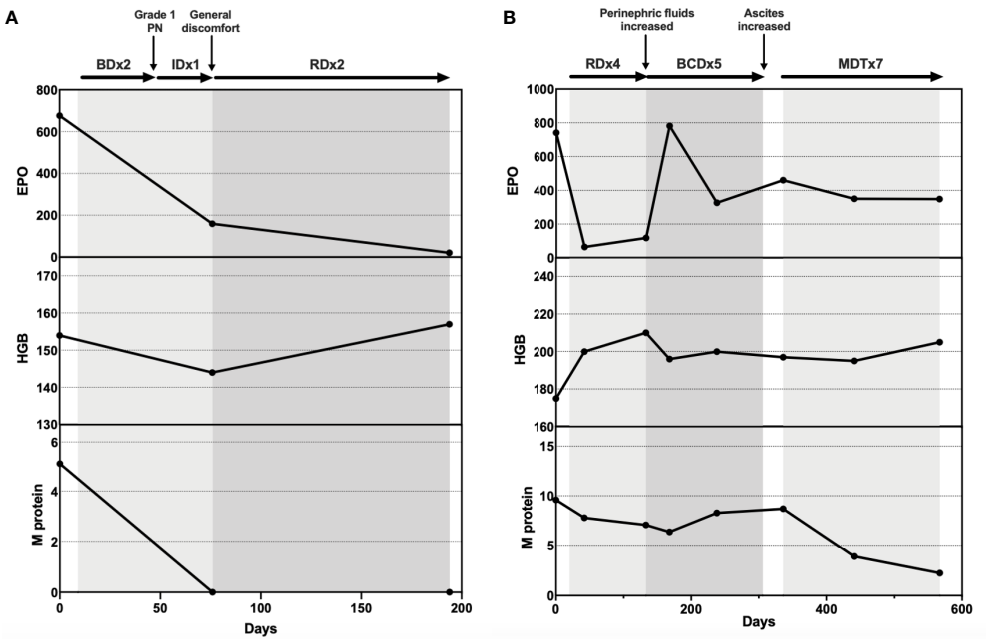

FIGURE 1
(A) Treatment response of Patient 1; **(B)** Treatment response of Patient 2.

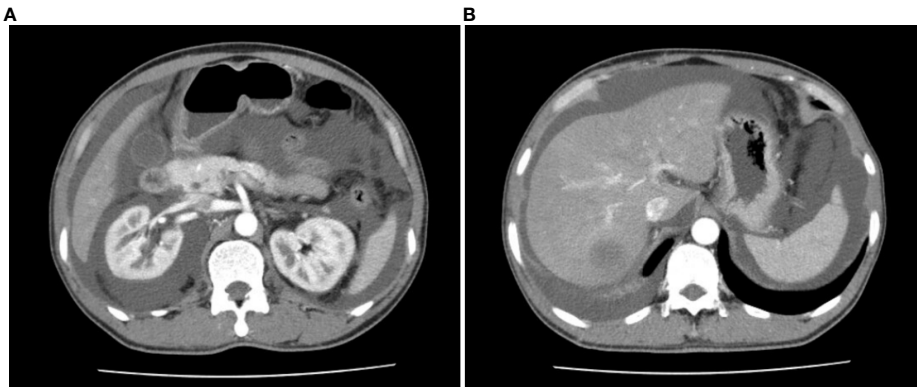

FIGURE 2
Enhanced CT scans of patient 2. **(A)** Perinephric fluids; **(B)** Abdominal fluids.

levels dropped continuously. However, his RBC counts and HGB level remained high. (Figure 1)

Patient 3

A 57 years old female with a seven-year history of dyspnea was presented to our department in 2021. The patient had been experiencing dyspnea and dizziness after physical activities since 2014. Four years later, in 2018, she developed rashes on her neck and chest. In 2020, she was hospitalized for dyspnea. Her pulmonary function test indicated type I respiratory failure and asthma. Her blood tests showed polycythemia and monoclonal gammopathy. Her bone marrow biopsy was normal. She was then initiated on asthma treatment and hydroxyurea treatment, to which she showed no response. During treatment, her dyspnea worsened. She was referred to our department for evaluation.

On admission, she had a SpO2 of 89%. Physical exams showed telangiectasis on her neck, chest, and abdomen. Peripheral cyanosis was found on the extremities. Skin pigmentation was found on her face and extremities. (Figure 3) Elevation of HGB level (181g/L) and monoclonal gammopathy (M protein% 35.4%, IgG-λ(+)) were confirmed by laboratory tests. Her EPO level was 209.77mIU/mL. Her TNFα level was elevated as well. Bone marrow biopsy revealed 10.5% plasma cells. Abdominal CT showed no sign of perinephric fluids. Chest CT indicated emphysema and possible interstitial lung disease. First-pass pulmonary perfusion scintigraphy confirmed intrapulmonary shunting (shunt fraction 10.4%).

The patient was diagnosed with TEMPI yndromee for three major and one minor criteria were met. Bd therapy was initiated. Her EPO (209.77 –> 56.55mIU/mL) and M protein (35.4% -> 7.2%) levels dropped dramatically after one course of Bd. Her HGB levels (181 –> 140g/L) and RBC counts (4.73 –> 4.32x10^{12}/L) also fell within the normal ranges. However, she developed swelling and pain in the right calf, which later progressed into cellulitis. Ultra-sound showed no sign of venous thrombosis. After abscess incision and drainage, the patient is now under skin grafting and careful monitoring of TEMPI syndrome.

Discussion

The TEMPI syndrome is a rare multisystem disease with unique cutaneous features and a signature set of clinical manifestations. It was first described in a case series of 6 patients in 2011 (1), where they shared five characteristics — telangiectasias, elevated EPO level and erythrocytosis, monoclonal gammopathy, perinephric fluid collections, and intrapulmonary shunting. Later, more cases were identified and reported as individual case reports across the globe (12), and TEMPI syndrome was officially categorized as a plasma cell disorder with paraneoplastic manifestations. Zhang et al. reviewed the first 15 published cases in 2018. It appears that TEMPI syndrome is an acquired disorder that slowly progresses and generally manifests after middle age. No gender, ethnicity, or geography predisposition was reported (13).

Almost all patients manifested telangiectasias, erythrocytosis, and monoclonal gammopathy, the three major criteria of TEMPI syndrome (12). The three patients we reported met all major criteria of TEMPI syndrome, although with distinct onset symptoms (Asymptomatic polycythemia; Skin pigmentation and abdominal distension; Dyspnea). Even though the diagnostic features are unique, misdiagnosis of PV, renal, pulmonary, or hematologic disorders appeared almost invariably throughout the cases. All of our patients had been misdiagnosed with PV and received hydroxyurea or phlebotomy treatment. The time between their disease onset and diagnosis of TEMPI syndrome spans from 5 to 7 years. Despite the rareness of the disease, early recognition and diagnosis are important. Proper treatment could prevent the progressive course of EPO increment, and the progression to

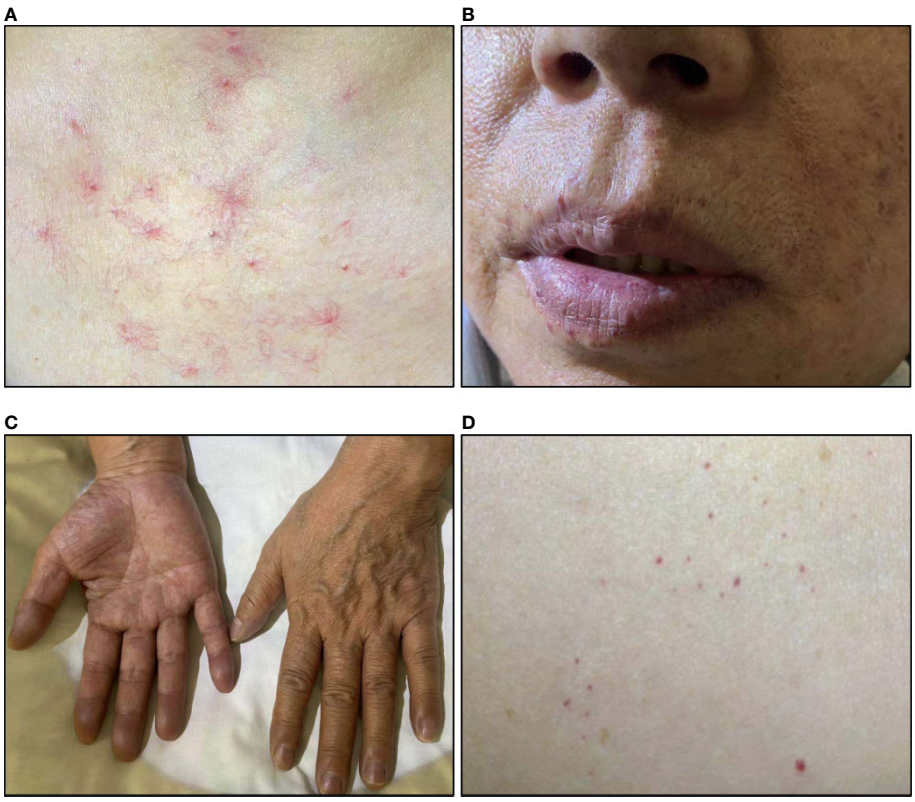

FIGURE 3
Skin changes of patient 3. **(A)** Telangiectasis on the neck and chest; **(B)** Telangiectasis on lips; **(C)** Cyanosis of fingers; **(D)** Rash on the abdomen.

more severe symptoms such as intrapulmonary shunting and perinephric fluids. Improper treatment with hydroxyurea and phlebotomy could lead to iron deficiency and microcytosis (12). From 2020 to 2022, our department has already diagnosed 3 new cases of TEMPI syndrome, which make us suspect there is more TEMPI patient unidentified. Early recognition and proper diagnosis of this disease require more awareness from hematologists, dermatologists, and general practitioners.

The less predominant clinical features and associated findings of TEMPI syndrome include venous thrombosis, spontaneous intracranial hemorrhage, liver hemangiomas, diarrhea, ascites, and pleural effusion (13). These sporadic symptoms are mostly considered coincidental. However, as the number of cases continues to grow, more associated symptoms might be discovered.

In our cases, patient 2 was presented with polyserosal effusion and a history of diarrhea, abdominal distension, and dyspnea. After careful examinations, no underlying diseases were found responsible for his polyserosal effusion. Patient 1, to a lesser extent, also had asymptomatic abdominal and pelvic fluids. It aroused our curiosity whether chest and abdominal fluids were associated with TEMPI syndrome. During the treatment of patient 2, a remarkable drop in M protein was observed, however, we did not see a simultaneous resolution of either chest and abdominal fluids or perinephric fluids.

We also noticed that all three patients demonstrated diffusive or localized skin pigmentation. Hyperpigmentation is commonly seen in patients with POEMS syndrome, yet has not been reported in TEMPI syndrome. Patient 1 was found to have localized facial pigmentation on admission. Patient 2 reported a seven–year history of whole-body skin pigmentation starting from the face and lips. Patient 3 was found to have diffusive skin pigmentation on admission. We wonder whether hyperpigmentation was one of the skin changes possibly associated with TEMPI syndrome that had been overlooked in the past. In POEMS syndrome, VEGF is a proposed candidate for contributing to skin changes (14). Increased VEGF and IL-6 levels were described in the previous cases (4). We did not measure VEGF level, but we did notice elevation of IL-6, IL-8, and TNFα in patient 1 and elevation of TNFα in patient 3. For patient 1 and 2, there were substantial improvements in telangiectasis during treatment. However, there was no self-reported improvement in skin pigmentation. For patient 3, no obvious change of either telangiectasias or skin pigmentation was observed during the two–month follow–up period. Pictures of her skin changes were documented for future reference.

Besides the clinical symptoms, little is known about the etiology and pathogenesis of TEMPI syndrome. One theory postulates that the syndrome is an autoimmune disease caused by antibodies, chemokines, or cytokines secreted by monoclonal plasma cells since plasma cell–directed therapy could reverse the manifestations (12). Khan et al. proposed that HIF-1α may play a role in the pathogenesis of TEMPI syndrome as well. Since bortezomib also affects the function of HIF-1α, inhibition of HIF-1α could also explain the resolution of symptoms (15). More recently, Sun et al. found that the expression of macrophage migration inhibitory factor (MIF) was significantly upregulated in three patients with TEMPI syndrome (16). Altogether, these hypotheses and findings suggest that multiple pathways might be involved in the pathophysiology of TEMPI syndrome. Due to the rareness of the disease, uncovering its etiology and pathogenesis will require international collaboration in collecting samples and data. We have not been able to collect research samples of the three patients, but we are open to sharing clinical data and possible research samples in the future.

Up till now, plasma cell-directed treatment is the only first–line therapeutic option for TEMPI syndrome (12). The complete and partial responses gained by bortezomib-based regimens have been revealed in multiple case reports (17–19). The alternative therapies that have been reported include daratumumab (20), lenalidomide (9), and autologous transplantation (21). Rapid and remarkable treatment response was seen in several patients. All symptoms of TEMPI syndrome appeared to be reversible under proper therapy (18). However, recurrence and refractory were also reported in multiple cases (7–9). Due to the lack of therapeutic experience, there are currently no treatment guidelines for those patients. Our limited experience suggested that personalized regimens need to be chosen and adjusted for patients by carefully monitoring their response. In our cases, Patient 1 reached satisfactory response with lenalidomide, while Patient 2's perinephric fluids progressed after four courses of Rd. Patient 2 was then treated with BCD, followed by MDT. After seven courses of MDT, a substantial drop in M protein and resolution of telangiectasia and serous fluids were finally observed. Patient 3 demonstrated rapid and dramatic response to bortezomib, but she developed infection and cellulitis after one course of Bd.

There is currently no prognostic marker for TEMPI syndrome. Since monoclonal gammopathy has been proposed to be the cause of TEMPI syndrome, M protein levels are carefully monitored throughout therapy. However, no clues of correlation between initial M protein level and treatment response was found. In patients who relapsed after initial therapy, the increase of EPO level seems to be the most sensitive marker (12). Nevertheless, EPO level before treatment did not predict disease severity or treatment response either. Up till now, the follow–up times are still too short to conclude long-term survival. Understanding the prognosis and outcomes of this rare disease will depend on the continued description of patients worldwide.

In conclusion, TEMPI syndrome is a rare disorder that can be reversible with timely diagnosis and appropriate treatment. We herein report the clinical presentation and treatment response of three new cases of TEMPI syndrome. Our observation showed that the possible associated symptoms and therapy responses varied among patients. More studies are in need to explore the etiology, pathogenesis, clinical manifestations, treatment, and prognosis of this ultra-rare disease.

Data availability statement

The original contributions presented in the study are included in the article/supplementary material. Further inquiries can be directed to the corresponding authors.

Ethics statement

Written informed consent was obtained from the participant for the publication of this case report.

Author contributions

Z-FX drafted the manuscript. All authors participated in patient management and data collection. JR, LC, and SW contributed to the preparation of figures. All authors contributed to the article and approved the submitted version.

Acknowledgments

Thanks are given to all the clinicians providing care and management to the patients.

Conflict of interest

The authors declare that the research was conducted in the absence of any commercial or financial relationships that could be construed as a potential conflict of interest.

Publisher's note

References

1. Sykes DB, Schroyens W, O'Connell C. The TEMPI syndrome–a novel multisystem disease. *N Engl J Med* (2011) 365(5):475–7. doi: 10.1056/NEJMc1106670

2. Wu JH, Viruni N, Chun J, Shanbhag S, Liu TYA. Ocular involvement in TEMPI syndrome. *Am J Ophthalmol Case Rep* (2022) 26:101534. doi: 10.1016/j.ajoc.2022.101534

3. Kubik T, Minoo P. TEMPI syndrome associated with IgM monoclonal gammopathy. *Blood* (2022) 139(8):1254. doi: 10.1182/blood.2021014393

4. Strobl J, Sinz C, Heil PM, Stary G, Weninger W. Cutaneous ulceration as primary presentation of TEMPI syndrome. *J Eur Acad Dermatol Venereol* (2021) 35(12):e891–4. doi: 10.1111/jdv.17539

5. Ruan Y, Zhao X, Pan M. Diffuse telangiectasia: A clue to the TEMPI syndrome. *JAAD Case Rep* (2021) 10:99–101. doi: 10.1016/j.jdcr.2021.02.022

6. Shizuku T, Matsui K, Yagi S, Iwabuchi S. The first case of TEMPI syndrome in Japan. *Intern Med* (2020) 59(14):1741–4. doi: 10.2169/internalmedicine.3547-19

7. Lor M, Cheng M, Liang B, Cheng CE. TEMPI syndrome with progressive telangiectasias associated with pulmonary deterioration. *JAMA Dermatol* (2020) 156(12):1379–80. doi: 10.1001/jamadermatol.2020.2668

8. Diral E, Parma M, Renso R, Pezzatti S, Terruzzi E, Perfetti P, et al. A fatal case of TEMPI syndrome, refractory to proteasome inhibitors and autologous stem cell transplantation. *Leuk Res* (2020) 97:106441. doi: 10.1016/j.leukres.2020.106441

9. Liang SH, Yeh SP. Relapsed multiple myeloma as TEMPI syndrome with good response to salvage lenalidomide and dexamethasone. *Ann Hematol* (2019) 98(10):2447–50. doi: 10.1007/s00277-019-03761-4

10. Pascart T, Herbaux C, Lemaire A, Soncin F, Hachulla E, Hatron PY, et al. Coexistence of rheumatoid arthritis and TEMPI syndrome: New insight in microangiogenic-related diseases. *Joint Bone Spine* (2016) 83(5):587–8. doi: 10.1016/j.jbspin.2015.06.011

11. Mohammadi F, Wolverson MK, Bastani B. A new case of TEMPI syndrome. *Clin Kidney J* (2012) 5(6):556–8. doi: 10.1093/ckj/sfs139

12. Sykes DB, O'Connell C, Schroyens W. The TEMPI syndrome. *Blood* (2020) 135(15):1199–203. doi: 10.1182/blood.2019004216

13. Zhang X, Fang M. TEMPI syndrome: Erythrocytosis in plasma cell dyscrasia. *Clin Lymphoma Myeloma Leuk* (2018) 18(11):724–30. doi: 10.1016/j.clml.2018.07.284

14. Dispenzieri A. POEMS syndrome. *Blood Rev* (2007) 21(6):285–99. doi: 10.1016/j.blre.2007.07.004

15. Khan S. The role of hypoxia-inducible factor-1 alpha in TEMPI syndrome. *NDT Plus* (2011) 4(6):454–5. doi: 10.1093/ndtplus/sfr143

16. Sun C, Xu J, Zhang B, Huang H, Chen L, Yan H, et al. Whole-genome sequencing suggests a role of MIF in the pathophysiology of TEMPI syndrome. *Blood Adv* (2021) 5(12):2563–8. doi: 10.1182/bloodadvances.2020003783

17. Kwok M, Korde N, Landgren O. Bortezomib to treat the TEMPI syndrome. *N Engl J Med* (2012) 366(19):1843–5. doi: 10.1056/NEJMc1202649

18. Schroyens W, O'Connell C, Sykes DB. Complete and partial responses of the TEMPI syndrome to bortezomib. *N Engl J Med* (2012) 367(8):778–80. doi: 10.1056/NEJMc1205806

19. Jasim S, Mahmud G, Bastani B, Fesler M. Subcutaneous bortezomib for treatment of TEMPI syndrome. *Clin Lymphoma Myeloma Leuk* (2014) 14(6):e221–3. doi: 10.1016/j.clml.2014.07.004

20. Sykes DB, Schroyens W. Complete responses in the TEMPI syndrome after treatment with daratumumab. *N Engl J Med* (2018) 378(23):2240–2. doi: 10.1056/NEJMc1804415

21. Kenderian SS, Rosado FG, Sykes DB, Hoyer JD, Lacy MQ. Long-term complete clinical and hematological responses of the TEMPI syndrome after autologous stem cell transplantation. *Leukemia* (2015) 29(12):2414–6. doi: 10.1038/leu.2015.298

frontiers | Frontiers in Oncology

TYPE Case Report
PUBLISHED 05 August 2022
DOI 10.3389/fonc.2022.934566

OPEN ACCESS

EDITED BY
Alessandro Gozzetti,
University of Siena, Italy

REVIEWED BY
Francesca Bacchiarri,
University of Siena, Italy
Apurva Patel,
Gujarat Cancer &Research Institute, India

*CORRESPONDENCE
Marco Lucioni
marco.lucioni@unipv.it

†These authors share first authorship

SPECIALTY SECTION
This article was submitted to Hematologic Malignancies, a section of the journal Frontiers in Oncology

RECEIVED 02 May 2022
ACCEPTED 08 July 2022
PUBLISHED 05 August 2022

CITATION
Bonometti A, Aronico N, Santacroce G, Fraticelli S, Lucioni M, Cartia CS, Vanoli A, Latorre MA, Arcaini L, Paulli M and Di Sabatino A (2022) Case report: A rare case of small bowel obstruction secondary to plasma cell myeloma.
Front. Oncol. 12:934566.
doi: 10.3389/fonc.2022.934566

Case Report: A rare case of small bowel obstruction secondary to plasma cell myeloma

Arturo Bonometti[1,2,3†], Nicola Aronico[4†], Giovanni Santacroce[4], Sara Fraticelli[2], Marco Lucioni[1,2*], Claudio Salvatore Cartia[5], Alessandro Vanoli[1,2], Mario Andrea Latorre[4], Luca Arcaini[2,5], Marco Paulli[1,2] and Antonio Di Sabatino[4]

[1]Unit of Anatomic Pathology, Fondazione Istituto di Ricovero e Cura a Carattere Scientifico (IRCCS) Policlinico San Matteo, University of Pavia, Pavia, Italy, [2]Department of Molecular Medicine, University of Pavia, Pavia, Italy, [3]Pathology Unit, Humanitas Clinical and Research Center Istituto di Ricovero e Cura a Carattere Scientifico (IRCCS), Rozzano, Italy, [4]First Department of Internal Medicine, Fondazione Istituto di Ricovero e Cura a Carattere Scientifico (IRCCS) Policlinico San Matteo, University of Pavia, Pavia, Italy, [5]Division of Hematology, Fondazione Istituto di Ricovero e Cura a Carattere Scientifico (IRCCS) Policlinico San Matteo, Pavia, Italy

Gastrointestinal (GI) involvement of plasma cell neoplasms is extremely rare. Herein, we describe the case of a 74-year-old Caucasian woman who came to our attention with abdominal pain, food vomiting, and weight loss of 10 kg over 1 year. A computed tomography scan of the abdomen revealed circumferential thickening of terminal ileum, for which the patient underwent an urgent 20-cm-long ileal resection. Histopathological and immunophenotypic analysis revealed a plasma cell neoplasm of the ileum. Subsequent investigations found a serum monoclonal immunoglobulin A component, an osteolytic lesion of the left jaw, and a clonal bone marrow plasma cell infiltrate carrying 1q21 amplification. Given the final diagnosis of plasma cell myeloma (PCM), the patient underwent a VMD (bortezomib, melphalan, and dexamethasone) chemotherapy regimen, achieving a complete remission after a 12-month treatment. For disease relapse, two further chemotherapy regimens were later attempted. At the last follow-up 4 years after the diagnosis, the patient is still alive. This case draws attention to the extramedullary presentation of plasma cell neoplasms, even if rare, as a prompt diagnosis seems to result in a better prognosis. In addition, it highlights the relevance of a multidisciplinary approach, involving gastroenterologists, hematologists, and pathologists, to the diagnosis and management of these neoplasms.

KEYWORDS

chemotherapy, intestinal occlusion, plasma cell myeloma, small bowel, extramedullary presentation

Introduction

Plasma cell neoplasms are a clinically heterogeneous group of clonal disorders of terminally differentiated B cells, often characterized by the secretion of monoclonal immunoglobulins (Ig), and include plasma cell myeloma (PCM), solitary plasmacytoma of bone, and extraosseous plasmacytoma (1).

PCM is the plasma cell neoplasm with the highest clinical burden and possibly the worst outcome, and its diagnosis is based on the detection of more than 10% of clonal bone marrow plasma cells or biopsy-proven bony or extramedullary plasmacytoma, and any one or more of the myeloma defining events, namely, CRAB (hypercalcemia, renal insufficiency, anemia, and bone lesions) features and biomarkers of malignancy (specifically more than 60% clonal plasma cells on bone marrow examination, serum involved/uninvolved free light chain ratio of 100 or greater, and more than one focal lesion on magnetic resonance) (2).

The bone is typically involved in PCM, but other organs may be infiltrated as well (1). Gastrointestinal (GI) involvement of plasma cell neoplasms seems infrequent, generally as a part of a multisystemic involvement (3), and it is described by few reports and a single large series (4–8). The liver seems to be the organ of the GI tract most affected, whereas stomach or intestine is far less reported as disease sites. Interestingly, GI involvement appears to be associated with adverse biological features (e.g., high lactate dehydrogenase levels, high risk karyotype, and plasmablastic cytology) and an aggressive behavior (4, 9).

Herein, we report a case of PCM presenting with ileal obstruction and diagnosed following emergency surgery.

Case presentation

A 74-year-old Caucasian woman referred to our centre in September 2017 for abdominal pain, food vomiting, and weight loss of 10 kg over 1 year. She had a medical history of arterial hypertension, hypercholesterolemia, obesity (with a body mass index of 31.2 and a body surface area of 1.89), primary osteoporosis, chronic Helicobacter pylori-unrelated gastritis, and smoking habit. Medications taken at home were antihypertensive drugs, hypolipidemic agents, and proton pump inhibitors. For osteoporosis, the patient was on calcium and vitamin D supplementation therapy. A previous exposure to radiation and chemical agents was excluded.

A computed tomography (CT) scan of the abdomen showed a small bowel circumferential wall thickening (Figure 1), for which the patient underwent an urgent ileal resection by laparoscopy. The surgical specimen consisted of a 20-cm-long segment of terminal ileum. At gross examination, the ileal wall displayed a 3-cm-long ulcerated lesion, determining a stenosis of the bowel lumen and infiltrating the mesentery through the visceral wall.

Microscopic analysis of the specimen (Figure 2) revealed a dense trans-parietal pleomorphic proliferation of mature plasma cells, consisting of small to large and multinucleated elements, some with Russel or Dutcher bodies, with ulceration of the bowel mucosa and infiltration of the perivisceral adipose tissue. All those elements stained positive for CD56, CD79a, CD138, MUM1, IgA and showed monoclonal restriction for the kappa (κ) light chain of Ig. CD5, CD20, CD45/LCA, Cyclin-D1, IgD, IgG, and IgM tested all negative as well as immunostaining for human herpes virus 8 (HHV8) and *in situ* hybridization for Epstein–Barr virus (EBV). The proliferative index of the neoplastic population (Mib1/Ki67) was estimated at around 40%. A moderate number of $CD3^+$ T lymphocytes were admixed to the plasma cell infiltrate. All the resected lymph nodes were spared, displaying reactive features.

Laboratory investigations were all within the limits (Table 1), with the exception of the serological presence of a monoclonal IgA-κ component equal to 1.2 g/dl with uninvolved normal Ig (IgG, 790 mg/dl; IgA, 1,380 mg/dl; IgM, 250 mg/dl) and antinuclear antibody positivity. Moreover, microscopic analysis of the bone marrow biopsy (Figure 3) showed a clonal plasma cell infiltrate (15% of bone marrow cellularity), consisting of small- to medium-sized plasma cells with aberrant expression of CD56 and monoclonal restriction for κ light chain of Ig, without amyloid deposits. Fluorescence *in situ* hybridization analysis documented the presence of 1q21 amplification.

A total body CT showed an osteolytic lesion of the left jaw, confirmed on positron emission tomography (PET) scan as secondary to the disease process. An upper GI endoscopy showing no pathological findings completed the diagnostic workup.

Our final diagnosis was PCM with ileal involvement. Therefore, the patient received chemotherapy according to the VMD scheme (i.e., bortezomib, 1.3 mg/m^2; melphalan, 0.12 mg/kg; and dexamethasone, 20 mg for nine cycles), achieving a complete remission in a 12-month period according to the International Myeloma Working Group consensus criteria (10). Thirty months later, a disease relapse was highlighted by the findings of increased monoclonal IgA-κ component, multiple lytic vertebral lesions showed by magnetic resonance imaging (MRI), and bone marrow plasma cell infiltration equal to 30%. Then, the patient underwent a second-line chemotherapy with Dara-Rd scheme (i.e., daratumumab, 16 mg/kg; lenalidomide, 5 mg per day; and dexamethasone, 20 mg for week) for 14 cycles achieving a partial remission. A third-line therapy was started on September 2021 due to only serological progressive disease without new lytic lesions based on PVD scheme (i.e., pomalidomide, 4 mg per day; bortezomib, 1.3 mg/m^2; and dexamethasone, 40 mg per week). At the last follow-up, 4 years after the diagnosis, the patient received the 10th cycle of PVD reaching at least a partial response.

The clinical course of the patient is summarized in Table 1.

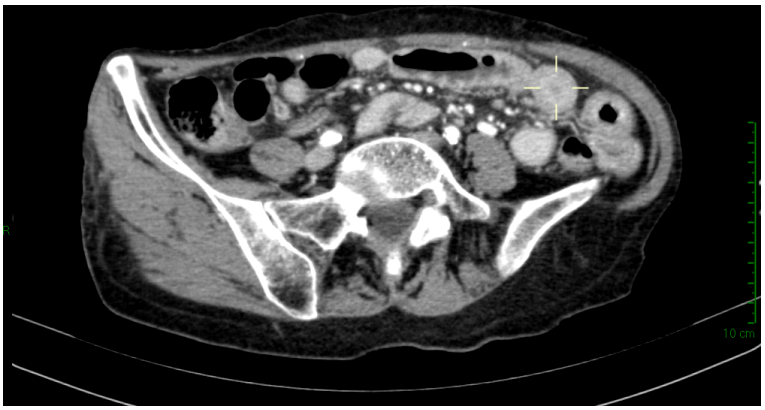

FIGURE 1
Abdominal computed tomography scan showing wall circumferential thickening (delimited by the pointer) at terminal ileum.

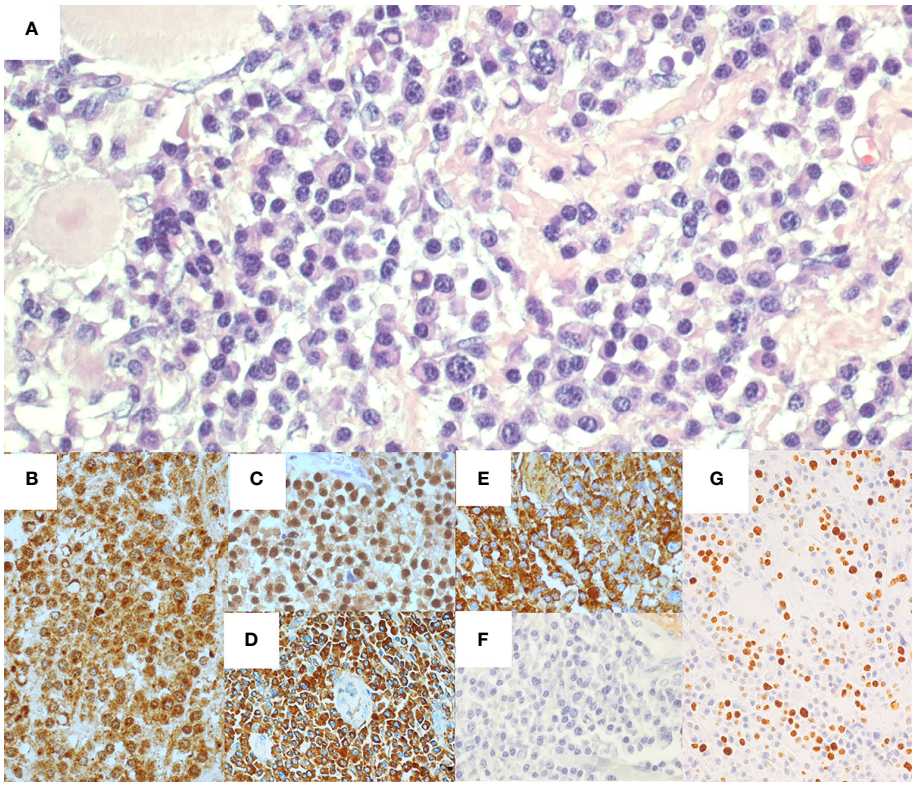

FIGURE 2
Histological and immunohistochemical features of ileal resection specimen. Hematoxylin-eosin staining **(A)** shows ileal wall infiltrated by a proliferation of pleomorphic plasma cells. Immunohistochemical staining presented $CD138^+$ **(B)**, $MUM1^+$ **(C)**, IgA^+ **(D)**, and monoclonal restriction for Kappa light chain of Ig **(E)**, whereas Lambda light chains of Ig tested negative **(F)**. The proliferative index (Mib1/Ki67) was around 40% **(G)**.

TABLE 1 Timeline of the disease and treatment.

Timeline	Diagnosis and Treatment	Outcome
September 2017	- *CT scan:* small bowel circumferential wall thickening - *Laparoscopic ileal resection:* proliferation of mature plasma cells	
November 2017	- *Bone marrow biopsy:* bone marrow involvement by plasma cell neoplasm (15%) - *Laboratory exams:* monoclonal IgA-κ component, 1.2 g/dl; TP, 7.6 g/dl; alb, 4.6 g/dl; γ–globulins, 1.7 g/dl; CBC (Hb, 13 g/dl; WBC, 7060/mmc; NEU, 3880/mmc; PLT, 221000/mmc); LDH, 144 UI/L; Beta-2 microglobulin, 3.7 mg/L; creatinine, 0.9 mg/dl; calcemia, 10.4 mg/dl; IFU + κ chain; normal urine exam; FLC κ, 239 mg/L; FLC lambda, 15.4 mg/L; ratio, 15.51; IgG, 790 mg/dl; IgA, 1,380 mg/dl; IgM, 250 mg/dl - *FISH analysis:* presence of 1q21 amplification - *Total body CT scan:* osteolytic lesion of the left jaw (confirmed on positron emission tomography)	Final diagnosis: plasma cell myeloma with ileal involvement
January 2018 to November 2018	- Chemotherapy with bortezomib, melphalan and dexamethasone (VMD for nine cycles)	Complete response based on IMWG criteria
May 2020	- *Serological and skeletal relapse:* multiple bone involvement with pathological vertebral fractures and presence of monoclonal IgA-κ component - *Bone marrow biopsy:* bone marrow involvement by plasma cell neoplasm (30%)	
July 2020 to July 2021	- Second-line chemotherapy with daratumumab, lenalidomide, and dexamethasone(Dara-Rd for14 cycles)	Progressive disease based on IMWG criteria (only serological)
September 2021 to ongoing	- Third-line chemotherapy with pomalidomide, bortezomib, and dexamethasone (PVD 10 cycles: ongoing)	Alive at last FU (April 2022)

CT, computed tomography; Ig, immunoglobulins; κ, kappa; TP, total proteins; alb, albumin; CBC, cell blood count; Hb, hemoglobin; WBC, leukocytes; NEU, neutrophils; PLT, platelet; IFU, immunofixation of urine; FLC, free light chain; FISH, fluorescence in situ hybridization; IMWG, International Myeloma Working Group; FU, follow-up.

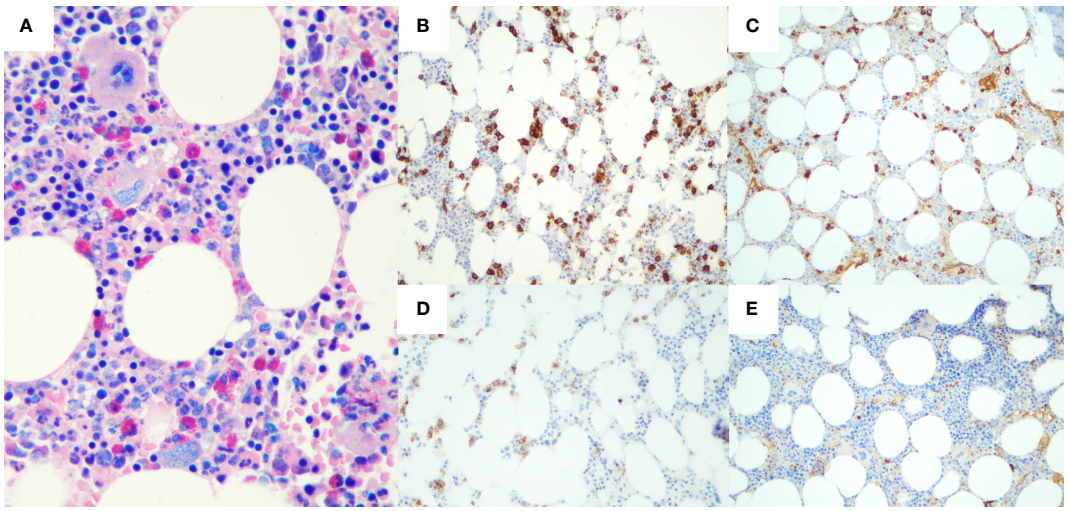

FIGURE 3
Histological and immunohistochemical features of bone marrow biopsy. Hematoxylin-eosin staining **(A)** shows a plasma cell infiltrate, accounting for 15% of bone marrow cellularity. Immunohistochemical staining presented $CD138^{+}$ **(B)**, with restriction for Kappa light chain of Ig **(C)**. Neoplastic plasma cells also aberrantly expressed CD56 **(D)**, whereas immunohistochemistry for Lambda light chain resulted completely negative **(E)**.

TABLE 2 Case reports of PCM with gastrointestinal tract involvement at presentation.

Pt	Sex	Age (Years)	GI Site	Clinical Presentation	BMPC Infiltration	Chromosomal Abnormalities	Therapy	Outcome (Time)	Ref
1	F	74	Ileum	Obstruction	15%	1q21	VMD, Dara-Rd, PVD	Alive (4 years)	Present case
2	n.a.	n.a.	Stomach and Rectum	Upper GI bleeding	n.a.	n.a.	n.a.	n.a.	4
3	n.a.	n.a.	Right Colon	Weight loss and Abdominal discomfort	n.a.	Complex	n.a.	n.a.	4
4	n.a.	n.a.	Rectum	Tenesmus and Hematochezia	n.a.	n.a.	n.a.	n.a.	4
5	M	79	Colon	Obstruction	n.a.	n.a.	Surgery	Dead (2 months)	13
6	M	68	Stomach	Upper GI bleeding	n.a.	n.a.	Refused	Dead (1 month)	14

BMPC, bone marrow plasma cell; F, female; GI, gastrointestinal; M, male; n.a., not available; PCM, plasma cell myeloma; Pt, patient; Ref, reference; Dara-Rd, daratumumab; lenalidomide and dexamethasone scheme; PVD, pomalidomide, bortezomib and dexamethasone scheme; VMD, bortezomib, melphalan, and dexamethasone scheme.

Discussion

Plasma cell neoplasms are categorized into four groups: PCM (including smoldering and non-secretory myeloma and plasma cell leukemia) and plasmacytoma [including solitary plasmacytoma of bone and extraosseous plasmacytoma (EP)] (1). EP is rare representing only 5% of all plasma cell neoplasms and generally involves mucous membranes of airways or GI tract and only rarely parenchimatous organs (11, 12). It is more common in men, with a male-to-female ratio of 4:1 with a median patient age of 55 years at diagnosis (11, 12). The diagnosis of EP needs to exclude a systemic involvement by a PCM, and it is therefore a diagnosis of exclusion. Therefore, EP needs to be distinguished by extraosseous involvement by a PCM (1). In such case, the most frequently involved tissues are soft tissues, skin, lymph nodes, liver, spleen, and kidneys. Conversely, GI involvement by a PCM is very rare. It most commonly occurs in the small intestine, followed by stomach, whereas the involvement of esophagus and colon—especially in ileo-cecal region—is exceedingly rare (1, 4, 6, 7, 9). In the literature, very few cases of multiple myeloma primarily presented with GI involvement are reported (Table 2). GI involvement by PCM may occur with loss of appetite, bleeding, abdominal discomfort, or obstruction (4, 13, 14). In such cases, histopathological examination of tissue samples is needed to address the diagnosis of plasma cell neoplasms, whereas imaging (CT scan, MRI, and PET-CT) together with laboratory examination and bone marrow biopsy may confirm the presence of a systemic involvement (4).

This is indeed the case of our patient, in which the ileal involvement by a plasma cell neoplasm emerged after the development of GI symptoms such as abdominal pain, food vomiting, and weight loss of 10 kg over 1 year. The diagnosis of a GI involvement by PCM can be difficult from both a clinical and histopathological point of view, as it can mimic a carcinoma or lymphoma.

Our first diagnostic hypothesis, based on the patient's age, clinical presentation, and CT finding of GI obstruction, was intestinal neoplasm. Given the ileal localization, a neuroendocrine tumor, an intestinal lymphoma, or an adenocarcinoma was highly suspected. The subsequent urgent ileal resection and histological examination led to the more unusual diagnosis of plasma cell neoplasia.

This case required a histopathological complex differential diagnosis between plasma cell neoplasms and lymphomas with predominant plasma cell differentiation and possible GI involvement, namely, marginal zone lymphoma and several high-grade B-cell lymphoma (i.e., plasmablastic lymphoma, EBV^+ diffuse large B-cell lymphoma, and $HHV8^+$ B-cell lymphoma) (1). In our patient, the morphologic and immunohistochemical features of the neoplastic infiltrate, the absence of large cells with blastic appearance, and the negativity for both EBV and HHV8 search suggested a PCM rather than the aforementioned entities. The integration with clinical features was necessary to conclude the differential diagnosis. In particular, the absence of history of immunosuppression ruled out the plasmablastic lymphoma, whereas the serological presence of a monoclonal IgA-κ component, the imaging detection of osteolytic lesions, and the bone marrow plasma cell infiltration allowed the final diagnosis of PCM.

From a clinical perspective, a differential diagnosis between PCM and extraosseous plasmacytoma was necessary. As mentioned above, serological and imaging examinations, associated with the bone marrow biopsy, showed the neoplasm systemic involvement in our patient, allowing the diagnosis of PCM and the exclusion of extraosseous plasmacytoma.

According to the available data, PCM with intestinal involvement has a poor prognosis, with a median survival of only a few months, despite the recent discovery of novel active agents (4, 9). In addition, the chromosome 1 abnormalities, such as the 1q21 amplification of our patient, frequently detected in PCM with extramedullary involvement, are typically associated with a worse prognosis (15, 16). Our patient, despite the

presence of such negative prognostic factors, is still alive at the last follow-up 4 years after diagnosis. We assume that early diagnosis of PCM by GI presentation, with limited bone co-involvement, and subsequent prompt targeted chemotherapy, resulted in a significant prognostic improvement.

In conclusion, although intestinal involvement of PCM is rare, it must be promptly identified, and a multidisciplinary approach, involving gastroenterologists, hematologists, and pathologists, is required to achieve a proper diagnosis and a successful management. In addition, this report highlights that an appropriate and early diagnosis is associated with a prognostic improvement, although further studies on a large number of patients are needed to better clarify this issue.

Data availability statement

The original contributions presented in the study are included in the article/supplementary material. Further inquiries can be directed to the corresponding author.

Ethics statement

The studies involving human participants were reviewed and approved by San Matteo Hospital Foundation Pavia Ethics Committee. The patients/participants provided their written informed consent to participate in this study. Written informed consent was obtained from the individual(s) for the publication of any potentially identifiable images or data included in this article.

Author contributions

AB, NA, and ML designed and drafted the report. AB, GS, AV, CC, SF, MAL, LA, and MP collected, analyzed, and interpreted the data; AS and MP critically revised the manuscript. All authors contributed to the article and approved the submitted version.

Funding

This project was funded by "San Matteo Hospital Foundation, Internal Medicine research fundings".

Conflict of interest

The authors declare that the research was conducted in the absence of any commercial or financial relationships that could be construed as a potential conflict of interest.

Publisher's note

All claims expressed in this article are solely those of the authors and do not necessarily represent those of their affiliated organizations, or those of the publisher, the editors and the reviewers. Any product that may be evaluated in this article, or claim that may be made by its manufacturer, is not guaranteed or endorsed by the publisher.

References

1. Swerdlow SH, Campo E, Harris NL, Jaffe ES, Pileri SA, Stein H, et al. *WHO classification of hemathopoietic and lymphoid tissues; revised 4th edition*. Lyon France: IARC Press . (2017) 585.

2. Rajkumar SV, Dimopoulos MA, Palumbo A, Blade J, Merlini G, Mateos MV, et al. International myeloma working group updated criteria for the diagnosis of multiple myeloma. *Lancet Oncol* (2014) 15:e538–48. doi: 10.1016/S1470-2045(14)70442-5

3. Oshima K, Kanda Y, Nannya Y, Kaneko M, Hamaki T, Suguro M, et al. Clinical and pathologic findings in 52 consecutively autopsied cases with multiple myeloma. *Am J Hematol* (2001) 67:1–5. doi: 10.1002/ajh.1067

4. Talamo G, Cavallo F, Zangari M, Barlogie B, Lee CK, Pineda-Roman M, et al. Clinical and biological features of multiple myeloma involving the gastrointestinal system. *Haematologica* (2006) 91:964–7. doi: https://doi.org/10.3324/%25x

5. Parnell K, Ahmed M, Smalligan RD, Nadesan S. Extramedullary plasmacytoma mimicking colon carcinoma: an unusual presentation and review of the literature. *BMJ Case Rep* (2015) 2015:bcr2015210973. doi: 10.1136/bcr-2015-210973

6. Griffiths AP, Shepherd NA, Beddall A, Williams JG. Gastrointestinal tumour masses due to multiple myeloma: a pathological mimic of malignant lymphoma. *Histopathology* (1997) 31:318–23. doi: 10.1046/j.1365-2559.1997.1610866.x

7. Hayes DW, Bennett WA, Heck FJ. Extramedullary lesions in multiple myeloma. *AMA Arch Pathol* (1952) 53:262–72.

8. Venizelos I, Theodoridou S, Vakalopoulou S, Perifanis V, Vyzantiadis T, Garipidou V. Acute large bowel pseudo-obstruction due to multiple myeloma. *Leuk Lymphoma* (2004) 45:1943–5. doi: 10.1080/10428190410001697322

9. Usmani SZ, Heuck C, Mitchell A, Szymonifka J, Nair B, Hoering A, et al. Extramedullary disease portends poor prognosis in multiple myeloma and is over-represented in high-risk disease even in the era of novel agents. *Haematologica* (2012) 97:1761–7. doi: 10.3324/haematol.2012.065698

10. Kumar S, Paiva B, Anderson KC, Durie B, Landgren O, Moreau P, et al. International myeloma working group consensus criteria for response and minimal residual disease assessment in multiple myeloma. *Lancet Oncol* (2016) 17(8):e328–46. doi: 10.1016/S1470-2045(16)30206-6

11. Güler N. Extramedullary plasmacytoma: tumor occurrence and therapeutic concepts. *Cancer* (2000) 88:240–2. doi: 10.1002/(SICI)1097-0142(20000101)88:1<240::AID-CNCR33>3.0.CO;2-W

12. Mjoli M, Vorajee N, Naidoo Y, Madiba T. Solitary extramedullary plasmacytoma of the colon, rectum and anus. *S Afr J Surg* (2016) 54:45–7.

13. Herbst A, Renner SW, Ringenberg QS, Fass R, Krouse RS. Multiple myeloma presenting with a colonic obstruction and bony lesions: a clinical dilemma. *J Clin Oncol* (2008) 26:5645–7. doi: 10.1200/JCO.2008.18.6239

14. Chim CS, Wong WM, Nicholls J, Chung LP, Liang R. Extramedullary sites of involvement in hematologic malignancies: case 3. hemorrhagic gastric plasmacytoma as the primary presentation in multiple myeloma. *J Clin Oncol* (2002) 20:344–7. doi: 10.1200/JCO.2002.20.1.344

15. Schmidt TM, Fonseca R, Usmani SZ. Chromosome 1q21 abnormalities in multiple myeloma. *Blood Cancer J* (2021) 11:83. doi: 10.1038/s41408-021-00474-8

16. Biran N, Malhotra J, Bagiella E, Cho HJ, Jagannath S, Chari A. Patients with newly diagnosed multiple myeloma and chromosome 1 amplification have poor outcomes despite the use of novel triplet regimens. *Am J Hematol* (2014) 89:616–20. doi: 10.1002/ajh.23705

frontiers | Frontiers in Oncology

TYPE Case Report
PUBLISHED 18 August 2022
DOI 10.3389/fonc.2022.902301

OPEN ACCESS

EDITED BY
Liren Qian,
Fifth Medical Center of the PLA General Hospital, China

REVIEWED BY
Sanfang Tu,
Southern Medical University, China
Ciprian Tomuleasa,
Iuliu Haţieganu University of Medicine and Pharmacy, Romania

*CORRESPONDENCE
Jun Xu
neurojun@126.com

SPECIALTY SECTION
This article was submitted to Hematologic Malignancies, a section of the journal Frontiers in Oncology

RECEIVED 10 May 2022
ACCEPTED 25 July 2022
PUBLISHED 18 August 2022

CITATION
Wang Y-L, Zhang Y and Xu J (2022) Sodium oligomannate combined with rivastigmine may improve cerebral blood flow and cognitive impairment following CAR-T cell therapy: A case report. *Front. Oncol.* 12:902301. doi: 10.3389/fonc.2022.902301

Sodium oligomannate combined with rivastigmine may improve cerebral blood flow and cognitive impairment following CAR-T cell therapy: A case report

Yan-Li Wang[1,2], Yuan Zhang[1] and Jun Xu[1,2]*

[1]Department of Neurology, Beijing Tiantan Hospital, Capital Medical University, Beijing, China, [2]China National Clinical Research Center for Neurological Diseases, Beijing Tiantan Hospital, Capital Medical University, Beijing, China

Chimeric antigen receptor-T (CAR-T) cell therapy is a breakthrough for B-cell hematological malignancies but is commonly associated with cytokine release syndrome and neurotoxicity and is occasionally complicated by neurological symptoms, such as cognitive disturbances. Currently, no effective treatments for CAR-T therapy-related cognitive impairment are available. Here, we present a 22-year-old patient with cognitive impairment who was treated with CAR-T cells as a salvage therapy for Burkitt lymphoma. One month after CAR-T cell infusion, he experienced memory loss that mainly manifested as forgetting recent-onset events. Two months of rehabilitation and hyperbaric oxygen therapy failed to provide clinical improvement. Subsequently, the patient improved with oral oxiracetam for 5 months. However, after 10 months of withdrawal, he showed significantly worse memory decline. Then, he began to take sodium oligomannate (22 February 2021). Follow-up testing at 6 and 12 months revealed maintenance of memory gains with sodium oligomannate alone or in combination with rivastigmine. Our case shows that CAR-T therapy may compromise cognitive function and that sodium oligomannate may have partial efficacy in restoring cognitive performance and activities of daily living. This may provide insights for further applications of sodium oligomannate for neurological symptoms, especially cognitive deficits following CAR-T cell therapy.

KEYWORDS

sodium oligomannate, cognitive impairment, cerebral blood flow, CAR-T, rivastigmine

Introduction

Burkitt lymphoma is a rare and highly aggressive B-cell neoplasm but is generally curable when treated with brief-duration, high-intensity chemotherapeutic regimens. However, some patients develop recurrence or fail to respond. Chimeric antigen receptor-T (CAR-T) cell therapy is an important innovative approach to treating hematological and other malignancies. However, cognitive impairment is an important symptom of neurotoxicity that is associated with a poor prognosis of CAR-T cell infusion (1). Currently, there is no effective intervention method, and this is the first case describing sodium oligomannate to control the progression of cognitive impairment after CAR-T cell therapy.

Case report

A 22-year-old man was admitted to the Cognitive Disorders Department of our hospital in February 2021 complaining of gradual memory deterioration for more than 1 year.

The patient underwent CAR-T immunotherapy (specific treatment options not available) for Burkitt lymphoma in March 2019, and 1 month postoperatively, he first developed memory loss, with the main cognitive symptom being a failure to remember recent events. The patient suffered a grand mal seizure in April 2019, which was followed by a significant worsening of cognitive impairment, manifested by not recognizing familiar people, such as his parents, and not recognizing common objects, such as birds in paintings. MMSE and MoCA scores before treatment are unavailable. From June to August 2019, the patient was treated with rehabilitation and hyperbaric oxygen in our hospital with no significant improvement in cognitive symptoms. Since October 2019, the patient was administered oxiracetam 0.8 g orally twice daily for 5 months. The patient's memory deterioration has improved, and he began to gradually recognize his parents and primary school and high school classmates and he can recall simple mobile phone passwords. However, the patient discontinued his medication due to the impact of COVID-19, and at month 15, he showed significantly worse memory decline, which primarily manifested as forgetting where to put things, emotional instability, and impaired daily living activities.

The study was approved by the Institutional Review Board of Beijing Tiantan Hospital of Capital Medical University (KY-2021-028-01). Informed consent was signed by the patient and his father. A timeline of the historical and current information is shown in Figure 1. Since February 2021, when the patient was seen in our outpatient clinic, the patient has been taking regular oral doses of sodium oligomannate (GV-971) 450 mg twice daily without any other medication. There were significant improvements in the overall condition of the patient, including improvements in the activities of daily living, more stable emotions, and increased MMSE and MoCA.

To further improve his cognition, the patient has been co-administering rivastigmine hydrogen tartrate capsules 3 mg twice daily since August 2021; in January 2022, the regimen of 3 mg capsules twice daily was substituted with a 9.5-mg transdermal patch once daily. These were the only medications that the patient received. In comparison to sodium oligomannate alone, the patient was stable with no significant cognitive improvement. The results of the patient's three neuropsychological examinations are shown in Table 1. The results for 14 cytokines and CAR-T cell copy numbers in peripheral blood samples from August 2021 are shown in eTables 1, 2. Figure 2 shows the comparison of cerebral perfusion findings with 3D arterial spin labeling (ASL) imaging before and after treatment with sodium oligomannate. Significantly, the hypoperfusion regions around the lesion improved following GV-971 treatment, and cerebral perfusion was stable during combination therapy with rivastigmine. Furthermore, Table 2 shows cerebral blood flow (CBF) assessed with ASL in cognitive regions. The patient's condition has improved steadily since the follow-up, with occasional

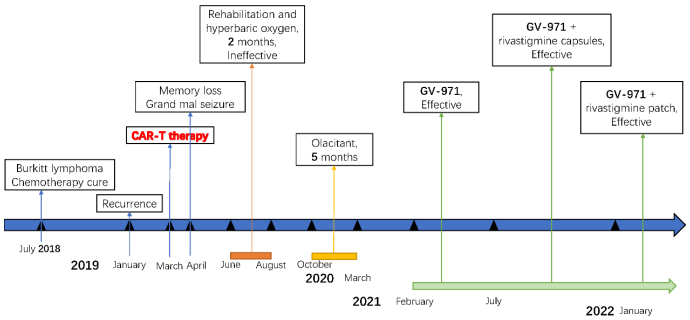

FIGURE 1
Medical history of the patient.

10.3389/fonc.2022.902301

TABLE 1 Neurophysiological follow-up.

Follow-up		9 February 2021	29 July 2021	18 January 2022
		T0	T1	T2
Mini-Mental State Examination, MMSE		23	26	26
Montreal Cognitive Assessment, MoCA-Beijing		21	23	23
Hopkins Verbal Learning Test, HVLT	Short-Delayed Recall	0	6	0
	Long-Delayed Recall	0	1	0
Cog-12 Questionnaire Investigation, Cog-12		23	21	24
Hamilton Anxiety Scale, HAMA		4	5	5
Hamilton Depression Scale, HAMD		3	2	6
Neuropsychiatric Inventory Questionnaire, NPI		5	4	16
Activities of Daily Living, ADL-20		27	24	30
Pittsburgh Sleep Quality Index, PSQI		0	0	1

fluctuations in symptoms. The patient's cranial MRI in August 2021 showed that abnormal signals were present in the bilateral insula, hippocampus, amygdala, subcallosal gyrus, left temporal lobe, anterior cingulate, and splenium cingulate, which were not markedly changed from 6 months before. In addition, a neurological examination revealed poor memory and executive function, without other obvious abnormalities.

Discussion

After choosing to stop taking oxiracetam for 10 months, his MMSE score was 23 and his MoCA score was 21. After 6 months on sodium oligomannate, the patient improved significantly, with MMSE scores ranging from 23 to 26 and MoCA scores ranging from 21 to 23. The combination of sodium oligomannate with rivastigmine did not show significant cognitive improvement, but the effects were stable. Currently, the patient has a normal digital memory, can basically take care of himself, can use computers and other tools, and can interact with people around him in a normal way.

CAR-T cell therapy as a treatment for Burkitt lymphoma is a nascent, burgeoning field. Consistent with our observations, a previous study also indicated cognitive difficulties following CAR-T cell therapy (2). The specific mechanism may involve several factors, such as cytokine release syndrome (CRS) and immune effector cell-associated neurotoxicity syndrome (ICANS) (3). CRS typically occurs in the first week after CAR T-cell infusion and ICANS in the second week after infusion, usually following the peak of CRS severity and lasting 5 to 10

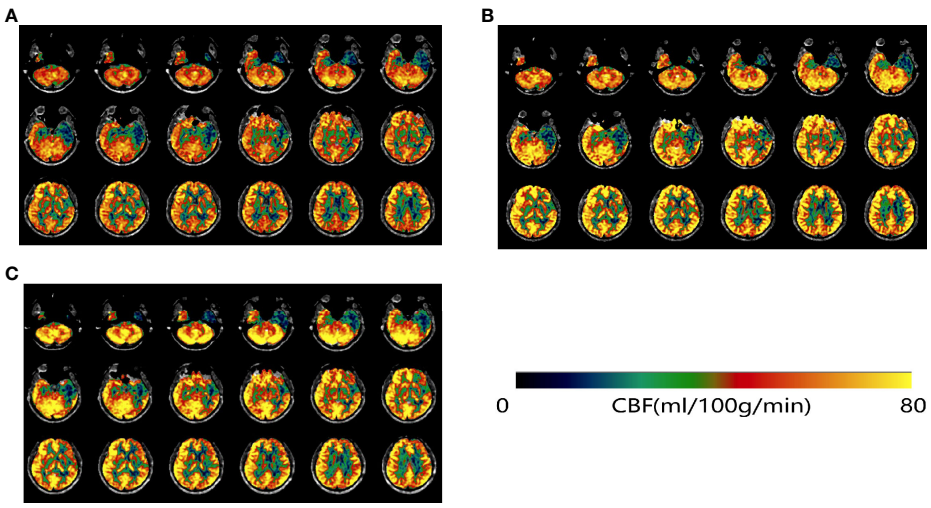

FIGURE 2
ASL-MRI on 9 February 2021 before GV-971 treatment **(A)**, 29 July 2021 **(B)**, and 18 January 2022 **(C)**. After treatment with GV-971 **(B, C)**, regions of low perfusion in green were visibly decreased.

TABLE 2 Cerebral blood flow follow-up.

Cognition-related regions	Left lobe			Right lobe		
(mL/100g/min)	T0	T1	T2	T0	T1	T2
Hippocampus	28.59	26.30	37.21	29.83	36.39	37.03
Posterior cingulate	53.60	61.54	62.65	56.01	64.23	62.82
Parahippocampal gyrus	31.59	32.37	30.05	35.13	45.92	41.12
Thalamus	41.07	47.78	39.16	51.00	51.00	48.96
Amygdala	22.56	23.74	39.00	26.56	31.85	36.50
Precuneus	50.24	55.94	53.00	55.34	59.04	58.36
Middle temporal gyrus	47.01	55.85	55.66	56.21	64.21	75.08

days (4). Mild ICANS (grades 1 and 2) is characteristic of aphasia, confusion, and impaired fine motor skills, and seizures, cerebral edema, and coma can manifest in severe cases (grades 3 and 4) (4). Both symptomatic treatment and supportive care are recommended to treat mild ICANS, whereas corticosteroids are the primary treatment strategy for severe ICANS (5, 6). Earlier administration of steroids could prevent severe effects without reducing CAR-T therapy efficacy (7). The severity of CRS is strongly correlated with the severity of ICANS, and approaches to CRS mitigation may subsequently reduce the risk of ICANS (8). Although tocilizumab has no effect on most ICANS, it is highly effective in the management of CRS (5, 9).

Although associations of early neurotoxicity with cognitive decline are significant, a large-scale cohort of patients receiving CAR-T cell therapy is needed to detect a correlation between acute neurotoxicity and long-term cognitive difficulties (2). There is also a study that found no cognitive toxicity of CAR-T cell treatment (10). The prevalence of cognitive difficulty following CAR-T cell therapy is higher among white individuals than among non-white patients, and a possible explanation for the discrepancies may arise from cultural differences (2).

A phase 3 clinical trial of sodium oligomannate demonstrated that GV-971 could effectively improve cognitive deficits in mild-to-moderate Alzheimer's dementia (11).

Sodium oligomannate could reduce the concentration of phenylalanine and alleviate Th1-related neuroinflammation and cognitive decline by effectively modulating the gut microbiota (12). It may play an important role in preserving dendritic spines and synaptic plasticity (13). In addition, it can also directly inhibit the formation of Aβ fibrils and decrease Aβ deposition in the brain (14, 15). There are no studies that have evaluated the relationship between GV-971 and CBF, and the mechanism of GV-971 in cerebrovascular disease has not been explored. Patients with encephalitis and Alzheimer's disease may exhibit regional CBF abnormalities, and CBF is a sensitive biomarker for the assessment of neuroinflammation and drug efficacy (16). This case strongly suggested that GV-971 might improve cognitive function by increasing cerebral blood flow.

Conclusion

These results indicated that sodium oligomannate exerts its protective effect on cognitive improvement following CAR-T cell therapy through the inhibition of neuroinflammation and an increase in cerebral perfusion. Importantly, a larger cohort is needed to verify the results.

Data availability statement

The original contributions presented in the study are included in the article/Supplementary Material. Further inquiries can be directed to the corresponding author.

Ethics statement

This study was reviewed and approved by Institutional Review Board of Beijing Tiantan Hospital of Capital Medical University (KY-2021-028-01). The patients/participants provided their written informed consent to participate in this study.

Author contributions

All authors have made a substantial contribution to the data collection and the drafting of the manuscript and reviewed and accepted the contents of the manuscript prior to its submission.

Funding

This study was supported by the National Natural Science Foundation (Grant Numbers 82071187, 81870821, 81471215), The National Key Research and Development Program of China (2021YFC2500103), Beijing Youth Talent Team Support Program (2018000021223TD08), National Key Research and Development Program (2019YFC01209028), and Beijing Natural Science Foundation grant (L182055).

Conflict of interest

The authors declare that the research was conducted in the absence of any commercial or financial relationships that could be construed as a potential conflict of interest.

Publisher's note

All claims expressed in this article are solely those of the authors and do not necessarily represent those of their affiliated organizations, or those of the publisher, the editors and the reviewers. Any product that may be evaluated in this article, or claim that may be made by its manufacturer, is not guaranteed or endorsed by the publisher.

Supplementary material

The Supplementary Material for this article can be found online at: https://www.frontiersin.org/articles/10.3389/fonc.2022.902301/full#supplementary-material

References

1. Lee EQ. Neurologic complications of cancer therapies. *Curr Neurol Neurosci Rep* (2021) 21:66. doi: 10.1007/s11910-021-01151-w

2. Ruark J, Mullane E, Cleary N, Cordeiro A, Bezerra ED, Wu V, et al. Patient-reported neuropsychiatric outcomes of long-term survivors after chimeric antigen receptor T cell therapy. *Biol Blood Marrow Transplant J Am Soc Blood Marrow Transplant* (2020) 26:34–43. doi: 10.1016/j.bbmt.2019.09.037

3. Brudno JN, Kochenderfer JN. Recent advances in CAR T-cell toxicity: Mechanisms, manifestations and management. *Blood Rev* (2019) 34:45–55. doi: 10.1016/j.blre.2018.11.002

4. Morris EC, Neelapu SS, Giavridis T, Sadelain M. Cytokine release syndrome and associated neurotoxicity in cancer immunotherapy. *Nat Rev Immunol* (2022) 22:85–96. doi: 10.1038/s41577-021-00547-6

5. Neelapu SS, Tummala S, Kebriaei P, Wierda W, Gutierrez C, Locke FL, et al. Chimeric antigen receptor T-cell therapy - assessment and management of toxicities. *Nat Rev Clin Oncol* (2018) 15:47–62. doi: 10.1038/nrclinonc.2017.148

6. Strati P, Ahmed S, Furqan F, Fayad LE, Lee HJ, Iyer SP, et al. Prognostic impact of corticosteroids on efficacy of chimeric antigen receptor T-cell therapy in large b-cell lymphoma. *BLOOD* (2021) 137:3272–6. doi: 10.1182/blood.2020008865

7. Shah NN, Johnson BD, Fenske TS, Raj RV, Hari P. Intrathecal chemotherapy for management of steroid-refractory CAR T-cell-associated neurotoxicity syndrome. *Blood Adv* (2020) 4:2119–22. doi: 10.1182/bloodadvances.2020001626

8. Freyer CW, Porter DL. Cytokine release syndrome and neurotoxicity following CAR T-cell therapy for hematologic malignancies. *J Allergy Clin Immunol* (2020) 146:940–8. doi: 10.1016/j.jaci.2020.07.025

9. Maus MV, Alexander S, Bishop MR, Brudno JN, Callahan C, Davila ML, et al. Society for Immunotherapy of Cancer (SITC) clinical practice guideline on immune effector cell-related adverse events. *J Immunother Cancer* (2020) 8(2): e001511. doi: 10.1136/jitc-2020-001511

10. Maillet D, Belin C, Moroni C, Cuzzubbo S, Ursu R, Sirven-Villaros L, et al. Evaluation of mid-term (6-12 months) neurotoxicity in b-cell lymphoma patients treated with CAR T cells: A prospective cohort study. *Neuro-oncology* (2021) 23:1569–75. doi: 10.1093/neuonc/noab077

11. Xiao S, Chan P, Wang T, Hong Z, Wang S, Kuang W, et al. A 36-week multicenter, randomized, double-blind, placebo-controlled, parallel-group, phase 3 clinical trial of sodium oligomannate for mild-to-moderate alzheimer's dementia. *Alzheimer's Res Ther* (2021) 13:62. doi: 10.1186/s13195-021-00795-7

12. Wang X, Sun G, Feng T, Zhang J, Huang X, Wang T, et al. Sodium oligomannate therapeutically remodels gut microbiota and suppresses gut bacterial amino acids-shaped neuroinflammation to inhibit alzheimer's disease progression. *Cell Res* (2019) 29:787–803. doi: 10.1038/s41422-019-0216-x

13. Ettcheto M, Busquets O, Cano A, Sánchez-Lopez E, Manzine PR, Espinosa-Jimenez T, et al. Pharmacological strategies to improve dendritic spines in alzheimer's disease. *J Alzheimer's Dis JAD* (2021) 82:S91–s107. doi: 10.3233/JAD-201106

14. Fan Y, Hu J, Li J, Yang Z, Xin X, Wang J, et al. Effect of acidic oligosaccharide sugar chain on scopolamine-induced memory impairment in rats and its related mechanisms. *Neurosci Lett* (2005) 374:222–6. doi: 10.1016/j.neulet.2004.10.063

15. Jiang RW, Du XG, Zhang X, Wang X, Hu DY, Meng T, et al. Synthesis and bioassay of β-(1,4)-D-mannans as potential agents against alzheimer's disease. *Acta Pharmacol Sin* (2013) 34:1585–91. doi: 10.1038/aps.2013.104

16. Miao A, Liu Q, Li Z, Liu W, Wang L, Ge J, et al. Altered cerebral blood flow in patients with anti-NMDAR encephalitis. *J Neurol* (2020) 267:1760–73. doi: 10.1007/s00415-020-09747-x

frontiers | Frontiers in Oncology

TYPE Case Report
PUBLISHED 29 August 2022
DOI 10.3389/fonc.2022.960914

OPEN ACCESS

EDITED BY
Emir Hadzijusufovic,
Ludwig Boltzmann Institute for Hematology and Oncology (LBI HO), Austria

REVIEWED BY
Ahmet Emre Eskazan,
Istanbul University-Cerrahpasa, Turkey
Zafar Iqbal,
King Saud Bin Abdulaziz University for Health Sciences (KSAU-HS), Saudi Arabia
Fabio Stagno,
University Hospital Polyclinic Vittorio Emanuele, Italy

*CORRESPONDENCE
Sabine Kayser
sabine.kayser@dkfz-heidelberg.de

SPECIALTY SECTION
This article was submitted to Hematologic Malignancies, a section of the journal Frontiers in Oncology

RECEIVED 03 June 2022
ACCEPTED 28 July 2022
PUBLISHED 29 August 2022

CITATION
Ramdohr F, Fabarius A, Maier B, Bretschneider D, Jauch A, Monecke A, Metzeler KH, Janssen JWG, Schlenk RF and Kayser S (2022) Atypical presentation of patients with chronic myeloid leukemia in chronic phase—Case report.
Front. Oncol. 12:960914.
doi: 10.3389/fonc.2022.960914

Atypical presentation of patients with chronic myeloid leukemia in chronic phase—Case report

Florian Ramdohr[1], Alice Fabarius[2], Bettina Maier[3], Daniela Bretschneider[1], Anna Jauch[4], Astrid Monecke[5], Klaus H. Metzeler[1], Johannes W. G. Janssen[4], Richard F. Schlenk[3,6,7] and Sabine Kayser[1,6*]

[1]Medical Clinic and Policlinic I, Hematology and Cellular Therapy, University Hospital Leipzig, Leipzig, Germany, [2]Department of Hematology and Oncology, University Hospital Mannheim, Heidelberg University, Mannheim, Germany, [3]Department of Internal Medicine V, University Hospital Heidelberg, Heidelberg, Germany, [4]Institute of Human Genetics, University Heidelberg, Heidelberg, Germany, [5]Department of Diagnostics, Institute of Pathology, University Hospital Leipzig, Leipzig, Germany, [6]NCT Trial Center, National Center of Tumor Diseases, German Cancer Research Center (DKFZ), Heidelberg, Germany, [7]Department of Medical Oncology, National Center of Tumor Diseases (NCT), Heidelberg University Hospital, Heidelberg, Germany

The presence of the translocation t(9;22)(q34;q11), leading to the *BCR::ABL1* fusion transcript, is the hallmark of chronic myeloid leukemia (CML). Nevertheless, atypical presentation at diagnosis can be challenging. However, although most patients with CML are diagnosed with the e13a2 or e14a2 *BCR::ABL1* fusion transcripts, about 5% of them carry rare *BCR::ABL1* fusion transcripts, such as e19a2, e8a2, e13a3, e14a3, e1a3, and e6a2. In particular, the e6a2 fusion transcript has been associated with clinically aggressive disease frequently presenting in accelerated or blast crisis phases. To date, there is limited evidence on the efficacy of front-line second-generation tyrosine kinase inhibitors for this genotype. Here, we report two patients, in whom the diagnosis of CML was challenging. The use of primers recognizing more distant exons from the common *BCR::ABL1* breakpoint region correctly identified the atypical *BCR::ABL1* e6a2 fusion transcript. Treatment with the second-generation tyrosine kinase inhibitor nilotinib was effective in our patient expressing the atypical e6a2 *BCR::ABL1* fusion transcript.

KEYWORDS

chronic myeloid leukemia (CML), atypical transcripts, BCR-ABL +, e6a2, tyrosine kinase inhibitors, outcome

Introduction

Chronic myeloid leukemia (CML) is a malignant disease of the hematologic stem cell. The hallmark of the disease is the translocation t(9;22)(q34.1;q11.2), leading to the *BCR::ABL1* fusion transcript (1–3). Nearly half of the patients are asymptomatic at diagnosis and discovered when a white blood cell (WBC) count performed as part of a routine analysis is found to be abnormal. Additionally, most patients are diagnosed within chronic phase and only roughly 5% are initially diagnosed with accelerated or blast phase.

Treatment with tyrosine kinase inhibitors (TKIs), particularly of the second generation, such as nilotinib or dasatinib, leads to high molecular remission rates (4).

However, there is growing evidence of cases with an atypical clinical presentation, mostly related to alternative transcripts, accounting for less than 1% of CML patients and their clinical significance is still under investigation (5–8). These uncommon variant transcripts can result in phenotypic variability and affect response to TKI therapy (9). The atypical e6a2 *BCR::ABL1* transcript produces a rare fusion protein, which confers a poor prognosis in CML due to its association with aggressive phenotype and early transformation, perhaps due to the lack of an important regulatory *BCR* sequence within the fusion proteins (6).

Atypical presentations of CML can further be due to an unusual laboratory presentation or a concurrent second malignant disease, obscuring the diagnosis and thus hampering a highly curable disease. We here present two cases of CML with atypical clinical presentation.

Case description

Case 1

The first patient, a 50-year-old man, presented in February 2019 due to fatigue. Laboratory evaluation revealed an elevated WBC count of 264.7 × 10^9/L, anemia of 7.4 g/dl, and increased platelets of 1,376 × 10^9/L. Differential blood cell count revealed a left shift with 10% myeloid blast cells, whereas basophils and eosinophils were absent. LDH value was heavily increased with 1,418 U/L (range, 125–248 U/L) and uric acid was 8.6 g/dl (range, 3.5–7.0 mg/dl). Bone marrow evaluation revealed 4% myeloid blast cells. Abdominal ultrasound showed hepatosplenomegaly with a spleen size of 18 × 9 cm as well as a liver size of 21 cm (craniocaudal). In suspicion of CML in chronic phase, therapy with hydroxyurea was started with 4 g/daily as well as supportive care to prevent tumor lysis syndrome. After transfusion of two packed red blood cells, the hemoglobin value rose sufficiently to 9.2 g/dl. Astonishingly, the initial PCR analysis, targeting the typical isoforms p210 and p190, was negative for *BCR::ABL*. However, fluorescence *in situ* hybridization (FISH) analysis on bone marrow revealed a reciprocal *BCR::ABL1* fusion in 99% of 500 cells counted (Figure 1A) and cytogenetic analysis was positive for translocation t(9;22)(q34;q11) in 14 metaphases as well (Figure 1B). Thus, the diagnosis of CML in chronic phase was made. The Sokal and ELTS scores were high risk. Interestingly, in a second attempt, quantitative real-time PCR, targeting the rare transcript e6a2, revealed a *BCR::ABL/ABL1* transcript ratio of 40.563% (Figure 1C). Unfortunately, patients with rare *BCR::ABL* transcripts cannot be measured according to International Scale (IS), since it is standardized only for those with standard transcripts e13a2 and e14a2. Of course, all analyses were performed according to good clinical and laboratory practice, e.g., all analyses were performed as double analyses, including negative and positive controls from peripheral blood of healthy persons (Figure 1). Scoring of molecular responses were calculated as published (10). After 9 days of hydroxyurea, WBC count declined sufficiently to 29/nl; however, the platelets rose from initially 1,376 × 10^9/L to 1,950 × 10^9/L. Hydroxyurea was stopped and switched to the second-generation TKI nilotinib 300 mg twice daily within the NILOdeepR trial (ClinicalTrials.gov Identifier: NCT02546674).

However, 10 days after TKI initiation, the platelets rose further to 3,262 × 10^9/L, whereas WBC count remained faintly stable at 32 × 10^9/L. After one more week of TKI therapy, platelets declined to 1,018 × 10^9/L and finally to 456 × 10^9/L after one more week of therapy. Consistently, WBC count dropped to 10 × 10^9/L and finally normalized. Hemoglobin value slightly decreased to minimally 8.1 g/dl, but started to raise spontaneously after a few weeks to 10.7 g/dl. Bone marrow evaluation after 3 months of therapy revealed a complete cytogenetic remission (CCR) with normal cytogenetics in 25 metaphases and a decline of the *BCR::ABL/ABL1* transcript ratio to 0.063% by quantitative PCR analysis. Peripheral blood count had normalized as well and both spleen and liver were not palpable. After 6 months of TKI therapy, the patient was still in CCR and also in molecular remission with 0% *BCR::ABL/ABL1* transcripts by quantitative PCR analysis. After 1 year of treatment with nilotinib within the NILOdeepR trial (ClinicalTrials.gov Identifier: NCT02546674), the patient achieved deep molecular remission (MR4.5) and continues in deep remission (MR5) since December 2021 (last follow-up in March 2022).

The patient was recently interviewed on his view concerning the disease and treatment approach. He described himself as being positive-thinking and future-oriented. At the time of CML diagnosis, he was worried, but his familiar background (two daughters) stimulated him to fight. He felt relieved that the whole course of therapy could be conducted ambulatory. His optimism grew already after the first month, when the blood values declined as expected. He is in deep molecular remission

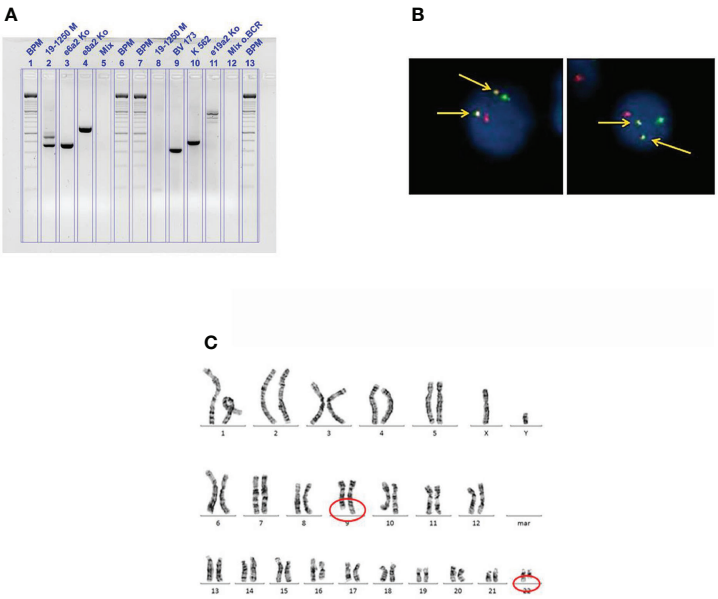

FIGURE 1
(A) Fluorescence *in situ* hybridization on bone marrow from case 1 showing a reciprocal *BCR::ABL1* fusion (arrows, indicated in yellow); red signal, probe for ABL on the long arm of chromosome 9 (9q34); green signal, probe for BCR on the long arm of chromosome 22 (22q11). **(B)** Cytogenetic analysis on bone marrow from case 1 showing the translocation t(9;22)(q34;q11). **(C)** Agarose gel analysis from cDNA extracted from peripheral blood from case 1 showing a positive result for the rare e6a2 transcript. BPM, base pair ladder (lines 1, 6, 7, and 13); 19-1250 M (lines 2 and 8), cDNA from patient 1; BV 173, K562, e19a2 (lines 9, 10, and 11), cDNA from *BCR::ABL1* positive cell-line controls; Mix (lines 5 and 12), negative controls; rare transcript controls (lines 3 and 4), e6a2 and e8a2.

without any symptoms. Currently, the patient is working again, feels healthy, and is confident about his future.

Case 2

The second patient, a 79-year-old man, was initially diagnosed with a triple-negative (*JAK2, CALR, MPL*) primary myelofibrosis in November 2019. Initially, cytogenetic analysis was not successful. At diagnosis, WBC count was only slightly increased (10.5×10^9/L; range, 3.5–9.8×10^9/L), and hemoglobin value (11.6 g/dl; range, 13.5–17.5 g/dl) as well as platelet counts slightly decreased (130×10^9/L; range, 140–360×10^9/L). Apart from that, the differential blood cell count was normal. Colonoscopy and x-ray of the chest were unremarkable. Due to hyperchromic, macrocytic anemia, therapy with vitamin B12 1,000 µg was initiated subcutaneously every 4 weeks. Gastroscopy 3 months later showed *Helicobacter pylori*-negative type A gastritis. Flow cytometry revealed 4% myeloid blast cells within peripheral blood. At that time, the patient received a transfusion with two packed red blood cells for the first time. Abdominal ultrasound showed mild hepatosplenomegaly with a spleen size of 14.5 × 7 cm. Bone marrow evaluation was performed in November 2020 due to progressive WBC count, and anemia was suggestive of primary myelofibrosis. PCR analysis was negative for *BCR::ABL*, *JAK2*, *CALR*, and *MPL* mutations. Astonishingly, flow cytometry was unremarkable at that time. CT scan in December 2020 showed progressive splenomegaly with a spleen size of 17 cm. A therapy with erythropoietin 20,000 IE once weekly was initiated in February 2021 and vitamin B12 was stopped. The patient did not receive a JAK2 inhibitor. Due to a progressive WBC count of 44.2×10^9/L, bone marrow evaluation was repeated in June 2021. Histopathology revealed a hypercellular bone marrow with pronounced megakaryo- and myelopoiesis, whereas erythropoiesis was strongly decreased, mild fibrosis (grade I), and 2% myeloid blast cells. Mast cells were not elevated in the bone marrow or peripheral blood. In molecular analysis, mutations in *ASXL1, EZH2, FLT3, RUNX1, STAG2, and TET2* could be detected. Thus, diagnosis was switched to atypical CML. Cytogenetic analysis revealed a trisomy 8 in 13 as well as a normal karyotype in 7 metaphases (47,XY+8[13]/46,XY[7]). Medical history included arterial hypertension, glaucoma, chronic renal failure (grade IV KDIGO), and benign prostate hyperplasia.

In August 2021, the patient was admitted to our department after syncope. At admission, his performance status was slightly decreased (ECOG 2). He showed signs of anemia with tachycardia (91 bpm at rest), pale skin, and a previously unknown cardiac murmur. Moreover, multiple purple lesions,

particularly at the head, were visible, which developed within a few weeks before admission. Physical examination revealed palpable hepatosplenomegaly.

The reason for the syncope turned out to be anemia of 6.6 g/dl (range, 13.5–17.5 g/dl). Furthermore, laboratory evaluation showed massively elevated WBC count of 249.4 × 10^9/L (range, 3.5–9.8 × 10^9/L), mild decreased platelets (127 × 10^9/L; range, 140–360 × 10^9/L), and an elevated lactate dehydrogenase (LDH) value of 1101.6 U/L (range, 125–248 U/L). Differential blood cell count showed a neutrophil left shift including 4% myeloid blast cells and a basophile count of 1.5%.

Due to leukocytosis, we started a cytoreductive treatment with hydroxycarbamide. With a daily dosage of 5 g, WBC count decreased from 249.4 to 97.6 × 10^9/L within 1 week. To prevent tumor lysis syndrome and due to known renal impairment, intravenous fluids, furosemide, and allopurinol as co-medications were administered.

Bone marrow evaluation showed hypoplastic erythropoiesis as well as myeloid blast cells of 10%, consistent with the previous diagnosis of atypical CML. However, cytogenetic analysis now revealed a balanced translocation t(9;22)(q34;q11) in 21 of 34 metaphases as well as a second, Philadelphia chromosome-negative clone with trisomy 8 in 3 and a normal karyotype in 10 metaphases (46,XY,t(9;22)(q34;q11)[21]/47,XY,+8[3]/46,XY[10]). Molecularly, *BCR::ABL* positivity was confirmed by PCR and FISH analyses (FISH positive in 68% of the interphase cells). The Sokal and ELTS scores were high risk.

To evaluate the skin lesions, we performed a skin biopsy. Histopathology showed a CD33-negative, CD34-negative, and CD117-positive myeloid blast cell population, which we interpreted within the context of the underlying CML.

Due to palpable hepatosplenomegaly, we performed an abdominal ultrasound, which confirmed the finding and additionally showed two splenic infarctions.

In summary, the diagnosis of *BCR::ABL*-positive CML in chronic phase was made and treatment with imatinib was started and hydroxycarbamide was terminated, once a WBC count of lower than 40 × 10^9/L was reached. In the following days, the performance status increased (ECOG 1) and the patient was discharged with a follow-up appointment with his local hemato-oncologist.

Re-admission to our hospital followed 18 days later with a drastically decreased performance status (ECOG 3) and acute on chronic renal failure. Although imatinib had been taken daily, WBC count had increased again to 47.7 × 10^9/L as compared to 23 × 10^9/L at discharge. Platelets were within normal range, but the patient was still anemic (hemoglobin value of 7.3 g/dl). Additionally, there was a mixed response of the skin lesions: some had disappeared, others increased, and some new lesions had occurred.

To exclude a treatment failure, we performed bone marrow evaluation, which again showed CML in chronic phase. No resistance mutation could be detected by PCR analysis, and the *BCR::ABL*-negative trisomy 8 subclone was found in 48% of the interphase cells by FISH analysis and in 1 of 25 metaphases (46,XY,t(9;22)(q34;q11)[9]/47,XY,+8[1]/46,XY[15]). We continued treatment with imatinib and re-initiated hydroxycarbamide due to the increased WBC count.

After a few days, the patient developed pneumocystis jirovecii pneumonia, which was treated with atovaquone/proguanil hydrochloride as well as corticosteroids. Due to progressive respiratory insufficiency, the patient had to be transferred to the intensive care unit. Unfortunately, the patient developed multi-organ with leading pulmonary failure. Pleural effusions were drained and showed myeloid blast cells. The patient had to be intubated and noradrenaline had to be used for circulatory support. Unfortunately, the patient died several days later due to multi-organ failure. An autopsy was performed, confirming pneumocystis jirovecii pneumonia (*via* positive PCR), but also showed several other interesting aspects.

First, the skin effusions showed a CD5, CD7, and CD8 expression (Figure 2A), leading to a CD8+ T-cell lymphoma of the skin with aberrant expression of CD117 and loss of CD2 (Figure 2B). Initially, CD117 positivity led to the assumption of CML skin involvement. The T-cell lymphoma was mainly limited to the skin, explaining the progressive skin nodules during treatment with imatinib.

Second, multiple organs showed a severe infiltration with myeloid precursors (Figure 3). Lung involvement (about 50% of the parenchyma), splenic involvement (90%), hepatic involvement (20%), and renal involvement (30%) (Figure 4) possibly explain the relatively sudden worsening of the performance status and multi-organ failure. Moreover, multiple lymph nodes, pleura, thyroid, prostate, and testicles were involved as well. However, the aggressive course of the disease with the invasion of multiple organs remains an obstacle.

Retrospective mutational analysis by next-generation sequencing at progressive disease showed mutations in *ASXL1* (c.1720-1G>C), *EZH2* (c.2069G>A; c.132delC), *STAG2* (c.436C>T; c2353G>T), and *TET2* (c.5038C>T). Additionally, two different *NRAS* mutations (c.35G>T; c.35G>A) with allele frequencies of 3% and 12% could be detected, whereas the mutations in *FLT3* and *RUNX1*, present at initial diagnosis, could not be detected.

Discussion

Our cases highlight the importance of a thorough investigation of the underlying diagnosis in patients with clinically unclear hematologic diseases but suspected CML.

In fact, the use of conventional multiplex RT-PCR usually fails to detect uncommon *BCR::ABL1* rearrangements due to the generation of atypical PCR products, which are often interpreted as nonspecific and may lead to misdiagnosis, thus excluding the patient from targeted therapy. While atypical transcripts in CML

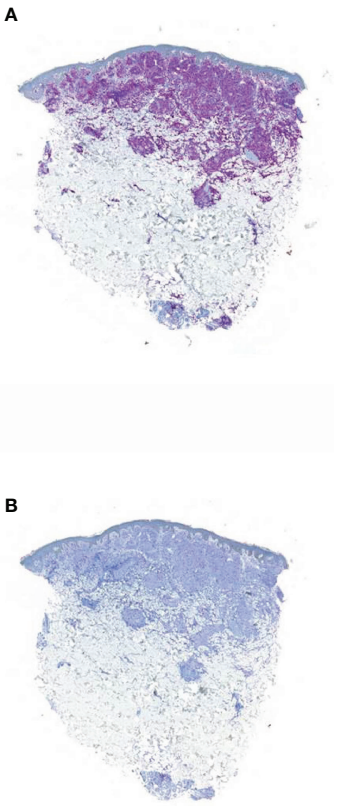

FIGURE 2
Immunohistochemistry of the skin biopsy from the second patient. **(A)** Infiltration of small cellular lymphoid cell components in CD 8 staining; scale bar, 500 µm. **(B)** Antigen loss of CD2 of the lymphoid infiltrates detected in hematoxylin and eosin staining; scale bar, 500 µm.

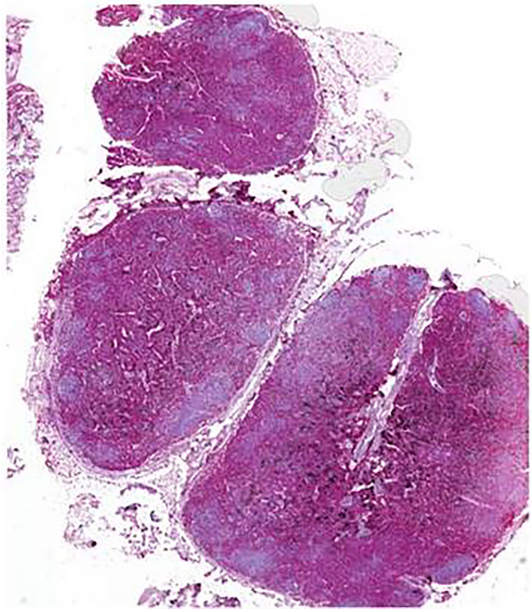

FIGURE 3
Lymph node biopsy from case 2 with myeloperoxidase staining showing infiltration of myeloid precursors; scale bar, 1,000 µm.

patients are increasingly reported (11–14), the outcome seems to be adverse in some of the more "frequent rare" mutations such as e1a2 (15, 16).

In 2019, Xue et al. evaluated the incidence and prognostic significance of CML patients with rare transcripts in a large cohort of 2,331 patients (15). Rare transcripts were found in 40 (1.7%) patients, including e1a2 (0.9%), e19a2 (0.4%), e13a3 (0.1%), and e14a3 (0.3%). Compared to patients with the typical transcript, those with the e1a2 transcript had an inferior response to TKIs [complete cytogenetic response rate (CCyR), 19.0% vs. 79.9%; $p < 0.001$] and an inferior 3-year overall survival (OS) rate (83.9% vs. 98.7%; $p < 0.001$). Patients with the e19a2 transcript had a high rate of early optimal response to TKIs, but most of them later lost CCyR due to *BCR::ABL1* mutations, resulting in a poor prognosis. Patients with the e13a3 or e14a3 transcripts responded well to TKIs and had a good outcome. However, the low patient number needs to be taken into account, when interpreting the data. Similarly, Gong et al. reported an inferior outcome for patients with e1a2 transcripts as compared to those with typical transcripts, such as e13a2 and e14a2 (16). Patients with e1a2 were more likely to develop CML with blast phase (61% vs 17.6%; $p < 0.001$) and the transcript was predictive for inferior OS ($p = 0.002$) as compared to patients with typical transcripts (16). In other cases with rare

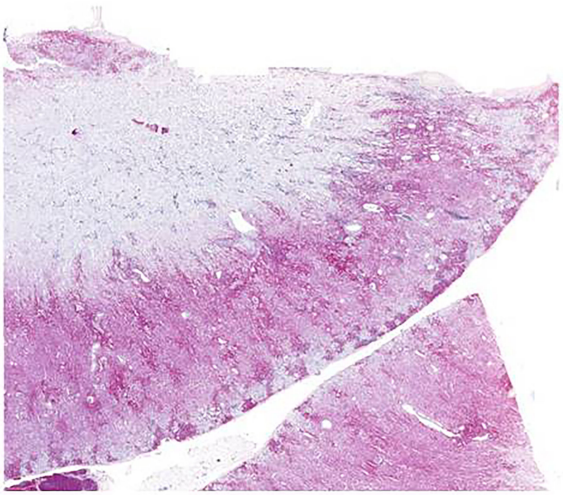

FIGURE 4
Renal biopsy from case 2 with myeloperoxidase staining showing infiltration of myeloid precursors; scale bar, 2,000 µm.

transcripts, the impact on outcome remains unclear due to their rarity and lack of data.

To date, there are only limited data on outcome of CML patients with the *BCR::ABL1* e6a2 transcript. Several case reports suggest an aggressive course of the disease with resistance to imatinib (17, 18) and dasatinib (18) treatment. In addition, three (50%) of six imatinib-treated CML patients with the *BCR::ABL* e6a2 transcript relapsed or did not respond (6, 19, 20). Two of them additionally developed imatinib resistance (19, 20) and one developed extramedullary disease (20). The short duration of response and rapid progression into advanced phase may indicate that the e6a2 *BCR::ABL* transcript has a higher transforming capacity than the standard major *BCR* transcript (e13a2 or e14a2 *BCR::ABL*). In our case, treatment with nilotinib within the NILOdeepR trial (ClinicalTrials.gov Identifier: NCT02546674), as second-generation TKI, led to a deep and enduring molecular remission, in line with a previous case report (21). Thus, the form of transcript should be considered when deciding on the optimal treatment approach. Our second case shows the diagnostic difficulty of an uncommon CML presentation. The initial diagnosis was a triple-negative primary myelofibrosis. The *JAK2* V617F mutation is specific for *BCR::ABL1* negative myeloproliferative neoplasm and occurs in approximately 50% of patients with primary myelofibrosis. However, mutational analysis was negative for *JAK2, CALR*, and *MPL* at diagnosis.

Initially, cytogenetic analyses revealed only trisomy 8 and no Philadelphia chromosome could be detected. However, repeated analysis in August 2021 showed the balanced translocation t(9;22) in 21 metaphases and in a small subclone trisomy 8. Thus, primary myelofibrosis and CML with *BCR::ABL* were separate clones, which evolved from a mutual precursor cell. This precursor was characterized by mutations in *TET2, EZH2, ASXL1*, and *STAG2*. Repeated analyses by next-generation sequencing revealed some overlapping mutations, but also discrepancies, since *NRAS* mutations evolved, whereas mutations in *FLT3* and *RUNX1*, present at initial diagnosis, could not be detected. In summary, this is a case of "branching" rather than "linear" evolution.

In addition, the secondary neoplasia of a T-cell non-Hodgkin's lymphoma (T-NHL) obscured the diagnosis, leading to the assumption of initial treatment failure. Although concurrent neoplasias are described in CML patients (22–25), they are still a diagnostic as well as therapeutic challenge. In our case, the atypical phenotype led to the assumption of CML infiltration of the skin, whereas autopsy revealed the diagnosis of a CD2-negative T-NHL. Interestingly, in autopsy, most organs showed an abundant infiltration with myeloid precursors, while sparing the skin, whereas the T-cell lymphoma mainly infiltrated the skin. The reason for this organ tropism remains elusive.

One reason for the large-scale infiltration of CML, despite being in chronic phase, might be driven by molecular abnormalities, such as *ASXL1* or *RUNX1* (26, 27). The impact on outcome of the other described mutations remains unclear (28–30). The known resistance to imatinib is consistent with our case and underlines the importance to evaluate the molecular profile, particularly in "atypical typical" cases.

In conclusion, in patients with suspected CML, the presence of rare transcripts needs to be taken into account to prevent the possibility of a misdiagnosis, thus preventing the patient from targeted therapy. Treatment with second-generation TKIs, such as nilotinib, seems to be effective in patients with the rare transcript e6a2. However, larger data, ideally from multicenter clinical trials, are needed in order to define the best treatment choice for patients with these rare transcripts.

Data availability statement

The raw data supporting the conclusions of this article will be made available upon reasonable request.

Ethics statement

Ethical review and approval was not required for the study on human participants in accordance with the local legislation and institutional requirements. Patients declare on their admission that their data may be used in anonymised form for scientific evaluations and for publications.

Author contributions

FR and SK were responsible for the concept of this paper, contributed to the literature search data collection, treated the patients, analysed and interpreted data, and wrote the manuscript. RS treated the patient and critically revised the manuscript. AF, BM, DB, AJ, AM, KM, and JWGJ performed research and critically revised the manuscript. All authors approved the submission.

Funding

The authors acknowledge support from the University of Leipzig within the program of Open Access Publishing.

Conflict of interest

The authors declare that the research was conducted in the absence of any commercial or financial relationships that could be construed as a potential conflict of interest.

Publisher's note

References

1. Rowley JD. Letter: A new consistent chromosomal abnormality in chronic myelogenous leukaemia identified by quinacrine fluorescence and giemsa staining. *Nature* (1973) 243(5405):290–3. doi: 10.1038/243290a0

2. Nowell PC, Hungerford DA. Chromosome studies on normal and leukemic human leukocytes. *J Natl Cancer Inst* (1960) 25:85–109.doi.org/10.1093/jnci/25.1.85

3. Shtivelman E, Lifshitz B, Gale RP, Canaani E. Fused transcript of abl and bcr genes in chronic myelogenous leukaemia. *Nature* (1985) 315(6020):550–4. doi: 10.1038/315550a0

4. Gugliotta G, Castagnetti F, Breccia M, Levato L, Intermesoli T, D'Adda M, et al. Treatment-free remission in chronic myeloid leukemia patients treated front-line with nilotinib: 10-year follow-up of the GIMEMA CML 0307 study. *Haematologica* (2022). doi: 10.3324/haematol.2021.280175

5. Massimino M, Stella S, Tirrò E, Consoli ML, Pennisi MS, Puma A, et al. Efficacy of dasatinib in a very elderly CML patient expressing a rare E13a3 BCR-ABL1 fusion transcript: A case report. *Anticancer Res* (2019) 39(7):3949–54. doi: 10.21873/anticanres.13548

6. Schultheis B, Wang L, Clark RE, Melo JV. BCR-ABL with an e6a2 fusion in a CML patient diagnosed in blast crisis. *Leukemia* (2003) 17(10):2054–5. doi: 10.1038/sj.leu.2403079

7. Branford S, Rudzki Z, Hughes TP. A novel BCR-ABL transcript (e8a2) with the insertion of an inverted sequence of ABL intron 1b in a patient with Philadelphia-positive chronic myeloid leukaemia. *Br J Haematol* (2000) 109 (3):635–7. doi: 10.1046/j.1365-2141.2000.02042.x

8. Hochhaus A, Reiter A, Skladny H, Melo JV, Sick C, Berger U, et al. A novel BCR-ABL fusion gene (e6a2) in a patient with Philadelphia chromosome-negative chronic myelogenous leukemia. *Blood* (1996) 88(6):2236–40. doi: 10.1182/blood.V88.6.2236.bloodjournal8862236

9. Langabeer SE. Is the BCR-ABL1 transcript type in chronic myeloid leukaemia relevant? *Med Oncol* (2013) 30(2):508. doi: 10.1007/s12032-013-0508-9

10. Cross NC, White HE, Colomer D, Ehrencrona H, Foroni L, Gottardi E, et al. Laboratory recommendations for scoring deep molecular responses following treatment for chronic myeloid leukemia. *Leukemia* (2015) 29(5):999–1003. doi: 10.1038/leu.2015.29

11. Ciftciler R, Saglam EA, Inanc A, Ozcebe O, Haznedaroglu IC. A unique case of complex variant translocation of t(6;9;22)(p22;q34;q11.2), der(19) in a newly diagnosed patient with chronic myeloid leukemia. *Cancer Genet* (2019) 237:78–81. doi: 10.1016/j.cancergen.2019.06.008

12. Liu B, Zhang W, Ma H. Complete cytogenetic response to nilotinib in a chronic myeloid leukemia case with a rare e13a3(b2a3) BCR-ABL fusion transcript: A case report. *Mol Med Rep* (2016) 13(3):2635–8. doi: 10.3892/mmr.2016.4826

13. Masuko M, Furukawa T, Abe T, Wada R, Maruyama S, Kitajima T, et al. A chronic myeloid leukemia patient with atypical karyotype and BCR-ABL e13a3 transcript caused by complex chromosome rearrangement. *Int J Hematol* (2009) 90 (2):230–4. doi: 10.1007/s12185-009-0368-4

14. Arun AK, Senthamizhselvi A, Mani S, Vinodhini K, Janet NB, Lakshmi KM, et al. Frequency of rare BCR-ABL1 fusion transcripts in chronicmyeloid leukemia patients. *Int J Lab Hematol* (2017) 39(3):235–42. doi: 10.1111/ijlh.12616

15. Xue M, Wang Q, Huo L, Wen L, Yang X, Wu Q, et al. Clinical characteristics and prognostic significance of chronic myeloid leukemia with rare BCR-ABL1 transcripts. *Leuk Lymphoma* (2019) 60(12):3051–7. doi: 10.1080/10428194.2019.1607329

16. Gong Z, Medeiros LJ, Cortes JE, Zheng L, Khoury JD, Wang W, et al. Clinical and prognostic significance of e1a2 BCR-ABL1 transcript subtype in chronic myeloid leukemia. *Blood Cancer J* (2017) 7(7):e583. doi: 10.1038/bcj.2017.62

17. Vefring HK, Gruber FXE, Wee L, Hovland R, Hjorth-Hansen H, Dahl TG, et al. Chronic myelogenous leukemia with the e6a2 BCR-ABL and lacking imatinib response: presentation of two cases. *Acta Haematol* (2009) 122(1):11–6. doi: 10.1159/000230037

18. Beel KA, Lemmens J, Vranckx H, Maertens J, Vandenberghe P. CML with e6a2 BCR-ABL1 transcript: an aggressive entity? *Ann Hematol* (2011) 90 (10):1241–3. doi: 10.1007/s00277-011-1169-4

19. Schnittger S, Bacher U, Kern W, Haferlach T, Hertenstein B, Haferlach C. A new case with rare e6a2 BCR-ABL fusion transcript developing two new resistance mutations during imatinib mesylate, which were replaced by T315I after subsequent dasatinib treatment. *Leukemia* (2008) 22(4):856–8. doi: 10.1038/sj.leu.2404949

20. Torres F, Ivanova-Dragoeva A, Pereira M, Veiga J, Rodrigues AS, Sousa AB, et al. An e6a2 BCR-ABL fusion transcript in a CML patient having an iliac chloroma at initial presentation. *Leuk. Lymphoma* (2007) 48(5):1034–7. doi: 10.1080/10428190701216402

21. Manzella L, Tirrò E, Vitale SR, Puma A, Consoli ML, Tambè L, et al. Optimal response in a patient with CML expressing BCR-ABL1 E6A2 fusion transcript with nilotinib therapy: A case report. *In Vivo* (2020) 34(3):1481–6. doi: 10.21873/invivo.11933

22. Faizan M, Anwar S, Ain RU, Zafar H, Saqlain N, Rathore Z. T Lymphoblastic lymphoma with BCR-ABL negative chronic myeloid leukaemia: a novel association. *Ecancermedicalscience* (2021) 15:1221. doi: 10.3332/ecancer.2021.1221

23. Gruszka AM, Rabascio C, Cannella L, Sammassimo S, Andreola G, Gregato G, et al. Molecular investigation of coexistent chronic myeloid leukaemia and peripheral T-cell lymphoma - a case report. *Sci Rep* (2015) 5:14829. doi: 10.1038/srep14829

24. Jamal E, El-Ashwah S, Ebrahim MA, Zaki MM, Saleh LM, El-Badrawy A, et al. Case report; meta-synchronous triple malignancy in primary diagnosed CML patient. *Am J Blood Res* (2020) 10(2):22–5.

25. Paczkowska E, Janowski M, Karpińska K, Ryłów M, Zdziarska B, Poncyljusz W, et al. Hodgkin Lymphoma as a secondary neoplasm during therapy for chronic myeloid leukaemia: Case report and review of the literature. *Onco Targets Ther* (2021) 14:2497–503. doi: 10.2147/OTT.S300320

26. Machnicki MM, Pepek M, Solarska I, Niesiobedzka-Krezel J, Seferynska I, Tybor JG, et al. ASXL1 mutations detectable at diagnosis may predict response to imatinib in patients with chronic myeloid leukemia. *Blood* (2019) 134 (Supplement_1):4148. doi: 10.1182/blood-2019-12983

27. Corm S, Biggio V, Roche-Lestienne C, Laï J-L, Yakoub-Agha I, Philippe N, et al. Coexistence of AML1/RUNX1 and BCR-ABL point mutations in an imatinib-resistant form of CML. *Leukemia* (2005) 19(11):1991–2. doi: 10.1038/sj.leu.2403931

28. Adnan-Awad S, Kankainen M, Mustjoki S. Mutational landscape of chronic myeloid leukemia: more than a single oncogene leukemia. *Leuk Lymphoma* (2021) 62(9):2064–78. doi: 10.1080/10428194.2021.1894652

29. Rinke J, Chase A, Cross NCP, Hochhaus A, Ernst T. EZH2 in myeloid malignancies. *Cells* (2020) 9(7):1639. doi: 10.3390/cells9071639

30. Kon A, Shih L-Y, Minamino M, Sanada M, Shiraishi Y, Nagata Y, et al. Recurrent mutations in multiple components of the cohesin complex in myeloid neoplasms. *Nat Genet* (2013) 45(10):1232–7. doi: 10.1038/ng.2731

frontiers | Frontiers in Oncology

TYPE Case Report
PUBLISHED 08 September 2022
DOI 10.3389/fonc.2022.1002333

OPEN ACCESS

EDITED BY
Liren Qian,
Fifth Medical Center of the PLA General Hospital, China

REVIEWED BY
Olle Thor,Hans Ringden,
Karolinska Institutet (KI), Sweden
Szymon Skoczen,
Jagiellonian University Medical College, Poland
Xiao-Dong Mo,
Peking University People's Hospital, China

*CORRESPONDENCE
Ting Zhang
zhangt@shchildren.com.cn
Zhibao Lv
lvzb@shchildren.com.cn

†These authors have contributed equally to this work

SPECIALTY SECTION
This article was submitted to Hematologic Malignancies, a section of the journal Frontiers in Oncology

RECEIVED 25 July 2022
ACCEPTED 19 August 2022
PUBLISHED 08 September 2022

CITATION
Wang Y, Liu J, Jiang B, Yuan C, Chen L, Zhang T and Lv Z (2022) Graft-versus-host disease complicated with small bowel obstruction in children: A case report. *Front. Oncol.* 12:1002333. doi: 10.3389/fonc.2022.1002333

Graft-versus-host disease complicated with small bowel obstruction in children: A case report

Yizhong Wang[1,2†], Jiangbin Liu[3†], Bingxin Jiang[1], Chenling Yuan[1], Licai Chen[3], Ting Zhang[1,2*] and Zhibao Lv[3*]

[1]Department of Gastroenterology, Hepatology and Nutrition, Shanghai Children's Hospital, School of Medicine, Shanghai Jiao Tong University, Shanghai, China, [2]Gut Microbiota and Metabolic Research Center, Institute of Pediatric Infection, Immunity and Critical Care Medicine, School of Medicine, Shanghai Jiao Tong University, Shanghai, China, [3]Department of General Surgery, Shanghai Children's Hospital, School of Medicine, Shanghai Jiao Tong University, Shanghai, China

Graft-versus-host disease (GvHD) is a severe complication following hematopoietic cell transplantation (HCT). The clinical manifestations of GvHD can affect multiple systems. Although gastrointestinal (GI) GvHD is common, GI obstruction complications are rare. Here, we present a case of GI-GvHD after HCT for acute myeloid leukemia (AML) in a young girl from China. The patient suffered from watery diarrhea, which progressed to bloody diarrhea 40 days after HCT. She experienced prolonged and repeated mucous or bloody stool after the withdrawal of cyclosporine and the gradual reduction in methylprednisolone. The plain abdominal radiography and computed tomographic (CT) scan showed apparent bowel wall thickening and intestinal stenosis 10 months after HCT. Finally, the patient underwent surgery to remove the small intestinal stenosis at the age of 26 months. The patient recovered with the help of appropriate medical therapies and nutritional support during hospitalization. She remained stable, and there was no recurrence of GI symptoms 16 months after the surgery. In summary, surgery may be an optimal treatment for GvHD patients with persistent bowel obstruction and failure of appropriate immunosuppressive therapies.

KEYWORDS

graft-versus-host disease, hematopoietic cell transplantation, bowel obstruction, child, leukemia

Abbreviations: AML, acute myeloid leukemia; GvHD, graft-versus-host disease; HCT, hematopoietic cell transplantation; GI, gastrointestinal; HLA, human leukocyte antigen; CT, computed tomographic.

Introduction

Graft-versus-host disease (GvHD) following hematopoietic cell transplantation (HCT) is a serious complication that can be life threatening to recipients. The occurrence of GvHD is attributable to the presence of immunocompetent T lymphocytes in the graft attacking the immunodeficient recipient tissue, ultimately causing host damage (1). Emerging evidence has revealed that multiple factors, including proinflammatory intracellular signaling activation, intestinal tissue regeneration defects, impaired antipathogen immunity, and dysbiosis of the gut microbiota, play critical roles in the pathogenesis of GvHD (2). The clinical manifestations of GvHD involve multiple systems, such as the skin, gastrointestinal (GI) tract, lungs, hepatobiliary system, musculoskeletal system, kidneys, eyes, and hematopoietic system (3). GI-GvHD, especially in the small intestine, is a leading cause of HCT-related morbidity and mortality in recipients (4). The clinical management of GvHD is complex and not standardized worldwide due to the limited results from well-designed, large-scale clinical studies. Immunosuppressive therapy is the most common intervention for the prophylaxis and treatment of GvHD, particularly acute GvHD that occurs in the short term after HCT (5). Recently, studies reported rare pediatric cases of small bowel obstruction caused by severe chronic intestinal GvHD that were managed efficiently with surgical intervention (6, 7). Here, we report a 26-month-old girl affected with small intestinal obstruction caused by chronic GI-GvHD after allogeneic HCT (allo-HCT) for acute myeloid leukemia (AML) who was treated successfully by surgery in China.

Case presentation

The patient was a girl diagnosed with AML and monosomy 7 at 10 months old (Figure 1). She received allo-HCT from a fully human leukocyte antigen (HLA)-matched unrelated donor (a 30-year-old female volunteer from the China Marrow Donor Program, 10/10 high resolution) after 4 months of chemotherapies with a standard protocol of DAE (DNR, Ara-C, and VP-16), IAE (IDA, Ara-C, and VP-16), MA (mito and Ara-C), and HA (Ara-C) based on the AML-SCMC-2009 protocol (8). Sustained cyclosporine (2.5 mg/kg) was used as prophylaxis for GvHD from 1 month before HCT until 5 months after HCT (Figure 1). She had no medical history of GI problems or GI allergies before HCT, and the patient was not complicated with GI manifestations during chemotherapy. On day 40 after HCT, the patient started to suffer from watery diarrhea, followed by bloody diarrhea, and was readmitted to our hospital. She had no fever, abdominal pain, cramps, or maculopapular rash. Abdominal ultrasonography revealed partial small-bowel wall thickening and lumen expansion. The colonoscopy was normal, and biopsy of the sigmoid colon showed chronic inflammation of the mucosa. Empiric antibiotic therapies (tigecycline and levofloxacin, followed by meropenem, vancomycin, and voriconazole) were first applied to treat possible intestinal infections. However, the diarrhea did not improve after 3 weeks of antibiotic therapy, and acute GI-GvHD was suspected. Then, the patient was treated with cyclosporine, basiliximab (once), and methylprednisolone, allowing a transient improvement of the GI symptoms (yellow loose stool, one to two times per day). During the withdrawal of cyclosporine and the gradual reduction in methylprednisolone (three courses of treatment, Figure 1), the patient experienced prolonged and repeated GI symptoms of mucous or bloody stool, along with recurrent hypoalbuminemia (albumin, 19.7–30.6 g/L). Albumin, gamma globulin, and frozen plasma were given to treat her hypoalbuminemia monthly.

Ten months after HCT, fever and abdominal pain followed by vomiting and diarrhea occurred. Plain abdominal radiography and abdominal ultrasound suggested intestinal obstruction. The pathogens of Epstein–Barr virus (EBV), TORCH, and cytomegalovirus (CMV) were all negative. Other causes of bloody diarrhea, including *Salmonella* and *Clostridium difficile*, were not detected in her feces. No sign of clinical manifestations was observed in other organs, including

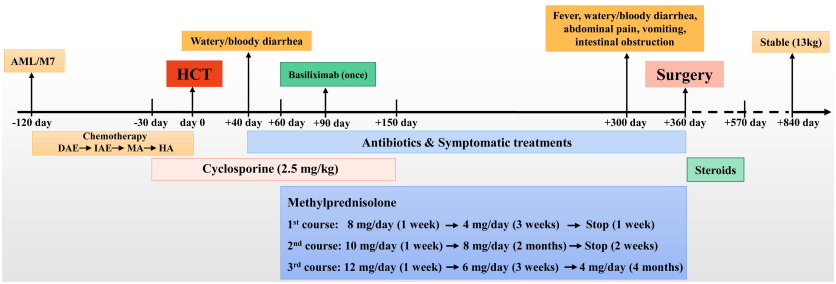

FIGURE 1
The timeline of the treatments. AML, acute myeloid leukemia; HCT, hematopoietic cell transplantation.

the skin, lungs, liver, kidneys, and eyes. The patient was treated with conservative medical treatments, including fasting, parenteral nutrition, and antibiotics (ceftriaxone, meropenem, and itraconazole), but the symptoms did not improve. Repeat plain abdominal radiography revealed bowel dilation exacerbation with an abnormal gas–liquid level (Figure 2A), and computed tomographic (CT) scan showed apparent bowel wall thickening and intestinal stenosis (Figure 2B). The patient underwent surgery to remove the small intestinal stenosis due to the ineffectiveness of medicinal treatments at the age of 26 months. At laparotomy, gross examination showed that the proximal small intestine was dilated, and the distal small intestinal wall was markedly thickened and edematous (Figure 3A). One ileal stenotic region of 20 cm was surgically removed (Figure 3B). The resected ileal tissue was stiff, and one stenosis with mucosal ulcerations was observed (Figures 3B, C). Pathological examination of the lesion location showed that the intestinal mucosa was substituted with granulation tissue with neutrophilic infiltration, and no crypts or epithelial cells were seen (Figure 4). Viral tests for cytomegalovirus and Epstein–Barr virus were all negative. Finally, the patient was diagnosed with GI-GvHD complicated with small bowel obstruction. An enteral diet was gradually given after flatus and bowel movement recovery. The patient significantly improved and was discharged after 57 days of hospitalization. The patient received steroids as maintenance treatment after discharge. The timeline of the treatments is summarized in Figure 1. As of this writing, the patient is 42 months old, her condition remains stable, and she weighs 13 kg (P14). The patient is monitored closely to be aware of symptoms recurrence and the development of chronic GvHD.

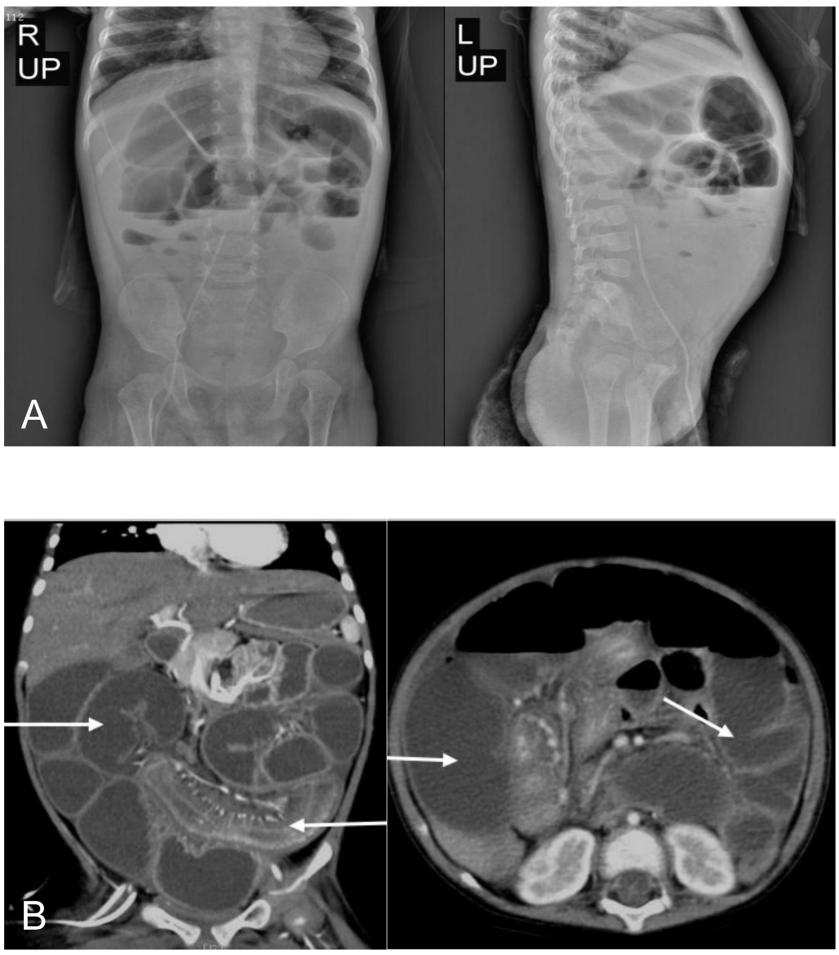

FIGURE 2
Bowel dilation, bowel wall thickening, and stenosis in the patient. **(A)** Abdominal radiograph showed bowel dilation with a gas–liquid level. **(B)** CT scan showed bowel dilation, thickening of the bowel wall, and small bowel stenosis.

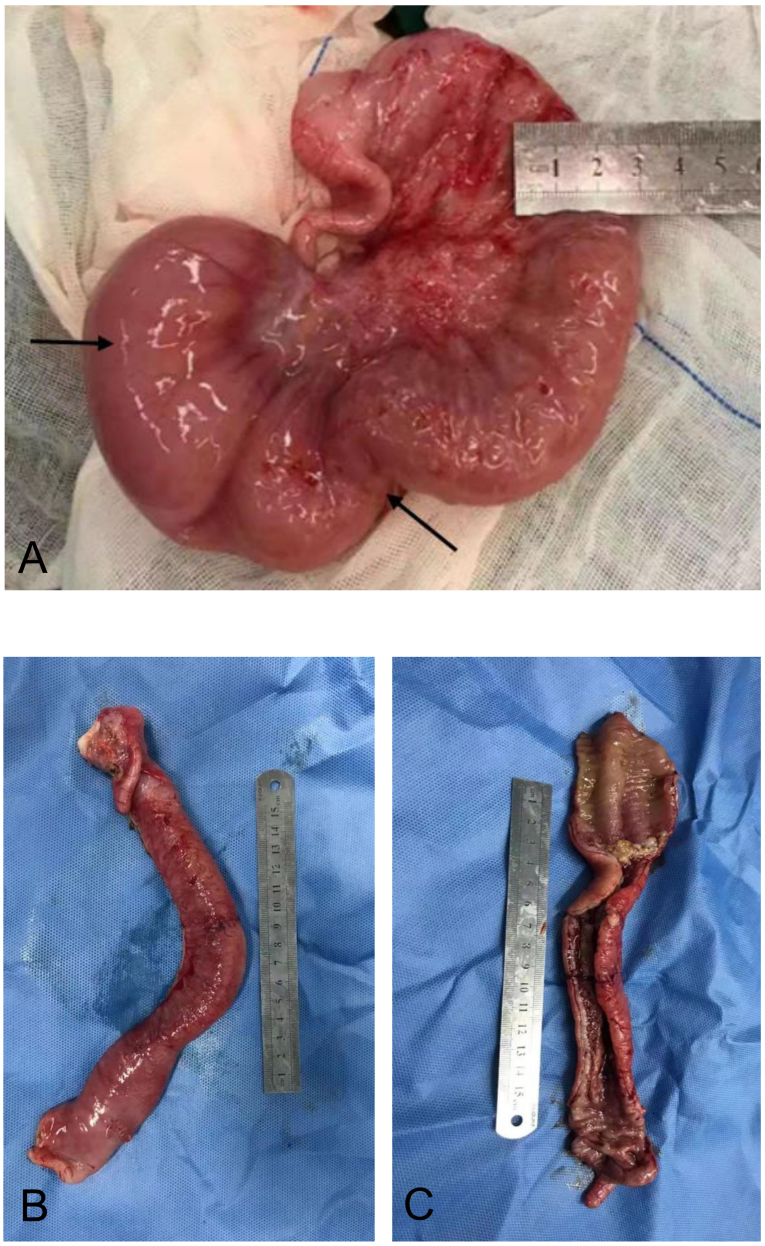

FIGURE 3
Surgical resection of the affected small intestine. **(A)** Small intestine wall thickening, edema, and stenosis. **(B)** Stiffness of the affected small intestine. **(C)** Reduction in the mucosal folds.

Discussion

GvHD is a systemic disorder caused by immunological rejection of host tissues by graft immune cells. It remains a major challenge after HCT due to its high morbidity and mortality. GvHD can affect multiple host organs, and the GI is one of the most frequently involved systems (3). GI-GvHD complicated with hemorrhage, perforation, or acute or chronic obstruction occurs in 20%–30% of all patients under HCT (6, 9). The common clinical manifestations of GI-GvHD include diarrhea, abdominal pain, nausea, vomiting, mucositis, and mucosal ulceration (10). Intestinal hemorrhage, perforation, and stricture with bowel obstruction can also occur in severe GI-GvHD (6, 7, 10), but they are rare. In this report, we describe a case of GI-GvHD following HCT for AML in a young child from China. Our patient suffered from watery diarrhea, which progressed to bloody diarrhea after 40 days of HCT. Although treatment with cyclosporine, basiliximab, and methylprednisolone allowed a transient improvement of the

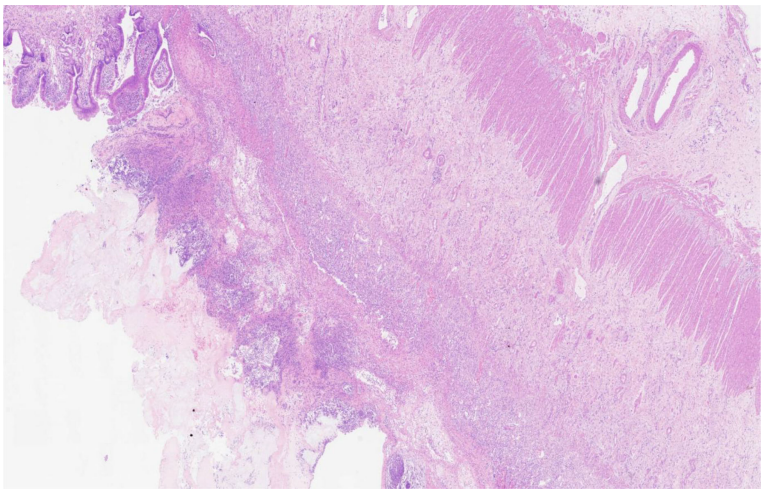

FIGURE 4
Histological examination showed crypt loss, marked inflammation, and associated architectural distortion (hematoxylin and eosin, 200×).

diarrhea, the patient experienced prolonged and repeated mucous or bloody stool after the withdrawal of cyclosporine and the gradual reduction in methylprednisolone. Plain abdominal radiography and CT scans showed apparent bowel wall thickening and intestinal stenosis 10 months after HCT. Finally, the patient underwent surgery to remove the small intestinal stenosis due to the ineffectiveness of internal medicinal treatments at the age of 26 months. The patient fully recovered, helped by appropriate medical therapies and nutritional support, after 57 days of hospitalization. She remained well and had no recurrence of GI symptoms as of 28 months after HCT and 16 months after surgery. The exact pathogenesis of GI-GvHD is still unclear. A recent study showed that high glucagon-like peptide-1 (GLP-1) levels in the early posttransplant phase reduced the risk of GI-GvHD by influencing the regeneration of injured epithelial barriers and ameliorating inflammatory responses (11). Furthermore, gut microbiota dysbiosis is associated with GI-GvHD. Burgos da Silva et al. showed that the preservation of fecal microbiome was correlated with reduced severity of GvHD (12).

Timely diagnosis and appropriate treatments are critical in the management of acute GvHD. The primary treatment should not be delayed in patients without classical constellation of symptoms. Biopsies may be helpful for the patients with unclear diagnosis. For patients with steroid-refractory acute GvHD, second-line treatments, such as extracorporeal photopheresis, anti-tumor necrosis factor antibodies (infliximab, etanercept), mammalian target of rapamycin inhibitors (sirolimus), mycophenolate mofetil, and interleukin-2 receptor antibodies (inolimomab, basiliximab), are needed to be considered and provided appropriately (13). Furthermore, alemtuzumab, pentostatin, mesenchymal stem cells, and methotrexate are suggested as third-line treatment options (13, 14). The patient not receiving timely second-line treatments was critical, as she was suspected with repeated intestinal infections after HCT. Transplant physicians should pay full attention to the management of patients without classical symptoms and steroid-refractory GvHD. The small bowel obstruction of our patient was most likely a presentation of persistent acute GI-GvHD, according to the Mount Sinai Acute GvHD International Consortium (MAGIC) criteria (15).

GvHD complicated with small bowel obstruction in children is rare (6, 7, 16–21). A systematic review conducted by Gutierrez et al. (6) summarized eight pediatric patients with intestinal GvHD who underwent surgical interventions due to small bowel obstruction. Tordjman et al. (7) presented four pediatric cases of small bowel obstruction after HCT with detailed gross and histological data and their genetic status. It was reported that pediatric patients who developed intestinal obstruction always had a history of severe acute GvHD with common symptoms of vomiting, diarrhea, or abdominal pain. Poor clinical response to immunosuppressive therapies leading to chronic GI-GvHD may be a high-risk factor for the development of intestinal obstruction and occlusion. Plain abdominal radiography and CT scans are important tools to observe intestinal obstructions and stenoses in patients with GI-GvHD. In addition, endoscopy and biopsy are helpful to reveal the GI condition of patients with persistent symptoms of vomiting, diarrhea, or abdominal pain (22). Similar to previously reported patients, our patient was less responsive to immunosuppressive therapies and was complicated by long-term GI-GvHD. Small bowel wall thickening and intestinal stenosis were observed 10 months after HCT. In cases of intensive medical treatment failure, surgery may be necessary to remove intestinal stenoses to

improve the patient's chance of survival. Several pediatric patients with small bowel obstruction related to GI-GvHD have been successfully managed by surgical resection of affected loops (6, 7). Nevertheless, the risks of surgical procedures in patients with GvHD should be evaluated prior to the operation, such as hemorrhage, infections, enterocutaneous fistulae, intestinal stricture, and adhesion. In patients complicated with surgery-related hemorrhage, infection, enterocutaneous fistulae, intestinal stricture, and adhesion, bowel obstruction recurrence is prone to arise (6).

In summary, we report a rare pediatric case of severe GI-GvHD complicated with small intestinal obstruction that was refractory to intensive medical treatments. She has been disease-free for 16 months since the surgical resection of the intestinal stenosis. Surgery can be an optimal treatment for GvHD patients with persistent bowel obstruction.

Data availability statement

The raw data supporting the conclusions of this article will be made available by the authors, without undue reservation.

Ethics statement

This study was reviewed and approved by Ethical Review Board of Shanghai Children's Hospital. Written informed consent to participate in this study was provided by the participants' legal guardian/next of kin.

Author contributions

TZ and ZL contributed to the study conception and design. JL, YC, and CL acquired the clinical data. YW and BJ drafted the manuscript. TZ and ZL edited and revised the manuscript. All authors contributed to the article and approved the submitted version.

Funding

This work was supported by the grants from the National Natural Science Foundation of China (grant number 81870373) and the Natural Science Foundation of Shanghai (grant number 22ZR1451800). The funders had no role in study design, data collection and analysis, decision to publish, or preparation of the manuscript.

Acknowledgments

The authors thank the family for participating and supporting this study.

Conflict of interest

The authors declare that the research was conducted in the absence of any commercial or financial relationships that could be construed as a potential conflict of interest.

Publisher's note

References

1. Nassereddine S, Rafei H, Elbahesh E, Tabbara I. Acute graft versus host disease: A comprehensive review. *Anticancer Res* (2017) 37(4):1547–55. doi: 10.21873/anticanres.11483

2. Zeiser R. Advances in understanding the pathogenesis of graft-versus-host disease. *Br J Haematol* (2019) 187(5):563–72. doi: 10.1111/bjh.16190

3. Ramachandran V, Kolli SS, Strowd LC. Review of graft-Versus-Host disease. *Dermatol Clin* (2019) 37(4):569–82. doi: 10.1016/j.det.2019.05.014

4. Ferrara JL, Smith CM, Sheets J, Reddy P, Serody JS. Altered homeostatic regulation of innate and adaptive immunity in lower gastrointestinal tract GVHD pathogenesis. *J Clin Invest* (2017) 127(7):2441–51. doi: 10.1172/JCI90592

5. Penack O, Marchetti M, Ruutu T, Aljurf M, Bacigalupo A, Bonifazi F, et al. Prophylaxis and management of graft versus host disease after stem-cell transplantation for haematological malignancies: Updated consensus recommendations of the European society for blood and marrow transplantation. *Lancet Haematol* (2020) 7(2):e157–67. doi: 10.1016/S2352-3026(19)30256-X

6. Gutierrez CA, Raval MV, Vester HR, Chaudhury S, von Allmen D, Rothstein DH. Surgical treatment of intestinal complications of graft versus host disease in the pediatric population: Case series and review of literature. *J Pediatr Surg* (2017) 52(11):1718–22. doi: 10.1016/j.jpedsurg.2017.06.022

7. Tordjman M, Ouachee M, Bonnard A, Tilea B, Yakouben K, Viala J, et al. Small bowel stenosis: a manifestation of chronic graft-versus-host disease in children? *Hum Pathol* (2018) 72:174–9. doi: 10.1016/j.humpath.2017.08.034

8. Tang Y, Luo C, Shen S, Xue H, Pan C, Hu W, et al. The efficacy and safety of a homoharringtonine-based protocol for children with acute myeloid leukemia: A retrospective study in China. *Pediatr Hematol Oncol* (2021) 38(2):97–107. doi: 10.1080/08880018.2020.1820649

9. Hings IM, Severson R, Filipovich AH, Blazar BR, Kersey JH, Ramsay NK, et al. Treatment of moderate and severe acute GVHD after allogeneic bone marrow transplantation. *Transplantation* (1994) 58(4):437–42. doi: 10.1097/00007890-199408270-00008

10. Malard F, Mohty M. New insight for the diagnosis of gastrointestinal acute graft-versus-host disease. *Mediators Inflammation* (2014) 2014:701013. doi: 10.1155/2014/701013

11. Ebbesen M, Kissow H, Hartmann B, Kielsen K, Sorensen K, Stinson SE, et al. Glucagon-like peptide-1 is associated with systemic inflammation in pediatric patients treated with hematopoietic stem cell transplantation. *Front Immunol* (2021) 12:793588. doi: 10.3389/fimmu.2021.793588

12. Burgos da Silva M, Ponce DM, Dai A, Devlin SM, Gomes AL, Moore GF, et al. Preservation of fecal microbiome is associated with reduced severity of graft-versus-Host disease. *Blood* (2022). doi: 10.1182/blood.2021015352

13. Dignan FL, Clark A, Amrolia P, Cornish J, Jackson G, Mahendra P, et al. Diagnosis and management of acute graft-versus-host disease. *Br J Haematol* (2012) 158(1):30–45. doi: 10.1111/j.1365-2141.2012.09129.x

14. Zhao K, Lou R, Huang F, Peng Y, Jiang Z, Huang K, et al. Immunomodulation effects of mesenchymal stromal cells on acute graft-versus-host disease after hematopoietic stem cell transplantation. *Biol Blood Marrow Transplant* (2015) 21(1):97–104. doi: 10.1016/j.bbmt.2014.09.030

15. Schoemans HM, Lee SJ, Ferrara JL, Wolff D, Levine JE, Schultz KR, et al. EBMT-NIH-CIBMTR task force position statement on standardized terminology & guidance for graft-versus-host disease assessment. *Bone Marrow Transplant* (2018) 53(11):1401–15. doi: 10.1038/s41409-018-0204-7

16. Gavel G, Marven S, Evans MJ, Walker J, Vora AJ. Obliterative enteritis complicating graft versus host disease. *Bone Marrow Transplant* (2003) 32 (11):1097–8. doi: 10.1038/sj.bmt.1704282

17. Faraci M, Dallorso S, Morreale G, Dini G, Castagnola E, Miano M, et al. Surgery for acute graft-versus-host disease of the bowel: description of a pediatric case. *J Pediatr Hematol Oncol* (2004) 26(7):441–3. doi: 10.1097/00043426-200407000-00008

18. Gassas A, Zaidman I, Schechter T, Doyle J. Beyond gastrointestinal graft-versus-host disease. a lesson to learn. *Pediatr Transplant* (2011) 15(7):E139–41. doi: 10.1111/j.1399-3046.2010.01327.x

19. Lieber J, Hauch H, Lang P, Handgretinger R, Blumenstock G, Seitz G, et al. Surgical management of stem cell transplantation-related complications in children. *Pediatr Transplant* (2012) 16(5):471–9. doi: 10.1111/j.1399-3046.2012.01708.x

20. Yoon JY, Kim H, Kang HJ, Park KD, Shin HY, Ahn HS. Chronic graft versus host disease with small bowel obstruction after unrelated hematopoietic stem cell transplantation in a patient with acute myeloid leukemia. *Korean J Hematol* (2012) 47(2):142–5. doi: 10.5045/kjh.2012.47.2.142

21. Grant CN, Nellis ED, Chahine AA. A case of small intestinal cast causing SBO in complicated intestinal graft-versus-host disease. *Pediatr Surg Int* (2014) 30 (6):685–8. doi: 10.1007/s00383-014-3515-9

22. Salomao M, Dorritie K, Mapara MY, Sepulveda A. Histopathology of graft-vs-Host disease of gastrointestinal tract and liver: An update. *Am J Clin Pathol* (2016) 145(5):591–603. doi: 10.1093/ajcp/aqw050

frontiers | Frontiers in Oncology

TYPE Case Report
PUBLISHED 13 September 2022
DOI 10.3389/fonc.2022.1012268

OPEN ACCESS

EDITED BY
Mario Tiribelli,
University of Udine, Italy

REVIEWED BY
Matteo Molica,
S. Eugenio, Rome, Italy
Ibrahim C. Haznedaroglu,
Hacettepe University Hospital, Turkey

*CORRESPONDENCE
Raffaella Pasquale
raffaella.pasquale@policlinico.mi.it

SPECIALTY SECTION
This article was submitted to Hematologic Malignancies, a section of the journal Frontiers in Oncology

RECEIVED 05 August 2022
ACCEPTED 22 August 2022
PUBLISHED 13 September 2022

CITATION
Pasquale R, Bucelli C, Bellani V, Zappa M, Iurlo A and Cattaneo D (2022) Case report: Pleural effusion during tyrosine-kinase inhibitor treatment in chronic myeloid leukemia: Not only a dasatinib-related adverse event.
Front. Oncol. 12:1012268.
doi: 10.3389/fonc.2022.1012268

Case report: Pleural effusion during tyrosine-kinase inhibitor treatment in chronic myeloid leukemia: Not only a dasatinib-related adverse event

Raffaella Pasquale[1]*, Cristina Bucelli[1], Valentina Bellani[1,2], Manuela Zappa[1], Alessandra Iurlo[1] and Daniele Cattaneo[1,2]

[1]Hematology Division, Foundation IRCCS Ca' Granda Ospedale Maggiore Policlinico, Milan, Italy, [2]Department of Oncology and Hemato-Oncology, University of Milan, Milan, Italy

The spectrum of TKI-related adverse events (AEs) is variable. Pleural effusion (PE) is a frequent AE attributable to dasatinib treatment, while it is only rarely associated with nilotinib. The pathogenetic mechanism leading to PE during nilotinib therapy is still unknown and its management has not yet been defined. To the best of our knowledge, only a limited number of similar case reports have already been reported in the literature so far. Here, we describe the case of a 41-year-old CML patient who developed PE during first-line nilotinib, successfully treated with steroids and nilotinib permanent discontinuation. We highlight the differences among our patient and the others, proposing therapeutic strategies to solve this rare but still possible AE, of which physicians should be aware.

KEYWORDS

adverse event, chronic myeloid leukemia, nilotinib, pleural effusion, tyrosine-kinase inhibitor

Introduction

BCR::ABL1-positive chronic myeloid leukemia (CML) is a myeloproliferative neoplasm with an incidence of 1-2 cases per 100.000 adults, which represents approximately 15% of newly diagnosed cases of leukemia in adults. This disease is characterized by a single reciprocal translocation between chromosomes 9 and 22, resulting in the formation of the Philadelphia (Ph) chromosome. *BCR::ABL1* fusion gene encodes a p210 protein (BCR::ABL1) with deregulated tyrosine kinase activity. Knowledge of this translocation was the basis for the development of drugs known as small molecule tyrosine-kinase inhibitors (TKIs) (1).

Currently, five TKIs are approved for CML treatment: original/generic imatinib, nilotinib, dasatinib, and bosutinib are recommended for both first and second or later lines, and ponatinib for second or subsequent lines, representing at the moment the only TKI that can be effectively used also in the case of the T315I point mutation. Each TKI has a distinct toxicity profile with most adverse effects (AEs) expressing 'off-target' toxicity of TKIs such as in the case of pleural effusion (PE) (Table 1) (2). This AE is reported only rarely during treatment with imatinib (1-2%) or bosutinib: considering in particular the latter TKI, PE has been reported in both the first and second or subsequent lines of treatment, with an incidence rate which varies from 1.9% to 6.1% (3–5). On the contrary, PE is a typical dasatinib-related AE with a higher incidence in patients showing baseline risk factors such as older age, history of pulmonary and/or hearth diseases, uncontrolled hypertension, hypercholesterolemia and/or autoimmune disorders (2, 6–9). In the DASISION trial, the incidence of PE at 5 years of follow-up was 28% in the dasatinib arm compared to 1% in the imatinib arm (10). A similar incidence of PE during dasatinib treatment was reported in real-life experiences, with a recurrence rate of 59.4% (11). In the ELN recommendations for the management of TKI-related AEs, recurrence of PE occurs in approximately 70% of the cases, thus representing the leading cause of dasatinib discontinuation (12).

As for nilotinib, it has a peculiar cardiovascular (CV) toxicity reported in 20% of patients, contraindicating its use in case of previous CV diseases, while other common side effects may include hypercholesterolemia and hyperglycemia (13). In the 10-year ENESTnd analysis, approximately 40% of nilotinib-treated patients experienced vascular events (14). In contrast, PE is rare during nilotinib: in the 6-month follow-up of an open-label Phase II clinical trial, only 1% of patients treated with nilotinib developed PE and all cases were Grade 1–2 in severity (15).

Case description

Here, we describe the case of a 41-year-old man with a history of esophageal achalasia affected by chronic phase (CP)-CML, high risk according to Sokal and low risk according to ELTS score. In July 2020 he was admitted to our hospital because of pain in left hypochondrium. Blood exams showed extreme leukocytosis [289.850/mmc with 5% of peripheral blood (PB) blasts] and thrombocytosis (903.000/mmc), associated with mild anemia and moderate splenomegaly (bipolar diameter of 17.5 cm at ultrasound examination). Given the diagnostic suspicion of a myeloid neoplasm, we searched for the *BCR::ABL1* p210 fusion transcript and the *JAK2*V617F mutation. The latter was not detected; on the contrary, a diagnosis of CML was made by means of qualitative PCR, which demonstrated the presence of a typical e14a2 (b3a2) *BCR::ABL1* p210 configuration. Bone marrow morphological analysis showed a CP-CML pattern, and cytogenetic studies revealed a 46,XY karyotype with the t(9;22)(q34;q11.2)[20/20], and no additional chromosomal abnormality. After previous debulking therapy with hydroxyurea, considering his young age, absence of any significant comorbidities and CML risk scores, first-line therapy with nilotinib 600 mg BID was started. After 3 months, the patient achieved an optimal response as defined in 2020 ELN recommendations (16), with a *BCR::ABL1* transcript level of 3.89% according to the International Scale (IS). However, at 6 months the patient complained about weight gain of 7 Kg and dyspnea on exertion, with no significant peripheral edema. An abdomen ultrasound showed neither hepato-splenomegaly nor ascites, while extensive bilateral PE with disventilative compression phenomena was collaterally detected. Chest X-ray confirmed this finding; even though there was no evidence of pericardial effusion in echocardiography, nilotinib was prudently discontinued. In addition, to exclude a concomitant lung infection, a CT scan was performed showing Grade 2 PE

TABLE 1 Adverse events during TKI therapy.

	IMATINIB	DASATINIB	NILOTINIB	BOSUTINIB	PONATINIB
Fluid retention	+++	–	–	+	–
Muscle cramps	+++	–	–	–	–
Fatigue	++	++	++	++	++
Rash	++	–	+++	+/-	+++
Nausea	++	+/-	+	+++	++
Diarrhea	++	–	–	+++	–
Increased pancreatic enzymes	–	–	++	+	+++
Hypertension	–	++	++	–	+++
Pleural effusion	–	+++	–	+	–
Arterial occlusive events	–	–	++	–	+++

+ means low frequent, ++ means intermediate frequent, +++ means high frequent, - means infrequent.

according to CTCAE v.4.0, and parenchymal thickening associated with shaded areas of peribronchiolar groundglass and signs of interstitial edema. Broncholwash excluded Aspergillus, respiratory viruses including SARS-CoV2, CMV-DNA, mycobacteria, Legionella pneumophila, Mycoplasma pneumoniae, Chlamydia pneumoniae, and Pneumocystis jirovecii infections. Interestingly, flow cytometry performed on broncholwash documented lymphoid cellularity for 11% distributed as follows: 66% T CD3+, CD4/CD8 = 1.6; 32% NK CD3-/CD16+; 2% B CD19+. No reactivity was instead detected for CD117 and/or CD34. Three days later, once an infectious etiology has been ruled out, steroid treatment with prednisone 25 mg QD was started. After 10 days a new chest X-ray was performed, documenting complete resolution of lung involvement together with an initial improvement in both dyspnea and body weight. Due to the severity of nilotinib toxicity and the optimal response already achieved, the drug was definitively discontinued and imatinib was started at the dosage of 400 mg QD. Imatinib therapy was well tolerated with no significant AE, in parallel with a progressive reduction in *BCR::ABL1* transcript level up to 0.7695% IS. However, after 6 months from imatinib start molecular evaluation showed a slight increase in *BCR::ABL1* transcript level till to 0.7924% IS, thus defining a warning response according to 2020 ELN recommendations (Figure 1) (16). Therefore, search for *ABL1* point mutations was performed, excluding any mutation known for conferring resistance to TKIs (including imatinib). Accordingly, considering the young age of the patient and the absence of any CV risk factors (score CHART 1%), third-line therapy with ponatinib at the dosage of 30 mg QD was started from September 2021. This new treatment did not lead to any significant toxicity and allowed the patient to achieve a progressive reduction in *BCR::ABL1* transcript level, till to the obtainment of a major molecular response (MMR).

Discussion

The most common non-hematological AEs of nilotinib are already well-known, including peripheral arterial occlusive diseases, followed by QTc interval prolongation, pancreatic enzymes, bilirubin and glucose blood levels elevation, gastrointestinal symptoms, pruritus, rash, headache, fatigue, arthralgia, nasopharyngitis, fever and night sweats; on the contrary, dasatinib has a peculiar pulmonary toxicity with a high incidence of PE estimated between 14% and 30% (17).

These AEs may be due to "off-target" effects; in particular, dasatinib-induced PE may be secondary to potent PDGFR-β inhibition in association with other possible mechanisms such as SRC inhibition (18). Indeed, it should be emphasized that PDGFR-β inhibition alone cannot cause serosal inflammation: for example, this AE is not associated with sorafenib which, however, also targets PDGFR-β.

One possible explanation is that dasatinib-related PE may be secondary to the cytotoxic T and NK cells expansion or to the action of other kinases (18). Indeed, PE is usually associated with dasatinib-induced non-malignant inflammatory lymphocytosis, which is often of NK type. The drug inhibits key kinases involved in the maturation of T and B lymphocytes, sometimes causing clonal expansion of large granular lymphocytes (LGL); the latter mainly involve NK or cytotoxic T cells, which can be detected in both PB and pleural fluid. This immunomodulatory effect, with lymphocytosis and clonal expansion of LGL, which are positively correlated with the onset of PE, has also been shown to be associated with a better response to treatment (19–21). As expected, patients with autoimmune diseases or previous immune-mediated AEs related to other TKIs are at increased risk of PE during dasatinib therapy (20, 21).

Regarding bosutinib, an orally active dual SRC and ABL1 TKI with minimal activity against PDGFR or c-KIT (22, 23), it

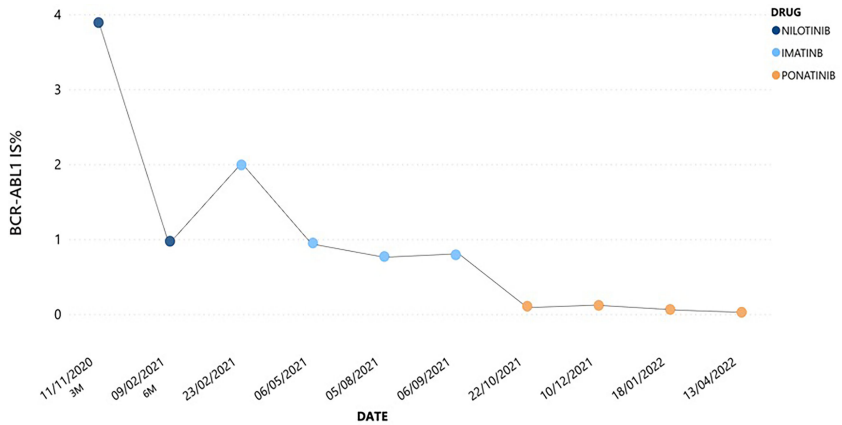

FIGURE 1
BCR::ABL1 transcript levels during the treatment with each TKIs.

has been more rarely associated with PE (24), both in real-life experiences (25) and in randomized clinical trials: more specifically, the incidence rate of PE ranged from 1.9% in the phase III BELA trial (26) to 6.1% in the phase IV BYOND study (4). Also considering the most recent BFORE trial, which compared bosutinib *vs.* imatinib for patients with newly diagnosed CP-CML, PE occurred in 5.2% of bosutinib-treated subjects, with the most promising risk factors for this AE, in addition to bosutinib treatment, represented by advanced age, smoking habit, and history of pulmonary events (5). The mechanism of action for bosutinib is unclear; however, major immunological changes during treatment do not seem to be the predominant factor (27).

Although the pathogenesis of dasatinib-induced PE has already been elucidated, the etiology of this AE during treatment with nilotinib has not yet been described (16).

Unlike dasatinib, nilotinib is a weaker PDGFR inhibitor, thus leading to a PE incidence of less than 1% in this setting (2), while inhibiting DDR1 phosphorylation expressed on bronchial epithelial cells in the same way as dasatinib (21, 28).

Information on this specific topic is rather scarce, being mainly represented by case reports. In 2012 Chakraborty et al. reported the case of a 66-year-old male CML patient with progressive dyspnea due to PE 2-3 months after initiation of second-line nilotinib treatment. Once cardiac and pulmonary etiologies were excluded, nilotinib was discontinued and the patient was treated for community-acquired pneumonia with only slight improvement. Despite the low incidence of PE with nilotinib, a short course of steroid was initiated with progressive resolution (29). In 2014 Teke et al. reported a similar case of a 68-year-old male patient with CML treated with nilotinib after imatinib discontinuation due to skin rash. After 5 years from nilotinib start, he developed PE associated with a suspicious lung mass. Catheter thoracostomy was performed detecting exudative pleural fluid enriched in lymphocytes, but without malignant cells. For suspected neoplasia, the patient underwent surgery with a preliminary diagnosis of pulmonary malignancy, then total decortication was performed, but the subsequent cytological and pathological evaluation was negative. After exclusion of any pulmonary and cardiac etiology, this serious complication was attributed to nilotinib and treatment with diuretic and steroid was started. After approximately 1.5–2 months on steroids, PE almost completely resolved and nilotinib was resumed at a reduced dose of 200 mg BID, then increased to 400 mg BID (30). More recently, Satoh et al. reported the case of a 23-year-old CML patient on nilotinib who had already suffered from PE during dasatinib a few years earlier. Due to respiratory failure, he was admitted to the ICU where endotracheal intubation and left chest drainage were performed. After extubation, the patient's condition gradually recovered and CML treatment was changed to ponatinib (31). Consequently, PE associated with nilotinib can be successfully treated in the same way as those related to dasatinib, including both steroids and diuretics, thus suggesting a similar pathogenetic mechanism, with inhibition of PDGFR among others. Despite the rarity of this AE, it should be considered once other possible cardiac or pulmonary causes have been ruled out. To support this specific etiology, Satoh et al. also looked for nilotinib in PB and pleural fluid and found it in both samples with a concentration of 927 and 2092 ng/mL, respectively, 60 hours after stopping nilotinib (31).

Consequently, as CML patients receiving TKIs can be expected to have a near-normal life expectancy and quality of life (QoL), individual characteristics of CML subjects, including comorbidities, lifestyle preferences, and TKI compliance, along with distinct 'off-target' TKI toxicities (which can lead to drug-related long-term morbidities) and molecular *BCR::ABL1* profile, are among the critical factors to consider when choosing the proper TKI, either as first, second or subsequent lines of therapy (2, 32–34).

All this considered, returning to our patient, it was decided not to restart nilotinib, even at half the standard dose, but to introduce imatinib for multiple reasons: firstly, unlike dasatinib and bosutinib, for which it is already known that they can be resumed at the same dose once the first episode of PE has resolved (12), no specific guidelines are now available for PE management during nilotinib. In support of this observation, Teke et al. resumed nilotinib at a reduced dose of 200 mg BID, then increased to 400 mg BID (30); on the contrary, Satoh et al. modified CML treatment in ponatinib (31). More important, given our patient's young age and the lack of information on the exact pathogenetic mechanisms of nilotinib-related PE, nilotinib continuation could have exposed the patient to long-term AEs, negatively impacting on his QoL and, consequently, on TKI compliance and efficacy.

Conclusions

In this case report, nilotinib was found to be the only possible cause of PE, after excluding other etiologies. However, unlike previous experiences, due to the severity of this rare AE and also considering the optimal response that the patient had already obtained, with the aim of preventing future PE recurrences, nilotinib was permanently discontinued with no new episodes during subsequent TKIs. In addition, some differences from other cases should be noted: firstly, this AE occurred during first-line therapy without concomitant medications. Overall, considering these experiences, it is not possible to hypothesize clear risk factors for nilotinib-induced PE with the sole exception of male sex. Indeed, differently from gender, older age does not seem to be prognostically relevant. The same was true for comorbidities: the first patient reported had coronary artery disease and hypertension, among others. The remaining patients, including the one described in this case report, had no significant comorbidities. Duration of treatment also does not appear to have an impact on PE risk as

patients developed this AE within 2-3 months to 5 years of starting nilotinib. An unmet clinical need may be the best management of this AE: apart from supportive care, i.e., steroids and diuretics, the real indication for switching from nilotinib to another TKI after a single episode of PE is still unclear. In our case, due to the severity of the clinical presentation of this rare AE and the progressive reduction in *BCR::ABL1* transcript level, in order to avoid new drug suspensions due to recurrences of PE, it was decided not to restart nilotinib, not even at a lower dosage, but to change the TKI by starting imatinib in the light of its safer toxicity profile. Unfortunately, due to an inadequate response to imatinib, once any known *ABL1* mutation was ruled out, given the patient's young age and the absence of any CV risk factors, third-line therapy with ponatinib was started at the dosage of 30 mg QD, allowing the patient to quickly achieve a MMR.

Data availability statement

The original contributions presented in the study are included in the article/supplementary material. Further inquiries can be directed to the corresponding author.

Ethics statement

Written informed consent was obtained from the individual(s) for the publication of any potentially identifiable images or data included in this article.

Author contributions

All authors listed have made a substantial, direct, and intellectual contribution to the work and approved it for publication.

Funding

This study was partially funded by Italian Ministry of Health - Current research IRCCS.

Conflict of interest

The authors declare that the research was conducted in the absence of any commercial or financial relationships that could be construed as a potential conflict of interest.

Publisher's note

References

1. Jabbour E, Kantarjian H. Chronic myeloid leukemia: 2022 update on diagnosis, therapy, and monitoring. *Am J Hematol* (2022) 97:1236–56. doi: 10.1002/ajh.26642

2. Iurlo A, Cattaneo D, Bucelli C, Breccia M. Dose optimization of tyrosine kinase inhibitors in chronic myeloid leukemia: A new therapeutic challenge. *J Clin Med* (2021) 10:515. doi: 10.3390/jcm10030515

3. Cortes JE, Kim DW, Kantarjian HM, Brümmendorf TH, Dyagil I, Griskevicius L, et al. Bosutinib versus imatinib in newly diagnosed chronic-phase chronic myeloid leukemia: results from the BELA trial. *J Clin Oncol* (2012) 30:3486–92. doi: 10.1200/JCO.2011.38.7522

4. Hochhaus A, Gambacorti-Passerini C, Abboud C, Gjertsen BT, Brümmendorf TH, Smith BD, et al. Bosutinib for pretreated patients with chronic phase chronic myeloid leukemia: primary results of the phase 4 BYOND study. *Leukemia* (2020) 34:2125–37. doi: 10.1038/s41375-020-0915-9

5. Brümmendorf TH, Cortes JE, Milojkovic D, Gambacorti-Passerini C, Clark RE, le Coutre P, et al. Bosutinib versus imatinib for newly diagnosed chronic phase chronic myeloid leukemia: final results from the BFORE trial. *Leukemia* (2022) 36:1825–33. doi: 10.1038/s41375-022-01589-y

6. Miura M. Therapeutic drug monitoring of imatinib, nilotinib, and dasatinib for patients with chronic myeloid leukemia. *Biol Pharm Bull* (2015) 38:645–54. doi: 10.1248/bpb.b15-00103

7. Suh KJ, Lee JY, Shin DY, Koh Y, Bang SM, Yoon SS, et al. Analysis of adverse events associated with dasatinib and nilotinib treatments in chronic-phase chronic myeloid leukemia patients outside clinical trials. *Int J Hematol* (2017) 106:229–39. doi: 10.1007/s12185-017-2225-1

8. Masiello D, Gorospe G, Yang AS. The occurrence and management of fluid retention associated with TKI therapy in CML, with a focus on dasatinib. *J Hematol Oncol* (2009) 2:46. doi: 10.1186/1756-8722-2-46

9. Cortes JE, Jimenez CA, Mauro MJ, Geyer A, Pinilla-Ibarz J, Smith BD. Pleural effusion in dasatinib-treated patients with chronic myeloid leukemia in chronic phase: Identification and management. *Clin Lymphoma. Myeloma Leuk* (2017) 17:78–82. doi: 10.1016/j.clml.2016.09.012

10. Cortes JE, Saglio G, Kantarjian HM, Baccarani M, Mayer J, Boqué C, et al. Final 5-year study results of DASISION: The dasatinib versus imatinib study in treatment-naive chronic myeloid leukemia patients trial. *J Clin Oncol* (2016) 34:2333–40. doi: 10.1200/JCO.2015.64.8899

11. Iurlo A, Galimberti S, Abruzzese S, Annunziata M, Bonifacio M, Latagliata R, et al. Pleural effusion and molecular response in dasatinib-treated chronic myeloid leukemia patients in a real-life Italian multicenter series. *Ann Hematol* (2018) 97:95–100. doi: 10.1007/s00277-017-3144-1

12. Steegmann JL, Baccarani M, Breccia M, Casado LF, García-Gutiérrez V, Hochhaus A, et al. European LeukemiaNet recommendations for the management and avoidance of adverse events of treatment in chronic myeloid leukaemia. *Leukemia* (2016) 30:1648–71. doi: 10.1038/leu.2016.104

13. Cortes J, Mauro M, Steegmann JL, Saglio G, Malhotra R, Ukropec JA, et al. Cardiovascular and pulmonary adverse events in patients treated with BCR-ABL inhibitors: Data from the FDA adverse event reporting system. *Am J Hematol* (2015) 90:E66–72. doi: 10.1002/ajh.23938

14. Kantarjian HM, Hughes TP, Larson RA, Kim DW, Issaragrisil S, le Coutre P, et al. Long-term outcomes with frontline nilotinib versus imatinib in newly

diagnosed chronic myeloid leukemia in chronic phase: ENESTnd 10-year analysis. *Leukemia* (2021) 35:440–53. doi: 10.1038/s41375-020-01111-2

15. Kantarjian HM, Giles F, Gattermann N, Bhalla K, Alimena G, Palandri F, et al. Nilotinib (formerly AMN107), a highly selective BCR-ABL tyrosine kinase inhibitor, is effective in patients with Philadelphia chromosome–positive chronic myelogenous leukemia in chronic phase following imatinib resistance and intolerance. *Blood* (2007) 110:3540–6. doi: 10.1182/blood-2007-03-080689

16. Hochhaus A, Baccarani M, Silver RT, Schiffer C, Apperley JF, Cervantes F, et al. European LeukemiaNet 2020 recommendations for treating chronic myeloid leukemia. *Leukemia* (2020) 34:966–84. doi: 10.1038/s41375-020-0776-2

17. *Highlights of prescribing information, FDA* . Available at: https://www.accessdata.fda.gov/drugsatfda_docs/label/2018/022068s029lbl.pdf (Accessed 17 Mar 2021).

18. Quintas-Cardama A, Kantarjian H, O'brien S, Borthakur G, Bruzzi J, Munden R, et al. Pleural effusion in patients with chronic myelogenous leukemia treated with dasatinib after imatinib failure. *J Clin Oncol* (2007) 25:3908–14. doi: 10.1200/JCO.2007.12.0329

19. de Lavallade H, Punnialingam S, Milojkovic D, Bua M, Khorashad JS, Gabriel IH, et al. Pleural effusions in patients with chronic myeloid leukaemia treated with dasatinib may have an immune-mediated pathogenesis. *Br J Haematol* (2008) 141:745–7. doi: 10.1111/j.1365-2141.2008.07108.x

20. Bergeron A, Rea D, Levy V, Picard C, Meignin V, Tamburini J, et al. Lung abnormalities after dasatinib treatment for chronic myeloid leukemia. *Am J Respir Crit Care Med* (2007) 176:814–8. doi: 10.1164/rccm.200705-715CR

21. Kelly K, Swords R, Mahalingam D, Padmanabhan S, Giles FJ. Serosal inflammation (pleural and pericardial effusions) related to tyrosine kinase inhibitors. *Targeting Oncol* (2009) 4:99–105. doi: 10.1007/s11523-009-0110-4

22. Puttini M, Coluccia AM, Boschelli F, Cleris L, Marchesi E, Donella-Deana A, et al. *In vitro* and *in vivo* activity of SKI-606, a novel src-abl inhibitor, against imatinib-resistant bcr-Abl1 neoplastic cells. *Cancer Res* (2006) 66:11314–22. doi: 10.1158/0008-5472.CAN-06-1199

23. Remsing Rix LL, Rix U, Colinge J, Hantschel O, Bennett KL, Stranzl T, et al. Global target profile of the kinase inhibitor bosutinib in primary chronic myeloid leukemia cells. *Leukemia* (2009) 23:477–85. doi: 10.1038/leu.2008.334

24. Cortes JE, Kantarjian HM, Mauro MJ, An F, Nick S, Leip E, et al. Long-term cardiac, vascular, hypertension, and effusion safety of bosutinib in patients with Philadelphia chromosome-positive leukemia resistant or intolerant to prior therapy. *Eur J Haematol* (2021) 106:808–20. doi: 10.1111/ejh.13608

25. Tiribelli M, Abruzzese E, Capodanno I, Sorà F, Trabacchi E, Iurlo A, et al. Efficacy and safety of bosutinib in chronic phase CML patients developing pleural effusion under dasatinib therapy. *Ann Hematol* (2019) 98:2609–11. doi: 10.1007/s00277-019-03802-y

26. Gambacorti-Passerini C, Cortes JE, Lipton JH, Dmoszynska A, Wong RS, Rossiev V, et al. Safety of bosutinib versus imatinib in the phase 3 BELA trial in newly diagnosed chronic phase chronic myeloid leukemia. *Am J Hematol* (2014) 89:947–53. doi: 10.1002/ajh.23788

27. Kreutzman A, Yadav B, Brummendorf TH, Gjertsen BT, Lee MH, Janssen J, et al. Immunological monitoring of newly diagnosed CML patients treated with bosutinib or imatinib first-line. *Oncoimmunology* (2019) 8:e1638210. doi: 10.1080/2162402X.2019.1638210

28. Weatherald J, Bondeelle L, Chaumais MC, Guignabert C, Savale L, Jaïs X, et al. Pulmonary complications of bcr-abl tyrosine kinase inhibitors. *Eur Respir J* (2020) 56:2000279. doi: 10.1183/13993003.00279-2020

29. Chakraborty K, Bossaer JB, Patel R, Krishnan K. Successful treatment of nilotinib-induced pleural effusion with prednisone. *J Oncol Pharm Pract* (2012) 19:175–7. doi: 10.1177/1078155212447530

30. Teke H.Ü, Akay OM, Şahin DG, Karagülle M, Gündüz E, Andjç N. Pleural effusion: a rare side effect of nilotinib–a case report. *Case Rep Med* (2014) 2014:203939. doi: 10.1155/2014/203939

31. Satoh K, Morisawa S, Okuyama M, Nakae H. Severe pleural effusion associated with nilotinib for chronic myeloid leukemia: cross-intollerance with tyrosin kinase inhibitors. *BMJ. Case Rep* (2021) 14:e243671. doi: 10.1136/bcr-2021-243671

32. Padula WV, Larson RA, Dusetzina SB, Apperley JF, Hehlmann R, Baccarani M, et al. Cost-effectiveness of tyrosine kinase inhibitor treatment strategies for chronic myeloid leukemia in chronic phase after generic entry of imatinib in the united states. *J Natl Cancer Inst* (2016) 108:djw003. doi: 10.1093/jnci/djw003

33. Yamamoto C, Nakashima H, Ikeda T, Kawaguchi S-I, Toda Y, Ito S, et al. Analysis of the cost-effectiveness of treatment strategies for CML with incorporation of treatment discontinuation. *Blood Adv* (2019) 3:3266–77. doi: 10.1182/bloodadvances.2019000745

34. Ciftciler R, Haznedaroglu IC. Tailored tyrosine kinase inhibitor (TKI) treatment of chronic myeloid leukemia (CML) based on current evidence. *Eur Rev Med Pharmacol Sci* (2021) 25:7787–98. doi: 10.26355/eurrev_202112_27625

frontiers | Frontiers in Oncology

TYPE Case Report
PUBLISHED 15 September 2022
DOI 10.3389/fonc.2022.1011023

OPEN ACCESS

EDITED BY
Osamu Imataki,
Kagawa University, Japan

REVIEWED BY
Chunling Wang,
Nanjing Medical University, China
Hong-Hu Zhu,
Zhejiang University, China

*CORRESPONDENCE
Lunhua Chen
clh68215@sina.com

SPECIALTY SECTION
This article was submitted to Hematologic Malignancies, a section of the journal Frontiers in Oncology

RECEIVED 03 August 2022
ACCEPTED 29 August 2022
PUBLISHED 15 September 2022

CITATION
Zhao J, Wang W, Yan L, Chen X, Li W, Li W, Chen T and Chen L (2022) Case Report: A rare case of acute myeloid leukemia with CPSF6–RARG fusion resembling acute promyelocytic leukemia. *Front. Oncol.* 12:1011023. doi: 10.3389/fonc.2022.1011023

Case report: A rare case of acute myeloid leukemia with CPSF6–RARG fusion resembling acute promyelocytic leukemia

Junmei Zhao[1], Wentao Wang[2], Li Yan[1], Xi Chen[1], Wen Li[1], Wanying Li[1], Tingting Chen[1] and Lunhua Chen[1]*

[1]Department of Hematology, Wuhan University Renmin Hospital, Wuhan, China, [2]Department of Infectious Diseases, Tongji Hospital, Tongji Medical College, Huazhong University of Science and Technology, Wuhan, China

Retinoic acid receptor gamma (*RARG*) gene rearrangement has been reported in several acute myeloid leukemia (AML) patients. They resemble classical acute promyelocytic leukemia (APL) patients in clinical features, morphology, and immunophenotype but do not carry the *promyelocytic leukemia* (*PML*)–*RARA* fusion gene. Importantly, almost all these APL-like AML patients show resistance to all-trans retinoic acid (ATRA), and no effective treatment is recommended for them. Here, we identified a case of AML resembling APL in clinical presentation and experimental findings carrying a rare cleavage and polyadenylation-specific factor 6 (CPSF6)-RARG fusion gene. The patient was insensitive to ATRA and ATO but responded well to homoharringtonine and cytarabine.

KEYWORDS

acute myeloid leukemia, CPSF6-RARG fusion, acute promyelocytic leukemia, resistance to ATRA, homoharringtonine

Introduction

Acute promyelocytic leukemia (APL) is a distinct subtype of acute myeloid leukemia (AML) characterized by abnormal accumulation of promyelocytes in bone marrow and coagulation abnormality. The hallmark of classic APL is the fusion gene and chimeric protein of promyelocytic leukemia and retinoic acid receptor-α (PML-RARA) caused by chromosome translocation t(15;17)(q24;q21) (1). PML-RARA oncoprotein inhibits the transcriptional activity of the *RARA* gene and disrupts the homeostatic function of PML, thus resulting in the proliferation of myeloid progenitors and maturation arrest at the promyelocytic stage (2). Importantly, the differentiation induction therapy with all-trans retinoic acid (ATRA) and arsenic trioxide (ATO) has strikingly improved the clinical outcome of classic APL patients. However, the *PML–RARA* fusion gene is absent in <2%

APL patients, which is classified into variant APL or AML resembling APL (3). Among these, RARA rearrangement is relatively common with *PLZF-RARA* accounting for 50% variant APL. Retinoic acid receptor beta (RARB) and retinoic acid receptor gamma (RARG) rearrangements have also been demonstrated to generate AML resembling APL (4–6). The genetic heterogeneity, leukemogenesis mechanism, and optimal treatment regimen of these subtypes of AML remained to be elucidated, which pose a challenge to the recognition and treatment of variant APL. Herein, we identified a rare case of AML resembling APL with the *CPSF6-RARG* fusion gene who was resistant to ATRA and ATO but sensitive to homoharringtonine and cytarabine (HA) treatment.

Case description

The patient was a 28-year-old man with no significant past medical history who presented with a 1-week history of petechiae. His blood count showed a white blood cell (WBC) count of 29.21 × 10^9/l, hemoglobin of 69 g/dl, and a platelet count of 103 × 10^9/l. Fibrinogen and D-dimer levels were 2.99 g/l and 44.22 mg/ml, respectively. PT and APTT were 12 and 25.9 s, respectively. Bone marrow (BM) smear showed the hypercellularity with 41% predominantly abnormal hypergranular promyelocytes without Auer rods (Figure 1A). Cytochemical staining revealed that the abnormal promyelocytes had strong reactivity to myeloperoxidase (MPO). Flow cytometric immunophenotyping showed that the blasts were positive for CD13, CD33, CD117, CD38 (partial), and CD64 (partial) but negative for HLA-DR, CD34, CD14, CD56, CD7, CD10, CD5, CD2, CD3, CD4, CD8, CD19, CD20, and CD138. Thus, the diagnostic impression of APL was initially established.

However, multiplex RT-qPCR showed that all of the myeloid-related fusion transcripts were negative, including *PML-RARα*, *FIP1L1-RARα*, *PLZF-RARα*, *NPM-RARA*, *NUMA-RARα*, *STAT5-RARα*, and *PRKAR1A-RARα*. Fluorescence *in situ* hybridization also failed to detect the *PML-RARA* fusion gene (Figure 1B). Cytogenetic studies did not detect the translocation of t (15;17) (q24;q21) (Figure 1C). Whole-genome sequencing (WGS) identified *K-RAS* mutations in this patient.

The patient was immediately treated with all-trans retinoic acid (ATRA), and arsenic trioxide (ATO) was started in addition to ATRA on day 2. After 28 days of treatment, there were still 39% abnormal promyelocytes in BM, indicating that the patient was resistant to ATRA and ATO. Then, one course of DA regimen (DNR 60 mg/m^2, d1–3, Ara-C 100 mg/m^2, d1–7) was used as induction therapy. Unfortunately, there was still no response. The patient received HA chemotherapy regimen (homoharringtonine 4 mg/day, d1–7, Ara-C 100 mg/m^2, d1–7) as reinduction therapy. The BM smear showed that the patient had achieved complete remission. Then, six courses of consolidation chemotherapy regimens were given as follows: 2 cycles of decitabine + CAG regimen (decitabine 20 mg/m^2, d1–5; aclarubicin 10 mg/m^2, d3–6; Ara-C 10 mg/m^2/q12h, d3–14; G-CSF 200 μg/day until WBC count was >20 × 109/l), 2 cycles of the HA regimen (homoharringtonine 4 mg/day, d1–7, Ara-C 100 mg/m^2, d1–7), and 2 cycles of the middle-dose cytarabine (2 g/m^2/q12h d1–3). Up to now, the patient remains alive and was leukemia-free at follow-up.

In order to identify the driver fusion gene, transcriptome sequencing (RNA-seq) of bone marrow cells was performed. After analyzing the data, the patient was shown to have a rare fusion transcript within chromosome 12, in which the exon 8 of *CPSF6* was fused to the exon 4 of *RARG* (Figures 2A, B). To confirm the fusion, RT-PCR was performed using cDNA and the following pair of primers was used: forward (at *CPSF6* exon 8), 5′-AGATTGCCTTCATGGAATTG-3′ and reverse (at *RARG* exon 4), 5′-GGTAGCCAGAGGACTTGT-3′. The PCR product was detected and analyzed by electrophoresis and Sanger sequencing, respectively (Figure 2C).

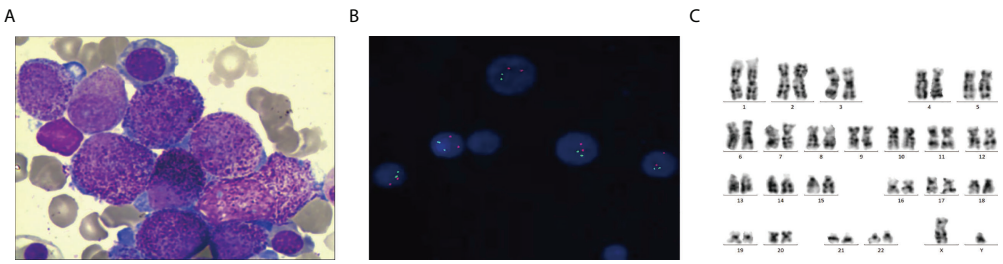

FIGURE 1
Morphology, FISH, and karyotyping analysis of the patient's AML bone marrow (BM) sample. **(A)** Promyelocytes with hypergranulated cytoplasm and invaginated nuclei (Wright–Giemsa-stained BM smear, 1,000× magnification). **(B)** *PML–RARA* fusion signals were not detected by Interphase FISH using *PML– RARA* dual-color, dual-fusion translocation probes. **(C)** G-banded karyotype showing 46, XY [20].

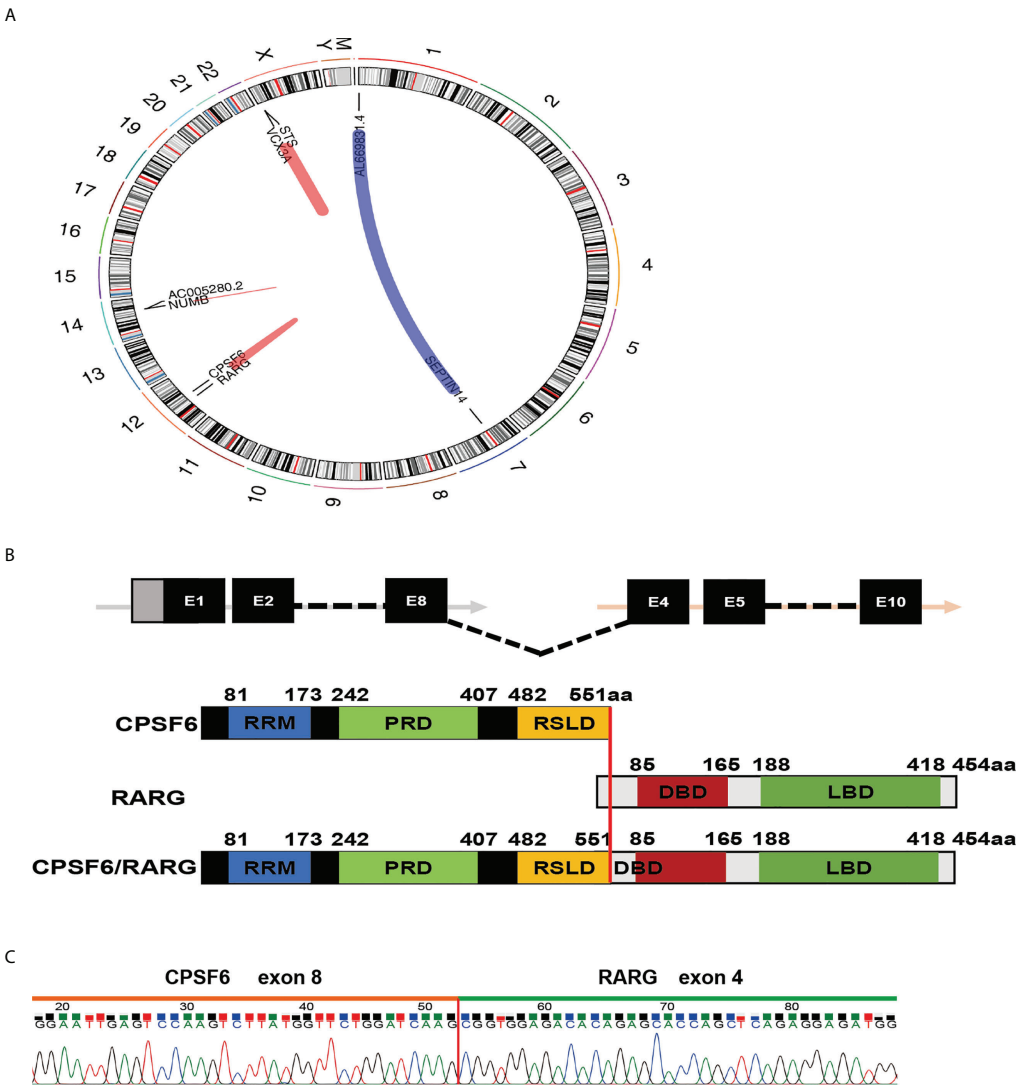

FIGURE 2
Molecular analysis of the CPSF6-RARG fusion. **(A)** Four fusion genes were found by analyzing RNA-sequencing data of the patient's BM sample using deFuse inspector software. **(B)** Schematic diagram of *CPSF6, RARG, CPSF6–RARG* fusion transcript, and the fusion protein of the patient. The breakpoint is indicated by a red line. **(C)** Sanger sequencing of the PCR product analysis of the *CPSF6–RARG* fusion transcript junctions revealed a fusion between exon 8 of the *CPSF6* gene and exon 4 of the *RARG* gene.

Discussion

Since 2018, six cases with *CPSF6-RARG* and one case with *RARG–CPSF6* have been reported (6–10). In previous studies, the fusing point was located at exon 4 of *CPSF6*; exon 1, exon 2, and exon 4 of *RARG*; exon 5 of *CPSF6*; exon 1 of *RARG*; intron 9 of *RARG*; and exon 6 of *CPSF6*, respectively. The present case provided the different transcript with *CPSF6* exon 8 fusing to *RARG* exon 4, further suggesting that the transcripts are highly varied.

All of the patients received ATRA therapy, but unfortunately, none showed any response to ATRA. In agreement with this, other RARG rearrangements also showed resistance to ATRA in clinic. Of note, *NUP98-RARG*-transformed murine HSPCs were sensitive to ATRA *ex vivo*. Additional chemotherapy drugs including cytarabine and/or anthracyclines were routinely recommended for high-risk APL patients in the course of induction therapy, but the regimen failed. Several patients received the salvage therapy after ineffective therapeutic regimen containing ATRA, and two patients showed a good treatment response. One patient achieved morphologic remission after a course of DA chemotherapy and received two courses of high-dose cytarabine therapy and two courses of standard 7 + 3 chemotherapy afterward and remained with complete remission until the last follow-up. Another patient underwent a course of HA treatment and achieved complete remission. In line

with previous reports with *CPSF6-RARG*/*RARG-CPSF6*, the present case showed similar clinical manifestations, cell morphology, and immunophenotype with APL. The patient was resistant to combined treatment including ATRA, ATO, and DA chemotherapy but showed a very good response to HA chemotherapy.

Cleavage and polyadenylation specificity factor 6 (CPSF6) interacts with CPSF5 through its RNA recognition motif to enhance RNA binding and direct RNA looping. Breast cancer cells hijacked CPSF6 to promote A-to-I RNA editing for driving tumorigenesis and contributing to tumor heterogeneity (11). However, the role of CPSF6 in leukemia remained to be figured out. Another fusion protein harboring CPSF6 is CPSF6-FGFR1, which has been reported in a patient with myeloproliferative syndrome (12).

RARG consists of a DNA-binding domain (also named as retinoic acid response elements) and a ligand-binding domain (LBD), which share 90% homology with RARA and RARB. Unlike RARA-inducing granulocytic differentiation, RARG primarily maintains a balance between the self-renewal and differentiation of hematopoietic stem cells (HSCs) (12). Loss of RARG leads to the reduction in long-term repopulating HSCs but an increase in more committed hematopoietic progenitors in BM. Walkley et al. also found that RARG was very critical for maintaining a normal BM microenvironment, and *RARG*$^{-/-}$ mice displayed the abnormal accumulation of granulocyte/macrophage progenitors and granulocytes in bone marrow and peripheral blood, which rapidly developed into myeloproliferative syndrome (13). In addition to *CPSF6-RARG*/*RARG–CPSF6*, four other *RARG* rearrangements, namely, *NUP98-RARG*, *PML-RARG*, *NPM1-RARG-NPM1*, and *HNRNPC-RARG*, have also been identified in these AML-resembling patients. *In vitro* and *in vivo* studies had already demonstrated the oncogenic potential of *PML-RARG* (14). However, almost all of these AML subtypes with *RARG* gene rearrangements do not respond to treatment with ATRA and ATO and there is no unified expert consensus at present. Daunorubicin, idarubicin, homoharringtonine, and cytarabine as the induction chemotherapy regimen may work. Allogeneic hematopoietic stem cell transplantation (allo-HSCT) may be a preferred post-remission therapy in these special types of AML. Considering that the patient was very young, we have recommended allo-HSCT several times, but the patient refused due to economical load.

In addition to *CPSF6–RARG* fusion, *K-NAS* mutation was also identified by WGS in the present patient. *K-NAS* mutation leads to the continuous activation of Ras protein and may cooperate with CPSF6–RARG to participate in tumorigenesis (15). Among the previous reports (six cases with *CPSF6-RARG* and one case with *RARG–CPSF6*), *WT1* mutation occurred in four of seven patients, implying that the frequency of *WT1* mutation was higher than other mutation. *K-NAS* mutation was identified in two cases, and *DNMT3A*, *EZH2*, *NEAT1*, *BMPR1A* mutation was identified in one case, respectively. *WT1* plays an important role in hematopoiesis, and its mutation may influence the sensitivity to ATRA (16). *EZH2* is a histone H3K27 methyltransferase involved in epigenetic gene silencing (17). It has been reported that one patient exhibited an APL phenotype without a fusion gene but had *EZH2*-D185H mutation detected by targeted next-generation sequencing (18). The alteration of EZH2 function may be responsible for APL-like phenotype by dysregulation of the RARA and RARG genes. These additional gene mutations were also critical in the pathogenesis of APL and ATRA resistance. However, it is confusing that although *FLT3*-ITD is the most common mutation in APL patients, accounting for 35%, this mutation has not been found in *CPSF6–RARG* fusion AML patients so far.

In conclusion, we identified a case of AML resembling APL with CPSF6-RARG transcript who was resistant to ATRA and ATO but sensitive to HA treatment. Our findings imply that the HA regimen may be effective for patients with RARG rearrangements. Exploring the mechanism of ATRA resistance and finding more effective drugs are the research focus for the future.

Data availability statement

The datasets presented in this article are not readily available because of ethical/privacy restrictions. Requests to access the datasets should be directed to the corresponding author.

Ethics statement

This study was reviewed and approved by Renmin Hospital of Wuhan University Institutional Review Board. The patients/participants provided their written informed consent to participate in this study.

Author contributions

JZ and WW designed the study, collected the material, analyzed the data, and wrote the manuscript. LY, WL, WYL, TC and XC collected the clinical samples and analyzed data. LC participated in analyzing the data and writing the manuscript. All authors contributed to the article and approved the submitted version.

Funding

This work was supported by the grants from the National Natural Science Foundation of China (82000109 and 81900168).

Conflict of interest

The authors declare that the research was conducted in the absence of any commercial or financial relationships that could be construed as a potential conflict of interest.

Publisher's note

References

1. Lo-Coco F, Avvisati G, Vignetti M, Thiede C, Orlando SM, Iacobelli S, et al. Retinoic acid and arsenic trioxide for acute promyelocytic leukemia. *N Engl J Med* (2013) 369(2):111–21. doi: 10.1056/NEJMoa1300874

2. Noguera NI, Catalano G, Banella C, Divona M, Faraoni I, Ottone T, et al. Acute promyelocytic leukemia: Update on the mechanisms of leukemogenesis, resistance and on innovative treatment strategies. *Cancers* (2019) 11(10):1591. doi: 10.3390/cancers11101591

3. Zhang X, Sun J, Yu W, Jin J. Current views on the genetic landscape and management of variant acute promyelocytic leukemia. *Biomark Res* (2021) 9(1):33. doi: 10.1186/s40364-021-00284-x

4. Osumi T, Tsujimoto SI, Tamura M, Uchiyama M, Nakabayashi K, Okamura K, et al. Recurrent RARB translocations in acute promyelocytic leukemia lacking RARA translocation. *Cancer Res* (2018) 78(16):4452–8. doi: 10.1158/0008-5472.can-18-0840

5. Ha JS, Do YR, Ki CS, Lee C, Kim DH, Lee W, et al. Identification of a novel PML-RARG fusion in acute promyelocytic leukemia. *Leukemia* (2017) 31(9):1992–5. doi: 10.1038/leu.2017.167

6. Liu T, Wen L, Yuan H, Wang Y, Yao L, Xu Y, et al. Identification of novel recurrent CPSF6-RARG fusions in acute myeloid leukemia resembling acute promyelocytic leukemia. *Blood* (2018) 131(16):1870–3. doi: 10.1182/blood-2017-11-818716

7. Zhang Z, Jiang M, Borthakur G, Luan S, Huang X, Tang G, et al. Acute myeloid leukemia with a novel CPSF6-RARG variant is sensitive to homoharringtonine and cytarabine chemotherapy. *Am J Hematol* (2020) 95(2): E48–e51. doi: 10.1002/ajh.25689

8. Han X, Jin C, Zheng G, Li Y, Wang Y, Zhang E, et al. Acute myeloid leukemia with CPSF6-RARG fusion resembling acute promyelocytic leukemia with extramedullary infiltration. *Ther Adv Hematol* (2021) 12:2040620720976984. doi: 10.1177/2040620720976984

9. Qin YZ, Huang XJ, Zhu HH. Identification of a novel CPSF6-RARG fusion transcript in acute myeloid leukemia resembling acute promyelocytic leukemia. *Leukemia* (2018) 32(10):2285–7. doi: 10.1038/s41375-018-0095-z

10. Miller CA, Tricarico C, Skidmore ZL, Uy GL, Lee YS, Hassan A, et al. A case of acute myeloid leukemia with promyelocytic features characterized by expression of a novel RARG-CPSF6 fusion. *Blood Adv* (2018) 2(11):1295–9. doi: 10.1182/bloodadvances.2017014183

11. Binothman N, Hachim IY, Lebrun JJ, Ali S. CPSF6 is a clinically relevant breast cancer vulnerability target: Role of CPSF6 in breast cancer. *EBioMedicine* (2017) 21:65–78. doi: 10.1016/j.ebiom.2017.06.023

12. Hidalgo-Curtis C, Chase A, Drachenberg M, Roberts MW, Finkelstein JZ, Mould S, et al. The t(1;9)(p34;q34) and t(8;12)(p11;q15) fuse pre-mRNA processing proteins SFPQ (PSF) and CPSF6 to ABL and FGFR1. *Genes Chromosomes Cancer* (2008) 47(5):379–85. doi: 10.1002/gcc.20541

13. Walkley CR, Olsen GH, Dworkin S, Fabb SA, Swann J, McArthur GA, et al. A microenvironment-induced myeloproliferative syndrome caused by retinoic acid receptor gamma deficiency. *Cell* (2007) 129(6):1097–110. doi: 10.1016/j.cell.2007.05.014

14. Marinelli A, Bossi D, Pelicci PG, Minucci S. A redundant oncogenic potential of the retinoic receptor (RAR) alpha, beta and gamma isoforms in acute promyelocytic leukemia. *Leukemia* (2007) 21(4):647–50. doi: 10.1038/sj.leu.2404572

15. Kim E, Ilic N, Shrestha Y, Zou L, Kamburov A, Zhu C, et al. Systematic functional interrogation of rare cancer variants identifies oncogenic alleles. *Cancer Discov* (2016) 6(7):714–26. doi: 10.1158/2159-8290.cd-16-0160

16. Conserva MR, Redavid I, Anelli L, Zagaria A, Specchia G, Albano F. RARG gene dysregulation in acute myeloid leukemia. *Front Mol Biosci* (2019) 6:114. doi: 10.3389/fmolb.2019.00114

17. Sashida G, Iwama A. Multifaceted role of the polycomb-group gene EZH2 in hematological malignancies. *Int J Hematol* (2017) 105(1):23–30. doi: 10.1007/s12185-016-2124-x

18. Coccaro N, Zagaria A, Orsini P, Anelli L, Tota G, Casieri P, et al. RARA and RARG gene downregulation associated with EZH2 mutation in acute promyelocytic-like morphology leukemia. *Hum Pathol* (2018) 80:82–6. doi: 10.1016/j.humpath.2018.02.023

frontiers | Frontiers in Oncology

TYPE Case Report
PUBLISHED 15 September 2022
DOI 10.3389/fonc.2022.970188

OPEN ACCESS

EDITED BY
Francesco Onida,
IRCCS Ca 'Granda Foundation Maggiore Policlinico Hospital, Italy

REVIEWED BY
Gioacchino Andrea Rotulo,
Bambino Gesù Children's Hospital (IRCCS), Italy
Arash Heidari,
Kern Medical Center, United States

*CORRESPONDENCE
Giuseppe Sconocchia
giuseppe.sconocchia@ift.cnr.it

SPECIALTY SECTION
This article was submitted to Hematologic Malignancies, a section of the journal Frontiers in Oncology

RECEIVED 15 June 2022
ACCEPTED 19 August 2022
PUBLISHED 15 September 2022

CITATION
Pasqualone G, Buzzatti E, Palmieri R, Savi A, Pascale MR, Borsellino B, Guarnera L, Buccisano F, Voso MT, Maurillo L, Sconocchia G, Venditti A and Del Principe MI (2022) Case report: A *Saprochaete clavata* (*Magnusiomyces clavatus*) severe infection effectively treated with granulocyte transfusion in a young patient with myeloid sarcoma. *Front. Oncol.* 12:970188. doi: 10.3389/fonc.2022.970188

Case report: A *Saprochaete clavata* (*Magnusiomyces clavatus*) severe infection effectively treated with granulocyte transfusion in a young patient with myeloid sarcoma

Gianmario Pasqualone[1], Elisa Buzzatti[1], Raffaele Palmieri[1], Arianna Savi[1], Maria Rosaria Pascale[1], Beatrice Borsellino[1], Luca Guarnera[1], Francesco Buccisano[1], Maria Teresa Voso[1], Luca Maurillo[1], Giuseppe Sconocchia[2]*, Adriano Venditti[1] and Maria Ilaria Del Principe[1]

[1]Hematology, Department of Biomedicine and Prevention, Università degli studi di Roma Tor Vergata, Rome, Italy, [2]Institute of Translational Pharmacology, Department of Biomedical Sciences, National Research Council (CNR), Rome, Italy

Myeloid sarcoma is a hematologic malignancy consisting of extramedullary tissue involvement by myeloid blasts, usually considered as acute myeloid leukemia and treated accordingly. The disease itself, together with chemotherapy and disease-associated factors, may have an impact in increasing the risk of developing severe and frequently life-threatening infections. Herein, we describe the case of a patient with a right breast skin lesion, histologically diagnosed myeloid sarcoma, who developed a severe disseminated fungal infection by *Saprochaete clavata* (*Magnusiomyces clavatus*), during the first consolidation course of chemotherapy. Despite maximum antifungal therapy, the infection progressed and the fungus continued to be isolated until granulocyte transfusion therapy was initiated. Our experience suggests that patients with profound and long-lasting neutropenia could benefit from granulocyte transfusions as additional therapy in severe fungal infections resistant to broad-spectrum antimicrobial therapy.

KEYWORDS

acute myeloid leukemia, invasive fungal infection, granulocyte transfusion, *Saprochaeta clavata*, *Magnusiomyces clavatus*, case report, myeloid sarcoma (MS)

Introduction

Acute myeloid leukemia (AML) is a malignant disorder caused by clonal expansion of hematopoietic cells abnormally or poorly differentiated, called blasts. These cells infiltrate and accumulate preferentially in the bone marrow (BM), with consequent impairment of normal hemopoiesis (1). AML categorization and classification rely on morphologic, immunophenotypic, cytogenetic, and molecular genetic analyses (2, 3). AML could be preceded or concurrent with an extramedullary localization of blasts, a condition defined as myeloid sarcoma (MS) (4).

MS is a rare malignant disease that could occur virtually in any anatomical site, most frequently in connective/soft tissues, gastrointestinal (GI) tract, spleen, and lymph nodes. Sanctuary sites, such as the central nervous system (CNS) and testis, could also be affected (4–6). Diagnosis can be challenging, and misdiagnosis is frequently reported: imaging (mostly computed tomography [CT], magnetic resonance imaging, F^{18}-fluorodeoxyglucose-positron-emission tomography [FDG-PET]) and most importantly immunohistochemical/cytochemical analysis are needed to confirm the clinical suspicion (5, 7). Therapeutic strategies in MS should consider tumor size and site, performance status (PS), patient's age, and comorbidities. To date, systemic chemotherapy (CHT) is considered the backbone of treatment.

Although data regarding the prognosis of MS in the setting of AML are limited and somewhat conflicting, it seems that the presence of extramedullary localization does not represent an independent prognostic feature of the underlying AML, so the outcome depends on the prognostic stratification of AML itself (4, 8, 9).

Patients diagnosed with hematological malignancies are subjects vulnerable to common and opportunistic infections because of several risk factors: besides the underlying malignancy, therapy-related immunosuppression, neutropenia, presence of central venous catheter (CVC), and the use of broad-spectrum antimicrobial therapy are additional elements to be considered. In such a context, invasive fungal infections (IFIs) represent a serious and life-threatening complication, requiring a timely identification and treatment.

Saprochaete clavata, formerly *Geotrichum clavatum* (often misidentified for *Saprochaete capitata*, formerly *Geotrichum capitatum/Magnusiomyces capitatus*, because of their close similarity), has recently emerged as a new threat among hemato-oncological patients with reported mortality rates up to 80%, with AML identified as the most common underlying malignancy (10–12). *S. clavata* infection is almost invariably identified in advanced phases of dissemination (positive blood cultures or organ infiltration). Despite that the site through which this pathogen enters the bloodstream is frequently unclear, respiratory or GI systems are likely to be preferential sites of colonization. Consequently, CHT-induced damage of the mucosal barrier promotes pathogen translocation (10, 12). There is no standard treatment for *S. clavata*, and no standardized European Committee on Antimicrobial Susceptibility Testing antifungal breakpoints are determined for this pathogen: therapy should be based on expert opinion and accurate interpretation of susceptibility tests. Antifungal combination therapy could represent an effective choice, but hematological recovery appears critical to enhance and accelerate clinical resolution (12, 13).

In this regard, cases of prolonged neutropenia and infection by multidrug-resistant or hard-to-treat pathogens might benefit from granulocyte transfusion (GTX). GTX is not a new therapeutic approach, but the interest around this strategy has consistently diminished due to the availability of new antibiotic and antifungal therapies (13, 14). However, several reports and case series have pointed out the effectiveness of this procedure, especially in situations of delayed neutrophil count recovery and failure of antimicrobial therapies (15, 16).

Here, we describe the case of a patient diagnosed with MS, who underwent systemic CHT and developed a severe IFI during the post-consolidation neutropenic phase. Despite maximal antifungal therapy, *S. clavata* continued to be isolated from blood cultures with progressive worsening of the patient's conditions. The introduction of GTX promptly reverted the clinical picture, with resolution of the infection.

Case description

The patient is a 24-year-old woman, who was referred to primary care in November 2020 because of a painless, indurated, purplish skin plaque of the right-side breast. Past medical history was uneventful, and she was only on oral contraceptives.

In May 2021, a punch biopsy of the lesion was diagnostic for MS, with immunohistochemistry positive for CD117, cKit, CD4, CD56, CD33, PGM1, and Bcl2 and negative for CD34, MPO, CD20, CD3, CD23, Tdt, and CD79a.

In June 2021, she was referred to our Institution and underwent an FDG PET-CT scan showing a slight and unspecific bilateral and symmetric nasopharyngeal uptake in addition to the known skin lesion. Thus, a biopsy of the nasopharynx was collected for diagnostic purposes. No fatigue, fever, night sweats, weight loss, or other constitutional symptoms were reported. Complete blood count (CBC) showed unremarkable results, and BM aspiration (BMA) showed a negative result for leukemic involvement, with a normal karyotype identified upon cytogenetic analysis. Lactate dehydrogenase and hepatic, renal, and coagulation profiles showed normal results. To relieve emerging pain and swelling, local radiotherapy of the breast skin lesion was started (24 Gy over 12 fractions).

In July 2021, histological examination of the nasopharyngeal biopsy confirmed the MS localization expressing the same

immunohistochemical profile of the primary breast lesion. In August 2021, the patient was hospitalized to proceed with restaging and to undergo systemic CHT.

A BM reassessment showed a 60% blast infiltrate with a CD45+, CD34+, CD33+, CD117+, CD64+, anti-HLA-DR +, CD4+, and CD56+ immunophenotypic profile. The cytogenetic study revealed the appearance of chromosome 4 trisomy (47, XX,+4 in 10/15 analyzed metaphases). The analysis of common fusion genes and mutations (BCR/ABL, RUNX1/RUNXT1, DEK/NUP214, CBFβ/MYH11, FLT3-ITD/TKD, and NPM1) showed a negative result for molecular abnormalities. The morphologic and phenotypic examination of cerebral spinal fluid excluded CNS involvement. According to the 2017 European LeukemiaNet recommendations, intermediate-risk AML with concurrent MS was the final diagnosis (2, 4).

Consequently, an FLAI induction CHT regimen (5 days of fludarabine 30 mg/m^2 daily; 5 days of cytarabine 2,000 mg/m^2 daily; 3 days of idarubicin 10 mg/m^2 daily) was initiated. Prophylactic posaconazole and filgrastim were given until neutrophil recovery.

During hospitalization (27 days), a single episode of febrile neutropenia occurred, which was effectively treated with a broad-spectrum antibiotic therapy (piperacillin/tazobactam 4.5 g/8 h for 14 days, with no isolates on blood cultures). Oral grade III mucositis (17) also occurred and resolved before discharge.

Upon full CBC recovery, the patient was reassessed and found to be in a BM complete remission (CR), with a complete clearance of the breast skin lesion.

Accordingly, she received a second course of FLAI as a consolidation therapy. Filgrastim (5 μg/kg/day) was started on day 9 from the first day of FLAI. On day 15, an episode of febrile neutropenia was recorded and treated with a broad-spectrum antibiotic therapy (piperacillin/tazobactam 4.5 g/8 h for 4 days, then meropenem 1 g/8 h because of persistence of fever). Fever was associated with elevation of procalcitonin (PCT: 2.38 ng/ml, reference values: 0.01–0.50 ng/ml).

Time curves of white blood cells (WBC), absolute neutrophil count (ANC), and procalcitonin (PCT) are shown in Figure 1.

On day 21, a high-resolution chest CT (HR-chest-CT) scan revealed a slight ground-glass-like area in the right upper lobe of unspecific significance. Due to persistent fever with negative blood cultures, vancomycin (500 mg/6 h) and liposomal amphotericin B (3 mg/kg/day) were empirically added. On day 28, she was placed on total parenteral nutrition due to grade III (17) mucositis with poor oral intake.

On day 29, *Saprochaete clavata* (*Magnusiomyces clavatus*) was isolated from a blood culture collected from CVC; serum galactomannan antigen (GM) showed a negative result. The susceptibility test showed minimum inhibitory concentration (MIC) values of 1 mg/l for amphotericin B, 1 mg/l for anidulafungin, 8 mg/l for caspofungin, 8 mg/l for fluconazole, 0.06 mg/l for itraconazole, 0.125 mg/l for posaconazole, and 0.125 mg/l for voriconazole. A new HR-chest CT disclosed a thickening of the previous right-upper-lobe finding to a nodule with ground-glass peripheral opacity, consistent with a diagnosis of fungal pneumonia. At this stage, we decided to remove CVC and to potentiate antifungal therapy by escalating the liposomal amphotericin B dosage (from 3 to 5 mg/kg/day) and with the addition of isavuconazole (loading dose of 200 mg/8 h for 48 h, then 200 mg/day). No recent consumption of food suspected of contamination was reported by the patient (10).

On day 31, because of emerging abdominal pain, an abdominal contrast-enhanced CT scan was performed, which documented multiple, sub-centimetric, hypodense, ubiquitously distributed round areas in the spleen and liver (Figure 2A) suggesting a disseminated *Saprochaete clavata* infection. A new BMA showed a markedly hypocellular BM, consistent with a persistent post-CHT aplasia.

On day 33, two additional blood cultures (collected from peripheral blood) showed a positive result for *S. clavata*. The day after, the clinical conditions worsened, developing septic shock. Considering the patient's critical status, the persistence of fever unresponsive to antifungal therapy, and blood culture positivity for *S. clavata*, we decided to screen potential donors for granulocyte harvest and transfusion (13, 16, 18, 19).

On day 35, *S. clavata* was also isolated from stool sample culture. Correlations between significant clinical events and laboratory tests are depicted in Figure 1.

On day 36, GTX was initiated and a rapid decrease in inflammatory markers (Figure 1) was observed, together with improvement of the patient's clinical condition. Afterward, no further *S. clavata*-positive hemocultures were found. In contrast with the improvement of clinical and laboratory parameters, the temperature curve did not show any improvement, continuing to exhibit at least two to four fever spikes per day.

On day 40, a new BMA was performed, confirming hypoplasia. Daily GTX was continued until day 47 and was stopped when a stable clinical condition was reached.

Forty-eight hours after GTX discontinuation, the patient rapidly worsened, developing generalized edema, septic shock, and respiratory distress. A total body CT scan displayed a further increase in the size of the lung nodule, now also showing a central necrotizing area and a worsening of the previous reported abdominal hypodense round lesions, with progression to confluent and liquefied patterns. Furthermore, three new nodular ring-enhancing lesions appeared in the subcortical CNS in the absence of neurologic signs or symptoms (Figure 2B).

Based on the evidence of infection recrudescence, on day 50, we resumed GTX with a pronounced and prompt improvement of both clinical condition and inflammatory markers (Figure 1). Weekly cytomegalovirus (CMV) quantitative molecular testing always showed a negative result. On day 54, a new BMA was consistent with CR.

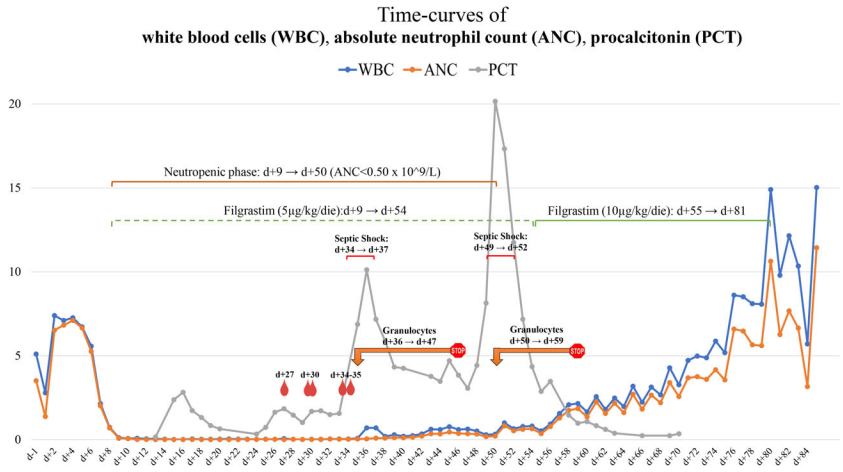

FIGURE 1
Timeline chart of WBC/ANC and blood cultures, GTX and PCT. Graphic representation of the WBC (blue line), ANC (orange line), and PCT (gray line) curves and their correlation with *Saprochaete clavata* isolation from blood cultures and GTX therapy. Hemocoltures positive for *Saprochaete clavata*; GTX interval. WBC, white blood count; GTX, granulocytes transfusion; PCT, procalcitonin.

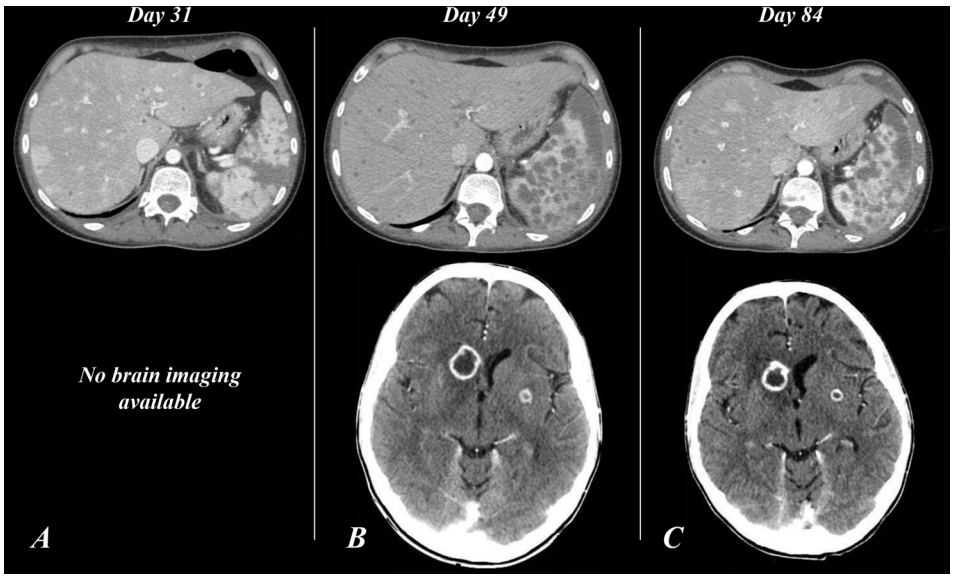

FIGURE 2
Contrast-enhanced CT scan of the abdomen **(A–C)** and the brain **(B, C)**. Panel A (*day 31*), finding of multiple, sub-centimetric, hypodense lesions involving the spleen and liver parenchymas. **(B)** (*Day 49*), spleen and liver enlargement; increase in number and size of the hypodense round lesions, some with confluent and liquefied patterns; new finding of nodular ring-enhancing lesions of the subcortical CNS with compression of the frontal (anterior) horn of the right lateral ventricle, and involvement of the left-side putamen. **(C)** (*Day 84*), confirmation of abdominal picture; stable brain lesions, expansion of the lesion surrounding with complete flattening of the frontal pole of the right lateral ventricle. CT, computed-tomography; CNS, central nervous system.

On day 55 (after 46 days of filgrastim 5 μg/kg/day), we decided to double the filgrastim dose in the attempt to accelerate neutrophil count reconstitution. After 2 days of filgrastim 10 μg/kg/day, ANC exceeded 1.0×10^9/l. GTX was continued until day 59. Indeed, after 21 total granulocyte units, we decided to stop granulocyte transfusion based on substantial clinical stability and ANC steadily at $>1.0 \times 10^9$/l.

The patient's general condition gradually improved, and the WBC count stabilized to normal values (Figure 1), so we decided to interrupt filgrastim administration (after 46 days with 5 μg/kg/day and 27 days with 10 μg/kg/day) and to repeat a contrast-enhanced total body CT scan (day 84), which showed stable brain lesions and cavitation of the lung nodule together with a significant reduction in pleural, pericardial, and free-abdominal effusions. Also, a marked and diffuse modification of spleen parenchyma (Figure 2C) was documented.

Intravenous antifungal combination therapy was administered until the day of discharge (day 86), then continued with oral isavuconazole. She is still in CR, under clinic follow-up, and her clinical condition is steadily improving.

Discussion and conclusion

FLAI is a well-known CHT regimen, frequently used in treating AML relapse. Burnett et al. (20) showed how the use of FAI as a first-line approach could lead to a greater amount of patients achieving an overall remission and CR after the first course of CHT, with reduction in relapse risk and prolongation of relapse-free survival when compared to standard therapy (20, 21). However, two courses of FLAI are more likely to be associated with greater hematological toxicity, so it should be considered in young patients (20, 21).

In this report, *S. clavata* was found to be responsible for disseminated and life-threatening infection in a young patient with AML, during a profound neutropenic phase after the second course of the FLAI CHT regimen. In line with available literature (10, 12, 22, 23), the susceptibility test has shown a high MIC for echinocandins and fluconazole and low for amphotericin B, itraconazole, posaconazole, and voriconazole (10, 12, 23–25). Not enough clinical data are available to assess the optimal treatment for this infection: a 2014 guideline for treatment of *S. clavata* infection recommended any formulation of amphotericin B ± other antifungals as the preferred approach (12, 22). Isavuconazole MIC was not tested in our case, but considering that the data about susceptibility to this agent are controversial (10, 12, 25), we tried to take advantage of its synergistic action with liposomal amphotericin B similar to other severe fungal infections (26).

The fungus continued to be isolated from blood cultures, and the infection progressed despite the antifungal combination therapy until the administration of GTX. Since the beginning of GTX, *S. clavata* was never isolated again (Figure 1). In addition to positive blood cultures, the isolation of *S. clavata* in stool (day 35) could indicate to consider the colonization of the GI tract as a reservoir from which the fungus may have reached the bloodstream (probably during GI mucositis). Serum GM turned out to be an unreliable marker of *S. clavata* infection (12).

Considering the critical conditions of the patient at the time of GTX arrangement, we decided to start screening for donors from both community and related individuals, to have the widest resources to continue GTX until the hematological recovery or complete resolution of the infection. A single granulocyte bag was obtained from each donor (granulocytapheresis), for a total of 21 granulocytes units received during the admission.

The effectiveness of this approach was demonstrated by the clear improvement (Figure 1) observed after the first course of GTX and confirmed by the sudden worsening of clinical condition upon GTX suspension. Hematological recovery was essential in restoring clinical condition and normalizing inflammatory markers. This could be the clue that antifungal alone might have a high failure rate unless supported by correcting factors (principally neutropenia) that expose the patients to the progression of the infection (13).

Three BMAs were performed during the hospitalization. The first evaluation (day 30) showed an aplastic BM in the absence of blasts, which was interpreted as a positive finding (AML was not the underlying cause of the delayed hematological recovery) even though a profound myelosuppression after the second course of FLAI was confirmed (20, 21). The two subsequent BMAs were still hypocellular, but both showed signs of initial multilineage recovery of hematopoiesis, without evidence of blast infiltrate. Despite these findings, the ANC curve exceeded 0.5×10^9/l only after 14 granulocyte units, reaching values steadily above 1.0×10^9/l after doubling of the filgrastim dose.

In this report, GTX proved to be a potential additional therapy in treating serious and antifungal-refractory fungal infections during the profound post-CHT neutropenic phase. Therefore, it suggests that this approach could be effective and should be considered in life-threatening infections.

In addition, this case also demonstrates that even combination antifungal therapy might not be sufficient in containing disseminated IFI unless it is accompanied by the patient's immune system recovery.

Patient perspective

The patient experienced a hard ordeal which led to a general worsening of her clinical condition (ECOG 2-3), together with a negative psychologic consequence in terms of motivation. Her clinical conditions have now substantially improved. At present, the patient is planned to receive a fully matched unrelated donor hematopoietic stem cell transplantation: her behavior is a

mixture of concern and expectation regarding her therapeutic plan.

Data availability statement

The original contributions presented in the study are included in the article/supplementary material. Further inquiries can be directed to the corresponding author.

Ethics statement

Written informed consent was obtained from the individual(s) for the publication of any potentially identifiable images or data included in this article.

Author contributions

All authors contributed to the clinical management of the patient. All authors wrote the manuscript, revised it critically and gave final approval to submit for publication.

Funding

GS is supported by the Italian Association for Cancer Research (AIRC) (grant IG-2020-24440), the Ministry of the University and Research (MUR)-European Union (TITAN project), and the Rome Foundation.

Conflict of interest

The authors declare that the research was conducted in the absence of any commercial or financial relationships that may represent a potential conflict of interest.

Publisher's note

All claims expressed in this article are solely those of the authors and do not necessarily represent those of their affiliated organizations, or those of the publisher, the editors and the reviewers. Any product that may be evaluated in this article, or claim that may be made by its manufacturer, is not guaranteed or endorsed by the publisher.

References

1. Döhner H, Weisdorf DJ, Bloomfield CD. Acute myeloid Leukemia1. *N Engl J Med* (2015) 373(12):1136–52. doi: 10.1056/NEJMra1406184

2. Döhner H, Estey E, Grimwade D, Amadori S, Appelbaum FR, Büchner T, et al. Diagnosis and management of AML in adults: 2017 ELN recommendations from an international expert panel. *Blood* (2017) 129(4):424–47. doi: 10.1182/blood-2016-08-733196

3. Short NJ, Rytting ME, Cortes JE. Acute myeloid leukaemia. *Lancet* (2018) 392 (10147):593–606. doi: 10.1016/S0140-6736(18)31041-9

4. Döhner H, Estey EH, Amadori S, Appelbaum FR, Büchner T, Burnett AK, et al. Diagnosis and management of acute myeloid leukemia in adults: Recommendations from an international expert panel, on behalf of the European LeukemiaNet. *Blood* (2010) 115(3):453–74. doi: 10.1182/blood-2009-07-235358

5. Almond LM, Charalampakis M, Ford SJ, Gourevitch D, Desai A. Myeloid sarcoma: Presentation, diagnosis, and treatment. *Clin Lymphoma Myeloma Leukemia* (2017) 17(5):263–7. doi: 10.1016/j.clml.2017.02.027

6. Goyal G, Bartley AC, Patnaik MM, Litzow MR, Al-Kali A, Go RS. Clinical features and outcomes of extramedullary myeloid sarcoma in the united states: Analysis using a national data set. *Blood Cancer J* (2017) 7:e592. doi: 10.1038/bcj.2017.79

7. Meyer HJ, Pönisch W, Schmidt SA, Wienbeck S, Braulke F, Schramm D, et al. Clinical and imaging features of myeloid sarcoma: A German multicenter study. *BMC Cancer* (2019) 19:1150. doi: 10.1186/s12885-019-6357-y

8. Bakst RL, Tallman MS, Douer D, Yahalom J. How I treat extramedullary acute myeloid leukemia. *Blood* (2011) 118(14):3785–93. doi: 10.1182/blood-2011-04-347229

9. Ganzel C, Manola J, Douer D, Rowe JM, Fernandez HF, Paietta EM, et al. Extramedullary disease in adult acute myeloid leukemia is common but lacks independent significance: Analysis of patients in ECOG-ACRIN cancer research group trials, 1980-2008. *J Clin Oncol* (2016) 34(29):3544–53. doi: 10.1200/JCO.2016.67.5892

10. Buchta V, Bolehovská R, Hovorková E, Cornely OA, Seidel D, Žák P. Saprochaete clavata invasive infections- a new threat to hematological-oncological patients. *Front Microbiol* (2019) 10. doi: 10.3389/fmicb.2019.02196

11. Del Principe MI, Sarmati L, Cefalo M, Fontana C, De Santis G, Buccisano F, et al. A cluster of geotrichum clavatum (Saprochaete clavata) infection in haematological patients: a first Italian report and review of literature. *Mycoses* (2016) 59(9):594–601. doi: 10.1111/myc.12508

12. El Zein S, Hindy JR, Kanj SS. Invasive saprochaete infections: An emerging threat to immunocompromised patients. *Pathogens* (2020) 9(11):922. doi: 10.3390/pathogens9110922

13. West KA, Gea-Banacloche J, Stroncek D, Kadri SS. Granulocyte transfusions in the management of invasive fungal infections. *Br J Haematol* (2017) 177:357–74. doi: 10.1111/bjh.14597

14. Higby DJ, Yates JW, Henderson ES, Holland JF. Filtration leukapheresis for granulocyte transfusion therapy: Clinical and laboratory studies. *N Engl J Med* (1975) 292:761–6. doi: 10.1056/NEJM197504102921501

15. Illerhaus G, Wirth K, Dwenger A, Waller CF, Garbe A, Brass V, et al. Treatment and prophylaxis of severe infections in neutropenic patients by granulocyte transfusions. *Ann Hematol* (2002) 81:273–81. doi: 10.1007/s00277-002-0439-6

16. Mousset S, Hermann S, Klein SA, Bialleck H, Duchscherer M, Bomke B, et al. Prophylactic and interventional granulocyte transfusions in patients with haematological malignancies and life-threatening infections during neutropenia. *Ann Hematol* (2005) 84:734–41. doi: 10.1007/s00277-005-1055-z

17. Cancer Therapy Evaluation Program (CTEP). Common terminology criteria for adverse events (CTCAE).v.5.0 [5x7]. *Cancer Ther Eval Program (CTEP)* (2017) 37.

18. Favre S, Rougeron A, Levoir L, Pérard B, Milpied N, Accoceberry I, et al. Saprochaete clavata invasive infection in a patient with severe aplastic anemia: Efficacy of voriconazole and liposomal amphotericin b with adjuvant granulocyte transfusions before neutrophil recovery following allogeneic bone marrow transplantation. *Med Mycol Case Rep* (2016) 11:21–3. doi: 10.1016/j.mmcr.2016.03.001

19. Catalano L, Fontana R, Scarpato N, Picardi M, Rocco S, Rotoli B. Combined treatment with amphotericin-b and granulocyte transfusion from G-CSF-stimulated donors in an aplastic patient with invasive aspergillosis undergoing bone marrow transplantation. *Haematologica* (1997) 82:71–2. doi: 10.3324/%25x

20. Burnett AK, Russell NH, Hills RK, Hunter AE, Kjeldsen L, Yin J, et al. Optimization of chemotherapy for younger patients with acute myeloid leukemia:

Results of the medical research council AML15 trial. *J Clin Oncol* (2013) 31 (27):3360–8. doi: 10.1200/JCO.2012.47.4874

21. Kantarjian H, Kadia T, DiNardo C, Daver N, Borthakur G, Jabbour E, et al. Acute myeloid leukemia: current progress and future directions. *Blood Cancer J* (2021) 11(2):41. doi: 10.1038/s41408-021-00425-3

22. Arendrup MC, Boekhout T, Akova M, Meis JF, Cornely OA, Lortholary O, et al. ESCMID and ECMM joint clinical guidelines for the diagnosis and management of rare invasive yeast infections. *Clin Microbiol Infect* (2014) 20 (Suppl 3):76–98. doi: 10.1111/1469-0691.12360

23. Noster J, Koeppel MB, Desnos-Olivier M, Aigner M, Bader O, Dichtl K, et al. Bloodstream infections caused by magnusiomyces capitatus and magnusiomyces clavatus: Epidemiological, clinical, and microbiological features of two emerging yeast species. *Antimicrob Agents Chemother* (2022) 66:e0183421. doi: 10.1128/AAC.01834-21

24. Desnos-Ollivier M, Bretagne S, Boullié A, Gautier C, Dromer F, Lortholary O. Isavuconazole MIC distribution of 29 yeast species responsible for invasive infections (2015–2017). *Clin Microbiol Infect* (2019) 25(5):634–43. doi: 10.1016/j.cmi.2019.02.007

25. Esposto MC, Prigitano A, Lo Cascio G, Ossi C, Grancini A, Cavanna C, et al. Yeast-like filamentous fungi: Molecular identification and *in vitro* susceptibility study. *Med Mycol* (2019) 57(7):909–13. doi: 10.1093/mmy/myy133

26. Gebremariam T, Gu Y, Singh S, Kitt TM, Ibrahim AS. Combination treatment of liposomal amphotericin b and isavuconazole is synergistic in treating experimental mucormycosis. *J Antimicrob Chemother* (2021) 7 (10):2636–9. doi: 10.1093/jac/dkab233

frontiers | Frontiers in Oncology

TYPE Case Report
PUBLISHED 16 September 2022
DOI 10.3389/fonc.2022.974307

OPEN ACCESS

EDITED BY
Jerry L. Spivak,
The Johns Hopkins Hospital, Johns Hopkins Medicine, United States

REVIEWED BY
Giorgio Alberto Croci,
University of Milan, Italy
Shih-Sung Chuang,
Chi Mei Medical Center, Taiwan

*CORRESPONDENCE
Kazuaki Yokoyama
k-yoko@ims.u-tokyo.ac.jp
Arinobu Tojo
tojo.adm@tmd.ac.jp

†These authors have contributed equally to this work and share first authorship

SPECIALTY SECTION
This article was submitted to Hematologic Malignancies, a section of the journal Frontiers in Oncology

RECEIVED 21 June 2022
ACCEPTED 18 August 2022
PUBLISHED 16 September 2022

CITATION
Kazama S, Yokoyama K, Ueki T, Kazumoto H, Satomi H, Sumi M, Ito I, Yusa N, Kasajima R, Shimizu E, Yamaguchi R, Imoto S, Miyano S, Tanaka Y, Denda T, Ota Y, Tojo A and Kobayashi H (2022) Case report: Common clonal origin of concurrent langerhans cell histiocytosis and acute myeloid leukemia.
Front. Oncol. 12:974307.
doi: 10.3389/fonc.2022.974307

Case report: Common clonal origin of concurrent langerhans cell histiocytosis and acute myeloid leukemia

Shintaro Kazama[1†], Kazuaki Yokoyama[2*†], Toshimitsu Ueki[1], Hiroko Kazumoto[1], Hidetoshi Satomi[3], Masahiko Sumi[1], Ichiro Ito[4], Nozomi Yusa[5], Rika Kasajima[6], Eigo Shimizu[7], Rui Yamaguchi[8], Seiya Imoto[7], Satoru Miyano[9], Yukihisa Tanaka[10], Tamami Denda[10], Yasunori Ota[10], Arinobu Tojo[11*] and Hikaru Kobayashi[1]

[1]Department of Hematology, Nagano Red Cross Hospital, Nagano, Japan, [2]Division of Molecular Therapy, Institute of Medical Science, Advanced Clinical Research Center, The University of Tokyo, Tokyo, Japan, [3]Department of Diagnostic Pathology and Cytology, Osaka International Cancer Institute, Osaka, Japan, [4]Department of Pathology, Nagano Red Cross Hospital, Nagano, Japan, [5]Department of Applied Genomics, Research Hospital, Institute of Medical Science, University of Tokyo, Tokyo, Japan, [6]Molecular Pathology and Genetics Division, Kanagawa Cancer Center Research Institute, Yokohama, Japan, [7]Division of Health Medical Data Science, Health Intelligence Center, Institute of Medical Science, University of Tokyo, Tokyo, Japan, [8]Division of Cancer Systems Biology, Aichi Cancer Center Research Institute, Nagoya, Japan, [9]Department of Integrated Data Science, Medical and Dental Data Science Center, Tokyo Medical and Dental University, Tokyo, Japan, [10]Department of Diagnostic Pathology, IMSUT Hospital, Institute of Medical Science, The University of Tokyo, Tokyo, Japan, [11]Department of Data Science and Faculty Affairs, Tokyo Medical and Dental University, Tokyo, Japan

Langerhans cell histiocytosis (LCH) and acute myeloid leukemia (AML) are distinct entities of blood neoplasms, and the exact developmental origin of both neoplasms are considered be heterogenous among patients. However, reports of concurrent LCH and AML are rare. Herein we report a novel case of concurrent LCH and AML which shared same the driver mutations, strongly suggesting a common clonal origin.An 84-year-old female presented with cervical lymphadenopathy and pruritic skin rash on the face and scalp. Laboratory tests revealed pancytopenia with 13% of blasts, elevated LDH and liver enzymes, in addition to generalised lymphadenopathy and splenomegaly by computed tomography. Bone marrow specimens showed massive infiltration of MPO-positive myeloblasts, whereas S-100 and CD1a positive atypical dendritic cell-like cells accounted for 10% of the atypical cells on bone marrow pathology, suggesting a mixture of LCH and AML. A biopsy specimen from a cervical lymph node and the skin demonstrated the accumulation of atypical cells which were positive for S-100 and CD1a. LCH was found in lymph nodes, skin and bone marrow; AML was found in peripheral blood and bone marrow (AML was predominant compared with LCH in the bone marrow).

Next generation sequencing revealed four somatic driver mutations (*NRAS*-G13D, *IDH2*-R140Q, and *DNMT3A*-F640fs/-I715fs), equally shared by both the lymph node and bone marrow, suggesting a common clonal origin for the

concurrent LCH and AML. Prednisolone and vinblastine were initially given with partial response in LCH; peripheral blood blasts also disappeared for 3 months. Salvage chemotherapy with low dose cytarabine and aclarubicin were given for relapse, with partial response in both LCH and AML. She died from pneumonia and septicemia on day 384. Our case demonstrates a common cell of origin for LCH and AML with a common genetic mutation, providing evidence to support the proposal to classify histiocytosis, including LCH, as a myeloid/myeloproliferative malignancy.

KEYWORDS

langerhans cell histiocytosis, acute myeloid leukemia, NRAS, MAPK pathway, histiocytic disorders, dendritic cells, BRAF V600E, inflammatory myeloid neoplasm

Introduction

Langerhans cell histiocytosis (LCH) and acute myeloid leukemia (AML) are distinct entities of blood neoplasms, and the exact developmental origin of both neoplasms is considered to be heterogenous among patients (1–6). However, to our knowledge, only ten cases of concurrent LCH and AML have been reported so far (2, 3, 7–11). Herein we report a novel case of concurrent AML and LCH which shared the same driver mutations, strongly suggesting a common clonal origin.

Case description

An 84 year-old female presented with cervical lymphadenopathy and pruritic skin rash on the face and scalp. She had no past history or family history of hematological or solid organ malignancies or other treatments. She had no fever but multiple lymph nodes were palpated bilaterally in the neck, axilla, and inguinal region. Laboratory tests revealed pancytopenia (WBC 2,520/μL including 13% blasts, 32% neutrophils, 6% eosinophils, 0% basophils, 3% monocytes, 46% lymphocytes, Hemoglobin (Hb) of 10.9 g/dL, and a platelet count of 92,000/μL) and elevated LDH (604 U/L) and liver enzymes (AST 51 U/L, ALT 39 U/L). Systemic lymphadenopathy and splenomegaly, but no other abnormal findings, were noted on computed tomography. Bone marrow specimens showing a massive infiltration of MPO-positive blasts including 53.5% of myeloblastic cells and 13.8% of monoblastic cells indicated the diagnosis of AML. Whereas, 9.1% of cellular components were occupied by MPO-negative atypical dendritic cell-like cells (Figures 1A–C). On flow cytometric analysis, monoclonal cells were positive for CD13, CD33, CD34, CD38, CD7, and TdT. On bone marrow pathology, S-100 and CD1a-positive atypical cells accounted for 10% of the blasts (Figures 1D, E), suggesting a mixture of AML and LCH. A biopsy specimen from a cervical lymph node demonstrated the accumulation of atypical round or horseshoe-shaped cells with indented or folded nuclei which were positive for S-100 and CD1a, and negative for MPO and CD34, confirming the diagnosis of LCH (Figures 1F, H–J). AML cells were absent not only on pathology, but also on flow cytometry in lymph nodes. Atypical cells were partially positive for langerin (Figure 1G), not suggestive of indeterminate cell histiocytosis (ICH). Around the atypical cells were scattered mononuclear cells positive for CD3, CD20, and CD68 (Figures 1K–M). Simultaneously, skin biopsy demonstrated atypical cells with an immunohistochemical profile similar to that in the lymph nodes, suggesting skin invasion of LCH. The atypical cells were negative for MPO and CD34, suggesting absence of skin invasion by the AML. The G-banding assay revealed a normal karyotype in both the bone marrow and lymph nodes.

LCH was found in lymph nodes, skin and bone marrow; AML was found in peripheral blood and bone marrow (AML was predominant compared with LCH in the bone marrow). Elevated liver enzymes and splenomegaly suggested the presence of hepatic and splenic lesions, but which tumor was responsible could not be determined.

Diagnostic assessment

Taken together, the patient was diagnosed with concurrent LCH and AML. Next generation sequencing with the TruSight Myeloid Sequencing Panel (Illumina) revealed four somatic driver mutations (*NRAS*-G13D, *IDH2*-R140Q, and *DNMT3A*-F640fs/-I715fs), equally found in both the lymph node and bone marrow (Table 1). *BRAF*-V600E was negative, which was also confirmed by immunohistochemistry staining (data not shown). The mutant allele frequencies were 24.6%-33.0% and 27.0%-38.5% in the lymph node and bone marrow, respectively. Assuming each mutant allele to be a single hit, 50-70% of tumor cells harbored each mutation, suggesting a common clonal origin of concurrent LCH and AML.

Prednisolone and vinblastine were initially given with partial response in LCH, additionally peripheral blood blasts

10.3389/fonc.2022.974307

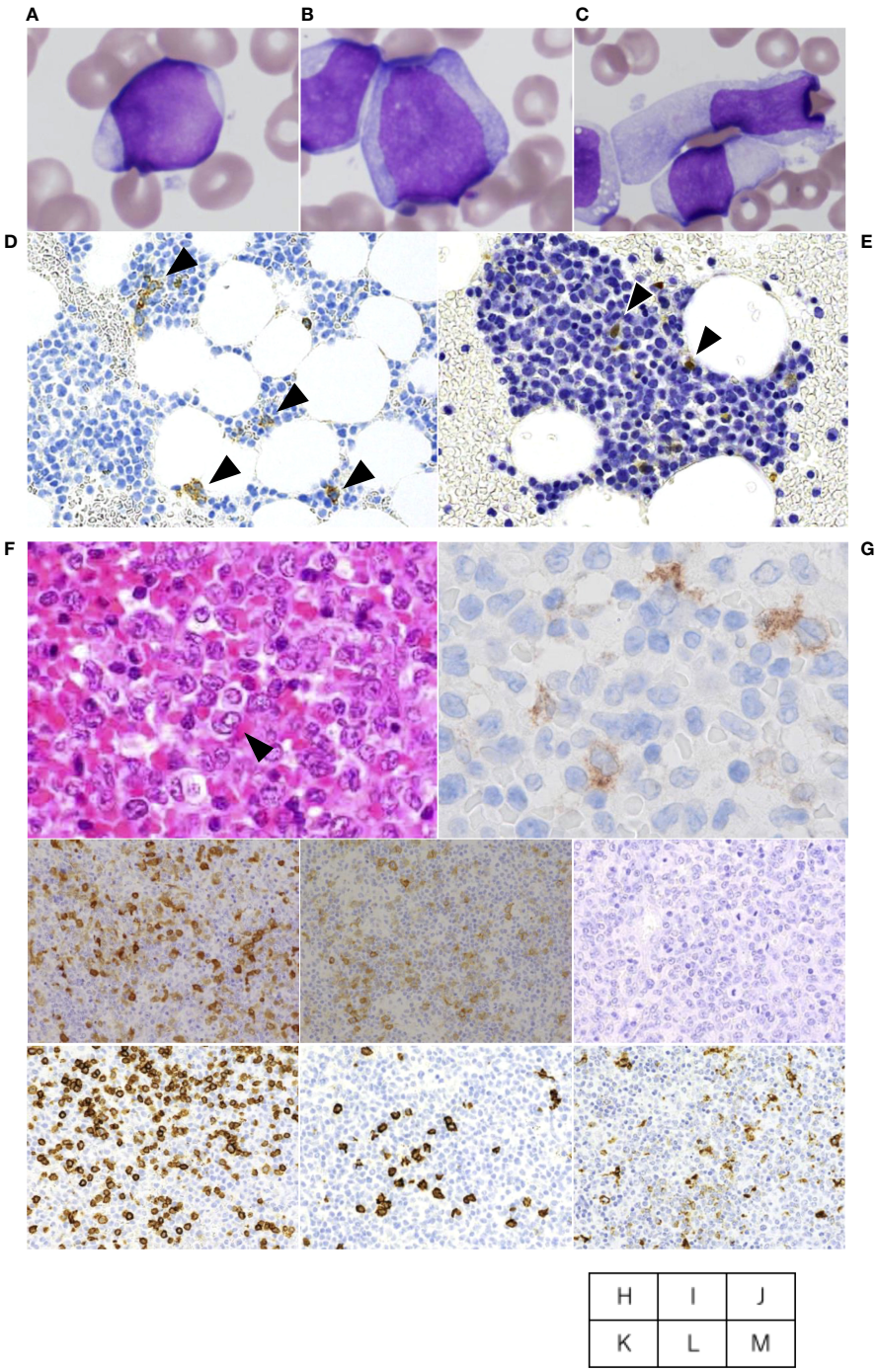

FIGURE 1
Cervical lymph node biopsy and bone marrow aspiration. The aspiration smears of bone marrow show myeloblastic cells accounted for 53.5% **(A)** and monoblastic cells accounted for 13.8% **(B)**, whereas dendritic cell-like atypical cells are also found at a frequency of 9.1% **(C)**. On bone marrow pathology, CD1a **(D)**- and S-100 **(E)**-positive atypical cells accounted for 10% of the blasts. Cervical lymph node biopsy specimen shows atypical cells with indented or folded nuclei like one indicated by arrowhead or other ones with mild folding **(F)**, and immunostaining was Langerin-partially positive **(G)**, S-100-positive **(H)**, CD1a-positive **(I)**, MPO-negative **(J)**. Around the atypical cells were scattered mononuclear cells positive for CD3 **(K)**, CD20 **(L)**, and CD68 **(M)** in the periphery.

TABLE 1 Results of genomic analysis of cervical lymph node biopsy and bone marrow aspiration by panel analysis.

Bone marrow (Total somatic mutations 3,885 ▷ Driver mutations 4)				
Amino acid mutations	*NRAS* p.G13D	*IDH2* p.G13D	*DNMT3A* p.F640fs	*DNMT3A* p.I715fs
Mutant allele frequency (%)	32.8	24.6	33.0	28.7
Lymph nodes (Total somatic mutations 2,468 ▷ Driver mutations 4)				
Amino acid mutations	*NRAS* p.G13D	*IDH2* p.R140Q	*DNMT3A* p.F640fs	*DNMT3A* p.I715fs
Mutant allele frequency (%)	30.9	27.0	37.1	38.5

disappeared for 3 months. From day 120, low dose cytarabine and aclarubicin were administered as a salvage chemotherapy with partial response in both LCH and AML. Subsequently, from day 253, the patient received low dose cytarabine and etoposide, which did not give rise to a durable response, and she died from pneumonia and septicemia on day 384 (Figure 2).

Discussion

Histiocytic disorders are a group of rare diseases characterized by organ infiltration by macrophages, dendritic cells, and monocytes (12). Gene mutations have been identified in a number of histiocytoses, including LCH and non-LCH (e.g., Erdheim-Chester disease (ECD), indeterminate cell histiocytosis, and histiocytic sarcoma) (5, 13–20), most of which are mutations in genes encoding proteins in the mitogen-activated protein kinase (MAPK) pathway (21). Therefore, the pathogenesis of histiocytic disorders, including LCH are mainly attributed to unregulated activation of the MAPK pathway (1, 22), and these disorders are clonal neoplastic diseases caused by this (23, 24). Activating mutations of MAPK pathway members are almost mutually exclusive. Among these, *BRAF* is a major target of mutation, and *BRAF*-V600E is most commonly observed in LCH (1). In contrast, mutation of *NRAS*, another member of the MAPK pathway, is rare in LCH, but one report stated that *NRAS* mutations were present in 40% of pulmonary LCH (25). Furthermore, genetic mutations in the MAPK pathway members including *NRAS* were identified in 57% of Langerhans cell sarcomas (26). *NRAS* mutations were more common in AML (10%) than LCH, and, in combination with *IDH2*, *DNMT3A* and other mutations, contribute to the pathogenesis of AML (27–29).

Cases of LCH combined with malignant neoplasms are rare and generally the subject of isolated case reports (2, 3). Most reports of AML associated with LCH are treatment-related AML after treatment for previous LCH. Only ten cases of simultaneous diagnosis of LCH and AML have been reported to date, most of which were characterized by generalized LCH, monocytic leukemia as the predominant type of associated AML, and poor prognosis, as in the present case (2, 3, 7–11). On the other hand, a high concomitant rate of myeloid neoplasm has been reported in non-LCH (e.g., 10.1% in ECD) (30, 31).

The exact cell of origin of histiocytic disorders, including LCH, is unknown. Allelic assessment of Langerhans cells in LCH clearly distinguished them from skin Langerhans cells (4), as *BRAF*-V600E mutations were identified in a subset of dendritic cells, mature monocytes, myeloid progenitor cells, and CD34+ cells in LCH and ECD patients. Therefore, it can be estimated myeloid progenitor cells are the cell of origin for histiocytic disorders (5, 32, 33). However, clinical and experimental evidence is lacking.

Recently, advances in genetic analysis have led to the discovery of commonly mutated genes in cases of histiocytic disorders and myeloid neoplasms, and the existence of a common cellular origin of histiocytic disorders and myeloid neoplasms has been proposed. In a review by Kemps PG et al. (34), mutated genes in histiocytic disorders and myeloid neoplasms have been reported in 30 cases (29, 33–55). A total of 31 cases, including one additional case of a common mutation found in LCH and primary myelofibrosis (39), including the present case are shown in Table 2. There have been five cases, of LCH occurring concurrently with a myeloid neoplasm, including the present case. Gene mutations of the MAPK pathway were frequently detected in LCH and non-LCH (30, 34, 35, 37, 40–44). There have been 5 cases of shared *NRAS* mutations, and one of them was at the same locus as the present case (*NRAS* p.G13D) (42). In this case, an adult female was diagnosed with ECD from skin lesions, and bone marrow biopsy revealed chronic myelomonocytic leukemia. The only mutation detected was *NRAS* p.G13D, which was common to both lesions, but *BRAF*-V600E was not examined.

Five cases of myeloid neoplasms have been suggested to have a common origin with LCH (2 cases of AML, 2 cases of polycrythemia vera, and 1 case of chronic myelomonocytic

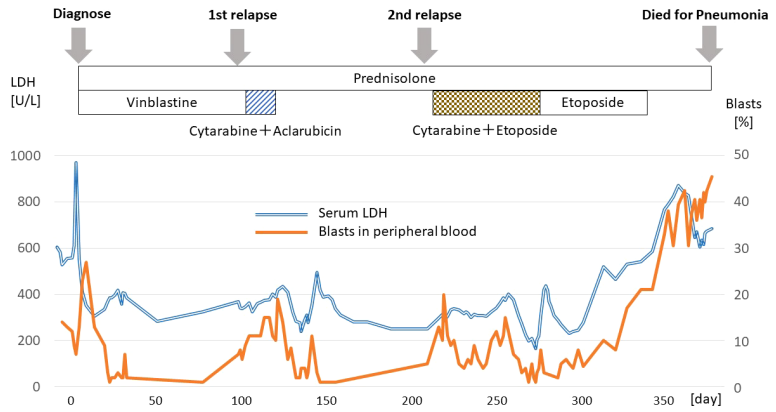

FIGURE 2
The timeline of diagnosis and treatment.

TABLE 2 Overview of reported cases with histiocytic disorders and additional myeloid neoplasms bearing the same genetic alteration(s).

No.	pediatric/adult	Histiocytic neoplasms	associated myeloid neoplasms	shared driver mutations	Reference
1	A	LCH	CMML	*BRAF*p.V600E	(34)
2	A	LCH	AML NOS	*ASXL1,IDH2 and STAG2* mutations	(35)
3	A	LCH	AML NOS	Trisomy 8,*KRAS*pA146T	(36)
4	A	LCH	PMF	*JAK2*p.V617F	(37)
5	A	LCH	PMF	*JAK2*p.V617F	(38)
6	A	Mixed LCH/ECD	ET	*JAK2*p.V617F	(29)
7	A	Mixed LCH/ECD	AML-M4	*TET2*p.L1819X and *SRSF2*p.L95P	(39)
8	A	ECD	AML-M5	*NRAS*p.Q61R	(33)
9	A	ECD	AML-M5	*BRAF*p.V600E	(33)
10	A	ECD	AML NOS	*BRAF*p.V600E	(40)
11	A	ECD	CMML	*BRAF*p.V600E, *TET2* and *SRSF2* mutations	(40)
12	A	ECD	CMML	*KRAS*p.G12D and *ASXL1*p.G642fs	(41)
13	A	ECD	CMML	*KRAS*p.G12D and *DNMT3A*p.Y623fs	(41)
14	A	ECD	CMML	*KRAS*p.G12D.*ASXL1*p.Y591X	(42)
15	A	ECD	CMML	*NRAS*p.G13D	(41)
16	A	ECD	CMML	*NRAS*p.Q61R	(29)
17	A	ECD	CMML	*NRAS*p.Q61R	(40)
18	A	ICH	CMML	*NRAS*p.G12V	(33)
19	A	ICH	CMML	*KRAS*p.G12R	(43)
20	A	ICH	CMML	*TET2*p.Q1466X and p.Q1523X,*ASXL1*p.K618X and *ZRS2*p.Q100X	(44)
21	P	JXG	JMML	*PTPN1*p.E76K	(45)
22	A	HS	CMML	*KRAS*p.A59E	(33)
23	N/A	HS	CMML	*TP53* mutation	(46)
24	A	HS	MDS	*TP53* and BCOR mutations	(47)
25	A	Atypical non LCH	AML MO	*RUNX1*p.R166X and p.P425L	(48)
26	A	MPDCN	MDS-MLD	*PTPN11*p.R501K	(49)
27	A	BPDCN	AML NOS	*TET2*p.C1642fs and p.A1810fs and *SRSF2*p.P95H	(50)
28	A	BPDCN	CMML	*TET2*p.G523fs, *SRSF2*p.P85L,*PHF6*p.Q251H	(51)
29	A	BPDCN	CMML	*TET2* p.Y1244fs and p.Q1810X and *SRSF2*p.P95H	(52)

(Continued)

TABLE 2 Continued

No.	pediatric/adult	Histiocytic neoplasms	associated myeloid neoplasms	shared driver mutations	Reference
30	N/A	BPDCN	CMML	*TET2* mutation	(53)
31	A	BPDCN	MDS-RARS	*TET2* mutation	(54)
32	A	LCH	AML	*NRAS*p.G13D,*IDH2*p.R140Q,*DNMTA*p.F640fs and p.1715fs	The present case

P, paediatric; A, adult; N/A, not available; LCH, Langerhans cell histiocytosis; ECD, Erdheim Chester disease; ICH, indeterminate cell histiocytosis; JXG, Juvenile xanthogranuloma; HS, histiocytic sarcoma; non-LCH, non-Langerhans cell histiocytosis; MPDCN, mature plasmacytoid dendritic cell neoplasm; BPDCN, blastic plasmacytoid dendritic cell neoplasm; CMML, chronic myelomonocytic leukemia; AML, acute myeloid leukemia; NOS, not otherwise specified; PMF, primary myelofibrosis; ET, essential thrombocytosis; JMML, juvenile myelomonocytic leukaemia; MDS, myelodysplastic syndromes; MLD, multilineage dysplasia; RARS, refractory anaemia with ring sideroblasts.

leukemia), thus, this is the third report of common gene mutation between LCH and AML. In the other two reports of shared mutation between LCH and AML, both adult males were diagnosed with LCH on skin biopsy and AML from bone marrow biopsy. One patient shared *ASXL1*, *IDH2*, and *STAG2* mutations (36), and the other shared *KRAS* mutation and trisomy 8 (37). Of note, in both cases, *BRAF*-V600E mutation was detected only in LCH cells. In the present case, allele frequencies of 4 driver mutations were comparable to each other as well as between LCH (lymph node) and AML (bone marrow), no genetic mutations present in only AML or LCH were detected, making it difficult to dissect the developmental process of LCH and AML. Thus, the present case provides important evidence that myeloid progenitors are the common origin of the two neoplasms, and reaffirms the importance of MAPK pathway activation in the pathogenesis of histiocytic disorders.

On the other hand, a different biological mechanism by which leukemic progenitor cells are misdirected into LCH by environmental factors was considered. This disease is an inflammatory myeloid neoplasm with features of both abnormal reaction processes and neoplastic processes. De Graaf et al. reported that inflammatory cytokines are expressed in LCH lesions (56). Kannourakis et al. extracted and cultured monocytes from the eosinophilic granuloma tissue of LCH patients, and found that such monocytes highly express inflammatory cytokines (57). In addition to a cytokine storm in local lesions, the levels of several pro-inflammatory cytokines in the serum of LCH patients are high, suggesting that cytokines are associated with the pathogenesis of LCH (58). LCH cells in the target tissues of LCH patients are surrounded by lymphocytic infiltrates and multinucleated giant cells, including T cells, macrophages, eosinophils, and B cells. Cytokines derived from LCH cells and T cells are considered to regulate the differentiation, maturation, and migration of myeloid dendritic cell precursors originating from hematopoietic stem cells (59, 60). In our case, the lymph node lesions also exhibited CD3-, CD20-, and CD68-positive mononuclear cell infiltrates around the LCH cells, suggesting that the microenvironment of these inflammatory cells played a role in the induction of LCH. Additionally, LCH lesions in this case were widely distributed in lymph nodes, but organs susceptible to LCH such as bone remained intact. Considering the common AML genotype and atypical LCH phenotype, there is one possible explanation for this case, that leukemic progenitor cells which migrated into lymph nodes could have been misguided toward LCH by environmental factors including the lymph node microenvironment and soluble factors.

According to the 2016 WHO classification, histiocytic disorders, including LCH and ECD, are classified as lymphoid neoplasms (61). This classification is based on several case reports describing individual patients with secondary malignant histiocytosis clonally associated with lymphoid neoplasms (62–66). However, with the recent development of genetic analysis techniques, the number of shared mutations in histiocytosis and myeloid neoplasms has surpassed those in lymphoid neoplasms (33).

Conclusion

In summary, our case demonstrates a common cell of origin for LCH and AML with a common genetic mutation, providing evidence to support the proposal to classify histiocytosis, including LCH, as a myeloid/myeloproliferative malignancy.

Data availability statement

The detailed clinical data and datasets presented in this article are not publicly available due to ethical and privacy restrictions. Requests to access the datasets should be directed to the corresponding authors.

Ethics statement

Written informed consent was obtained from the [individual(s) AND minor(s)' legal guardian/next of kin] for

the publication of any potentially identifiable images or data included in this article.

Author contributions

SK, TU, HKa, HS, MS, II, YT, TD, YO, and HKo were involved in the description of clinical information. KY, NY, ES, RY, SI, SM, and AT were involved in the data analysis. All authors contributed to the article and approved the submitted version.

Acknowledgments

We would like to thank Editage (www.editage.com) for English language editing.

Conflict of interest

The authors declare that the research was conducted in the absence of any commercial or financial relationships that could be construed as a potential conflict of interest.

Publisher's note

References

1. Allen CE, Parsons DW. Biological and clinical significance of somatic mutations in langerhans cell histiocytosis and histiocytic neoplastic disorders. *Hematol Am Soc Hematol Educ Program* (2015) 2015:559–64. doi: 10.1182/asheducation-2015.1.559

2. Egeler RM, Neglia JP, Puccetti DM, Brennan CA, Nesbit ME. Association of langerhans cell histiocytosis with malignant neoplasms. *Cancer* (1993) 71 (3):865–73. doi: 10.1002/1097-0142(19930201)71:3<865::aid-cncr2820710334>3.0.co;2-0

3. Egeler RM, Neglia JP, Aricò M, Favara BE, Heitger A, Nesbit ME, et al. The relation of langerhans cell histiocytosis to acute leukemia, lymphomas, and other solid tumors. the LCH-malignancy study group of the histiocyte society. *Hematol Oncol Clin North Am* (1998) 12(2):369–78. doi: 10.1016/s0889-8588(05)70516-5

4. Allen CE, Li L, Peters TL, Leung HCE, Yu A, Man TK, et al. Cell-specific gene expression in langerhans cell histiocytosis lesions reveals a distinct profile compared with epidermal langerhans cells. *J Immunol* (2010) 184(8):4557–67. doi: 10.4049/jimmunol.0902336

5. Berres ML, Lim KPH, Peters T, Price J, Takizawa H, Salmon H, et al. BRAF-V600E expression in precursor versus differentiated dendritic cells defines clinically distinct LCH risk groups. *J Exp Med* (2014) 211(4):669–83. doi: 10.1084/jem.20130977

6. Allen CE, Merad M, McClain KL. Langerhans-cell histiocytosis. *N Engl J Med* (2018) 379(9):856–68. doi: 10.1056/NEJMra1607548

7. Egeler RM, Neglia JP, Arico M, Favara BE, Heitger A, Nesbit ME. Acute leukemia in association with langerhans cell histiocytosis. *Med Pediatr Oncol* (1994) 23(2):81–5. doi: 10.1002/mpo.2950230204

8. Pina-Oviedo S, Torres-Cabala CA, Miranda RN, Tetzlaff MT, Singh S, Rapini RP, et al. Concomitant cutaneous langerhans cell histiocytosis and leukemia cutis. *Am J Dermatopathol* (2017) 39(5):388–92. doi: 10.1097/DAD.0000000000000775

9. Yohe SL, Chenault CB, Torlakovic EE, Asplund SL, McKenna RW. Langerhans cell histiocytosis in acute leukemias of ambiguous or myeloid lineage in adult patients: Support for a possible clonal relationship. *Mod Pathol* (2014) 27 (5):651–6. doi: 10.1038/modpathol.2013.181

10. Hwang YY, Tsui P, Leung RYY, Kwong YL. Disseminated langerhans cell histiocytosis associated with acute myeloid leukaemia: Complete remission with daunorubicin and cytarabine. *Ann Hematol* (2013) 92(2):267–8. doi: 10.1007/s00277-012-1555-6

11. Bohn OL, Feldman JL, Heaney ML, Teruya-Feldstein J. Acute myeloid leukemia with t(9;11) (p22;q23) and synchronous langerhans cell histiocytosis. *Int J Surg Pathol* (2014) 22(2):172–6. doi: 10.1177/1066896913487985

12. Emile JF, Abla O, Fraitag S, Horne A, Haroche J, Donadieu J, et al. Revised classification of histiocytoses and neoplasms of the macrophage-dendritic cell lineages. *Blood* (2016) 127(22):2672–81. doi: 10.1182/blood-2016-01-690636

13. Durham BH. Molecular characterization of the histiocytoses: neoplasia of dendritic cells and macrophages. *Semin Cell Dev Biol* (2019) 86:62–76. doi: 10.1016/j.semcdb.2018.03.002

14. Badalian-Very G, Vergilio JA, Degar BA, MacConaill LE, Brandner B, Calicchio ML, et al. Recurrent BRAF mutations in langerhans cell histiocytosis. *Blood* (2010) 116(11):1919–23. doi: 10.1182/blood-2010-04-279083

15. Haroche J, Charlotte F, Arnaud L, Deimling AV, Hélias-Rodzewicz Z, Hervier B, et al. High prevalence of BRAF V600E mutations in erdheim-Chester disease but not in other non-langerhans cell histiocytoses. *Blood* (2012) 120 (13):2700–3. doi: 10.1182/blood-2012-05-430140

16. Chakraborty R, Hampton OA, Shen X, Simko SJ, Shih A, Abhyankar H, et al. Mutually exclusive recurrent somatic mutations in MAP2K1 and BRAF support a central role for ERK activation in LCH pathogenesis. *Blood* (2014) 124 (19):3007–15. doi: 10.1182/blood-2014-05-577825

17. Sahm F, Capper D, Preusser M, Meyer J, Stenzinger A, Lasitschka F, et al. BRAFV600E mutant protein is expressed in cells of variable maturation in langerhans cell histiocytosis. *Blood* (2012) 120(12):e28–34. doi: 10.1182/blood-2012-06-429597

18. Satoh T, Smith A, Sarde A, Lu HC, Mian S, Trouillet C, et al. B-RAF mutant alleles associated with langerhans cell histiocytosis, a granulomatous pediatric disease. *PloS One* (2012) 7(4):e33891. doi: 10.1371/journal.pone.0033891

19. Brown NA, Furtado LV, Betz BL, Kiel MJ, Weigelin HC, Lim MS, et al. High prevalence of somatic MAP2K1 mutations in BRAF V600E-negative langerhans cell histiocytosis. *Blood* (2014) 124(10):1655–8. doi: 10.1182/blood-2014-05-577361

20. Nelson DS, Quispel W, Badalian-Very G, Halteren AGSV, Bos CVD, Bovée JVMG, et al. Somatic activating ARAF mutations in langerhans cell histiocytosis. *Blood* (2014) 123(20):3152–5. doi: 10.1182/blood-2013-06-511139

21. Durham BH, Rodrigo EL, Picarsic J, Abramson D, Rotemberg V, Munck SD, et al. Activating mutations in CSF1R and additional receptor tyrosine kinases in histiocytic neoplasms. *Nat Med* (2019) 25(12):1839–42. doi: 10.1038/s41591-019-0653-6

22. Berres ML, Merad M, Allen CE. Progress in understanding the pathogenesis of langerhans cell histiocytosis: Back to histiocytosis X? *Br J Haematol* (2015) 169 (1):3–13. doi: 10.1111/bjh.13247

23. Fletcher CDM, Bridge JA, Hogendoorn PCW, Mertens F. *WHO classification of tumours of soft tissue and bone. 4th ed* Vol. Volume 5. . Lyon: IARC (2013).

24. Swerdlow S, Campo E, Harris N, Jaffe ES, Pileri SA, Stein H, et al. *WHO classification of tumours of haematopoietic and lymphoid tissues. Revised 4th ed* Vol. Volume 2. . Lyon: IARC (2017).

25. Mourah S, How-Kit A, Meignin V, Gossot D, Lorillon G, Bugnet E, et al. Recurrent NRAS mutations in pulmonary langerhans cell histiocytosis. *Eur Respir J* (2016) 47(6):1785–96. doi: 10.1183/13993003.01677-2015

26. Shanmugam V, Griffin GK, Jacobsen ED, Fletcher CDM, Sholl LM, Hornick JL. Identification of diverse activating mutations of the RAS-MAPK pathway in histiocytic sarcoma. *Mod Pathol* (2019) 32(6):830–43. doi: 10.1038/s41379-018-0200-x

27. Cox AD, Fesik SW, Kimmelman AC, Luo J, Der CJ. Drugging the undruggable RAS: mission possible? *Nat Rev Drug Discov* (2015) 13(11):828–51. doi: 10.1038/nrd4389

28. Wang S, Wu Z, Li T, Li Y, Wang W, Hao Q, et al. Mutational spectrum and prognosis in NRAS-mutated acute myeloid leukemia. *Sci Rep* (2020) 10(1):12512. doi: 10.1038/s41598-020-69194-6

29. Rodriguez-Viciana P, Tetsu O, Oda K, Okada J, Rauen K, McCormick F. Cancer targets in the ras pathway. *Cold Spring Harb Symp Quant Biol* (2005) 70:461–8. doi: 10.1101/sqb.2005.70.044

30. Papo M, Diamond EL, Cohen-Aubart F, Emile JF, Roos-Weil D, Gupta N, et al. High prevalence of myeloid neoplasms in adults with non-langerhans cell histiocytosis. *Blood* (2017) 130(8):1007–13. doi: 10.1182/blood-2017-01-761718

31. Kommalapati A, Tella SH, Durkin M, Go RS, Goyal G. Histiocytic sarcoma: a population-based analysis of incidence, demographic disparities, and long-term outcomes. *Blood* (2018) 131(2):265–8. doi: 10.1182/blood-2017-10-812495

32. Milne P, Bigley V, Bacon CM, Néel A, McGovern N, Bomken S, et al. Hematopoietic origin of langerhans cell histiocytosis and erdheim-Chester disease in adults. *Blood* (2017) 130(2):167–75. doi: 10.1182/blood-2016-12-757823

33. Durham BH, Roos-Weil D, Baillou C, Cohen-Aubart F, Yoshimi A, Miyara M, et al. Functional evidence for derivation of systemic histiocytic neoplasms from hematopoietic stem/progenitor cells. *Blood* (2017) 130(2):176–80. doi: 10.1182/blood-2016-12-757377

34. Kemps PG, Hebeda KM, Pals ST, Verdijk RM, Lam KH, Bruggink AH, et al. Spectrum of histiocytic neoplasms associated with diverse hematological malignancies bearing the same oncogenic mutation. *J Pathol Clin Res* (2021) 7 (1):10–26. doi: 10.1002/cjp2.177

35. Konstantinou MP, Lucas P, Uthurriague C, Severino-Freire M, Spenatto N, Gaudin C, et al. Langerhans cell histiocytosis associated with chronic myelomonocytic leukemia both harboring the same BRAF V600E mutation: efficacy of vemurafenib. *J Eur Acad Dermatol Venereol* (2021) 35(2):e120–1. doi: 10.1111/jdv.16850

36. Khurana S, Sluzevich JC, He R, Reimer DK, Kharfan-Dabaja MA, Foran JM, et al. Association between highgrade myelodysplastic syndrome and cutaneous langerhans cell histiocytosis suggested by next-generation sequencing. *JAMA Dermatol* (2020) 156(7):817–9. doi: 10.1001/jamadermatol.2020.0544

37. Wang X, Wang Z. Revealing homologous clonality by synchronous trisomy 8 in langerhans cell histiocytosis and acute myeloid leukemia. *Blood* (2019) 134 (1):5040. doi: 10.1182/blood-2019-127883

38. Bonometti A, Bagnoli F, Fanoni D, Venegoni L, Corti L, Bianchi P, et al. JAK2-mutated langerhans cell histiocytosis associated with primary myelofibrosis treated with ruxolitinib. *Hum Pathol* (2018) 73:171–5. doi: 10.1016/j.humpath.2017.10.017

39. Holst JM, Enemark MB, Plesner TL, Pedersen MB, Ludvigsen M, d'Amore F. Coexisting BRAF-mutated langerhans cell histiocytosis and primary myelofibrosis with shared JAK2 mutation. *Case Rep Hematol* (2021). doi: 10.1155/2021/6623706

40. Ghobadi A, Miller CA, Li T, O'Laughlin M, Lee YS, Ali M, et al. Shared cell of origin in a patient with erdheim–Chester disease and acute myeloid leukemia. *Haematologica* (2019) 104(8):e373–5. doi: 10.3324/haematol.2019.217794

41. Tzankov A, Kremer M, Leguit R, Orazi A, Walt JVD, Gianelli U, et al. Histiocytic cell neoplasms involving the bone marrow: summary of the workshop cases submitted to the 18th meeting of the European association for haematopathology (EAHP) organized by the European bone marrow working group, Basel 2016. *Ann Hematol* (2018) 97 (11):2117–28. doi: 10.1007/s00277-018-3436-0

42. Bonnet P, Chasset F, Moguelet P, Abisror N, Itzykson R, Bouaziz JD, et al. Erdheim-Chester disease associated with chronic myelomonocytic leukemia harboring the same clonal mutation. *Haematologica* (2019) 104(11):e530–3. doi: 10.3324/haematol.2019.223552

43. Goyal G, Liu Y, Ravindran A, Al-Kali A, Go RS, Patnaik MM, et al. Concomitant erdheim-Chester disease and chronic myelomonocytic leukaemia: genomic insights into a common clonal origin. *Br J Haematol* (2019) 187(2):e51–4. doi: 10.1111/bjh.16177

44. Loghavi S, Curry JL, Garcia-Manero G, Patel KP, Xu J, Khoury JD, et al. Chronic myelomonocytic leukemia masquerading as cutaneous indeterminate dendritic cell tumor: expanding the spectrum of skin lesions in chronic myelomonocytic leukemia. *J Cutan Pathol* (2017) 44(12):1075–9. doi: 10.1111/cup.13039

45. Santos-Briz A, Medina-Miguelañez M, Moyano-Bueno D, Viñolas-Cuadros A, Martínez TG, Izquierdo MM, et al. Indeterminate dendritic cell tumor as cutaneous involvement of chronic myelomonocytic leukemia successfully treated with phototherapy. *Am J Dermatopathol* (2020) 42(11):876–80. doi: 10.1097/DAD.0000000000001703

46. Bátai B, Krizsán S, Gángó A, Hegyi L, Csóka M, Erdélyi DJ, et al. Juvenile myelomonocytic leukaemia presentation after preceding juvenile xanthogranuloma harbouring an identical somatic PTPN11 mutation. *Pediatr Blood Cancer* (2020) 67 (9):e28368. doi: 10.1002/pbc.28368

47. Facchetti F, Pileri SA, Lorenzi L, Tabanelli V, Rimsza L, Pittaluga S, et al. Histiocytic and dendritic cell neoplasms: what have we learnt by studying 67 cases. *Virchows Arch* (2017) 471(4):467–89. doi: 10.1007/s00428-017-2176-1

48. Tashkandi H, Dogan A. Histiocytic sarcoma arising in patient with history of clonally-related germ cell tumour and myelodysplastic syndrome. *Br J Haematol* (2020) 188(4):482. doi: 10.1111/bjh.16372

49. Mugairi AA, Turki SA, Salama H, Ahmadi KA, Abuelgasim KA, Damlaj M. Isolated bone marrow non-langerhans cell histiocytosis preceding RUNX1-mutated acute myeloid leukemia: Case report and literature review. *Am J Clin Pathol* (2019) 151(6):638–46. doi: 10.1093/ajcp/aqz018

50. Bodmer A, Menter T, Juskevicius D, Arranto C, Wenzel F, Dirnhofer S, et al. Sharing of a PTPN11 mutation by myelodysplastic bone marrow and a mature plasmacytoid dendritic cell proliferation provides evidence for their common myelomonocytic origin. *Virchows Arch* (2017) 470(4):469–73. doi: 10.1007/s00428-017-2075-5

51. Luskin MR, Kim AS, Patel SS, Wright K, LeBoeuf NR, Lane AA, et al. Evidence for separate transformation to acute myeloid leukemia and blastic plasmacytoid dendritic cell neoplasm from a shared ancestral hematopoietic clone. *Leuk Lymphoma* (2020) 61(9):2258–61. doi: 10.1080/10428194.2020.1755856

52. Patnaik MM, Lasho T, Howard M, Finke C, Ketterling RL, Al-Kali A, et al. Biallelic inactivation of the retinoblastoma gene results in transformation of chronic myelomonocytic leukemia to a blastic plasmacytoid dendritic cell neoplasm: Shared clonal origins of two aggressive neoplasms. *Blood Cancer J* (2018) 8(9):82. doi: 10.1038/s41408-018-0120-5

53. Brunetti L, Battista VD, Venanzi A, Schiavoni G, Martelli MP, Ascani S, et al. Blastic plasmacytoid dendritic cell neoplasm and chronic myelomonocytic leukemia: a shared clonal origin. *Leukemia* (2017) 31(5):1238–40. doi: 10.1038/leu.2017.38

54. Sukegawa S, Sakata-Yanagimoto M, Matsuoka R, Momose H, Kiyoki Y, Noguchi M, et al. Blastic plasmacytoid dendritic cell neoplasm accompanied by chronic myelomonocytic leukemia successfully treated with azacitidine. *Rinsho Ketsueki* (2018) 59(12):2567–73. doi: 10.11406/rinketsu.59.2567

55. Krause JR, Baugh L, Swink A, Burchet M. Blastic plasmacytoid dendritic cell neoplasm following acquired erythropoietic protoporphyria. *Baylor Univ Med Cent Proc* (2017) 30(4):450–1. doi: 10.1080/08998280.2017.11930225

56. Graaf JHD, Tamminga RY, Dam-Meiring A, Kamps WA, Timens W. The presence of cytokines in langerhans' cell histiocytosis. *J Pathol* (1996) 180(4):400–6. doi: 10.1002/(SICI)1096-9896(199612)180:4<400::AID-PATH701>3.0.CO;2-W

57. Kannourakis G, Abbas A. The role of cytokines in the pathogenesis of langerhans cell histiocytosis. *Br J Cancer Suppl* (1994) 23:S37–40.

58. Feng C, Li Y, Ke H, Peng X, Guo H, Zhan L, et al. Immune microenvironment in langerhans cell histiocytosis: Potential prognostic indicators. *Front Oncol* (2021) 11:631682. doi: 10.3389/fonc.2021.631682

59. Egeler RM, Favara BE, Meurs MV, Laman JD, Claassenet E. Differential *In situ* cytokine profiles of langerhans-like cells and T cells in langerhans cell histiocytosis: Abundant expression of cytokines relevant to disease and treatment. *Blood* (1999) 94(12):4195–201.

60. Rizzo FM, Cives M, Simone V, Silvestris F. New insights into the molecular pathogenesis of langerhans cell histiocytosis. *Oncologist* (2014) 19(2):151–63. doi: 10.1634/theoncologist.2013-0341

61. Swerdlow SH, Campo E, Pileri SA, Harris NL, Stein H, Siebert R, et al. The 2016 revision of the world health organization classification of lymphoid neoplasms. *Blood* (2016) 127(20):2375–90. doi: 10.1182/blood-2016-01-643569

62. Feldman AL, Arber DA, Pittaluga S, Martinez A, Burke JS, Raffeld M, et al. Clonally related follicular lymphomas and histiocytic/ dendritic cell sarcomas: evidence for transdifferentiation of the follicular lymphoma clone. *Blood* (2008) 111 (12):5433–9. doi: 10.1182/blood-2007-11-124792

63. West DS, Dogan A, Quint PS, Tricker-Klar ML, Porcher JC, Ketterling RP, et al. Clonally related follicular lymphomas and langerhans cell neoplasms: Expanding the spectrum of transdifferentiation. *Am J Surg Pathol* (2013) 37 (7):978–86. doi: 10.1097/PAS.0b013e318283099f

64. Shao H, Xi L, Raffeld M, Feldman AL, Ketterling RP, Knudson R, et al. Clonally related histiocytic/dendritic cell sarcoma and chronic lymphocytic leukemia/small lymphocytic lymphoma: A study of seven cases. *Mod Pathol* (2011) 24(11):1421–32. doi: 10.1038/modpathol.2011.102

65. Chen W, Jaffe R, Zhang L, Hill C, Block AM, Sait S, et al. Langerhans cell sarcoma arising from chronic lymphocytic lymphoma/small lymphocytic leukemia: Lineage analysis and BRAF V600E mutation study. *N Am J Med Sci* (2013) 5(6):386–91. doi: 10.4103/1947-2714.114172

66. Ratei R, Hummel M, Anagnostopoulos I, Jähne D, Arnold R, Dörken B, et al. Common clonal origin of an acute b-lymphoblastic leukemia and a langerhans' cell sarcoma: Evidence for hematopoietic plasticity. *Haematologica* (2010) 95(9):1461–6. doi: 10.3324/haematol.2009.021212

frontiers | Frontiers in Oncology

TYPE Case Report
PUBLISHED 23 September 2022
DOI 10.3389/fonc.2022.1013046

OPEN ACCESS

EDITED BY
Justin Watts,
University of Miami, United States

REVIEWED BY
Riccardo Masetti,
University of Bologna, Italy
Liyun Chen,
The First Affiliated Hospital of Soochow University, China

*CORRESPONDENCE
Junmin Li
ljm10378@rjh.com.cn
Kankan Wang
kankanwang@shsmu.edu.cn

†These authors have contributed equally to this work

SPECIALTY SECTION
This article was submitted to Hematologic Malignancies, a section of the journal Frontiers in Oncology

RECEIVED 06 August 2022
ACCEPTED 02 September 2022
PUBLISHED 23 September 2022

CITATION
Chen L, Zhu H, Zhu Y, Jin W, Dong F, Li J, Hu J, Chen Q, Wang K and Li J (2022) Case Report: Successful therapy with all-*trans* retinoic acid combined with chemotherapy followed by hematopoietic stem cell transplantation for acute promyelocytic leukemia carrying the *BCOR-RARA* fusion gene. *Front. Oncol.* 12:1013046. doi: 10.3389/fonc.2022.1013046

Case Report: Successful therapy with all-*trans* retinoic acid combined with chemotherapy followed by hematopoietic stem cell transplantation for acute promyelocytic leukemia carrying the *BCOR-RARA* fusion gene

Li Chen†, Hongming Zhu†, Yongmei Zhu†, Wen Jin, Fangyi Dong, Jianfeng Li, Jiong Hu, Qiusheng Chen, Kankan Wang* and Junmin Li*

Shanghai Institute of Hematology, State Key Laboratory of Medical Genomics, National Research Center for Translational Medicine at Shanghai, Ruijin Hospital Affiliated to Shanghai Jiao Tong University School of Medicine, Shanghai, China

Acute promyelocytic leukemia (APL) is characterized by the balanced translocation of chromosomes 15 and 17, resulting in the formation of *PML-RARA* fusion gene. More than 98% of APL have *PML-RARA* fusion, and less than 2% have other types of *RARA* gene partners, which named variant APL (vAPL). In the present study, we reported a vAPL with *BCOR-RARA*, which was the third case of *BCOR-RARA* APL published. The patient achieved complete remission (CR) with all-*trans* retinoic acid (ATRA) monotherapy, and molecular CR with ATRA plus standard chemotherapy. After that, he underwent allogeneic hematopoietic stem cell transplantation (allo-HSCT) and ATRA maintenance and maintained a molecular CR status. This case provided valuable insights into the accurate identification of vAPL. Moreover, ATRA combined with chemotherapy followed by allo-HSCT was suggested as an optimal choice for those vAPL patients who had a high risk of relapse.

KEYWORDS

acute promyelocytic leukemia, variant, BCOR-RARA, all-trans retinoic acid, allogeneic hematopoietic stem cell transplantation

Introduction

Acute promyelocytic leukemia (APL) is characterized by a clonal expansion of abnormal promyelocytes in bone marrow. The majority of the patients manifest the t(15;17) translocation forming the *PML-RARA* fusion gene, regarded as classical APL. In a small number of APL cases, *RARA* is fused with an alternative gene partner, such as *ZBTB16, NPM1*, and *STAT5B*, termed as variant APL (vAPL). To date, at least 16 *RARA* variant gene partners have been identified, most of which have been reported as rare cases or even a single case, in addition to *ZBTB16* (1–3). Most patients with vAPL are insensitive to arsenic trioxide (ATO) and/or all-*trans* retinoic acid (ATRA), and their prognosis is far worse than classical APL (4, 5). To our knowledge, 2 cases of APL with *BCOR-RARA* have been published, and here we report the third case.

Case presentation

The patient was a 47-year-old man who was admitted to a local hospital (the First Affiliated Hospital of Nanchang University) in April 2021. He suffered from dizziness, fatigue and exertional dyspnea for 2 weeks. A full blood count showed a white blood cell count of 10.05×10^9/L, a hemoglobin level of 53 g/L, and a platelet count of 108×10^9/L. The prothrombin time and activated partial thromboplastin time were within the normal range. Fibrinogen and D-dimer levels were 4.43 g/L (reference range 2-4 g/L) and 5.43 mg/L (reference < 0.5 mg/L), respectively. The morphological analysis of bone marrow (BM) showed extreme hyperplasia with 82.5% of hypergranular promyelocytes, and no Auer rod was found in his promyelocytes (Figure 1A). Flow cytometry revealed that the abnormal cells expressed CD13, CD33, CD117, CD38, CD56, but lacked the expression of CD34, CD15, CD14 and HLA-DR. The patient was proposed to be diagnosed as APL and was treated with ATRA. However, both the reverse transcription-polymerase chain reaction (RT-PCR) and fluorescence *in situ* hybridization (FISH) failed to provide any evidence of the *PML-RARA* fusion transcript in his BM. As a result, he suspended ATRA treatment and came to Ruijin Hospital affiliated to Shanghai Jiao Tong University School of Medicine. The karyotype analysis indicated 42, X, -Y, -15, -16, -18[cp12] (Figure 1B). Results of a multiplex RT-PCR panel covering 49 fusion genes commonly found in myeloid leukemia, including *PML-RARA*, *PLZF-RARA*, *NPM1-RARA*, *STAT5b-RARA*, *NuMA1-RARA*, *PRKARIA-RARA* and *FIPIL1-RARA*, were negative. Then, we performed RNA sequencing (RNA-Seq) on BM samples from our patient, and found the existence of the *BCOR-RARA* fusion transcript, in which exon 12 of *BCOR* was fused with exon 3 of *RARA* (Figures 1C, D). Furthermore, we performed targeted next-generation sequencing (NGS) covering 100 genes reportedly mutated in myeloid leukemia. We found mutations of *NRAS*, *KRAS*, *FLT3*-ITD, *FLT3*-TKD in his blasts. Hence, the patient was diagnosed with vAPL and continued induction therapy with ATRA. At the same time, hydroxyurea was used to control leukocytes and dexamethasone was used to prevent differentiation syndrome. Four weeks after hospitalization (June 9, 2021), the BM smear showed 10% of promyelocytes, 20.5% of abnormal neutrophilic myelocytes with nucleocytoplasmic imbalance, 3% of metamyelocytes and 4.5% of neutrophilic stab granulocytes. The patient was then discharged from our hospital and continued to take ATRA. On June 28, 2021, the BM smear showed complete remission (CR), and minimal residual disease (MRD) measured by flow cytometry was less than 0.01%, but *BCOR-RARA* measured by RT-PCR was still positive. The patient was then treated with ATRA plus idarubicin (IDA) (ATRA 20 mg twice daily, days 1-14, IDA 8 mg/m^2 days 1-3) for 2 courses. The third consolidation course of chemotherapy plus ATRA after 2 courses of ATRA plus IDA had been intensified by adding cytarabine (ATRA 20 mg twice daily, days 1-14, IDA 8 mg/m^2 days 1-2, cytarabine 100 mg/m^2 days 1-5) because of the failure of molecular remission, and finally his *BCOR-RARA* turned negative. Then, he underwent related haploidentical allogeneic hematopoietic stem cell transplantation (allo-HSCT) on November 9, 2021. The conditioning regimen included fludarabine 30 mg/m^2/d from day -6 to day -2, busulfan 3.2 mg/kg/d from day -6 to day -5 and melphalan 70 mg/m^2/d from day -3 to day -2. The graft-versus-host disease (GVHD) prophylaxis consisted of cyclophosphamide 50 mg/kg on day 3 and day 4 followed by tacrolimus 0.05 mg/kg divided into 2 doses per day from day 5 (6). However, a single dose of 2.5 mg/kg anti-thymoglobulin (ATG) after neutrophil engraftment was omitted because of pneumorrhagia on day 12. After that he received ATRA maintenance for 1 year (ATRA 20 mg twice daily, days 1-14, every month). Until now, he has maintained a molecular CR status for more than 9 months after HSCT. Figure 2 shows the detailed events of the clinical episode for the patient.

Discussion

APL variants account for 2% of APL, and the expansion in the detection of *RARA* partners might be attributed to the advancements in transcriptome sequencing. These variants are different from the classical APL in many ways, including the clinical presentations, morphological and cytochemical characteristics, and immunophenotyping, which could delay the final diagnosis of vAPL. vAPL often poses a management challenge as there are no defined guidelines. The outcome seems to be suboptimal in a number of cases with poor response to ATRA and ATO, such as *ZBTB16-RARA*. Still, fusions, such as *NPM1-RARA* and *FIP1L1-RARA*, are sensitive to ATRA, and fusions, such as *TTMV-RARA*, are sensitive to both ATRA and ATO combination therapy (4, 7). Generally, these variants should be treated with a combination of ATRA and chemotherapy (anthracyclines), with the possible use of AML protocols in known resistant variants (4, 8, 9).

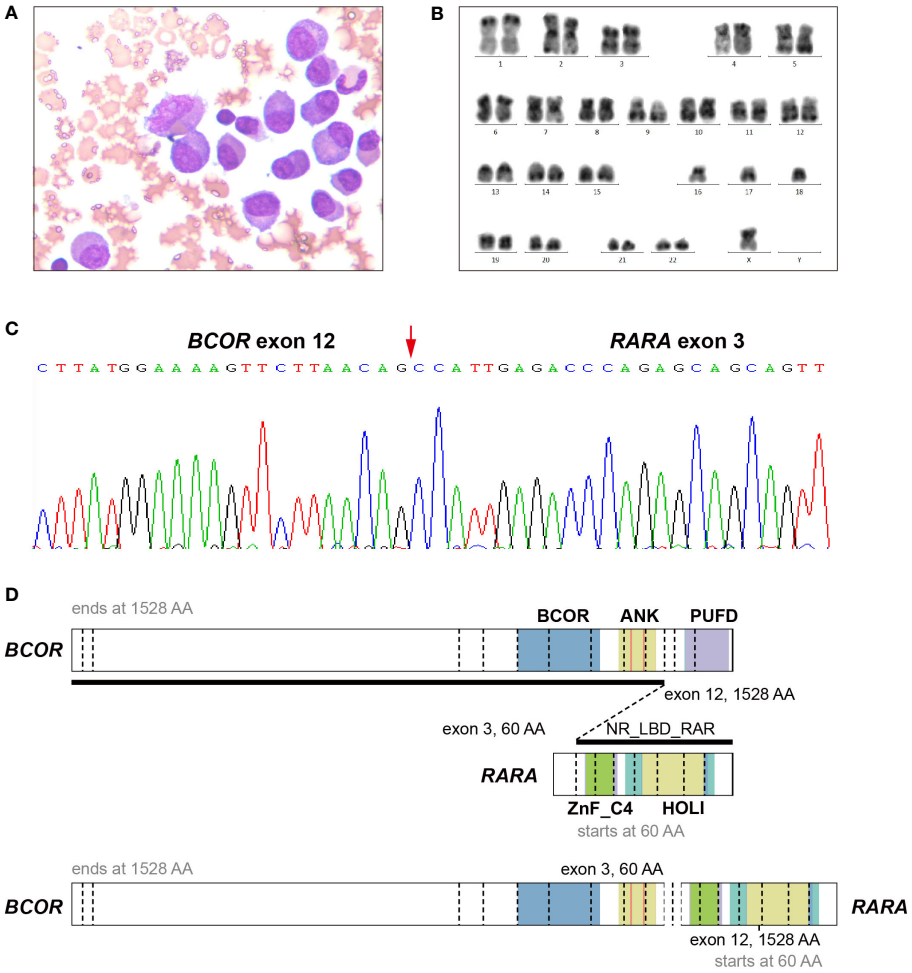

FIGURE 1
Morphology, cytogenetic and Molecular analysis of a bone marrow sample of the APL patient with BCOR-RARA. **(A)** May-Giemsa staining. Original magnification × 400. **(B)** Karyotype analysis. 42, X, -Y, -15, -16, -18 was detected in the patient. **(C)** BCOR-RARA fusion sequence at the junction site. An in-frame BCOR-RARA transcript is shown with corresponding exon numbers. The junction is indicated by a red arrowhead. **(D)** Schematic representation of BCOR, RARA, and the BCOR-RARA fusion protein. BCOR-RARA protein retains both BCOR and ANK of BCOR and ZnF_C4 and NR_LBD of RARA. ANK, ankyrin repeats; PUFD, PCGF Ub-like fold discriminator of BCOR; NR_LBD_RAR, the ligand binding domain (LBD) of retinoic acid receptor (RAR); ZnF_C4, c4 zinc finger in nuclear hormone receptors; HOLI, Ligand binding domain of hormone receptors.

APL with *BCOR-RARA* is quite rare among vAPL. Our results showed that this kind of vAPL could also be accompanied by common gene mutations in classical APL or other acute myeloid leukemia (AML), which may also be one of the reasons for high risk of relapse. Although these patients could achieve remission after ATRA combined with traditional chemotherapy, they could barely be cured.

BCOR is a transcriptional corepressor by the interaction of the proto-oncoprotein, BCL6 and plays critical roles in myeloid differentiation (8). The incidence of *BCOR* mutations is about 3.8% to 5.0% in adult *de novo* AML (10), and loss-of-function mutations in *BCOR* serve as an independent risk factor for poor outcomes of AML (11). The subcellular localization of BCOR-RARA is distinct with wild-type BCOR, likely destroying the function of wild-type BCOR (10). The difference in ATRA sensitivity might be related to variation in corepressors (12). *BCOR-RARA*, similar to *PML-RARA*, has a high affinity for corepressor molecules, thereby requiring high levels of ATRA to induce release of the corepressor complex and allow transcription and differentiation to proceed. Therefore, patients with *BCOR-RARA* can achieve CR with the same therapy as patients of classical APL (13). Our patient also achieved hematological remission with ATRA monotherapy.

The morphology of blast cells of our patient did not show the rectangular and round cytoplasmic inclusion bodies as reported by Yamamoto et al., but the immunophenotyping by flow cytometry was similar to that of the other 2 patients, with expression of CD13, CD33 and lack of HLA-DR, which may

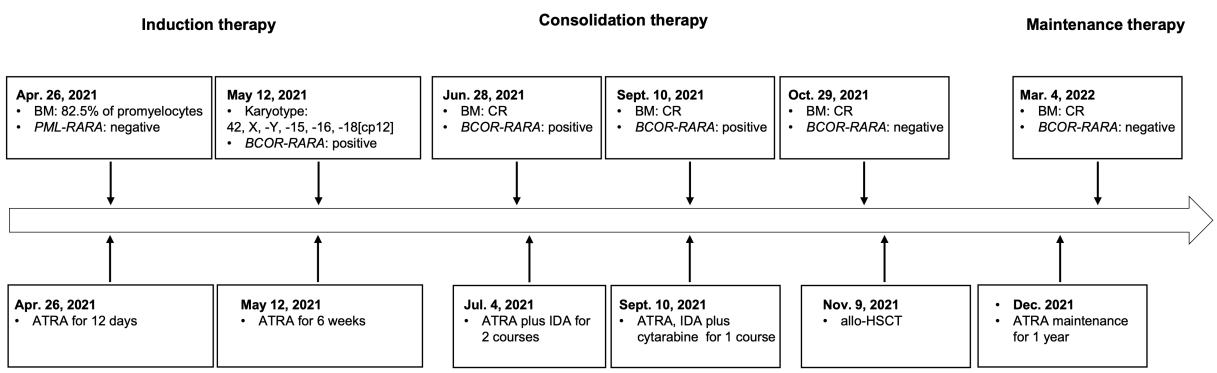

FIGURE 2
Timeline with the main events of the clinical episode for the patient.

be a feature of APL with *BCOR-RARA*. Besides, our patient and the one described by Yamamoto et al. had a strong expression of CD56, while the other one did not (Table 1). It has been reported that CD56 is frequently expressed in some variant APL forms (13, 15). In addition, our patient had mutated *NRAS*, *KRAS*, *FLT3*-ITD and *FLT3*-TKD. *BCOR*-mutated AML patients usually exhibit a high rate of *N-RAS* and *K-RAS* mutations (36.8%). Moreover, *BCOR*-mutated cases show a lower remission rate, overall survival and relapse-free survival, as compared with cases of wild-type. HSCT seems to abrogate the adverse prognostic impact of *BCOR* mutations (10). Although *BCOR* mutations were undetected in our patient, the

TABLE 1 Comparison of clinical features of the three cases of acute promyelocytic leukemia with *BCOR-RARA* fusion.

Author (year) (Refs.)	Present study	Yamamoto Y (2010) (12)	Satoshi Ichikawa (2015) (14)
Age	47	45	71
Gender	Male	Male	Male
Lab test			
WBC (×10^9/L)	10.05	25.3	leukocytosis
Hb (g/L)	53	121	anemia
PLT (×10^9/L)	108	116	normal
DIC	APTT, PT normal; Fg 4.43 g/L; DD 5.43 mg/L	INR 1.58, APTT 33.7s, Fg 52 mg/dL, FDP 50.6 mg/L	trivial
BM morphology	hypergranular promyelocytes, no Auer rod	peculiar rectangular and round cytoplasmic inclusion bodies in APL cells	not characteristic of APL, few Auer bodies, no faggot cells
Karyotype	42, X, -Y, -15, -16, -18	t(X;17)(p11;q12)	45, - Y, t(X;17)(p11.4;q21)
Flow cytometry	CD13+, CD33+, CD117+, CD38+, CD56+, CD34-, CD15-, CD14-, HLA-DR-	CD13+, CD33+, CD56+, HLA-DR-	CD13+, CD33+, HLA-DR-, CD34-, CD56-, and CD11c-
NGS	mutations of *NRAS, KRAS, FLT3-ITD, FLT3-TKD*	NA	NA
Treatment			
Induction treatment	ATRA only	ATRA + IDA + cytarabine	IDA + cytarabine
Achieve CR	Yes	Yes	Yes
Consolidation treatment	ATRA + IDA 2 courses, ATRA + IDA + cytarabine 1 course	MTN + cytarabine, DNR + cytarabine, IDA + cytarabine	ATRA + chemotherapy 3 courses
Transplantation	allogeneic HSCT	cord-blood transplantation	No
Outcome	mCR	CR3	mCR maintained for 1 year
Survival (months)	> 15	> 41	> 12

WBC, white blood cell; Hb, Hemoglobin; PLT, platelet; DIC, disseminated intravascular coagulation; BM, bone marrow; NGS, next-generation sequencing; CR, complete remission; APTT, activated partial thromboplastin time; PT, prothrombin time; Fg, Fibrinogen; DD, D-dimer; INR, international normalized ratio; FDP, fibrin/fibrinogen degradation products; APL, acute promyelocytic leukemia; NA, not available; ATRA, all-trans retinoic acid; IDA, idarubicin; MTN, mitoxantrone; DNR, daunorubicin; HSCT, hematopoietic stem cell transplantation; mCR, molecule complete remission.

fusion of *BCOR* and *RARA* may affect the function of *BCOR* gene by altering the subcellular location of wild-type BCOR. *FLT3*-ITD mutation is a poor prognostic factor not only for AML, but also for APL in the era of ATRA combined with chemotherapy (16). Recently, we analyzed the genomics and transcriptomics in 348 newly diagnosed APL patients and found that *NRAS* mutation was an independent adverse prognostic factor for APL (17). We did not find t(X;17)(p11;q12) chromosomal translocation by conventional chromosome banding test, but complex karyotype with 42, X, -Y, -15, -16, -18. These genomic and chromosomal abnormalities further supported the indication to allogeneic transplantation for this patient.

Our previous studies have shown that the addition of targeted drugs could reduce the intensity of chemotherapeutics, thereby alleviating severe myelosuppression caused by chemotherapy. Therefore, the patient was applied with ATRA plus IDA as consolidation for 2 courses, the same as the scheme of non-ATO group for low- and intermediate-risk APL patients in the APL2012 study (NCT01987297) (18). Nevertheless, *BCOR-RARA* was still positive, suggesting that ATRA plus anthracycline was not enough to clear MRD in such cases. We added cytarabine to the ATRA plus IDA regime as the third consolidation, and the *BCOR-RARA* fusion gene of the patient turned negative eventually. Therefore, it is suggested that ATRA combined with traditional AML chemotherapy may be a better option for APL with *BCOR-RARA*.

Although patients with *BCOR-RARA* could achieve promising short-term efficacy by ATRA plus chemotherapy, relapse still remains a major concern for patients. All the 3 patients received ATRA-chemotherapy-based treatment. The first case of APL with *BCOR-RARA* was reported with 2 episodes of relapse, and achieved the third remission by intensive chemotherapy plus cord-blood transplantation. The second case maintained molecular remission by intensive chemotherapy plus ATRA for 1 year so far, and long-term follow-up was anticipated (12, 14). The detailed treatment and outcome of the 3 patients are shown in Table 1. Transplantation was rarely used as a modality for vAPL, given the short-term follow-up and small number of the cases, but the benefit has been discussed in some variants with the high relapse rate, like *STAT5B-RARA* (9) and very young cases, like *TTMV-RARA* (7). Our patient had even stronger indications for transplantation due to complicated chromosome karyotype and poorly prognostic mutated genes. Besides, he continued taking ATRA as maintenance after transplantation since this setting of APL was sensitive to ATRA.

Future considerations for vAPL should include 1) the improvement of fast detection for these variants, not only the popularization of genetic sequencing, but also the use of artificial intelligence tools for deep learning of morphologic features just as in classical APL (2, 19, 20) the investigation of more therapies that might provide a better outcome, including hypomethylating agents, Bcl-2 inhibitors and hematopoietic cell transplantation.

In summary, our detailed analysis of this rare case of vAPL has showed that ATRA combined with traditional chemotherapy could bring good short-term outcome to APL patients with *BCOR-RARA*. Furthermore, allo-HSCT was administered as an optimal choice to cure the patient considering a high risk of relapse.

Data availability statement

The datasets presented in this article are not readily available because of ethical/privacy restrictions. Requests to access the datasets should be directed to the corresponding author.

Ethics statement

The studies involving human participants were reviewed and approved by the Ethics Committee of Ruijin Hospital in Shanghai. The patients/participants provided their written informed consent to participate in this study.

Author contributions

JuL designed the study. LC, HZ and YZ wrote the paper. KW revised the manuscript. FD and QC followed the patient. JH performed allogeneic hematopoietic stem cell transplantation for the patient. WJ and JiL performed the molecular studies. All authors contributed to the article and approved the submitted version.

Funding

National Natural Science Foundation of China (No. 81800141, 81890994, 81770144 and 81870110). Science and Technology Commission of Shanghai Municipality (No. 19DZ1910702).

Conflict of interest

The authors declare that the research was conducted in the absence of any commercial or financial relationships that could be construed as a potential conflict of interest.

Publisher's note

References

1. Zhu HH, Yang MC, Wang F, Lou YJ, Jin J, Li K, et al. Identification of a novel NUP98-RARA fusion transcript as the 14th variant of acute promyelocytic leukemia. *Am J Hematol* (2020) 95(7):e184–6. doi: 10.1002/ajh.25807

2. Wang Z, Wen L, Zhang L, Xu X, Chen X, Yao L, et al. Identification of a novel TNRC18-RARA fusion in acute promyelocytic leukemia lacking t(15;17)(q24;q12)/PML-RARA. *Mol Carcinog* (2021) 60(2). doi: 10.1002/mc.23276

3. Liu M, Zhao X, Pan W, Qian Z, Du M, Wang LM, et al. A novel HNRNPC-RARA fusion in acute promyelocytic leukaemia lacking PML-RARA rearrangement, sensitive to venetoclax-based therapy. *Br J Haematol* (2021) 195 (2):e123–8. doi: 10.1111/bjh.17642

4. Geoffroy MC, de The H. Classic and variants APLs, as viewed from a therapy response. *Cancers (Basel)* (2020) 12(4):967. doi: 10.3390/cancers12040967

5. Cicconi L, Testi AM, Montesinos P, Rego E, Zhu HH, Takahashi H, et al. Characteristics and outcome of acute myeloid leukemia with uncommon retinoic acid receptor-alpha (RARA) fusion variants. *Blood Cancer J* (2021) 11(10):167. doi: 10.1038/s41408-021-00561-w

6. Jiang JL, Chen M, Wang LN, Wan M, Gao WH, Wang L, et al. Double alkylators based conditioning reduced the relapse rate after allogeneic peripheral blood stem cell transplantation in adult patients with myeloid malignancies: A single arm phase II study. *Bone Marrow Transplant* (2022) 57(5):843–5. doi: 10.1038/s41409-022-01643-4

7. Astolfi A, Masetti R, Indio V, Bertuccio SN, Messelodi D, Rampelli S, et al. Torque teno mini virus as a cause of childhood acute promyelocytic leukemia lacking PML/RARA fusion. *Blood* (2021) 138(18):1773–7. doi: 10.1182/blood.2021011677

8. Mannan A, Muhsen IN, Barragan E, Sanz MA, Mohty M, Hashmi SK, et al. Genotypic and phenotypic characteristics of acute promyelocytic leukemia translocation variants. *Hematol Oncol Stem Cell Ther* (2020) 13(4):189–201. doi: 10.1016/j.hemonc.2020.05.007

9. Guarnera L, Ottone T, Fabiani E, Divona M, Savi A, Travaglini S, et al. Atypical rearrangements in APL-like acute myeloid leukemias: Molecular characterization and prognosis. *Front Oncol* (2022) 12:871590. doi: 10.3389/fonc.2022.871590

10. Sportoletti P, Sorcini D, Falini B. BCOR gene alterations in hematologic diseases. *Blood* (2021) 138(24):2455–68. doi: 10.1182/blood.2021010958

11. Eckardt JN, Stasik S, Kramer M, Rollig C, Kramer A, Scholl S, et al. Loss-of-Function mutations of BCOR are an independent marker of adverse outcomes in intensively treated patients with acute myeloid leukemia. *Cancers (Basel)* (2021) 13 (9):2095. doi: 10.3390/cancers13092095

12. Yamamoto Y, Tsuzuki S, Tsuzuki M, Handa K, Inaguma Y, Emi N. BCOR as a novel fusion partner of retinoic acid receptor alpha in a t(X;17)(p11;q12) variant of acute promyelocytic leukemia. *Blood* (2010) 116(20):4274–83. doi: 10.1182/blood-2010-01-264432

13. Adams J, Nassiri M. Acute promyelocytic leukemia: A review and discussion of variant translocations. *Arch Pathol Lab Med* (2015) 139(10):1308–13. doi: 10.5858/arpa.2013-0345-RS

14. Ichikawa S, Ichikawa S, Ishikawa I, Takahashi T, Fujiwara T, Harigae H. Successful treatment of acute promyelocytic leukemia with a t(X;17)(p11.4;q21) and BCOR-RARA fusion gene. *Cancer Genet* (2015) 208(4):162–3. doi: 10.1016/j.cancergen.2015.01.008

15. Sainty D, Liso V, Cantu-Rajnoldi A, Head D, Mozziconacci MJ, Arnoulet C, et al. A new morphologic classification system for acute promyelocytic leukemia distinguishes cases with underlying PLZF/RARA gene rearrangements. *Blood* (2000) 96(4):1287–96.

16. Picharski GL, Andrade DP, Fabro A, Lenzi L, Tonin FS, Ribeiro RC, et al. The impact of Flt3 gene mutations in acute promyelocytic leukemia: A meta-analysis. *Cancers (Basel)* (2019) 11(9):1311. doi: 10.3390/cancers11091311

17. Lin X, Qiao N, Shen Y, Fang H, Xue Q, Cui B, et al. Integration of genomic and transcriptomic markers improves the prognosis prediction of acute promyelocytic leukemia. *Clin Cancer Res* (2021) 27(13):3683–94. doi: 10.1158/1078-0432.CCR-20-4375

18. Chen L, Zhu HM, Li Y, Liu QF, Hu Y, Zhou JF, et al. Arsenic trioxide replacing or reducing chemotherapy in consolidation therapy for acute promyelocytic leukemia (APL2012 trial). *Proc Natl Acad Sci U.S.A.* (2021) 118 (6):e2020382118. doi: 10.1073/pnas.2020382118

19. Sidhom JW, Siddarthan IJ, Lai BS, Luo A, Hambley BC, Bynum J, et al. Deep learning for diagnosis of acute promyelocytic leukemia *via* recognition of genomically imprinted morphologic features. *NPJ Precis Oncol* (2021) 5(1):38. doi: 10.1038/s41698-021-00179-y

20. Cheli E, Chevalier S, Kosmider O, Eveillard M, Chapuis N, Plesa A, et al. Diagnosis of acute promyelocytic leukemia based on routine biological parameters using machine learning. *Haematologica* (2022) 107(6):1466–9. doi: 10.3324/haematol.2022.280406

frontiers | Frontiers in Oncology

TYPE Case Report
PUBLISHED 28 September 2022
DOI 10.3389/fonc.2022.912696

OPEN ACCESS

EDITED BY
Esther Natalie Oliva,
Grande Ospedale Metropolitano Bianchi Melacrino Morelli, Italy

REVIEWED BY
Daniela Damiani,
Hematology and Stem Cell Transplant, Italy
Benjamin Moskoff,
UC Davis Health, United States

*CORRESPONDENCE
Qingsheng Li
wshsyh604@163.com
Zhengqi Huang
drhuangzq120@163.com

†These authors have contributed equally to this work

SPECIALTY SECTION
This article was submitted to Hematologic Malignancies, a section of the journal Frontiers in Oncology

RECEIVED 04 April 2022
ACCEPTED 07 September 2022
PUBLISHED 28 September 2022

CITATION
Long Z, Ruan M, Wu W, Zeng Q, Li Q and Huang Z (2022) The successful combination of grapefruit juice and venetoclax in an unfit acute myeloid leukemia patient with adverse risk: A case report.
Front. Oncol. 12:912696.
doi: 10.3389/fonc.2022.912696

The successful combination of grapefruit juice and venetoclax in an unfit acute myeloid leukemia patient with adverse risk: A case report

Zhangbiao Long†, Min Ruan†, Wei Wu, Qingshu Zeng, Qingsheng Li* and Zhengqi Huang*

Department of Hematology, The First Affiliated Hospital of Anhui Medical University, Hefei, China

Venetoclax combined with hypomethylating agents such as azacitidine and decitabine is the standard regime for the elderly patient with acute myeloid leukemia (AML) unfit for intensive induction therapy. However, many patients struggle with finances and forgo treatments due to the high costs of venetoclax. In this study, we performed the regime with azacitidine, low-dose venetoclax, and grapefruit juice on an unfit AML patient with TP53 mutation. The peak venetoclax concentration (C_{max}) and side effects on the patient were also monitored. The patient achieved complete remission with the venetoclax C_{max} within the effective concentration range (1,000–3,000 ng/ml) and maintained durable remission until recently. Febrile neutropenia, thrombocytopenia, and pneumonia appeared during the first cycle and were recovered by stimulating agents and antibiotic treatment. This improvement combination approach by drug-food interaction may enlighten other similarly patients with AML, especially those in low-middle income countries.

KEYWORDS

grapefruit, venetoclax, AML – acute myeloid leukaemia, unfit, adverse risk

Introduction

Elderly patients with acute myeloid leukemia (AML) have a dismal outcome and cannot tolerate conventional intensive induction chemotherapy. Taking the place of supportive care, venetoclax combination with hypomethylating agents such as azacitidine and decitabine is currently becoming the preferred regime for these patients (1). Previous studies investigated the overall response rate was approximately 66–73%, and the median overall survival was 14.7–17.5 months in *de novo* unfit patients with AML (2–4). In recent years, venetoclax has been approved in China and other countries for elderly

patients with AML unfit for intensive induction therapy. Actually, the price remains too expensive (5). For instance, the cost of venetoclax is currently 38,880 RMB yuan per month in China. Due to the high costs of venetoclax, many patients face considerable financial struggles. These patients usually forgo treatments and succumb to death at last.

A strategy to reduce the cost of venetoclax is dose reduction. Venetoclax is an oral agent, primarily metabolized by cytochrome P450 enzyme (CYP3A4) (6). Several previous studies revealed that concurrent use of CYP3A4 inhibitors such as azole antifungal agents and venetoclax could reduce the metabolism of venetoclax, thus increasing its exposure (7, 8). The recommended dose of venetoclax is 100 mg once daily for patients receiving a strong concomitant CYP3A4 inhibitor (i.e., posaconazole or voriconazole) (9). When the venetoclax dose was reduced to 100 mg once daily from 400 mg once daily, the cost of venetoclax reduced to 9720 RMB yuan per month. Although some researchers recommended antifungal treatment for AML patients with grade 4 neutropenia, only a portion of patients with AML required azole antifungal treatment or prophylaxis during the first few cycles (3, 10–12).

Some foods can be considered a practical approach to enhancing the plasma concentration and effect of CYP3A4 substrates. Grapefruit juice is the most common food that can strongly inhibit CYP3A4 (13, 14). The simultaneous use of grapefruit juice and CYP3A4 substrate was an advanced strategy and also a challenge in clinical management. Here, we present an unfit newly diagnosed patient with AML who has low income and could not tolerate the high price of venetoclax. She has adopted the solution with the combination of grapefruit juice 200 ml 3 times daily, venetoclax 100 mg once daily, and azacitidine 75 mg/m^2 on days 1–7 of each 28-day cycle. We detected the patient's peak venetoclax concentration (C_{max}) to ensure appropriate drug exposure and reduce drug toxicity. In addition, we monitored the QTc interval, liver function, and renal function to avoid severe side effect. Eventually, the patient achieved complete remission and sustained durable remission until this present.

Case report

The patient was a 70-year-old woman. In July 2021, she came to the outpatient department of our hospital because of progressive dizziness and fatigue for 3 months without any cause. Initial blood routine test results showed pancytopenia (Table 1). A bone marrow aspiration was performed at our hospital. The bone marrow smears showed 42.5% large-sized blasts with fine chromatin and occasional prominent nucleoli (Figure 1). Flow cytometry of the bone marrow revealed positive for CD34, HLA-DR, myeloperoxidase, CD33, CD13, CD117, and CD7 and negative for Cy79α, CD19, CyCD3, and CD5. Cytogenetic analysis of the bone marrow identified a normal karyotype (46, XX) without a (15;17) chromosomal translocation. Next-generation sequencing of the bone marrow showed a frameshift mutation in TP53 (NM_000546: exon5: c.388dupC: p.Leu130fs) and did not identify a mutation in other genes. The MICM results of bone marrow were consistent with the WHO classification of AML, not otherwise specified.

The patient was generally evaluated for the subsequent treatment. The AML risk stratification by the genetics of this patient was adverse due to TP53 mutation. The Eastern Cooperative Oncology Group (ECOG) performance status was 2. The age and current situation suggested that the patient was ineligible for intensive chemotherapy. The preferred therapy of the patient was a hypomethylating agent combined with venetolcax. However, the patient was poor and could not afford the regular venetoclax dose of 400 mg once daily. After the patient's agreement, informed consent was obtained from the patient and the approval of the Ethics committee of our hospital. We performed the improved therapy with the combination of azacitidine (75 mg/m^2 subcutaneously on days 1–7 of each 28-day cycle), venetoclax (100 mg orally once daily), and grapefruit juice (200 ml orally 3 times daily) for this patient. To ensure the effectiveness of the reduced dose of venetoclax, we monitored the patient's peak venetoclax concentration (C_{max}) every week in the first cycle. The venetoclax C_{max} was 1,440 ng/ml at 7 days and 1,920 ng/ml at 14 days after the treatment and was within the effective concentration range (1,000–3000 ng/ml) (8, 15). In consequence, adherence to this regime was processed in the treatment. Febrile neutropenia and thrombocytopenia with grade 4 appeared 2 weeks after the therapy and completely recovered rapidly after the treatment with stimulating agents. The patient got pneumonia on day 14 after the initiation of treatment and recovered after the antibiotic treatment. The laboratory tests, including blood cell counting, liver function, renal function, and ECG were performed during the entire treatment period to monitor the side effect. The liver and renal functions were normal, and the QTc interval was 450 ms.

The bone marrow aspiration was performed on day 21. The bone marrow smears and immunology results revealed normal without leukemia cells. The patient continued this regime for five cycles to the current presentation and sustained durable remission. There was always no morphologic or phenotypic evidence of AML relapsed (Figure 2). A notable side effect was not detected during the subsequent treatment and follow-up period.

Discussion

Along with the application of novel target drugs, the management strategy of AML patients who were unfit for intensive induction therapy has changed from previous best supportive care to the regime of which combination of multiple targeted drugs. As a selective inhibitor of B cell lymphoma 2

10.3389/fonc.2022.912696

TABLE 1 The baseline laboratory data of the patient.

Variable	Baseline value	Reference range
White blood cell count (/ml)	810	3500-9500
Differential count (%)		
Neutrophils	23.5	40-75
Lymphocytes	64.2	20-50
Eosinophils	0	0.4-8
Basophils	1.2	0-1
Monocytes	11.1	3-10
Hemoglobin (g/dl)	8.2	11.5-15
Platelet count (/ml)	77000	125000-350000
Alanine aminotransferase (U/L)	16	7-40
Aspartate aminotranferase (U/L)	15	13-35
Alkaline aminotransferase (U/L)	62	35-100
Albumin (g/L)	40.4	40-55
Globulin (g/L)	21.1	20-40
Lactate dehydrogenase (U/L)	212	120-250
Uric acid (μmol/L)	257	155-357
Urea (mmol/L)	5.08	2.6-7.5
Creatinine (μmol/L)	48	41-73

regulatory protein (Bcl-2), venetoclax has become a backbone drug in the regime for unfit AML patients. It can be combined with hypomethylating agents or reduced dose chemotherapy, such as low-dose cytarabine, resulting in a high-response rate and prolonged overall survival in unfit AML patients (16). Venetoclax has been approved by the Chinese national medical products administration but has not been covered by Chinese medical insurance. Thus, reducing the costs that enable venetoclax to be applicable to many low-income patients is a challenge for clinical practice. In this present case, we added grapefruit juice to the regime venetolcax plus azacitidine and carefully monitored the concentration of venetoclax. The clinical data showed that grapefruit juice could effectively improve the C_{max} of venetoclax and obtain an ideal clinical effect. So it is a successful treatment for this patient.

Based on previous studies, the venetoclax concentration was positively correlated with the AUC curve and reflected the venetoclax exposure (7, 17). In this study, grapefruit juice can significantly increase the C_{max} of venetoclax and improve its effectiveness. We avoided the repeated detection of venetoclax concentration at multiple time points daily to reduce the iatrogenic anemia and cost. In the subsequent clinical trials, it can be considered to verify the pharmacokinetics of venetoclax by detecting the concentration at several time points. For this patient, we have significantly reduced the treatment cost. For other patients taking a sufficient dose of venetoclax, the current monthly cost is 38,880 RMB yuan, whereas that of this patient was 9,720 RMB yuan.

To monitor the side effects caused by grapefruit juice during the therapy period, we detected laboratory and imaging examinations, such as ECG. There was no QTc interval prolonged, and another abnormal result was found. The application of antibacterial was adequate for the infection of the patient. Thus, we did not use other CYP3A4 inhibitors in the whole treatment process. It is worth noting that if an azole antifungal agent such as posaconazole was used for prophylaxis or treatment, the application of grapefruit juice should be temporarily interrupted to avoid excessive venetoclax concentration. In addition, the concurrent use of azole antifungal agents also can decrease the venetoclax dose and reduce the costs, but not superior to grapefruit juice. There were several reasons. First, antifungal prophylaxis is not a universal recommendation but applies to patients with grade 4 neutropenia (neutrophil $< 0.5 \times 10^9$/L), whereas some AML patients without grade 4 neutropenia were not mandatory for antifungal prophylaxis (3, 10, 11, 18). Second, antifungal prophylaxis is usually applied during the myelosuppression period, ceased when recovery from neutropenia, rather than during the entire venetoclax plus azacitidine treatment period

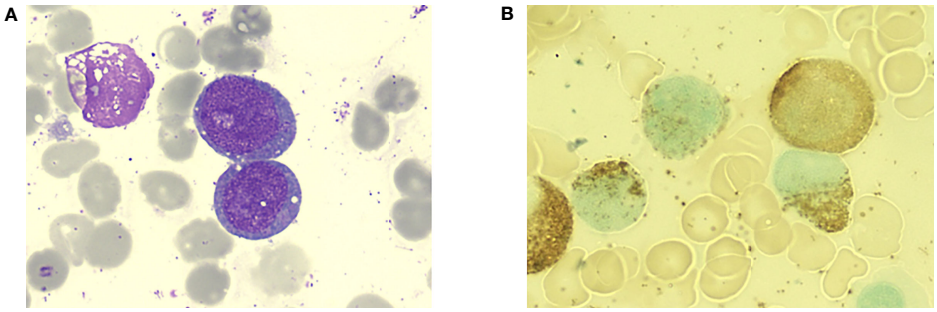

FIGURE 1
Bone marrow aspiration of the patient at the initial diagnosis. **(A)** Large-sized myeloid blasts with slight nuclear irregularities and scant granular cytoplasm (Wright-Giemsa staining, 1000×). **(B)** Peroxidase staining of the blasts was positive.

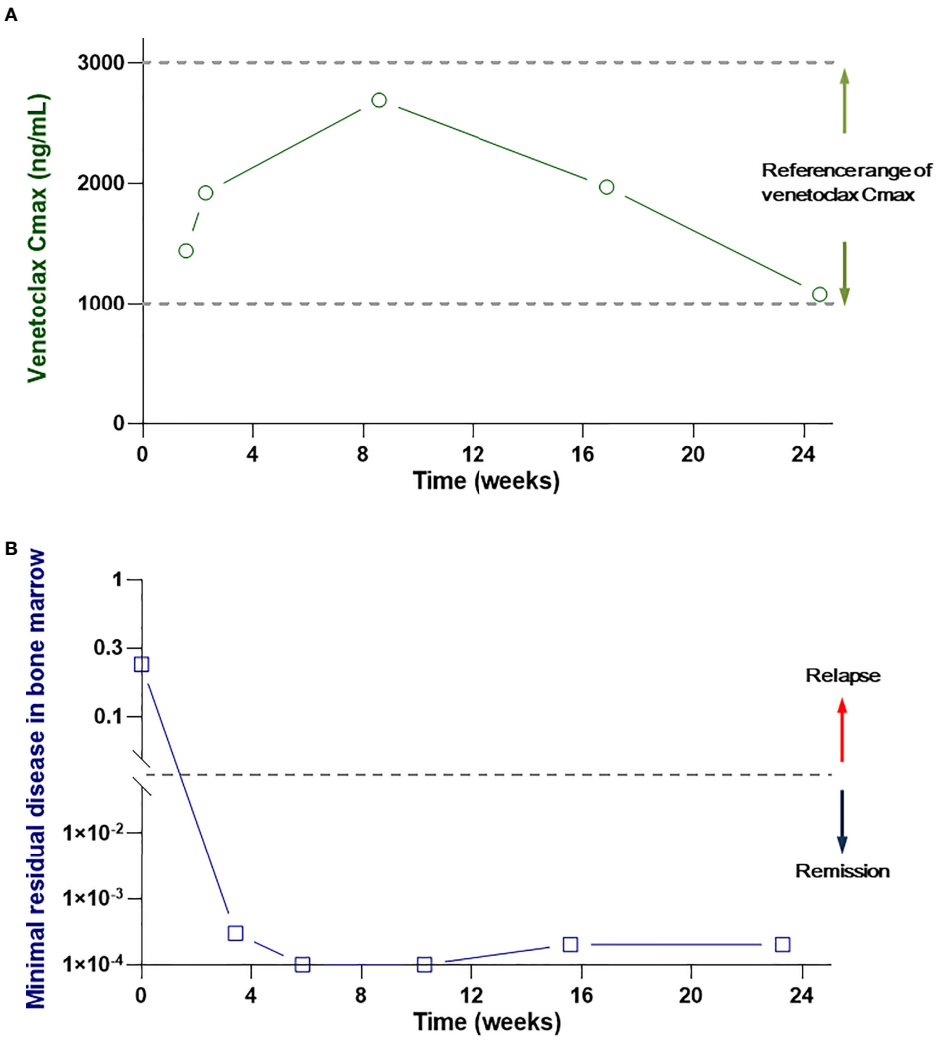

FIGURE 2
(A) The peak venetoclax concentration in the patient's serum. **(B)** MRD in the patient's bone marrow during the treatment and follow-up period.

(10). Furthermore, a real-world observational study revealed significantly prolonged thrombocytopenia in AML patients with concomitant venetoclax and azole antifungals (9). Third, some institutions administer non-azole antifungal prophylaxis for AML patients rather than azole prophylaxis (19). In a retrospective study of 119 patients with AML, only 49 (41%) patients received azole-based antifungal prophylaxis (12). Fourth, the azole agents are more expensive than grapefruit juice. Thus, the treatment costs actually increase when combined with azole antifungals.

The patient herein achieved complete remission and sustained durable remission after the treatment of this regime, but another unknown was how long will this regime's effects last? Venetoclax has shown a promising remission effect in patients with AML, but these patients' progression-free survival has not yet been satisfied (20, 21). The patient in this study was an older woman with adverse prognostic gene mutation. Therefore, after remission, allogeneic hematopoietic stem cell transplantation is a curable approach for the patient. During the treatment and follow-up period, monitoring minimal residual disease by flow cytometry, digital PCR, or qRT-PCR was essential to alert the recurrence. Furthermore, the patients had a frameshift mutation in TP53. As a preclinical study demonstrated, applying sublethal venetoclax in AML may enhance the risk of disease progression. In contrast, sufficiently lethal treatment could maximize the outcomes of AML patients with TP53 mutation (22). A higher dose venetoclax strategy may be applied in future treatment but remains a challenge due to the

deficiency of clinical evidence. A previous study demonstrated that TP53 deficiency impairs sensitivity to combined venetoclax. High-dose idarubicin and co-targeting MCL1 could enhance venetoclax activity in AML (23). Therefore, a regime containing these agents can be an intelligent choice. Further integration of the TP53 target agent into the current administration may be an objective for future studies (24, 25).

There were several limits to this research. First, the patients achieved complete remission and kept relapse free during the follow-up period. However, the follow-up is not long enough to assess the long-term efficacy of this approach. Second, we did not detect the venetoclax concentration at multiple time points and thus, did not collect adequate parameters to evaluate the venetoclax pharmacokinetics. Third, a single case may not enough to demonstrate the clinical safety and efficacy of grapefruit juice plus dose-adjusted venetoclax, a large sample, and long-term clinical trial were needed to confirm the results.

To the best of our knowledge, this is the first case of the combination of CYP3A4 inhibitor food and venetoclax in an AML patient. The efficacy and side effects need to be verified in further studies. The costs and feasibility of the novel drugs should be considered by physicians, especially those in developing countries. Furthermore, the food–drug interaction model presented in this study may provide a reference for other disorders.

Conclusions

In this study, we reported that a patient with AML who could not afford expensive costs achieved complete remission with acceptable side effect by the regime with azacitidine, low-dose venetoclax, and grapefruit juice. This combination approach may enlighten other similar patients, especially those in low-middle income countries.

Data availability statement

The raw data supporting the conclusions of this article will be made available by the authors, without undue reservation.

Ethics statement

This study was reviewed and approved by the ethics committee of the first affiliated hospital of Anhui medical university. The patients/participants provided their written informed consent to participate in this study. Written informed consent was obtained from the individual(s) for the publication of any potentially identifiable images or data included in this article.

Author contributions

QL, ZH and ZL designed the study and wrote the manuscript. ZL, MR and QZ collected the data and treated the patient. MR and WW performed examination and helped analyze examinational data. All authors contributed to the article and approved the submitted version.

Funding

This study was supported by grants from the National natural science foundation (81900118).

Conflict of interest

The authors declare that the research was conducted in the absence of any commercial or financial relationships that could be construed as a potential conflict of interest.

Publisher's note

All claims expressed in this article are solely those of the authors and do not necessarily represent those of their affiliated organizations, or those of the publisher, the editors and the reviewers. Any product that may be evaluated in this article, or claim that may be made by its manufacturer, is not guaranteed or endorsed by the publisher.

References

1. Pollyea DA, Amaya M, Strati P, Konopleva MY. Venetoclax for AML: Changing the treatment paradigm. *Blood Adv* (2019) 3(24):4326–35. doi: 10.1182/bloodadvances.2019000937

2. DiNardo CD, Pratz K, Pullarkat V, Jonas BA, Arellano M, Becker PS, et al. Venetoclax combined with decitabine or azacitidine in treatment-naive, elderly patients with acute myeloid leukemia. *Blood* (2019) 133(1):7–17. doi: 10.1182/blood-2018-08-868752

3. DiNardo CD, Jonas BA, Pullarkat V, Thirman MJ, Garcia JS, Wei AH, et al. Azacitidine and venetoclax in previously untreated acute myeloid leukemia. *N Engl J Med* (2020) 383(7):617–29. doi: 10.1056/NEJMoa2012971

4. DiNardo CD, Pratz KW, Letai A, Jonas BA, Wei AH, Thirman M, et al. Safety and preliminary efficacy of venetoclax with decitabine or azacitidine in elderly patients with previously untreated acute myeloid leukaemia: A non-randomised, open-label, phase 1b study. *Lancet Oncol* (2018) 19(2):216–28. doi: 10.1016/S1470-2045(18)30010-X

5. Patel KK, Zeidan AM, Shallis RM, Prebet T, Podoltsev N, Huntington SF. Cost-effectiveness of azacitidine and venetoclax in unfit patients with previously untreated acute myeloid leukemia. *Blood Adv* (2021) 5(4):994–1002. doi: 10.1182/bloodadvances.2020003902

6. Megias-Vericat JE, Solana-Altabella A, Ballesta-Lopez O, Martinez-Cuadron D, Montesinos P. Drug-drug interactions of newly approved small molecule inhibitors for acute myeloid leukemia. *Ann Hematol* (2020) 99(9):1989–2007. doi: 10.1007/s00277-020-04186-0

7. Freise KJ, Shebley M, Salem AH. Quantitative prediction of the effect of CYP3A inhibitors and inducers on venetoclax pharmacokinetics using a physiologically based pharmacokinetic model. *J Clin Pharmacol* (2017) 57 (6):796–804. doi: 10.1002/jcph.858

8. Agarwal SK, DiNardo CD, Potluri J, Dunbar M, Kantarjian HM, Humerickhouse RA, et al. Management of venetoclax-posaconazole interaction in acute myeloid leukemia patients: Evaluation of dose adjustments. *Clin Ther* (2017) 39(2):359–67. doi: 10.1016/j.clinthera.2017.01.003

9. Rausch CR, DiNardo CD, Maiti A, Jammal NJ, Kadia TM, Marx KR, et al. Duration of cytopenias with concomitant venetoclax and azole antifungals in acute myeloid leukemia. *Cancer* (2021) 127(14):2489–99. doi: 10.1002/cncr.33508

10. Cornely OA, Maertens J, Winston DJ, Perfect J, Ullmann AJ, Walsh TJ, et al. Posaconazole vs. fluconazole or itraconazole prophylaxis in patients with neutropenia. *N Engl J Med* (2007) 356(4):348–59. doi: 10.1056/NEJMoa061094

11. DiNardo CD, Wei AH. How I treat acute myeloid leukemia in the era of new drugs. *Blood* (2020) 135(2):85–96. doi: 10.1182/blood.2019001239

12. Aldoss I, Dadwal S, Zhang J, Tegtmeier B, Mei M, Arslan S, et al. Invasive fungal infections in acute myeloid leukemia treated with venetoclax and hypomethylating agents. *Blood Adv* (2019) 3(23):4043–9. doi: 10.1182/bloodadvances.2019000930

13. Dolton MJ, Roufogalis BD, McLachlan AJ. Fruit juices as perpetrators of drug interactions: The role of organic anion-transporting polypeptides. *Clin Pharmacol Ther* (2012) 92(5):622–30. doi: 10.1038/clpt.2012.159

14. Chen M, Zhou SY, Fabriaga E, Zhang PH, Zhou Q. Food-drug interactions precipitated by fruit juices other than grapefruit juice: An update review. *J Food Drug Anal* (2018) 26(2S):S61–71. doi: 10.1016/j.jfda.2018.01.009

15. Salem AH, Agarwal SK, Dunbar M, Enschede SL, Humerickhouse RA, Wong SL. Pharmacokinetics of venetoclax, a novel BCL-2 inhibitor, in patients with relapsed or refractory chronic lymphocytic leukemia or non-Hodgkin lymphoma. *J Clin Pharmacol* (2017) 57(4):484–92. doi: 10.1002/jcph.821

16. Wei AH, Strickland SAJr., Hou JZ, Fiedler W, Lin TL, Walter RB, et al. Venetoclax combined with low-dose cytarabine for previously untreated patients with acute myeloid leukemia: Results from a phase Ib/II study. *J Clin Oncol* (2019) 37(15):1277–84. doi: 10.1200/JCO.18.01600

17. Freise KJ, Jones AK, Menon RM, Verdugo ME, Humerickhouse RA, Awni WM, et al. Relationship between venetoclax exposure, rituximab coadministration, and progression-free survival in patients with relapsed or refractory chronic lymphocytic leukemia: Demonstration of synergy. *Hematol Oncol* (2017) 35 (4):679–84. doi: 10.1002/hon.2373

18. Jonas BA, Pollyea DA. How we use venetoclax with hypomethylating agents for the treatment of newly diagnosed patients with acute myeloid leukemia. *Leukemia* (2019) 33(12):2795–804. doi: 10.1038/s41375-019-0612-8

19. Rausch CR, DiPippo AJ, Jiang Y, DiNardo CD, Kadia T, Maiti A, et al. Comparison of mold active triazoles as primary antifungal prophylaxis in patients with newly diagnosed acute myeloid leukemia in the era of molecularly targeted therapies. *Clin Infect Dis* (2022) 3:1–8. doi: 10.1093/cid/ciac230

20. Graveno ME, Carulli A, Freyer CW, Mangan BL, Nietupski R, Loren AW, et al. Venetoclax in combination with hypomethylating agents or low dose cytarabine for relapsed and refractory acute myeloid leukemia. *Leukemia Lymphoma* (2022) 63(7):1645–50. doi: 10.1080/10428194.2022.2042688\

21. De Bellis E, Imbergamo S, Candoni A, Lico A, Tanasi I, Mauro E, et al. Venetoclax in combination with hypomethylating agents in previously untreated patients with acute myeloid leukemia ineligible for intensive treatment: A real-life multicenter experience. *Leukemia Res* (2022) 114:106803. doi: 10.1016/j.leukres.2022.106803

22. Thijssen R, Diepstraten ST, Moujalled D, Chew E, Flensburg C, Shi MX, et al. Intact TP-53 function is essential for sustaining durable responses to BH3-mimetic drugs in leukemias. *Blood* (2021) 137(20):2721–35. doi: 10.1182/blood.2020010167

23. Teh TC, Nguyen NY, Moujalled DM, Segal D, Pomilio G, Rijal S, et al. Enhancing venetoclax activity in acute myeloid leukemia by co-targeting MCL1. *Leukemia* (2018) 32(2):303–12. doi: 10.1038/leu.2017.243

24. Cluzeau T, Sebert M, Rahme R, Cuzzubbo S, Lehmann-Che J, Madelaine I, et al. Eprenetapopt plus azacitidine in TP53-mutated myelodysplastic syndromes and acute myeloid leukemia: A phase II study by the groupe francophone des myelodysplasies (GFM). *J Clin Oncol* (2021) 39(14):1575–83. doi: 10.1200/JCO.20.02342

25. Yan W, Zhang Y, Zhang J, Liu S, Cho SJ, Chen X. Mutant p53 protein is targeted by arsenic for degradation and plays a role in arsenic-mediated growth suppression. *J Biol Chem* (2011) 286(20):17478–86. doi: 10.1074/jbc.M111.231639

frontiers | Frontiers in Oncology

TYPE Case Report
PUBLISHED 30 September 2022
DOI 10.3389/fonc.2022.945060

OPEN ACCESS

EDITED BY
Mario Tiribelli,
University of Udine, Italy

REVIEWED BY
Pooja Arora,
University of Delhi, India
Sohinee Sarkar,
Royal Children's Hospital, Australia

*CORRESPONDENCE
Laura Ballotta
laura.ballotta@asugi.sanita.fvg.it

†These authors have contributed equally to this work

SPECIALTY SECTION
This article was submitted to Hematologic Malignancies, a section of the journal Frontiers in Oncology

RECEIVED 16 May 2022
ACCEPTED 29 August 2022
PUBLISHED 30 September 2022

CITATION
Ballotta L, Simonetti O, D'Agaro P, Segat L, Koncan R, Martinez-Orellana P, Dattola F, Orsini E, Marcello A, Dal Monego S, Licastro D, Misin A, Mohamed S, Sbisà E, Lucchini E, De Sabbata GM, Zaja F and Luzzati R (2022) Case report: Long-lasting SARS-CoV-2 infection with post-COVID-19 condition in two patients with chronic lymphocytic leukemia: The emerging therapeutic role of casirivimab/imdevimab. *Front. Oncol.* 12:945060. doi: 10.3389/fonc.2022.945060

Case report: Long-lasting SARS-CoV-2 infection with post-COVID-19 condition in two patients with chronic lymphocytic leukemia: The emerging therapeutic role of casirivimab/imdevimab

Laura Ballotta[1,2*†], Omar Simonetti[3†], Pierlanfranco D'Agaro[1,4], Ludovica Segat[4], Raffaella Koncan[1,4], Pamela Martinez-Orellana[5], Federica Dattola[5,6], Emanuele Orsini[5], Alessandro Marcello[5], Simeone Dal Monego[7], Danilo Licastro[7], Andrea Misin[3], Sara Mohamed[2], Eugenio Sbisà[2], Elisa Lucchini[2], Giovanni Maria De Sabbata[2], Francesco Zaja[1,2] and Roberto Luzzati[1,3]

[1]Dipartimento Clinico di Scienze Mediche, Chirurgiche e della Salute, Università degli Studi di Trieste, Trieste, Italy, [2]Unità Complessa Operativa (UCO) Ematologia, Azienda Sanitaria Universitaria Giuliano Isontina, Trieste, Italy, [3]Struttura Complessa (SC) Malattie Infettive, Azienda Sanitaria Universitaria Giuliano Isontina, Trieste, Italy, [4]Unità Complessa Operativa (UCO) Igiene e Sanità Pubblica, Azienda Sanitaria Universitaria Integrata Giuliano Isontina, Trieste, Italy, [5]Laboratory of Molecular Virology, International Centre for Genetic Engineering and Biotechnology (ICGEB), AREA Science Park, Trieste, Italy, [6]Department of Life Sciences, Università degli Studi di Trieste, Trieste, Italy, [7]Biomedicine, AREA Science Park, Trieste, Italy

Post-coronavirus disease 2019 (post-COVID-19) condition, previously referred to as long COVID, includes a post-acute syndrome defined by the presence of non-specific symptoms occurring usually 3 months from the onset of the acute phase and lasting at least 2 months. Patients with chronic lymphocytic leukemia (CLL) represent a high-risk population for COVID-19. Moreover, the response to SARS-CoV-2 vaccination is often absent or inadequate. The introduction of monoclonal antibodies (mAbs) in the treatment landscape of COVID-19 allowed to reduce hospitalization and mortality in mild–moderate SARS-CoV-2 infection, but limited data are available in hematological patients. We here report the effective use of casirivimab/imdevimab (CI) in the treatment of two CLL patients with persistent infection and post-COVID-19 condition. Full genome sequencing of viral RNA from nasopharyngeal swabs was performed at the time of COVID-19 diagnosis and before the administration of CI. Both patients experienced persistent SARS-CoV-2 infection with no seroconversion for 8 and 7 months, respectively, associated with COVID symptoms. In both cases after the infusion of CI, we observed a rapid negativization of the nasal swabs, the resolution of post-COVID-19 condition, and the development of both the IgG against the trimeric spike

protein and the receptor-binding domain (RBD) of the spike protein. The analysis of the viral genome in the period elapsed from the time of COVID-19 diagnosis and the administration of mAbs showed the development of new mutations, especially in the *S* gene. The genome variations observed during the time suggest a role of persistent SARS-CoV-2 infection as a possible source for the development of viral variants. The effects observed in these two patients appeared strongly related to passive immunity conferred by CI treatment permitting SARS-CoV-2 clearance and resolution of post-COVID-19 condition. On these grounds, passive anti-SARS-CoV-2 antibody treatment may represent as a possible therapeutic option in some patients with persistent SARS-CoV-2 infection.

KEYWORDS

chronic lymphocyte leukemia, COVID - 19, monoclonal antibodies, casirivimab/imdevimab, post COVID-19 condition

Introduction

Although most of the patients affected by the coronavirus disease 2019 (COVID-19) fully recovered within a few weeks, a large proportion of them, up to 76% at 6 months, reported at least one symptom of a post-COVID-19 condition (1). Post-COVID-19 condition (previously referred to as long COVID) occurs in individuals with a history of probable or confirmed severe acute respiratory syndrome coronavirus 2 (SARS-CoV-2) infection usually 3 months from the onset of COVID-19, with symptoms that last for at least 2 months and cannot be explained by an alternative diagnosis. The common symptoms include fatigue, shortness of breath, and cognitive dysfunction among others and generally have an impact on everyday functioning. The symptoms may be new onset following initial recovery from an acute COVID-19 episode or persist from the initial illness, and these symptoms may also fluctuate or relapse over time (2).

Patients with hematological malignancies represent a high-risk population for COVID-19 because of immunodeficiency related to their disease (e.g., hypogammaglobulinemia, dysfunction of the innate and adaptive immune system), immunosuppressive therapies (3), and frequent hospital admissions. A recent meta-analysis on 3,337 hematologic patients with COVID-19 demonstrated a death risk of 34% for adult patients and 4% for pediatric patients. Additionally, the pooled risk of death for lymphoma and chronic lymphocytic leukemia (CLL) patients was 32% and 31%, respectively (4). Furthermore, adult patients with cancer, including hematological patients, are likely to develop post-COVID-19 complications, particularly respiratory symptoms and residual fatigue, in about 15% of the cases with high rates of cessation or modification of anticancer treatment and subsequent impairment of prognosis and survival (5).

Based on these data, hematological patients represent a high-priority population for vaccination in order to mitigate COVID-19 morbidity and mortality. Unfortunately, the experiences of these patients resulted in suboptimal antibody responses following COVID-19 vaccination. For instance, the serologic response to the BNT162b2 mRNA COVID-19 vaccine was about 40% in CLL patients with a lower response rate in patients actively treated with Bruton's tyrosine kinase inhibitors (BTKs) or venetoclax +/− anti-CD20 antibodies (6).

Since the beginning of the COVID-19 pandemic in 2020, the therapy for COVID-19 has focused on the acute viral phase of SARS-CoV-2 infection. The availability of an effective antiviral is even more crucial for unvaccinated patients as well as for immunocompromised patients not responding effectively to vaccination. Various therapeutic options have been explored for patients with COVID-19, including convalescent plasma and immunomodulators, with contrasting results (7–10). In the last year, the therapeutic strategies for COVID-19 have been enriched. With the aim to reduce viral load, prevent hospitalization, and ameliorate the symptoms of COVID-19, the U.S. Food and Drug Administration (FDA) and the European Medicines Agency (EMA) had issued the emergency use authorization (EUA) for monoclonal antibodies (mAbs) targeting the SARS-CoV-2 spike protein. In particular, the combination of bamlanivimab and etesevimab, casirivimab and imdevimab (REGN-COV2), and sotrovimab has been shown to prevent hospitalization and mortality in high-risk outpatients with mild-to-moderate COVID-19 (11–13). Though data regarding the use of mAbs in early COVID-19 cases are more robust (11–13), limited data on their use in immunocompromised patients with prolonged SARS-CoV-2 infection are available (14, 15). Here, we present our experience on the use of mAbs in the treatment of two

patients affected by CLL and post-COVID-19 condition with long-term persistently positive SARS-CoV-2 infection.

Case 1

On 17 January 2021, a 66-year-old man was admitted to the emergency department due to fever, asthenia, ageusia, anosmia, diarrhea, and dyspnea. This patient had a history of type 2 diabetes on metformin therapy and was followed by our hematological department since June 2019 for an untreated CLL associated with severe hypogammaglobulinemia. At diagnosis, the biologic characterization of CLL cells showed unmutated heavy chain variable (IGHV), and the fluorescence *in situ* hybridization (FISH) analysis was positive for trisomy of chromosome 12 with no further alterations of chromosomes 11, 13, and 17 and TP53 wild type. A nasal swab was positive for molecular testing [reverse transcription-polymerase chain reaction (RT-PCR)] of SARS-CoV-2. Arterial blood gas showed hypoxia with pO_2 equal to 57 mmHg in ambient air, and chest X-ray and pulmonary computed tomography (CT) revealed a bilateral interstitial pneumonia. The patient was admitted to the Infectious Diseases (ID) unit for oxygen supply (e.g., high-flow nasal oxygen, HFNC), dexamethasone, and enoxaparin prophylaxis. At admission, his blood tests were as follows: white blood cells 44×10^9/L, neutrophils 2×10^9/L, lymphocytes 41×10^9/L, hemoglobin 87 g/L, platelet count 256×10^9/L, C-reactive protein 106.8 mg/L, D-dimer 2,597 ng/ml, total proteins 60 g/L with severe hypogammaglobulinemia (gamma globulin 6.9%, IgG 4.45 g/L), and stable mild paraproteinemia IgG lambda (1 g/L). During the subsequent period of hospitalization, the patient required a course of antibiotic therapy with piperacillin/tazobactam and gentamycin for hospital-acquired pneumonia. He improved progressively, and 30 days after the admission, the patient was discharged with nasal swabs RT-PCR-positive for SARS-CoV-2. During the following 5 months, the patient continued to complain of dysgeusia, anosmia, dyspnea, asthenia, and foot paraesthesia with a slight impairment in maintaining an erect posture and in walking. Such symptoms were attributable to the post-COVID-19 condition and required a multidisciplinary approach. Nasopharyngeal swab RT-PCR was repeated monthly and gave persistent positive results in detecting SARS-CoV-2 infection. Full genome sequencing was performed on two different patients' samples collected on 25 February (hCoV-19/Italy/FVG-TS-36474928/2021) and on 24 May 2021 (hCoV-19/Italy/FVG-TS-64028678/2021), and these samples were stored at −80°C until processed, together, in the same analytical session [cycle threshold value (Ct) was S 18, N 19, *Orf1ab* 18 for the first sample and S 17, N 18, *Orf1ab* 17 for the second sample]. In both cases, the B.1.177 variant (Pango v.3.1.20 2022-02-28) was identified (for the materials and method, see Supplemental). Interestingly, careful inspection of the sequences identified 21 polymorphisms including the amino-acid T95I (nt 21846) in the spike gene that has been observed in several variants of concern (VOC) including BA.1 (Omicron) (Table 1). A reverse mutation was observed in two positions (nt 17333 and 27826). In 13 sites, the frequency of mutated nucleotide ranged from 20% to 59%, suggesting the emergence at different times. In six sites, a polymorphism was detected in both samples, but the proportion of the mutant nucleotide increased in the second sample from 32% to 72%. Excluding the two reverse mutations, the non-synonymous/synonymous mutation ratio was 13/6, suggesting an ongoing positive selection pressure, and this was higher in the *S* gene (7/1) than the *M* gene (2/1) or *ORF1ab* (4/2). The second swab was also inoculated in Vero E6 cells, and viable virus was recovered demonstrating the infectivity of the sample.

Due to the persistence of SARS-CoV-2 infection, in this patient, we investigated the tissue reservoir harboring the infectious virus. Cells obtained by a nasopharyngeal brush in May 2021 were subjected to single-cell RNA sequencing (scRNA-seq). A total of 2,838 cells were recovered from the analysis, which were clustered and classified based on their expression patterns, as shown in Figure 1. The most represented cellular types were epithelial cells (N = 2,128) and immune cells, including neutrophils (N = 304), T cells (N = 165), B cells (N = 111), macrophages (N = 42), and monocytes (N = 21). As shown in Figure 1, viral RNAs were identified mostly in epithelial cells (red dots, N = 14/16), with residual positivity also in macrophages and T cells (N = 1 each, respectively).

The patient did not develop an anti-SARS-CoV-2 humoral response on plasma collected 6 months after the primary infection; more specifically, no IgG anti-S1-RBD was present in July 2021, while only low levels of IgG against the trimeric spike protein were detected. Due to the persistence of upper respiratory tract SARS-CoV-2 infection and symptoms consistent with post-COVID-19 condition, off-labeled anti-SARS-CoV-2 casirivimab/imdevimab (1,200 mg/1,200 mg) was administered intravenously in the outpatient service of the ID unit on July 28. This therapy was well-tolerated without any adverse reaction. After mAb infusion, the patient had a rapid clinical improvement with the resolution of all post-COVID-associated symptoms in the subsequent 3 weeks. On August 6, the patient had positive anti-spike IgG antibodies, confirmed by two independent immunochemiluminescent tests (see Supplemental). Anti-trimeric spike protein IgG was positive with 2,080 BAU/ml, as well as IgG anti-S1-RBD with 185,311 AU/ml values. Furthermore, two successive RT-PCR nasal swabs performed on September 4 and 8 did not detect SARS-CoV-2, and the virus could not be isolated in Vero E6 cells. The patient has been doing well during the next 4-month follow-up period. A timeline including the clinical and virological courses is presented in Figure 2.

10.3389/fonc.2022.945060

TABLE 1 Comparative mutation analysis of the two sequences from patient 1.

Nucleotide position	Ref. seq (nt)	Sample 25/02 (nt)	No. of reads	% mutation	AA	Sample 24/05 (nt)	No. of reads	% mutation	AA	Gene	Mut. type
487	G	G	6,127		Ser	K	7,998	48%	Ser	*ORF1ab*	S
2534	G	G	1,453		Val	R	1,949	50%	Val/Ile	*ORF1ab*	NS
10369	C	C	1,713		Arg	Y	2,018	24%	Arg	*ORF1ab*	S
12561	A	A	4,307		Gln	W	5,300	44%	Gln/Leu	*ORF1ab*	NS
12570	T	T	3,635		Val	K	4,699	57%	Val/Gly	*ORF1ab*	NS
17333	C	Y	4,988	55% (T)	Met/Thr	C	5,691		Thr	*ORF1ab*	NS
21572	T	T	109	4% (C)	Phe	Y	91	76%	Phe/Leu	*S* (S1)	NS
21846	C	C	1,280		Thr	Y	1,216	36%	Thr/Ile	*S* (S1)	NS
21998	C	C	347	9% (T)	His	Y	643	52%	His/Tyr	*S* (S1)	NS
22191	T	T	877		Ile	Y	1,188	49%	Ile/Thr	*S* (S1)	NS
22986	C	C	155		Ala	Y	331	59%	Ala/Val	*S* (RBD)	NS
23009	G	G	155	8%	Val	R	331	40%	Val/Ile	*S* (RBD)	NS
23580	G	G	6,132		Ser	S	5,789	49%	Ser/Thr	*S* (S1)	NS
24034	C	C	234		Asp	Y	289	53%	Asp	*S* (S1)	S
25421	T	T	5,609		Ile	K	5,894	38%	Ile/Ser	*ORF3a*	NS
25728	C	C	759		Val	Y	778	46%	Val	*ORF3a*	S
26527	C	C	146	18% (T)	Ala	Y	269	50%	Ala/Val	*M*	NS
26847	A	A	1,736	2% (T)	Met	W	1,599	52%	Met/Leu	*M*	NS
26939	A	A	1,790		Val	R	1,699	20%	Val	M	S
27826	T	Y	7,485	43% (C)	Met/Thr	T	6,284		Met	*ORF7b*	NS
27972	C	Y	12,915	22% (T)	Gln/Stop	Y	13,408	59% (T)	Gln/Stop	*ORF8*	S

The polymorphisms identified are indicated together with variation percentages. IUPAC codes are used for nucleotides and amino acids. S/NS means synonymous/non-synonymous mutations.

Case 2

On 17 May 2021, a 67-year-old man presented to the emergency room of our hospital with fever, dyspnea, asthenia, skin, and mucous hemorrhagic manifestations. The patient had a previous diagnosis of CLL (unmutated IGHV gene, positive for 11q deletion with no further alterations of chromosomes 12, 13, and 17 and TP53) that was treated with six cycles of fludarabine, cyclophosphamide, and rituximab (FCR) achieving a complete response in April 2016. Because of progressive symptomatic disease in 2018, he started second-line therapy with ibrutinib with a persistent partial response. During the last 5 years, the patient experienced several bacterial and viral infectious episodes (viral stomatitis, varicelliform herpes zoster with residual neuritis, bacterial infection of the oral cavity, and *Pseudomonas aeruginosa* infection of the nasal cavities). Furthermore, he was vaccinated for COVID-19 with the second dose performed on 9 May 2021 (BNT162b2 mRNA vaccine). At the time of admission to the emergency room, a nasal swab confirmed SARS-CoV-2 infection; blood tests showed moderate anemia (hemoglobin 87 g/L), leukopenia (white blood cells 2.59 × 10 (9)/L, neutrophils 1.08 × 10 (9)/L, lymphocytes 1.45 × 10 (9)/L), severe thrombocytopenia (platelet count 17 × 10 (9)/L), increased acute-phase reactants (C-reactive

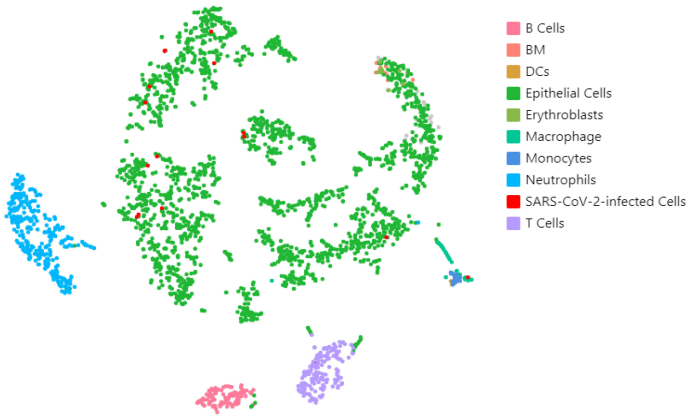

FIGURE 1
Single-cell transcriptome analysis of nasal brush isolated from a chronic SARS-CoV-2 infection. The two-dimensional t-distributed stochastic neighbor embedding (t-SNE) plot, based on n = 2,838 cells, shows the distribution of SARS-CoV-2-infected cells (red dots) into each cluster, representing a different cell type.

protein 192.1 mg/L, procalcitonin 2 ng/ml, and D-dimer level 41,791 ng/ml FEU). Oxygen saturation was 92% and a chest X-ray and a pulmonary CT confirmed interstitial pneumonia. The patient was admitted to the ID unit; ibrutinib therapy was stopped, while treatment with amoxicillin and clarithromycin was started together with supplemental oxygen, methylprednisolone therapy, and red blood cell (RBC) and platelet transfusions. During hospitalization, respiratory failure

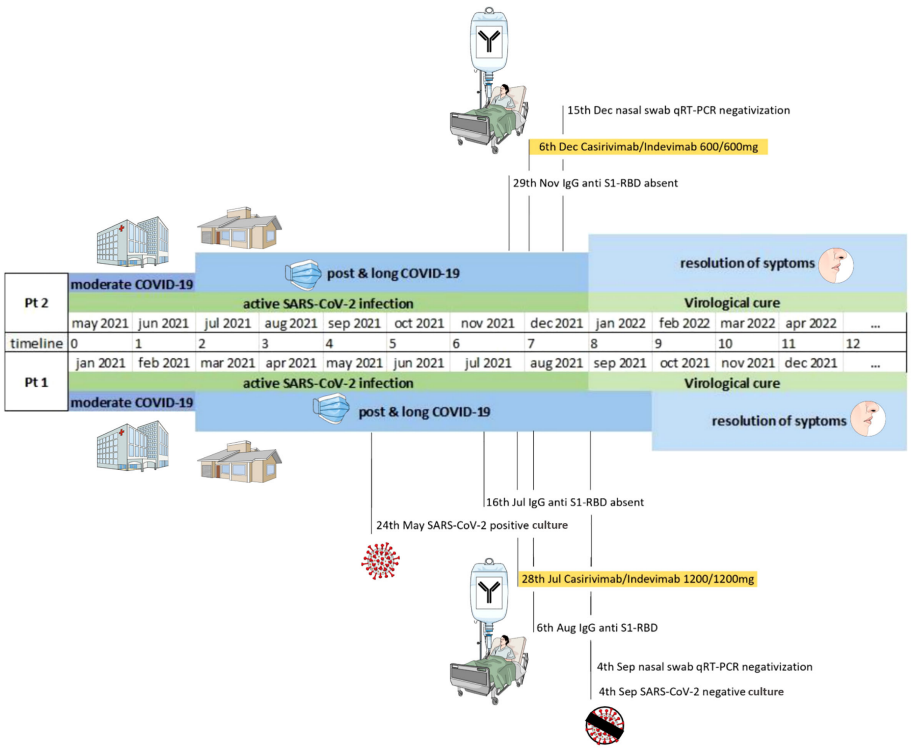

FIGURE 2
Timeline including the virological course and COVID-19-related symptoms in patients 1 and 2.

progressively improved and on May 26, he was transferred to a rehabilitation facility with a positive nasal swab for COVID-19. In the following months, he experienced post-COVID-19 condition with exertional dyspnea, asthenia, and hyposthenia of the leg. Due to the progressive increase of lymphocytosis, SARS-CoV-2 infection, and reduced bone marrow reserve, he was persistently pancytopenic requiring RBC and platelet transfusions until July 2021.

A monthly nasal swab for SARS-CoV-2 showed persistent positivity, and on 29 November 2021, serological testing for SARS-CoV-2 was negative (IgG anti-S1-RBD). Full genome sequencing was performed in two different patients' samples collected on 21 May (hCoV-19/Italy/FVG-GO-36863251/2021) and on 21 July 2021 (hCoV-19/Italy/FVG-GO-36998512/2021), and these samples were stored at −80°C until processed, together, in the same analytical session as described in the methods (see Supplemental) (Ct was S 18.2, *Orf1ab* 19.4 for the first sample and N 21, *Orf1ab* 22 for the second sample). The sequences were deposited in the Global Initiative on Sharing All Influenza Data (GISAID) with accession ID EPI_ISL_7015624.2 and EPI_ISL_7015625.2, respectively. In both cases, the variant B.1.1.7 (Pango v.3.1.20 2022-02-28) was identified. Careful analysis of the sequences identified 19 mutations including a 6-nucleotide deletion in positions 22289–22294 (Table 2). A reverse mutation was observed in two positions (nt 22337 and 23009), and excluding the reverse mutations and deletion, the non-synonymous/synonymous mutation ratio was 7/3. The second swab was also inoculated in Vero E6 cells, and viable virus was recovered demonstrating the infectivity of the sample.

On 6 December 2021, the patient was treated with casirivimab/imdevimab (600mg/600 mg) with good tolerance; a nasal swab for SARS-CoV-2 performed 4 days later was negative. Because of progressive disease, on 30 December 2021, he resumed ibrutinib therapy with no response; on March 2022, BTK and phospholipase Cγ2 (PLCG2) mutations of acquired resistance to ibrutinib therapy were detected. Currently, in April 2022, the patient is in fair clinical conditions, and he started venetoclax therapy. A timeline including the clinical and virological courses is presented in Figure 2.

TABLE 2 Comparative mutation analysis of the two sequences from patient 2.

Nucleotide position	Ref. seq (nt)	Sample 21/05 (nt)	No. of reads	% mutation	AA	Sample 21/07 (nt)	No. of reads	% mutation	AA	Gene	Mut. type
2676	C	Y	538	66%	Pro/Leu	T	7,551	100%	Leu	*ORF1ab*	NS
4230	C	Y	569	70% (T)	Thr/Ile	T	6,051	100%	Ile	*ORF1ab*	NS
5648	A	A	714		Lys	C	8,353	90%	Gln	*ORF1ab*	NS
9515	C	C	693		Leu	T	8,551	100%	Leu	*ORF1ab*	S
9779	T	T	153	15% (A)	Phe/Ile	A	1,476	100%	Ile	*ORF1ab*	NS
13348	G	G	593		Val	T	4,701	89%	Val	*ORF1ab*	S
19862	C	Y	147	31% (T)	Ala/Val	T	1,381	100%	Val	*ORF1ab*	NS
22289	G	G	823		Ala	DEL	12,451	100%	*	*S*	
22290	C	C	821		Ala	DEL	12,452	100%	*	*S*	
22291	T	T	820		Ala	DEL	12,452	100%	*	*S*	
22292	T	T	819		Leu	DEL	12,452	100%	*	*S*	
22293	T	T	819		Leu	DEL	12,458	100%	*	*S*	
22294	A	A	820		Leu	DEL	12,463	100%	*	*S*	
22337	A	W	655	63% (T)	Thr/Ser	A	3,666		Thr	*S*	NS
23009	G	K	123	56% (T)	Val/Lys	G	735		Val	*S*	NS
23012	G	G	123		Glu	A	737	100%	Lys	*S*	NS
25440	G	G	747		Lys	S	10,817	23%	Lys/Asn	*ORF3a*	NS
27720	T	Y	837	47% (C)	Phe	C	10,299	100%	Phe	*ORF7a*	S
27915	G	G	3,830	18% (A)	Gly/Arg	G	54,181		Gly	*ORF8*	NS

The polymorphisms identified are indicated together with variation percentages. IUPAC codes are used for nucleotides and amino acids. S/NS means synonymous/non-synonymous mutations.
*ref seq NC_045512.2.

Discussion

Data from the COVID-19 pandemic have clearly indicated that patients with hematological malignancies are associated with a higher risk to develop multiorgan complications and a significant increased mortality rate upon SARS-CoV-2 infection (3, 4). Because of their immune-incompetent status, secondary to the characteristic of hematological disease and/or treatments adopted to cure it, these patients frequently fail to develop anti-SARS-CoV-2 antibodies or cellular response to primary infection leading to prolonged viral replication (6). The same immune defect leads frequently to an impaired immune response to SARS-CoV-2 vaccination.

Several experiences highlighted this issue; 19 patients with lymphoma treated with chemotherapy regimens, including anti-CD20 antibodies, have been found to show persistent SARS-CoV-2 infection (median duration 65 days, range 3 weeks–12 months), and most of them did not develop anti-SARS-CoV-2 antibodies (16). Similarly, a persistent PCR positivity (defined as SARS-CoV-2 RNA detection ≥30 days after initial positivity) has been observed in 51 (13.9%) of 214 lymphoma patients in a 1-year period of observation. In this series, the risk factors independently associated with prolonged infection were lymphopenia, treatment with anti-CD20 antibodies within 1 year, and cellular therapy including hematopoietic stem cell transplantation (HSCT) (17). Hueso et al. reported a small cohort of lymphoma patients (15) with profound B-cell lymphopenia and prolonged SARS-CoV-2 infection treated with convalescent plasma. The median duration of COVID-19 symptoms was 56 days (range 7–83), and all patients failed to develop SARS-CoV-2 antibodies (18). Other case series described prolonged SARS-CoV-2 infection associated with clinical relapse of COVID-19; for instance, in a patient diagnosed with mantle cell lymphoma (MCL), a blastoid variant was described. He was previously treated with two cycles of bendamustine, cytarabine, and rituximab and experienced persistent SARS-CoV-2 viremia associated with four clinical relapses of COVID-19 effectively treated with remdesivir (19).

On these grounds, the long-term persistent positivity of the SAR-CoV-2 swab observed in our two CLL patients was not surprising. Even though case 1 did not receive any chemotherapy, he had severe hypogammaglobulinemia with the inability to produce neutralizing antibodies (15, 16). As a matter of fact, immunodeficiency in CLL is multifactorial and mediated by T-cell defects, suboptimal complement activity, neutrophil and natural killer cell dysfunction, and altered normal B-cell activity (20). The second patient has been treated with multiple regimens including FCR and, subsequently, ibrutinib due to the progressive disease. Both FCR and ibrutinib are two well-known therapeutic regimens associated with profound immune depression and a higher risk to develop common or opportunistic infections in CLL patients. In particular, patients receiving ibrutinib or, similarly, other BTK inhibitors, which nowadays are more and more adopted as first-line or salvage therapy in CLL, have been associated with a very high risk of COVID-19 complications and mortality (6, 21, 22). The second patient was vaccinated with two doses of mRNA vaccine, the last one on 9 May 2021 before the onset of COVID-19 but unfortunately without achieving active immunization.

Both cases had long complained of symptoms with multiple organ impairment following COVID-19 pneumonia; they did not develop anti-SARS-CoV-2 plasma humoral response and showed persisting positive nasopharyngeal RT-PCR for SARS-CoV-2 for 236 and 199 days, respectively. As suggested by Proal and colleagues (23), SARS-CoV-2 may cause chronic symptoms because it persists in different tissue reservoirs after acute infection as confirmed by the identification of SARS-CoV-2 inert viral RNA and/or proteins. The cell culture obtained by a nasal brush of case 1 detected viral RNA predominantly in epithelial cells but, at a lower extent, also in macrophages and T cells. These findings confirm that SARS-CoV-2 preferentially infects nasal epithelial cells, as already demonstrated by the high levels of angiotensin-converting enzyme 2 (ACE2) expression in this cell type (24). While SARS-CoV-2 infection has been reported also for macrophages by scRNA-seq analysis (25), viral infection of T cells on the contrary has not been reported.

Although data about SARS-CoV-2-acquired mutations in hematological patients are scarce, preliminary experiences demonstrated that persistent viral infection may promote intrahost viral evolution as a consequence of several acquired mutations, particularly in the spike gene. This effect may lead to the emergence of SARS-CoV-2 variants (26, 27) that could negatively impact patients' clinical outcome, particularly in immunosuppressed hosts. In our two patients, indeed, nasopharyngeal swab samples obtained 2 and 3 months apart showed an increasing number of mutations suggestive of an ongoing positive selection pressure, especially in the *S* gene.

To the best of our knowledge, this is the first analysis reporting the successful outcome of persisting SARS-CoV-2 infection associated with post-COVID-19 condition in hematologic patients treated with anti-SARS-CoV-2 mAbs. Following therapy with casirivimab/imdevimab, nasopharyngeal RT-PCR for SARS-CoV-2 became quickly negative in both patients; at the same time, post-COVID-19 condition symptoms progressively improved until completely disappearing in both patients.

There are two case reports in the literature on SARS-CoV-2 persistent infection treated successfully with mAbs; however, such patients were not found to be affected by long COVID (14, 15). On the contrary, despite the proven effectiveness of monoclonal antibodies, secondary acquired mutations of SARS-CoV-2 following monoclonal antibody therapy are emerging as an immune escape resistance mechanism in patients with B-cell malignancies (28).

At present, there are no evidence-based guidelines indicating how to manage persistent COVID-19 infection in asymptomatic as well as post-COVID-19 patients. Although we cannot exclude that the virological and clinical cure of our patients was just a matter of time, the strong time relationship between mAb infusion and viral disappearance is consistent with the favorable effect of mAb therapy in these patients.

In conclusion, our data show that the recovery of our patients might be due to passive immunity conferred by mAb treatment permitting SARS-CoV-2 clearance and resolution of post-COVID-19 condition. Controlled studies are needed to confirm this therapeutic strategy in immunocompromised patients with persisting viral infection and post-COVID-19 condition. Moreover, the variations observed in the sequences obtained in the two samples collected at 2- and 3-month intervals from both patients suggest a role of persistent SARS-CoV-2 infection as a possible source for the development of viral variants.

Data availability statement

The datasets presented in this study can be found in online repositories. The names of the repository/repositories and accession number(s) can be found in the article/Supplementary Material.

Ethics statement

This study was reviewed and approved by Regional Ethics Committee (Unique Regional Ethical Committee, Friuli Venezia-Giulia 16 April 2020), No. CEUR 2020-OS-072. Written informed consent for participation was not required for this study in accordance with the national legislation and the institutional requirements.

Author contributions

LB and OS collected the patient data and wrote the manuscript. PDA analyzed NGS sequencing data and critically revised the manuscript. LS and RK performed SARS-CoV-2 real time PCR and NGS sequencing. PMO performed viral isolation. EO, FD, SDM performed single-cell RNA sequencing. AMa and DL collected and analyzed data and revised the manuscript. FZ and RL critically revised the manuscript and approved the final version of the paper. All the other authors contributed to the article and approved the submitted version.

Acknowledgments

We thanked Fondazione Cassa di Risparmio di Trieste for the purchase of the Illumina MiSeq sequencer (Chromium 10x Genomics testing) and Generali SpA for the support.

Conflict of interest

Dr. LB received honoraria for giving lectures at medical meetings from AbbVie. Dr. FZ received advisory board fees or honoraria for giving lectures at medical meetings from Roche, Celgene, Janssen, Sandoz, Gilead, Novartis, AbbVie, Amgen, Sobi, Argenx, Grifols, Takeda, and BeiGene.

The remaining authors declare that the research was conducted in the absence of any commercial or financial relationships that could be construed as a potential conflict of interest.

Publisher's note

Supplementary material

The Supplementary Material for this article can be found online at: https://www.frontiersin.org/articles/10.3389/fonc.2022.945060/full#supplementary-material

References

1. Huang C, Huang L, Wang Y, Li X, Ren L, Gu X, et al. 6-month consequences of COVID-19 in patients discharged from hospital: A cohort study. *Lancet* (2021) 397(10270):220–32. doi: 10.1016/S0140-6736(20)32656-8

2. WHO. *A clinical case definition of post COVID-19 condition by a Delphi consensus, 6 October 2021* . Available at: https://www.who.int/publications/i/item/WHO-2019-nCoV-Post_COVID-19_condition Clinical_case_definition-2021.1 (Accessed 3 March 2022).

3. Maschmeyer G, De Greef J, Mellinghoff SC, Nosari A, Thiebaut-Bertrand A, Bergeron A, et al. Infections associated with immunotherapeutic and molecular targeted agents in hematology and oncology. A position paper by the European conference on infections in leukemia (ECIL). *Leukemia* (2019) 33(4):844–62. doi: 10.1038/s41375-019-0388-x

4. Vijenthira A, Gong IY, Fox TA, Booth S, Cook G, Fattizzo B, et al. Outcomes of patients with hematologic malignancies and COVID-19: A systematic review

and meta-analysis of 3377 patients. *Blood* (2020) 136(25):2881–92. doi: 10.1182/blood.2020008824

5. Pinato DJ, Tabernero J, Bower M, Scotti L, Patel M, Colomba E, et al. Prevalence and impact of COVID-19 sequelae on treatment and survival of patients with cancer who recovered from SARS-CoV-2 infection: evidence from the OnCovid retrospective, multicentre registry study. *Lancet Oncol* (2021) 22 (12):1669–80. doi: 10.1016/S1470-2045(21)00573-8

6. Herishanu Y, Avivi I, Aharon A, Shefer G, Levi S, Bronstein Y, et al. Efficacy of the BNT162b2 mRNA COVID-19 vaccine in patients with chronic lymphocytic leukemia. *Blood* (2021) 137(23):3165–73. doi: 10.1182/blood.2021011568

7. Cavalcanti AB, Zampieri FG, Rosa RG, Azevedo LCP, Veiga VC, Avezum A, et al. Hydroxychloroquine with or without azithromycin in mild-to-Moderate covid-19. *N Engl J Med* (2020) 383(21):2041–52. doi: 10.1056/NEJMoa2019014

8. Beigel JH, Tomashek KM, Dodd LE, Mehta AK, Zingman BS, Kalil AC, et al. Remdesivir for the treatment of covid-19 - final report. *N Engl J Med* (2020) 383 (19):1813–26. doi: 10.1056/NEJMoa2007764

9. Salama C, Han J, Yau L, Reiss WG, Kramer B, Neidhart JD, et al. Tocilizumab in patients hospitalized with covid-19 pneumonia. *N Engl J Med* (2021) 384(1):20–30. doi: 10.1056/NEJMoa2030340

10. Joyner MJ, Senefeld JW, Klassen SA, Mills JR, Johnson PW, Theel ES, et al. Effect of convalescent plasma on mortality among hospitalized patients with COVID-19: Initial three-month experience. *medRxiv [Preprint]*. (2020) 12:2020.08.12.20169359. doi: 10.1101/2020.08.12.20169359

11. Gupta A, Gonzalez-Rojas Y, Juarez E, Crespo Casal M, Moya J, Falci DR, et al. Early treatment for covid-19 with SARS-CoV-2 neutralizing antibody sotrovimab. *N Engl J Med* (2021) 385(21):1941–50. doi: 10.1056/NEJMoa2107934

12. Dougan M, Nirula A, Azizad M, Mocherla B, Gottlieb RL, Chen P, et al. Bamlanivimab plus etesevimab in mild or moderate covid-19. *N Engl J Med* (2021) 385(15):1382–92. doi: 10.1056/NEJMoa2102685

13. Weinreich DM, Sivapalasingam S, Norton T, Ali S, Gao H, Bhore R, et al. REGN-COV2, a neutralizing antibody cocktail, in outpatients with covid-19. *N Engl J Med* (2021) 384(3):238–51. doi: 10.1056/NEJMoa2035002

14. Rabascall CX, Lou BX, Navetta-Modrov B, Hahn SS. Effective use of monoclonal antibodies for treatment of persistent COVID-19 infection in a patient on rituximab. *BMJ Case Rep* (2021) 14(8):e243469. doi: 10.1136/bcr-2021-243469

15. Drouin AC, Theberge MW, Liu SY, Smither AR, Flaherty SM, Zeller M, et al. Successful clearance of 300 day SARS-CoV-2 infection in a subject with b-cell depletion associated prolonged (B-DEAP) COVID by REGEN-COV anti-spike monoclonal antibody cocktail. *Viruses* (2021) 13(7):1202. doi: 10.3390/v13071202

16. Yasuda H, Mori Y, Chiba A, Bai J, Murayama G, Matsushita Y, et al. Resolution of one-year persisting COVID-19 pneumonia and development of immune thrombocytopenia in a follicular lymphoma patient with preceding rituximab maintenance therapy: A follow-up report and literature review of cases with prolonged infections. *Clin Lymphoma Myeloma Leuk.* (2021) 21(10): e810–6. doi: 10.1016/j.clml.2021.07.004

17. Lee CY, Shah MK, Hoyos D, Solovyov A, Douglas M, Taur Y, et al. Prolonged SARS-CoV-2 infection in patients with lymphoid malignancies. *Cancer Discov* (2021) 12(1):62–73. doi: 10.1101/2021.08.25.21262417

18. Hueso T, Pouderoux C, Péré H, Beaumont AL, Raillon LA, Ader F, et al. Convalescent plasma therapy for b-cell-depleted patients with protracted COVID-19. *Blood* (2020) 136(20):2290–5. doi: 10.1182/blood.2020008423

19. Sepulcri C, Dentone C, Mikulska M, Bruzzone B, Lai A, Fenoglio D, et al. The longest persistence of viable SARS-CoV-2 with recurrence of viremia and relapsing symptomatic COVID-19 in an immunocompromised patient-a case study. *Open Forum Infect Dis* (2021) 8(11):ofab217. doi: 10.1093/ofid/ofab217

20. Schliffke S, Sivina M, Kim E, von Wenserski L, Thiele B, Akyuz N, et al. Dynamic changes of the normal b lymphocyte repertoire in CLL in response to ibrutinib or FCR chemo-immunotherapy. *Oncoimmunology* (2018) 7(4):e1417720. doi: 10.1080/2162402X.2017.1417720

21. Bagacean C, Letestu R, Al-Nawakil C, Brichler S, Lévy V, Sritharan N, et al. Humoral response to mRNA anti-COVID-19 vaccines BNT162b2 and mRNA-1273 in patients with chronic lymphocytic leukemia. *Blood Adv* (2022) 6(1):207–11. doi: 10.1182/bloodadvances.2021006215

22. Borgogna C, Bruna R, Griffante G, Martuscelli L, De Andrea M, Ferrante D, et al. Patterns of neutralizing humoral response to SARS-CoV-2 infection among hematologic malignancy patients reveal a robust immune response in anti-cancer therapy-naive patients. *Blood Cancer J* (2022) 12(1):8. doi: 10.1038/s41408-022-00608-6

23. Proal AD, VanElzakker MB. Long COVID or post-acute sequelae of COVID-19 (PASC): An overview of biological factors that may contribute to persistent symptoms. *Front Microbiol* (2021) 12:698169. doi: 10.3389/fmicb.2021.698169

24. Sungnak W, Huang N, Bécavin C, Berg M, Queen R, Litvinukova M, et al. SARS-CoV-2 entry factors are highly expressed in nasal epithelial cells together with innate immune genes. *Nat Med* (2020) 26(5):681–7. doi: 10.1038/s41591-020-0868-6

25. Grant RA, Morales-Nebreda L, Markov NS, Swaminathan S, Querrey M, Guzman ER, et al. Circuits between infected macrophages and T cells in SARS-CoV-2 pneumonia. *Nature* (2021) 590(7847):635–41. doi: 10.1038/s41586-020-03148-w

26. Truong TT, Ryutov A, Pandey U, Yee R, Goldberg L, Bhojwani D, et al. Increased viral variants in children and young adults with impaired humoral immunity and persistent SARS-CoV-2 infection: A consecutive case series. *EBioMedicine* (2021) 67:103355. doi: 10.1016/j.ebiom.2021.103355

27. Nussenblatt V, Roder AE, Das S, de Wit E, Youn JH, Banakis S, et al. Year-long COVID-19 infection reveals within-host evolution of SARS-CoV-2 in a patient with b cell depletion. *medRxiv [Preprint]*. (2021) 5:2021.10.02.21264267. doi: 10.1101/2021.10.02.21264267

28. Pommeret F, Colomba J, Bigenwald C, Laparra A, Bockel S, Bayle A, et al. Bamlanivimab + etesevimab therapy induces SARS-CoV-2 immune escape mutations and secondary clinical deterioration in COVID-19 patients with b-cell malignancies. *Ann Oncol* (2021) 32(11):1445–7. doi: 10.1016/j.annonc.2021.07.015

frontiers | Frontiers in Oncology

TYPE Case Report
PUBLISHED 18 October 2022
DOI 10.3389/fonc.2022.1031500

OPEN ACCESS

EDITED BY
Arpad Szallasi,
Semmelweis University, Hungary

REVIEWED BY
Agota Szepesi,
Semmelweis University, Hungary
Sam Sadigh,
Brigham and Women's Hospital and Harvard Medical School, United States

*CORRESPONDENCE
Yan Wang
qfsyywy@163.com
Qian Liu
pluto2999@163.com

†These authors have contributed equally to this work and share first authorship

SPECIALTY SECTION
This article was submitted to Hematologic Malignancies, a section of the journal Frontiers in Oncology

RECEIVED 30 August 2022
ACCEPTED 03 October 2022
PUBLISHED 18 October 2022

CITATION
Bi Y, Feng S, Shang J, Liu Q and Wang Y (2022) Case report: simultaneous occurrence of primary pulmonary lymphoma and opportunistic infections in a patient with chronic myeloid leukemia. *Front. Oncol.* 12:1031500. doi: 10.3389/fonc.2022.1031500

Case report: Simultaneous occurrence of primary pulmonary lymphoma and opportunistic infections in a patient with chronic myeloid leukemia

Yazhen Bi[1†], Saran Feng[2†], Jinyu Shang[3], Qian Liu[2*] and Yan Wang[2*]

[1]Department of Hematology, Shandong Provincial Qianfoshan Hospital, Shandong University, Jinan, China, [2]Department of Hematology, The First Affiliated Hospital of Shandong First Medical University & Shandong Provincial Qianfoshan Hospital, Jinan, China, [3]Graduate School, Shandong First Medical University, Jinan, China

Background: The occurrence of primary pulmonary lymphoma (PPL) as a secondary malignancy in patients diagnosed with chronic myeloid leukemia (CML) is extremely rare. As the clinical manifestations are atypical, most patients with PPL tend to be misdiagnosed with pneumonia. When the radiographic features of PPL and pulmonary infection overlap, clinicians can be confused about the diagnosis. Here, we report the first case of coexistence of PPL and opportunistic infections in a patient with CML in chronic phase (CML-CP).

Case presentation: A 55-year-old woman presented with three weeks of hemorrhage of the oral mucosa at the Department of Hematology. After undergoing various examinations, she was diagnosed with CML-CP and was started on imatinib (400 mg/daily). Due to sudden respiratory distress, the patient was admitted to the respiratory intensive care unit 11 months later. Chest computed tomography (CT) revealed ground-glass opacities, patchy shadows, and multiple nodules in both lungs and enlarged mediastinal lymph nodes. The combination of biapenem and voriconazole antibiotic treatments was effective. The patient's respiratory distress was relieved, but there was intermittent coughing. In the following time, the patient developed a fever, and the imaging findings indicated progression of the disease in both lungs. Bronchoalveolar lavage (BAL) identified pathogens of multiple opportunistic infections. The coexistence of lymphomatoid granulomatosis (LYG) was not confirmed in this patient until a second CT-guided biopsy was performed. Ultimately, the patient underwent chemotherapy in time and is currently alive today.

Conclusions: When the patient's recurrent respiratory symptoms and imaging findings do not coincide, secondary tumors should be considered in addition to infection as a diagnosis. In these cases, multiple pathological tissue biopsies should be performed.

KEYWORDS

chronic myeloid leukemia, primary pulmonary lymphoma, opportunistic infections, antibiotic therapy, biopsy, pathology

Introduction

Chronic myeloid leukemia (CML) is a clonal hematopoietic stem cell disorder, characterized by the *BCR-ABL1* fusion gene leading to an aberrant chimeric tyrosine kinase (TK). TK inhibitors (TKIs) can help improve the disease-free survival time in patients with CML. However, the risk of secondary malignancies due to increased survival time of these patients is increased. The cumulative incidence of simultaneous occurrence of CML and other secondary cancers in a singular case has been reported to be less than 5% (1). These mainly comprise cancers of the male genital system and digestive system (2). However, to our knowledge, the diagnosis of primary pulmonary lymphoma (PPL) as a secondary neoplasm during therapy for CML in chronic phase (CML-CP) is extremely rare.

PPL is an uncommon neoplasm that represents 3–4% of all extranodal lymphomas, less than 1% of all lymphomas, and less than 0.5% of all primary pulmonary tumors (3). The rare and nonspecific clinical features of PPL often cause delay and neglect in diagnosis, which negatively affect treatment. A previous study reported a patient who presented with pneumonia-like imaging findings, with a delay in diagnosis of up to 11 years (4). It is common for hematological diseases to be complicated by opportunistic infections, with lung infections being the most common (5). In patients with hematological malignancies, a pulmonary infection may overshadow primary pulmonary lymphoma, posing a challenge for clinicians to diagnose and treat (6). Early identification of the second tumor is particularly important in case of co-infection, to improve outcomes with better treatment options. Here, we present an extremely rare case of simultaneous occurrence of PPL and opportunistic infections in a patient with CML, after 16 months of the primary diagnosis.

Abbreviations: PPL, primary pulmonary lymphoma; CML, chronic myeloid leukemia; CML-CP, CML in chronic phase; CT, computed tomography; BAL, bronchoalveolar lavage; LYG, lymphomatoid granulomatosis; TK, chimeric tyrosine kinase; TKIs, TK inhibitors; NGS, next-generation sequencing; RT-PCR, quantitative reverse transcription polymerase chain reaction; EBV, Epstein–Barr virus; PET/CT, positron emission tomography/computed tomography; FDG, fludeoxyglucose.

Case description

A 55-year-old woman with no past medical history presented with three weeks of hemorrhage of the oral mucosa at the Department of Hematology in August 2019. There were no complaints of fever, cough, fatigue, or ostalgia. Vital signs revealed a temperature of 36.5°C, heart rate of 80 beats/min, respiratory rate of 20 breaths/min, and blood pressure of 125/81 mmHg. The physical examination revealed unremarkable findings. Laboratory test results revealed a white blood cell count of 88.13×10^9/L (normal range, 3.5–9.5×10^9/L) with 67% neutrophils, 2% lymphocytes, 5% basophils, 1% eosinophils, 1% monocytes, 14% myelocytes, 10% metamyelocytes, with an erythrocyte count of 4.18×10^{12}/L (normal range, 3.8–5.1×10^{12}/L) and a platelet count of 640×10^9/L (normal range, 125–350×10^9/L). The lactate dehydrogenase level was 647 U/L (normal range, 135–214 U/L), while erythrocyte sedimentation rate, procalcitonin, liver, and renal function tests were normal. The abdominal ultrasound showed an enlarged spleen. Bone marrow examination showed markedly proliferated granulocytes. The quantitative reverse transcription polymerase chain reaction (RT-PCR) test for *BCR/ABL p210* was positive at the time of diagnosis. Chromosomal analysis revealed 46, XX, t (9,22) (q34; q11). The patient was diagnosed with CML-CP and was started on imatinib (400 mg/daily).

Due to sudden respiratory distress, she was admitted again 11 months later. Her temperature was 36.5°C, heart rate was 137 beats/min, respiratory rate was 34 breaths/min, and blood pressure was 89/64 mmHg. Her cough started 2 months before admission. A physical examination revealed moist rales at the base of the lung. Sputum culture revealed *Stenotrophomonas maltophilia*, filamentous fungi, and traces of *Aspergillus fumigatus*. Routine blood tests showed a white blood cell count of 6.78 $\times10^9$/L, an erythrocyte count of 4.00×10^{12}/L, and a platelet count of 269×10^9/L. A peripheral blood smear revealed no abnormal cells. Procalcitonin was 1.035 ng/mL (normal range, 0–0.05 ng/mL). The serum IgM test for toxoplasma, rubella virus, cytomegalovirus, herpes simplex virus and parvovirus B19 (TORCH) was negative. Influenza, mycoplasma pneumoniae, T cell spot test, Epstein–Barr virus (EBV), cytomegalovirus plasma 1-3-β-d glucan test, and plasma

galactomannan tests were also negative. An electrocardiogram showed sinus tachycardia. There were no abnormalities on the cardiac ultrasound. Chest computed tomography (CT) revealed ground-glass opacities, patchy shadows, and multiple nodules in both lungs and enlarged mediastinal lymph nodes (Figure 1A). She was diagnosed with septic shock and was treated with biapenem and voriconazole. The combination of antibiotic treatments was effective. The patient's respiratory distress was relieved; however, intermittent coughing remained. Another chest CT showed decreased patchy shadows and multiple nodules in both lungs (Figures 1B, C).

She was readmitted 3 months later due to a fever (maximum of 38.5℃). A CT scan showed an increase of the masses in the left lung compared with previous findings (Figures 1D, G). CT-guided percutaneous lung biopsy was conducted on October 28, 2020. The pathological examination showed extensive necrosis of the examined tissue. Periodic acid-silver methenamine staining was negative. Simultaneously, she underwent flexible fiberoptic bronchoscopy, which showed thick and yellow secretions. BAL fluid was sent for next-generation sequencing (NGS), which revealed EBV and *Actinomyces odontolyticus*. The patient received penicillin sodium and acyclovir for anti-infective treatment. The patient's symptoms improved, and she was discharged home from the hospital.

One month later, the patient presented with worsening cough, white sputum, and intermittent fever (maximum of 38.5°C), and was readmitted. CT revealed a reduction in the size of the masses in the upper lobe of the left lung (Figure 1E) and an increase in the size of the masses in the lower lobe of the left lung compared with the previous scan (Figure 1H). Therefore, a second bronchoscopy and bronchoalveolar lavage were performed. Bronchoscopy revealed a white substance in the entrance of the dorsal segment of the left lower lobe. The BAL fluid was sent for NGS, which revealed EBV and *Enterobacter cloacae complex Hoffmann cluster III*. The patient underwent a second CT-guided percutaneous lung biopsy. Histopathological examination of the biopsied lung tissue showed proliferation and vascular infiltration of polymorphic lymphoid cells (Figure 2). Immunohistochemical staining showed that the tumor cells were positive for Pax5, CD20, Bcl-2, EBER and (60%) Ki-67 and negative for Bcl-6, c-MYC, CD10, TdT, CD34, CD117, and MPO. MUM-1 staining was positive (20%); admixed T cells were positive for CD3 and CD7; tuberculosis-polymerase chain reaction was negative; and staining of mycobacteria and fungi were negative. Positron emission tomography/computed tomography (PET/CT) revealed an 18 F-fludeoxyglucose (FDG) increased uptake in the dorsal segment, posterior basal segment, and lateral basal segment of the left lower lobe

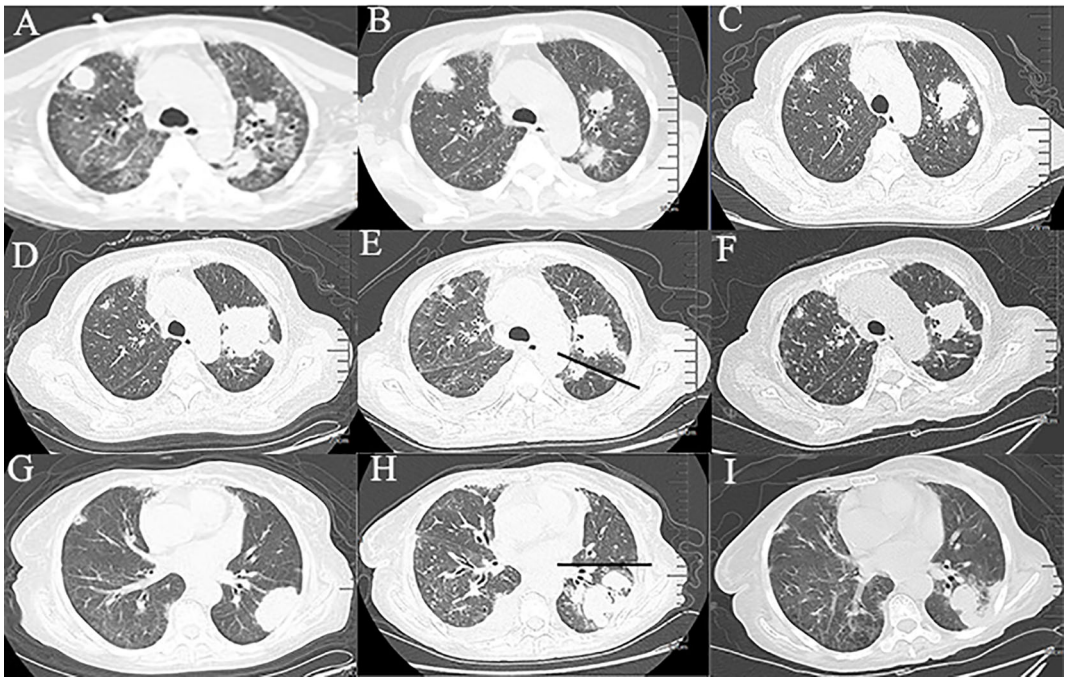

FIGURE 1
Chest computed tomography at different time periods. **(A–C)** Changes of ground-glass opacities, patchy shadows, and multiple nodules in both lungs within 50 days. **(D, E)** Changes of masses in the upper lobe of the left lung within 20 days. (The straight line indicates the left interlobar fissure). **(G, H)** Changes of the masses in the lower lobe of the left lung within 20 days. (The straight line indicates the interlobar fissure). **(F, I)** Imaging findings after 2 courses of chemotherapy.

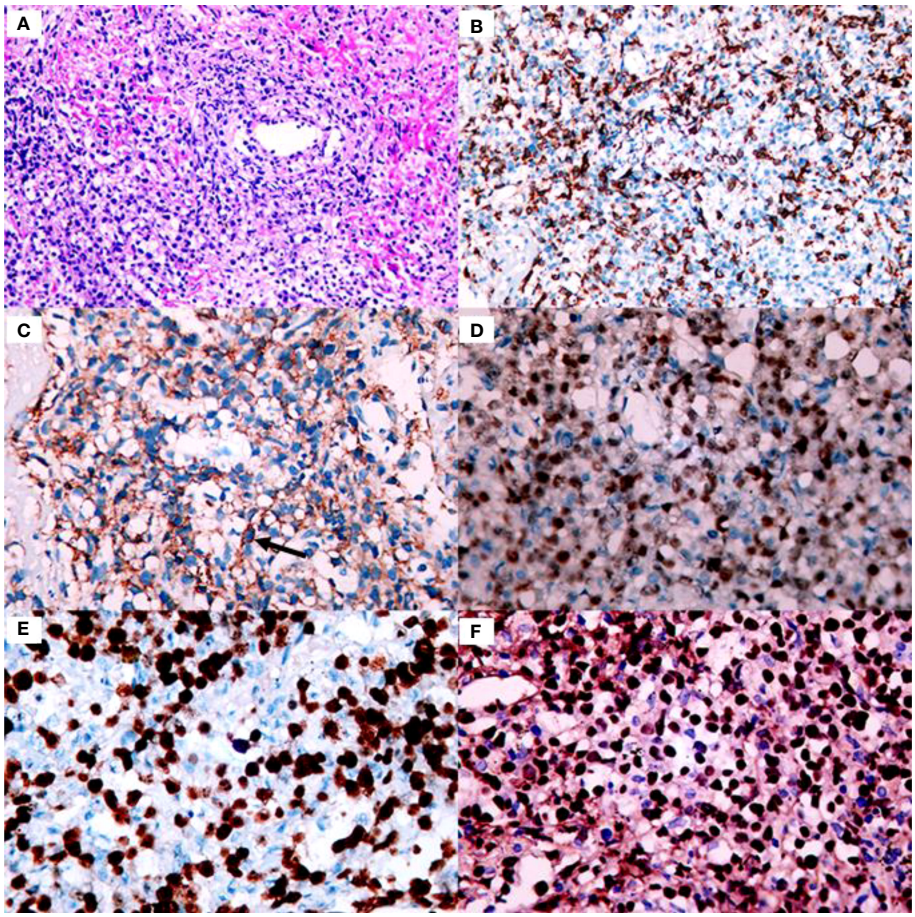

FIGURE 2
Histology and immunohistochemistry of the core biopsy from the lung is consistent with lymphomatoid granulomatosis grade 3.
(A) Proliferation and vascular infiltration of polymorphic lymphoid cells (×200 magnification). **(B)** Admixed T cells were positive for CD3 (×200 magnification). **(C)** Scattered CD20 positive large B-cells are detected-with arrows on the picture (×400 magnification). **(D)** The large cells are strongly stained with Pax5 (×400 magnification). **(E)** The large cells are positive for Ki-67 (×400 magnification). **(F)** The number of EBER positive cells is above 50/HPF consistent with garde 3 lymphomatoid granulomatosis (×400 magnification).

(Figure 3). FDG uptake was not detected in the mediastinal lymph nodes, thus excluding secondary lung infiltration of nodal/mediastinal DLBCL (Figures 3G–I). Bone marrow aspiration did not show involvement of lymphoma cells. *BCR-ABL* (RT-PCR) was 0.0%. Furthermore, laboratory results showed an EBV DNA load of 2.07×10^4 IU/mL (normal range, <5000 IU/mL) and lactate dehydrogenase level of 348 U/L. The patient was diagnosed with lymphomatoid granulomatosis (grade 3). She stopped imatinib treatment and instead received R-CHOP (rituximab, cyclophosphamide, doxorubicin, vincristine, and prednisone) therapy. Her clinical manifestations improved, and chest CT scan revealed a reduction of the multiple nodules and masses in both lungs after 2 courses of chemotherapy (Figures 1F, I). Moreover, five months following imatinib withdrawal, flumatinib was then administered as a treatment for CML. The hematological remission of CML was maintained, and *BCR-ABL* transcript level remained undetectable by RT-PCR. As of August 16, 2022, the patient was still alive.

Discussion

We experienced a case of a patient who presented with hemorrhage of the oral mucosa and was diagnosed with CML and treated with imatinib. After 11 months, she developed respiratory distress. The initial diagnosis of the patient was a pulmonary infection. After multiple antibiotic treatments, the patient's pulmonary symptoms and imaging manifestations improved. However, the patient developed fever and the imaging findings continued to progress in both lungs. BAL showed pathogens of multiple opportunistic infections. A

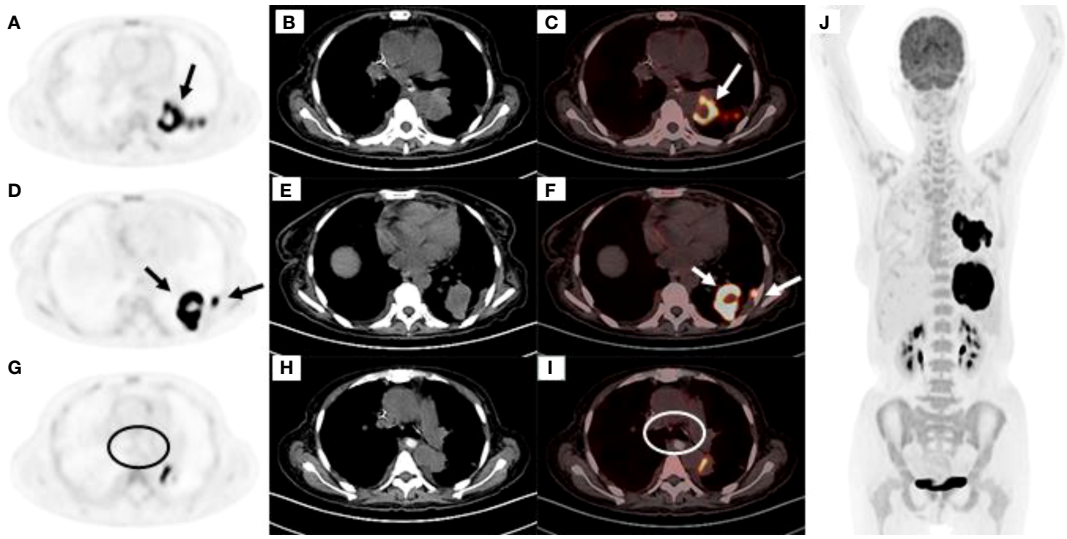

FIGURE 3
(A–C) High FDG uptake at the dorsal segment of the left lower lobe **(A)** PET image, **(B)** CT mediastinal window, **(C)** PET and CT fusion images. **(D–F)** High FDG uptake at the posterior basal segment and lateral basal segments of the left lower lobe **(D)** PET image, **(E)** CT mediastinal window, **(F)** PET and CT fusion images. **(G–I)** No FDG uptake was observed in the mediastinal lymph nodes as shown within the circle **(G)** PET image, **(H)** CT mediastinal window, **(I)** PET and CT fusion images. **(J)** Except for the left lung tumor, there was no obviously high metabolism in other parts of the body.

second CT-guided biopsy was performed to establish the coexistence of PPL. Finally, the patient underwent chemotherapy in time and is currently alive.

With the success of TKI therapy, the prognosis of patients with CML has remarkably improved. However, secondary therapy-related malignancies may be an associated concern. Sasaki et al. demonstrated that compared with the general population, 13,276 patients with newly diagnosed CML had an increased incidence of a second malignancy (2). Pathogenic theories of these relations remain unclear. Lymphomatoid granulomatosis (LYG) is an EBV-driven B-cell lymphoproliferative disease and is often associated with immunosuppression or immunodeficiency states (7). The main site of involvement is the lungs. Salmons et al. (8). and Yazdi et al. (9). have presented case reports describing LYG following imatinib administration. Both cases were secondary to gastrointestinal stromal tumors. It has been shown that imatinib affects the function of T-lymphocytes and peripheral blood progenitor cells (10, 11). Whether imatinib-induced immunosuppression further promotes LYG development should be considered (8). However, some studies suggest that long-term TKI therapy for patients does not increase the incidence of secondary cancers (1, 12). Pina-Oviedo et al. (13) described a patient with chronic myeloid leukemia, diagnosed with LYG, after 24 years of treatment with interferon and cytarabine. Cytarabine was discontinued and imatinib was used to treat CML. Surprisingly, the patient underwent spontaneous remission of LYG. Therefore, a fear of the possibility of a second tumor secondary to CML should not be a reason for discontinuing TKI therapy. The etiology of coexistence of two haematopoietic malignancies may involve tumor-associated immune deficiency, side effects of therapy, host genetic predisposition, environmental exposures or a combination of these factors (8). Vigilant regular follow-ups are needed in the diagnosis and treatment of patients with CML (14).

PPL is infrequent and defined as a clonal lymphoproliferative disorder that affects one or both lungs (parenchyma and/or bronchi) without extra-pulmonary involvement at the time of diagnosis or over the following three months (15). PPL is rarer than secondary pulmonary lymphoma. The median age for PPL diagnosis is 60 years, and it is more common among woman (15). Mucosa-associated lymphoid tissue lymphoma is the most frequent subtype, accounting for 60% to 80% of all the PPLs, followed by diffuse large B-cell lymphoma (10-25%). Others rare types of PPLs include LYG, mantle B-cell lymphoma and follicular lymphoma (16). About 36% of cases are asymptomatic at the time of diagnosis (17). There are no specific clinical symptoms of PPL. Common symptoms include cough, fever, bloody sputum, dyspnea, and chest pain (18). In previous reports, the imaging findings of PPL were consolidations, ground-glass opacities, and single/multiple nodules, with perilymphatic and/or bronchovascular spread (19). As the clinical manifestations are atypical, most patients are initially misdiagnosed with pulmonary tuberculosis, pneumonia, fungal infections, or lung cancer.

The lung is a common site of opportunistic infections. The risk for an opportunistic infection is influenced by the exposure, host defenses, and interactions between the intrinsic virulence properties of microorganisms and the immune system (20).

When pulmonary opportunistic infections occur in patients with hematologic malignancies, they often deteriorate rapidly and evolve to respiratory failure. Several reports have suggested that imatinib may damage the immune system, increasing the risk of infections such as varicella, herpes zoster, and hepatitis B (21). The possibility of infection was considered, and based on the sputum culture and BAL, we identified pathogens of multiple opportunistic infections, including *Stenotrophomonas maltophilia*, filamentous fungi, *Aspergillus fumigatus*, EBV, *Actinomyces odontolyticus*, and *Enterobacter cloacae complex Hoffmann cluster III*. After anti-infective treatment, the patient's clinical manifestations were significantly improved. Afterward, the patient's symptoms and imaging findings worsened, which prompted an alternative diagnosis. There are also some cases of co-diagnosed lymphoma and infections, such as invasive pulmonary aspergillosis (6), tuberculosis (22), and *Aspergillus fumigatus* (23). Regardless of the etiology, timely diagnosis and treatment are crucial. After two lung biopsies, we finally established the diagnosis of LYG. Lymphoma may be missed and misdiagnosed when a hematological tumor and infection overlap in the same site.

Our case is the first report of the simultaneous occurrence of PPL and pulmonary infection in a patient with CML. To provide some references for early detection and diagnosis, we offer the following suggestions: First, in the presence of pulmonary symptoms, such as cough, in patients with pre-existing hematologic disorders, the presence of a second neoplasm should be considered in addition to pulmonary infection. Second, when a CT scan shows pneumonia-like imaging findings, it is difficult to differentiate PPL from pneumonia. In our case, after anti-infective treatment, the patient's symptoms, signs, and imaging findings improved, causing misinterpretation of the findings as recovery. When the patient's recurrent respiratory symptoms and imaging do not coincide, repeated actively pathological tissue biopsies should be conducted. At last, the accurate diagnosis of PPL requires histopathological examination. The common methods include CT-guided percutaneous lung biopsy, an open thoracotomy or a video-assisted thoracoscopic lung biopsy, and flexible fiberoptic bronchoscopy.

In conclusion, when CML is diagnosed, the presence of lung lesions may lead to consideration of a secondary infection, causing clinicians to overlook other possible diagnoses. Diagnosing concurrent PPL and pulmonary infection is challenging. When the patient's recurrent respiratory symptoms and imaging do not match, alternative diagnoses should be considered. In such cases, repeated pathological tissue biopsies should be performed.

Data availability statement

The original contributions presented in the study are included in the article/supplementary material. Further inquiries can be directed to the corresponding authors.

Ethics statement

The studies involving human participants were reviewed and approved by the Shandong Provincial Qianfoshan Hospital. The patients/participants provided their written informed consent to participate in this study. Written informed consent was obtained from the individual(s) for the publication of any potentially identifiable images or data included in this article.

Author contributions

YB and SF searched relevant references and drafted the manuscript. JS collected part of the data. QL and YW originated the work, made comments, and revised the manuscript. All authors contributed to the article and approved the submitted version.

Acknowledgments

The authors thank the patient for allowing us to understand her condition and write this case report.

Conflict of interest

The authors declare that the research was conducted in the absence of any commercial or financial relationships that could be construed as a potential conflict of interest.

Publisher's note

References

1. Verma D, Kantarjian H, Strom SS, Rios MB, Jabbour E, Quintas-Cardama A, et al. Malignancies occurring during therapy with tyrosine kinase inhibitors (TKIs) for chronic myeloid leukemia (CML) and other hematologic malignancies. *Blood* (2011) 118:4353–8. doi: 10.1182/blood-2011-06-362889

2. Sasaki K, Kantarjian HM, O'Brien S, Ravandi F, Konopleva M, Borthakur G, et al. Incidence of second malignancies in patients with chronic myeloid leukemia in the era of tyrosine kinase inhibitors. *Int J Hematol* (2019) 109:545–52. doi: 10.1007/s12185-019-02620-2

3. Kim D, Elgeti T, Penzkofer T, Steffen IG, Jensen LJ, Schwartz S, et al. Enhancing the differentiation of pulmonary lymphoma and fungal pneumonia in hematological patients using texture analysis in 3-T MRI. *Eur Radiol* (2021) 31:695–705. doi: 10.1007/s00330-020-07137-5

4. Yu JY, Ma TG, Li YL, Ma L, Gao R, Liu J. An 11 years delayed diagnosis of primary pulmonary diffuse large b cell lymphoma. *Chin Med J (Engl)* (2019) 132:2000–1. doi: 10.1097/CM9.0000000000000378

5. Hardak E, Avivi I, Berkun L, Raz-Pasteur A, Lavi N, Geffen Y, et al. Polymicrobial pulmonary infection in patients with hematological malignancies: prevalence, co-pathogens, course and outcome. *Infection* (2016) 44:491–7. doi: 10.1007/s15010-016-0873-3

6. Shao L, Jiang L, Wu S, Yu L, Wang L, Huang X. Simultaneous occurrence of invasive pulmonary aspergillosis and diffuse large b-cell lymphoma: case report and literature review. *BMC Cancer* (2020) 20:15. doi: 10.1186/s12885-019-6471-x

7. Melani C, Jaffe ES, Wilson WH. Pathobiology and treatment of lymphomatoid granulomatosis, a rare EBV-driven disorder. *Blood* (2020) 135:1344–52. doi: 10.1182/blood.2019000933

8. Salmons N, Gregg RJ, Pallalau A, Woolhouse I, Geh I, Taniere P. Lymphomatoid granulomatosis in a patient previously diagnosed with a gastrointestinal stromal tumour and treated with imatinib. *J Clin Pathol* (2007) 60:199–201. doi: 10.1136/jcp.2005.036541

9. Yazdi AS, Metzler G, Weyrauch S, Berneburg M, Bitzer M, Muller-Hermelink HK, et al. Lymphomatoid granulomatosis induced by imatinib-treatment. *Arch Dermatol* (2007) 143:1222–3. doi: 10.1001/archderm.143.9.1222

10. Miranda MB, Lauseker M, Kraus MP, Proetel U, Hanfstein B, Fabarius A, et al. Secondary malignancies in chronic myeloid leukemia patients after imatinib-based treatment: long-term observation in CML study IV. *Leukemia* (2016) 30:1255–62. doi: 10.1038/leu.2016.20

11. Hehlmann R, Muller MC, Lauseker M, Hanfstein B, Fabarius A, Schreiber A, et al. Deep molecular response is reached by the majority of patients treated with imatinib, predicts survival, and is achieved more quickly by optimized high-dose imatinib: results from the randomized CML-study IV. *J Clin Oncol* (2014) 32:415–23. doi: 10.1200/JCO.2013.49.9020

12. Pilot PR, Sablinska K, Owen S, Hatfield A. Epidemiological analysis of second primary malignancies in more than 9500 patients treated with imatinib. *Leukemia* (2006) 20:148. doi: 10.1038/sj.leu.2404025

13. Pina-Oviedo S, Miranda RN, Medeiros LJ. Cancer therapy-associated lymphoproliferative disorders: An under-recognized type of immunodeficiency-associated lymphoproliferative disorder. *Am J Surg Pathol* (2018) 42:116–29. doi: 10.1097/PAS.0000000000000954

14. Cai Z, Liu S, Zi J, Ma J, Ge Z. A case of primary gastric diffuse large b-cell lymphoma occurring in chronic myeloid leukemia. *Onco Targets Ther* (2019) 12:5917–23. doi: 10.2147/OTT.S212838

15. Pina-Oviedo S, Weissferdt A, Kalhor N, Moran CA. Primary pulmonary lymphomas. *Adv Anat Pathol* (2015) 22:355–75. doi: 10.1097/PAP.0000000000000090

16. Hu M, Gu W, Chen S, Mei J, Wang W. Clinical analysis of 50 cases of primary pulmonary lymphoma: A retrospective study and literature review. *Technol Cancer Res Treat* (2022) 21:15330338221075529. doi: 10.1177/15330338221075529

17. Borie R, Wislez M, Antoine M, Fleury-Feith J, Thabut G, Crestani B, et al. Clonality and phenotyping analysis of alveolar lymphocytes is suggestive of pulmonary MALT lymphoma. *Respir Med* (2011) 105:1231–7. doi: 10.1016/j.rmed.2011.03.018

18. Cadranel J, Wislez M, Antoine M. Primary pulmonary lymphoma. *Eur Respir J* (2002) 20:750–62. doi: 10.1183/09031936.02.00404102

19. Cozzi D, Dini C, Mungai F, Puccini B, Rigacci L, Miele V. Primary pulmonary lymphoma: imaging findings in 30 cases. *Radiol Med* (2019) 124:1262–9. doi: 10.1007/s11547-019-01091-z

20. Kumar R, Ison MG. Opportunistic infections in transplant patients. *Infect Dis Clin North Am* (2019) 33:1143–57. doi: 10.1016/j.idc.2019.05.008

21. Daniels JM, Vonk-Noordegraaf A, Janssen JJ, Postmus PE, van Altena R. Tuberculosis complicating imatinib treatment for chronic myeloid leukaemia. *Eur Respir J* (2009) 33:670–2. doi: 10.1183/09031936.00025408

22. Sachdev R, Duggal R, Agrawal K, Goel S. Coexistent nodal diffuse Large b-cell lymphoma with extrapulmonary tuberculosis: A rare case. *Int J Surg Pathol* (2016) 24:70–2. doi: 10.1177/1066896915604458

23. Malhotra P, Singh K, Gill P, Sahni S, Makaryus M, Talwar A. Pseudomembranous tracheitis caused by aspergillus fumigatus in the setting of high grade T-cell lymphoma. *Respir Med Case Rep* (2017) 21:42–5. doi: 10.1016/j.rmcr.2017.03.016

frontiers | Frontiers in Oncology

TYPE Case Report
PUBLISHED 24 October 2022
DOI 10.3389/fonc.2022.983585

OPEN ACCESS

EDITED BY
Liren Qian,
Fifth Medical Center of the PLA General Hospital, China

REVIEWED BY
Julie Bruneau,
Assistance Publique Hopitaux De Paris, France
Daisuke Niino,
University of Occupational and Environmental Health Japan, Japan

*CORRESPONDENCE
Yanhui Liu
Yanhuiliu1124@163.com

†These authors have contributed equally to this work and share first authorship

SPECIALTY SECTION
This article was submitted to Hematologic Malignancies, a section of the journal Frontiers in Oncology

RECEIVED 01 July 2022
ACCEPTED 03 October 2022
PUBLISHED 24 October 2022

CITATION
Zhang F, Li W, Cui Q, Chen Y and Liu Y (2022) Angioimmunoblastic T-cell lymphoma with extensive follicular dendritic cell and fibroblastic reticular cell network proliferation mimicking follicular dendritic cell sarcoma: A case report with pathologic, immunophenotypic, and molecular findings.
Front. Oncol. 12:983585.
doi: 10.3389/fonc.2022.983585

Angioimmunoblastic T-cell lymphoma with extensive follicular dendritic cell and fibroblastic reticular cell network proliferation mimicking follicular dendritic cell sarcoma: A case report with pathologic, immunophenotypic, and molecular findings

Fen Zhang†, Wenyu Li†, Qian Cui, Yu Chen and Yanhui Liu*

Department of Pathology, Guangdong Provincial People's Hospital, Guangdong Academy of Medical Sciences, Guangzhou, China

Angioimmunoblastic T-cell lymphoma (AITL) is a common type of nodal peripheral T-cell lymphoma, which always presents with extensive follicular dendritic cell (FDC) meshwork. Here, we report a case of AITL combined with extensive spindle cell meshwork. Spindle cells occupied were positive for the FDC markers CD21, CD23, and CD35. Furthermore, some cells were positive for desmin and smooth muscle actin (SMA), suggesting the differentiation of fibroblastic reticular cell (FRC). Interestingly, the proliferation of spindle cells was so extensive that was easily misdiagnosed as FDC sarcoma (FDCS). Next-generation sequencing showed that the common mutations reported in AITL, including *RHOA*, *TET2*, and *IDH2*, were also detected in this case, while the genes that are recurrently mutated in FDCS were not detected. Regrettably, the patient died 19 months later. Overall, we highlight the unusual morphologic features in an AITL patient with extensive FDC and FRC network that may be misdiagnosed as FDCS, and careful morphological observation and immunochemical and molecular examinations are crucial for an accurate diagnosis.

KEYWORDS

angioimmunoblastic T-cell lymphoma, follicular dendritic cell, mutation, diagnosis, morphology

Introduction

Angioimmunoblastic T-cell lymphoma (AITL) is a rare aggressive malignant tumor derived from mature T-follicular helper (TFH) cells. It is the second most common type of peripheral T-cell lymphomas (PTCLs) and accounts for about 20% (1). Patients with AITL are always diagnosed with advanced stages, and the 5-year survival is only about 30% (2). Generally, the diagnosis of AITL is confirmed by experienced pathologists according to the results of biopsies. The lymph node architecture is partially or totally effaced by small to medium atypical T cells that are typically positive for CD2, CD3, CD4, CD5, CD10, BCL6, C-X-C motif chemokine ligand 13 (CXCL13), ICOS, and programmed cell death 1 (PD-1). The neoplastic cells always congregate near high endothelial venules and are surrounded by expended follicular dendritic cell (FDC) meshwork and inflammatory cell infiltrates (3). However, a small subset of AITL cases still remains difficult to diagnose, and exploitation of the potent supplementary diagnostic methods is of importance.

Nodal FDC sarcoma (FDCS) is a very rare entity usually affecting cervical and abdominal lymph nodes and is generally considered as an indolent tumor with weak aggressiveness (4). Expansion of FDC is common in AITL patients, but discrimination of the unusual expanded FDC meshwork and FDCS is quite difficult. Previously, Benharroch et al. (5) reported a Jewish case who presented with the combination of AITL and FDCS, but the possibility of AITL with an excessively expanded FDC meshwork could not be excluded by the author based on the results of histological examination. Rogges et al. (6) recently reported an Italian patient diagnosed with AITL and FDC expansion, who excluded FDCS based on the results of histopathology and mutation profile. Similarly, we report a Chinese female patient who was diagnosed with AITL with extensive FDC networks mimicking FDCS. She progressed to recurrence and refractory disease and died from AITL after 19 months of the diagnosis.

Case presentation

A 40–45-year-old woman arrived for consultation with facial swelling that affected eating and breathing as well as the palpable "nodules" in both groins in June 2017. Figure 1 summarizes the important events of this patient according to the timeline. Generalized lymphadenopathy and multiple nodules in the bilateral parotid glands [standard uptake value (SUV)max 17.2] were found, as examined by the PET-CT. However, nasopharyngeal biopsy and right cervical lymph node fine-needle aspiration showed no evidence of tumor. In addition, no monoclonal bands were found as detected by serum immunofixation electrophoresis. Thus, she was clinically diagnosed as having plasmacytosis and given prednisone and methotrexate. Meanwhile, she received Chinese herbal medicine from another hospital. Cervical lymph node enlargement regressed, while the bilateral inguinal lymph node size remained unchanged after the treatment.

One year later, the patient presented with significantly enlarged inguinal lymph nodes on both sides, increased local skin temperature, local tenderness, surface redness, and left lower extremity edema. A right inguinal lymph node biopsy was carried out. The normal structure of the lymph node was effaced (Figure 2A), with hyperplasia of several kinds of cells and perinodal infiltration. In most of the areas, the proliferation of spindle cells was dominant, with vortex distribution (Figure 2B). Some areas were dominated by medium-sized lymphoid tumor cells with mild atypia, unclear cell boundary, and abundant pale cytoplasm (Figure 2C). Affluent branching of high endothelial small vessels, mixed with small lymphocytes, plasma cells (Figure 2D), eosinophils, and neutrophils was seen in the background (Figure 2E), together with few scattered large immunoblastic cells (Figure 2F). The immunohistochemistry (IHC) staining demonstrated that the spindle cells were positive for complement C3d receptor 2 (CD21) (Figure 3A), CD23 (Figure 3B), CD35 (Figure 3C), and desmin (Figure 3D) and

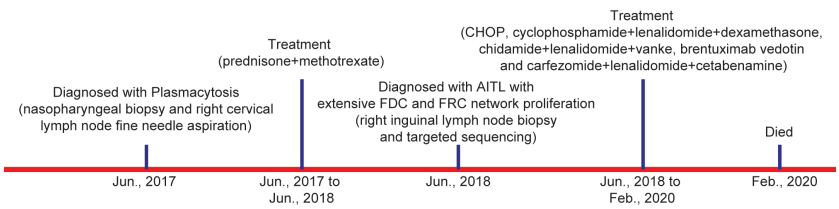

FIGURE 1
Diagnosis and treatment process of the patient. (AITL, angioimmunoblastic T-cell lymphoma; FDC, follicular dendritic cell; FRC, fibroblastic reticular cell).

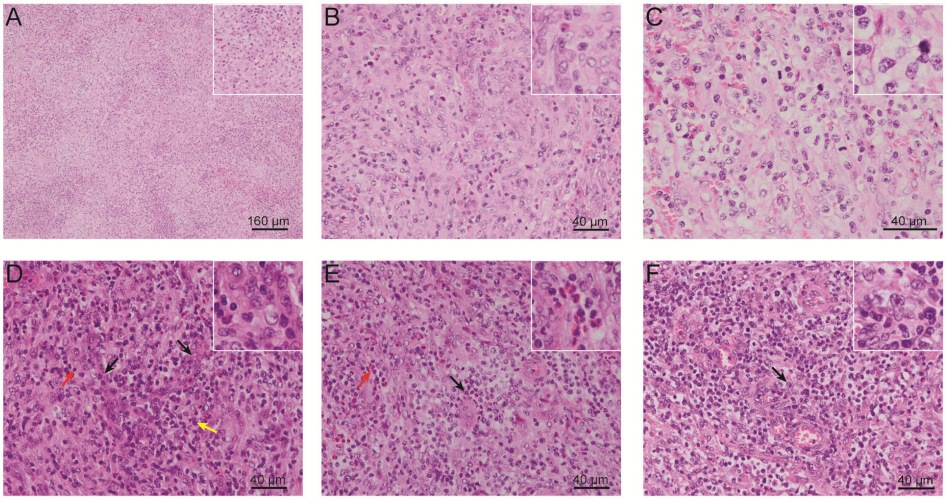

FIGURE 2
Representative H&E-stained images of the patient's right inguinal lymph node. **(A)** Cell hyperplasia and perinodal infiltration. **(B)** Vortex distribution of spindle cells. **(C)** Medium-sized lymphoid tumor cells with mild atypia, unclear cell boundary, and abundant pale cytoplasm. Abundant branching of high endothelial small vessels, mixed with **(D)** small lymphocytes and plasma cells, **(E)** eosinophils and neutrophils, and **(F)** few scattered large immunoblastic cells. (H&E, Eosin & Hematoxylin).

partially positive for SMA (Figure 3E). The lymphoid tumor cells were positive for CD3 (Figure 4A), CD4, CD10 (Figure 4B), PD-1 (Figure 4C), CXCL13 (Figure 4D), and T cell receptor, bF1 (*TCRbF1*) and negative for CD20, CD8, and T cell receptor, g (TCRg). The Ki-67 index of the tumor cells was about 60%, while majority of the spindle cells were negative for Ki-67 staining (Figures 4E, F). *In situ* hybridization for Epstein-Barr virus (EBV)-encoded small RNA (EBER) showed that a few

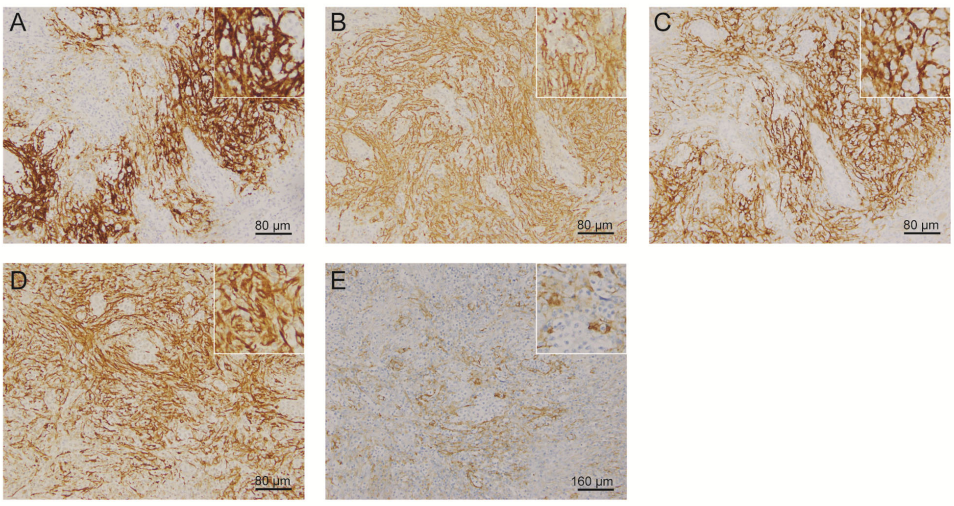

FIGURE 3
Representative IHC staining images of spindle cells. Spindle cells were positive for **(A)** CD21, **(B)** CD23, **(C)** CD35, **(D)** desmin, and **(E)** SMA. (IHC, immunohistochemistry; SMA, smooth muscle actin).

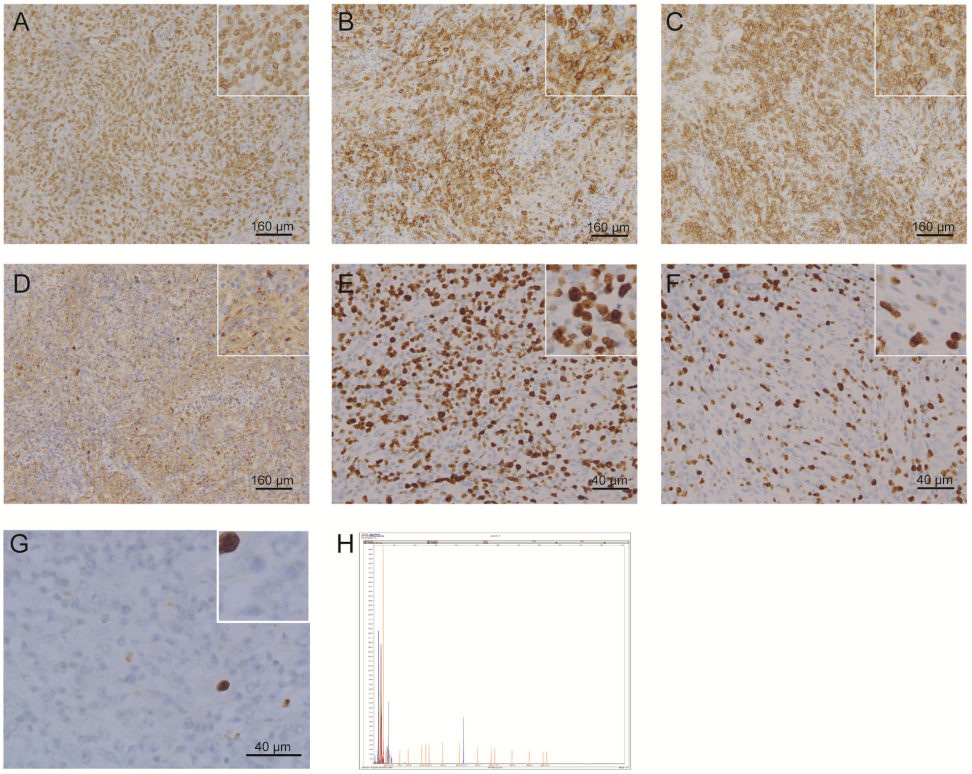

FIGURE 4
Representative IHC staining images and detection of clonal rearrangement of the *TCR* gene in lymphoid tumor cells. Lymphoid tumor cells were positive for **(A)** CD3, **(B)** CD10, **(C)** PD-1, and **(D)** CXCL13. **(E, F)** Lymphoid tumor cells were positive for Ki-67, while most of the spindle cells were negative for Ki-67 staining. **(G)** A few scattered immunoblastic large cells were positive for EBER. **(H)** Clonal rearrangement of *TCRβ* was observed. (IHC, immunohistochemistry; TCR, T cell receptor; PD-1, programmed cell death 1; CXCL13, C-X-C motif chemokine ligand 13; EBER, Epstein-Barr virus encoded small RNA).

scattered immunoblastic large cells were positive for EBER (Figure 4G). Clonal rearrangement of *TCRβ* gene was detected (Figure 4H).

To further describe the characteristics of this case, we also carried out next-generation sequencing (DNA sequencing) to detect the mutation profile of the lymph node sample. Mutations of 571 lymphoma-related genes (Supplementary Table S1) were detected on Novaseq (Illumina, San Diego, CA, USA). Variants, including single-nucleotide variations (SNVs) and Indels (insertion and deletion), were screened by Shanghai Rightongene Biotechnology Co., Ltd. (Shanghai, China), based on the following filter conditions: 1) SNVs or Indels with a variant allele frequency (VAF) ≥1% were retained; 2) SNVs or Indels with a mutation allele frequency (MAF) ≥0.001 in databases of the 1000 Genomes (1KG) Project (7), ExAC_ALL, and ExAC_EAS (8) were removed; 3) SNVs or Indels including stopgain, stoploss, frameshift, non-frameshift, and splicing sites were retained; 4) missense variants that are predicted to be deleterious by SIFT and PolyPhen-2 were retained. According to this, mutations in *RHOA*, *TET2*, *IDH2*, *ERG*, *JAK1*, *EGFR*, *MUC4*, *MYH11*, *PKP2*, *ARHGAP29*, *CCND1*, and *SAMD9* genes were detected (Table 1).

Based on the results of histological examination and mutational characteristics, the diagnosis of AITL (at a stage of IV) with extensive FDC and fibroblastic reticular cell (FRC) network proliferation was confirmed in July 2018.

The anti-AITL therapeutic schedules for this patient were complex (Figure 1). First, she received CHOP (cyclophosphamide, Adriamycin, vincristine, and prednisone) combined with 20 mg chidamide for six cycles. After the first cycle of chemotherapy, skin pruritus was relieved, as well as the swelling of the left lower extremity. However, the disease progressed. Then, she was injected with gemcitabine hydrochloride. Two cycles later, the CT examination indicated that she achieved stable disease (SD). Unluckily, the patient developed fever and infection and was treated with moxifloxacin. Also, she was given cyclophosphamide, lenalidomide, and dexamethasone owing to the increased pleural effusion and poor mental state. Following one cycle of the treatment, she achieved SD but had a cough that was so

10.3389/fonc.2022.983585

TABLE 1 Summary of the results for the targeted NGS screening.

Gene	cDNA change	Protein change	VAF	Minor allele frequency[a]			Functional prediction[b]	
				1KG	ExAC_ALL	ExAC_EAS	SIFT	PolyPhen-2
RHOA	c.50G>T	p.Gly17Val	11.97%	0	0	0	Damaging	Damaging
TET2	c.4138C>T	p.His1380Tyr	9.80%	0.0004	0.0001	0	Damaging	Damaging
TET2	c.5604delT	p.His1868fs	11.52%	0	0	0	–	–
IDH2	c.516G>C	p.Arg172Ser	9.24%	0	0	0	Damaging	Damaging
ERG	c.874A>T	p.Lys292*	38.59%	0	0.00004	0.0005	–	–
JAK1	c.2635C>T	p.Arg879Cys	1.08%	0	0.00002	0.0001	Damaging	Damaging
EGFR	c.2033C>T	p.Thr678Met	7.78%	0	0.00003	0	Damaging	Damaging
MUC4	c.11918G>T	p.Ser3973Ile	40.06%	0	0.0001	0	–	Damaging
MYH11	c.3172C>T	p.Arg1058Trp	45.30%	0	0	0	Damaging	Damaging
PKP2	c.1943T>C	p.Phe648Ser	7.21%	0	0	0	Damaging	Damaging
ARHGAP29	c.221C>A	p.Thr74Asn	35.05%	0	0.00005	0.0006	Damaging	Damaging
CCND1	c.409C>A	p.Leu137Met	47.00%	0	0.00002	0.0004	Damaging	Damaging
SAMD9	c.689G>A	p.Arg230His	43.20%	0.0002	0.0002	0	Damaging	Damaging

[a]Minor allele frequencies were estimated according to the databases of the 1000 Genomes (1KG) Project, ExAC_ALL, and ExAC_EAS.
[b]Variant pathogenicity was assessed by the SIFT and PolyPhen-2 tools. *Stopgain. cDNA, complementary DNA; IKG, 1,000 genomes project; ExAC_EAS, ExAC_East Asian.

frequent to lie at night. Then, the treatment regimen was changed into chidamide, lenalidomide, and Velcade. Disappointingly, the disease progressed again, and brentuximab vedotin (a monoclonal antibody of CD30) was given. Three cycles later, the symptoms were not improved, and multiple lung lesions in both lungs were detected. Based on this, she was diagnosed as having recurrent refractory AITL. Subsequently, salvage therapy (carfezomide, lenalidomide, and cetabenamine) was recommended. Cough and sputum were improved after the treatment. Regrettably, she died from AITL in February 2020.

Discussion

In the present study, we reported a Chinese female patient who was diagnosed as having AITL combined with extensive spindle cell network. This patient was diagnosed as having plasmacytosis without detectable tumor cells 1 year before the diagnosis. Several research groups assessed the behavior of plasma cells in AITL, which ranged from reactive plasmacytosis to striking clonal proliferation (9–11). The performance status of AITL patients with exuberant polyclonal plasmacytosis was significantly worse compared to those in AITL patients without exuberant polyclonal plasmacytosis, but patients with plasmacytosis responded well to chemotherapy and immunosuppressants and had a favorable outcome (10). This case was biopsied twice at the initial onset of disease. However, the nasopharyngeal site was often infected and inguinal lymph nodes presented with more necrotic area, which affected the diagnosis. Thus, how to take biopsy to improve the diagnostic success rate still remains a big challenge for clinicians.

It was uncertain whether the extensive proliferation of spindle cells was an accompanying tumor or not at first. The proliferation of spindle cells was more extensive than other AITL cases, which was easily misdiagnosed as FDCS. In this case, the morphology of spindle cells was gentle without atypia and mitosis, and most of the spindle cells were negative for Ki-67 staining while the Ki-67 index of tumor cells was about 60%. Thus, FDCS was excluded for which the Ki-67 index was always less than 30%. Moreover, parts of the spindle cells expressed desmin and SMA, suggesting that FRCs existed. Similarly, the proliferation of both FDC and FRC in AITL has been reported by Jones et al. (12). Recently, Benharroch et al. (5) reported a Jewish case who was diagnosed with the combination of AITL and FDCS only based on the histopathology. However, the authors acknowledged that they cannot provide sufficient evidence to exclude excessive FDC meshwork proliferation from FDCS. Also, Starkey et al. (13) described an elderly male patient with peripheral T-cell lymphoma (PTCL) accompanied by an excessive FDC network mimicking FDCS. Such cases of extensive FDC hyperplasia challenge pathological examination alone.

Next-generation sequencing emerges as a reliable method for the adjuvant diagnosis of lymphoma. It has been demonstrated that *TET2*, $RHOA^{G17V}$, *DNMT3A*, and *IDH2* are the most common mutated genes in AITL, with a mutation frequency of 80% (14–18), 50%–70% (15–19), 20%–40% (15–18, 20), and 20%–30% (15–18, 21), respectively. Among them, *TET2*, *DNMT3A*, and *IDH2* are three genes encoding epigenetic enzymes (18). *RHOA* encodes a small GTPase in either active GTP-bound or inactive GDP-bound forms. The mutation of $RHOA^{G17V}$ induces the phosphorylation of VAV1 (a guanine exchange factor) and then promotes the enhancement of T-cell receptor (TCR) signaling *in vitro* (22). In this case,

mutations in *TET2*, *RHOA*^{G17V}, and *IDH2* genes were detected, further confirming the diagnosis of AITL.

Recently, Rogges et al. (6) reported an expansion of FDC in a patient with AITL based on the results of both histopathology and mutational profile. Mutations in genes (i.e., *RHOA*, *DNMT3A*, *TET2*, and *IDH2*) associated with AITL were detected, while the mutations in genes recurrent in FDCS, such as the nuclear factor (NF)κB pathway-involving genes (*BIRC3*, *NFKBIA*, *TRAF3*, *SOCS3*, *CYLD*, and *TNFAIP3*) and tumor suppressor genes (*CDKN2A*, *RB1*, and *TP53*) (23), were detected. Consistently, mutations in *RHOA*, *TET2*, *IDH2*, *ERG*, *JAK1*, *EGFR*, *MUC4*, *MYH11*, *PKP2*, *ARHGAP29*, *CCND1*, and *SAMD9* genes were detected in our patient, none of which was involved in FDCS. These results emphasize the importance of next-generation sequencing in the diagnosis of lymphoma, as well as the differential diagnosis of the expanded FDC meshwork and FDCS.

This patient received various anticancer regimens, including CHOP, gemcitabine hydrochloride, chidamide, lenalidomide, Velcade, and monoclonal antibodies against CD30. However, the curative effect was unsatisfactory, the disease progressed, and the patient died, suggesting a poor prognosis of this case with AITL and extensive FDC and FRC networks.

Taken together, this study described a rare case of AITL combined with extensive FDC and FRC networks mimicking FDCS in a female patient. This case highlights the heterogeneity of the clinical presentation of AITL, and a combination of histological examination and next-generation sequencing may help the clinical diagnosis and initiate treatment of this kind of disease. It is crucial to include more of the same cases to summarize the features of AITL combined with extensive FDC and FRC networks and thereafter to develop efficient treatment methods.

Data availability statement

The original contributions presented in the study are included in the article/Supplementary Material. Further inquiries can be directed to the corresponding author.

Ethics statement

The studies involving human participants were reviewed and approved by Guangdong Provincial People's Hospital/Guangdong Academy of Medical Sciences. The patients/participants provided their written informed consent to participate in this study. Written informed consent was obtained from the individual(s) for the publication of any potentially identifiable images or data included in this article.

Author contributions

YL, FZ, and WL contributed to the study conception and design. Material preparation, data collection and analysis were performed by YL, FZ, WL, QC, YC, and YL. The first draft of the manuscript was written by FZ and WL. All authors reviewed the manuscript. All authors contributed to the article and approved the submitted version.

Funding

This study was supported by Natural Science Foundation of Guangdong Province (no. 2019A1515011643).

Acknowledgments

We thank Shanghai Rightongene Biotechnology Co. Ltd. (Shanghai, China) for assisting in molecular detection.

Conflict of interest

The authors declare that the research was conducted in the absence of any commercial or financial relationships that could be construed as a potential conflict of interest.

Publisher's note

Supplementary material

The Supplementary Material for this article can be found online at: https://www.frontiersin.org/articles/10.3389/fonc.2022.983585/full#supplementary-material

References

1. Vose J, Armitage J, Weisenburger D. International peripheral T-cell and natural Killer/T-cell lymphoma study: Pathology findings and clinical outcomes. *J Clin Oncol: Off J Am Soc Clin Oncol* (2008) 26(25):4124–30. doi: 10.1200/JCO.2008.16.4558

2. Bellei M, Federico M. The outcome of peripheral T-cell lymphoma patients failing first-line therapy: A report from the prospective international T-cell project. *Haematologica* (2019) 104(4):e178. doi: 10.3324/haematol.2019.218305

3. Moskowitz AJ. Practical treatment approach for angioimmunoblastic T-cell lymphoma. *J Oncol Pract* (2019) 15(3):137–43. doi: 10.1200/JOP.18.00511

4. Dalia S, Jaglal M, Chervenick P, Cualing H, Sokol L. Clinicopathologic characteristics and outcomes of histiocytic and dendritic cell neoplasms: The Moffitt cancer center experience over the last twenty five years. *Cancers* (2014) 6 (4):2275–95. doi: 10.3390/cancers6042275

5. Benharroch D, Zekzer M, Nalbandyan K. Angioimmunoblastic T-cell lymphoma: A questionable association with follicular dendritic cell sarcoma. *Case Rep Hematol* (2017) 2017:9601094. doi: 10.1155/2017/9601094

6. Rogges E, Pelliccia S, Lopez G, Barresi S, Tafuri A, Alaggio R, et al. Angioimmunoblastic T-cell lymphoma with exuberant Cd30-positive follicular dendritic cell proliferation in a sars-Cov-2 patient: The role of mutational analysis to exclude an associated follicular dendritic cell sarcoma. *Int J Mol Sci* (2022) 23 (16):9346. doi: 10.3390/ijms23169349

7. Abecasis GR, Altshuler D, Auton A, Brooks LD, Durbin RM, Gibbs RA, et al. A map of human genome variation from population-scale sequencing. *Nature* (2010) 467(7319):1061–73. doi: 10.1038/nature09534

8. Zou J, Valiant G, Valiant P, Karczewski K, Chan SO, Samocha K, et al. Quantifying unobserved protein-coding variants in human populations provides a roadmap for Large-scale sequencing projects. *Nat Commun* (2016) 7:13293. doi: 10.1038/ncomms13293

9. Singh N, Sharma A, Pasricha S, Agrawal N, Bhurani D, Gupta G, et al. Florid plasmacytosis in angioimmunoblastic T cell lymphoma: A diagnostic conundrum. *Indian J Hematol Blood Transfusion: Off J Indian Soc Hematol Blood Transfusion* (2018) 34(1):188–90. doi: 10.1007/s12288-017-0824-x

10. Nagoshi H, Kuroda J, Kobayashi T, Maegawa S, Chinen Y, Kiyota M, et al. Clinical manifestation of angioimmunoblastic T-cell lymphoma with exuberant plasmacytosis. *Int J Hematol* (2013) 98(3):366–74. doi: 10.1007/s12185-013-1411-z

11. Sokol K, Kartan S, Johnson WT, Alpdogan O, Nikbakht N, Haverkos BM, et al. Extreme peripheral blood plasmacytosis mimicking plasma cell leukemia as a presenting feature of angioimmunoblastic T-cell lymphoma (Aitl). *Front Oncol* (2019) 9:509. doi: 10.3389/fonc.2019.00509

12. Jones D, Jorgensen JL, Shahsafaei A, Dorfman DM. Characteristic proliferations of reticular and dendritic cells in angioimmunoblastic lymphoma. *Am J Surg Pathol* (1998) 22(8):956–64. doi: 10.1097/00000478-199808000-00005

13. Starkey CR, Corn AI, Porensky RS, Viswanatha D, Wilson CS. Peripheral T-cell lymphoma with extensive dendritic cell network mimicking follicular dendritic cell tumor: A case report with pathologic, immunophenotypic, and molecular findings. *Am J Clin Pathol* (2006) 126(2):230–4. doi: 10.1309/Q1YK-AU1X-XEN3-NVKQ

14. Quivoron C, Couronne L, Della Valle V, Lopez CK, Plo I, Wagner-Ballon O, et al. Tet2 inactivation results in pleiotropic hematopoietic abnormalities in mouse and is a recurrent event during human lymphomagenesis. *Cancer Cell* (2011) 20 (1):25–38. doi: 10.1016/j.ccr.2011.06.003

15. Sakata-Yanagimoto M, Enami T, Yoshida K, Shiraishi Y, Ishii R, Miyake Y, et al. Somatic rhoa mutation in angioimmunoblastic T cell lymphoma. *Nat Genet* (2014) 46(2):171–5. doi: 10.1038/ng.2872

16. Odejide O, Weigert O, Lane AA, Toscano D, Lunning MA, Kopp N, et al. A targeted mutational landscape of angioimmunoblastic T-cell lymphoma. *Blood* (2014) 123(9):1293–6. doi: 10.1182/blood-2013-10-531509

17. Wang C, McKeithan TW, Gong Q, Zhang W, Bouska A, Rosenwald A, et al. Idh2r172 mutations define a unique subgroup of patients with angioimmunoblastic T-cell lymphoma. *Blood* (2015) 126(15):1741–52. doi: 10.1182/blood-2015-05-644591

18. Chiba S, Sakata-Yanagimoto M. Advances in understanding of angioimmunoblastic T-cell lymphoma. *Leukemia* (2020) 34(10):2592–606. doi: 10.1038/s41375-020-0990-y

19. Yoo HY, Sung MK, Lee SH, Kim S, Lee H, Park S, et al. A recurrent inactivating mutation in rhoa gtpase in angioimmunoblastic T cell lymphoma. *Nat Genet* (2014) 46(4):371–5. doi: 10.1038/ng.2916

20. Palomero T, Couronne L, Khiabanian H, Kim MY, Ambesi-Impiombato A, Perez-Garcia A, et al. Recurrent mutations in epigenetic regulators, rhoa and fyn kinase in peripheral T cell lymphomas. *Nat Genet* (2014) 46(2):166–70. doi: 10.1038/ng.2873

21. Cairns RA, Iqbal J, Lemonnier F, Kucuk C, de Leval L, Jais JP, et al. Idh2 mutations are frequent in angioimmunoblastic T-cell lymphoma. *Blood* (2012) 119 (8):1901–3. doi: 10.1182/blood-2011-11-391748

22. Fujisawa M, Sakata-Yanagimoto M, Nishizawa S, Komori D, Gershon P, Kiryu M, et al. Activation of rhoa-Vav1 signaling in angioimmunoblastic T-cell lymphoma. *Leukemia* (2018) 32(3):694–702. doi: 10.1038/leu.2017.273

23. Griffin GK, Sholl LM, Lindeman NI, Fletcher CD, Hornick JL. Targeted genomic sequencing of follicular dendritic cell sarcoma reveals recurrent alterations in nf-kappab regulatory genes. *Modern Pathol: Off J United States Can Acad Pathol Inc* (2016) 29(1):67–74. doi: 10.1038/modpathol.2015.130

frontiers | Frontiers in Oncology

TYPE Case Report
PUBLISHED 24 October 2022
DOI 10.3389/fonc.2022.932254

OPEN ACCESS

EDITED BY
Jose-Maria Ribera,
Germans Trias i Pujol Health Science Research Institute (IGTP), Spain

REVIEWED BY
Monica Balzarotti,
Humanitas Research Hospital, Italy
Michele Merli,
University of Insubria, Italy
Maria Chiara Tisi,
San Bortolo Hospital, Italy

*CORRESPONDENCE
Jianmin Yang
chhyangjianmin@163.com

SPECIALTY SECTION
This article was submitted to Hematologic Malignancies, a section of the journal Frontiers in Oncology

RECEIVED 29 April 2022
ACCEPTED 29 September 2022
PUBLISHED 24 October 2022

CITATION
Ye M, Gao L, Wang T, Yu J, Gui J and Yang J (2022) CD19 chimeric antigen receptor T-cell therapy following autologous stem cell transplantation against relapsed or refractory Burkitt lymphoma/leukemia: A case report and literature review.
Front. Oncol. 12:932254.
doi: 10.3389/fonc.2022.932254

CD19 chimeric antigen receptor T-cell therapy following autologous stem cell transplantation against relapsed or refractory Burkitt lymphoma/leukemia: A case report and literature review

Mingyu Ye, Lei Gao, Tao Wang, Jiechen Yu, Jiaping Gui and Jianmin Yang*

Department of Hematology, The First Affiliated Hospital of Naval Medical University, Shanghai, China

Burkitt lymphoma or leukemia (BL) is a highly aggressive non-Hodgkin lymphoma. Older age (over 60 years old) and the presence of high-risk factors (such as abdominal mass, high levels of the serum lactic dehydrogenase, Ann Arbor stage II-IV and so on) usually predict a poorer outcome. Chimeric antigen receptor T cells (CART) have achieved remarkable success in the treatment of B-cell leukemia and lymphoma. Here, for the first time, we report a 61-year-old, high-risk BL patient with autologous stem cell transplantation (ASCT) bridging therapy prior to CART as consolidation therapy. Our findings demonstrate that the combination of ASCT and CART for BL is safe and feasible.

KEYWORDS

Burkitt lymphoma, leukemia, CD19, chimeric antigen receptor T-cell, autologous stem cell transplantation

Abbreviations: ASCT, Autologous stem cell transplantation; BL, Burkitt lymphoma or leukemia; CART, Chimeric antigen receptor T cells; CR, complete remission; IRB, Institutional review board; OS, Overall survival; PFS, Progression-free survival; VDCP, Vindesine, daunorubicin, cyclophosphamide, and dexamethasone.

Introduction

Burkitt lymphoma/leukemia (BL) is a highly aggressive non-Hodgkin lymphoma characterized by rapidly progressive tumors with high extranodal involvement (1). It has been established that following dose-intensive chemotherapy, the three year-progression-free survival (PFS) and overall survival (OS) rates are 64 and 70%, respectively. However, the proportion of patients with BL who were over 60 years old was 24%, and the three-year PFS rate was only 56% (2). Age is an important predictor of outcome, as treatment-related mortality is high in older patients. For relapsed or refractory patients, high dose chemotherapy and autologous stem cell transplantation (ASCT) are recommended as salvage therapies.

In recent years, chimeric antigen receptor T cells (CART) have yielded unprecedented success with B-cell malignancies, with a complete remission (CR) rate of 81–93% (3, 4) in B-cell acute lymphoblastic leukemia and 40–59% in B-cell non-Hodgkin lymphoma (5–7). However, few studies have reported the potential of CART against BL.

The present case study is the first to report the treatment of a high-risk patient with BL with a combination of ASCT and CART therapy and the patient has now been in remission for 4 years. In this report, we describe the clinical course, including cytokine monitoring after CART infusion and the follow-up of expression of CD19 CAR T-cell expansion in peripheral blood. Our findings demonstrate that the combination of autologous stem cell transplantation and chimeric antigen receptor T-cells for Burkitt lymphoma is safe and feasible.

Case report

A 61-year-old man exhibiting fever (38.5°C), bleeding gums, and pain in the upper abdomen was admitted to the Department of Hematology, Changhai Hospital on August 31, 2016. A complete blood count test revealed the following: white blood cell count: 27.25×10^9/L, hemoglobin level: 139 g/L, and platelet count: 13×10^9/L. Additional laboratory tests showed that the serum lactic dehydrogenase level was 2246 U/L (upper limit of normal: 310 U/L). The patient was diagnosed with BL by bone marrow aspiration and biopsy tests, with 79% lymphoma cells in the bone marrow. The cells expressed CD19, CD20, CD10, CD22, and CD38, and had a 47, XY,dup (1), t (8, 14)+18 (10)/46,XY (10) karyotype. Computed tomography revealed multiple enlarged lymph nodes in the neck, mediastinum, and retroperitoneum. Contrast magnetic resonance imaging revealed leukemia with multiple enlarged lymph nodes in the hilar area, mesenteric area, and retroperitoneum.

The patient received induction therapy with VDCP (vindesine, daunorubicin, cyclophosphamide, and dexamethasone) on September 1, 2016. Then, he was administered with six courses of alternative therapy with Hyper-CVAD-A (cyclophosphamide, vindesine, doxorubicin, and dexamethasone), MAVP (methotrexate, cytarabine, vindesine, and dexamethasone), and central nervous system prophylaxis. One month after the last round of therapy, B-ultrasound showed that the inguinal lymph nodes were enlarged; the largest was 2.3 × 0.6 cm.

Therefore, the patient was enrolled in our clinical trials of ASCT bridging CD19 CART as consolidation therapies (NCT02672501). Peripheral blood lymphocyte separation and collection after a bone marrow aspiration biopsy showed complete remission, followed by CE regimen chemotherapy (cyclophosphamide 2g day1-2 and etoposide 330mg day1-2). When the patient's blood routine level dropped to the lowest level, G-CSF (granulocyte-colony stimulating factor) 400ug were injected for 4 consecutive days. Peripheral blood mononuclear cells were collected using apheresis. The conditioning therapy for the patient undergoing ASCT was CEAC (semustine, etoposide, cytarabine, and cyclophosphamide), which included semustine (250 mg/m^2) on day -6, cytarabine (500 mg/m^2) every 12 h, and etoposide (300 mg/m^2) and cyclophosphamide (1.0 g/m^2) from days -5 to -2. The patient developed fever(37.8°C) and nasal congestion on day-4, and recovered after cefoperazone-sulbactam treatment. Autologous hematopoietic stem cells were infused on day 0 with a mononuclear cell dose of 4.2×10^8/kg and a CD34$^+$ cell dose of 2.69×10^6/kg. On day +5, he developed fever(38.2°C) due to agranulocytosis, which returned to normal after 2 days of cefoperazone-sulbactam treatment. Additionally, 6×10^6/kg CART cells were infused 7 d after ASCT. The CART products included 32.8% CD45$^+$CD62L$^+$ naive CART cells, 44.7% CD45RA$^-$CD62L$^+$ central memory CART cells, and 15.9% CD45RA$^-$CD62L$^-$ effector memory CART cells. Grade 1 cytokine release syndrome was reached according to the Penn grading scale, because the patient developed a high fever with a body temperature of 39°C 2 h after infusion (8). Vancomycin was added to prevent infection and body temperature returned to normal 2 days later without using steroids and tocilizumab. No manifestations of neurotoxicity and other adverse effects in this patient. The time of neutrophil and platelet engraftment was 10 days and 11 days after ASCT, respectively. Cytokine monitoring after infusion of CART is shown in Figure 1. The patient achieved CR and has been in remission for four years. The follow-up is still ongoing. The treatment regimen of the patient is depicted in Figure 2.

The *in vivo* expansion and persistence of CART cells were monitored by reverse transcription polymerase chain reaction (Figure 3). CART cells reached their first peak 6 d after infusion and then dropped. The second peak was observed at 38 months after infusion, when the patient showed enlargement of the inguinal lymph nodes (the largest was 2.8 × 0.5 cm); moreover, the expression of *CAR* decreased as the lymph nodes shrunk to their normal size. At the follow-up 48 months after the patient's CART infusion, the expression of *CAR* persisted *in vivo*,

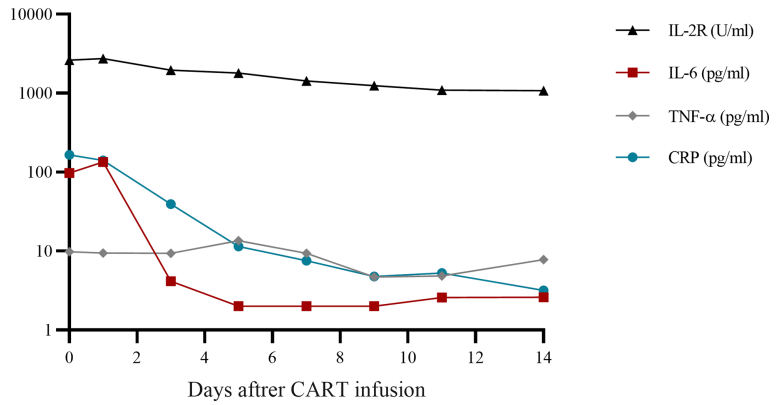

FIGURE 1
Cytokine monitoring after CART infusion. CART, chimeric antigen receptor T-cell; IL, interleukin; TNF, tumor necrosis factor; CRP, C-reactive protein.

reaching to 2.55×10^5 copies/ug gDNA in the bone marrow and 7.78×10^4 copies/ug gDNA in the peripheral blood.

Discussion

This case study is the first to report the treatment of a 61-year old, high-risk BL patient with ASCT combined with CART cell therapy and show that the patient achieved CR without any severe adverse events. This confirmed the safety and feasibility of using a combination of ASCT and CART cell therapy for BL. In addition, we observed long-term persistence of CART cells in the BM and peripheral blood. The effect of CART against BL is relatively unexplored (Table 1); therefore, our study provides novel insights into the potential applications of the therapy.

Compared to the patients in previously reported cases of CART against BL, the patient in the present study was older. Our treatment plan may be a better choice to improve the low PFS rate in older patients who rely solely on chemotherapy. In previously reported cases, most patients required a second or even third round of CART treatment. However, in our case study, because the persisting CART cells helped prevent tumor relapse, the patient sustained CR and did not require any other further treatment.

The long-term persistence of CART cells might be attributed to two mechanisms. First, CART products in this patient showed a high proportion of naive(32.8%) and memory(44.7%) CART cells. Studies have shown that compared with T central memory cells, T memory stem cells from the $CD45RA^+$ T cell population with high CD62L expression are more durable and effective against tumors (14). The naivety of CART cells can increase the effect of immunotherapy (15). In addition, the CART product in our study uses 4-1BB as the costimulatory domain. Compared to CD28 CART cells, 4-1BB CART cells show more memory phenotypes, express lower levels of depletion markers, and can retain effector functions for a long time under chronic antigen stimulation (16). Second, we believe that ASCT and its high dose transplantation conditioning decreased tumor burden, depleted the immunosuppressive microenvironment of lymphoma and deeply deplete regulatory T cells that inhibit CAR T-cell function,which enhanced CART cell persistence (17).

In summary, our novel combination of ASCT and CART therapy successfully cured a high-risk Burkitt lymphoma patient. In future, we will elucidate the mechanism behind persistence of

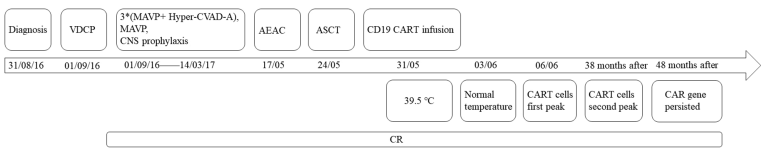

FIGURE 2
Timeline of treatment and efficacy. *multiply: six courses of alternative therapy with Hyper-CVAD-A (cyclophosphamide, vindesine, doxorubicin, and dexamethasone), MAVP (methotrexate, cytarabine, vindesine, and dexamethasone).

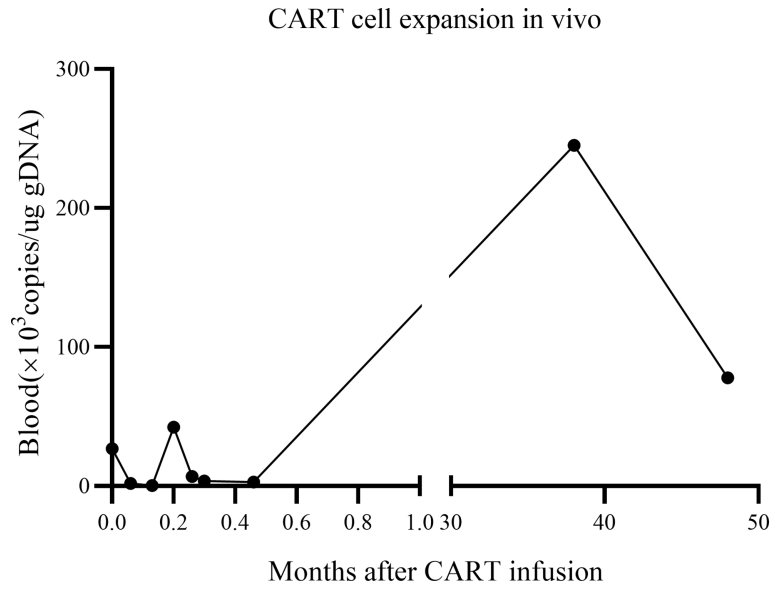

FIGURE 3
CART cell expansion *in vivo*. CART, chimeric antigen receptor T-cell.

TABLE 1 Treatment and outcomes from prior trials of CART cell therapy for Burkitt lymphoma (Literature review).

Published online	Number of patients	Age (years)	IPI/ Stage	Target	co-stimulatory domains	CRS	Response	HSCT	Survival months
18th, Jan., 2021 (9)	6	21-34	3 IPI4, 1 IPI3, 2 IPI1	CD19+CD22	CD28 and 4-1BB	5(I) 1(III)	1CR, 2PR, 1SD, 2PD	1	1-37^{+} [a]
25th, Jun., 2020 (10)	5	6-10	3 stageIV, 2 stageIII	3 CD19, 1 CD19+CD22, 1CD19+CD22 +CD20	4-1BB	3(III), 2(I)	5CR	none	5^{+}-14^{+} [b]
26th, Apr., 2018 (11)	1	32	StageIV	CD19	CD28	II	CR	1	0 [c]
25th, Feb., 2021 (12)	1 [d]	1.7	StageIV	CD19	4-1BB	II	CR	none	16^{+}
20th, May., 2022 (13)	28	17-70	3 StageI-II, 25 StageIII-IV	CD19/CD22	CD28 and 4-1BB	16(I) 11(II-IV)	16CR 3PR 12PD	13	0-60^{+}

[a] The CR patient received allo-HSCT and is in ongoing remission at 37 months, the SD patient died after 4.5 months of disease progression, one of the PD patients died after a month of therapy, another three patients were enrolled into another clinical trial (CAR22/19-T cells following auto-HSCT), two of them showed no response to this clinical trial, whereas the third is under remission at 22 months.
[b] A median follow-up of 331 d, ranging from 149 to 428 days; all patients remained in CR.
[c] Died of sepsis on the 9th day after HSCT.
[d] A male patient was diagnosed with BL-PTLD after undergoing living liver transplantation.
IPI/Stage, international prognostic index or Ann Arbor stage; PTLD, post-transplant lymphoproliferative disorder; HSCT, hematopoietic stem cell transplantation.

CART cells and apply our treatment method to more high-risk Burkitt lymphoma patients to improve their prognosis.

Data availability statement

The original contributions presented in the study are included in the article/supplementary material. Further inquiries can be directed to the corresponding author.

Ethics statement

The studies involving human participants were reviewed and approved by the National Natural Science Foundation of China. The patients/participants provided their written informed consent to participate in this study.

Author contributions

Treatment decision-making and discussions: LG, JYa. Data collection and analysis: MY, JYu, TW, and JG. Manuscript writing: MY and TW. Final approval of manuscript: JYa. All authors contributed to the article and approved the submitted version.

Funding

We would like to acknowledge the funding support of the National Natural Science Foundation of China (Grant No. 81770209) and Shanghai 2021 "Action Plan of Technological Innovation" Biomedical Science and Technology Support Special Project (21S11906100).

Acknowledgments

Firstly, I would like to extend my sincere gratitude to my supervisor, JMY, for his instructive advice and useful suggestions on my thesis and I am deeply grateful for his help in the completion of this thesis. I am also deeply indebted to all the other tutors and teachers in Translation Studies for both their direct and indirect help to me. Special thanks should go to my friends who have put considerable time and effort into their comments on the draft. Finally, I am indebted to my parents for their continuous support and encouragement.

Conflict of interest

The authors declare that the research was conducted in the absence of any commercial or financial relationships that could be construed as a potential conflict of interest.

Publisher's note

All claims expressed in this article are solely those of the authors and do not necessarily represent those of their affiliated organizations, or those of the publisher, the editors and the reviewers. Any product that may be evaluated in this article, or claim that may be made by its manufacturer, is not guaranteed or endorsed by the publisher.

References

1. Crombie J, LaCasce A. The treatment of burkitt lymphoma in adults. *Blood* (2021) 137(6):743–50. doi: 10.1182/blood.2019004099

2. Evens AM, Danilov A, Jagadeesh D, Sperling A, Kim SH, Vaca R, et al. Burkitt lymphoma in the modern era: real-world outcomes and prognostication across 30 US cancer centers. *Blood* (2021) 137(3):374–86. doi: 10.1182/blood.2020006926

3. Park JH, Rivière I, Gonen M, Wang X, Sénéchal B, Curran KJ, et al. Long-term follow-up of CD19 CAR therapy in acute lymphoblastic leukemia. *N Engl J Med* (2018) 378:449–59. doi: 10.1056/NEJMoal1709919

4. Maude SL, Laetsch TW, Buechner J, Rives S, Boyer M, Bittencourt H, et al. Tisagenlecleucel in children and young adults with b-cell lymphoblastic leukemia. *N Engl J Med* (2018) 378:439–48. doi: 10.1056/NEJMoal1709866

5. Schuster SJ, Bishop MR, Tam CS, Waller EK, Borchmann P, McGuirk JP, et al. Tisagenlecleucel in adult relapsed or refractory diffuse large b-cell lymphoma. *N Engl J Med* (2019) 380:45–56. doi: 10.1056/NEJMoal804980

6. Schuster SJ, Svoboda J, Chong EA, Nasta SD, Mato AR, Anak Ö, et al. Chimeric antigen receptor T cells in refractory b-cell lymphomas. *N Engl J Med* (2017) 377:2545–54. doi: 10.1056/NEJMoa1708566

7. Locke FL, Ghobadi A, Jacobson CA, Miklos DB, Lekakis LJ, Oluwole OO, et al. Long-term safety and activity of axicabtagene ciloleucel in refractory large b-cell lymphoma (ZUMA-1): a single-arm, multicentre, phase 1–2 trial. *Lancet Oncol* (2019) 20:31–42. doi: 10.1016/S1470-2045(18)30864-7

8. Porter D, Frey N, Wood PA, Weng Y, Grupp SA. Grading of cytokine release syndrome associated with the CAR T cell therapy tisagenlecleucel. *J Hematol Oncol* (2018) 11:35. doi: 10.1186/s13045-018-0571-y

9. Zhou X, Ge T, Li T, Huang L, Cao Y, Xiao Y, et al. CAR19/22 T cell therapy in adult refractory burkitt's lymphoma. *Cancer Immunol Immunother* (2021) 70:2379–84. doi: 10.1007/s00262-021-02850-6

10. Zhang W, Yang J, Zhou C, Hu B, Jin L, Deng B, et al. Early response observed in pediatric patients with relapsed/refractory burkitt lymphoma treated with chimeric antigen receptor T cells. *Blood* (2020) 135(26):2425–27. doi: 10.1182/blood.2019002008

11. Avigdor A, Shouval R, Jacoby E, Davidson T, Shimoni A, Besser M, et al. CAR T cells induce a complete response in refractory burkitt lymphoma. *Bone Marrow Transplant* (2018) 53:1583–85. doi: 10.1038/s41409-018-0235-0

12. Wang T, Feng M, Luo C, Wan X, Pan C, Tang J, et al. Successful treatment of pediatric refractory burkitt lymphoma PTLD after liver transplantation using anti-CD19 chimeric antigen receptor T-cell therapy. *Cell Transplant* (2021) 30:963689721996649. doi: 10.1177/0963689721996649

13. Jiaying Wu, Yang C, Qi Z, Wanying L, Xiaoxi Z, Xi M, et al. Chimeric antigen receptor-modified T cell immunotherapy for relapsed and refractory adult burkitt lymphoma. *Front Immunol* (2022) 13:879983. doi: 10.3389/fimmu.2022.879983

14. Gattinoni L, Klebanoff CA, Restifo NP. Paths to stemness: building the ultimate antitumour T cell. *Nat Rev Cancer* (2012) 12:671–84. doi: 10.1038/nrc3322

15. Golubovskaya V, Wu L. Different subsets of T cells, memory, effector functions, and CAR-T immunotherapy. *Cancers* (2016) 8(3):36. doi: 10.3390/cancers8030036

16. Sievers NM, Dörrie J, Schaft N. CARs: beyond T cells and T cell-derived signaling domains. *Int J Mol Sci* (2020) 21(10):3525. doi: 10.3390/ijms21103525

17. Wang T, Gao L, Wang Y, Zhu W, Xu L, Wang Y, et al. Hematopoietic stem cell transplantation and chimeric antigen receptor T cell for relapsed or refractory diffuse large b-cell lymphoma. *Immunotherapy* (2020) 12(13):997–1006. doi: 10.2217/imt-2020-0075

frontiers | Frontiers in Oncology

TYPE Case Report
PUBLISHED 31 October 2022
DOI 10.3389/fonc.2022.986957

OPEN ACCESS

EDITED BY
Anna Maria Testi,
Sapienza University of Rome, Italy

REVIEWED BY
Lorenzo Muccioli,
University of Bologna, Italy
Maurizio Aricò,
Department of Pediatrics, Italy

*CORRESPONDENCE
Xueping Zhu
zhuxueping4637@hotmail.com

SPECIALTY SECTION
This article was submitted to Hematologic Malignancies, a section of the journal Frontiers in Oncology

RECEIVED 05 July 2022
ACCEPTED 06 October 2022
PUBLISHED 31 October 2022

CITATION
Sun W, Fu C and Zhu X (2022) Acute necrotizing encephalopathy associated with lymphoma-associated hemophagocytic lymphohistiocytosis: A case report and literature review. *Front. Oncol.* 12:986957. doi: 10.3389/fonc.2022.986957

Acute necrotizing encephalopathy associated with lymphoma-associated hemophagocytic lymphohistiocytosis: A case report and literature review

Wenqiang Sun, Changchang Fu and Xueping Zhu*

Department of Neonatology, Children's Hospital of Soochow University, Suzhou, China

Damage associated with lymphoma-associated hemophagocytic lymphohistiocytosis (LA-HLH) to the central nervous system (CNS) is not uncommon. However, the combination with brain damage resembling acute necrotizing encephalopathy (ANE) is rarely reported. Herein, we introduce the diagnosis and treatment of a case of ANE associated with LA-HLH in our hospital and review the relevant literature. After treatment, the child was discharged with only dysarthria and decreased sucking ability. The child is now discharged from the hospital for 6 months with regular follow-up. There were no disease recurrence signs. LA-HLH and ANE were related to cytokine storm. Therefore, early steroid application is essential for treating these diseases.

KEYWORDS

hemophagocytic lymphohistiocytosis, lymphoma, acute necrotizing encephalopathy, cytokines, steroids

Introduction

Hemophagocytic syndrome (HPS), also called hemophagocytic lymphohistiocytosis (HLH), is an inflammatory syndrome depicting excessive and abnormal T lymphocytes and mononuclear phagocyte activation. Moreover, there is a massive release of inflammatory factors accompanying hemophagocytosis of tissues and organs, including the primary and secondary categories (1). Lymphoma-associated hemophagocytic lymphohistiocytosis (LA-HLH) is a common cause of secondary HLH (2). Acute necrotizing encephalopathy (ANE) is considered one of the most critical subtypes of acute encephalopathy (3). It has a mortality rate of up to 30%, and

most surviving cases suffer from moderate to severe disability. Damage associated with LA-HLH to the central nervous system (CNS) is not uncommon, but the combination with ANE is rarely reported (4–6). In this study, we reported a case of ANE associated with an LA-HLH and reviewed the relevant literature to discuss the disease's clinical features and treatment points.

Case description

A 10-year-old female patient was admitted for the first time to our hospital due to a persistent high fever for 19 days. The girl was born to healthy, non-consanguineous parents without any family history of neurological and hematological disorders. There were no abnormalities in the patient's birth history. She developed a persistent high fever (up to 40.2°C) for 19 days and showed no improvement after treatment with second-generation cephalosporin in other hospitals. On admission, her blood pressure was 102/68 mmHg (1 mmHg = 0.133 kPa), pulse was 102 beats/min, and body temperature was 39.3°C. She had a moderately anemic appearance with multiple enlarged lymph nodes of the neck, axilla, and groin and also had hepatosplenomegaly. Blood investigations (Table 1) revealed the following: decreased white blood cell count, 3.86×10^9/L; percentage of lymphocytes (LY%), 36.8%; absolute neutrophil count, 1.98×10^9/L; hemoglobin, 92 g/L; and fibrinogen, 2.12 g/L. PCT was significantly elevated (5.6 μg/L). Magnetic resonance imaging (MRI) and computed tomography (CT) (Figures 1A–E) showed multiple enlarged lymph nodes of the mediastinum and the axilla. MRI (Figures 1F, G) indicated edema around the dorsal extensor tendons of the 2nd to 5th metacarpals in the right hand and soft tissue swelling around the right wrist. Bone marrow cell morphology (Figure 2A) on the second day of admission suggested that the proliferation of bone marrow was active. Flow cytometry analyzed 10.9% of the mature lymphocyte population in the bone marrow, with 0.2% of the $CD5^+CD10^-$ mature clonal B-lymphocyte population being visible. After 8 days of anti-infection treatment with third-generation cephalosporin, the child's fever has not improved. Blood investigations (Table 1) revealed the following: decreased white blood cell count, 1.23×10^9/L; LY%, 49.6%; absolute neutrophil count, 1.12×10^9/L; hemoglobin, 75 g/L; and fibrinogen, 1.16 g/L. In addition, natural killer (NK) cell activity was decreased. The patient had elevated triglycerides (3.21 mmol/L), lactate dehydrogenase (789 U/L), ferritin (1,102.5 pmol/L), soluble CD25 (sCD25) (1,668.8 pg/ml), interleukin-6 (IL-6) (138.2 pg/ml), and TNF-α (16.7 ng/ml). The microbiological investigations ruled out bacterial, viral, and fungal infections, including EBV. Autoantibody and antinuclear antibodies were negative. Whole-exome sequencing did not identify primary HLH-associated genes. Bone marrow cell morphology (Figure 2B) revealed phagocytic cells. In addition, bone marrow cell morphology revealed a small number of abnormal lymphocytes with an oval-like cell cytosol, and a few granules in the cell cytoplasm were seen. Flow cytometry analysis of 12.7% of the mature lymphocyte population in the bone marrow, with 4.8% of the $CD5^+CD10^-$ mature clonal B-lymphocyte population (FSC increased), revealed the following: expression of CD19, FMC-7, CD10, CD20, KAPPA, CD38, and CD45; weak expression of CD22; and no expression of CD4, CD8, CD3, LAMBDA, CD56, CD5, CD57, CD200, CD79b, CD23, CD103, and CD11c. The bone marrow fluorescence *in-situ* hybridization (FISH) test

TABLE 1 Routine blood and CSF investigations of the patient.

	Reference value	First day	Sixth day	Early stages of ANE	Discharge
WBC	(4–10) × 10^9/L	3.86	1.23	1.03	13.39
LY	(20–40) %	36.8	49.6	10.8	21.6
NE	(50–75) × 10^9/L	1.98	1.12	1.03	11.26
Hb	(110–140) g/L	92	75	77	107
Plt	(100–300) × 10^9/L	198	143	139	433
Fib	(2–4) g/L	2.12	1.16	1.05	2.33
TG	(0–1.7) mmol/L	2.02	2.16	3.21	2.06
LDH	(172–382) U/L	668.2	789.0	1015.2	507.6
ALT	(5–35) U/L	36.2	39.8	114	43.2
SF	(22–640) pmol/L	688.4	1,102.5	2,472.1	672.1
sCD25	() pg/ml	–	1,668.8	1,356.4	Negative
IL-6	(0–5.9) pg/ml	–	138.2	–	Negative
TNF-α	(0.74–1.54) ng/ml	–	16.7	–	Negative
CSF protein	(120–600) mg/L	–	–	2,355	Negative
CSF IL-6	(0–5.9) pg/ml	–	–	98.6	Negative
CSF TNF-α	(0.74–1.54) ng/ml	–	–	15.3	Negative

WBC, white blood cell; LY%, percentage of lymphocytes; NE, neutrophil; Hb, hemoglobin; Plt, platelet; Fib, fibrinogen; TG, triglycerides; LDH, lactate dehydrogenase; SF, serum ferritin; sCD25, soluble CD25; IL-6, interleukin-6; CSF, cerebrospinal fluid; –, not done.

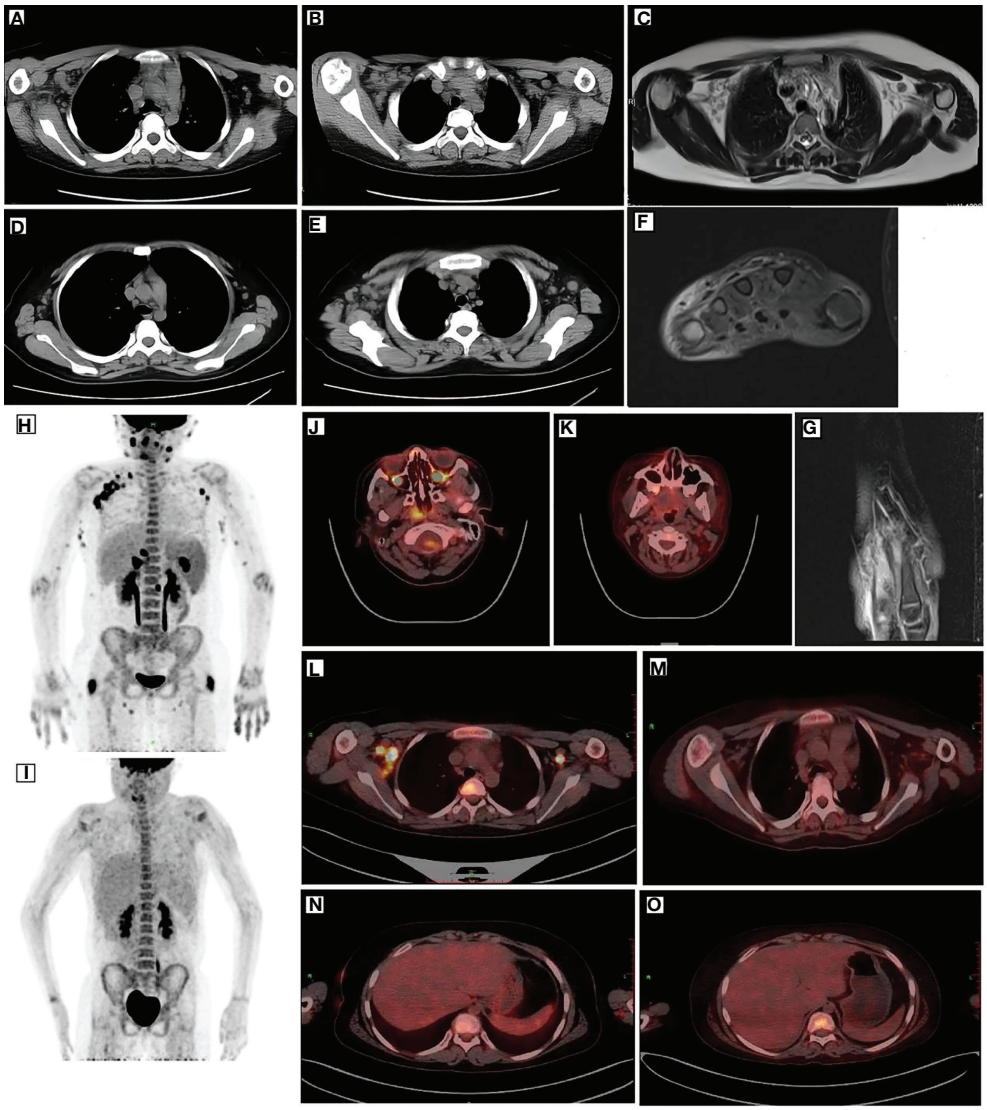

FIGURE 1
Imaging of the patient. CT **(A, B)**, MRI **(C)**, and PET **(L)** revealed multiple enlarged lymph nodes in the mediastinum and axilla with elevated glucose metabolism. After remission, CT **(D, E)** and PET **(M)** showed smaller lymph nodes than before and decreased glucose metabolism. Before treatment, PET **(H)** depicted multiple lymph node enlargements and tissue involvement with abnormally increased glucose metabolism. After remission, PET **(I)** revealed a significant reduction in the original lymph node and tissue lesions and decreased glucose metabolism. After remission, PET **(J, L)** indicated elevated FDG metabolism in the posterior nasopharyngeal wall and central bone marrow **(K, M)**, suggesting normal FDG metabolism. MRI **(F, G)** indicated edema around the dorsal extensor tendons of the 2nd to 5th metacarpals of the right hand and soft tissue swelling around the right wrist. PET **(N)** depicted increased liver volume. Moreover, repeat PET **(O)** after remission indicated increased liver volume and diffused hypodensity of the liver parenchyma. CT, computed tomography; MRI, magnetic resonance imaging; PET, positron emission tomography.

suggested 29% positive c-MYC rearrangement. Positron emission tomography (PET) (Figures 1H–O) depicted multiple systemic enlarged lymph nodes coupled with abnormally high glucose metabolism, hepatosplenomegaly, significant myeloproliferative neoplasm, and infiltrated connective muscle tissue. This patient was evaluated by our surgeons, and they stated that the patient's superficial lymph nodes were not big enough to yield a positive finding through a minimally invasive puncture biopsy. Moreover, performing an open-chest operation for biopsy was too traumatic, the localization was also challenging, and the patient's parents refused it as well. Despite the lack of pathological biopsy, the diagnosis of B-cell lymphoma was considered more likely in combination with immunophenotyping analysis and FISH testing in the child. The patient did not show a significant decrease in trilineage cells at the beginning of the disease course, had a significantly higher LY% of peripheral blood, and

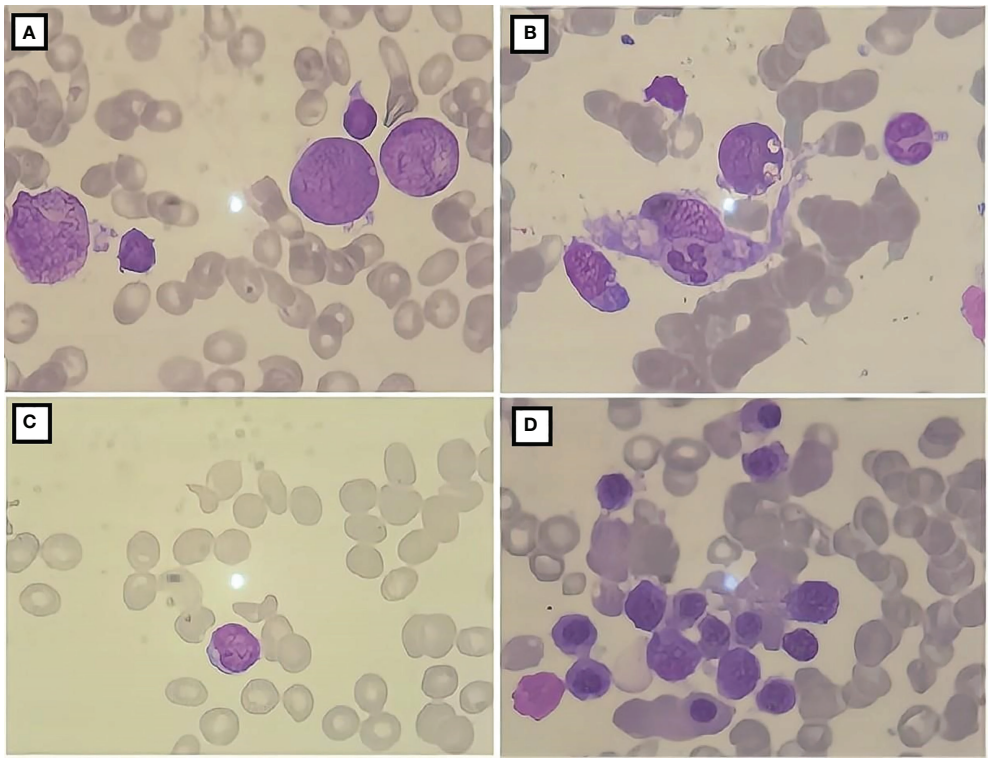

FIGURE 2
Bone marrow cell morphology of the patient. **(A)** The proliferation of bone marrow is active; **(B)** the presence of phagocytic cells; **(C)** severely diminished nucleated cell proliferation; **(D)** active bone marrow nucleated cell proliferation.

did not show phagocytosis on bone marrow cell morphology after admission. In addition, based on the patient's family history and genetic testing, it is not likely to be genetic HLH. Therefore, we considered HLH and lymphoma to be associated in this child.

During the first day of the CCHG-HLH-2018 chemotherapy regimen, the patient developed hyperthermia (40.6°C), vomiting, and decreased blood pressure (72/44 mmHg; 1 mmHg = 0.133 kPa), which improved through fluid infusion. The following morning, she also developed a rapid and progressive deterioration of consciousness, dysphagia, and dysarthria. On examination, the patient's bilateral pupils were equally sized, but the light reflex was sluggish. The patient had limb weakness (R and L, lower, proximal predominant), and the right knee jerk reflex was ±. Blood investigations (Table 1) depicted the following results: decreased white blood cell count, 1.11×10^9/L; absolute neutrophil count, 1.03×10^9/L; hemoglobin, 77 g/L; platelet count, 139×10^9/L; and fibrinogen, 1.05 g/L. She also had elevated triglycerides (3.21 mmol/L), lactate dehydrogenase (LDH) (1,015.2 U/L), glutamate transaminase (114 U/L), ferritin (2,472.1 pmol/L), and sCD25 (1,356.4 pg/ml). The cerebrospinal fluid (CSF) evaluation showed elevated opening pressure, normal cell count, and elevated protein level (2,355 mg/L), IL-6 (98.6 pg/ml), and TNF-α (15.3 ng/ml). CSF microbiology testing, culture, and "next-generation" sequencing (NGS) technology were negative. CT revealed low-density areas bilaterally in the thalami. MRI (Figures 3A, B) showed high-intensity brainstem and thalamus areas on T2-weighted images (T2WI), which indicated edema. After 2 weeks, the MRI (Figures 3C, D) still depicted symmetrical brain damage, and the thalamic damage revealed the typical "concentric circle" sign. Therefore, the final diagnosis was ANE.

After 41 days of treatment, the child's condition improved significantly. Primary treatments included chemotherapy, immunoglobulin (1 g/kg), steroid, mannitol, albumin, and fibrinogen. Additionally, the muscle strength of the limbs recovered more than before, all of which was V−, but dysarthria persisted with decreased sucking ability. Routine blood examinations (Table 1) showed the following: white blood cell count of 13.39×10^9/L, absolute neutrophil count of 11.26×10^9/L, hemoglobin of 107 g/L, and platelet count of 433×10^9/L; decreased ferritin levels (672.1 pmol/L); normal fibrinogen and serum cytokine levels; and normal CSF, biochemical markers, and cytokines. Moreover, NK cell activity improved from the initial examination. Three weeks after the start of chemotherapy, bone marrow cell morphology

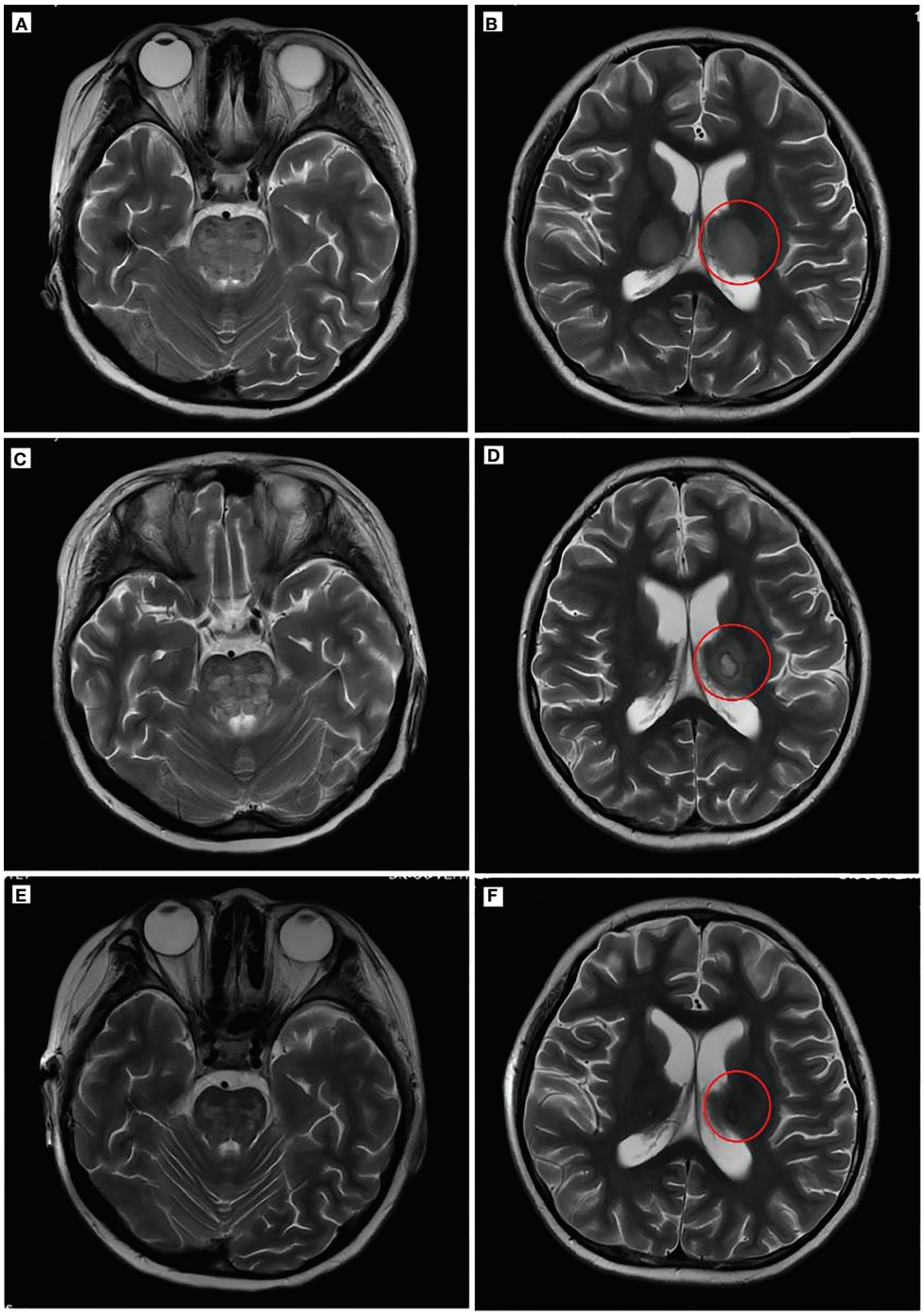

FIGURE 3
Brain imaging of the patient. T2WI **(A, B)** showed a high brainstem density and thalamus density (red circle). Brain T2WI **(C, D)** 2 weeks after ANE diagnosis indicated brainstem edema and typical "concentric circles" (red circles) within the thalamus. T2WI **(E, F)** after remission indicated the disappearance of edema and damage in the thalamus and brainstem. T2WI, T2-weighted MRI; PET, positron emission tomography; ANE, acute necrotizing encephalopathy.

(Figure 2C) indicated severe hypoplasia of bone marrow nucleated cells without phagocytic cells. Three days before discharge, bone marrow cell morphology (Figure 2D) revealed active proliferation of myeloid nucleated cells, normal morphology of all the cells, and no phagocytic cells. Necrotic lesions were still visible on brain MRI (Figures 3E, F) but significantly improved from the previous examination. PET showed that the original lymph nodes and soft tissue lesions

significantly improved, and the glucose metabolism was significantly lower. The sequela of the child during follow-up 2 months after being discharged was only slow speech. Six months after being discharged, the patient was followed up and had fluent speech without neurological involvement. The patient and her guardians were satisfied with the treatment results, and the patient was followed up regularly, with no signs of disease recurrence. The parents also intended to have their child undergo allogeneic hematopoietic stem cell transplantation (allo-PBSCT). The patient's disease progression and treatment flow chart are shown in Figure 4.

Discussion

HLH patients are characterized by persistent fever, bicytopenia, and hemophagocytosis in the bone marrow, liver, spleen, and lymph node tissues. HLH was first reported by Scott et al. in 1939. The incidence of the disease varies by age and race, with 1.2/1,000,000 in the European and Japanese populations and 1/100,000 in the US population (1, 7). The disease occurs in children and infants with a rapid onset, rapid progression, and poor prognosis. HLH is associated with a series of pathological changes due to the overactivation of the body's macrophages, lymphocytes, and other immune cells. The common causes of HLH include genetic susceptibility, viral infections, autoimmune diseases, and malignancies, including lymphomas (2). The clinical manifestations, laboratory tests, and imaging examinations of this child meet the diagnostic criteria of HLH (8). Meanwhile, the case of HLH should be distinguished from genetic HLH. The peripheral blood of the child and her parents was analyzed by whole-exome sequencing, focusing on familial HLH (FHLH) and HLH associated with immunodeficiency disease (9), and no relevant abnormal mutations were found. There were no HLH patients in the child's family. Therefore, it is not likely to be genetic HLH.

The pathological changes of neurological damage in HLH mainly include degeneration and necrosis due to lymphocyte and macrophage infiltration in the meningeal, cerebrovascular, and brain tissues. The most common brain injury imaging features of HLH are widespread brain atrophy, leukoaraiosis, and demyelinating encephalopathy. However, other specific findings include brain hemorrhage and edema (10, 11). Acute necrotizing encephalopathy associated with HLH is not uncommon (12–14). ANE was first proposed by Mizuguchi et al. in 1995 (5). Patients present acute viral infection, with further neurological manifestations such as twitching and consciousness disorder. These clinical symptoms are often accompanied by systemic inflammatory response syndrome (SIRS) manifestations such as shock, multiple organ dysfunction syndrome (MOD), and disseminated intravascular coagulation (DIC). ANE patients have a mortality rate of up to 30%, and the survivors often have moderate to severe disabilities. Brain imaging of ANE often reveals symmetric, multifocal CNS lesions, particularly in the thalamus and brainstem (4, 6, 15). A wide range of disorders should be considered in the differential diagnosis, including Leigh disease, Reye syndrome, Japanese encephalitis, hemorrhagic encephalitis, and acute disseminated encephalomyelitis. The patient presented with recurrent high fever and gradually developed dysphagia, dysarthria, consciousness disorder, and decreased muscle strength. Brain MRI showed symmetric thalamic and brainstem edema. Moreover, the typical "concentric circle" sign was seen on the repeated brain MRI 2 weeks later, consistent with the pathological changes of ANE (16), excluding hemorrhagic encephalitis, acute disseminated encephalomyelitis, and Japanese encephalitis. Leigh disease and Reye syndrome were not considered in children without hyperammonemia and lactic acidosis (17). After 1 day of chemotherapy, the child presented with neurological involvement, and ANE caused by the drugs could not be entirely excluded. However, ANE caused by chemotherapy drugs has not been reported and requires further research.

The pathogenesis of ANE is still unclear. A cytokine storm may play an essential role in the development of ANE. Cytokine storms are life-threatening systemic inflammatory syndromes involving elevated levels of circulating cytokines,

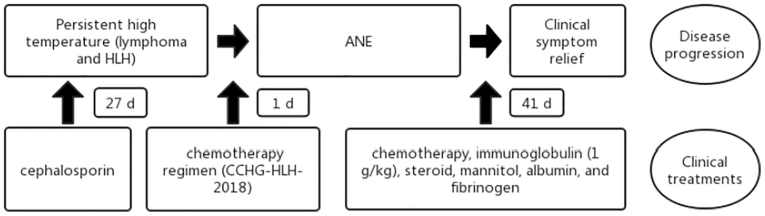

FIGURE 4
Flowchart of the patient disease progression and clinical treatments. HLH, hemophagocytic lymphohistiocytosis; ANE, acute necrotizing encephalopathy.

immune cell hyperactivation, and secondary organ dysfunction, including the brain (18). The patient had elevated peripheral blood inflammatory factor levels prior to the onset of neurological involvement (IL-6 138.2 pg/ml, TNF-α 16.7 pg/ml). After the presentation of encephalopathy, her cerebrospinal fluid inflammatory factor levels were significantly elevated, and the brain MRI showed extensive cerebral edema (IL-6 98.6 pg/ml, TNF-α 15.3 pg/ml). IL-6 and TNF-α dominated the elevated inflammatory factors in the patient. There is evidence that high levels of IL-6 are neurotoxic (19). Moreover, elevated TNF-α levels can damage vascular endothelial cells, disrupt the blood–brain barrier (BBB), and induce myelin and oligodendroglia necrosis (20, 21). In a nutshell, peripheral inflammation may lead to BBB disruption, which induces CNS inflammatory response and further aggravates the destruction of the BBB, forming a vicious cycle that results in encephalopathy eventually (22, 23). Pensato et al. (24) defined CySE as follows: encephalopathy with acute or subacute onset, association with cytokine storm (as defined by Fajgenbaum et al.), and exclusion of other causes that might independently account for the severity of neurological manifestations. The clinical symptoms and brain imaging of the patient improved after steroid treatment. The cytokine levels in the serum and CSF were normalized, indicating proinflammatory cytokine overactivation and overexpression of SCKRs in HLH patients and could be associated with ANE development.

HLH treatment mainly includes remission therapy induction and etiological therapy. Induction remission therapy controls the cytokine storm to prevent HLH, and the etiological treatment can correct the underlying immunodeficiency in preventing HLH recurrence (1, 8). After a treatment course, this child's clinical symptoms and related tests indicated HLH remission. ANE is extremely rare in HLH patients. The early application of steroids in ANE therapy to antagonize the cytokine storm is considered effective in clinical treatment (25, 26). In this case, steroid treatment was initiated early in ANE, and only dysarthria and decreased sucking ability remained after symptom resolution. Therefore, the early application of steroids in HLH patients could reduce ANE incidence and minimize the risk of death in established ANE patients. The child is now discharged from the hospital for 6 months with regular follow-up. There were no disease recurrence signs. Routine blood, lipid levels, liver function, ferritin, IL-6, and sCD25 were normal, and bone marrow cytology continues to indicate remission. The parents intend to have their child undergo allo-PBSCT.

The combination of LA-HLH with ANE could be associated with cytokine storm. Therefore, patients with HLH should be vigilant about developing ANE when presenting clinical manifestations of CNS involvement. Early steroid application to antagonize the cytokine storm has a better therapeutic effect on HLH. Moreover, it could also prevent the development of ANE and reduce the risk of death.

Data availability statement

The original contributions presented in the study are included in the article/supplementary material. Further inquiries can be directed to the corresponding author.

Author contributions

WS participated in the study design and writing of the manuscript. CF participated in clinical data collection and carried out the interpretation of the data. XZ participated in the data analysis, data interpretation, and manuscript writing. All authors read and approved the final manuscript.

Acknowledgments

We would like to thank the patient for consenting to the publication of this case.

Conflict of interest

The authors declare that the research was conducted in the absence of any commercial or financial relationships that could be construed as a potential conflict of interest.

Publisher's note

References

1. La Rosee P, Horne A, Hines M, von Bahr Greenwood T, Machowicz R, Berliner N, et al. Recommendations for the management of hemophagocytic lymphohistiocytosis in adults. *Blood* (2019) 133(23):2465–77. doi: 10.1182/blood.2018894618

2. Sangineto M, Perrone A, Agosti P, Boccuti V, Campobasso A, Sabbà C. Hemophagocytic lymphohistiocytosis, an unclear nosologic entity: Case report of an adult man with rising of amylase and lipase and spinal cord infiltration. *Hematol Rep* (2017) 9(1):6859. doi: 10.4081/hr.2017.6859

3. Hoshino A, Saitoh M, Oka A, Okumura A, Kubota M, Saito Y, et al. Epidemiology of acute encephalopathy in Japan, with emphasis on the association of viruses and syndromes. *Brain Dev* (2012) 34(5):337–43. doi: 10.1016/j.braindev.2011.07.012

4. Bassuk AG, Burrowes DM, McRae W. Acute necrotizing encephalopathy of childhood with radiographic progression over 10 hours. *Neurology* (2003) 60 (9):1552–3. doi: 10.1212/01.WNL.0000058757.52327.17

5. Mizuguchi M, Abe J, Mikkaichi K, Noma S, Yoshida K, Yamanaka T, et al. Acute necrotising encephalopathy of childhood: a new syndrome presenting with multifocal, symmetric brain lesions. *J Neurol Neurosurg Psychiatry* (1995) 58 (5):555–61. doi: 10.1136/jnnp.58.5.555

6. Yamamoto H, Okumura A, Natsume J, Kojima S, Mizuguchi M. A severity score for acute necrotizing encephalopathy. *Brain Dev* (2015) 37(3):322–7. doi: 10.1016/j.braindev.2014.05.007

7. Brisse E, Matthys P, Wouters CH. Understanding the spectrum of haemophagocytic lymphohistiocytosis: Update on diagnostic challenges and therapeutic options. *Br J Haematol.* (2016) 174(2):175–87. doi: 10.1111/bjh.14144

8. Henter J, Horne A, Aricó M, Egeler RM, Filipovich AH, Imashuku, et al. HLH-2004: Diagnostic and therapeutic guidelines for hemophagocytic lymphohistiocytosis. *Pediatr Blood Cancer* (2007) 48(2):124–31. doi: 10.1002/pbc.21039

9. Ponnatt TS, Lilley CM, Mirza KM. Hemophagocytic lymphohistiocytosis. *Arch Pathol Lab Med* (2022) 146(4):507–19. doi: 10.5858/arpa.2020-0802-RA

10. Rego I, Severino M, Micalizzi C, Faraci M, Pende D, Dufour C, et al. Neuroradiologic findings and follow-up with magnetic resonance imaging of the genetic forms of haemophagocytic lymphohistiocytosis with CNS involvement. *Pediatr Blood Cancer* (2012) 58(5):810–4. doi: 10.1002/pbc.23405

11. Fitzgerald NE, MacClain KL. Imaging characteristics of hemophagocytic lymphohistiocytosis. *Pediatr Radiol* (2003) 33(6):392–401. doi: 10.1007/s00247-003-0894-9

12. Akiyoshi K, Hamada Y, Yamada H, Kojo M, Izumi T. Acute necrotizing encephalopathy associated with hemophagocytic syndrome. *Pediatr Neurol* (2006) 34(4):315–8. doi: 10.1016/j.pediatrneurol.2005.08.030

13. Radmanesh F, Rodriguez-Pla A, Pincus MD, Burns JD. Severe cerebral involvement in adult-onset hemophagocytic lymphohistiocytosis. *J Clin Neurosci* (2020) 76:236–7. doi: 10.1016/j.jocn.2020.04.054

14. Dai D, Wen F, Liu S, Zhou S. Brain damage resembling acute necrotizing encephalopathy as a specific manifestation of haemophagocytic lymphohistiocytosis - induced by hypersensitivity. *Ital J Pediatr* (2016) 42(1):79. doi: 10.1186/s13052-016-0286-z

15. Seo H, Hwang S, Choe BH, Cho MH, Park SP, Kwon S, et al. Clinical spectrum and prognostic factors of acute necrotizing encephalopathy in children. *J Korean Med Sci* (2010) 25(3):449–53. doi: 10.3346/jkms.2010.25.3.449

16. Albayram S, Bilgi Z, Selcuk H, Selcuk D, Cam H, Koçer N. Diffusion-weighted MR imaging findings of acute necrotizing encephalopathy. *AJNR Am J Neuroradiol* (2004) 25(5):792–7.

17. Mizuguchi M. Acute necrotizing encephalopathy of childhood: A novel form of acute encephalopathy prevalent in Japan and Taiwan. *Brain Dev* (1997) 19 (2):81–92. doi: 10.1016/S0387-7604(96)00063-0

18. Fajgenbaum DC, June CH. Cytokine storm. *N Engl J Med* (2020) 383 (23):2255–73. doi: 10.1056/NEJMra2026131

19. Sugaya N. Influenza-associated encephalopathy in Japan: Pathogenesis and treatment. *Pediatr Int* (2000) 42(2):215–8. doi: 10.1046/j.1442-200x.2000.01200.x

20. Sato N, Goto T, Haranaka K, Satomi N, Nariuchi H, Mano-Hirano Y, et al. Actions of tumor necrosis factor on cultured vascular endothelial cells: morphologic modulation, growth inhibition, and cytotoxicity. *J Natl Cancer Inst* (1986) 76(6):1113–21.

21. Selmaj KW, Raine CS. Tumor necrosis factor mediates myelin and oligodendrocyte damage *in vitro*. *Ann Neurol* (1988) 23(4):339–46. doi: 10.1002/ana.410230405

22. Perrin P, Collongues N, Baloglu S, Bedo D, Bassand X, Lavaux T, et al. Cytokine release syndrome-associated encephalopathy in patients with COVID-19. *Eur J Neurol* (2021) 28(1):248–58. doi: 10.1111/ene.14491

23. Huang X, Hussain B, Chang J. Peripheral inflammation and blood-brain barrier disruption: effects and mechanisms. *CNS Neurosci Ther* (2021) 27(1):36–47. doi: 10.1111/cns.13569

24. Pensato U, Muccioli L, Cani I, Janigro D, Zinzani PL, Guarino M, et al. Brain dysfunction in COVID-19 and CAR-T therapy: Cytokine storm-associated encephalopathy. *Ann Clin Transl Neurol* (2021) 8(4):968–79. doi: 10.1002/acn3.51348

25. Okumura A, Mizuguchi M, Aiba H, Tanabe T, Tsuji T, Ohno A, et al. Delirious behavior in children with acute necrotizing encephalopathy. *Brain Dev* (2009) 31(8):594–9. doi: 10.1016/j.braindev.2008.09.002

26. Kawashima H, Togashi T, Yamanaka G, Nakajima M, Nagai M, Aritaki K, et al. Efficacy of plasma exchange and methylprednisolone pulse therapy on influenza-associated encephalopathy. *J Infect* (2005) 51(2):E53–6. doi: 10.1016/j.jinf.2004.08.017

frontiers | Frontiers in Oncology

TYPE Case Report
PUBLISHED 24 November 2022
DOI 10.3389/fonc.2022.1021786

OPEN ACCESS

EDITED BY
Arpad Szallasi,
Semmelweis University, Hungary

REVIEWED BY
Xiao-Dong Mo,
Peking University People's Hospital, China
Donglin Yang,
Chinese Academy of Medical Sciences and Peking Union Medical College, China

*CORRESPONDENCE
Jian Ge
gejian52@163.com

†These authors have contributed equally to this work

SPECIALTY SECTION
This article was submitted to Hematologic Malignancies, a section of the journal Frontiers in Oncology

RECEIVED 24 August 2022
ACCEPTED 02 November 2022
PUBLISHED 24 November 2022

CITATION
Ni J, Zhou J, Long Z, Chen X, Chen X, Hong J, Liang X, Li Q, Xia R and Ge J (2022) Anti-CD19 chimeric antigen receptor T-cell followed by interferon –α therapy induces durable complete remission in donor cell-derived acute lymphoblastic leukemia: A case report. *Front. Oncol.* 12:1021786. doi: 10.3389/fonc.2022.1021786

Anti-CD19 chimeric antigen receptor T-cell followed by interferon–α therapy induces durable complete remission in donor cell-derived acute lymphoblastic leukemia: A case report

Jing Ni[1,2†], Junjie Zhou[1†], Zhangbiao Long[1], Xin Chen[1], Xiaowen Chen[1], Jian Hong[1], Xinglin Liang[1], Qingsheng Li[1], Ruixiang Xia[1] and Jian Ge[1*]

[1]Department of Hematology, The First Affiliated Hospital of Anhui Medical University, Hefei, Anhui, China, [2]Department of Hematology, Xuanwu Hospital, Capital Medical University, Beijing, China

Donor cell-derived leukemia (DCL) is a special type of relapse after allogeneic hematopoietic stem cell transplantation (allo-HSCT). Patients with DCL generally have a poor prognosis due to resistance to conventional chemotherapy. Here, we report a case of donor cell-derived acute lymphoblastic leukemia after umbilical cord blood transplantation. The patient didn't respond to induction chemotherapy. She then received anti-CD19 CAR-T cell therapy and achieved MRD-negative complete remission (CR). However, MRD levels rose from negative to 0.05% at 5 months after CAR-T cell therapy. Higher MRD levels were significantly associated with an increased risk of leukemia recurrence. Afterward, preemptive interferon-α treatment was administrated to prevent disease recurrence. To date, the patient has maintained MRD-negative CR for 41 months. Our results suggested that anti-CD19 CAR-T cells followed by interferon-α therapy are effective in treating donor cell-derived acute lymphoblastic leukemia. This report provides a novel strategy for the treatment of DCL.

KEYWORDS

chimeric antigen receptor T cell, interferon-α, durable complete remission, donor cell-derived leukemia, post-transplant recurrence

Introduction

Leukemia relapse remains one of the most common causes of posttransplant mortality (1). The relapse clone is usually host-derived. Rarely, acute leukemia can also develop *de novo* in donor-derived cells, which is known as donor cell-derived leukemia (DCL). Since the first case of DCL was published in 1971, reports of DCL have accelerated in recent years (2, 3). Available data suggested that DCL accounts for approximately 5% of posttransplant relapses (4). The prognosis of DCL was poor, with a median survival time of 6 months after diagnosis (5). A second allogeneic hematopoietic stem cell transplantation (allo-HSCT) after successful re-induction remission seems to be an effective means for achieving long-term survival. However, most DCL patients are resistant to chemotherapy and fail to achieve remission again. Furthermore, a second allo-HSCT is also difficult to implement due to the patient's poor physical function, lack of suitable donors, etc.

CD19-targeted chimeric antigen receptor T-cell (CAR-T cell) therapy is a promising treatment for relapsed/refractory B-cell acute lymphoblastic leukemia (r/r B-ALL) with a high complete remission (CR) rate of 70–90% (6, 7). Nevertheless, the long-term efficacy of CAR-T cell therapy remains unsatisfactory due to the high recurrence rate, with a median event-free survival of only 6.1 months (8). There is a growing need for new strategies to prevent relapse and maintain sustained remission after CAR-T cell therapy.

Interferon-α is a biological agent with anti-leukemic effects (9, 10). Previous studies have demonstrated that interferon-α reduces the relapse of leukemia and improves long-term survival after chemotherapy and allo-HSCT (11, 12). However, whether the use of interferon-a following CAR-T cell therapy can reduce relapse has not been reported in clinical settings. In this paper, we for the first time present a successful case of treating donor cell-derived B-ALL with anti-CD19 CAR-T cell therapy followed by interferon-α. The patient achieved minimal residual disease (MRD) -negative CR after CAR-T cell therapy. However, MRD rose 5 months after CAR-T cell therapy. Subsequent treatment with interferon-α allowed the patient to regain undetectable MRD. To date, the patient has remained CR for 41 months after CAR-T cells followed by interferon-α therapy.

Case description

An 18-year-old female was admitted to the hospital with abdominal pain on January 31, 2016. Routine blood test revealed white blood cell count of 102.52×10^9/L, hemoglobin levels of 6.9 g/dL, and platelet count of 57×10^9/L. Bone marrow smear and flow cytometry identified 90% of blast cells expressing CD34, HLA-DR, CD19, CD10, and CD22. Cytogenetic analysis showed a normal 46, XX karyotype. RT-PCR analysis did not detect any gene rearrangements, such as ETV6, KMT2A, ABL1, ABL2, JAK2, IKZF1, CRLF2, PDGFR*B*, TCF3, ZNF384, and CSFF1R. Therefore, the patient was diagnosed with B-ALL (common-B, poor-risk group). On February 9, she received induction chemotherapy with VIP regimen (vincristine, idarubicin, and dexamethasone) and successfully achieved CR. Next, consolidation chemotherapy including VILP (VIP+ asparaginase) and hyper-CVAD regimen was performed. The patient refused allo-HSCT at the time of the first CR. In November 2016, bone marrow examination showed 41% lymphoblastic cells, indicating leukemia relapse. After re-induction therapy with VILP regimen, the patient attained her second CR. She subsequently underwent an umbilical cord blood transplantation (UCBT) in May 2017. Allografts were from a 4/6 HLA-matched unrelated umbilical cord blood according to low-resolution. The doses of total nucleated cells and CD34+ cells infused were 3.9×107/kg and 3.0×105/kg, respectively. The conditioning regimen included intravenous busulfan at 3.2 mg/kg/d for 4 days, cyclophosphamide at 60 mg/kg daily for 2 days, and fludarabine at 30 mg/m2 daily for 4 days. Cyclosporine and mycophenolate mofetil were used for GVHD prophylaxis. Neutrophil and platelet engraftment was observed on day 22 and day 37 after umbilical cord blood infusion, respectively. The patient maintained CR for 19 months with complete donor chimerism and without graft-versus-host disease. However, in January 2019, 21% of lymphoblasts were detected in the bone marrow by morphological analysis and flow cytometry (Figure 1). The patient relapsed again after UCBT. Intriguingly, chimerism testing using short tandem repeats still showed complete donor chimerism at this time point. This was termed "donor cell-derived leukemia"(DCL). Chemotherapy with VIP regimen failed to induce remission (32% lymphoblasts in bone marrow). The patient had no opportunity for second transplantation due to lack of available donors. CAR-T cell therapy was recommended for the patient. She was enrolled in our clinical trial of anti-CD19 CAR-T cell therapy (ChiCTR1800016315). After informed consent, peripheral blood lymphocytes were collected from the patient to prepare anti-CD19 CAR-T cells, which were engineered by Gracell Biotechnologies of Shanghai, China. The patient received lymphodepletion pretreatment with FC regimen (fludarabine 30 mg/m2 daily for 3 days, cyclophosphamide 300 mg/m2 daily for 3 days) from March 13, 2019 to March 15, 2019. After the lymphodepletion pretreatment, anti-CD19 CAR-T cells were infused at a total dose of 2.0×10^6/kg for 3 consecutive days (0.2×10^6/kg at day 0, 0.6×10^6/kg at day 1, 1.2×10^6/kg at day 2). Body temperature, cytokine levels, and c-reactive protein (CRP) were monitored (Figures 2A, B). The patient developed a fever with a maximum body temperature of 38°C on day 6. The temperature rose to 39°C and the blood pressure dropped to 83/58 mmHg on day 7. According to the standard of the American Society for Transplantation and Cellular Therapy (ASTCT), the patient was diagnosed with grade 2 cytokine release syndrome (CRS) (13). Non-steroidal anti-inflammatory drugs (NSAIDs)

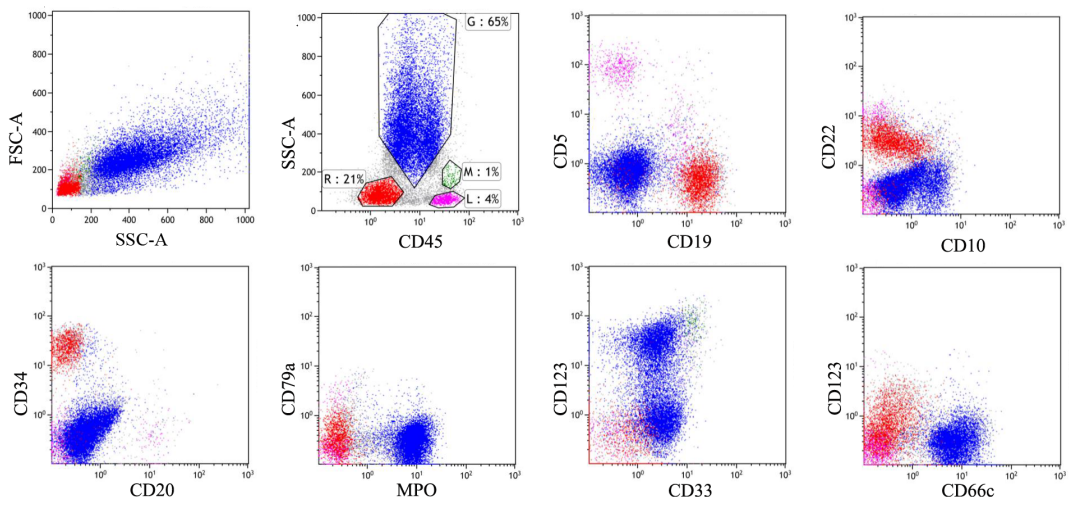

FIGURE 1
Immunophenotypic analysis by flow cytometry revealed a common B-cell acute lymphoblastic leukemia. There were 21% lymphoblasts expressing CD19+ in the bone marrow at the time of post-transplant recurrence, represented in red.

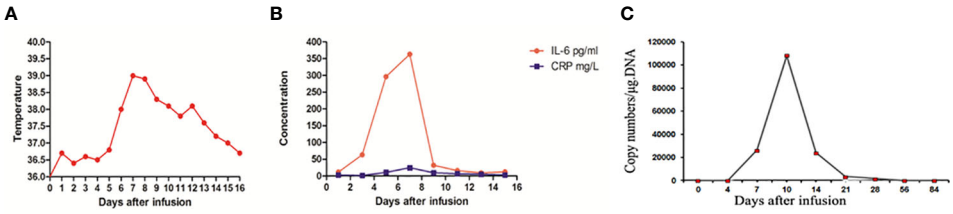

FIGURE 2
Clinical evolutions after CAR-T cells infusion. **(A)** Measures of body temperature after CAR-T cells infusion, the plot showed the maximum temperature was 39°C on day 7. **(B)** Levels of cytokines IL-6 and CRP were monitored at the indicated time points after CAR-T cells infusion. IL-6 and CRP peaked on day 7. **(C)** The vector copy number of anti-CD19 CAR in peripheral blood was detected by PCR. The highest anti-CD19 CAR DNA copy number was 108,140 copies/μg DNA on day 10. IL-6, interleukin-6; CRP, C reactive protein; PCR, polymerase chain reaction.

and tocilizumab (8 mg/kg) were used for CRS. Afterward, the temperature dropped gradually and returned to normal after a week. The highest serum level of interleukin 6 (IL-6) was 363 pg/mL on day 7. The copy number of anti-CD19 CAR in peripheral blood reached its peak on day 10, which was 1.08×10^5 copies/μg.DNA (Figure 2C). On April 4, 2019 (day 17), the bone marrow smear found no lymphoblast, and FCM revealed MRD negative (MRD<0.01% by 8-color flow cytometry). On day 118 after CAR-T cells infusion, the copy number of CAR was not detected. The patient remained in MRD-negative status for 5 months. On August 20, 2019, flow cytometry examination showed MRD levels of 0.05% for 2 consecutive bone marrow samples within a 1-month interval. The immunophenotype of MRD was CD34+CD10+CD19+CD22+ CD58dim CD20-CD123-. Given the increased MRD levels, the patient was given 3 million IU of interferon-α-2b, three times a week. She achieved MRD negative again after 42 days of interferon-alpha treatment. Interferon-α-2b was used for 2 years. Notably, analysis of immune cell subsets from peripheral blood showed a significant increase in the proportion of $CD16^+$ $CD56^+$ NK cells. To date, the patient has maintained CR for 41 months after CAR-T cells followed by interferon-α therapy. No adverse reactions were observed during interferon-α treatment. The patient is still under follow-up now. The main clinical process of the patient is summarized in Figure 3.

Discussion

Here, we reported a case of donor cell-derived B-ALL treated with anti-CD19 CAR-T cells followed by interferon-α treatment. The patient developed DCL 20 months after UCBT. Leukemia

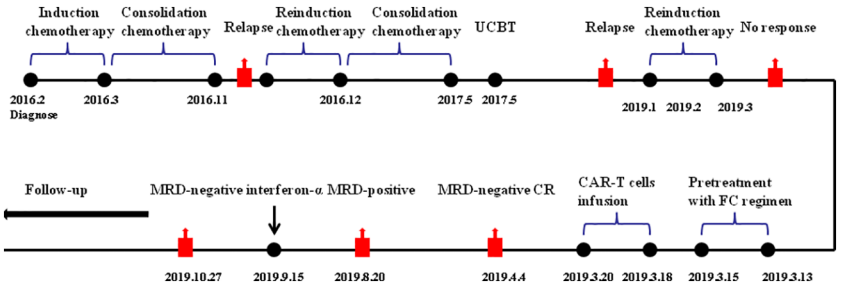

FIGURE 3
Summary of clinical course. FC, fludarabine and cyclophosphamide regimen; CAR-T cell, chimeric antigen receptor T cell; MRD, minimal residual disease; IFN- α, interferon-α.

cells were resistant to chemotherapy at this time. She then received anti-CD19 CAR-T cell therapy and achieved MRD-negative CR. However, after 5 months of CAR-T cell therapy, MRD levels rose to 0.05%. Based on the sensitivity of EuroFlow 8-color flow cytometry, MRD ≥0.01% was defined as MRD positive (14). The rising MRD levels indicated an increased rate of leukemia recurrence (15). Fortunately, the patient regained MRD-undetectable after interferon-α treatment. To date, the patient has remained in CR for 41 months. Our case suggested that CAR-T cell therapy followed by interferon-α had excellent clinical efficacy in DCL. To the best of our knowledge, this is the first successful clinical case of DCL treated with CAR-T cell therapy followed by interferon-α.

DCL is a rare and serious complication after allo-HSCT. UCBT was a risk factor for DCL compared to bone marrow transplantation. DCL following UCBT tends to be resistant to chemotherapy and the prognosis is very poor (5). The median interval between the occurrence of DCL following CBT was 14.5 months (16). Consistent with the characteristics reported in previous studies, the patient in our case developed DCL 20 months after CBT and was resistant to chemotherapy. Mechanistically, impaired immune surveillance by reduced functional T-lymphocytes in the recipient microenvironment was considered to promote the occurrence of DCL (16). Thus, restoring donor T cell functions, such as adoptive T cell therapy may be a promising approach for DCL therapy. Adoptive cell therapy using CAR-T cells has demonstrated impressive responses in treating r/r B-ALL. Thus, anti-CD19 CAR-T cell therapy was used to treat donor cell-derived B-ALL in this case. As expected, the patient achieved MRD-negative CR.

Despite the high remission rate, the long-term survival of B-ALL patients after CAR-T cell therapy is still unsatisfactory. Relapse remains a major challenge, especially for patients who are MRD positive after CAR-T cell therapy. Park et al. found that all 9 patients with MRD-positive CR after CAR-T cell therapy experienced relapse, indicating a 100% relapse rate (8). Bridging to allo-HSCT is considered an important means to reduce relapse after CAR-T cell therapy (17). However, a substantial proportion of patients are not eligible for allo-HSCT due to lack of suitable donors, patients' poor physical function, and so on. Here, MRD level of this patient was significantly elevated after 5 months after CAR-T cell therapy. A second allo-HSCT was not feasible due to lack of suitable donors. Therefore, there is a strong need to adopt novel therapeutic approaches to prevent relapse in this patient.

Interferon-α is a cytokine that can directly inhibit the proliferation of leukemia cells (11). More importantly, it has an immunoregulatory function, which is a crucial mechanism against leukemia. Interferon-α induces the activation and maturation of DCs, enhances cytotoxic activities of natural killer cells, and amplifies the proliferation and activation of T lymphocytes (18). It also significantly increases human $CD8^+$T cells exhibiting a surface phenotype of T central memory cells, which helps induce profound and sustained remission in leukemia patients (19). Based on the immunomodulatory effect, interferon-α promotes sustained remission by increasing the number of memory T cells and NK cells in patients with chronic myeloid leukemia (20). Interferon-α also promotes the graft-versus-leukemia effect. Therefore, it is used as an adjuvant or maintenance treatment after allo-HSCT to clear MRD and reduce the recurrence of leukemia (12, 21). Of note, several studies have reported synergistic effects between interferon-α and cell therapy. For example, interferon-α was found to increase the efficacy of donor lymphocyte infusion in posttransplant patients (22). Interferon-α enhanced the killing effects of CAR-T cells *in vitro* by increasing CAR-T cell activation and cytokine production (23). However, the clinical application of CAR-T cells combined with interferon-α treatment has not been reported. In this report, we observed that CAR-T cell followed by interferon-α therapy induced a durable remission in this patient with DCL. The mechanism underlying the efficacy of interferon-α in the case requires exploration. We found that the copy numbers of CAR were not detected when interferon-α was used, indicating that

interferon-α did not work by enhancing CAR-T activity. The patient remained in complete donor chimerism, suggesting that interferon-α might induce a graft-versus-leukemia effect through immunomodulation.

In conclusion, the present case suggested that anti-CD19 CAR-T cell followed by interferon-α treatment was effective in donor cell-derived B-ALL. Based on the possible mechanism, we envision that not only for patients with DCL, but also for all leukemia patients who relapse after allo-HSCT, sequential interferon-α therapy helps maintain durable remission if the patient achieves complete remission and donor chimerism after CAR-T cell therapy. Although the results of this report are encouraging, more studies are required to evaluate the efficacy of this treatment strategy.

Data availability statement

The original contributions presented in the study are included in the article/Supplementary Material. Further inquiries can be directed to the corresponding author.

Ethics statement

Written informed consent was obtained from the individual for the publication of any potentially identifiable images or data included in this article.

Author contributions

JN and JZ drafted the manuscript. ZL, XinC, XiaC, JH, and XL took care of the patient. JN,QL and JG collected clinical data. JN and JG analyzed the data. RX and JG revised the manuscript. All authors contributed to the article and approved the submitted version.

Funding

This work was supported by Key research and development plan of Anhui Province(Grant No. 201904a07020057), Natural Science Foundation of Anhui province (Grant No. 2108085MH270), Research Foundation of Anhui Provincial Institute of Translational Medicine(Grant No. 2021zhyx-C32), Research Foundation of Anhui Medical University (Grant No.2020xkj166 and No.2021xkj154), Clinical Trial Initiative Projects of The first Affiliated Hospital of Anhui Medical University(Grant No. LCYJ2021YB009).

Conflict of interest

The authors declare that the research was conducted in the absence of any commercial or financial relationships that could be construed as a potential conflict of interest.

Publisher's note

All claims expressed in this article are solely those of the authors and do not necessarily represent those of their affiliated organizations, or those of the publisher, the editors and the reviewers. Any product that may be evaluated in this article, or claim that may be made by its manufacturer, is not guaranteed or endorsed by the publisher.

References

1. Spyridonidis A, Labopin M, Schmid C, Volin L, Yakoub-Agha I, Stadler M, et al. Outcomes and prognostic factors of adults with acute lymphoblastic leukemia who relapse after allogeneic hematopoietic cell transplantation. An analysis on behalf of the acute leukemia working party of EBMT. *Leukemia* (2012) 26(6):1211–7. doi: 10.1038/leu.2011.351

2. Fialkow PJ, Thomas ED, Bryant JI, Neiman PE. Leukaemic transformation of engrafted human marrow cells *in vivo*. *Lancet* (1971) 1(693):251–5. doi: 10.1016/s0140-6736(71)90998-6

3. Engel N, Rovo A, Badoglio M, Labopin M, Basak GW, Beguin Y, et al. European Experience and risk factor analysis of donor cell-derived leukaemias/MDS following haematopoietic cell transplantation. *Leukemia* (2019) 33(2):508–17 doi: 10.1038/s41375-018-0218-6

4. Boyd CN, Ramberg RC, Thomas ED. The incidence of recurrence of leukemia in donor cells after allogeneic bone marrow transplantation. *Leuk Res* (1982) 6 (6):833–7. doi: 10.1016/0145-2126(82)90067-4

5. Shiozaki H, Yoshinaga K, Kondo T, Imai Y, Shiseki M, Mori N, et al. Donor cell-derived leukemia after cord blood transplantation and a review of the literature: Differences between cord blood and BM as the transplant source. *Bone marrow Transplant* (2014) 49(1):102–9. doi: 10.1038/bmt.2013.127

6. Maude SL, Frey N, Shaw PA, Aplenc R, Barrett DM, Bunin NJ, et al. Chimeric antigen receptor T cells for sustained remissions in leukemia. *N Engl J Med* (2014) 371(16):1507–17. doi: 10.1056/NEJMoa1407222

7. Lee DW, Kochenderfer JN, Stetler-Stevenson M, Cui YK, Delbrook C, Feldman SA, et al. T Cells expressing CD19 chimeric antigen receptors for acute lymphoblastic leukaemia in children and young adults: A phase 1 dose-escalation trial. *Lancet* (2015) 385(9967):517–28. doi: 10.1016/S0140-6736(14)61403-3

8. Park JH, Rivière I, Gonen M, Wang X, Sénéchal B, Curran KJ, et al. Long-term follow-up of CD19 CAR therapy in acute lymphoblastic leukemia. *N Engl J Med* (2018) 378(5):449–59. doi: 10.1056/NEJMoa1709919

9. Webster JA, Robinson TM, Blackford AL, Warlick E, Ferguson A, Borrello I, et al. A randomized, phase II trial of adjuvant immunotherapy with durable TKI-free survival in patients with chronic phase CML. *Leuk Res* (2021) 111:106737. doi: 10.1016/j.leukres.2021.106737

10. Healy FM, Dahal LN, Jones JRE, Floisand Y, Woolley JF. Recent progress in interferon therapy for myeloid malignancies. *Front Oncol* (2021) 11:769628. doi: 10.3389/fonc.2021.769628

11. Jiang H, Liu XH, Kong J, Wang J, Jia JS, Lu SY, et al. Interferon-α as maintenance therapy can significantly reduce relapse in patients with favorable-risk

acute myeloid leukemia. *Leuk Lymphoma* (2021) 62(12):2949–56. doi: 10.1080/10428194.2021.1948027

12. Shen MZ, Zhang XH, Xu LP, Wang Y, Yan CH, Chen H, et al. Preemptive interferon-α therapy could protect against relapse and improve survival of acute myeloid leukemia patients after allogeneic hematopoietic stem cell transplantation: Long-term results of two registry studies. *Front Immunol* (2022) 13:757002. doi: 10.3389/fimmu.2022.757002

13. Lee DW, Santomasso BD, Locke FL, Ghobadi A, Turtle CJ, Brudno JN, et al. ASTCT consensus grading for cytokine release syndrome and neurologic toxicity associated with immune effector cells. *Biol Blood Marrow Transplant* (2019) 25 (4):625–38. doi: 10.1016/j.bbmt.2018.12.758

14. Weng XQ, Shen Y, Sheng Y, Chen B, Wang JH, Li J, et al. Prognostic significance of monitoring leukemia-associated immunophenotypes by eight-color flow cytometry in adult b-acute lymphoblastic leukemia. *Blood Cancer J* (2013) 3 (8):e133. doi: 10.1038/bcj.2013.31

15. Borowitz MJ, Wood BL, Devidas M, Loh ML, Raetz EA, Salzer WL, et al. Prognostic significance of minimal residual disease in high risk b-ALL: A report from children's oncology group study AALL0232. *Blood* (2015) 126(8):964–71. doi: 10.1182/blood-2015-03-633685

16. Kato M, Yamashita T, Suzuki R, Matsumoto K, Nishimori H, Takahashi S, et al. Donor cell-derived hematological malignancy: A survey by the Japan society for hematopoietic cell transplantation. *Leukemia* (2016) 30(8):1742–5. doi: 10.1038/leu.2016.23

17. Jiang H, Li C, Yin P, Guo T, Liu L, Xia L, et al. Anti-CD19 chimeric antigen receptor-modified T-cell therapy bridging to allogeneic hematopoietic stem cell transplantation for relapsed/refractory b-cell acute lymphoblastic leukemia: An open-label pragmatic clinical trial. *Am J Hematol* (2019) 94(10):1113–22. doi: 10.1002/ajh.25582

18. Zitvogel L, Galluzzi L, Kepp O, Smyth MJ, Kroemer G. Type I interferons in anticancer immunity. *Nat Rev Immunol* (2015) 15(7):405–14. doi: 10.1038/nri3845

19. Ramos HJ, Davis AM, Cole AG, Schatzle JD, Forman J, Farrar JD. Reciprocal responsiveness to interleukin-12 and interferon-alpha specifies human CD8+ effector versus central memory T-cell fates. *Blood* (2009) 113 (22):5516–25. doi: 10.1182/blood-2008-11-188458

20. Ilander M, Kreutzman A, Rohon P, Melo T, Faber E, Porkka K, et al. Enlarged memory T-cell pool and enhanced Th1-type responses in chronic myeloid leukemia patients who have successfully discontinued IFN-α monotherapy. *PloS One* (2014) 9(1):e87794. doi: 10.1371/journal.pone.0087794

21. Fan S, Shen MZ, Zhang XH, Xu LP, Wang Y, Yan CH, et al. Preemptive immunotherapy for minimal residual disease in patients with t (8;21) acute myeloid leukemia after allogeneic hematopoietic stem cell transplantation. *Front Oncol* (2022) 11:773394. doi: 10.3389/fonc.2021.773394

22. Mo X, Zhang X, Xu L, Wang Y, Yan C, Chen H, et al. Interferon-α salvage treatment is effective for patients with acute leukemia/myelodysplastic syndrome with unsatisfactory response to minimal residual disease-directed donor lymphocyte infusion after allogeneic hematopoietic stem cell transplantation. *Front Med* (2019) 13(2):238–49. doi: 10.1007/s11684-017-0599-3

23. Young PA, Yamada RE, Trinh KR, Vasuthasawat A, De Oliveira S, Yamada DH, et al. Activity of anti-CD19 chimeric antigen receptor T cells against b cell lymphoma is enhanced by antibody-targeted interferon-alpha. *J Interferon Cytokine Res* (2018) 38(6):239–54. doi: 10.1089/jir.2018.0030

frontiers | Frontiers in Oncology

TYPE Case Report
PUBLISHED 25 November 2022
DOI 10.3389/fonc.2022.1027585

OPEN ACCESS

EDITED BY
Ahmad Antar,
Almoosa Specialist Hospital, Saudi Arabia

REVIEWED BY
Yan-Hua Zheng,
Fourth Military Medical University (Air Force Medical University), China
Joshua Richter,
Icahn School of Medicine at Mount Sinai, United States

*CORRESPONDENCE
Yun Liang
liangyun@zju.edu.cn

SPECIALTY SECTION
This article was submitted to Hematologic Malignancies, a section of the journal Frontiers in Oncology

RECEIVED 25 August 2022
ACCEPTED 07 November 2022
PUBLISHED 25 November 2022

CITATION
Li X, Wang W, Zhang X and Liang Y (2022) Multiple myeloma with isolated central nervous system relapse after autologous stem cell transplantation: A case report and review of the literature.
Front. Oncol. 12:1027585.
doi: 10.3389/fonc.2022.1027585

Multiple myeloma with isolated central nervous system relapse after autologous stem cell transplantation: A case report and review of the literature

Xian Li, Weiqin Wang, Xiaohong Zhang and Yun Liang*

Department of Hematology, The Second Affiliated Hospital, College of Medicine, Zhejiang University, Hangzhou, China

Patients with multiple myeloma (MM) rarely present with central nervous system (CNS) involvement as a manifestation of extramedullary disease (EMD), a condition that is associated with poor prognosis. CNS relapse without evidence of systemic involvement is even rarer, and there is no standardized treatment because there are only few case reports. We present a 47-year-old female who was diagnosed with nonsecretory multiple myeloma (NSMM) 9 years previously. She had a complete remission after receiving aggressive therapies, including high-dose chemotherapy and autologous stem cell transplantation (ASCT). However, after 7 years of progression-free survival, she had CNS relapse without evidence of systemic involvement. We switched to a salvage regimen consisting of high-dose methotrexate with lenalidomide. She achieved rapid clinical improvement, with a reduction in cerebrospinal fluid plasmacytosis of more than 80%, and no notable side effects. Our description of this unique case of a patient with MM and isolated CNS relapse after ASCT provides a reference for physicians to provide more appropriate management of these patients. We also reviewed previously reported cases and summarized the outcomes of isolated CNS relapse after ASCT, and discuss the pathogenesis and possible treatment strategies for MM with isolated CNS relapse.

KEYWORDS

multiple myeloma, isolated central nervous system relapse, autologous stem cell transplantation, pathogenesis and treatment, case report

Introduction

Multiple myeloma (MM) is characterized by the monoclonal proliferation of plasma cells (PCs) in bone marrow (1). Despite the use of established treatments followed by autologous stem cell transplantation (ASCT) and improvements in patient outcomes during recent years, MM is still incurable (2). Relapse in most patients is characterized as a medullary monoclonal proliferation, and 3.4% to 35% of these patients present with extramedullary disease (EMD) (3). Central nervous system (CNS) involvement is a very rare aggressive presentation of EMD, and occurs in only about 1% of patients (4). CNS relapse without evidence of systemic involvement is even rarer, with only few case reports, and these patients face a very poor prognosis, with a median survival time less than 6 months (5).

The present study describes a female who had MM with isolated CNS relapse after ASCT, and faced a poor prognosis despite the use of aggressive therapy. There is no standard treatment for CNS localization of multiple myeloma (CNS-MM) (4, 6) due to the rarity of this presentation. Thus, we also conducted a literature review to summarize the outcomes of other MM patients who had isolated CNS relapse after ASCT and examined the pathogenesis and possible treatment strategies for this condition.

Case report

A 38-year-old female with lumbago was diagnosed with nonsecretory multiple myeloma (NSMM) in December 2012. At that time, bone marrow specimens indicated 74% infiltration of plasma cells, and flow cytometry analysis showed abnormal plasma cells, which were positive for CD38, CD56, CD138, and cytoplasmic λ light-chain. Serum immunofixation (IFE) showed no detectable monoclonal component, a blood examination showed no anemia or renal dysfunction, and the levels of lactate dehydrogenase (LDH) and β_2 microglobulin (β_2-MG) were normal. Whole body bone imaging showed diffuse abnormal signals in the ribs, spinal vertebrae, and ilium. These findings led to a diagnosis of NSMM, with stage I based on the International Staging System (ISS) and stage IIIA based on the Durie-Salmon (DS) staging system. The patient received 4 courses of bortezomib, dexamethasone, and thalidomide (VDT) and achieved a complete response (CR).

After a treatment-free period of 4 months, she presented again with low backache. Bone marrow flow cytometry indicated that 6.5% of the plasma cells were abnormal, indicative of medullary recurrence. She then received 8 courses of different chemotherapies: 4 courses of vincristine, doxorubicin, and dexamethasone (VAD); 3 courses of vincristine, dexamethasone, cyclophosphamide, and thalidomide (VDCT); and 1 course of thalidomide, dexamethasone, cis-platin, doxorubicin, cyclophosphamide, and etoposide (DTPACE). After treatment, she achieved a partial response (PR) with regression of bone pain and 1% plasma cells in bone marrow.

In July 2014, she was given ASCT with preconditioning using semustine, busulphan, and etoposide (Me-CCNu + Bu + VP-16) and maintained a PR. However, 5 months after ASCT, she developed right-lower limb pain. Whole body bone imaging at that time showed a new focus in the right femoral region, and the bone marrow had 14% plasma cells with a normal level of the M protein based on immunofixation electrophoresis (IFE). Thus, melphalan and prednisolone (MP) therapy was initiated. There were no detectable myeloma cells in the bone marrow after 6 courses of this therapy. Thalidomide (100 mg orally) maintenance therapy was then administered for 2 years, and she had no further relapse.

In May 2022, she presented again and reported the sudden onset of dizziness, staggering gait, and loss of hearing. Physical examination revealed that she had clear poor hearing. The muscular strength tension of limbs was normal. Physiological reflexes were existent without any pathological ones. No enlargement of lymph nodes, liver, or spleen was found. Brain magnetic resonance imaging (MRI) showed cerebrospinal meninges and auditory nerve thickening (Figure 1A). Positron emission tomography/computerized tomography (PET/CT) showed multiple cerebrospinal meninges with increased ^{18}F-flurodeoxyglucose metabolism, but no other site of disease involvement (Figures 1B, C). Further examination showed she had no abnormalities in the hemogram, M-protein level, renal function, LDH level, and β_2-MG level. A bone marrow analysis showed no chromosomal abnormalities and no increased number of abnormal plasma cells. However, her cerebrospinal fluid (CSF) was positive for plasma cells (Figure 2A), and a lumbar puncture showed the CSF had a protein content of 213.8 mg/dL (normal range: 20–40), glucose of 50 mg/dL (normal range: 50–60), and 42×10^6 nucleated cells/L (normal range: 0–8×10^6). These findings indicated that the relapse was localized to the CNS.

We advised high-dose methotrexate (HD-MTX) therapy with lenalidomide (25 mg orally). After one course of salvage therapy, she achieved rapid clinical improvement without any notable side effects, such as hematological toxicity or peripheral neuropathy. Furthermore, this treatment reduced the CSF plasmacytosis by more than 80% (Figure 2B). The timeline of the patient is summarized in Figure 3.

Discussion

ASCT after induction therapy is a common standard treatment for eligible MM patients because it can induce durable remission and improve long-term survival. Nonetheless, MM is still an incurable disease. Although most patients who experience relapse have proliferation of monoclonal plasma cells, mainly in the bone marrow, about

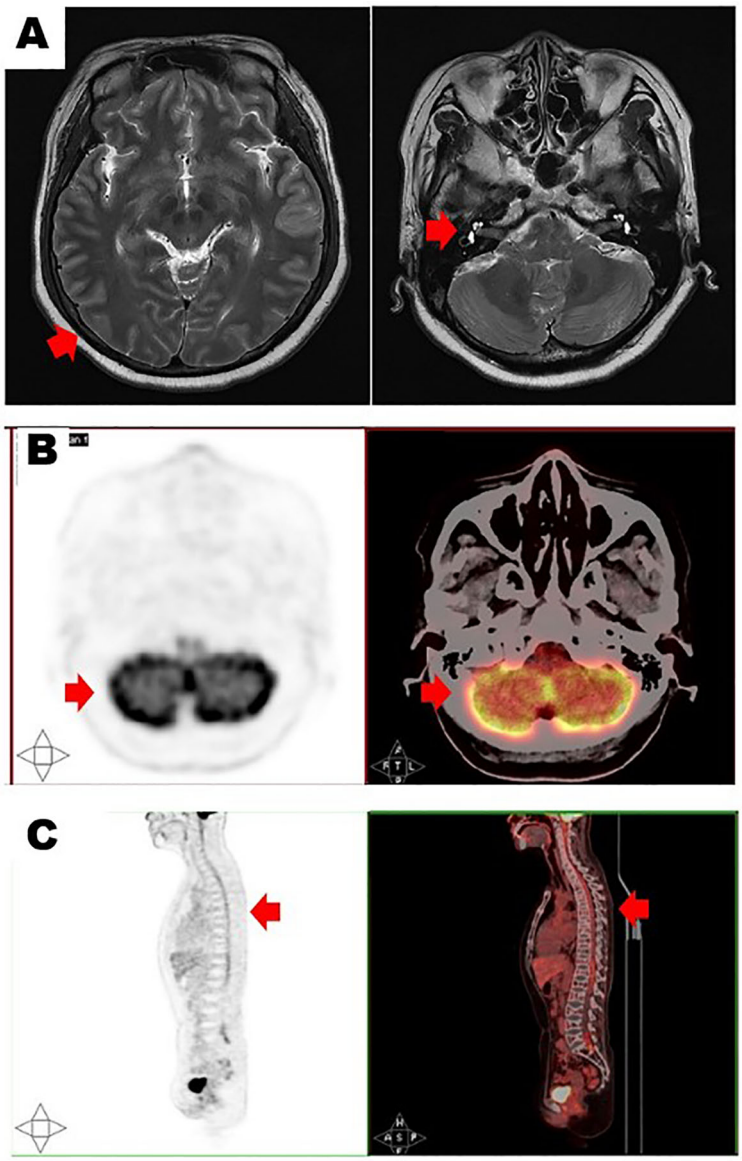

FIGURE 1
Brain magnetic resonance imaging **(A)** showed cerebrospinal meninges (left, red arrow) and auditory nerve thickening (right, red arrow). Positron emission tomography/computerized tomography in transverse section **(B)** and longitudinal section **(C)** showed multiple cerebrospinal meninges with increased 18F-flurodeoxyglucose metabolism (red arrows).

3.4% to 35% of these patients present with EMD (1, 3). CNS involvement is a specific presentation of extramedullary extraosseous, and occurs in only about 1% of patients (4). The median survival time of these patients is only 4 to 7 months, even when aggressive therapy is given (4, 7). CNS relapse without evidence of systemic involvement after ASCT is even rarer in patients who have MM, and there are only a few case reports in the literature.

Certain clinical factors are associated with increased risk of CNS-MM, including lambda subtype, elevated LDH, elevated β_2-MG, EMD, plasma cell leukemia, and chromosomal abnormalities (deletion of 17p or 13q) (4, 8, 9). We performed a comprehensive search of the literature and identified 14 cases (Tables 1, 2). Most of these patients had ISS stage III disease at diagnosis, but the myeloma subtype was variable. There were more patients with high LDH and β_2-MG levels than with normal levels. Only one patient had plasma cell leukemia. The median time from ASCT to CNS disease was 6 months (range: 2.5–84), and most patients died after developing CNS disease, with a

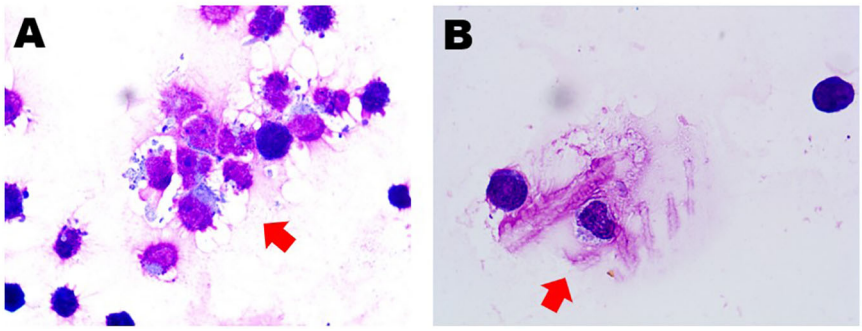

FIGURE 2
Cerebrospinal fluid smear showed the presence of abnormal plasma cells (red arrows) before **(A)** and after **(B)** salvage therapy.

median survival post-CNS relapse of 6 months (range: 0.3–29). Cytogenetic results were available in 7 patients: 4 patients had 17p deletion (17p-), 2 patients had 1q21 amplification (1q21+), and 2 patients had translocation (4, 14). These cytogenetic abnormalities may be related to isolated CNS relapse after ASCT for MM. This is consistent with the observations from previous studies (4). One cohort study showed that deletion of chromosome 17p13,1 (p53) was present in 89% of the CNS-MM patients and associated with metastatic features of myeloma cells (20). Moreover, investigators found that amplification of 1q21 was associated with disease progression and poor prognosis in MM despite the use of novel regimens (21). Patients with 1q21+ showed a high incidence of aggressive features, including an unusually high CNS involvement incidence (11%) and early onset of CNS disease (22). Our patient, who had bone marrow expression of CD56 had no EMD or circulating plasma cells at baseline. Our patient differed from other previously described patients in that she had normal levels of LDH and β_2-MG and no cytogenetic abnormalities. Because factors that apparently increase the risk for CNS involvement were not present in our patient, we examined the possible reasons why she developed such aggressive disease.

The mechanism leading to isolated CNS relapse post-ASCT is uncertain. One hypothesis is that malignant plasma cells are transmitted by blood or plasma cell precursors, and then spread in the cerebrospinal meninges. In the past decade, therapies using novel agents and ASCT have improved the progression-free survival of MM patients, and it seems likely that this has led to the appearance of new patterns of relapse. The downregulation of CD56 adhesion molecules after first-line therapy could allow MM cells to escape the bone marrow environment and establish distant plasma cell metastasis, including in the CNS (18). Patients with plasma cell leukemia have abnormal plasma cells in the circulating blood, and the presence of these circulating plasma cells increases the risk of hematogenous spread. This supports our first hypothesis that malignant plasma cells are transmitted in the blood, and then spread to the cerebrospinal meninges (23). A second hypothesis is that plasmacytoma infiltrated adjacent skull lytic lesions. These patients mainly have parenchymal infiltration, varying from 39% to 65% in some cohorts (5, 24). Finally, a series of reports showed that clonal heterogeneity could play a role in CNS-MM. In particular, high dose chemotherapy for ASCT might select for extramedullary drug-resistant clonal populations, thus leading to relapse without bone marrow

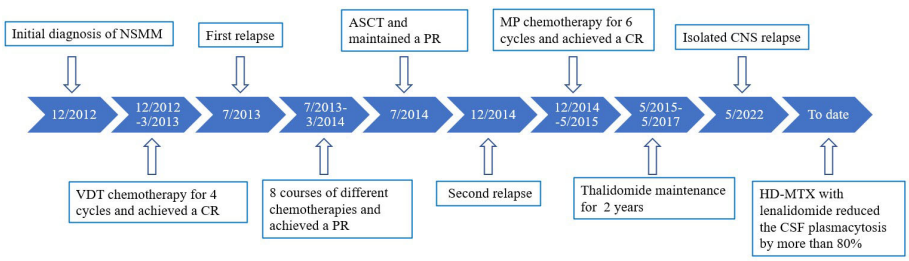

FIGURE 3
Timeline of the patient's diagnosis and treatments.

TABLE 1 Published case reports of patients with multiple myeloma who had isolated CNS relapse after ASCT.

Patient No. (Reference)	1 (10)	2 (11)	3 (12)	4 (13)	5 (14)	6 (15)	7 (15)	8 (16)
Age, years	39	55	32	58	29	49	66	66
Gender	Male	Male	Female	Male	Male	Male	Male	Male
Myeloma type	IgA-λ	IgG-κ	IgA-κ	IgA-κ	IgG-κ	IgG-λ	IgA-λ	IgG-κ
Stage								
DS	IIIB	IIIB	IIIA	IIIB	IIIB	IIIA	IIIA	IIIB
ISS					III	III	III	III
Plasma cell CD56 status	NA	NA	NA	NA	+	+	–	–
LDH	>ULN	>ULN	>ULN	NA	NA	NA	NA	NA
β_2-MG	≤ULN	NA	>ULN	>ULN	>ULN	NA	NA	NA
Cytogenetic abnormalities	NA	NA	NA	NA	NA	17p-, 1q21+	1q21+	NA
Plasma cell leukemia	yes	no	no	no	no	no	no	no
Treatments prior to ASCT, n	5	3	4	6	4	4	4	4
High-dose therapy	Mel	Mel	Mel	Bu/Mel/CY	Mel	Mel	Mel	NA
Time to relapse post-ASCT	3 months	3 months	10 weeks	7 years	6 months	9 months	6 months	8 months
Parenchymal	yes	no	no	yes	yes	yes	yes	NA
Treatment for CNS-MM	IT	BCNU/CY/IT/RT/ ASCT	IT	IT/Dexa	CTAD/IT/RT	Surgery/RT DPACE/RD/ DVD	IT/RT	IT/RT/ Dexa
Best response to CNS-MM treatment	PD	CR	PD	CR	SD	PR	CR	CR
Survival post-CNS relapse	9 days	7 months	8 days	11 months	3 months	29 months	12 months	10 months
Patient No. (Reference)	**9** (16)	**10** (17)	**11** (8)	**12** (18)	**13** (19)	**14 (current case)**		
Age, years	40	58	56	62	46	38		
Gender	Female	Male	Female	Female	Female	Female		
Myeloma type	IgA-κ	IgG-κ	IgA-κ	IgG-λ	IgA-λ	nonsecretory		
Stage								
DS	IIIB	IIIB		IIIB	IIIB	IIIA		
ISS	III	III	III			I		
Plasma cell CD56 status	+	NA	NA	+	+	+		
LDH	NA	>ULN	NA	≤ULN	NA	≤ULN		
β_2-MG	NA	>ULN	NA	≤ULN	>ULN	≤ULN		
Cytogenetic abnormalities	17p-, t (4;14)	17p-, t (4;14)	hyperdiploid karyotype	17p-	NA	None		
Plasma cell leukemia	no	no	no	no	no	no		
Treatments prior ASCT, n	3	4	3	4	2	12		
High-dose therapy	NA	Mel	NA		Mel	Bu		

(Continued)

TABLE 1 Continued

Patient No. (Reference)	1 (10)	2 (11)	3 (12)	4 (13)	5 (14)	6 (15)	7 (15)	8 (16)
Time to relapse post-ASCT	8 months	5 months	4 months	7 years	6 months	7 years		
Parenchymal	NA	no	yes	yes	yes	no		
Treatment for CNS-MM	Dexa	DKBP-BD	VTD-PACE	IT/Dexa/PD	Chemotherapy*/IT/RT	HD-MTX/lenalidomide		
Best response to CNS-MM treatment	SD	CR	PR	CR	PR			
Survival post CNS relapse	2 months		2 months	11 months	5 months			

DS, Durie Salmon Staging system; ISS, International Staging System; LDH, lactate dehydrogenase; β_2-MG, β_2 microglobulin; ASCT, autologous stem cell transplatation; CNS-MM, central nervous system localization of multiple myeloma; NA, not available; ULN, upper limit of normal; PD, progressive disease; CR, complete response; SD, stable disease; PR, partial response; Mel, melphalan; CY, cyclophosphamide; BU, busulfan; IT, intrathecal chemotherapy; BCNU, carmustine; RT, radiotherapy; MP, melphalan and prednisolone; HDT, high dose therapy; Dexa, dexamethasone; CTAD, cyclophosphamide, thalidomide, adriamycin, and dexamethasone; DPACE, dexamethasone, cisplatin, doxorubicin, cyclophosphamide and etoposide; RD, lenalidomide and dexamethasone; DVD, daratumumab, bortezomib, and dexamethasone; DKBP,BD, dexamethasone, carfilzomib, bendamustine, pomalidomide, clarithromycin, and daratumumab; VTD-PACE, bortezomib, thalidomide, dexamethasone, cis,platin, doxorubicin, cyclophosphamide, and etoposide; PD, pomalidomide and dexamethasone; Chemotherapy*, topotecan, temozolomide and dexamethasone; HD-MTX, high-dose methotrexate.

involvement (14, 25, 26). Our patient received first-line ASCT after aggressive therapy, and had none of the factors associated with risk for CNS involvement at baseline. After our patient achieved a 7-year progression-free survival, the selection of plasma cells with an atypical homing behavior and the absence of immunoglobulin secretion may have led to the isolated CNS relapse. We hypothesize that her relapse may have been from a new clone, rather than the clone responsible for the initial diagnosis.

There is currently no standard treatment for CNS-MM. Traditional therapeutic strategies include chemotherapy, surgery, radiotherapy, and intrathecal injection, but evidence supporting their efficacy is limited and durable remission is rare (27). Previous studies of systemic chemotherapy agents (methotrexate, cytarabine, edabixin, azathioprine and thiotepa) that can penetrate the blood-brain barrier (BBB) may provide a rapid therapeutic effect (8, 28). However, due to their CNS toxicity and low efficacy in MM patients who have chromosome 17p-, treatments consisting of traditional chemotherapy drugs alone are insufficient. Given the known radiosensitivity of malignant plasma cells, craniospinal irradiation is frequently used to treat parenchymal CNS-MM lesions (29). Although this treatment modality is associated with a statistically significantly longer survival (9), hematologic toxicity is a potential concern, especially in the cases who prior exposure to several myelosuppressive chemotherapy agents and ASCT (30).

Although novel agents have improved the outcomes of patients with CNS-MM (31), most conventional anti-myeloma drugs have relatively poor CNS penetration. A literature review of the penetration of novel myeloma-active drugs into the CSF reported that some immunomodulatory drugs (IMiDs) entered the CSF. For example, thalidomide can be detected in CSF after oral administration (32) and the lenalidomide and pomalidomide concentrations in CSF can reach 11% to 49% of the peak concentration in blood. Thus, these drugs may have good CSF activity against lymphoma and myeloma when there is CNS involvement (33–36). In addition, similar studies showed that one-third of lenalidomide-resistant patients still responded to pomadodomide, particularly those with MM with chromosome 17p- and/or translocation (4, 14) (37, 38).

Few proteasome inhibitors can penetrate the BBB, limiting their efficacy in patients with CNS-MM (27). Marizomib and carfilzomib are novel next-generation proteasome inhibitors that can pass through the BBB and may be effective in CNS-MM. For example, an animal study of radiolabeled marizomib reported the CNS level was 30% of that in the blood (39). Case reports (40) showed that marizomib provided clinical and radiological improvements, so it may be an effective approach for treatment of CNS-MM. Some case series also reported that carfilzomib was effective in the clearance of myeloma cells from CSF (41).

Some studies examined the ability of monoclonal antibodies to improve the outcomes of patients with CNS-MM. Although the penetration of systemic daratumumab (anti-CD38 monoclonal antibody) into the CNS was limited, it produced durable responses in some case reports. It is possible that the BBB becomes more permeable in certain disease states, such as when there is disruption of the meninges (28, 42).

In addition to monoclonal antibodies, the recently developed B-cell maturation antigen, chimeric antigen receptor T cell (BCMA CAR-T) therapy is a novel treatment strategy for relapsed/refractory(R/R) CNS-involved MM. For example, Wang et al. identified the presence of BCMA CAR-T cells in CSF (43). The mechanisms responsible for the higher CD4/CD8 ratio in CSF than in peripheral blood may regulate the

TABLE 2 Summary of multiple myeloma cases who had isolated CNS relapse after ASCT (n=14).

Characteristic	n	%
Gender		
Male	9	64
Female	5	36
Age, median years (range)	52 (29,66)	
Myeloma type		
IgA-λ	3	21
IgA-κ	4	29
IgG-λ	2	14
IgG-κ	4	29
Nonsecretory	1	7
Cytogenetics		
17p-	4	29
1q21+	2	14
t (4;14)	2	14
Not evaluated	7	
LDH		
>ULN	4	29
≤ULN	2	14
Not evaluated	8	
β_2-MG		
>ULN	5	36
≤ULN	3	21
Not evaluated	6	
Plasma cell leukemia	1	7
Time to relapse post ASCT, median months (range)	6 (2.5,84)	
Treatment for CNS-MM		
Intrathecal	9	64
Radiotherapy	6	43
Proteasome inhibitors	3	21
Immunomodulatory drugs	6	43
Anti-CD38 monoclonal antibody	2	14
ASCT	1	7
Survival post CNS relapse, median months (range)	6 (0.3,29)	

ULN, upper limit of normal.

penetration of CD4 + and CD8 + CAR-T cells across the BBB and their proliferation in CSF to kill myeloma cells. Several studies investigated the effects of BCMA CAR-T cells on CNS-MM patients and reported remarkable clinical remissions (43, 44). Closer monitoring of patients may help in the early identification of CAR-T neurotoxicity, thus making immune effector cell-associated neurotoxicity syndrome (ICANS) more predictable and controllable (45). BCMA CAR-T therapy appears to be a safe and effective for treatment for R/R CNS-MM, but the duration of remission is a remaining problem.

Although the optimal therapy for CNS-MM is uncertain because of the rarity of this condition, aggressive management is necessary. Examination of individualized combinations of chemotherapy, targeted drugs, monoclonal antibodies, CAR-T cells, and local therapy could lead to further improvements of outcomes.

Conclusion

Our study describes a case of CNS-MM following ASCT, with no evidence of systemic involvement. High dose methotrexate and lenalidomide (which can cross the BBB) produced a rapid response and effectively cleared myeloma cells from the CSF, but the duration of this remission must be addressed. Isolated CNS relapse after ASCT in MM is extremely rare. Even with novel therapies, the survival time after CNS-MM remains poor, and the optimal method for management of these patients is an open question because of the rarity of this condition. Further studies are required to identify factors associated with CNS relapse after ASCT and the underlying mechanism, and to determine improved methods of prophylaxis and management.

Data availability statement

The original contributions presented in the study are included in the article/supplementary material. Further inquiries can be directed to the corresponding author.

Ethics statement

The studies involving human participants were reviewed and approved by The Medical Ethics Committee of The Second Affiliated Hospital, College of Medicine, Zhejiang University. The patients/participants provided their written informed consent to participate in this study. Written informed consent was obtained from the individual(s) for the publication of any potentially identifiable images or data included in this article.

Author contributions

XL, WW, and YL contributed to the design and conception of the study; XL and WW contributed to data collection; XL contributed to writing the initial drafting of the manuscript; XZ and YL reviewed and edited the original draft. All authors contributed to manuscript revision and read and approved the submitted version.

Conflict of interest

The authors declare that the research was conducted in the absence of any commercial or financial relationships that could be construed as a potential conflict of interest.

Publisher's note

References

1. Palumbo A, Anderson K. Multiple myeloma. *N Engl J Med* (2011) 364:1046–60. doi: 10.1056/NEJMra1011442

2. Kumar SK, Rajkumar V, Kyle RA, van Duin M, Sonneveld P, Mateos MV, et al. Multiple myeloma. *Nat Rev Dis Primers* (2017) 3:17046. doi: 10.1038/nrdp.2017.46

3. Gagelmann N, Eikema DJ, Iacobelli S, Koster L, Nahi H, Stoppa AM, et al. Impact of extramedullary disease in patients with newly diagnosed multiple myeloma undergoing autologous stem cell transplantation: A study from the chronic malignancies working party of the EBMT. *Haematologica* (2018) 103:890–7. doi: 10.3324/haematol.2017.178434

4. Jurczyszyn A, Grzasko N, Gozzetti A, Czepiel J, Cerase A, Hungria V, et al. Central nervous system involvement by multiple myeloma: A multi-institutional retrospective study of 172 patients in daily clinical practice. *Am J Hematol* (2016) 91:575–80. doi: 10.1002/ajh.24351

5. Chen CI, Masih-Khan E, Jiang H, Rabea A, Cserti-Gazdewich C, Jimenez-Zepeda VH, et al. Central nervous system involvement with multiple myeloma: Long term survival can be achieved with radiation, intrathecal chemotherapy, and immunomodulatory agents. *Br J Haematol* (2013) 162:483–8. doi: 10.1111/bjh.12414

6. Majd N, Wei X, Demopoulos A, Hormigo A, Chari A. Characterization of central nervous system multiple myeloma in the era of novel therapies. *Leuk Lymphoma* (2016) 57:1709–13. doi: 10.3109/10428194.2015.1122786

7. Abdallah AO, Atrash S, Shahid Z, Jameel M, Grazziutti M, Apewokin S, et al. Patterns of central nervous system involvement in relapsed and refractory multiple myeloma. *Clin Lymphoma Myeloma Leuk* (2014) 14:211–4. doi: 10.1016/j.clml.2013.11.004

8. Varga G, Mikala G, Gopcsa L, Csukly Z, Kollai S, Balázs G, et al. Multiple myeloma of the central nervous system: 13 cases and review of the literature. *J Oncol* (2018) 2018:3970169. doi: 10.1155/2018/3970169

9. Nieuwenhuizen L, Biesma DH. Central nervous system myelomatosis: Review of the literature. *Eur J Haematol* (2008) 80:1–9. doi: 10.1111/j.1600-0609.2007.00956.x

10. Petersen SL, Wagner A, Gimsing P. Cerebral and meningeal multiple myeloma after autologous stem cell transplantation. a case report and review of the literature. *Am J Hematol* (1999) 62:228–33. doi: 10.1002/(sici)1096-8652(199912)62:4<228::aid-ajh5>3.0.co;2-3

11. Veinstein A, Brizard A, Randriamalala E, Babin P, Preud'homme JL, Guilhot F. Central nervous system relapses after autologous stem cell transplantation for myeloma. report of two cases. *Hematol Cell Ther* (1997) 39:327–30. doi: 10.1007/s00282-997-0327-6

12. Ulusakarya A, Youssef A, Bayle C, Vantelon JM, Munck JN. Plasma cell meningitis after an autograft in a patient with multiple myeloma. *Leuk Lymphoma* (1999) 34:633–4. doi: 10.3109/10428199909058496

13. Seftel MD, Maguire J, Voss N, Woodhurst WB, Dalal BI, Shepherd JD. Intra-cerebral relapse following prolonged remission after autologous stem cell transplantation for multiple myeloma. *Leuk Lymphoma* (2002) 43:2399–403. doi: 10.1080/1042819021000040125

14. Mittal A, Pushpam D, Kumar L. Isolated central nervous system relapse of multiple myeloma post autologous stem cell transplant- a rare presentation. *Leuk Res Rep* (2020) 14:100207. doi: 10.1016/j.lrr.2020.100207

15. Bergantim R, Bastos J, Soares MJ, Carvalho B, Soares P, Marques C, et al. Aggressive central nervous system relapse after autologous stem cell transplant in multiple myeloma: Case reports and literature review. *Case Rep Hematol* (2020) 2020:8563098. doi: 10.1155/2020/8563098

16. Gangatharan SA, Carney DA, Prince HM, Wolf MM, Januszewicz EH, Ritchie DS, et al. Emergence of central nervous system myeloma in the era of novel agents. *Hematol Oncol* (2012) 30:170–4. doi: 10.1002/hon.1021

17. Mousavi-Fatemi K, Maleki N. Management of central nervous system involvement in multiple myeloma after autologous hematopoietic stem cell transplantation. *Leuk Res Rep* (2020) 14:100210. doi: 10.1016/j.lrr.2020.100210

18. Marini A, Carulli G, Lari T, Buda G, Lambelet P, Ciancia EM, et al. Myelomatous meningitis evaluated by multiparameter flow cytometry: Report of a case and review of the literature. *J Clin Exp Hematop* (2014) 54:129–36. doi: 10.3960/jslrt.54.129

19. Annibali O, Nobile C, Greco R, Cellini F, Quattrocchi CC, Tirindelli MC, et al. The combination topotecan, temozolomide and dexamethasone associated with radiotherapy as treatment of central nervous system myeloma relapse. *Int J Hematol* (2009) 89:513–6. doi: 10.1007/s12185-009-0277-6

20. Chang H, Sloan S, Li D, Keith Stewart A. Multiple myeloma involving central nervous system: high frequency of chromosome 17p13.1 (p53) deletions. *Br J Haematol* (2004) 127:280–4. doi: 10.1111/j.1365-2141.2004.05199.x

21. Schmidt TM, Fonseca R, Usmani SZ. Chromosome 1q21 abnormalities in multiple myeloma. *Blood Cancer J* (2021) 11:83. doi: 10.1038/s41408-021-00474-8

22. Biran N, Malhotra J, Bagiella E, Cho HJ, Jagannath S, Chari A. Patients with newly diagnosed multiple myeloma and chromosome 1 amplification have poor outcomes despite the use of novel triplet regimens. *Am J Hematol* (2014) 89:616–20. doi: 10.1002/ajh.23705

23. Gundesen MT, Lund T, Moeller HEH, Abildgaard N. Plasma cell leukemia: Definition, presentation, and treatment. *Curr Oncol Rep* (2019) 21:8. doi: 10.1007/s11912-019-0754-x

24. Katodritou E, Terpos E, Kastritis E, Delimpasis S, Symeonidis AS, Repousis P, et al. Lack of survival improvement with novel anti-myeloma agents for patients with multiple myeloma and central nervous system involvement: The Greek myeloma study group experience. *Ann Hematol* (2015) 94:2033–42. doi: 10.1007/s00277-015-2484-y

25. Keats JJ, Chesi M, Egan JB, Garbitt VM, Palmer SE, Braggio E, et al. Clonal competition with alternating dominance in multiple myeloma. *Blood* (2012) 120:1067–76. doi: 10.1182/blood-2012-01-405985

26. Zeiser R, Deschler B, Bertz H, Finke J, Engelhardt M. Extramedullary vs medullary relapse after autologous or allogeneic hematopoietic stem cell transplantation (HSCT) in multiple myeloma (MM) and its correlation to clinical outcome. *Bone Marrow Transplant* (2004) 34:1057–65. doi: 10.1038/sj.bmt.1704713

27. Egan PA, Elder PT, Deighan WI, O'Connor SJM, Alexander HD. Multiple myeloma with central nervous system relapse. *Haematologica* (2020) 105:1780–90. doi: 10.3324/haematol.2020.248518

28. Elhassadi E, Murphy M, Hacking D, Farrell M. Durable treatment response of relapsing CNS plasmacytoma using intrathecal chemotherapy, radiotherapy, and daratumumab. *Clin Case Rep* (2018) 6:723–8. doi: 10.1002/ccr3.1451

29. Tsang RW, Campbell BA, Goda JS, Kelsey CR, Kirova YM, Parikh RR, et al. Radiation therapy for solitary plasmacytoma and multiple myeloma: Guidelines from the international lymphoma radiation oncology group. *Int J Radiat Oncol Biol Phys* (2018) 101:794–808. doi: 10.1016/j.ijrobp.2018.05.009

30. Kauffmann G, Buerki RA, Lukas RV, Gondi V, Chmura SJ. Case report of bone marrow-sparing proton therapy craniospinal irradiation for central nervous system myelomatosis. *Cureus* (2017) 9:e1885. doi: 10.7759/cureus.1885

31. Touzeau C, Moreau P. How I treat extramedullary myeloma. *Blood* (2016) 127:971–6. doi: 10.1182/blood-2015-07-635383

32. Vicari P, Ribas C, Sampaio M, Arantes AM, Yamamoto M, Filho JB, et al. Can thalidomide be effective to treat plasma cell leptomeningeal infiltration? *Eur J Haematol* (2003) 70:198–9. doi: 10.1034/j.1600-0609.2003.00022.x

33. Bladé J, Fernández de Larrea C, Rosiñol L, Cibeira MT, Jiménez R, Powles R., et al. Soft-tissue plasmacytomas in multiple myeloma: Incidence, mechanisms of extramedullary spread, and treatment approach. *J Clin Oncol* (2011) 29:3805–12. doi: 10.1200/JCO.2011.34.9290

34. Devoe CE, Li JY, Demopoulos AM. The successful treatment of a recurrent intracranial, dural-based plasmacytoma with lenalidomide. *J Neurooncol* (2014) 119:217–20. doi: 10.1007/s11060-014-1475-5

35. Li Z, Qiu Y, Personett D, Huang P, Edenfield B, Katz J, et al. Pomalidomide shows significant therapeutic activity against CNS lymphoma with a major impact on the tumor microenvironment in murine models. *PloS One* (2013) 8:e71754. doi: 10.1371/journal.pone.0071754

36. Selene I, Jose J, Malik MN, Qureshi A, Anwer F. Presentation patterns and management strategies for central nervous system involvement in multiple myeloma: A systematic review of literature. *Blood* (2018) 132:1951. doi: 10.1182/blood-2018-99-109923

37. Leleu X, Karlin L, Macro M, Hulin C, Garderet L, Roussel M, et al. Pomalidomide plus low-dose dexamethasone in multiple myeloma with deletion 17p and/or translocation (4,14): IFM 2010-02 trial results. *Blood* (2015) 125:1411–7. doi: 10.1182/blood-2014-11-612069

38. Mussetti A, Dalto S, Montefusco V. Effective treatment of pomalidomide in central nervous system myelomatosis. *Leuk Lymphoma* (2013) 54:864–6. doi: 10.3109/10428194.2012.718343

39. Di K, Lloyd GK, Abraham V, MacLaren A, Burrows FJ, Desjardins A, et al. Marizomib activity as a single agent in malignant gliomas: Ability to cross the blood-brain barrier. *Neuro Oncol* (2016) 18:840–8. doi: 10.1093/neuonc/nov299

40. Badros A, Singh Z, Dhakal B, Kwok Y, MacLaren A, Richardson P, et al. Marizomib for central nervous system-multiple myeloma. *Br J Haematol* (2017) 177:221–5. doi: 10.1111/bjh.14498

41. Espinoza R, Nolasco DB, Alejandro S, Nidia Z, Eduardo C, Candelaria M, et al. Report of 5 cases of extramedullary myeloma with central nervous system involvement treated with a combination of Carfilzomib/Thalidomide/Dexamethasone as a first line treatment at a single institution in Mexico. *Blood* (2016) 128:5704. doi: 10.1182/blood.V128.22.5704.5704

42. Zajec M, Frerichs KA, van Duijn MM, Nijhof IS, Stege CAM, Avet-Loiseau H, et al. Cerebrospinal fluid penetrance of daratumumab in leptomeningeal multiple myeloma. *Hemasphere* (2020) 4:e413. doi: 10.1097/HS9.0000000000000413

43. Wang Y, Zu C, Teng X, Yang L, Zhang M, Hong R, et al. BCMA CAR-T therapy is safe and effective for Refractory/Relapsed multiple myeloma with central nervous system involvement. *J Immunother* (2022) 45:25–34. doi: 10.1097/CJI.0000000000000391

44. Wang Y, Wang L, Zeng Y, Hong R, Zu C, Yin ETS, et al. Successful BCMA CAR-T therapy for multiple myeloma with central nervous system involvement manifesting as cauda equina syndrome-a wandering road to remission. *Front Oncol* (2021) 11:755584. doi: 10.3389/fonc.2021.755584

45. Gust J, Hay KA, Hanafi LA, Li D, Myerson D, Gonzalez-Cuyar LF, et al. Endothelial activation and blood-brain barrier disruption in neurotoxicity after adoptive immunotherapy with CD19 CAR-T cells. *Cancer Discovery* (2017) 7:1404–19. doi: 10.1158/2159-8290.CD-17-0698

frontiers | Frontiers in Oncology

TYPE Case Report
PUBLISHED 29 November 2022
DOI 10.3389/fonc.2022.1023785

OPEN ACCESS

EDITED BY
Arpad Szallasi,
Semmelweis University, Hungary

REVIEWED BY
Peifeng Li,
960th Hospital of the PLA, China
Mike Barbeck,
Technical University of Berlin, Germany

*CORRESPONDENCE
Yoshiya Sugiura
yoshiya.sugiura@med.toho-u.ac.jp

†These authors have contributed equally to this work and share first authorship

SPECIALTY SECTION
This article was submitted to Hematologic Malignancies, a section of the journal Frontiers in Oncology

RECEIVED 24 August 2022
ACCEPTED 02 November 2022
PUBLISHED 29 November 2022

CITATION
Otsuka-Kamakura N, Sugiura Y, Yamazaki T, Shimizu N and Hiruta N (2022) Case report: Plasmablastic neoplasm with multinucleated giant cells—Analysis of stemness of the neoplastic multinucleated giant cells. *Front. Oncol.* 12:1023785. doi: 10.3389/fonc.2022.1023785

Case report: Plasmablastic neoplasm with multinucleated giant cells—Analysis of stemness of the neoplastic multinucleated giant cells

Narumi Otsuka-Kamakura[1†], Yoshiya Sugiura[1,2,3*†], Toshiki Yamazaki[1], Naomi Shimizu[4] and Nobuyuki Hiruta[1,2,3]

[1]Department of Pathology, Sakura Hospital, Toho University Medical Center, Sakura, Japan, [2]Department of Surgical Pathology, Sakura Hospital, Toho University Medical Center, Sakura, Japan, [3]Division of Pathology, The Cancer Institute, Japanese Foundation for Cancer Research, Tokyo, Japan, [4]Department of Hematology, Sakura Hospital, Toho University Medical Center, Sakura, Japan

Cancer stem cells have the capability of self-renewal and multipotency and are, therefore, associated with tumor heterogeneity, resistance to chemoradiation therapy, and metastasis. The hypothesis that multinucleated giant cells, which often emerge following chemo- and/or radiotherapy, serve as cancer stem cells has not been fully evaluated. Although a previous study demonstrated that these cells functioned as stem cells, only low levels of Yamanaka factors were expressed, contrasting with the high expression seen from their gestated first-generation mononuclear cells. Herein, we report a case of a plasmablastic neoplasm with multinucleated giant cells that were analyzed for stemness to test the above hypothesis. The patient was a male in his 80s who had a plasmablastic neoplasm that was not easily distinguishable as plasmablastic lymphoma versus plasma cell myeloma of plasmablastic type. Lymph node biopsy showed predominant mononuclear cell proliferation with admixed multinucleated giant cells. Immunohistochemistry and *in situ* hybridization showed that both multinucleated and mononuclear cells had the same profile: CD138(+), light chain restriction of κ>λ, cyclin D1(+), CD68(-), EBER-ISH (+). These results suggested that both cell types were neoplastic. In accordance with the previous study, the multinucleated giant cells showed low expression of Yamanaka factors, which were highly expressed in some of the mononuclear cells. Furthermore, the multinucleated giant cells showed a much lower proliferative activity (Mib1/Ki67 index) than the mononuclear cells. Based on these results, the multinucleated giant cells were compatible with cancer stem cells. This case is expected to expand the knowledge base regarding biology of cancer stem cells.

KEYWORDS

plasmablastic neoplasm, multinucleated giant cell, cancer stem cell, Yamanaka factors, Mib1/Ki67 index

Introduction

Plasmablastic lymphoma (PBL) is an aggressive B-cell lymphoma with plasmablastic features that occurs in immunodeficient patients and is usually associated with Epstein-Barr virus (EBV) infection. It was first reported as lymphoma of the oral cavity in a human immunodeficiency virus (HIV)-infected patient (1). However, many cases have since then been reported that involve different localizations while also occurring in patients who are HIV-negative (2).

Plasma cell myeloma (PCM) is a plasma cell neoplasm that commonly produces monoclonal immunoglobulin (M-protein). Some cases of extraosseous PCM showing severe atypia are classified as plasmablastic PCM (PPCM). It is often difficult to differentiate between PBL and PPCM (Supplemental Table 1) (3); thus, in such cases, a diagnosis of plasmablastic neoplasm (PBN) is made (4). There have been several reports of cases of PBL or PBN containing neoplastic multinucleated giant cells (5–7).

Recent *in vitro* and *in vivo* studies mainly conducted in cases of ovarian cancer have proposed the hypothesis that multinucleated giant cells serve as cancer stem cells and are associated with resistance to chemotherapy and the potential for metastasis (8, 9). To the best of our knowledge, this hypothesis has not been tested using surgical pathological analysis.

Herein, we present a case of PBN predominantly consisting of mononuclear cells with admixed multinucleated giant cells that were analyzed for stemness to test the above hypothesis.

Case description

A man in his 80s presented to our hospital with a chief complaint of a cervical mass. He had a history of angina and idiopathic interstitial pneumonia but had no overt immune deficiency. Physical examination showed enlarged lymph nodes on the right side of the neck. Computed tomography revealed enlarged cervical lymph nodes and involvement of the mandible and Th1 vertebral body (Supplemental Figure 1). Blood analysis showed increased serum immunoglobulin G (IgG) levels (Supplemental Table 2), and serum immunofixation electrophoresis detected IgG-κ type M-protein (Supplemental Figure 2) which demonstrates the results of serum immunofixation electrophoresis). A fine-needle aspiration biopsy of a cervical lymph node was performed, and the cytological findings suggested plasma cell neoplasm (Figure 1). Excisional lymph node biopsy was also performed, and the chromosome analysis revealed a deletion in chromosome 1 and two marker chromosomes (Supplemental Table 2), while chromosome 8 was not involved. The final pathological diagnosis was PBN, as described below. The tumor was chemotherapy-resistant, and the patient died 4 months after diagnosis.

Cytological and histological analysis

For cytological analysis, the cervical lymph node specimen obtained using fine needle aspiration was sprayed on glass slides, and the excisional biopsy specimen was sliced and placed on glass slides. These glass slides were quickly fixed with ethanol for Papanicolaou staining or air-dried and fixed with methanol for Giemsa staining. For histological analysis, tissues were processed following standard procedures. Formalin-fixed paraffin-embedded blocks were cut into 4-μm-thick sections and stained with hematoxylin and eosin.

The analysis showed diffusely proliferating mononuclear cells admixed with multinucleated giant cells. Because of the marked tumor invasion, the original architecture of the lymph node was almost lost. The mononuclear cells had eccentric round nuclei and a basophilic cytoplasm, exhibiting features of plasmablastic or plasma cells. The nuclei had prominent nucleoli and manifested anisokaryosis and irregular chromatin distribution. The multinucleated giant cells had dozens of nuclei, mimicking osteoclasts (Figure 1).

Immunohistochemistry and EBV detection

For immunohistochemistry, unstained specimens were submerged in either a sodium citrate buffer at 97˚C for 20 min or Tris-EDTA buffer at 95°C for 45 minutes or incubated with proteinase K at 37°C for 30 min to retrieve epitopes. Immunostaining was performed using Envision TM FLEX Target Retrieval Solution, High pH (50×) (Agilent, Santa Clara, CA, USA). Specimens underwent immunostaining for CD138, multiple myeloma oncogene-1, CD20, CD79a, CD68, Epstein-Barr nuclear antigen 2 (EBNA2), Cyclin D1, IgG, light chain restriction of κ and λ, cytokeratin AE1/AE3, octamer-binding transcription factor 4 (OCT4), Krüppel-like factor 4 (KLF4), c-Myc, SRY (sex-determining region Y)-box 2 (SOX2), and Mib1/Ki67 (Supplemental Table 3 which shows the primary antibodies used).

EBV RNA was detected using EBV-encoded RNA *in-situ* hybridization (EBER-ISH). The paraffin-embedded sections (thickness, 4 μm) were dewaxed with xylene, treated with proteinase K, and hybridized with fluorescein isothiocyanate-labeled EBER peptide nucleic acid probe (Agilent). After incubation with anti-fluorescein isothiocyanate-conjugated rabbit polyclonal antibody and polymer horseradish peroxidase-labeled anti-rabbit IgG antibody, slides were covered with diaminobenzidine + chromogen (Agilent).

The results are shown in Table 1. First, we assessed the line of differentiation (Table 1A). Both the mononuclear and multinucleated cells were positive for CD138 (Figure 2A) and revealed light chain restriction of κ>λ (Figure 2B), suggesting

10.3389/fonc.2022.1023785

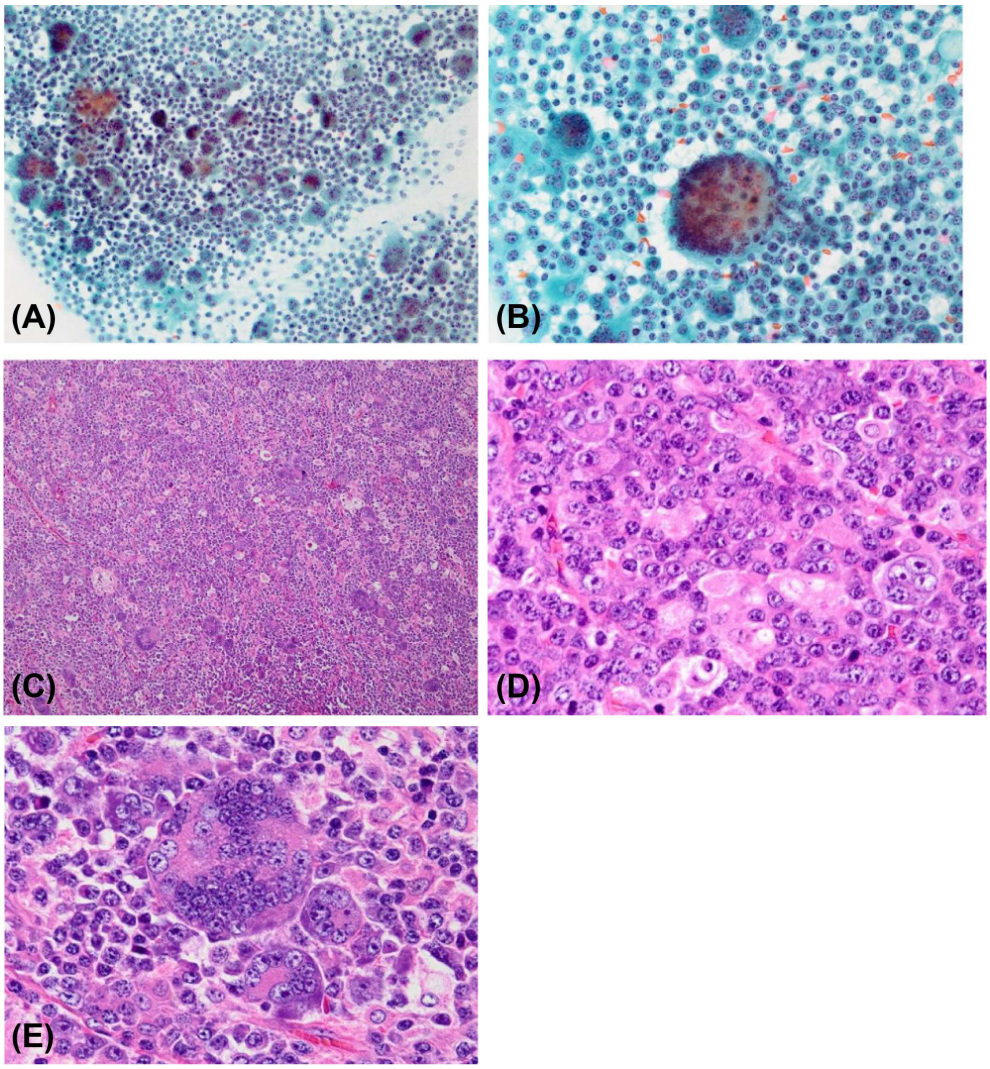

FIGURE 1
Cytological findings. **(A)** Proliferation of mononuclear cells admixed with multinucleated giant cells (Papanicolaou staining, original magnification ×20); **(B)** Multinucleated giant cells with dozens of nuclei (Papanicolaou staining, original magnification ×40). Histological findings. **(C)** The lymph node was almost replaced by the tumor, and its original architecture was lost (hematoxylin and eosin staining; original magnification ×10); **(D)** Predominant mononuclear neoplastic cells with prominent nucleoli and basophilic cytoplasm (hematoxylin and eosin staining; original magnification ×60); **(E)** Multinucleated giant cells with dozens of nuclei (hematoxylin and eosin staining; original magnification ×60).

monoclonal plasma cell proliferation. Furthermore, both cell types were positive for cyclin D1 (Figure 2C) and EBER-ISH (Figure 2D). However, both cell types were negative for CD68, a marker for histiocytes (Figure 2E). These results suggested that not only the mononuclear cells but also the multinucleated giant cells were neoplastic. The multinucleated giant cells were not considered osteoclasts because they expressed features of plasma cell neoplasms while lacking histiocytic features. The neoplastic cells were positive for EBER-ISH, suggesting PBL, but were also positive for cyclin D1, which suggested PPCM. In addition, they did not express EBNA2, a finding that did not support immune suppression and PBL. Due to this inconsistency, we could not differentiate between PBL and PPCM.

Next, we evaluated the stemness of the mononuclear and multinucleated cells (Table 1B). Some of the mononuclear cells exhibited strong cytoplasmic immunopositivity to OCT4, which was not the case with any of the multinucleated cells (Figure 2F). As for c-Myc, the mononuclear cells showed stronger nuclear immunopositivity than the multinucleated cells (Figures 2G, H). Among the multinucleated cells, those with a larger number of nuclei (Figure 2G) showed weaker positivity than those with a smaller number of nuclei (Figure 2H). As for KLF4, some of the

TABLE 1 Immunohistochemistry and *in situ* hybridization results.

A. Markers for diagnosis

Positive	Weakly positive	Negative	
CD138	CD3	ALK	CD7
CD38	CD56	CD10	CD79a
c-Myc	TIA-1	CD2	CD8
CyclinD1		CD20	Cytokeratin (AE1/AE3)
EBER-ISH		CD30	EMA
MUM-1		CD4	Granzyme B
κ>>λ		CD5	PAX-5
		CD68 (KP-1)	SOX2
		CD68 (PGM-1)	S-100
			TdT

B. Markers for stemness and proliferative activity

Markers	Mononuclear cells	Multinucleated giant cells
OCT4	Negative	Positive (strong and partial)
c-MYC	Positive (weak and partial)	Positive (strong and partial)
KLF4	Negative	Positive (strong and partial)
SOX2	Negative	Negative
CD44	Positive	Positive
Mib1/Ki67	Very low	Very high

These results were common for multinucleated giant cells and mononuclear cells.
EBER-ISH, Epstein-Barr virus-encoded RNA *in-situ* hybridization; MUM-1, multiple myeloma oncogene-1; ALK, anaplastic lymphoma kinase; EMA, epithelial membrane antigen; PAX-5, paired box 5; SOX2, SRY-box transcription factor 2; TdT, terminal deoxynucleotidyl transferase.
Oct4, octamer-binding transcription factor 4; KLF4, Krüppel-like factor 4; SOX2, SRY-box transcription factor 2.

mononuclear cells showed nuclear positivity, while multinucleated cells were consistently negative (Figure 2I). Both mononuclear and multinucleated cells were strongly positive for CD44 (Figure 2J) and negative for SOX2. Furthermore, the mononuclear cells had a high Mib1/Ki67 index, while multinucleated cells were scarcely positive (Figure 2K).

We have summarized these results in Figure 3 and compared them to the results of previous studies (8, 10). This comparison is explained in detail in the discussion.

Fluorescent *in situ* hybridization

Unstained sections (thickness, 4 μm) were "pretreated" using a Histology Fluorescent *in situ* hybridization (FISH) kit (GSP Laboratory, Kobe, Japan). Next, they were subjected to hybridization with BAC clone-derived probes for CCND1 and IGH, with a CKS1β dual-color probe set (Agilent) or with a c-Myc dual-color probe set (Abbott). The names of BAC clones used will be provided upon request. Hybridized slides were then stained with DAPI (4,6-diamidino-2-phenylindole, dihydrochloride) and examined using a fluorescence microscope BX51 (Olympus, Tokyo, Japan).

Split of CCND1 and/or IGH is a genetic marker for PPCM. However, neither was detected using FISH. Split of c-Myc is a genetic marker for PBL. However, it was not detected either. Moreover, amplification of CKS1β, a poor prognostic factor for PPCM (11), was also not detected.

Discussion

In the present case, the patient was diagnosed with PBN, comprising predominantly proliferating mononuclear cells with admixed multinucleated giant cells, both of which were confirmed to be neoplastic. The analysis of stemness indicated that the multinucleated giant cells were compatible with cancer stem cells.

Diagnosis, in this case, was challenging owing to the difficulty in differentiating between PBL and PPCM. The EBER-ISH positivity suggested PBL; however, there were no indicators of immune suppression as the patient had no history of HIV infection or organ transplantation, and the tumor cells were negative for EBNA2, an indicator of immune suppression (12). Without immune suppression, a diagnosis of PBL was not strongly suggested. Furthermore, approximately 50% of PBLs harbor a rearrangement of c-Myc on chromosome 8 (13–15),

10.3389/fonc.2022.1023785

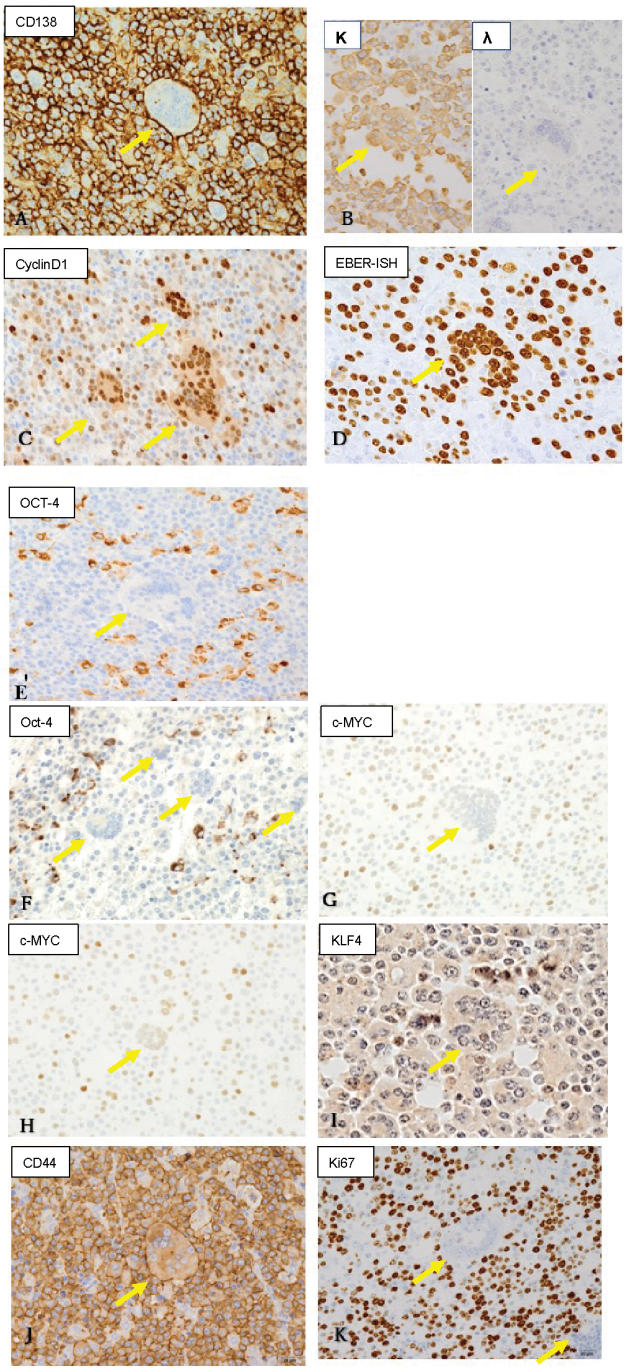

FIGURE 2
Immunohistochemistry and Epstein-Barr virus-encoded RNA (EBER) in-situ hybridization findings (original magnification ×40). Yellow arrows indicate multinucleated cells. Both multinucleated giant cells and mononuclear cells were positive for **(A)** CD138 (a plasma cell marker; membranous positive), **(B)** light chain restriction of κ>λ (suggesting monoclonality), **(C)** cyclin D1 (a marker for plasma cell myeloma), and **(D)** EBER (suggesting Epstein-Barr virus-associated neoplasm). **(E)** Both cell types were negative for CD68 (a histiocyte marker). **(F)** Mononuclear cells were positive, but multinuclear giant cells were negative for OCT4 (Yamanaka factor). **(G, H)** c-Myc (Yamanaka factor) expression was stronger in mononuclear than in multinucleated cells, and multinucleated cells with a larger number of nuclei **(G)** showed weaker positivity than those with a smaller number of nuclei **(H)**. **(I)** KLF4 (Yamanaka factor) was positive in some of the mononuclear cells, but negative in the multinucleated giant cells. **(J)** CD44 (a marker for cancer stem cells) was positive in both cell types. **(K)** Mib1/Ki67 showed strong positivity in the mononuclear cells, while the multinucleated cells were almost negative.

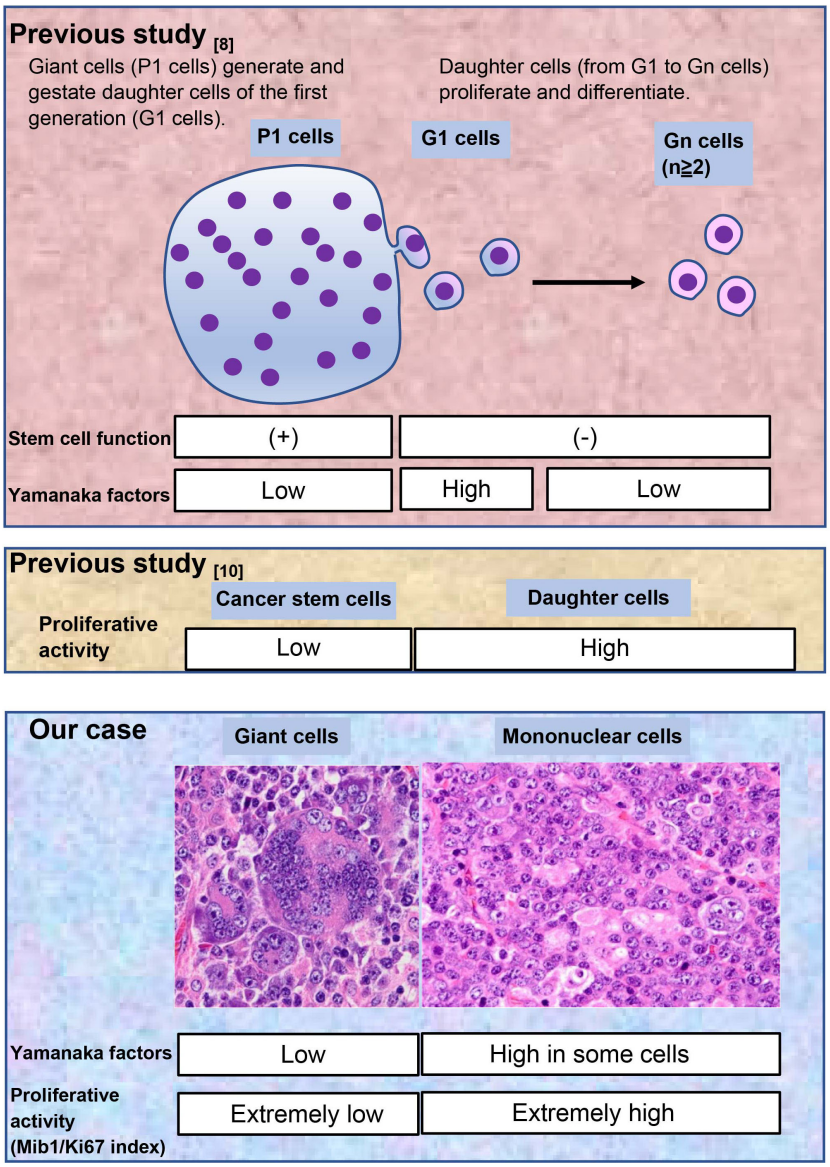

FIGURE 3
Comparison of our case with previous studies.

while, in this case, there was no abnormality in chromosome 8. In addition, the expression of cyclin D1 suggested PPCM, but the cytogenetic analyses did not detect translocation or amplification of CCND1. Hence, the final pathological diagnosis was PBN.

Adult stem cells are associated with the capacity for self-renewal and multipotency. In neoplasms, putative cancer stem cells play these roles. Following chemo- and/or radiotherapy, multinucleated giant cells often emerge as cancer stem cells and are associated with tumor heterogeneity, therapy resistance, and metastasis (8, 9). Nonetheless, the hypothesis that neoplastic multinucleated giant cells serve as cancer stem cells has not been fully evaluated. We tested this hypothesis using the Yamanaka factors and Mib1/Ki67.

First, we evaluated the Yamanaka factors (OCT4, SOX2, KLF4, and c-Myc), which are implicated in cancer cell stemness (16, 17). The tumor consisted of mononuclear and multinucleated giant cells, and we assessed the stemness of both cell lineages. In a previous study on post-chemotherapy ovarian cancer, neoplastic multinucleated giant cells, designated as P1 cells, generated and gestated mononuclear daughter cells, designated as Gn cells (G1 cells were the first generation of Gn cells), and these cells were involved in drug resistance (8). Although P1 cells had stem cell functions, stem

cell markers such as CD44 and Yamanaka factors were more strongly expressed in G1 than in P1 cells in that study. This unexpected phenomenon has not yet been fully explained. In concordance with the previous study (8), in our case, the stem cell markers OCT4, c-Myc, and KLF4 were more strongly expressed in the mononuclear than in the multinucleated giant cells. Moreover, SOX2 was negative in both cell types.

Next, we evaluated the proliferative activity. Stem cells generally grow slowly and have low proliferating activity (10). We used the Mib1/Ki67 index as an indicator of proliferative activity. In our case, mononuclear and multinucleated giant cells had a very high and very low Mib1/Ki67 index, respectively, which was interpreted as supportive evidence for the stemness of the multinucleated giant cells. Based on these results, we concluded that the multinucleated giant cells (P1 cells) were cancer stem cells.

Previous studies on neoplastic multinucleated giant cells have been conducted primarily after chemo- or radiation therapy. According to the study on ovarian cancer, multinucleated giant cells were rarely seen in untreated patients and markedly increased after chemotherapy (8).

In our case, there were several multinucleated giant cells even before chemotherapy, suggesting that the phenomenon of maternal multinucleated giant cells gestating mononuclear cells is not limited to the post-chemotherapy period. Moreover, we used formalin-fixed paraffin-embedded specimens for the analysis, ensuring high accessibility. The same analyses can be conducted on multiple cases at a low cost.

Considering the persisting scarcity of knowledge on cancer stem cells, we believe that the present case will add insight to the biology of cancer stem cells.

Data availability statement

The original contributions presented in the study are included in the article/Supplementary Material. Further inquiries can be directed to the corresponding author.

Ethics statement

The studies involving human participants were reviewed and approved by The Ethics Committee of Toho University. The patients/participants provided their written informed consent to participate in this study. Written informed consent was obtained from the individual(s) for the publication of any potentially identifiable images or data included in this article.

Author contributions

NO-K and YS contributed to conception and design of the study. NO-K and TY conducted the immunohistochemical and molecular biological experiments. NO-K and YS were involved in the data analyses. NO-K wrote the first draft of the manuscript. YS wrote sections of the manuscript. NS and NH reviewed the manuscript. All authors contributed to manuscript revision, read, and approved the submitted version.

Acknowledgments

The authors thank Dr. Kengo Takeuchi from the Cancer Institute, Japanese Foundation for Cancer Research, for his insightful suggestions. The authors are also grateful to Ms. Satoko Baba for preparing tests using fluorescent *in situ* hybridization. We would like to thank Editage (www.editage.com) for English language editing.

Conflict of interest

The authors declare that the research was conducted in the absence of any commercial or financial relationships that could be construed as a potential conflict of interest.

Publisher's note

Supplementary material

The Supplementary Material for this article can be found online at: https://www.frontiersin.org/articles/10.3389/fonc.2022.1023785/full#supplementary-material

References

1. The Delecluse HJ, Anagnostopoulos I, Dallenbach FE, Hummel M, Marafioti T, Schneider U, et al. Plasmablastic lymphomas of the oral cavity: a new entity associated with the human immunodeficiency virus infection. *Blood* (1997) 89:1413–20. doi: 10.1182/blood.V89.4.1413

2. Lopez A, Abrisqueta P. Plasmablastic lymphoma: current perspectives. *Blood Lymphat Cancer* (2018) 8:63–70. doi: 10.2147/BLCTT.S142814

3. Ahn JS, Okal R, Vos JA, Smolkin M, Kanate AS, Rosado FG. Plasmablastic lymphoma versus plasmablastic myeloma: an ongoing diagnostic dilemma. *J Clin Pathol* (2017) 70:775–80. doi: 10.1136/jclinpath-2016-204294

4. Campo E, Stein H, Harris NL. Plasmablastic lymphoma. In: Swerdlow SH, Campo E, Harris NL, Jaffe ES, Pileri SA, Stein H, et al, eds. WHO Classification of Tumours of Haematopoietic and Lymphoid Tissues, Revised, *4th Edition*. Lyon, France: IARC (2017). p. 321–322.

5. Guijarro F, Rozman M, Matutes E. Multinucleated giant myeloma cells after failure of daratumumab therapy. *Br J Haematol* (2018) 181:432. doi: 10.1111/bjh.15139

6. Ghattas S, Salisbury J. Giant multinucleated plasma cells in relapsed plasma cell myeloma. *eJHaem* (2020) 1:16–7. doi: 10.1002/jha2.35

7. Harankhedkar S, Gupta R, Rahman K. Pleomorphic multinucleated plasma cells simulating megakaryocytes in an anaplastic variant of myeloma. *Turk J Haematol* (2018) 35:150–1. doi: 10.4274/tjh.2017.0329

8. Díaz-Carballo D, Saka S, Klein J, Rennkamp T, Acikelli AH, Malak S, et al. A distinct oncogenerative multinucleated cancer cell serves as a source of stemness and tumor heterogeneity. *Cancer Res* (2018) 78:2318–31. doi: 10.1158/0008-5472.CAN-17-1861

9. Pienta KJ, Hammarlund EU, Brown JS, Amend SR, Axelrod RM. Cancer recurrence and lethality are enabled by enhanced survival and reversible cell cycle arrest of polyaneuploid cells. *Proc Natl Acad Sci USA* (2021) 118:e2020838118. doi: 10.1073/pnas.2020838118

10. Shiokawa D, Sakai H, Ohata H, Miyazaki T, Kanda Y, Sekine S, et al. Slow-cycling cancer stem cells regulate progression and chemoresistance in colon cancer. *Cancer Res* (2020) 80:4451–64. doi: 10.1158/0008-5472.CAN-20-0378

11. Bahmanyar M, Qi X, Chang H. Genomic aberrations in anaplastic multiple myeloma: high frequency of 1q21(CKS1B) amplifications. *Leuk Res* (2013) 37:1726–8. doi: 10.1016/j.leukres.2013.09.025

12. Brink AA, Dukers DF, Van den Brule AJ, Oudejans JJ, Middeldorp JM, Meijer CJ, et al. Presence of Epstein-Barr virus latency type III at the single cell level in post-transplantation lymphoproliferative disorders and AIDS related lymphomas. *J Clin Pathol* (1997) 50:911–8. doi: 10.1136/jcp.50.11.911

13. Bogusz AM, Seegmiller AC, Garcia R, Shang P, Ashfaq R, Chen W. Plasmablastic lymphomas with MYC/IgH rearrangement: report of three cases and review of the literature. *Am J Clin Pathol* (2009) 132:597–605. doi: 10.1309/AJCPFUR1BK0UODTS

14. Taddesse-Heath L, Meloni-Ehrig A, Scheerle J, Kelly JC, Jaffe ES. Plasmablastic lymphoma with MYC translocation: evidence for a common pathway in the generation of plasmablastic features. *Mod Pathol* (2010) 23:991–9. doi: 10.1038/modpathol.2010.72

15. Valera A, Balagué O, Colomo L, Martínez A, Delabie J, Taddesse-Heath L, et al. IG/MYC rearrangements are the main cytogenetic alteration in plasmablastic lymphomas. *Am J Surg Pathol* (2010) 34:1686–94. doi: 10.1097/PAS.0b013e3181f3e29f

16. Takahashi K, Yamanaka S. Induction of pluripotent stem cells from mouse embryonic and adult fibroblast cultures by defined factors. *Cell* (2006) 126:663–76. doi: 10.1016/j.cell.2006.07.024

17. Fatma H, Siddique HR. Pluripotency inducing yamanaka factors: role in stemness and chemoresistance of liver cancer. *Expert Rev Anticancer Ther* (2021) 21:853–64. doi: 10.1080/14737140.2021.1915137

frontiers | Frontiers in Oncology

TYPE Case Report
PUBLISHED 05 December 2022
DOI 10.3389/fonc.2022.1069977

OPEN ACCESS

EDITED BY
Ahmad Antar,
Almoosa Specialist Hospital,
Saudi Arabia

REVIEWED BY
Tamar Tadmor,
Technion Israel Institute of Technology, Israel
Gábor Barna,
Semmelweis University, Hungary

*CORRESPONDENCE
Giovanni D'Arena
giovannidarena@libero.it
Daniela Lamorte
daniela.lamorte@crob.it

SPECIALTY SECTION
This article was submitted to Hematologic Malignancies, a section of the journal Frontiers in Oncology

RECEIVED 14 October 2022
ACCEPTED 14 November 2022
PUBLISHED 05 December 2022

CITATION
Valvano L, D'Auria F, Grieco V, Statuto T, Nozza F, Pietrantuono G, Villani O, D'Arena G and Lamorte D (2022) Case report: Hematologic malignancies concomitant diagnosis of hairy cell leukemia and chronic lymphocytic leukemia: A rare association.
Front. Oncol. 12:1069977.
doi: 10.3389/fonc.2022.1069977

Case report: Hematologic malignancies concomitant diagnosis of hairy cell leukemia and chronic lymphocytic leukemia: A rare association

Luciana Valvano[1], Fiorella D'Auria[2], Vitina Grieco[1], Teodora Statuto[1], Filomena Nozza[1], Giuseppe Pietrantuono[3], Oreste Villani[3], Giovanni D'Arena[4]* and Daniela Lamorte[5]*

[1]Laboratory of Clinical and Advanced Diagnostics, Centro di Riferimento Oncologico della Basilicata (IRCCS CROB), Rionero in Vulture, Italy, [2]Laboratory of Clinical Pathology, Centro di Riferimento Oncologico della Basilicata (IRCCS CROB), Rionero in Vulture, Italy, [3]Hematology and Stem Cell Transplantation Unit, Centro di Riferimento Oncologico della Basilicata (IRCCS CROB), Rionero in Vulture, Italy, [4]Hematology, P. O. S. Luca, ASL, Salerno, Italy, [5]Laboratory of Preclinical and Translational Research, Centro di Riferimento Oncologico della Basilicata (IRCCS CROB), Rionero in Vulture, Italy

A case of concomitant hairy cell leukemia (HCL) and chronic lymphocytic leukemia (CLL) in a 50- year-old man was reported. Flow cytometry and droplet digital PCR (ddPCR) were used to detect the B-Raf proto-oncogene (BRAF) V600E mutation. The HCL population was the predominant component. The patient was first treated with cladribine and then with rituximab and achieved HCL partial remission. Importantly, the high sensitivity of our flow cytometric approach allowed the detection of a small population "P3," in addition to the typical HCL and CLL clones. The P3 clone changed over time, from an HCL-like to a CLL-like immunophenotype. This case is added to the few other cases of synchronous HCL and CLL already reported in the literature and underlines the importance of analyzing chronic lymphoproliferative disorders by highly sensitive diagnostic techniques, like the multicolor flow cytometry and ddPCR, to evaluate the possible association between HCL and CLL at diagnosis.

KEYWORDS

hairy cell leukemia, chronic lymphocytic leukemia, flow cytometry, BRAF V600E mutation, droplet digital PCR

Introduction

Hairy cell leukemia (HCL) is a rare neoplasm representing 2% of all lymphoid leukemia (1). The median age at diagnosis is 55 years, and it predominantly affects men. Typically, HCL patients show cytopenias, splenomegaly, a low percentage of circulating hairy cells, and diffuse leukemic bone marrow infiltration. The B-RAf proto oncogene (BRAF) V600E point mutation occurs in 97% of HCL patients and is responsible for the typical "hairy" appearance of the HCL cells (1). This mutation constitutively activates the RAS-RAF-MEK-ERK signaling pathway, inducing cellular proliferation and survival. Hairy cells have a typical pattern of B-cell antigen expression (CD19+, CD20+, and CD22+) with the coexpression of CD11c, CD25, and CD103. Although the association of HCL with other neoplasms is well known, the simultaneous diagnosis of HCL and other tumors is very rare. A case of concomitant diagnosis of HCL and B-cell chronic lymphocytic leukemia (CLL) was reported and compared with other literature-reported ones.

Case presentation

A 50-year-old man was referred to our center because of fatigue for approximately 2 months, neutropenia, anemia, and thrombocytopenia (Table 1). Pale skin and splenomegaly were also found at physical examination. A peripheral blood (PB) smear showed lymphocytes (90%), neutrophils (10%), and 0% monocytes. Two distinct monoclonal B-cell populations were detected by flow cytometry immunophenotypic analyses. The predominant population, approximately 66% of the white blood cell (WBC) count, was consistent with HCL: $CD19^{+high}$, $CD20^{+high}$, $CD5^{-}$, $CD23^{-}$, $CD43^{-}$, $CD10^{-}$, $CD103^{+}$, $CD25^{+}$, $CD11c^{+}$, $CD79b^{+}$, $CD200^{+}$, $FMC7^{+}$, $CD22^{+high}$, and $sIg\lambda^{+high}$. A smaller population (approximately 17%) showed the $CD19^{+intermediate}$, $CD20^{+low}$, $CD5^{+intermediate}$, CD23+, CD43+, CD10-, CD103-, CD25-, CD11c-, CD79b-, CD200+, FMC7+/-, $CD22+^{low}$, and $sIg\kappa+^{low}$ immunophenotype, consistent with monoclonal B-cell lymphocytosis (MBL), typical B-CLL-like (Table 2, Figure 1A). The hairy cells were counted as monocytes by automated blood cell counters (Table 1). There were 90% of hairy cells with a minimal localization of small-sized lymphocytes found upon morphological examination of the bone marrow (BM). Two distinct monoclonal B-cell populations, consistent with HCL and MBL, were also found in the BM by flow cytometry analyses. The BRAF V600E mutation evaluated by droplet digital PCR (ddPCR) was found with 38% marrow involvement. Fluorescence in situ hybridization (FISH) analysis performed on fixed nuclei using the commercially available Vysis CLL FISH Probe Kit showed the deletion of chromosome 13 and the presence of wild-type Tp53 and ATM genes. Finally, the diagnosis of a composite predominant HCL with a minor clone of MBL CLL-like was made.

The patient was treated with cladribine after informed consent was given. At +3 months after the diagnosis (t1), he achieved partial remission (PR) with moderate neutropenia and thrombocytopenia and the resolution of anemia (Table 1). The immunophenotyping of BM aspirate revealed an HCL population reduction to 0.9%, while the CLL population was 16% among WBCs (Table 2, Figure 1B). Likewise, the persistence of the BRAF V600E mutation (1%) was described (Table 2). For that reason, additional four weekly cycles followed by another four biweekly cycles of rituximab were also given, followed by a watch-and-wait approach on the PR status. Either cladribine or rituximab was well tolerated without relevant side effects.

The persistence of the two pathological B-cell populations (HCL and MBL, both without CD20 surface expression) was detected in the BM 1 month after the end of rituximab treatment (t2) (Table 2, Figure 1C). The BRAF V600E mutation was still detectable (Table 2). At +8 months (t3), the flow cytometric examination of the PB sample again evidenced the presence of both HCL and MBL populations, both positive for CD20 (Table 2, Figure 1D).

At the last follow-up (+27 months: t4), the percentage of the BRAF V600E mutation found on the PB was 0.65% and the immunophenotyping analysis of the PB confirmed the presence of both HCL and CLL populations (Table 2, Figure 1E). In this case, indeed, the number of clonal B cells was found higher than 5.000/μl, consistent with the diagnosis of CLL. Moreover, a third

TABLE 1 Complete blood cell count of our case at diagnosis (t0) and after therapy (t1–t4).

CBC	t_0	t_1	t_2	t_3	t_4
Hemoglobin	8.1 g/dl (L)	13.5 g/dl (N)	15.8 g/dl (N)	15.5 g/dl (N)	15.8 g/dl (N)
Absolute neutrophil count	0.5×10^3/μl (L)	1×10^3/μl (L)	3.4×10^3/μl (N)	1.3×10^3/μl (L)	0.8×10^3/μl (L)
Absolute lymphocyte count	4.8×10^3/μl (N)	1.5×10^3/μl (N)	0.7×10^3/μl (L)	2.4×10^3/μl (N)	5.8×10^3/μl (H)
Absolute monocyte count	13.9×10^3/μl (H)	0×10^3/μl (L)	0×10^3/μl (L)	0.1×10^3/μl (L)	0.1×10^3/μl (L)
Platelet count	56×10^3/μl (L)	128×10^3/μl (L)	169×10^3/μl (N)	131×10^3/μl (N)	107×10^3/μl (L)

N, normal value; L, low value; H, high value; and CBC, complete blood cell.
The high value of the monocyte count at t0 refers to the hairy cell count obtained by automated blood cell counters.

TABLE 2 Percentage of the three clonal populations detected by flow cytometric analysis on white blood cells (WBCs) and of the BRAF V600E mutation performed on the peripheral blood (PB) and/or bone marrow (BM) at diagnosis (t0) and after treatment (t1–t4).

Time	Clone	% on WBC	% BRAF V600E
t0 (PB)	HCL	65.85	
	CLL	17.32	
	P3	n.i.	
t0 (BM)	HCL	55.3	38
	CLL	19	
	P3	n.i.	
t1 (BM)	HCL	0.91	1
	CLL	15.68	
	P3	0.94	
t2 (BM)	HCL	0.69	2.3
	CLL	11.69	
	P3	1.54	
t3 (PB)	HCL	0.24	0.25
	CLL	24.9	
	P3	0.23	
t4 (PB)	HCL	0.85	0.65
	CLL	34.8	
	P3	1.29	

PB, peripheral blood; BM, bone marrow; WBCs, white blood cells; and n.i., not identified.

clone (P3: 1.3% of WBCs) was identified owing to the particular expression (intermediate intensity) of the λ light chain in a portion of CD5+ B cells (Table 2, Figure 1E). The P3 population showed an MBL/B-CLL phenotype with a characteristic intensity of CD20 and CD19 markers that was used for the gating strategy. In particular, P3 expressed CD19$^{+intermediate}$, CD20$^{+intermediate}$, CD23^{+}, CD5^{+high}, CD25^{-}, CD11c^{-}, CD43^{+}, CD103^{-}, CD79b^{+low}, FMC7^{+low}, sIgκ^{-}, and sIgλ$^{+intermediate}$ immunophenotype (Figure 1E). Based on this result, we researched P3 analyzing the previous flow cytometric files. Figure 1 shows the gating strategy and the immunophenotype of the three populations at different time points. P3 was absent at diagnosis (t0) and appeared in post-therapy samples (Figure 1). In particular, we found a P3 clone (0.94% of WBCs) in t1 at first evaluation after cladribrine treatment (Figure 1B, Table 2). It showed an HCL-like immunophenotype: CD19$^{+ intermediate}$, CD20$^{+intermediate}$, CD23^{-}, CD5^{-}, CD25$^{+intermediate}$, CD11c^{+}, CD103^{+}, sIgκ^{-}, and sIgλ$^{+intermediate}$ (Figure 1B). For this reason, we hypothesized that the P3 population may have originated from the HCL clone. In t2 (+1 month after the end of rituximab treatment), P3 was 1.5% of WBCs and it showed the same immunophenotype of t1 except for CD20 that was absent (Table 2, Figure 1C). P3 was also identified in t3 (8 months after the end of rituximab treatment) representing 0.23% of WBCs and showing the same immunophenotype of t1 (Table 2,

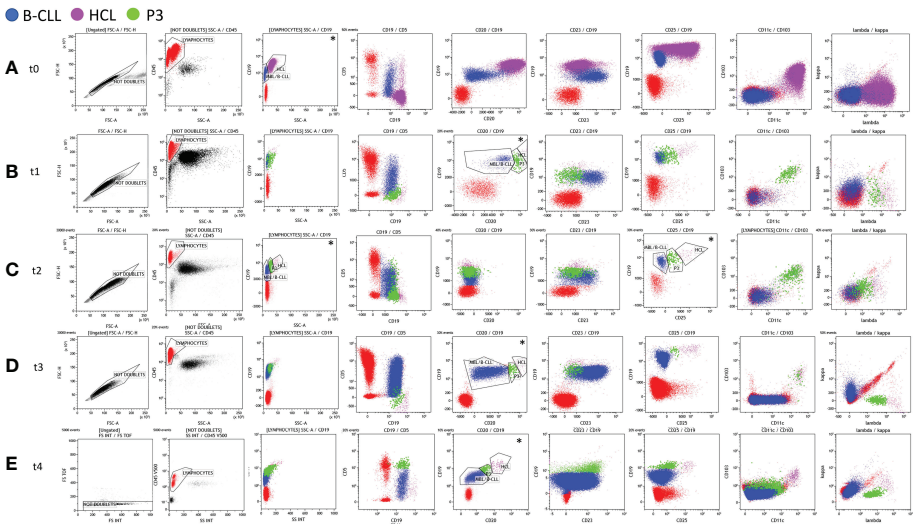

FIGURE 1
Immunophenotyping analysis of the bone marrow (BM) aspirate (t0, t1, and t2) and peripheral blood (PB) (t3 and t4) carried out at diagnosis (t0 – panel **A**), at first evaluation after cladribine therapy (t1 – panel **B**), and after rituximab treatment (t2 – panel **C**, t3 – panel **D**, and t4 – panel **E**).Any debris, dead cells, and clumps or doublets were excluded using forward scatter (FSC)-height (FSC-H) by FSC-area (FSC-A) parameters (black gate, "Not Doublets"). CD45+ lymphocytes (red gate) were gated on CD45 *vs*. the side scatter (SSC) dot plot on the Not Doublets gate. Hairy cell leukemia (HCL), monoclonal B-cell lymphocytosis (MBL)/B-cell chronic lymphocytic leukemia (B-CLL), and P3 populations (fuchsia, blue, and green gates, respectively) were identified from the lymphocyte gate. The expression of some specific markers (CD19, CD20, and CD25) and the physical parameter of SSCs were exploited to identify the three clonal populations (see the dot plots marked with *). At t0 **(A)**, the HCL and MBL/B-CLL clones were identified by the different expression of CD19 *vs*. SSC. At t1 **(B)**, t3 **(D)**, and t4 **(E)**, the three B-cell clones were identified by coexpression at the variable intensity of the CD19 and CD20 markers. At t2 **(C)**, following treatment with rituximab, the gating strategy was based on the different intensities of the expression of CD19 *vs*. CD25 and/or CD19 *vs*. SSC.

Figure 1D). Finally, we established to monitor the patient with a watch-and-wait approach until disease progression (HCL or CLL diseases).

Discussion

Although the coexistence of HCL and second tumors, including other hematological malignancies, has been already described, the simultaneous diagnosis of HCL and CLL is considered quite rare (2). From 2002 to date, to the best of our knowledge, only 11 cases of synchronous diagnosis of HCL and CLL have been published (Table 3) (2–4, 6–10). A new case of concomitant diagnosis of HCL and CLL has been reported here and compared with literature-reported ones. All patients were men with pancytopenia and splenomegaly. In our case, the HCL population was the predominant component in both the PB and BM at diagnosis. Only two other cases (2 and 10) showed similar data, while in all other cases, the CLL population was predominant in the PB and the HCL population was predominant in the BM (Table 3) (2, 8). Since HCL cells are typically rare in the PB, the use of highly sensitive diagnostic

TABLE 3 Clinical characteristics of simultaneous diagnosis of hairy cell leukemia (HCL) and B-cell chronic lymphocytic leukemia (CLL) cases.

Case	Age	Sex	Treatment	Outcome	Predominant B-cell population in PB	Predominant B-cell population in BM	BRAF V600E mutation	Secondary tumors	Reference no.
1	50	M	I. Cladribine II. Rituximab	HCL partial remission, stable CLL	HCL	HCL	Yes (ddPCR)		Our case
2	59	M	I. DCF II. 2-CDA	HCL in remission, stable CLL	HCL	HCL	Not reported		(2)
3	72	M	I. Splenectomy II. Trametinib and dabrafenib	Not reported	Not reported	HCL	Yes (immunohistochemistry)		(3)
4	77	M	I. Cladribine	HCL in remission, CLL immunophenotype occupying 5% of BM	HCL	CLL	Yes (NGS)		(4)
5	75	M	Patient declined therapy	Not reported	CLL	CLL/SLL	Not reported		(5)
6	69	M	Rituximab	HCL in remission, stable CLL	CLL (CD19+/CD20-/CD5+/CD23+/dim surface κ+/CD25-/CD103-)	HCL	Not reported	Thyroid cancer and multiple pulmonary and pleural nodes	(6)
7	43	M	Cladribine	Worsening lymphadenopathy	CLL (CD19+/CD20+/CD5+/CD23+/moderate-density λ+)	HCL	Not reported		(6)
8	79	M	Treated for lung cancer	Transfer to another facility	CLL	HCL	Not reported		(6)
9	83	M	I. Cholambucil and prednisone II. 2-CDA III. Fludarabine, cytoxan, and G-CSF IV. Rituximab	Stable HCL, CLL in remission	CLL		Not reported		(7)
10	54	M	I. Cladribine II. Rituximab	HCL in remission, residual CLL	HCL	HCL	Yes (allele-specific PCR)		(8)
11	63	M	I. 2-CDA (1 year after diagnosis)	Decrease of HCL population; stable CLL	CLL	HCL	Not reported		(9)
12	72	M	Pentostatin and rituximab	Residual HCL, CLL in remission	Not reported	HCL	Not reported		(10)

M, male; DCF, deoxycoformycin; 2-CDA, 2-chloroadenosine; G-CSF, granulocyte colony-stimulating factor; HCL, hairy cell leukemia; B-CLL, B-cell chronic lymphocytic leukemia; BRAF, B-Raf proto oncogene; ddPCR, droplet digital PCR; and NGS = next-generation sequencing.

techniques, including multicolor flow cytometry and allele-specific PCR, were useful for their detection. Different molecular techniques, like ddPCR and next-generation sequencing, are recently introduced as sensitive approaches for assessing the BRAF V600E mutation in HCL patients. In our case, we analyzed both the PB and BM aspirate samples by flow cytometry using a stain–lyse-no wash technique and a comprehensive seven-color antibody panel (FITC/PE/PerCP-Cy5.5/PE-Cy7/APC/APC-H7/V500 fluorescent conjugates) and evaluated the BRAF V600E mutation by ddPCR. The high sensitivity of our flow cytometric approach allowed the detection of a small population "P3," in addition to the typical HCL and CLL clones. The P3 population was absent at diagnosis and it appeared in post-therapy samples (Figure 1). P3 showed an immunophenotype intermediate between HCL and CLL although its features changed over time (Figure 1). In particular, at the first evaluation (t1), P3 showed an HCL-like immunophenotype and it differed from the HCL clone mainly for the intensity expression of CD19, CD20, CD25, and the λ light chain. For this reason, we hypothesized that the P3 population may have originated from the HCL clone. From t1 to t3, the P3 immunophenotype remained the same with the only exception of CD20 that became negative in t2 following rituximab treatment. At the last follow-up (t4), the P3 immunophenotype changed assuming predominantly CLL-like features. In particular, it expressed $CD23^{+}$, $CD5^{+high}$ without CD25, CD11c, and CD103 (Figure 1). However, unlike CLL, it was positive for the λ light chain.

Zhang et al. previously described a case of composite HCL and CLL showing three distinct B-cell populations at diagnosis (case 4, Table 3) (4). The third population expressed CD11c and bright CD20 and lacked CD25 and CD103. Unlike what was described in our case, the authors did not tell of any immunophenotyping change in their third population but described a low-variant allele frequency for the BRAF V600E mutation in their P3 population at diagnosis. Unfortunately, we could not sort out our P3 clone so we could not evaluate the possible presence of the BRAF V600E mutation. However, although the BRAF V600E mutation represents the genetic cause of HCL and it allows the differential diagnosis between the HCL and other B-cell neoplasms, including the HCL variant and splenic marginal zone lymphoma; it was evaluated only in two other cases reported in literature. In particular, Liptrot et al. (case 10) combined a six-color immunophenotypic analysis with an allele-specific PCR approach to detect the HCL cells and to assess the BRAF V600E mutation, and Francischetti and Calvo (case 3) detected the said mutation by immunohistochemistry (Table 3) (3, 8). Only case 10 received the same treatment as our patient (cladribine and rituximab), achieving HCL remission but with the persistence of the CLL clone (8). However, while no evidence of the BRAF V600E mutation was detected in case 10 after treatment, in our case, the same mutation was still detectable (0.65%) by ddPCR, 27 months after the end of rituximab treatment. Cases 2, 4, and 6 also described patients who achieved HCL remission but with the persistence of CLL after treatment, although they were differently treated (Table 3) (2, 4, 6). Cases 9 and 12 were the only two cases that reported CLL remission and the persistence of a small HCL population in the BM after different courses of therapy (7, 10). However, although the large availability of new therapeutic agents has improved the survival of HCL patients, HCL is often associated with an increased risk of second tumor development, including lymphomas, chronic lymphocytic leukemia/small lymphocytic lymphoma (CLL/SLL), chronic myelogenous leukemia (CML), lymphoma, and thyroid cancer (6). Among all cases of the simultaneous diagnosis of HCL and CLL, only one patient (case 6) developed second malignancies (Table 3). In particular, case 6 developed papillary thyroid cancer and multiple pulmonary/pleural nodes 51 months after diagnosis and he passed away. Additionally, case 8 described a patient with the concurrent diagnosis of HCL, CLL, and a third neoplasm, specifically lung adenocarcinoma (Table 3). In this case, the patient was treated for lung cancer first and he was lost to follow-up. Finally, a particular case of composite HCL and CLL was case 11: a patient with simultaneous B- and T-cell disorders at diagnosis (9). In particular, the patient showed three clones, namely, HCL, CLL, and $CD4^{++}/CD8^{+}$ T-cell large granular lymphocytosis. A decrease in the percentage of HCL subpopulation and a stable percentage of CLL cells were reported after the 2-CDA therapy.

All patients were treated for HCL or for their simultaneous neoplasms, except for case 5 because the patient declined all kinds of therapy (5).

In conclusion, our case is added to the few other cases of synchronous HCL and CLL already reported in the literature and underlines the importance of analyzing chronic lymphoproliferative disorders by highly sensitive diagnostic techniques, like the multicolor flow cytometry and ddPCR, to evaluate the possible association between HCL and CLL at diagnosis and to monitor minimal residual disease after therapy.

Data availability statement

The original contributions presented in the study are included in the article. Further inquiries can be directed to the corresponding authors.

Ethics statement

Ethical review and approval was not required for the study on human participants in accordance with the local

legislation and institutional requirements. Written informed consent was obtained from the individual for the publication of any potentially identifiable images or data included in this article.

Author contributions

LV, FD'A and TS performed flow cytometric analyses and analyzed the data. VG performed droplet digital PCR to detect the BRAF V600E mutation. FN performed the FISH analysis. GP and OV monitored the patient in all phases of the disease. DL performed literature search and wrote the original draft, and GD'A revised the manuscript. All authors contributed to the article and approved the submitted version.

Funding

This work was supported by the Italian Ministry of Health - Ricerca Corrente 2022.

Acknowledgments

We thank the patient and his family for giving consent to this case report.

Conflict of interest

The authors declare that the research was conducted in the absence of any commercial or financial relationships that could be construed as a potential conflict of interest.

Publisher's note

References

1. Falini B, Tiacci E. New treatment options in hairy cell leukemia with focus on BRAF inhibitors. *Hematol Oncol* (2019) 1:30–3737. doi: 10.1002/hon.2594

2. Giné E, Bosch F, Villamor N, Rozman M, Colomer D, López-Guillermo A, et al. Simultaneous diagnosis of hairy cell leukemia and chronic lymphocytic leukemia/small lymphocytic lymphoma: A frequent association? *Leukemia* (2002) 16(8):1454–9. doi: 10.1038/sj.leu.2402553

3. Francischetti IMB, Calvo KR. Hairy cell leukemia coexistent with chronic lymphocytic leukemia. *Blood* (2019) 3133(11):1264. doi: 10.1182/BLOOD-2018-12-885145

4. Zhang R, Accola MA, Johnson JC, Rehrauer WM, Xiao J, Yang DT. Clonality and mutational profiling of a case of composite hairy cell leukemia and chronic lymphocytic leukemia. *J Hematop* (2017) 10:81–6. doi: 10.1007/s12308-017-0301-3

5. Rastogi P, Jeyaraman P, Sachdeva MU, Malhotra P, Ahluwalia J. Synchronous hairy cell leukemia and chronic lymphocytic leukemia: A case report with a brief review of literature. *Blood Res* (2018) 53(2):160–3. doi: 10.5045/br.2018.53.2.160

6. Verma V, Giri S, Bhatt VR, Amador-Ortiz C, Armitage JO. Synchronous or metachronous hairy cell leukemia and chronic lymphocytic leukemia: A case series and literature review. *Front Oncol* (2017) 6:270. doi: 10.3389/fonc.2016.00270

7. Sokol L, Agosti SJ. Simultaneous manifestation of chronic lymphocytic leukemia (CLL) and hairy cell leukemia (HCL). *Am J Hematol* (2004) 75 (2):107–9. doi: 10.1002/ajh.10459

8. Liptrot S, O'Brien D, Langabeer SE, Quinn F, Mackarel AJ, Elder P, et al. An immunophenotypic and molecular diagnosis of composite hairy cell leukaemia and chronic lymphocytic leukaemia. *Med Oncol* (2013) 30(4):692. doi: 10.1007/s12032-013-0692-7

9. Garrido P, Jiménez P, Sánchez C, Valero F, Balanzategui A, Almagro M, et al. Molecular and flow cytometry characterization during the follow-up of three simultaneous lymphoproliferative disorders: Hairy cell leukemia, monoclonal b-cell lymphocytosis, and CD4 ++/CD8 +/-dim T-large granular lymphocytosis - a case report. *Cytom Part B - Clin Cytom* (2011) 80 B(3):195–200. doi: 10.1002/cyto.b.20579

10. Obiorah IE, Francischetti IMB, Wang HW, Ahn IE, Wang W, Raffeld M, et al. Concurrent chronic lymphocytic leukemia/small lymphocytic lymphoma and hairy cell leukemia: Clinical, pathologic and molecular features. *Leuk Lymphoma* (2020) 61(13):3177–87. doi: 10.1080/10428194.2020.1797007

frontiers | Frontiers in Oncology

TYPE Case Report
PUBLISHED 07 December 2022
DOI 10.3389/fonc.2022.1014671

OPEN ACCESS

EDITED BY
Ahmad Antar,
Almoosa Specialist Hospital, Saudi Arabia

REVIEWED BY
Guangsheng He,
Nanjing Medical University, China
Gianni Binotto,
University of Padua, Italy

*CORRESPONDENCE
Gaël Vermeersch
gael.vermeersch@uzleuven.be

SPECIALTY SECTION
This article was submitted to Hematologic Malignancies, a section of the journal Frontiers in Oncology

RECEIVED 10 August 2022
ACCEPTED 04 November 2022
PUBLISHED 07 December 2022

CITATION
Vermeersch G, Delforge M, Havelange V, Graux C, Michaux L and Devos T (2022) Case report: Chronic neutrophilic leukemia associated with monoclonal gammopathies. A case series and review of genetic characteristics and practical management. *Front. Oncol.* 12:1014671. doi: 10.3389/fonc.2022.1014671

Case report: Chronic neutrophilic leukemia associated with monoclonal gammopathies. A case series and review of genetic characteristics and practical management

Gaël Vermeersch[1]*, Michel Delforge[1], Violaine Havelange[2], Carlos Graux[3], Lucienne Michaux[4] and Timothy Devos[1,5]

[1]Department of Hematology, University Hospitals Leuven, KU Leuven, Leuven, Belgium, [2]Department of Hematology, Université Catholique de Louvain Saint-Luc, Woluwe-Saint-Lambert, Belgium, [3]Department of Hematology, Université Catholique de Louvain, CHU UCL Namur - site Godinne, Yvoir, Belgium, [4]Center for Human Genetics, KU Leuven, Leuven, Belgium, [5]Department of Microbiology and Immunology, Laboratory of Molecular Immunology (Rega Institute), KU Leuven, Leuven, Belgium

Chronic neutrophilic leukemia (CNL) is a rare but potentially aggressive *BCR::ABL1* negative myeloproliferative neoplasm, characterized by sustained mature, neutrophilic leukocytosis. The discovery of key driver mutations in the colony-stimulating-factor-3 receptor (*CSF3R*) gene resulted in the updated World Health Organization (WHO) diagnostic criteria in 2016. A significant number of CNL cases have been associated with plasma cell dyscrasias, predominantly multiple myeloma (MM) and monoclonal gammopathy of unknown significance (MGUS). Compared to pure CNL, mutated *CSF3R* is infrequently reported in CNL cases associated with monoclonal gammopathies (MG). Until now it remains unclear whether CNL and occurring plasma cell neoplasms are clonally related or CNL is developing secondary to the underlying dyscrasia. Owing to its rarity, currently no standard of care management exists for CNL and MG-associated CNL. In this case series we report the multi-center experience of five MG-associated CNL cases with a median age of diagnosis of 69 years. Three patients (66%) showed predominance of lambda light chain expression. Four (80%) eventually evolved to MM, and one CNL-MGUS patient developed secondary acute myeloid leukemia (AML). Mutated *CSF3R* was present in the patient who developed AML but was absent in other cases. To assess possible associated genetic aberrations we performed recurrent analysis with next-generation sequencing (NGS). Two patients (40%) deceased with a median time of survival of 8 years after CNL diagnosis. Three (60%) are currently in follow-up with no reoccurring leukocytosis. This case series, followed by a short review, provides a long-term clinical and genetic overview of five CNL cases associated with MG.

KEYWORDS

myeloproliferative disorders, chronic neutrophilic leukemia, monoclonal gammopathy, multiple myeloma, myeloid malignancy, myeloproliferative neoplasm

Introduction

Chronic neutrophilic leukemia (CNL) is an infrequent *BCR::ABL1* negative myeloproliferative neoplasm (MPN) defined by sustained, mature neutrophilia and bone marrow hypercellularity with granulocytic hyperplasia (1, 2). Approximately 200 CNL cases have been described; however, many of these do not meet the current diagnostic criteria (3). The identification of key driver mutations in the colony-stimulating-factor-3 receptor (*CSF3R*) gene resulted in the updated diagnostic criteria by the World Health Organization (WHO) in 2016 (4, 5). *CSF3R* is mutated in up to 80% of CNL cases (6). Approximately 32% of CNL cases are associated with plasma cell dyscrasias, wherein *CSF3R* tends to be less frequently mutated (1, 7). It remains unclear whether both entities should be considered clonally related or neutrophilia is provoked by the plasma cell dyscrasia (1). The majority of CNL-associated paraproteinemias express lambda light chains (8). The lack of genetic markers and arbitrary WHO-diagnostic criteria, such as leukocyte count, challenges the diagnosis. This case series provides a long-term clinical and genetic overview of five CNL cases associated with monoclonal gammopathies (MG). Four patients developed multiple myeloma (MM), and one patient developed secondary acute myeloid leukemia (AML).

Case description

Case 1

In 2012, a 61-year-old woman was referred due to persistent, incremental neutrophilia since 2009. Medical history included no major abnormalities. At presentation medical therapy comprised estriol cream and alprazolam. She had one sibling diagnosed with polycythemia vera (PV). Ultrasound excluded hepatosplenomegaly. Serum electrophoresis and immunofixation identified immunoglobulin G (IgG) kappa-type paraproteinemia (cfr. Table 1 for results of the full blood analysis from all patients). Bone marrow biopsy showed hypercellularity without dysplasia. Karyotyping resulted normal. Positron emission tomography-computed tomography (PET-CT) showed no bone lesions. No therapy was initiated. In 2016, MGUS evolved to MM "Revised International Staging System" stadium I (R-ISS). M-peak rose from 10 to 32 g/L. Bone marrow biopsy showed right-shifted hypercellularity (90%) with approximately 73.3% segmented neutrophils and central plasmacytosis of 35% without central blast excess. Amyloidosis was excluded by Congo Red staining. Next-generation sequencing (NGS) and fluorescence *in situ* hybridization (FISH) resulted normal. Initiation of bortezomib-thalidomide-dexamethasone (VTD) resulted in a very good partial response (VGPR) after six cycles. Autologous hematopoietic stem cell transplantation (HSCT) was executed in 2017. Six months later, MM progressed and FISH revealed a mono-allelic loss of 17p13/*TP53* (February 2018). Daratumumab-lenalidomide-dexamethasone (DRd) was started as the patient showed intolerance towards carfilzomib-lenalidomide-dexamethasone (KRd). Six months afterwards, fourth-line therapy with bendamustine was started as PET-CT showed disease progression. The patient died due to progressive multiple myeloma, respectively 9 and 3 years after CNL and MM diagnosis. No reoccurrence of peripheral blood leukocytosis ≥25 × 10^9/L was observed after the initiation of VTD and following therapies.

Case 2

A 74-year-old man, known with IgA-type MGUS since 2003 and persistent neutrophilic leukocytosis since 2009, was diagnosed with spinal located diffuse large B-cell lymphoma (DLBCL) subtype ABC in 2013 (KI67 20%–25%, karyotype (46, XY[20]). Familial anamnesis did not include hemato-oncological pathologies. Medical therapy at presentation comprised nebivolol (2.5 mg QD) and spironolacton/altizide (12.5 mg/7.5 mg QD). Biochemical analysis showed leukocytosis of 43.69 × 10^9/L (90.7% neutrophils) with M-spikes in both β- and γ-fractions.

Bone marrow biopsy revealed hypercellularity with increased representation of the myeloid lineage (mature and immature) and local clustering (5%–10%) of monotypic plasma cells (kappa-type, CD20-). Karyotyping resulted normal. Clonality between the spinal located DLBCL and bone marrow tissue was proved by polymerase chain reaction (PCR) (*IGH/IGK*).

Thus, the patient was diagnosed with bone marrow involved DLBCL, CNL, and MGUS. Six cycles of rituximab-cyclophosphamide-doxorubicin-vincristin-prednisone (R-CHOP), followed by rituximab monotherapy (administered twice), were given. In addition, intrathecal chemotherapy (methotrexate, cytarabine, and hydrocortisone) was administered three times. During therapy, bone marrow biopsy showed minimal CD5+ positivity (<0.1% all nucleated cells (ANC)) and isolated loss of the Y-chromosome (45,X,-Y [3]/46,XY[7]). *CSF3R* mutations were absent. Complete remission (CR) of DLBCL was obtained on PET-CT scan by September 2014. Asymptomatic neutrophilic leukocytosis remained during remission (>30 × 10^9/L; >80% neutrophils).

In February 2016, an increasing absolute neutrophil count of 48.5 × 10^9/L and M-spike were observed (IgA 13.5g/L). Urine kappa FLCs were not calculable. In June 2020, MGUS progressed to MM, type IgA kappa (R-ISS III, IgA 36.60 g/L); the total number of leukocytes normalized. Cytogenetic analysis showed

TABLE 1 Overview of clinical and laboratory findings at presentation and follow-up.

	Patient 1 (F)		Patient 2 (M)			Patient 3 (F)		Reference range	Patient 4 (M)				Reference range	Patient 5 (F)			Reference range
	2012	2016	2013	2016	2020	Jul/2018	Nov/2018		Mar/2019	May/2019	Jun/20	Aug/21		Jan/20	Jul/20	Oct/20	
Stage of disease	CNL +MGUS	CNM+MM	CNL+DLBCL+MGUS	CNL +MGUS	CNL +MM	CNL	CNL +MM		CNL	CNL +AML	Relapse AML	1 y post HSCT		CNL +smoldering MM	CNL +MM	CNL +MM	
Age (years)	61	65	74	77	81	73	73		69	69	70	71		66	66	67	
B-symptoms	Yes	No	No	No	No	Yes	No		No	No	No	No		Yes	No	No	
Hepatosplenomegaly (ultrasound)	No	No	No	No	No	Yes	No		No	No	No	No		No	No	No	
Treatment	/	VTD, KRd, DRd, bendamustine	R-CHOP, R, intrathecal MTX, ARA-C&HCT	/	/	/	VMP		/	/	DAC +HSCT	/		/	VRD	VRD cycle 3	
YoS after diagnosis	9 y	3 y	7 y	4 y	<1 month	>4 y	>4 y		>3 y	>3 y	>3 y	>1 y		>2 y	>2 y	>1 y	
Current status	Deceased		Deceased			Alive			Alive					Alive			
Laboratory findings																	
Hb (g/L)	122	101	116	109	70	109	93	120–160	116	83	88	109	133–176	104	132	132	122–150
RBC count (10^12/L)	4.03	3.16	3.72	3.49	2.3	3.52	2.82	3.9–5.6	3.41	2.47	2.58	3.16	4.10–5.70	2.95	4.37	4.29	4.0–6.0
MCV (fL)	94.8	98.4	93.3	93.4	91.3	96.2	104.3	76.0–96.0	100.3	99.6	103.5	106.0	80.1–99.8	105.8	93.6	94.4	85.0–95.0
WBC count (10^9/L)	41.32	17.71	43.69	53.14	7.98	65.2	60.85	4.0–10.0	13.62	18.54	1.57	4.15	3.70–9.50	41.54	34.15	11.63	4.0–10.0
Neutrophils %	87.8	74.7	90	91.3	73	89.1	88	38.0–77.0	70.1	74.6	19.5	47.8	45.0–70.0	87.5	80.7	67.6	40.0–70.0
Eosinophils %	0.3	0.6	0.3	0.3	1	0	0	≤6.0	3.1	2	0	1.7	1.0–6.0	0	0.5	1.8	0.5–6.0
Basophils %	0.3	0.1	0.3	0.1	0	0	0	≤1.0	0.8	3.3	0.7	0.7	0.0–2.0	0	0.4	0.4	0.1–2.0
Lymphocytes %	8.2	19.5	5.2	5.7	19	3.2	5	20–50	19.7	10.7	75.8	36.1	20.0–45.0	3.6	10.1	16.7	20.0–50.0
Monocytes%	3.5	5.1	3.6	2.6	3	4.5	7	2.0–10.0	6.3	2.7	3.3	<1.0	2.0–12.0	2.2	4.1	11.1	5.0–10.0
Blasts %	/	/	/	/	/	/	/	/	<1.0	2.7	<1.0	<1.0	<1.0	/	/	/	/
eGFR (CKD-EPI mL/min/1.73m^2)	>90	101	27	27	17	46	60	/	94	108	133.72	71.56	/	59	82	63	/
LDH (U/L)	160	163	/	139	247	260	232	135–250	/	198	124	201	120–246	261	177	202	<250
Vitamin B12 (ng/L)	>2000	/	/	/	196	>2000	/	191–663	/	928	/	/	239–931	>2000	/	/	196–729
M-spike (g/L)	10.1	32.1	/	/	/	/	/	/	/	/	/	/	/	9.6	14.23	5.5	/
IgG (g/L)	18.4	42	/	2.13	2.19	/	3.87	7.51–15.60	/	2.53	/	7.00	0.88–4.10	15.2	16.61	10.52	7.0–16.0
IgA (g/L)	0.6	0.16	/	13.5	36.6	/	0.71	0.82–4.53	/	11.97	/	0.16	6.90–14.00	0.71	0.66	0.59	0.7–0.4
IgM (g/L)	0.57	0.19	/	0.05	<0.04	/	0.10	0.46–3.04	/	1.12	/	0.06	0.34–2.10	0.57	0.55	0.44	0.4–2.3

(Continued)

10.3389/fonc.2022.1014671

10.3389/fonc.2022.1014671

TABLE 1 Continued

	Patient 1 (F)		Patient 2 (M)		Patient 3 (F)		Reference range	Patient 4 (M)			Reference range	Patient 5 (F)			Reference range
Serum k/λ	1.37	/	/	/	1.306	/	0.066	0.399–0.984	/	/	/	0.399–0.984	/	/	1.29	0.399–0.984
Urine k/λ	/	/	/	Nc	Nc	/	Nc	0.7–6.2	/	/	/	0.7–6.2	/	/	/	0.7–6.2
Blood film	Left-shifted, TG, DB	/	Left-shifted, TG	/	TG	Left-shifted, TG,DB	TG, DB		/	/	/		/	/	/	

AML, acute myeloid leukemia; ARA-C, cytarabine; CNL, chronic neutrophilic leukemia; DAC, decitabine; DB: Döhle bodies; DRd, daratumumab-lenalidomide-dexamethasone; F, female; Hb, hemoglobin; HCT, hydrocortisone; HSCT, hematopoietic stem cell transplantation; Ig, immunoglobulin; KRd, carfilzomib-lenalidomide-dexamethasone; MGUS, monoclonal gammopathy of unknown significance; MCV, mean corpuscular volume; MTX, methotrexate; M, male; MM, multiple myeloma; Nc, not calculable; Nd, not detected; RBC, red blood cell; R-CHOP, rituximab-cyclophosphamide-doxorubicin-vincristin-prednison; TG, toxic granulations; US, ultrasound; VMP, bortezomib-melphalan-prednisone; VRD, bortezomib-lenalidomide-dexamethasone; VTD, bortezomib-thalidomide-dexamethasone; Y, years; YoS, Years of survival; /, not determined.

hyperdiploidy with gain on chromosome 1q. *CSF3R*-analysis was not performed at this stage. Bone marrow biopsy showed hypercellularity and right-shifted myeloid cells with normal morphology. There was plasmocytosis of 55.7% ANC. The patient preferred no further therapies and deceased shortly after, roughly 7 years after CNL diagnosis.

Case 3

In 2018, a 73-year-old woman was referred due to persistent leukocytosis for 1 year. Medical therapy comprised acetylsalicylic acid (80 mg QD), bisoprolol (2.5 mg QD), and rosuvastatin (10 mg QD). Besides significant weight loss (>10% within 12 months), no B-symptoms were present. Blood film analysis confirmed the presence of left-shifted neutrophilia with toxic granulations and Döhle bodies. Bone marrow biopsy showed hypercellularity (>95%) with myeloid hyperplasia, plasmacytosis of 10%–15% (lambda positive), and bone marrow fibrosis grade 1. Karyotyping resulted normal. NGS revealed mutated *ASXL1* (c.1934dup;p.Gly646Trpfs*12)(VAF 26%); *CSF3R* appeared normal (Table 2). The tentative diagnosis of CNL was made. No therapy was initiated.

Four months later, the patient was diagnosed with lambda light chain MM (R-ISS I). Biochemical analysis revealed neutrophilic leukocytosis, hypogammaglobulinemia, and a normal β_2-microglobulin concentration. Serum lambda FLCs were significantly increased (free λ: 276 mg/L (ref. 10–34) (Table 1)). There was significant proteinuria (6.79 g/24 h) with prominent lambda excretion (9816 mg/24 h). Bone marrow biopsy showed hypercellularity with segmented neutrophils (36.3% ANC) and increased central plasmocytosis (13.7% ANC) without blastosis. Congo Red staining resulted normal. Karyotyping revealed hyperdiploidy with gain on chromosomes 5, 7, 9, and 15. FISH detected IGH/14q32 rearrangement. Bortezomib-melphalan-prednisone (VMP) was initiated and halted after nine cycles as biochemical CR and minimal residual disease on PET-CT were obtained. Currently, more than 4 years after CNL and MM diagnosis, the patient is stable. Peripheral blood leukocyte count is $<25 \times 10^9$/L.

Case 4

In 2019, a 69-year-old man was referred due to incremental neutrophilic leukocytosis and fatigue since several months. Medical history included diabetes mellitus type 2. Medical therapy comprised sitagliptin/metformin (50 mg/1000 mg BID), rosuvastatin (10 mg QD), and allopurinol (100 mg QD). Biochemical analysis showed normocytic anemia with concurrent neutrophilic leukocytosis and 2.7% blasts. Electrophoresis and immunofixation indicated MGUS (IgG lambda type). Bone marrow biopsy showed hypercellularity

TABLE 2 Genetic and molecular findings at diagnosis and follow-up.

	Patient 1 (F)			Patient 2 (M)			Patient 3 (F)		Patient 4 (M)		Patient 5 (F)	
	2012	2016	2018	2013	During R-CHOP (2014)	2020	Jul/18	Nov/18	May/19	Jun/20	Jul/19	Jan/20
Stage of disease	CNL +MGUS	CNL +MM	During follow-up	CNL +MGUS +DLBCL	CNL +MGUS +DLBCL	MM	CNL	CNL +MM	CNL+AML	Relapse AML	Smoldering MM	CNL +MM
Karyotyping	46,XX [10]	/	/	46,XY [3]	45,X,-Y [3] 46,XY [7]	/	46,XX [10]	46,XX, +5,+7, +9,+15	47,XY,-7,+14,+r, inc[2] 46,sl,-r[5] 46,sdl,del(12) (p11p13)[4]	46,XY,-7,del (12) (p11p13), +14[2] 46,XY, t (17;22) (q12; q12)[3] 46,XY[5]	46,XX[28]	46,XX [25]
FISH	/	Normal**	17p13/ *TP53*$^{+}$ *IGH*$^{-}$	/	/	*IGH*/ 14q32^{-}	/	*IGH*/ 14q32^{+} *FGFR*3 [t(4;14)]$^{-}$ *MAF* [t (14;16)]$^{-}$ **	/	/	Duplication 1q^{+} Deletion 16q23^{+} t(4;14)$^{-}$ t(14;16)$^{-}$ *TP53*$^{-}$ **	*BCR::ABL1*$^{-}$
PCR/NGS	*BCR::ABL1*$^{-}$* *FLT3*-ITD^{-} *TP53*$^{-}$ V617F *JAK2*$^{-}$	*CSF3R*$^{-}$ *ASXL1*$^{-}$ V617F *JAK2*$^{-}$ *SETBP1*$^{-}$ *TP53*$^{-}$ ***	/	*IGH*/ *IGK*$^{+}$* *BCR-ABL1*$^{-}$ BCL2/ *IGH*$^{-}$	*CSF3R*$^{-}$ *ASXL1*$^{-}$ V617F *JAK2*$^{-}$ *SETBP1*$^{-}$ *TP53*$^{-}$ ***	+1q	*ASXL1*$^{+}$* (c.1934dup; p.Gly646Trpfs*12) *BCR-ABL*$^{-}$ *CSF3R*$^{-}$ V617F *JAK2*$^{-}$ *FLT3*-ITD^{-} *TP53*$^{-}$ ***	/	*CSF3R*$^{+}$ * (c.1853C>T; p.(Thr618Ile)) *SETBP1*$^{+}$ (c.2615T>C; p.(Ile871Thr)) *U2AF1*$^{+}$ (c.470A>C; p.(GLn157Pro)) *BCR::ABL1*$^{-}$ *ASXL1*$^{-}$ V617F *JAK2*$^{-}$ *FLT3*-ITD^{-} *TP53*$^{-}$ ***	/	*BCR::ABL1*$^{-}$ *CSF3R*$^{-}$ *AXSL1*$^{-}$ V617F *JAK2*$^{-}$ *FLT3*-ITD^{-} *TP53*$^{-}$ *IGH*$^{-}$ ***	*BCR::ABL1*$^{-}$ *CSF3R*$^{-}$ *AXSL1*$^{-}$ V617F *JAK2*$^{-}$ *FLT3*-ITD^{-} *TP53*$^{-}$ ***

*With "$^{-}$"indicating the absence of a mutation; "$^{+}$" indicating the presence of a mutation; **Cfr. Appendix 1 for the complete list of screened regions/loci by fluorescence *in situ* hybridization (FISH); ***Cfr. Appendix 2 for the complete list of screened genes by next-generation sequencing (NGS); "/" indicating "not determined".

with blast excess (20%). Cytogenetic analysis identified a complex karyotype with monosomy of chromosome 7, trisomy of chromosome 14, and deletion of p12 (Table 2). *CSF3R* (44%), *SETBP1* (45%), and *U2AF1* (42%) appeared mutated. The diagnosis of AML secondary to CNL was made. Complete morphologic and cytogenetic remission was obtained after eight cycles of decitabine. Planned allogeneic HSCT was postponed due to flu and the SARS-CoV-2 pandemic. The patient relapsed several months later. Cytogenetic analysis detected the reoccurrence of previous described mutations in combination with a new translocation t(17;22) (Table 2). Despite that no CR was obtained after remission-reinduction, allogeneic HSCT was performed. Bone marrow analysis 2 and 4 months afterwards showed no blast excess; mutated *CSF3R* was absent. The patient recovered and is currently, more than 2 years after HSCT, in CR. Paraproteinemia and neutrophilic leukocytosis did not reoccur.

Case 5

In 2020, a 66-year-old woman presented with recurrent headaches, fever and generalized myalgia/arthralgia since several months. Clinical investigation was unremarkable. Familial anamnesis did not include hemato-oncological abnormalities. There was no use of medicines. Medical history included successfully treated mammary carcinoma in 2010 (surgical resection, radio- and hormonal therapy; CR at presentation). In 2019, the patient developed auto-immune aortitis, successfully treated with corticoids. A few months later, the patient was diagnosed with smoldering MM (IgG lambda). Bone marrow biopsy then showed hypercellularity with a strong representation of the granulocytic lineage in intermediary and mature stages, toxic granulations, and sea-blue histiocytes. Central plasmocytosis was 10.5%. No central blast excess was observed. Cytogenetic and molecular analysis

resulted normal. Since the diagnosis of smoldering MM, there was persistent neutrophilia. Given the suspicion of CNL, the patient was shortly treated with hydroxycarbamide, which was rapidly stopped due to provoked cytopenia. Relapse of breast carcinoma was excluded and PET-CT resulted normal.

A few months later, smoldering MM evolved into MM (R-ISS II). Treatment with bortezomib-lenalidomide and dexamethasone (VRD) was initiated and resulted in partial response (PR). The patient refused intensification with autologous HSCT. VRD was stopped after three cycles due to neurological complications. According to patient requirement, low-dose lenalidomide (5 mg) was continued in monotherapy and PR was maintained. Under lenalidomide, the patient progressively developed nephrotic syndrome. Renal biopsy showed glomerulonephritis with mesangial IgA deposits, probably not related to the hematologic condition. Currently, the patient is in follow-up; leukocyte count remains normal.

Methods

Five patients diagnosed with CNL between 2012 and 2020 were included in this study. In retrospect, CNL diagnosis was based on the 2016 WHO diagnostic criteria (4). Cytogenetic and molecular analysis of patients 1–3 was performed at the University Hospitals Leuven, Belgium. Cytogenetic analysis of patient 4 was performed at *Université Catholique de Louvain*, CHU UCL Namur, Belgium. Molecular analysis of patient 4 was performed at the University Hospitals Leuven. Cytogenetic analysis of patient 5 was performed at *Université Catholique de Louvain Saint-Luc*, Woluwe-Saint-Lambert, Belgium. Molecular analysis of patient 5 was performed at *Institut de Pathologie et de Génétique* (IPG), Charleroi, Belgium. We report cytogenetic and molecular analyses at diagnosis and during follow-up. Used probes and screened genes by FISH and NGS are clarified in the appendices. Patients 1–3 are treated at the University Hospitals Leuven. Patient 4 is treated at Université Catholique de Louvain, CHU UCL Namur, and patient 5, at Université Catholique de Louvain Saint-Luc, Woluwe-Saint-Lambert.

Results

In this series the median age of CNL diagnosis is 69 years, 40% of patients (n = 2) are men; 20% (n = 1) of patients carried mutated *CSF3R*. B-symptoms and splenomegaly were present in 40% (n = 2) and 20% (n = 1) of patients, respectively. Three patients (66%) showed a predominance of lambda light chain expression. Four patients (80%) evolved to multiple myeloma. Hydroxycarbamide was shortly initiated in one patient. All patients received treatments focusing on associated malignancies such as AML and MM, among these 40% (n = 2) underwent HSCT. Two patients died after a median time of survival of 8 years after CNL diagnosis. Three patients (66%) are currently in follow-up (approximately 3 years after diagnosis) and show no signs of reoccurring leukocytosis.

Discussion and review of the literature

CNL laboratory features and epidemiology

In 1920, CNL was first described as "polymorphonuclear neutrophil hyperleukocytosis" (9). Roughly 200 CNL cases are currently reported in literature; however, many cases may not meet the WHO-defined diagnostic criteria (1, 3). The lack of cytogenetic markers has complicated accurate diagnosis in the past. Recent identification of oncogenic driver mutations in *CSF3R* resulted in the updated WHO diagnostic criteria in 2016 (1, 4, 5).

Besides the presence of mutated *CSF3R*, the diagnostic criteria include a peripheral blood leukocytosis of $\geq 25 \times 10^9$/L with ≥80% neutrophils (segmented and band), <10% peripheral neutrophil precursors, absence of monocytosis/eosinophilia/basophilia, and rarely observed peripheral myeloblasts. Arber et al. provide a complete list of the current diagnostic criteria (4, 7, 10). Levels of vitamin B12 and lactate dehydrogenase (LDH) are frequently elevated but are no solid criteria. Neutrophil morphology typically presents with non-specific characteristics such as toxic granulations and Döhle bodies (8, 11). Bone marrow biopsy shows hypercellularity with increased numbers of normal maturating neutrophilic granulocytes. Chronic myeloid leukemia and other *BCR::ABL1* negative MPNs must be excluded; rearrangement of *PDGFRA, PDGFRB, FGR*, or *PCM1::JAK2* should be absent. Without mutated *CSF3R*, the diagnosis is possible if persistent non-reactive neutrophilia (≥3 months) is present. In this context, demonstrated myeloid clonality by cytogenetic or molecular analysis is preferred (4, 10).

When strictly applied, only cases 1–3 and 5 meet the CNL criteria concerning leukocytosis. In case 4, even before the diagnosis of AML, peripheral blood leukocytosis was $<25 \times 10^9$/L with <80% neutrophils. However, the persistence of leukocytosis (>3 months) without an identifiable cause of reactive neutrophilia combined with mutated *CSF3R* strongly supports the CNL diagnosis. In AML, the incidence of mutated *CSF3R* is approximately 1%. This case emphasizes the risk of an arbitrary leukocyte number as an absolute criterion for diagnosis (5, 12).

Elliott et al., analyzing 40 WHO-defined CNL cases, reported a median age of 66 years (range 16–86). The majority of these cases were men (56%) (3). In our series two of five patients (40%) were male and the median age of diagnosis was 69 years. Splenomegaly, which is removed as a solid criterion in the current WHO criteria, was present in one of five (20%).

Mutated *CSF3R* as key driver in CNL

CSF3R is the gene coding for the receptor of colony-stimulating-factor-3 (CSF3), a primary neutrophil growth factor. Mutated *CSF3R* is considered as a solid CNL-defining criterion. In CNL, the mutational frequency of *CSF3R* is approximately 60%–80%, with *CSF3R*T618I as the most frequent reported mutation (7, 13). *CSF3R*T618I occurs in the extracellular or transmembrane domain of the receptor and results in the activation of the JAK-STAT pathway; which explains the marked clinical improvement after the initiation of ruxolitinib in some patients. Other mutations preferentially activate the SRC tyrosine kinase. We refer to Maxson et al. for qualitative information about *CSF3R* (5, 6, 13). In MG-associated CNL, the incidence of mutated *CSF3R* appears to be significantly lower; however, data is scarce (7).

CNL and plasma cell disorders

According to the WHO diagnostic criteria, plasma cell neoplasms should be excluded in the absence of mutated *CSF3R* (4). Nevertheless, up to 32% of CNL cases report concurrent plasma cell dyscrasias, with the predominance of lambda light chain expression (66% or 3/5 in our series) (1). All patients showed sign of MG at the time of CNL diagnosis; 80% (4/5) eventually evolved into MM. Larger data sets are necessary to evaluate whether patients with CNL-associated MGUS carry an inherent higher risk to evolve into MM.

It is unclear whether MG-associated CNL has to be considered as a genuine myeloproliferative neoplasm or neutrophilic reaction, for example, secondary to production of plasma cell-derived cytokines such as G-CSF (1). Quantification of G-CSF serum concentration was not performed in our series but could be useful. The lower frequency of mutated *CSF3R*, combined with the longer median time of survival in MG-associated CNL, may indicate different etiopathogenesis (1, 7). Only patient 4 carried mutated *CSF3R*. MG-associated CNL shows a median time of survival of approximately 5 years, compared to 24 months in true CNL (3, 7, 14). Patients 1 and 2 show a median time of survival of 8 years after CNL diagnosis. Patients 3, 4, and 5 are in follow-up, roughly 3 years after CNL diagnosis.

Some authors stress the few reported chromosomal abnormalities and better survival as evidence for a provoked neutrophilic reaction in MG-associated CNL (14, 15). However, Nedeljkovic et al. reported the presence of a homozygous *JAK2*V617F mutation in a patient with CNL associated with plasma cell myeloma, demonstrating molecular evidence of clonality in the absence of mutated *CSF3R* (16). Mutated *ASXL1* in patient 3 at the time of CNL diagnosis is a sign of clonality in the absence of mutated *CSF3R*.

Cytogenetic abnormalities

Karyotype

Y-chromosome loss, as in patient 2, is frequently reported in patients with hematological disorders. It remains unknown whether Y-chromosome loss should be considered as an age-related phenomenon or cytogenetic marker for malignancy (17). Copy number alterations, resulting in gain of chromosomes such as +5, +7, +9, and +15 in patient 3, are one of the most prominent perturbations in MM. The gain on chromosomes 9 and 15 may play an important role in MGUS transformation (18). Abnormalities of chromosome 1 are observed in approximately 25% of patients at MM diagnosis. The gain on 1q, as in patients 2 and 5, is associated with inferior survival (19).

At CNL diagnosis, patient 4 carried monosomy 7, trisomy 14 and 12p-deletion. This latter is associated with progression to post-MPN AML (20). Trisomy 14 is a rare cytogenetic abnormality in myeloid neoplasms such as AML. Isolated trisomy 14 is indicated as an early event in leukemogenesis; however, more research on its clinicopathological features is needed. Monosomy 7 is frequently reported in myeloid malignancies and is detected in previous CNL-cases who developed secondary AML (3, 21, 22). The translocation t (17;22)(q12;q12), which occurred in patient 4 during AML relapse, is associated with myelodysplastic syndrome (MDS) (23).

Additional mutations

Specific mutations may indicate a negative prognosis in CNL, even if, by our knowledge, currently no mutations are validated as prognostic markers. Mutated *ASXL1* as in patient 3, resulting in disrupted epigenetic regulation, is associated with a negative prognosis in CNL. Mutational frequency is varying from 30% to 81% (1, 22).

Mutated *TP53* is characterized as a negative prognostic factor in myeloid and lymphoid malignancies (24, 25). Monoallelic loss of *TP53* was detected in patient 1 during follow-up; the patient deceased 2 years afterwards. The relevance of mutated *TP53* in MG-associated CNL is unclear.

Rearrangements involving the *IGH locus* on chromosome 14q32 frequently occur in MM and are associated with standard risk (26). Translocations in 14q32 less frequently co-occur with hyperdiploid chromosomes such as in patient 3 (27).

SETBP1, considered as a driver oncogene, is mutated in approximately 33% of CNL cases (7). It is associated with poor prognosis in various myeloproliferative phenotypes, including secondary AML as in patient 4. Whether mutated *SETBP1* is associated with poor survival in CNL is unknown (22, 28).

A limited number of cases report the presence of *JAK2*V617F mutations in CNL; little is known about its true prevalence in WHO-defined CNL cases (7, 29–34). *JAK2*V617F and *CSF3R*T618I appear to be mutually exclusive (7, 10, 35). None of the patients in our series carried *JAK2*V617F.

Mutated spliceosome-associated genes such as *SRSF2* and *U2AF1* have been reported in CNL. Meggendorfer et al. report a *SRSF2* mutational frequency of 21% (4/14 cases); others report a frequency of 0% (0/10) (35–37). Patient 4 carried the Glutamin (Gln)157pro mutation in the *U2AF1* gene at the moment of CNL and AML diagnosis. Mutated *U2AF1* results in predisposition to AML (38, 39). Other CNL-associated mutations, such as *TET2* and *RUNX1*, were absent in our cases. *TET2* mutations have an estimated mutational frequency of 29% in CNL (1, 36). Previous authors postulated that cooperating *RUNX1* and *CSF3R* mutations in CNL may result in disease progression, resistance to ruxolitnib and may act as an early marker of AML transformation (40, 41).

Management

CNL

Currently, no standard of care management exists for CNL. Historically, splenic irradiation and splenectomy were performed to reduce tumor bulk and abdominal discomfort. Nevertheless, splenectomy is associated with worsening of neutrophilia in CNL. The only potentially curative treatment is HSCT (1). Allogeneic HSCT showed a one-year overall survival rate of 40% in patients with CNL. However, data regarding clinical outcomes and the most optimal regimens of HSCT are scarce (3, 10, 42, 43). In our series, autologous and allogeneic HSCTs were performed in patient 1 due to progressive MM and in patient 4 due to AML, not CNL specifically.

The use of "7+3" induction chemotherapy in CNL has not been able to induce hematological remission. One report describes a young patient in the blast phase who attained a second chronic phase following induction chemotherapy (anthracycline and cytarabine) (44).

Cytoreductive agents, such as hydroxyurea and interferon-alpha (IFN-α), have demonstrated efficacy in controlling leukocytosis and splenomegaly. Currently, hydroxyurea is the most frequently used first-line agent; nonetheless, 25% of patients appear to be refractory (3, 35). Few reports mention durable remission and good tolerability after IFN-α initiation (45–47). No IFN-α is used in our series as it is not reimbursed in our country.

Promising targeted therapies are being investigated since the identification of mutated *CSF3R*. Depending on the mutation downstream signaling pathways through JAK-STAT or SRC tyrosine kinase are activated, these may be inhibited by ruxolitinib and dasatinib, respectively (5, 10, 42). An overall response rate of 32% was observed in patients with *CSF3R*-mutated CNL treated with ruxolitinib; patients harboring *CSF3R*T618I were most likely to respond (48). None of these agents were used in our series.

MG-associated CNL

As in CNL, there is no standard of care management for MG-associated CNL (1). No specific anti-myeloma regimen can be recommended, but conventional chemotherapy, immunomodulatory drugs, proteasome inhibitors, and anti-CD38 monoclonal antibodies may reduce neutrophil counts to a variable extent. However, it is difficult to discriminate a direct effect on the CNL clone from an indirect reduction by the suppression of the malignant plasma cell clone. Keeping in mind the more favorable prognosis of MG-associated CNL, treatment strategies in our series were primarily focused on associated plasma cell dyscrasias and AML.

In patient 1, autologous HSCT was performed after VTD therapy. Subsequently, the patient received therapy existing out of KRd, DRd, and bendamustine due to MM progression. No reoccurrence of neutrophilia was observed after the initiation of VTD and following therapies. However, as various therapies were administered in a short time frame, no conclusion on the effectivity of individual therapies in CNL can be made. As mentioned, HSCT in patient 1 and 4 was performed due to progressive MM and AML respectively, not CNL specifically.

Decitabine, a demethylating agent, was initiated in patient 4 and resulted in complete morphologic and cytogenetic remission after eight cycles. Previous authors reported complete remission and suggested decitabine as a potential effective therapeutic agent in patients with secondary AML; nonetheless, data is scarce (49).

Bortezomib, a proteasome inhibitor, was administered in patients 1, 3, and 5 for the treatment of MM. To our knowledge, only one previous case report describes the use of bortezomib in CNL-MM, resulting in the complete resolution of both leukocytosis and MG (50). Reduced neutrophil count is a common observation in the use of bortezomib. Bortezomib could act directly through the effect on proteasomes in neutrophils, or indirectly through its influence on cytokine concentration. The administration of bortezomib in patients 1 and 3 resulted in a VGPR, while in patient 5 a partial response was achieved. Data of immunomodulatory drugs in MG-associated CNL, such as thalidomide and lenalidomide in patients 1 and 5 of our series, are scarce. The number of leukocytes normalized in all of these patients.

Conclusion

Chronic neutrophilic leukemia is a rare but potentially aggressive myeloproliferative neoplasm with a median survival of approximately 24 months. A non-negligible number of CNL cases are diagnosed with plasma cell dyscrasias; these patients show a more favorable prognosis with a median survival of 5 years. The discovery of oncogenic *CSF3R* driver mutations raised the diagnostic accuracy of CNL and resulted in the updated WHO diagnostic criteria in 2016. *CSF3R* tends to be less frequently mutated in CNL associated with monoclonal gammopathies (MG), challenging the diagnosis. Better survival and lower *CSF3R* mutational frequency may suggest a different

etiopathogenesis between pure CNL and MG-associated CNL. Owing to the rarity of CNL, there is no defined standard of care. Currently, hematopoietic stem cell transplantation (HSCT) is the only curative treatment. This series provides an overview of cytogenetic evolution and treatment in MG-associated CNL. More knowledge about occurring mutations and the order of acquisition will hopefully result in better therapeutic approaches and outcomes.

Data availability statement

The raw data supporting the conclusions of this article will be made available by the authors, without undue reservation.

Ethics statement

Written informed consent was obtained from the individual(s) for the publication of any potentially identifiable images or data included in this article.

Author contributions

GV: data curation (equal), formal analysis (equal), visualization (equal), writing-original draft (lead), writing-review and editing (supporting). MD: data curation (equal), formal analysis (equal), visualization (equal), writing-original draft (supporting), writingreview and editing (supporting). VH: data curation (equal), formal analysis (equal), visualization (equal), writing-original draft (supporting), writing-review and editing (supporting). CG: data curation (equal), formal analysis (equal), visualization (equal), writingoriginal draft (supporting), writing-review and editing (supporting). LM: data curation (equal), formal analysis (equal), visualization (equal), writing-original draft (supporting), writing-review and editing (supporting). TD: data curation (equal), formal analysis (equal), visualization (equal), writing-original draft (lead), writing-review and editing (lead).

Conflict of interest

The authors declare that the research was conducted in the absence of any commercial or financial relationships that could be construed as a potential conflict of interest.

Publisher's note

All claims expressed in this article are solely those of the authors and do not necessarily represent those of their affiliated organizations, or those of the publisher, the editors and the reviewers. Any product that may be evaluated in this article, or claim that may be made by its manufacturer, is not guaranteed or endorsed by the publisher.

References

1. Szuber N, Elliott M, Tefferi A. Chronic neutrophilic leukemia: 2022 update on diagnosis, genomic landscape, prognosis, and management. *Am J Hematol* (2022) 97:491-505. doi: 10.1002/ajh.26481

2. Thomopoulos TP, Symeonidis A, Kourakli A, Papageorgiou SG, Pappa V. Case report: Chronic neutrophilic leukemia associated with monoclonal gammopathies: Case series and review of genetic characteristics and practical management. *Front Oncol* (2022) 12:891961/BIBTEX. doi: 10.3389/FONC.2022.891961/BIBTEX

3. Elliott MA, Hanson CA, Dewald GW, Smoley SA, Lasho TL, Tefferi A. WHO-defined chronic neutrophilic leukemia: A long-term analysis of 12 cases and a critical review of the literature. *Leukemia* (2005) 19:313–7. doi: 10.1038/sj.leu.2403562

4. Arber DA, Orazi A, Hasserjian R, Thiele J, Borowitz MJ, Le Beau MM, et al. The 2016 revision to the world health organization classification of myeloid neoplasms and acute leukemia. *Blood* (2016) 127:2391–405. doi: 10.1182/blood-2016-03-643544

5. Maxson JE, Gotlib J, Pollyea DA, Fleischman AG, Agarwal A, Eide CA, et al. Oncogenic CSF3R mutations in chronic neutrophilic leukemia and atypical CML. *N Engl J Med* (2013) 368:1781–90. doi: 10.1056/NEJMoa1214514

6. Maxson JE, Tyner JW. Genomics of chronic neutrophilic leukemia. *Blood* (2017) 129:715–22. doi: 10.1182/blood-2016-10-695981

7. Pardanani A, Lasho TL, Laborde RR, Elliott M, Hanson CA, Knudson RA, et al. CSF3R T618I is a highly prevalent and specific mutation in chronic neutrophilic leukemia. *Leukemia* (2013) 27:1870–3. doi: 10.1038/leu.2013.122

8. Bain BJ, Ahmad S. Chronic neutrophilic leukaemia and plasma cell-related neutrophilic leukaemoid reactions. *Br J Haematol* (2015) 171:400–10. doi: 10.1111/bjh.13600

9. Tuohy E. A case of splenomegaly with polymorphonuclear neutrophil hyperleukocytosis. *Am J Med Sci* (1920), 160:18–25. doi: 10.1097/00000441-192007000-00003

10. Elliott MA, Tefferi A. Chronic neutrophilic leukemia: 2018 update on diagnosis, molecular genetics and management. *Am J Hematol* (2018) 93:578–87. doi: 10.1002/ajh.24983

11. Elliott MA, Dewald GW, Tefferi A, Hanson CA. Chronic neutrophilic leukemia (CNL): A clinical, pathologic and cytogenetic study. *Leukemia* (2001) 15:35–40. doi: 10.1038/sj.leu.2401993

12. Dao KHT, Tyner JW, Gotlib J. Recent progress in chronic neutrophilic leukemia and atypical chronic myeloid leukemia. *Curr Hematol Malig Rep* (2017) 12:432–41. doi: 10.1007/s11899-017-0413-y

13. Maxson JE, Luty SB, MacManiman JD, Paik JC, Gotlib J, Greenberg P, et al. The colony-stimulating factor 3 receptor T640N mutation is oncogenic, sensitive toJAKInhibition, and mimics T618i. *Clin Cancer Res* (2016) 22:757–64. doi: 10.1158/1078-0432.CCR-14-3100

14. Ito T, Kojima H, Otani K, Komeno T, Mitsuhashi S, Hasegawa Y, et al. Chronic neutrophilic leukemia associated with monoclonal gammopathy of undetermined significance. *Acta Haematol* (1996) 95:140–3. doi: 10.1159/000203863

15. Standen GR, Jasani B, Wagstaff M, Wardrop CAJ. Chronic neutrophilic leukemia and multiple myeloma: An association with λ light chain expression. *Cancer* (1990) 66:162–6. doi: 10.1002/1097-0142(19900701)66:1<162

16. Nedeljkovic M, He S, Szer J, Juneja S. Chronic neutrophilia associated with myeloma: Is it clonal? *Leuk Lymph* (2014) 55:439–40. doi: 10.3109/10428194.2013.809080

17. Forsberg LA. Loss of chromosome y (LOY) in blood cells is associated with increased risk for disease and mortality in aging men. *Hum Genet* (2017) 136:657–63. doi: 10.1007/s00439-017-1799-2

18. Aktas Samur A, Minvielle S, Shammas M, Fulciniti M, Magrangeas F, Richardson PG, et al. Deciphering the chronology of copy number alterations in multiple myeloma. *Blood Cancer J* (2019) 9:39. doi: 10.1038/s41408-019-0199-3

19. Giri S, Huntington SF, Wang R, Zeidan AM, Podoltsev N, Gore SD, et al. Chromosome 1 abnormalities and survival of patients with multiple myeloma in the era of novel agents. *Blood Adv* (2020) 4:2245–53. doi: 10.1182/bloodadvances.2019001425

20. Klampfl T, Harutyunyan A, Berg T, Gisslinger B, Schalling M, Bagienski K, et al. Genome integrity of myeloproliferative neoplasms in chronic phase and during disease progression. *Blood* (2011) 118:167–76. doi: 10.1182/blood-2011-01-331678

21. Inaba T, Honda H, Matsui H. The enigma of monosomy 7. *Blood* (2018) 131:2891–8. doi: 10.1182/blood-2017-12-822262

22. Elliott MA, Pardanani A, Hanson CA, Lasho TL, Finke CM, Belachew AA, et al. ASXL1 mutations are frequent and prognostically detrimental in CSF3R -mutated chronic neutrophilic leukemia. *Am J Hematol* (2015) 90:653–6. doi: 10.1002/ajh.24031

23. Antic D, Impera L, Fekete MD, Djordjevic V, Storlazzi CT, Elezovic I. Novel chromosomal translocation (17;22)(q12;q12) in a case of myelodisplastic syndrome characterized with signs of hemolytic anemia at presentation. *Gene* (2012) 493:161–4. doi: 10.1016/j.gene.2011.11.002

24. Xu-Monette ZY, Jeffrey Medeiros L, Li Y, Orlowski RZ, Andreeff M, Bueso-Ramos CE, et al. Dysfunction of the TP53 tumor suppressor gene in lymphoid malignancies. *Blood* (2012) 119:3668–83. doi: 10.1182/blood-2011-11-366062

25. Cumbo C, Tota G, Anelli L, Zagaria A, Specchia G, Albano F. TP53 in myelodysplastic syndromes: Recent biological and clinical findings. *Int J Mol Sci* (2020) 21:3432. doi: 10.3390/ijms21103432

26. Rajkumar SV. Multiple myeloma: 2018 update on diagnosis, risk-stratification, and management. *Am J Hematol* (2018) 93:1091–110. doi: 10.1002/ajh.25117

27. Smadja NV, Leroux D, Soulier J, Dumont S, Arnould C, Taviaux S, et al. Further cytogenetic characterization of multiple myeloma confirms that 14q32 translocations are a very rare event in hyperdiploid cases. *Genes Chromosomes Cancer* (2003) 38:234–9. doi: 10.1002/gcc.10275

28. Shou LH, Cao D, Dong XH, Fang Q, Wu Y, Zhang Y, et al. Prognostic significance of SETBP1 mutations in myelodysplastic syndromes, chronic myelomonocytic leukemia, and chronic neutrophilic leukemia: A meta-analysis. *PloS One* (2017) 12:e0171608. doi: 10.1371/journal.pone.0171608

29. Gajendra S, Gupta R, Chandgothia M, Kumar L, Gupta R, Chavan SM. Chronic neutrophilic leukemia with V617F JAK2 mutation. *Indian J Hematol Blood Transfus* (2014) 30:139–42. doi: 10.1007/s12288-012-0203-6

30. Imashuku S, Kudo N, Kubo K, Saigo K, Okuno N, Tohyama K. Rituximab for managing acquired hemophilia a in a case of chronic neutrophilic leukemia with the JAK2 kinase V617F mutation. *J Blood Med* (2012) 3:157. doi: 10.2147/jbm.s37631

31. Kako S, Kanda Y, Sato T, Goyama S, Noda N, Shoda E, et al. Early relapse of JAK2 V617F-positive chronic neutrophilic leukemia with central nervous system infiltration after unrelated bone marrow transplantation. *Am J Hematol* (2007) 82:386–90. doi: 10.1002/ajh.20805

32. Lea NC, Lim Z, Westwood NB, Arno MJ, Gäken J, Mohamedali A, et al. Presence of JAK2 V617F tyrosine kinase mutation as a myeloid-lineage-specific mutation in chronic neutrophilic leukaemia. *Leukemia* (2006) 20:1324–6. doi: 10.1038/sj.leu.2404240

33. Mc Lornan DP, Percy MJ, Jones AV, Cross NCP, Mc Mullin MF. Chronic neutrophilic leukemia with an associated V617F JAK2 tyrosine kinase mutation. *Haematologica* (2005) 90:1696–7. doi: 10.3324/%x

34. Steensma DP, Dewald GW, Lasho TL, Powell HL, McClure RF, Levine RL, et al. The JAK2 V617F activating tyrosine kinase mutation is an infrequent event in both "atypical" myeloproliferative disorders and myelodysplastic syndromes. *Blood* (2005) 106:1207–9. doi: 10.1182/blood-2005-03-1183

35. Szuber N, Tefferi A. Chronic neutrophilic leukemia: New science and new diagnostic criteria. *Blood Cancer J* (2018) 8:19. doi: 10.1038/s41408-018-0049-8

36. Meggendorfer M, Haferlach T, Alpermann T, Jeromin S, Haferlach C, Kern W, et al. Specific molecular mutation patterns delineate chronic neutrophilic leukemia, atypical chronic myeloid leukemia, and chronic myelomonocytic leukemia. *Haematologica* (2014) 99:e244–6. doi: 10.3324/haematol.2014.113159

37. Ouyang Y, Qiao C, Chen Y, Zhang SJ. Clinical significance of CSF3R, SRSF2 and SETBP1 mutations in chronic neutrophilic leukemia and chronic myelomonocytic leukemia. *Oncotarget* (2017) 8:20834–41. doi: 10.18632/oncotarget.15355

38. Dao KHT, Tyner JW. What's different about atypical CML and chronic neutrophilic leukemia? *Hematology* (2015) 2015:264–71. doi: 10.1182/asheducation-2015.1.264

39. Yoshida K, Sanada M, Shiraishi Y, Nowak D, Nagata Y, Yamamoto R, et al. Frequent pathway mutations of splicing machinery in myelodysplasia. *Nature* (2011) 478:64–9. doi: 10.1038/nature10496

40. Nooruddin Z, Miltgen N, Wei Q, Schowinsky J, Pan Z, Tobin J, et al. Changes in allele frequencies of CSF3R and SETBP1 mutations and evidence of clonal evolution in a chronic neutrophilic leukemia patient treated with ruxolitinib. *Haematologica* (2017) 102:e207–9. doi: 10.3324/haematol.2016.163089

41. Stoner RC, Press RD, Maxson JE, Tyner JW, Dao KHT. Insights on mechanisms of clonal evolution in chronic neutrophilic leukemia on ruxolitinib therapy. *Leukemia* (2019) 34:1684–8. doi: 10.1038/s41375-019-0688-1

42. Venugopal S, Mascarenhas J. Chronic neutrophilic leukemia: Current and future perspectives. *Clin Lymph Myeloma Leuk* (2019) 19:129–34. doi: 10.1016/j.clml.2018.11.012

43. Itonaga H, Ota S, Ikeda T, Taji H, Amano I, Hasegawa Y, et al. Allogeneic hematopoietic stem cell transplantation for the treatment of BCR-ABL1-negative atypical chronic myeloid leukemia and chronic neutrophil leukemia: A retrospective nationwide study in Japan. *Leuk Res* (2018) 75:50–7. doi: 10.1016/J.LEUKRES.2018.11.003

44. Hasle H, Olesen G, Kerndrup G, Philip P, Jacobsen N. Chronic neutrophil leukaemia in adolescence and young adulthood. *Br J Haematol* (1996) 94:628–30. doi: 10.1046/J.1365-2141.1996.7082329.X

45. Zhang X, Pan J, Guo J. Presence of the JAK2 V617F mutation in a patient with chronic neutrophilic leukemia and effective response to interferon alfa-2b. *Acta Haematol* (2013) 130:44–6. doi: 10.1159/000345851

46. Yassin MA, Kohla S, Al-Sabbagh A, Soliman AT, Yousif A, Moustafa A, et al. A case of chronic neutrophilic leukemia successfully treated with pegylated interferon alpha-2a. *Clin Med Insights: Case Rep* (2015) 8:33–6. doi: 10.4137/CCRep.s22820

47. Meyer S, Feremans W, Cantiniaux B, Capel P, Huygen K, Dicato M. Successful alpha-2b-interferon therapy for chronic neutrophilic leukemia. *Am J Hematol* (1993) 43:307–9. doi: 10.1002/ajh.2830430416

48. Dao KHT, Gotlib J, Deininger MMN, Oh ST, Cortes JE, Collins RH, et al. Efficacy of ruxolitinib in patients with chronic neutrophilic leukemia and atypical chronic myeloid leukemia. *J Clin Oncol* (2020) 38:1006–18. doi: 10.1200/JCO.19.00895

49. Shi J, Ni Y, Li J, Qiu H, Miao K. Concurrent chronic neutrophilic leukemia blast crisis and multiple myeloma: A case report and literature review. *Oncol Lett* (2015) 9:2208. doi: 10.3892/OL.2015.3043

50. Taiwo E, Wang H, Lewis R. Treatment of coexisting chronic neutrophilic leukemia and light chain multiple myeloma with hydroxyurea, bortezomib, and dexamethasone. *Case Rep Hematol* (2014) 2014:1–3. doi: 10.1155/2014/869395

10.3389/fonc.2022.1014671

Appendix 1

A. List of screened regions/genes by Fluorescent In Situ Hybridization (FISH) in patient 1

LSI *CDKN2A*(9p21)(SO)/*CEP9(SG)* [9p21/9p11.1-9q11.1, Abbott], LSI *TP53*(SO)/*CEP17*(SG) [17p13/17p11.1-17q11.1, Abbott], LSI *IGH*(DC BA) [14q32, Abbott], *CEP9*(SO) [9p11.1-q11.1, Abbott], *CKS1B*(SG)/*CEP1*(SO) [1q21/1p11.1-1q11.1, CME + Abbott]

B. *List of screened regions/genes by Fluorescent In Situ Hybridization (FISH) in patient 2*

XL *IGH*(DC BA) [14q32, Metasystems]

C. *List of screened regions/genes by Fluorescent In Situ Hybridization (FISH) in patient 3*

LSI *IGH*(DC BA) [14q32, Vysis], LSI *IGH*(SG)/*CMAF*(SO) (DC DF) [14q32/16q23, Vysis], LSI *IGH*(SG)/*CCND1*-XT(SO) (DC DF) [14q32/11q13, Vysis], LSI *IGH*(SG)/*FGFR3*(SO) (DC DF) [14q32/4p16, Vysis]

D. *List of screened regions/genes by Fluorescent In Situ Hybridization (FISH) in patient 5*

LSI 4q12 (*FIP1L1*-PDGFRA) [Vysis tri-color rearrangement probe], LSI *PDGFRB* [Vysis], LSI *JAK2* [Kreatech], LSI *FGFR1* [Zytovision], LSI *BCR*/ABL(ES) [9q34.1/22q11.23, Vysis], *TPI* 17p13.1/*CEP17*(D17Z1) [Metasystems], *IGH/FGFR3* (DC DF) [14q32/4p16, Metasystems], *IGH/MAF* (DC DF) [14q32/16q23, Metasystems]

Appendix 2

A. List of screened genes by Next-Generation Sequencing (NGS) in patient 1,2, 3 & 4.

ABL1, ASXL1, ATRX, BCOR, BCORL1, BRAF, CALR, CBL, CBLB, CBLC, CDKN2A, CSF3R, *CUX1, DNMT3A, ETV6, EZH2, FBXW7, FLT3, GATA1, GATA2, GNAS, IDH1, IDH2, IKZF1, JAK2, KMD6A, KIT, KRAS, MPL, MYD88, NOTCH1, NPM1, NRAS, PDGFRA, PHF6, PTEN, PTPN11, RAD21, RUNX1, SETBP1, SF3B1, SMC1A, SMC3, SRSF2, STAG2, TET2, TP53, U2AF1, WT1, ZRSR2*

B. *List of screened genes by Next-Generation Sequencing (NGS) in patient 5*

ASXL1, CEBPA, DNMT3A, FLT3, IDH1, IDH2, cKIT, NPM1, RUNX1, TET2, TP53, WT1, SF3B1, SRSF2, U2AF1, JAK2, MPL, CALR, EZH2, SETBP1, CSF3R

frontiers | Frontiers in Oncology

TYPE Case Report
PUBLISHED 08 December 2022
DOI 10.3389/fonc.2022.986144

OPEN ACCESS

EDITED BY
Yuqian Sun,
Peking University People's Hospital, China

REVIEWED BY
Xiaoxia Hu,
Ruijin Hospital, China
David Gomez-Almaguer,
Autonomous University of Nuevo León, Mexico

*CORRESPONDENCE
Hongmei Ning
ninghongmei72@sina.com

†These authors have contributed equally to this work

SPECIALTY SECTION
This article was submitted to Hematologic Malignancies, a section of the journal Frontiers in Oncology

RECEIVED 04 July 2022
ACCEPTED 04 November 2022
PUBLISHED 08 December 2022

CITATION
Zheng W, Wu Y, Guan L, Cheng L, Hu Y, Tan M, Yang Y and Ning H (2022) Case report: First report of haploidentical allogeneic hematopoietic stem cell transplantation from donors with mild alpha-thalassemia for acute leukemia. *Front. Oncol.* 12:986144. doi: 10.3389/fonc.2022.986144

Case report: First report of haploidentical allogeneic hematopoietic stem cell transplantation from donors with mild alpha-thalassemia for acute leukemia

Wenshuai Zheng[1†], Yamei Wu[2†], Lixun Guan[1†], Longcan Cheng[1], Yalei Hu[1], Min Tan[1], Yuhui Yang[1] and Hongmei Ning[3*]

[1]Department of Hematology, Hainan Hospital of Chinese PLA General Hospital, Sanya, China, [2]Department of Hematology, Seventh Medical Center of Chinese PLA General Hospital, Beijing, China, [3]Senior Department of Hematology, Fifth Medical Center of Chinese PLA General Hospital, Beijing, China

For acute leukemia (AL) with adverse prognostic factors, allogeneic hematopoietic stem cell transplantation (allo-HSCT) is the standard care option after the first complete remission. Meanwhile, as the success of haploidentical HSCT (haplo-HSCT), haploidentical donors (HIDs) become a reliable choice. However, there have been no reports on haplo-HSCT from HIDs with mild alpha(α)-thalassemia for AL yet. In the present report, we first describe two cases of successful haplo-HSCT from HIDs with mild α-thalassemia for AL.

KEYWORDS

haploidentical donors, thalassemia, acute leukemia, successful, haploidentical allogeneic hematopoietic stem cell transplantation

Introduction

Acute leukemia (AL) is a heterogeneous disease characterized by impaired differentiation and increased proliferation of myeloid progenitor cells (1). Allogeneic hematopoietic stem cell transplantation (allo-HSCT) is the standard care option for AL with adverse prognostic factors (2, 3). For the donor selection of allo-HSCT, human leukocyte antigen (HLA)-matched sibling donors (MSDs) are generally preferred, with haploidentical donors (HIDs) and matched unrelated donors (MUDs) as alternatives (4). In China, due to the shortage of MSDs and MUDs, haploidentical HSCT (haplo-HSCT)

has achieved great success (5). Nevertheless, in areas where thalassemia is endemic, it is inevitable that part of the HIDs have thalassemia. Currently, the safety and efficacy of haplo-HSCT from HIDs with mild alpha(α)-thalassemia for AL is unknown. We first report two cases of AL patients received haplo-HSCT from HIDs with mild α-thalassemia.

Case presentation

Two patients were diagnosed as AL and received haplo-HSCT from HIDs with mild α-thalassemia. The patients charts were screened for patient history and actual clinical data and laboratory findings. Both patients were female, aged 18 and 56 years with HIDs. The detailed patients' and donors' characteristics are shown in Table 1. Patient 1 was diagnosed as mixed phenotype acute leukemia (MPAL) with two blast populations of distinct lineages (B lymphoid/myeloid) and had multiple gene mutations with poor prognosis. Patient 2 was diagnosed as acute myeloid leukemia (AML) classified as high risk group. We considered allo-HSCT for them and performed HLA typing and blood tests of their family members to find a suitable donor. For patient 1, we fund two HIDs and no MSDs and MUDs were identified. Her elder son is a HID with positive hepatitis B virus (HBV) infection (HBV DNA = 1.84 × 10 (6)/ml) and younger son is a HID with mild anemia. The detection of thalassemia revealed that her younger son is a patient with mild α-thalassemia. Since her elder son had positive HBV infection and younger son had hematological stability with hemoglobin (Hb) levels maintained at approximately 11-12 g/dL, we recommended her younger son as HID of haplo-HSCT. For patient 2, HLA typing showed that her father, mother and little brother are HIDs and no MSDs and MUDs were identified. Her father and little brother also had mild anemia with Hb levels maintained at approximately 10-12 g/dL. The detection of thalassemia revealed that both of her father and little brother are patients with α-thalassemia. Because her family refused to use her mother as donor, we choosed the younger donor as her HID. The course of therapy, conditioning regimen and graft-versus-host disease (GVHD) prophylaxis can be seen in Table 1. Peripheral blood stem cells (PBSCs) were harvested from HIDs after four days of granulocyte colony stimulating factor (G-CSF). For patient 1, the total nucleated cell, CD34+, and CD3+ cell counts were 8.9 × 10(8)/kg, 7.1 × 10(6)/kg, and 2.9 × 10(8)/kg, respectively. White blood cell (WBC) was engrafted on +14 day and platelet was engrafted on +12 day (The day of WBC engraftment was defined as the first of three consecutive days on which the granulocyte count exceeded 0.5 × 10 (8)/L. The day of platelet engraftment was defined as the first of seven consecutive days on which the platelet count exceeded 20 × 10 (8)/L without platelet infusion). For patient 2, the total nucleated cell, CD34+, and CD3+ cell counts were 7.97 × 10(8)/kg, 9.12 × 10(6)/kg, and 2.5 × 10(8)/kg, respectively. Both WBC and platelet were engrafted on +9 day. In both patients, regimen-associated toxicities, such as anorexia, enteritis and infection, were mild and there were II degree cutaneous acute GVHD which was controlled by first-line treatment with glucocorticoids. The 1, 2, 3, 6 month follow-up of patient 1 and 1, 2, 3, 6, 9, 12, 18, 24, 36 month follow-up of patient 2 showed that bone marrow examination were normocellular

TABLE 1 The clinic characteristics of patients and donors.

Patients	Age	Diagnosis	Karyotype	Mutation	Treatment and remission	Conditioning regimen	Immunosuppression	Donors	Age	Sex	Thalassemia type
Patient 1	56	MPAL	46, XX[20]	*IDH2*, *NRAS*, *WT1*, *EZH2*	DA+VP, NR DA+AZA, CR MRD(-) DA+AZA, CR MRD(-) DA+AZA, CR MRD(-)	Fludarabine (30 mg/m^2 -6 to -3d) Carmustine (300 mg/m^2 -6d) Busulfan (0.8 mg/kg/6h -5 to -3d)	Tacrolimus (0.015 mg/kg/12h from +5d with drug level monitoring) Cyclophosphamide (50mg/kg +3 to +4 d) MMF (1g/12h +5 to +28d)	Donor 1	30	Man	- -$^{SEA/}$αα
Patient 2	18	AML	45, X, -X, t (8: 21) (q22: q22), arr (4) × 3 [20]	*C-kit*	DA, PR IAC, CR MRD(+) DA, CR MRD(-)	Busulfan (0.8 mg/kg/6h -10 to -8d) Cytarabine (4 g/m^2 -6 to -5d); Cyclophosphamide (50 mg/kg -4 to -3d) Anti-thymoglobulin (1.5 mg/kg -5d, 2.5 mg/kg -4 to -3d, 3.5 mg/kg -2d)	CSA (2 mg/kg/12h from -10d with drug level monitoring) MTX (10 mg/m^2 +1, +3, +6, and +11d) MMF (1g/12h -10d to +28d)	Donor 2	11	Man	- -$^{SEA/}$αα

AML, acute myeloid leukemia; AZA, azacitidine; CR, complete remission; CSA, cyclosporine A; DA, daunorubicin + cytarabine; GVHD, graft-versus-host disease; IAC, Idarubicin +cytarabine+cladribine; MRD, minimal residual disease; MMF, mycophenolate mofetil; MPAL, mixed phenotype acute leukemia; MTX, methotrexate; NR, non-remission; PR, partial remission; VP, vincristine+prednison.

marrow, and chimerism analysis by variable-number tandem repeat were full donor chimerism. No chronic GVHD were observed. The detection of thalassemia showed that both patients converted to donors' thalassemia type with mild microcytic hypochromic anemia in which Hb levels maintained at approximately 10-12 g/dL without transfusion.

Discussion

The treatment of AL involves initial induction therapy and post-remission therapy. The goal of post-remission therapy is to prevent relapse of the disease. The two commonly strategies of post-remission are additional post-remission cytotoxic chemotherapies or allo-HSCT. The choice of therapy is determined by the unique risks and benefits provided by each treatment.

In our cases, patient 1 was diagnosed as MAPL. Clinically, the outcomes for MPAL are worse than both acute lymphoblastic leukemia (ALL) and AML (7). In addition, patient 1 didn't get CR after first course chemotherapy. Patient 2 has karyotype of monomer, which was classified as high risk group. So we recommended allo-HSCT for them to decrease the choice of relapse. But both patients were lack of suitable MSDs and MUDs. Under the circumstances, haplo-HSCT is an alternative option. A systematic review showed that the relapse, survival, and acute GVHD were not significantly different between MSD-HSCT and haplo-HSCT using post transplantation cyclophosphamide (PT-Cy) (9). Wang et al. reported that the haplo-HSCT and MSD-HSCT groups exhibited comparable 3-year non-relapse mortality, disease free survival and overall survival in intermediate/high-risk AML (6).

In our cases, because of some reasons as above, we choosed the younger son of patient 1 and the little brother of patient 2 as donor, however, both donors had mild α-thalassemia. In areas where thalassemia is endemic, this is an inevitable situation sometimes. According to the suitability criteria for adult related donors, hematopoietic stem cell collections from individuals with red blood cell abnormalities such as spherocytosis and elliptocytosis are generally not recommended; however, subjects with mild α-thalassemia, or β-thalassemia are suitable hematopoietic stem cell donors (8). Nevertheless, to our best knowledge, no case of AL patients undergoing haplo-HSCT from HIDs with mild α-thalassemia have been reported yet. Despite having α-thalassemia phenotype, the two donors had sufficiently stable hematology. After careful consideration, we opted haplo-HSCT for them.

α-thalassaemia is inherited as an autosomal recessive disorder characterised by a microcytic hypochromic anaemia, and a clinical phenotype varying from almost asymptomatic to a lethal haemolytic anaemia (10). It is probably the most common monogenic gene disorder in the world and is especially frequent in Mediterranean countries, South-East Asia, Africa, the Middle East and in the Indian subcontinent (10). Mild α-thalassemia is usually asymptomatic but sometimes involves mild anemia which does not require treatment (10). However, considering the pathophysiology of α-thalassemia, our main concern was the risk of poor engraftment of erythrocytes after HSCT and the efficiency of the mobilization of PBSCs in patients with thalassemia. Mi YJ et al. reported a rare case in which allo-HSCT for a 7-year-old severe aplastic anemia patient from a MSD with mild β-thalassemia was performed successful. In this case, the engraftment of erythrocytes was evident, good performance status has been observed throughout the 5 years after HSCT and the PBSCs mobilized by G-CSF were sufficient (11). Li K et al. also reported that for the efficiency of mobilization of PBCSs in patients with thalassemia, there were no significant differences in the CD34+ cell subsets and lymphocyte subsets after G-CSF administration when compared with those in healthy donors (12).

In our cases, PBSCs were harvested from donors' peripheral blood after four days of G-CSF administration to the day of transplantation. The total nucleated cell and CD34+ cell counts were sufficient and the donors had no complication. Both patients' WBC and platelet were engrafted successfully and no further blood transfusions have been required to this day.

Conclusion

Our findings suggest that HIDs with mild α-thalassemia could be suitable donors of allo-HSCT for AL and the mobilization and collection of PBSCs in patients with mild α-thalassemia are feasible.

Data availability statement

The datasets presented in this study can be found in online repositories. The names of the repository/repositories and accession number(s) can be found in the article/supplementary material.

Ethics statement

Written informed consent was obtained from the individual(s) for the publication of any potentially identifiable images or data included in this article.

Author contributions

WZ and HN conceived and designed the study, interpreted the results, wrote the paper and gave critical comments. LC, YH, MT, YY collected the data. YW and LG wrote the paper and gave critical comments. All authors contributed to the article and approved the submitted version.

Acknowledgments

The authors thank the patient for allowing us to understand her condition and write this case report.

Conflict of interest

The authors declare that the research was conducted in the absence of any commercial or financial relationships that could be construed as a potential conflict of interest.

Publisher's note

All claims expressed in this article are solely those of the authors and do not necessarily represent those of their affiliated organizations, or those of the publisher, the editors and the reviewers. Any product that may be evaluated in this article, or claim that may be made by its manufacturer, is not guaranteed or endorsed by the publisher.

References

1. Arber DA, Orazi A, Hasserjian R, Thiele J, Borowitz MJ, Le Beau MM, et al. The 2016 revision to the world health organization classification of myeloid neoplasms and acute leukemia. *Blood* (2016) 127:2391–405. doi: 10.1182/blood-2016-03-643544

2. Pollyea DA, Bixby D, Perl A, Bhatt VR, Altman JK, Appelbaum FR, et al. NCCN guidelines insights: Acute myeloid leukemia, version 2.2021. *J Natl Compr Canc Netw* (2021) 19:16–27. doi: 10.6004/jnccn.2021.0002

3. Brown PA, Shah B, Advani A, Aoun P, Boyer MW, Burke PW, et al. Acute lymphoblastic leukemia, version 2.2021, NCCN clinical practice guidelines in oncology. *J Natl Compr Canc Netw* (2021) 19:1079–109. doi: 10.6004/jnccn.2021.0042

4. Duarte RF, Labopin M, Bader P, Basak GW, Bonini C, Chabannon C, et al. Indications for haematopoietic stem cell transplantation for haematological diseases, solid tumours and immune disorders: current practice in Europe. *2019. Bone Marrow Transplant* (2019) 54:1525–52. doi: 10.1038/s41409-019-0516-2

5. Lv M, Chang YJ, Huang XJ. Everyone has a donor: Contribution of the Chinese experience to global practice of haploidentical hematopoietic stem cell transplantation. *Front Med* (2019) 13:45–56. doi: 10.1007/s11684-017-0595-7

6. Wang Y, Liu QF, Xu LP, Liu KY, Zhang XH, Ma X, et al. Haploidentical vs identical-sibling transplant for AML in remission: A multicenter, prospective study. *Blood* (2015) 125:3956–62. doi: 10.1182/blood-2015-02-627786

7. Maliha K, Rabbia S, Kiran N. An update on classification, genetics, and clinical approach to mixed phenotype acute leukemia (MPAL). *Ann Hematol* (2018) 97:945–53. doi: 10.1007/s00277-018-3297-6

8. Worel N, Buser A, Greinix HT, Hägglund H, Navarro W, Pulsipher MA, et al. Suitability criteria for adult related donors: A consensus statement from the worldwide network for blood and marrow transplantation standing committee on donor issues. *Biol Blood Marrow Transplant* (2015) 21:2052–60. doi: 10.1016/j.bbmt.2015.08.009

9. Meybodi MA, Cao W, Luznik L, Bashey A, Zhang X, Romeeet R, et al. HLA-haploidentical vs matched-sibling hematopoietic cell transplantation: A systematic review and meta-analysis. *Blood Adv* (2019) 3:2581–5. doi: 10.1182/bloodadvances.2019000614

10. Kattamis A, Kwiatkowski JL, Aydinok Y. Thalassaemia. *Lancet* (2022) 399:2310–24. doi: 10.1016/S0140-6736(22)00536-0

11. Jung MY, Lim YT, Lim H, Hah JO, Lee JM. Successful hematopoietic stem cell transplantation from a matched related donor with beta-thalassemia minor for severe aplastic anemia. *Children (Basel)* (2020) 7:E162. doi: 10.3390/children7100162

12. Li K, Wong A, Li CK, Shing MM, Chik KW, Tsang KS, et al. Granulocyte colony-stimulating factor-mobilized peripheral blood stem cells in beta-thalassemia patients: Kinetics of mobilization and composition of apheresis product. *Exp Hematol* (1999) 27:526–32. doi: 10.1016/s0301-472x(98)00045-9

frontiers | Frontiers in Oncology

TYPE Case Report
PUBLISHED 15 December 2022
DOI 10.3389/fonc.2022.1074913

OPEN ACCESS

EDITED BY
Shimin Hu,
University of Texas MD Anderson Cancer Center, United States

REVIEWED BY
Madhu M. Ouseph,
Cornell University, United States
Zhihong Hu,
University of Texas Health Science Center at Houston, United States

*CORRESPONDENCE
Hongxing Liu
starliu@pku.edu.cn

SPECIALTY SECTION
This article was submitted to Hematologic Malignancies, a section of the journal Frontiers in Oncology

RECEIVED 20 October 2022
ACCEPTED 23 November 2022
PUBLISHED 15 December 2022

CITATION
Chen X, Wang F, Zhou X, Zhang Y, Cao P, Ma X, Yuan L, Fang J, Liu M, Liu M, Chen J, Chen Q, Wu P, Lu Y, Ma X and Liu H (2022) Torque teno mini virus driven childhood acute promyelocytic leukemia: The third case report and sequence analysis. *Front. Oncol.* 12:1074913. doi: 10.3389/fonc.2022.1074913

Torque teno mini virus driven childhood acute promyelocytic leukemia: The third case report and sequence analysis

Xue Chen[1], Fang Wang[1], Xiaosu Zhou[2], Yang Zhang[1], Panxiang Cao[1], Xiaoli Ma[1], Lili Yuan[1], Jiancheng Fang[1], Mingyue Liu[1], Ming Liu[1], Jiaqi Chen[1], Qihui Chen[3], Ping Wu[1], Yue Lu[4], Xiujuan Ma[1] and Hongxing Liu[1,2]*

[1]Division of Pathology & Laboratory Medicine, Hebei Yanda Lu Daopei Hospital, Langfang, China, [2]Molecular Medicine Research Center, Beijing Lu Daopei Institute of Hematology, Beijing, China, [3]Department of Research and Development, Beijing Geneprofile Technologies Co., Ltd, Beijing, China, [4]Department of Bone Marrow Transplantation, Hebei Yanda Lu Daopei Hospital, Langfang, China

In this manuscript, we report torque teno mini virus (TTMV) as a cause of acute promyelocytic leukemia (APL) lacking *PML*::*RARA* in a 3-year-old boy. Astolfi et al. firstly identified partial integration of the TTMV genome into *RARA* intron 2, which resulted in in-frame *TTMV*::*RARA* fusion in two APL-like pediatric cases without *PML*::*RARA* in November 2021. This fascinating report identified an unexpected exogenous genetic cause of APL and could be of great importance for diagnosing and managing APL. Here we report the third childhood APL-like case caused by TTMV integration and investigate the location and structure of the integrated TTMV sequence. These findings suggest *TTMV*::*RARA* is a recurrent cause of APL lacking *PML*::*RARA*. Considering the widespread prevalence of TTMV in the population, more *TTMV*::*RARA* positive APL-like cases might remain to be identified. Establishing a bioinformatic analysis strategy optimized for the highly variable TTMV genome sequence may facilitate the identification of *TTMV*::*RARA* by whole transcript sequencing. An effective PCR protocol to identify *TTMV*::*RARA* based on a profound analysis of the conservation of TTMV segments in the fusion transcript is also expected. Also, further investigation is needed to elucidate the oncogenic mechanisms of TTMV integration and the clinical features of *TTMV*::*RARA* positive patients.

KEYWORDS

acute promyelocytic leukemia, torque teno mini virus, *RARA*, *TTMV*::*RARA*, whole-transcriptome sequencing

Introduction

Astolfi et al. (1, 2) firstly reported torque teno mini virus (TTMV) as a cause of childhood acute promyelocytic leukemia (APL) lacking *PML*::*RARA* fusion. They identified partial integration of the TTMV genome into the intron 2 of the human *RARA* gene, which resulted in in-frame *TTMV*::*RARA* fusion transcripts in two APL-like pediatric cases without *PML*::*RARA* fusion. This is a fascinating report because it identified an unexpected exogenous genetic cause of APL and could be of great importance for diagnosing and managing APL, especially given the widespread recessive carriage and transmission of TTMV in the population.

To explore whether there were more *TTMV*::*RARA* positive APL-like cases, we retrospectively performed a principal component analysis comparing 74 *PML*::*RARA*-positive APL cases, 343 oncogenic fusion gene negative AML cases, and 50 healthy controls in our whole-transcriptome sequencing (WTS) cohort (3). The result showed that one AML case was separated from other AML cases while clustered adjacent to the APL cohort (Figure 1A).

Case description

The index case was a 3-year-old boy initially admitted to a local hospital because of persistent fever and headache. Blood tests showed white blood cell count of 36.76×10^9/L, hemoglobin level of 86 g/L, and platelet count of 117×10^9/L. Prothrombin time and activated partial thromboplastin time were 13.3 s (reference, 9.4 - 12.5 s) and 23.6 s (reference, 25.1 - 38.0 s), respectively. Morphologic examination of bone marrow (BM) smears disclosed infiltration by 73.6% of hyper-granular promyelocytes. Flow cytometry (FCM) revealed 84.1% of myeloblasts (positive for CD13, CD33, CD45, CD117, CD123, CD64, and cMPO; partially positive for CD34; negative for HLA-DR, CD11b, CD16, and other T- or B-lymphoid related markers). The presumptive initial diagnosis of this patient was APL. However, both reverse transcription PCR (RT-PCR) and fluorescence *in situ* hybridization failed to detect the *PML*::*RARA* fusion in the BM, and the karyotype was normal. Next-generation sequencing mutation analysis of 86 genes that are frequently mutated in hematological malignancies revealed *FLT3*-ITD mutation.

Given the clinical suspicion of APL, the patient was immediately treated with ATRA and hydroxyurea. The white blood cell count increased to 128.52×10^9/L after four-day treatment, and induction chemotherapy (daunorubicin, cytarabine, and etoposide) was started concomitantly. ATRA was discontinued seven days after ATRA initiation due to the absence of *PML*::*RARA*. Follow-up monitoring 21 days after induction chemotherapy showed 13% of myeloblasts and promyelocytes in BM. Then he received consolidation therapy (idarubicin, cytarabine, and etoposide) and achieved complete remission (CR).

However, one month after achieving CR, the patient suffered from recurrent fever and was admitted to our hospital. BM morphology examination showed that 60% of nucleated cells were blast cells with abundant purple granules, irregular nuclei, and cytoplasmatic budding, while negative for Auer rods (Figure 1B). The karyotype was normal, and an in-house established protocol of WTS screening for oncogenic fusion genes reported a negative result (3). The patient was started on induction chemotherapy and achieved remission by day 39. Then he underwent haploidentical hematopoietic stem cell transplantation with his father as the donor but relapsed 50 days later with multiple metastases and gave up treatment.

Following the retrospective cluster analysis, we performed a manual investigation of the *RARA* transcript sequence in WTS data of this case. Alignment of the WTS data in integrative genomics viewer (IGV) revealed abundant *RARA* fusion transcripts with a 5' extension from *RARA* exon 3, which is not homologous to any human sequence (Figure 2A). Further

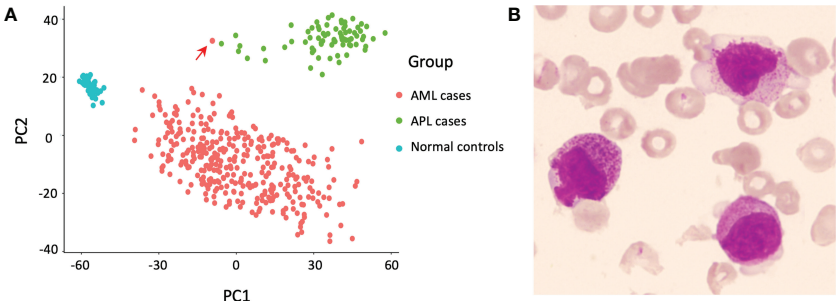

FIGURE 1
Discovery of the index case. **(A)** Principal component analysis revealed one relapsed acute myeloid leukemia (AML) case (indicated by the red arrow) separate from other AML cases, but adjacent to the cluster of acute promyelocytic leukemia (APL) cases. **(B)** Morphology of the bone marrow (BM) smear at relapse, Wright's stain.

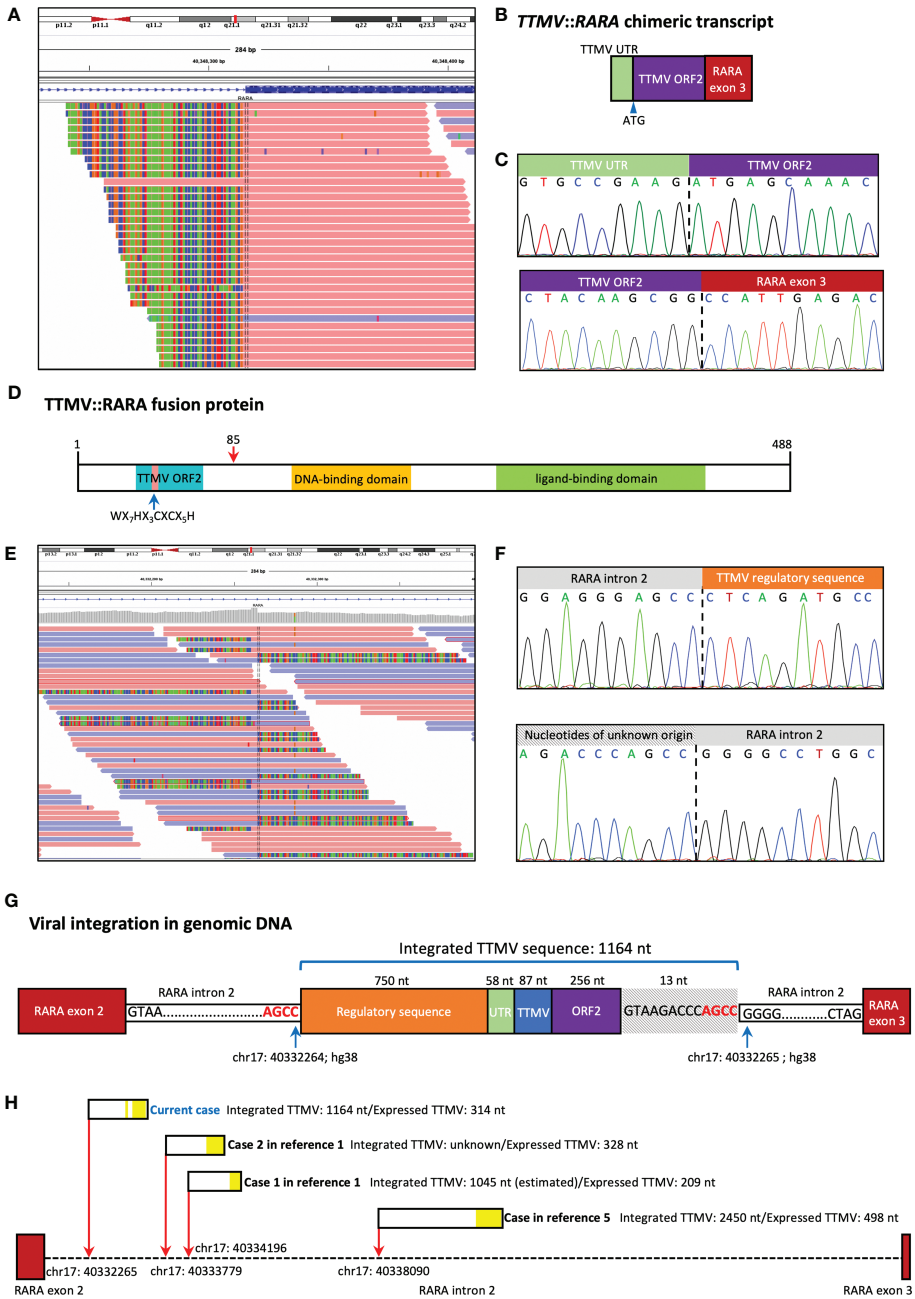

FIGURE 2
TTMV integration structure of our case. **(A)** Alignment of the whole transcript sequencing (WTS) data in integrative genomics viewer (IGV) revealed abundant *RARA* fusion transcripts with a 5′ extension from *RARA* exon 3, which is not homologous to any human sequence. **(B)** Schematic representation of the fusion between the TTMV sequence and *RARA* exon 3. The chimeric transcript includes TTMV open reading frame 2 (ORF2) and an upstream conserved untranslated region (UTR), in-frame with *RARA* exon 3. **(C)** Sanger sequencing confirmed the existence of the *TTMV::RARA* fusion transcript. **(D)** The predicted structure of the TTMV::RARA fusion protein. The blue arrow indicates the highly conserved TTMV ORF2 motif. The red arrow at position 85 indicates the fusion site. **(E)** Whole genome sequencing (WGS) revealed the insertion was located at chr17: 40332265 (hg38) in *RARA* intron 2. **(F)** Sanger sequencing confirmed the two genomic junction sequences. **(G)** Schematic representation of the location and structure of the integrated TTMV sequence. **(H)** TTMV insertion characteristics in the 4 cases reported to date. The red arrows show the insertion positions of TTMV sequence in *RARA* intron 2 (hg38). The black rectangles show the integrated TTMV sequences, and the yellow blocks within them show the nucleotides expressed in the *TTMV::RARA* fusion transcript.

TABLE 1 Summary of clinical and laboratory characteristics in the 4 reported cases with *TTMV*::*RARA* fusion.

Literature	Sex	Age (y)	Diagnosis	Initial WBC, $\times 10^9$/L	Fibrinogen	D-dimer	PT (second)	APTT (second)	Morphology	Immunotyping	Karyotype	RARA break-apart probe	Gene mutation	Treatment	Outcome
2021 Astolfi et al. (1)	F	6	Hypergranular APL	2.8	↓	↑	↑	↑	BM: hypercellularity with 85% abnormal promyelocytes with Aure rods	CD33+, CD13+, CD38+, CD99+, MPO+, HLA-DR^{low}	Normal karyotype	RARA rearrangements (-)	NA	ATRA+ATO +chemotherapy +HSCT	CR
2021 Astolfi et al. (1)	NA	3	AML	NA	NA	NA	NA	NA	NA	NA	Normal karyotype	NA	(-)	NA	NA
2022 Sala-Torra et al. (5)	M	39	AML with APL characteristics	NA	↓	↑	↑	NA	PB: circulating promyelocytic blasts with abundant azurophilic granules.	CD33+, MPO+, CD34-, HLA-DR-	46, XY, i(17)(q10)[18]/47, XY, 18, i(17)(q10)[2]	NA	NA	chemotherapy	NA
Our case	M	3	APL	36.76	NA	NA	↑	↓	BM: 73.6% hyper-granular promyelocytes	CD33+, CD13+, CD117, CD64+, MPO+, CD34 partially positive, HLA-DR-, CD11b-, CD16-	Normal karyotype	NA	*FLT3*-ITD	ATRA +chemotherapy +HSCT	Death

AML, acute myeloid leukemia; APL, acute promyelocytic leukemia; APTT, activated partial thromboplastin time; ATO, arsenic trioxide; ATRA, all-trans retinoic acid; BM, bone marrow; CR, complete remission; F, female; HSCT, hematopoietic stem cell transplantation; M, male; NA, not available; PB: peripheral blood; PT, prothrombin time; WBC, white blood cell count; ↑, higher than the reference value; ↓, below the reference value.

10.3389/fonc.2022.1074913

analysis revealed the exogenous sequence started with 58 nucleotides that aligned to the untranslated region (UTR) of TTMV, followed by 256 nucleotides starting with a start codon (ATG) and revealed a significant alignment to different TTMV isolates (83% coverage, 93% to 94% identity), in-frame with the full *RARA* exon 3. RT-PCR and Sanger sequencing confirmed the existence of the *TTMV*::*RARA* fusion transcript (Figures 2B, C). This full-length *TTMV*::*RARA* fusion transcript was predicted to encode a fusion protein containing 488 amino acids (Figure 2D). The putative N terminal 85 polypeptide sequence showed 54% identity and 45% coverage to TTMV open reading frame 2 (ORF2) and displayed the conserved motif $WX_7HX_3CXCX_5H$, which were shared among all anelloviruses. The RARA part of the fusion protein was consistent with *PML*::*RARA* and all other RARA fusions.

Whole genome sequencing (WGS) and Sanger sequencing confirmed the insertion of 1164 bp exogenous fragment at chr17: 40332265 in *RARA* intron 2, which aligned to parts of the TTMV genome (Figures 2E, F). There were 750 nucleotides and 87 nucleotides derived from TTMV genomic sequences upstream and downstream of the TTMV UTR region, respectively. Also, there were 13 nucleotides not belonging to any known TTMV isolates downstream of TTMV ORF2, all of which were removed during splicing (Figure 2G). PCR and Sanger sequencing also confirmed the existence of the same genomic fusion sequence in the archived DNA samples at primary diagnosis. The integrated viral sequence possessed the two 15-nt conserved sequences (CGAATGGCTGAGTTT and AGGGGCAATTCGGGC) in the UTR of all TTVs (4). The last four bases (AGCC) of *RARA* intron 2 sequence 5' to the insertion site were the same as the four 3' terminal bases of the inserted sequence, suggesting there might be a microhomologous recombination mechanism that mediated the viral sequence integration (Figure 2G).

Discussion

We here report the third childhood APL-like case caused by the integration of TTMV fragment into the *RARA* locus. The first case was a 6-year-old girl diagnosed as hypergranular APL based on the characteristic morphologic features. The patient received CR after treatment combining standard AML induction therapy and ATRA, followed by 3 high-dose cytabine-based courses of consolidation therapy. She relapsed 8 months later and achieved CR after receiving combination of ATRA and ATO. Then she underwent HSCT and was alive at 4 years after HSCT. The second case was a 3-year-old AML child reported in the same literature. *TTMV*::*RARA* fusion in this patient was identified by a retrospective in silico analysis in a WTS database of 22 pediatric cytogenetically normal AML cases and the laboratory and clinical data were not detailly described (1, 2). Recently, Sala-Torra et al. (5) reported *TTMV*::*RARA* fusion in a 39-year-old man diagnosed as AML with APL characteristics but without *PML*::*RARA*. He was initially treated with the standard 7 +3 regimen and showed induction failure. He then received mitoxantrone, etoposide, and cytarabine with decitabine and venetoclax with a response. Table 1 provides patient characteristics of all reported cases, including the current case, and the TTMV insertion characteristics in the 4 cases reported to date was summarized in Figure 2H. These findings suggest *TTMV*::*RARA* is a recurrent cause of APL lacking *PML*::*RARA* fusion.

Considering the widespread prevalence of TTMV in the population, more *TTMV*::*RARA* positive APL-like cases might remain to be identified. Establishing a bioinformatic analysis strategy optimized for the highly variable TTMV genome sequence may facilitate the identification of *TTMV*::*RARA* by WTS data analysis. An effective PCR protocol to identify *TTMV*::*RARA* is also worth expecting, but this should be based on a profound analysis of the conservation of TTMV segments in the fusion transcript. Also, further investigation is needed to elucidate the oncogenic mechanisms of TTMV integration and the clinical features of *TTMV*::*RARA* positive patients. The first reported case was successfully treated with ATRA and ATO and subsequent HSCT. However, as ATRA was coupled with chemotherapy and HSCT, it is almost impossible to assess the contribution of ATRA. The outcomes of the other two reported cases were not available. In addition, our patient in the current case report died after giving up treatment and the efficiency of ATRA was unclear since ATRA was used only for 7 days. Therefore, further studies into the optimal therapeutic approaches for patients with *TTMV*::*RARA* are urgently needed.

Data availability statement

The datasets presented in this article are not readily available because of ethical/privacy restrictions. Requests to access the datasets should be directed to the corresponding author.

Ethics statement

The studies involving human participants were reviewed and approved by The Institutional Review Board and Ethical Committee of the Hebei Yanda Lu Daopei Hospital. Written informed consent to participate in this study was provided by the participants' legal guardian/next of kin.

Author contributions

HL designed the research; XC designed molecular studies and wrote the paper; PC, JF, QC, and XiuM performed bioinformatics analysis; FW, YZ, JC, and MingL supervised clinical and experimental findings; XZ, XiaM, LY, and MingyL performed molecular studies; YL was involved in the management of the patient and provided clinical data. PW

performed morphological analysis. All authors reviewed the manuscript and contributed to the final draft.

Acknowledgments

We thank the patient in this study.

Conflict of interest

Author QC is employed by Beijing Geneprofile Technologies Co,.Ltd.

The remaining authors declare that the research was conducted in the absence of any commercial or financial relationships that could be construed as a potential conflict of interest.

Publisher's note

References

1. Astolfi A, Masetti R, Indio V, Bertuccio SN, Messelodi D, Rampelli S, et al. Torque teno mini virus as a cause of childhood acute promyelocytic leukemia lacking PML/RARA fusion. *Blood* (2021) 138(18):1773–7. doi: 10.1182/blood.2021011677

2. Rau RE. A viral cause of APL. *Blood* (2021) 138(18):1653–5. doi: 10.1182/blood.2021013630

3. Chen X, Wang F, Zhang Y, Ma X, Cao P, Yuan L, et al. Fusion gene map of acute leukemia revealed by transcriptome sequencing of a consecutive cohort of 1000 cases in a single center. *Blood Cancer J* (2021) 11(6):112. doi: 10.1038/s41408-021-00504-5

4. Okamoto H, Nishizawa T, Tawara A, Peng Y, Takahashi M, Kishimoto J, et al. Species-specific TT viruses in humans and nonhuman primates and their phylogenetic relatedness. *Virology* (2000) 277(2):368–78. doi: 10.1006/viro.2000.0588

5. Sala-Torra O, Beppu LW, Abukar FA, Radich JP, Yeung C. TTMV-RARA fusion as a recurrent cause of AML with APL characteristics. *Blood Adv* (2022) 6 (12):3590–2. doi: 10.1182/bloodadvances.2022007256

frontiers | Frontiers in Oncology

TYPE Case Report
PUBLISHED 21 December 2022
DOI 10.3389/fonc.2022.1046878

OPEN ACCESS

EDITED BY
Osamu Imataki,
Kagawa University, Japan

REVIEWED BY
Liang Wang,
Beijing Tongren Hospital, Capital Medical University, China
Bin Li,
Fujian Provincial Cancer Hospital, China

*CORRESPONDENCE
Yifei Li
785290652@qq.com

†These authors have contributed equally to this work

SPECIALTY SECTION
This article was submitted to Hematologic Malignancies, a section of the journal Frontiers in Oncology

RECEIVED 17 September 2022
ACCEPTED 05 December 2022
PUBLISHED 21 December 2022

CITATION
Qiu B, Lin C, Wu L and Li Y (2022) A case report of synchronous triple primary malignancies: Diffuse large B-cell lymphoma, rectal adenocarcinoma and hepatocellular carcinoma. *Front. Oncol.* 12:1046878. doi: 10.3389/fonc.2022.1046878

A case report of synchronous triple primary malignancies: Diffuse large B-cell lymphoma, rectal adenocarcinoma and hepatocellular carcinoma

Beixuan Qiu[1†], Cheng Lin[2], Lupeng Wu[3] and Yifei Li[1*†]

[1]Department of XingLin General Surgery, First Affiliated Hospital of Xiamen University, Xiamen, China, [2]Department of Hematology, First Affiliated Hospital of Xiamen University, Xiamen, China, [3]Department of Hepatobiliary & Pancreatovascular Surgery, First Affiliated Hospital of Xiamen University, Xiamen, China

A 59-year-old man was admitted to our hospital in August 2020 because of fever with night sweats and weight loss. The patient was eventually diagnosed with synchronous triple primary malignancies: diffuse large B-cell lymphoma (DLBCL), rectal adenocarcinoma and hepatocellular carcinoma (HCC), which has not been reported previously. The patient initially received six cycles of R-Gemox chemotherapy targeting DLBCL, the response to the treatment was partial remission. We continued six cycles of R-CHOP therapy, and DLBCL achieved a complete remission to treatment. During R-CHOP chemotherapy, PD-1 inhibitor (Sintilimab) was used to control the disease progression of HCC, which was effective and tolerable. Subsequently, he successfully completed curative intent Dixon operation and right hemihepatectomy. The diagnosis and treatment for like these synchronous triple primary malignancies are a huge challenge, herein we provide our experience in this regard.

KEYWORDS

multiple primary malignancies, diffuse large B-cell lymphoma, rectal cancer, hepatocellular carcinoma, diagnosis, treatment

Abbreviations: MPM, multiple primary malignancies; DLBCL, diffuse large B-cell lymphoma; HCC, hepatocellular carcinoma; GA, gastric adenocarcinoma; SA, sigmoid adenocarcinoma; MDS, myelodysplastic syndrome; RA, rectal adenocarcinoma; PNT, pancreatic neuroendocrine tumour.

Introduction

Warren and Gates first defined multiple primary malignancies (MPM) as two or more histopathologically distinct malignancies in the same individual. MPM are classified as synchronous when tumors are diagnosed within 6 months of each other, otherwise as metachronous (1). Metachronous presentation is more frequent than synchronous, with a ratio of about 2-4 (2, 3). MPM mainly involve breast, lung, prostate, and melanoma. Synchronous lymphoma and solid digestive system tumor are a relatively rare scenario (3). Cases of patients with coexistence of 2 malignancies, such as colorectal cancer with diffuse large B-cell lymphoma (DLBCL), hepatocellular carcinoma (HCC) with DLBCL, rectal cancer with HCC, have been reported (4, 5). However, to our knowledge, there is no reported case of synchronous triple primary malignancies involving rectal cancer, HCC and DLBCL. Here we report for the first time an extremely unusual case with these 3 malignancies coexisting in the same patient. No diagnosis and treatment standards for this type of case have been established. This study aims to provide our experience on one case in this regard.

Case presentation

A 59-year-old man was admitted to the general surgery department of the First Affiliated Hospital of Xiamen University in August 2020, due to fever to 38.5°C, accompanied with night sweats and weight loss of 7kg over the past 1 month. The patient had no personal and family history of malignant neoplasm. An abdominal contrast-enhanced computed tomography (CT) scan taken at another hospital a few days before admission revealed the following: a space-occupying lesion of the rectal; one diameter 15-mm hypervascular lesion with arterial phase enhancement followed by portal venous phase washout in couinaud segment 8 (S8) of liver; multiple low-density shadows scattered in the liver parenchyma; and multiple hypovascular nodules in spleen.

After admission, routine laboratory test results showed that lactate dehydrogenase: 1331 u/L (normal range, 120-250 u/mL), albumen was 29 g/L (normal range, 40-55 g/L), and C-reactive protein was 76.8 ng/L (normal range, 0-6 ng/L). The virological examination indicated the patient was infected with hepatitis B virus (HBV). The remaining parameters including tumor markers were in the normal range. Positron emission tomography-computed tomography (PET-CT) exposed multiple abnormal fluorodeoxyglucose (FDG) uptake in rectum (standardised uptake value (SUV)max 6.7), liver (SUVmax 6.4), spleen (SUVmax 5.5), bone (SUVmax 12.0), left parotid gland (SUV max 21.2) and multiple enlarged lymph nodes in the bilateral cervical and periclavicular, right hilar, mediastinal, retroperitoneal, para-aortic, bilateral internal and external iliac regions (SUVmax 20.7) (Figures 1A, E). However, PET-CT showed that liver S8 had no metabolic uptake, which had an enhanced lesion in previous CT. From the above B-symptoms and radiological findings, the patient was considered to have a hematological disease involved multiple organs, and then was transferred to the Department of Hematology in our hospital for further examinations and treatments.

PET-CT guided percutaneous needle biopsies of retroperitoneal enlarged lymph nodes and Hepatic S6 nodule were performed. Histopathological examination of biopsies from both the retroperitoneal enlarged lymph nodes and liver lesions revealed DLBCL (Figure 2A), with CD20(+), CD30(30%+), Bcl-2(+), Bcl-6 (+), MUM-1(+), c-Myc(30–60%+), P53(40%+). The Ki67 proliferation index was 80%. *In situ* hybridization showed EBER was negative. Bone marrow biopsy of L4 vertebrae was positive for lymphoma (Figure 2B). In order to exclude other primary diseases, further colonoscopy and biopsy were performed. The colonoscopy showed a hard-intraluminal ulcerated mass in the rectum, approximately 8cm from the anal verge, and the biopsy of the lesion suggested moderately differentiated adenocarcinoma (Figure 3). Based on pathology and PET scan findings, the patient was diagnosed with synchronous primary stage IV DLBCL and rectal adenocarcinoma.

After considering the tumor burden of both diseases and the performance status of the patient, it was decided to initially treat the stage IV DLBCL given that the lymphoma was more likely to affect survival than the asymptomatic rectal cancer. He received six cycles of chemotherapy with R-Gemox (rituximab, gemcitabine, oxaliplatin), and was good tolerance. An interim PET-CT showed that the majority of enlarged lymph nodes and bone metastases with high uptake of FDG disappeared, and the rest significantly shrinked. There was no metabolic uptake in the liver, spleen and left parotid gland. PET-CT revealed a slight rise uptake value in the rectum (SUVmax 7.9). In all, the response to DLBCL treatment was assessed as partial remission (PR), and the rectal cancer was relatively stable. However, follow-up abdominal enhancement CT exposed that the hepatic S8 lesion showed in previous CT scan has a rapid progression measuring longest diameter 51mm with imaging characteristics of "quick wash-in and wash-out" (Figures 4A, B), which strongly suggested HCC. Liver needle biopsy confirmed that the S8 lesion was HCC (Figure 5). The diagnosis time interval between DLBCL and HCC was less than 5 months. Finally, the patient was diagnosed with synchronous triple primary malignancies: DLBCL, rectal adenocarcinoma and HCC.

A multidisciplinary team of hematologist, oncologists, general surgeon and hepatobiliary surgeon proposed a combination therapy plan, comprising R-CHOP (rituximab, cyclophosphamide, doxorubicin, vincristine and prednisolone) targeting DLBCL plus PD-1 inhibitor sintilimab (200mg every 3 weeks) targeting HCC. After six cycles of combined therapy, follow-up PET-CT found that DLBCL was complete remission (CR) to the therapy this time, and abdominal CT showed a

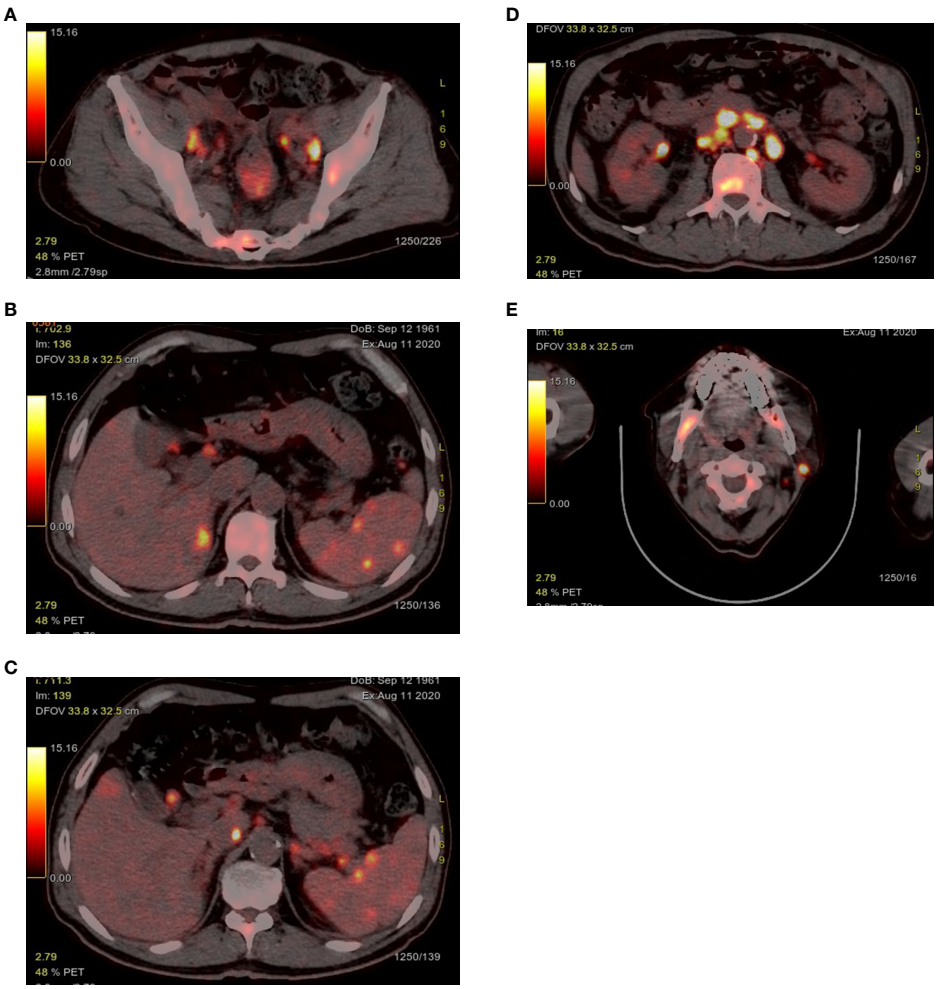

FIGURE 1
PET-CT exposed abnormal FDG uptake in the rectum **(A)**, liver and spleen **(B, C)**, bone **(A, D, E)**, left parotid gland **(E)** and multiple enlarged lymph nodes.

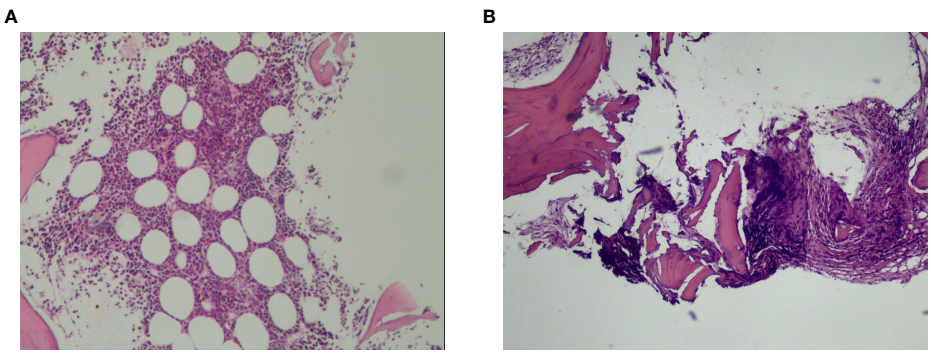

FIGURE 2
Histopathological examination of biopsies from both the retroperitoneal enlarged lymph nodes and liver lesions revealed diffuse large B- cell lymphoma **(A)**. Bone marrow biopsy of L4 vertebrae was positive for lymphoma **(B)**.

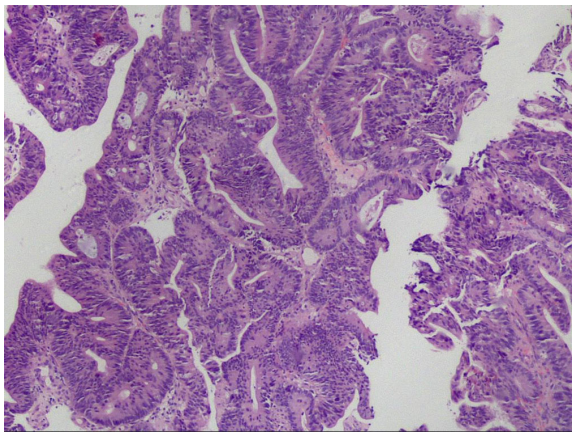

FIGURE 3
The colonoscopic biopsy suggested moderately differentiated adenocarcinoma.

reduction of more than 20% of the HCC mass, which was evaluated as PR.

With the cure of DLBCL and relief of HCC, laparoscopic Dixon operation was performed to treat rectal cancer in June 2021. The post-operative course was uneventful. The patient was discharged 6 days after the operation. Pathological examination confirmed a moderately differentiated adenocarcinoma, with tumor-free circumferential and distal margins, without lymph nodes metastases (pT3N0M0, stage IIA). Immunohistochemistry revealed Ki-67(80%+), MLH1(+), MSH2(+), PMS2(+), MSH6(+). Postoperative adjuvant chemotherapy was considered unnecessary.

One month later, enhanced magnetic resonance imaging (MRI) detected the second progression of S8 HCC with a size of 74 mm, and a diameter 20mm new tumor was found in the S6 of liver, which was considered an intrahepatic metastasis of HCC. Then, radical right hemihepatectomy was performed in August 2021, and postoperative histological analysis of specimens from both S8 and S6 of the liver was compatible with HCC. Some four months after resection, MRI detected local recurrence, and he underwent percutaneous microwave ablation (MVA). The process was mundane and the patient was dismissed one day after the operation. Two months after MVA, contrast-enhanced ultrasound showed that the recurrent tumor was completely inactivated. She remains alive and well without evidence of any tumor recurrence till now. (The medical process is shown in Table 1).

Discussion

Synchronous MPM refer to two or more tumors occurring within 6 months of each other. The following three criterias have been proposed by Warren and Gates to characterise MPM, (i) each tumour must be distinct from the other; (ii) each must have well-defined malignancy characteristics; (iii) the probability that one is a metastasis derived from the other must be excluded (1). Our case met all these criteria. Therefore, we can state that the patient in this report suffered from synchronous MPM consisting of three tumors. The previously similar reported instances of synchronous triple primary malignancies including lymphoma and solid digestive system tumors are listed in Table 2 (6–8).

Aetiological factors with MPM may include genetic predisposition and family cancer syndromes, immunosuppression, immunodeficiencies and infection, hormonal factors, environmental and lifestyle exposures, carcinogenic effects of prior cancer treatments (9). Andersen et al. suggested that chronic HBV infection was associated with all-type cancer, but not non-Hodgkin's lymphoma (10). Therefore, HBV infection may contribute to some extent to the development of synchronous rectal cancer and HCC in our case. Michele et al. reported that

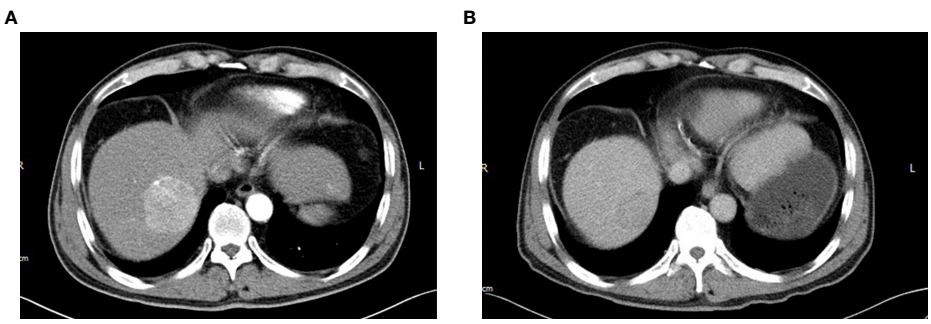

FIGURE 4
After six cycles of R-Gemox chemotherapy, follow-up abdominal enhancement CT exposed that the hepatic S8 lesion has a rapid progression measuring longest diameter 51mm with arterial phase enhancement **(A)** with portal venous phase washout **(B)**.

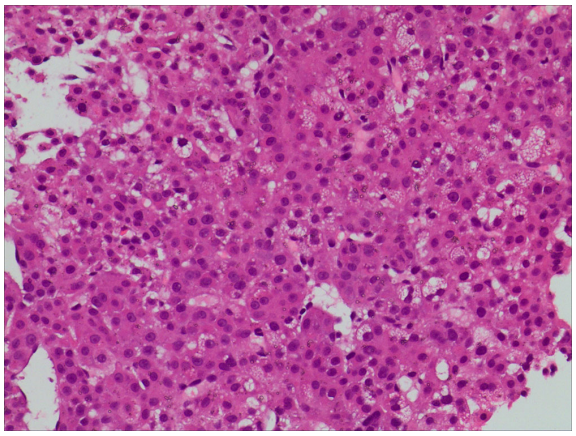

FIGURE 5
Pathological examination of liver needle biopsy confirmed that the S8 lesion was hepatocellular carcinoma.

among MPM with HCC, B cell neoplasms are associated with HCC more frequently than other cancers, and at a higher incidence than in the general population (11). Besides, a partial Bccip defect is found to be a risk factor for spontaneous hepatocellular carcinoma and B-lymphoma development (12). These findings attempted to explain the phenomenon of the coexistence of HCC and DLBCL. With regards to colorectal tumor and lymphoma, Barron and Localio suggested that patients with lymphoma have an increased incidence of synchronous colorectal carcinoma, and lymphoma may be the initial event which suppresses the patient's defenses against the development of colorectal carcinoma (13). In addition, Hirano et al. observed a case that both colon cancer and lymphoma showed microsatellite DNA instability, sharing alteration in a locus of chromosome 7 (D7S501) (14). Nonetheless, the rarity of such cases prevents any firm conclusion regarding the pathophysiology of the relationship between these 3 coexistent malignancies of rectal cancer, HCC, DLBCL.

Diagnosis of synchronous MPM may be difficult and one of these malignancies could be missed by the practitioner in some clinical situations. Such missed cases have been reported. A 61-year-old male was diagnosed with follicular lymphoma by an excision biopsy of cervical enlarged lymph node. PET-CT showed focal pathological uptake in the stomach, which was considered an infiltration of lymphoma into the stomach. After two cycles of R-CHOP chemotherapy, PET-CT indicated residual FDG uptake in the stomach. Subsequently, gastroscopic biopsy was performed. Astonishingly, histopathology revealed gastric tubular adenocarcinoma, and no infiltration of lymphoma to the stomach was found (05). Risio et al. reported a similar case of postoperative pathologically confirmed DLBCL of the colon with synchronous liver metastasis, which was considered preoperatively to be metastatic colorectal adenocarcinoma due to no liver biopsy (15). Therefore, clinicians should be aware of the possibility of MPM, whenever a patient with multiple lesions distributed in different organs. Biopsy is necessary for suspicious lesions, especially multiple lesions of different organs, because preoperative diagnosis can be challenging to the radiologist. During the initial diagnostic work-up in our case, abdominal CT revealed multiple low-density foci without enhancement in the liver, and these lesions showed hypermetabolism in the PET-CT. After a liver biopsy, it was confirmed that these low-density foci were DLBCL. Meanwhile CT images revealed one 1.5cm hypervascular space-occupying lesion with "quick wash-in and wash-out" in S8 of the liver, which has obvious heterogeneity compared with other liver DLBCL lesions. However, since PET-CT revealed no abnormal uptaken radioactivity in the S8 lesion, the liver biopsy was not performed on this lesion before the treatment of DLBCL, leading to that HCC was not immediately diagnosed. These clinical observations highlight the need for more focus on the investigation of the diagnosis for MPM. Multidisciplinary collaboration between the different specialists should be performed for careful investigations and accurate diagnosis.

Treatment protocols for MPM are not well established, even more so is the treatment for the synchronous presentation of rectal cancer, HCC, DLBCL. Colorectal cancer is the third most frequently diagnosed cancer and the second most lethal cancer worldwide (16). Treatments for early rectal cancer include curative intent colectomy, neoadjuvant therapy (17). Primary liver cancer ranks sixth in terms of incidence, but third in terms of mortality in the world (16). For HCC, the common treatments include surgical resection, ablation, transarterial chemoembolization, target immunotherapy (18). DLBCL is the most common subtype of non-Hodgkin's lymphoma. It is one of the aggressive lymphomas that can be cured, even in advanced cases. R-CHOP chemotherapy is the most appropriate treatment (19). When our patient was diagnosed with synchronous rectal cancer and DLBCL, curative intent colectomy was infeasible at that time, thus the systemic treatment regimens must consist of drugs targeting these two different kinds of tumors. Gemcitabine plus oxaliplatin (Gemox) has shown significant antitumor activity in solid digestive system tumors (20). On the other hand, rituximab plus gemcitabine and oxaliplatin (R-Gemox) is highly effective in non-Hodgkin's lymphoma (21). So, we chose R-Gemox as initial therapy, which was effective and tolerable. However, during R-Gemox chemotherapy, the HCC had a rapid progression with the longest diameter from 15 to 51mm. Surgical resection is the gold standard for treatment of primary liver cancer. However, the patient was not candidates for hepatic resection because of aggressive lymphoma. Microwave ablation (MVA) is an effective treatment for patients with early-stage HCC, especially tumor smaller than 20mm, which is comparable with hepatic resection. And

TABLE 1 The timeline of diagnosis and treatment process.

Date	Medical process	Result
July 8, 2020	Onset of disease	Fever, night sweats and weight loss
August 8, 2020	Abdominal enhancement CT	A space-occupying lesion of the rectal; one diameter 15-mm hypervascular lesion with arterial phase enhancement followed by portal venous phase washout in couinaud segment 8 (S8) of liver; multiple low-density shadows scattered in the liver parenchyma; and multiple hypovascular nodules in spleen.
August 10, 2020	Routine blood tests	Lactate dehydrogenase: 1331 u/L (normal range, 120-250 u/mL), Albumen: 29 g/L (normal range, 40-55 g/L) C-reactive protein: 76.8 ng/L (normal range, 0-6 ng/L) HBsAg: positive
August 12, 2020	PET-CT	Multiple abnormal FDG uptake in rectum, spleen, bone, left parotid gland and multiple enlarged lymph nodes in the bilateral cervical and periclavicular, right hilar, mediastinal, retroperitoneal, para-aortic, bilateral internal and external iliac regions. Image diagnosis: Lymphoma
August 13, 2020	Transfer to	Hematology department
August 14, 2020	Biopsies	Retroperitoneal enlarged lymph nodes, hepatic S6 nodule and bone marrow: histopathological examination confirmed DLBCL
August 16, 2020	Colonoscopy	A hard-intraluminal ulcerated mass in the rectum, approximately 8cm from the anal verge, and the biopsy suggested moderately differentiated adenocarcinoma
August 22, 2020	Diagnosis	1.DLBCL(Stage IV) 2.Rectal adenocarcinoma
August 25, 2020 to January 22, 2021	Chemotherapy	R-Gemox (rituximab, gemcitabine, oxaliplatin)
January 28, 2021	PET-CT and abdominal enhancement CT	DLBCL : Partial remission, Rectal adenocarcinoma:Disease stability Abdominal enhancement CT: Hepatic S8 lesion has a rapid progression measuring longest diameter 51mm with imaging characteristics of “quick wash-in and wash-out”
January 30, 2021	Liver needle biopsy	Histopathological examination confirmed that the S8 lesion was HCC
February 5, 2021	Updated diagnosis	1.DLBCL(Stage IV) 2.Rectal adenocarcinoma 3. HCC
February 7, 2021	Multidisciplinary conference	Multidisciplinary team proposed a combination therapy plan, comprising R-CHOP (rituximab, cyclophosphamide, doxorubicin, vincristine and prednisolone) targeting DLBCL plus PD-1 inhibitor sintilimab (200mg every 3 weeks) targeting HCC.
February 8, 2021 to June 22, 2021	Combination therapy	R-CHOP+ PD-1 inhibitor
June 26, 2021	PET-CT and abdominal enhancement CT	DLBCL : Complete remission, Rectal adenocarcinoma:Disease stability, HCC::Partial remission
June 29, 2021	Surgery	Laparoscopic Dixon operation
July 22, 2021	Abdominal enhancement MRI	Progression of S8 HCC with a size of 74 mm, and a diameter 20mm new tumor was found in the S6 of liver
August 18, 2021	Surgery	Radical right hemihepatectomy
December 22, 2021	Follow-up MRI	Local recurrence of surgical margin
December 28, 2021	Ablation	Percutaneous microwave ablation
August 10, 2022	Last follow-up	Alive with disease-free

TABLE 2 The previously reported examples of synchronous triple primary malignancies including lymphoma and solid digestive system tumors.

Author	Year	Age/Gender	MPM	Treatment	Prognosis
Chong (06)	2010	80/M	DLBCL	No treatment	Died 30 days after diagnosis
			HCC		
			GA		
Wang (07)	2019	78/M	DLBCL	Radical resection	Died of stroke about 1year after diagnosis
			SA	Radical resection	
			MDS	4 cycles of chemotherapies	
Dayer (08)	2021	67/F	DLBCL	R- CHOP chemotherapy	Alive after 1- year follow- up
			RA	Rectal endoscopic excision of the colorectal tumour	
			PNT	Laparoscopic pancreatectomy	
Present case	2022	59/M	DLBCL	R-GEMOX and R-CHOP chemotherapy	Alive 2 years after diagnosis
			RA	Radical resection	
			HCC	Sintilimab targeted therapy right hemihepatectomy microwave ablation	

percutaneous MVA has become a recognized treatment approach because of its efficacy, reproducibility, low complication rates, and availability (22). If we provided early detection and timely accurate diagnosis when the diameter of S8 lesion was 15mm, and MVA was performed in the initial treatment modality, the patient may have a better outcome, even avoiding right hemihepatectomy. Therefore, successful treatment of MPM required a good multidisciplinary collaboration to provide timely correct diagnosis and the best therapeutic strategy based on the diagnosis.

In summary, this is an unusual presentation of multiple primary malignancies of rectal adenocarcinoma, DLBCL and HCC. The study of this case may provide useful information regarding the diagnosis and treatment of patients with similar conditions. We concluded the following points (1): Clinicians must keep in mind that patients with multi-organ simultaneous lesions may suffer from MPM (2). We suggest a scrupulous biopsy of suspicious lesions in patient with multiple lesions of different organs to improve the diagnostic accuracy (3). The standard diagnosis and treatment protocols for MPM remain unclear. To handle these complex cases, require a multidisciplinary team with expertise and effective teamwork.

Data availability statement

The original contributions presented in the study are included in the article/supplementary material. Further inquiries can be directed to the corresponding author.

Ethics statement

Written informed consent was obtained from the individual(s) for the publication of any potentially identifiable images or data included in this article.

Author contributions

BQ and YL contributed equally to this article. BQ wrote the first draft of the manuscript. BQ and CL collected the data. YL and LW revised the manuscript. YL contributed to conception and design of the study and designed the manuscript. All authors contributed to the article and approved the submitted version.

Acknowledgments

We thank Doctor Yanming Zhou (Department of Gastrointestinal Surgery, The First Affiliated Hospital of Xiamen University, Xiamen, China) for his critical help of the study.

Conflict of interest

The authors declare that the research was conducted in the absence of any commercial or financial relationships that could be construed as a potential conflict of interest.

Publisher's note

References

1. Warren S, Gates O. Multiple primary malignant tumors: A survey of the literature and statistical study. *Am J Cancer.* (1932) 16:1358–414.

2. Alhamadh MS, Alanazi RB, Algarni ST, Alhuntushi AAR, Alshehri MQ, Chachar YS, et al. A descriptive study of the types and survival patterns of Saudi patients with multiple primary solid malignancies: A 30-year tertiary care center experience. *Curr Oncol* (2022) 29:4941–55. doi: 10.3390/curroncol29070393

3. Liu YL, Cadoo KA, Mukherjee S, Khurram A, Tkachuk K, Kemel Y, et al. Multiple primary cancers in patients undergoing tumor-normal sequencing define novel associations. *Cancer Epidemiol Biomarkers Prev* (2022) 31:362–71. doi: 10.1158/1055-9965.EPI-21-0820

4. Di Stasi M, Sbolli G, Fornari F, Cavanna L, Rossi S, Buscarini E, et al. Extrahepatic primary malignant neoplasms associated with hepatocellular carcinoma: high occurrence of b cell tumors. *Oncology.* (1994) 51:459–64. doi: 10.1159/000227383

5. Meng J, Pan H, Li X, Liu T, Liu Z, Li Q, et al. Diagnosis and treatment of synchronous lymphoma and digestive system carcinoma: Report of four cases and literature review. *Front Oncol* (2019) 9:1367. doi: 10.3389/fonc.2019.01367

6. Chong VH, Idros A, Telisinghe PU. Triple synchronous gastrointestinal malignancies: a rare occurrence. *Singapore Med J* (2010) 51:e176–7. doi: 10.1136/bcr-2017-219237

7. Wang W, Li P. Coexistence of colon adenocarcinoma, diffuse large b-cell lymphoma, and myelodysplastic syndrome: A case report. *Med (Baltimore).* (2019) 98:e16742. doi: 10.1097/MD.0000000000016742

8. Dayer N, Fasquelle F, Salati E, Dietrich G. Multiple primary malignancies: synchronous lymphoma, pancreatic neuroendocrine tumour and colorectal cancer. *BMJ Case Rep* (2021) 14(6):e241938. doi: 10.1136/bcr-2021-241938

9. Copur MS, Manapuram S. Multiple primary tumors over a lifetime. *Oncol (Williston Park)* (2019) 33(7):629384.

10. Andersen ES, Omland LH, Jepsen P, Krarup H, Christensen PB, Obel N, et al. Risk of all-type cancer, hepatocellular carcinoma, non-Hodgkin lymphoma and pancreatic cancer in patients infected with hepatitis b virus. *J Viral Hepat.* (2015) 22:828–34. doi: 10.1111/jvh.12391

11. Xu W, Liao W, Ge P, Ren J, Xu H, Yang H, et al. Multiple primary malignancies in patients with hepatocellular carcinoma: A largest series with 26-year follow-up. *Med (Baltimore).* (2016) 95:e3491. doi: 10.1097/MD.0000000000003491

12. Lu H, Ye C, Feng X, Liu J, Bhaumik M, Xia B, et al. Spontaneous development of hepatocellular carcinoma and b-cell lymphoma in mosaic and heterozygous Brca2 and Cdkn1a interacting protein knockout mice. *Am J Pathol* (2020) 190:1175–87. doi: 10.1016/j.ajpath.2020.01.020

13. Barron BA, Localio SA. A statistical note on the association of colorectal cancer and lymphoma. *Am J Epidemiol.* (1976) 104:517–22. doi: 10.1093/oxfordjournals.aje.a112324

14. Hirano K, Yamashita K, Yamashita N, Nakatsumi Y, Esumi H, Kawashima A, et al. Non-hodgkin's lymphoma in a patient with probable hereditary nonpolyposis colon cancer: report of a case and review of the literature. *Dis Colon Rectum.* (2002) 45:273–9. doi: 10.1007/s10350-004-6161-9

15. Risio D, Percario R, Legnini M, Caldaralo F, Angelucci D, Marinelli C, et al. Diffuse large b-cell lymphoma of the colon with synchronous liver metastasis: A rare case report mimicking metastatic colorectal adenocarcinoma. *BMC Surg* (2014) 14:75. doi: 10.1186/1471-2482-14-75

16. Sung H, Ferlay J, Siegel RL, Laversanne M, Soerjomataram I, Jemal A, et al. Global cancer statistics 2020: GLOBOCAN estimates of incidence and mortality worldwide for 36 cancers in 185 countries. *CA Cancer J Clin* (2021) 71:209–49. doi: 10.3322/caac.21660

17. Keller DS, Berho M, Perez RO, Wexner SD, Chand M. The multidisciplinary management of rectal cancer. *Nat Rev Gastroenterol Hepatol* (2020) 17:414–29. doi: 10.1038/s41575-020-0275-y

18. Benson AB, D'Angelica MI, Abbott DE, Anaya DA, Anders R, Are C, et al. Hepatobiliary cancers, version 2.2021, NCCN clinical practice guidelines in oncology. *J Natl Compr Canc Netw* (2021) 19:541–65. doi: 10.6004/jnccn.2021.0022

19. Lehrich BM, Abiri A, Goshtasbi K, Birkenbeuel J, Yasaka TM, Papagiannopoulos P, et al. Treatment modalities and survival outcomes for sinonasal diffuse Large b-cell lymphoma. *Laryngoscope.* (2021) 131:E2727–35. doi: 10.1002/lary.29584

20. Ziras N, Potamianou A, Varthalitis I, Syrigos K, Tsousis S, Boukovinas I, et al. Multicenter phase II study of gemcitabine and oxaliplatin (GEMOX) as second-line chemotherapy in colorectal cancer patients pretreated with 5-fluorouracil plus irinotecan. *Oncology.* (2006) 70:106–14. doi: 10.1159/000092956

21. Meriggi F, Zaniboni A. Gemox: a widely useful therapy against solid tumors-review and personal experience. *J Chemother* (2010) 22:298–303. doi: 10.1179/joc.2010.22.5.298

22. Izzo F, Granata V, Grassi R, Fusco R, Palaia R, Delrio P, et al. Radiofrequency ablation and microwave ablation in liver tumors: An update. *Oncologist.* (2019) 24:e990–e1005. doi: 10.1634/theoncologist.2018-0337

frontiers | Frontiers in Oncology

TYPE Case Report
PUBLISHED 04 January 2023
DOI 10.3389/fonc.2022.1083500

OPEN ACCESS

EDITED BY
Kikkeri N. Naresh,
Fred Hutchinson Cancer Research Center, United States

REVIEWED BY
Shahin Sayed,
Aga Khan University Hospital, Kenya
Sam Sadigh,
Brigham and Women's Hospital, Harvard Medical School, United States

*CORRESPONDENCE
Mitsuhiro Kawano
sk33166@gmail.com

SPECIALTY SECTION
This article was submitted to Hematologic Malignancies, a section of the journal Frontiers in Oncology

RECEIVED 29 October 2022
ACCEPTED 14 December 2022
PUBLISHED 04 January 2023

CITATION
Yoshida M, Zoshima T, Hara S, Takahashi Y, Nishioka R, Ito K, Mizuhima I, Inoue D, Nakada S and Kawano M (2023) Case report: Rosai-Dorfman disease with rare extranodal lesions in the pelvis, heart, liver and skin. *Front. Oncol.* 12:1083500. doi: 10.3389/fonc.2022.1083500

Case report: Rosai-Dorfman disease with rare extranodal lesions in the pelvis, heart, liver and skin

Misaki Yoshida[1], Takeshi Zoshima[1], Satoshi Hara[1], Yoshinori Takahashi[1], Ryo Nishioka[1], Kiyoaki Ito[1], Ichiro Mizuhima[1], Dai Inoue[2], Satoko Nakada[3] and Mitsuhiro Kawano[1]*

[1]Department of Rheumatology, Kanazawa University Graduate School of Medical Sciences, Kanazawa, Japan, [2]Department of Radiology, Kanazawa University Graduate School of Medical Sciences, Kanazawa, Japan, [3]Department of Diagnostic Pathology, Kanazawa University Hospital, Kanazawa, Japan

Rosai-Dorfman disease (RDD), a rare form of non-Langerhans cell histiocytosis, can involve systemic extranodal lesions. Skin lesions are the most common, whereas intrapelvic, cardiac, and hepatic lesions are infrequent. The present study describes a 74-year-old woman with multiple extranodal lesions in the pelvis, heart, liver, and skin that were successfully treated with glucocorticoid therapy. She had experienced fever and persistent inflammation without cervical lymphadenopathy for several months and ^{18}F-fluorodeoxyglucose (FDG) positron emission tomography (PET) showed abnormal FDG uptake in the left cheek; cervical, axillary, inguinal lymph nodes; periatrium; and pelvis. She was diagnosed with RDD based on skin and pelvic biopsies. Although this was an atypical case without bilateral cervical lymphadenopathy, the FDG-PET detection of inflammatory lesions led to selection of suitable biopsy sites, and pathological examination led to a correct diagnosis. Findings in this patient indicate that RDD can present with an atypical distribution of infrequent extranodal lesions, with attention required to prevent a delayed diagnosis.

KEYWORDS

Rosai-Dorfman disease, histiocytosis, extranodal lesion, cervical lymphadenopathy, fever of unknown origin

Introduction

Rosai-Dorfman disease (RDD) is a non-Langerhans cell histiocytosis characterized by bilateral cervical lymphadenopathy, fever, and an inflammatory response. It is rare, with a prevalence of 1 in 200,000. The mean age at onset is between the 20s and 30s, although some patients have been reported to develop RDD in their 70s. RDD is more

common among people of African descent while the skin lesions are more common among Asian people (1). RDD has also been associated with rheumatic diseases and malignancies (1). Furthermore, fever or inflammation of unknown origin could be the first manifestation of RDD (2, 3). Pathological confirmation is required for the diagnosis of RDD, with this disease being characterized by the proliferation of histiocytes that are positive for S-100 protein and CD68 and negative for CD1a, as well as emperipolesis (4). Generally, RDD patients with only skin or lymph node lesions do not require treatment, as about 50% experience spontaneous remission. Surgical resection is the treatment of choice for patients with a single lesion. However, patients with severe conditions, disseminated extranodal lesions, or refractory disease are treated with immunosuppressive drugs, such as glucocorticoids.

Extranodal lesions have been reported in 43% of patients with RDD. These lesions can develop in almost all organs and adversely affect patient prognosis. About 67% of patients have only extranodal lesions (5, 6), whereas approximately 20% have lesions in multiple organs. The number of damaged organs correlates with patient prognosis (4). The most common extranodal sites include the skin (10–52%), bones (5–25%), head and neck (11–22%), kidneys (9%), and central nervous system (5–8%) (4, 6). Lesions in the heart and pelvis, however, are uncommon, and, to our knowledge, there have been no reports of their simultaneous development.

The present study describes an elderly woman who was diagnosed with RDD and had multiple extranodal lesions, including in the heart and pelvis, without bilateral cervical lymphadenopathy, a typical lesion of RDD. She had experienced inflammation of unknown origin for several months and was finally diagnosed with RDD with heart, pelvis, skin, and liver lesions. She was successfully treated with glucocorticoid. Although this was an atypical case without bilateral cervical lymphadenopathy, the detection of inflammatory lesions using ^{18}F-fluorodeoxyglucose (FDG)-positron emission tomography (PET) led to the final diagnosis.

Case report

A 74-year-old woman was admitted to our hospital for closer examination of chronic inflammation. She had been treated for hypertension and type 2 diabetes for 16 years. Four years prior to hospitalization, she experienced a slight elevation of serum C-reactive protein (CRP) concentration, to around 0.5 mg/dL, but she was asymptomatic. Two years prior, she developed lower leg edema, which gradually worsened. One year previously, she developed puffy fingers and abnormal nailfold capillaries, and was positive for serum anti-centromere antibody but not Raynaud's phenomenon. She was suspected of having systemic sclerosis but did not fulfill the classification criteria (7). Ten months prior, erythema developed on her face and limbs. A skin biopsy of the left lower leg revealed infiltration of inflammatory cells, mainly histiocytes, in the superficial intradermal area and infiltration of small lymphocytes and plasma cells in the perivascular area. Although the cause was not identified, the skin lesions improved following application of topical glucocorticoids. Nine months previously, she had developed dyspnea on exertion. Although a chest X-ray revealed cardiac dilatation, there was no evidence of pulmonary congestion. Treadmill exercise electrocardiogram showed transient atrial fibrillation. Chest computed tomography (CT) revealed pleural effusion, whereas echocardiography showed no asynergy. She was suspected of having mild congestive heart failure caused by paroxysmal atrial fibrillation. Her dyspnea improved after treatment with bisoprolol, apixaban, furosemide, and spironolactone. Eight months prior, her body temperature was 37°C and her serum CRP level was elevated to 4.78 mg/dL. Systemic CT showed a contrast-enhanced intra-pelvic mass with irregular margins, along with peripheral enhancement (Figure 1A), but no other lesions in the heart, liver, or lymph nodes. Magnetic resonance imaging (MRI) showed an intra-pelvic mass with low-intensity signals on T2-weighted images and heterogeneous high-intensity signals on diffusion-weighted images (Figure 1B). Intra-pelvic thickening of the peritoneum was also observed. Cervical cytology revealed the absence of malignant cells. Because a pelvic abscess was suspected, antibiotics were prescribed, but there were no improvements in serum CRP levels or the size of the pelvic lesion. Her serum CRP level persisted at around 2 mg/dL, accompanied by a weight loss of 5 kg in 6 months. One month prior to admission, a white keratotic nodule appeared on her left cheek. FDG-PET-CT revealed abnormal FDG uptake in the left cheek; cervical, axillary, and inguinal lymph nodes; periatrium, colon, and pelvis (Figures 1C–F). These PET-CT results suggested that malignant lymphoma was highly likely.

On admission, cervical lymphadenopathy was not observed. A murmur (Levine II/VI) was heard at the left second sternal border. Abdominal examination yielded normal results. Bilateral lower leg edema was detected. Facial erythema had disappeared, and the erythema on both legs had changed to brownish or yellowish pigmentation. Laboratory examination revealed elevated levels of serum CRP (2.72 mg/dL) and soluble interleukin-2 receptor (965 U/mL). The patient was positive for anti-centromere antibodies, but there was no evidence of other rheumatic diseases including IgG4-related disease or infections (Table 1). Echocardiography showed hyperechoic thickening at the interatrial septum and irregular thickening with heterogeneous echoic brightness at the left atrial wall behind the aorta. Electrocardiography-gated contrast-enhanced CT revealed homogeneous wall thickening around the left atrium (Figure 1G). Abdominal ultrasonography showed a homogeneous hypoechoic nodule (Figure 1H). Contrast-enhanced CT and gadolinium ethoxybenzyl diethylenetriamine pentaacetic acid (Gd-EOB-DTPA)-enhanced MRI demonstrated

10.3389/fonc.2022.1083500

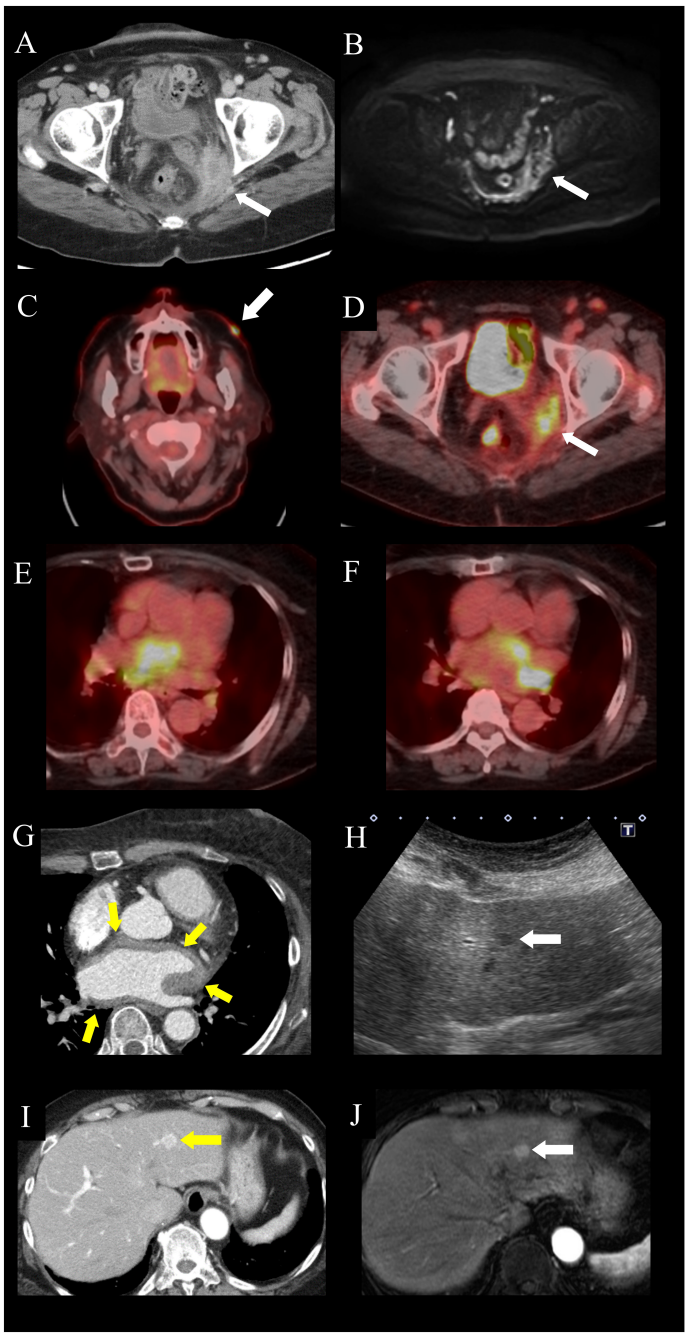

FIGURE 1
Images of extranodal lesions in the patient with Rosai-Dorfman disease. **(A, B)** Pelvic lesion. **(A)** Computed tomography (CT) scan showing an intra-pelvic mass enhanced predominantly in the peripheral zone. **(B)** Magnetic resonance imaging (MRI), of the intra-pelvic mass, showing heterogeneous high-intensity signals on diffusion-weighted imaging, accompanied by peritoneal thickening. **(C–F)** 18F-fluorodeoxyglucose-positron emission tomography (FDG-PET)-CT of the **(C)** facial skin lesion (arrow), with a maximum standardized uptake value (SUVmax) of 10.7, **(D)** pelvic lesion (arrow), with an SUVmax of 6.2, and **(E, F)** peri-atrial lesion spreading from the interatrial septum to the left atrium, with an SUVmax of 25. **(G)** Electrocardiography-gated contrast-enhanced CT, showing homogeneous wall thickening around the left atrium (arrows). **(H–J)** Hepatic lesion. **(H)** Ultrasonography, showing a homogeneous hypoechoic nodule (arrow). **(I)** Contrast-enhanced CT imaging, showing a hypervascular nodule in the left lateral hepatic segment. (arrow). **(J)** Gadolinium ethoxybenzyl diethylenetriamine pentaacetic acid-enhanced MRI, showing a homogeneously enhanced nodule in the arterial phase (arrow).

10.3389/fonc.2022.1083500

TABLE 1 Laboratory Data on Admission.

	Value	Normal range
Urinalysis		
Protein	(–)	(–)
Occult blood	(–)	(–)
Blood count		
White blood cells (/μL)	8,260	3,300-8,800
Neutrophil (%)	80.7	
Eosinophil (%)	1.6	
Lymphocyte (%)	13.1	
Hemoglobin (g/dL)	9.5	13.5-17.0
Platelet (/μL)	32.3×10^4	$13.0\text{-}35.0\times10^4$
Erythrocyte sedimentation rate (mm/h)	54	3-15
Serum chemistry		
BUN (mg/dL)	17	8.0-20.0
Cr (mg/dL)	0.79	0.60-1.00
Na (mEq/L)	141	135-149
K (mEq/L)	3.9	3.5-4.9
Cl (mEq/L)	105	96-108
AST (IU/L)	18	13-33
ALT (IU/L)	9	8-42
LDH (IU/L)	167	119-229
Total protein (g/dL)	7	6.7-8.3
Albumin (g/dL)	3.5	4.0-5.0
HbA1c(%)	7.5	5.6-5.9
Immunological findings		
CRP (mg/dL)	2.72	0-0.3
IgG (mg/dL)	2,098	870-1,700
IgG4 (mg/dL)	90.6	4.8-105
IgA (mg/dL)	217	110-410
IgM (mg/dL)	85	46-260
C3 (mg/dL)	111	65-135
C4 (mg/dL)	31	13-35
CH50 (U/mL)	69	25.0-48.0
Soluble interleukin-2 receptor (U/mL)	965	157-474
Anti-nuclear antibody	×80 (AC, H)	<40
Anti-RNP antibody (U/mL)	(–)	(–)
Anti-SS-A antibody (U/mL)	<10.0	<10.0

(Continued)

TABLE 1 Continued

	Value	Normal range
Anti-Scl-70 antibody (U/mL)	<10.0	<10.0
Anti-centromere antibody (U/mL)	24.8	<10.0
Anti-RNA polymerase III antibody	(–)	(–)
Anti-ARS antibody	(–)	(–)
MPO-ANCA (IU/mL)	<1.0	<1.0
PR3-ANCA (IU/mL)	<1.0	<1.0
NT-proBNP (pg/mL)	3,597	<125
HBsAg (IU/mL)	<0.001	<0.05
HBsAb (IU/mL)	<0.1	<10
HBcAb	(–)	(–)
HCVAb	(–)	(–)
Interferon-gamma release assay	(–)	(–)
β-D-glucan (pg/mL)	<6.0	<11.0
Cytomegalovirus antigen	(–)	(–)

a hyper vascular nodule approximately 10 mm in diameter in the left lateral hepatic segment (Figures 1I, J). These lesions had not been detected in images acquired 6 months before hospitalization. Lower gastrointestinal endoscopy did not reveal any lesions. Skin biopsy of the left cheek showed diffuse aggregations of large round histiocytes in the upper dermis just beneath the epidermis. Some histiocytes engulfed lymphocytes and neutrophils, a finding compatible with emperipolesis. Immunohistochemistry revealed that these histiocytes were positive for CD68 and S-100 protein (Figure 2). There was no evidence of histiocytosis other than RDD. In addition, malignant cells were not observed and there were no indications of clonal proliferation of kappa and lambda chains. The ratio of IgG4-positive cells to CD138-positive cells was approximately 10%. CT-guided biopsy of the pelvic mass (Supplemental Figure 1) and re-examination of the skin biopsy of the leg obtained before hospitalization showed similar findings. Next-generation sequencing analysis for mutations in the MAPK pathway was not performed. However, based on these histological findings, the patient was diagnosed with RDD involving the pelvis, skin, heart, liver, and lymph nodes.

The patient was started on treatment with 50 mg/day prednisolone (0.75 mg/kg/day). Nine days later, her serum CRP levels normalized. Fourteen days later, however, she developed an arterial flutter, which was successfully treated with electrical cardioversion, bisoprolol, and verapamil. A follow-up PET-CT scan six months later showed significantly reduced FDG uptake by the above-mentioned lesions (Figure 3). Furthermore, abdominal ultrasonography revealed that the liver nodule had disappeared.

Discussion

This report describes an elderly patient who presented with RDD involving the pelvis, heart, liver, skin, and lymph nodes. This patient was difficult to diagnose because she only had extranodal lesions, such as pelvic and cardiac lesions, which are infrequently associated with RDD, and showed no evidence of bilateral cervical lymphadenopathy.

Pelvic lesions are rare in patients with RDD and have been described only in case reports (8). CT findings are non-specific, but invasive masses have been reported to surround the kidneys, ureters, and blood vessels, as has soft tissue with lymphadenopathy (9). The incidence rate of intraperitoneal lesions, including those in the pelvis, is 4% (8). The onset of intraperitoneal lesions occurs during the seventh and eighth decades of life (8). When only intraperitoneal lesions are detected, it is important to exclude neoplastic lesions other than RDD (9). In this case, pelvic pathology was consistent with RDD, with these lesions considered pelvic manifestations of RDD.

Cardiac lesions are also rare extranodal lesions of RDD, being observed in only about 0.1% of patients with RDD (10). Cardiac lesions have been classified into three types: intracardiac masses, pericardial/epicardial involvement, and pulmonary arterial involvement (11). An analysis of 15 patients showed that the mean age of these patients was 49.5 years (range, 22–79 years) and that intracardiac masses were the most common cardiac lesions, being observed in nine (60%) of these 15 patients (11). In addition, 8 patients (53%) had no lesions other than cardiac lesions. The most common symptoms were chest pain

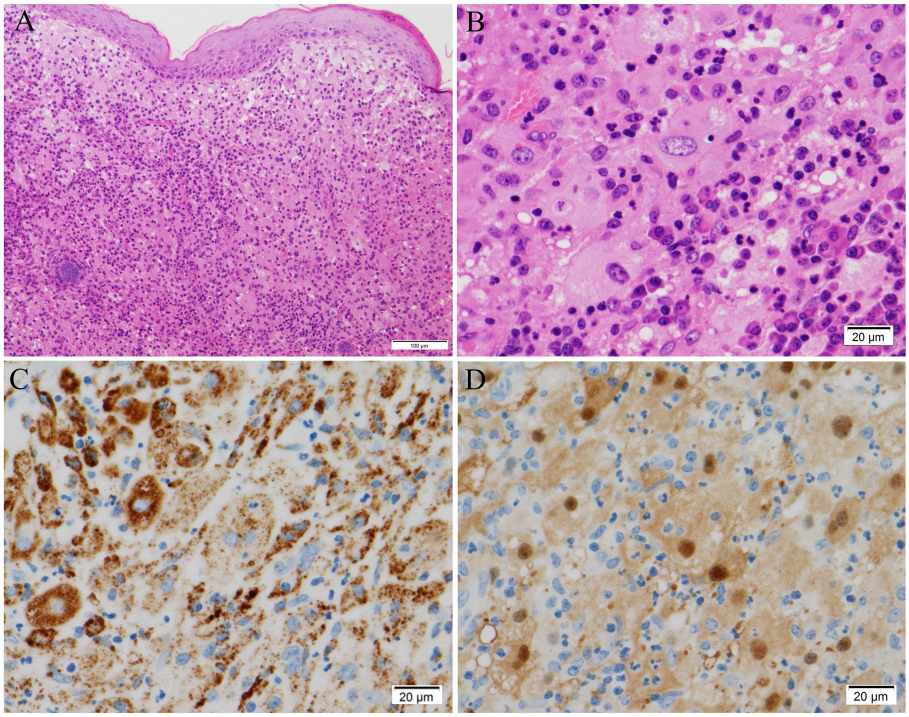

FIGURE 2
Histological findings of the facial skin biopsy. **(A, B)** Hematoxylin and eosin staining, showing **(A)** large round cells aggregated diffusely in the upper dermis immediately beneath the epidermis, and **(B)** emperipolesis, in which lymphocytes and neutrophils are engulfed. **(C, D)** Immunohistochemical analysis, showing that the large round cells were positive for **(C)** CD68 and **(D)** S-100 protein. Original magnifications: × 100 **(A)**, × 400 **(B–D)**. Scale bars: 100 μm **(A)** and 20 μm **(B–D)**.

and shortness of breath, followed by palpitations and edema. Nine patients underwent surgical resection, including six with intracardiac masses and three with pulmonary artery masses. Glucocorticoids were administered to three patients, one each with an intracardiac mass, pericardial/epicardial lesion, and pulmonary arterial mass. Although the observation period was not reported, all patients treated surgically were alive at the time of last follow-up, suggesting that surgical removal of these lesions is associated with a favorable prognosis. However, four (27%) of these patients died. Although the present patient did not undergo cardiac biopsy, her cardiac lesion was consistent with RDD, probably because the cardiac lesion improved along with her other lesions, following treatment with glucocorticoid.

Hepatic lesions are infrequent in patients with RDD patients, being reported in only 1–5% (4, 6). These patients show single or multiple hepatic nodules, or hepatomegaly (8, 9, 12). One report described 11 patients with gastrointestinal lesions, including five with hepatic lesions (12). Four of the latter had other extranodal lesions, including two with cardiac lesions, similar to the present patient.

Recently, RDD has been diagnosed at ages older than previously reported. A report describing 423 RDD patients published in 1990 showed that most cases of RDD developed in childhood, with an average age of onset of 20–30 years; age at diagnosis was not reported (4). In contrast, a report of 64 patients published in 2020 showed that the median age at diagnosis was 50 years (interquartile range [IQR] 2–79 years), with the median period from onset to diagnosis being 7 months (IQR 0–128 months) (6). Moreover, a report of 10 patients at a single facility published in 2019 showed that the mean age was 56 years (IQR 20–81 years) (13). The present patient was diagnosed with RDD at age 74 years.

The diagnosis of RDD may be delayed because of its low prevalence and late recognition. RDD is a rare disease that is often undiagnosed at early stages (14). There are many differential diagnoses, including infections with, for example, acid-fast bacilli and fungi; and malignant diseases, including malignant lymphoma; Erdheim-Chester disease; and IgG4-related disease. Each extranodal lesion has a differential diagnosis (1). Furthermore, emperipolesis may occur in other conditions such as malignant lymphoma, leukemia, myelodysplasia, and myeloma. For diagnosis with RDD, immunohistochemical analyses including positive for S-100 and CD68 and negative for CD1a are important (1, 4). One of the typical findings of RDD is cervical lymphadenopathy; however, many recent reports have described patients with

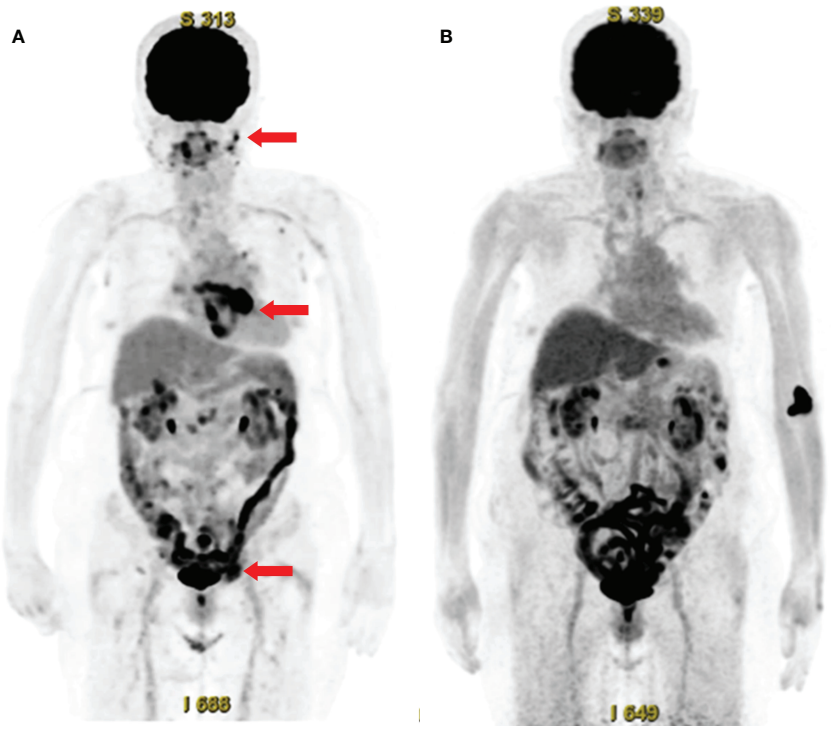

FIGURE 3
Whole-body ^{18}F-fluorodeoxyglucose (FDG)-positron emission tomography with computed tomography (PET-CT) before and after treatment. **(A)** FDG-PET-CT before treatment, showing abnormal FDG uptake in the facial skin, peri-atrial, pelvic (arrows), cervical, axillary, and inguinal lymph nodes, and colon. **(B)** Follow-up FDG-PET-CT after treatment, showing the disappearance of abnormal FDG uptake.

RDD without lymphadenopathy (6). Moreover, some patients with RDD, such as the present patient, present with fever or inflammation of unknown origin (2, 3).

FDG-PET-CT has been shown useful for the identification of sites that can be biopsied and for the evaluation of responses to treatment (1). The present patient underwent biopsies of areas of the skin and pelvic lesions with abnormal FDG uptake. However, the cardiac and hepatic lesions were not biopsied because of the risk of hemorrhage when direct oral anticoagulants were administered. Because these cardiac and hepatic lesions appeared at the same time as the other RDD lesions and their responses to glucocorticoid treatment were similar, they were diagnosed as RDD-associated lesions. In addition, diagnosis may be delayed in patients with atypical distribution of infrequent lesions, such as the present patient.

In conclusion, this report describes a rare case of RDD in an elderly patient with extranodal lesions in the pelvis, heart, liver, and skin. Although this presentation was atypical without bilateral cervical lymphadenopathy, detection of inflammatory lesions using FDG-PET led to the selection of suitable biopsy sites, with subsequent pathological examination resulting in a correct diagnosis. These findings indicate that RDD may present with an atypical distribution of infrequent extranodal lesions, with attention being required to prevent a delayed diagnosis.

Data availability statement

The raw data supporting the conclusions of this article will be made available by the authors, without undue reservation.

Ethics statement

The studies involving human participants were reviewed and approved by Kanzawa University Hospital. The patients/participants provided their written informed consent to participate in this study.

Author contributions

MY, TZ, and MK wrote the draft and revised it. SH, YT, RN, KI, IM, DI, and SN provided some important advice for the

draft. All authors contributed to the article and approved the submitted version.

Conflict of interest

The authors declare that the research was conducted in the absence of any commercial or financial relationships that could be construed as a potential conflict of interest.

Publisher's note

All claims expressed in this article are solely those of the authors and do not necessarily represent those of their affiliated organizations, or those of the publisher, the editors and the reviewers. Any product that may be evaluated in this article, or claim that may be made by its manufacturer, is not guaranteed or endorsed by the publisher.

Supplementary material

The Supplementary Material for this article can be found online at: https://www.frontiersin.org/articles/10.3389/fonc.2022.1083500/full#supplementary-material

SUPPLEMENTARY FIGURE 1
Histological findings of the pelvic lesion. **(A, B)** Hematoxylin and eosin staining revealed lymphoplasmacytic infiltration in fat tissue and scattered histiocytes with emperipolesis. **(C)** Immunohistochemical analysis for S-100 protein showing histiocytes with emperipolesis. Original magnifications: × 100 (A), × 400 **(B, C)**.

References

1. Abla O, Jacobsen E, Picarsic J, Krenova Z, Jaffe R, Emile JF, et al. Consensus recommendations for the diagnosis and clinical management of rosai-Dorfman-Destombes disease. *Blood* (2018) 131:2877–90. doi: 10.1182/blood-2018-03-839753

2. Cunha BA, Lortholary O, Cunha CB. Fever of unknown origin: a clinical approach. *Am J Med* (2015) 128:1138.e1–1138.e15. doi: 10.1016/j.amjmed.2015.06.001

3. Rew SY, Jang HC, Park KH, Ahn JS, Kim GE, Choi YD, et al. A case of rosai-dorfman disease with highly elevated serum ferritin. *Ann Lab Med* (2012) 32:158–61. doi: 10.3343/alm.2012.32.2.158

4. Foucar E, Rosai J, Dorfman R. Sinus histiocytosis with massive lymphadenopathy (Rosai-dorfman disease): review of the entity. *Semin Diagn Pathol* (1990) 7:19–73.

5. Dalia S, Sagatys E, Sokol L, Kubal T. Rosai-dorfman disease: tumor biology, clinical features, pathology, and treatment. *Cancer Control* (2014) 21:322–7. doi: 10.1177/107327481402100408

6. Goyal G, Ravindran A, Young JR, Shah MV, Bennani NN, Patnaik MM, et al. Clinicopathological features, treatment approaches, and outcomes in rosai-dorfman disease. *Haematologica* (2020) 105:348–57. doi: 10.3324/haematol.2019.219626

7. van den Hoogen F, Khanna D, Fransen J, Johnson SR, Baron M, Tyndall A, et al. 2013 Classification criteria for systemic sclerosis: an American college of rheumatology/European league against rheumatism collaborative initiative. *Ann Rheum Dis* (2013) 72:1747–55. doi: 10.1136/annrheumdis-2013-204424

8. Mar WA, Yu JH, Knuttinen MG, Horowitz JM, David O, Wilbur A, et al. Rosai-dorfman disease: Manifestations outside of the head and neck. *AJR Am J Roentgenol* (2017) 208:721–32. doi: 10.2214/AJR.15.15504

9. Karajgikar J, Grimaldi G, Friedman B, Hines J. Abdominal and pelvic manifestations of rosai-dorfman disease: a review of four cases. *Clin Imaging* (2016) 40:1291–5. doi: 10.1016/j.clinimag.2016.09.006

10. Gaitonde S. Multifocal, extranodal sinus histiocytosis with massive lymphadenopathy: An overview. *Arch Pathol Lab Med* (2007) 131:1117–21. doi: 10.5858/2007-131-1117-MESHWM

11. O'Gallagher K, Dancy L, Sinha A, Sado D. Rosai-dorfman disease and the heart. *Intractable Rare Dis Res* (2016) 5:1–5. doi: 10.5582/irdr.2015.01047

12. Lauwers GY, Perez-Atayde A, Dorfman RF, Rosai J. The digestive system manifestations of rosai-dorfman disease (sinus histiocytosis with massive lymphadenopathy): Review of 11 cases. *Hum Pathol* (2000) 31:380–5. doi: 10.1016/s0046-8177(00)80254-3

13. Sathyanarayanan V, Issa A, Pinto R, Fayad LE, Loghavi S, Hagemeister F, et al. Rosai-dorfman disease: The MD Anderson cancer center experience. *Clin Lymphoma Myeloma Leuk* (2019) 19:709–14. doi: 10.1016/j.clml.2019.06.013

14. Azari-Yaam A, Abdolsalehi MR, Vasei M, Safavi M, Mehdizadeh M. Rosai-dorfman disease: A rare clinicopathological presentation and review of the literature. *Head Neck Pathol* (2021) 15:352–60. doi: 10.1007/s12105-020-01183-7

frontiers | Frontiers in Oncology

TYPE Case Report
PUBLISHED 12 January 2023
DOI 10.3389/fonc.2022.1100577

OPEN ACCESS

EDITED BY
Arpad Szallasi,
Semmelweis University, Hungary

REVIEWED BY
Alexander J Ambinder,
Johns Hopkins Medicine, United States
Tamar Tadmor,
Technion Israel Institute of Technology, Israel

*CORRESPONDENCE
Aasems Jacob
aasems.jacob@pikevillehospital.com
Anna E. Johnson
Anna.johnson@uky.edu
Athul Raj Raju
drathulraj.raju@gmail.com

SPECIALTY SECTION
This article was submitted to Hematologic Malignancies, a section of the journal Frontiers in Oncology

RECEIVED 16 November 2022
ACCEPTED 16 December 2022
PUBLISHED 12 January 2023

CITATION
Johnson AE, Raju AR, Jacob A and Hildebrandt GC (2023) Case report: A case of classic hairy cell leukemia with CNS involvement treated with vemurafenib.
Front. Oncol. 12:1100577.
doi: 10.3389/fonc.2022.1100577

Case report: A case of classic hairy cell leukemia with CNS involvement treated with vemurafenib

Anna E. Johnson[1]*, Athul Raj Raju[2]*, Aasems Jacob[2]* and Gerhard C. Hildebrandt[3]

[1]Department of Internal Medicine, University of Kentucky, Lexington, KY, United States, [2]Department of Hematology and Oncology, Pikeville Medical Center, Pikeville, KY, United States, [3]Division of Hematology and Medical Oncology, University of Missouri, Columbia, MO, United States

Hairy cell leukemia (HCL) is a rare mature B-cell lymphoproliferative disorder and most often presents as classic hairy cell leukemia. This entity is characterized by an indolent course and the presence of the *BRAF* V600E mutation. We report the case of an 80-year-old man with a history of classical hairy cell leukemia who presented with fatigue, dizziness, shortness of breath, blurring of vision, and headache. His initial diagnosis was 9 years prior, and he received treatments with cladribine, pentostatin, and rituximab. The workup showed an elevated white blood cell count with atypical lymphocytes, anemia, and thrombocytopenia. A peripheral blood smear confirmed HCL relapse, and a magnetic resonance imaging (MRI) of the brain showed diffuse, nonenhancing masses in the supratentorial and infratentorial regions of the brain. He was initiated on treatment with vemurafenib, with improvements in his white blood cell count and a recovery of his platelet count and hemoglobin. A repeat MRI of the brain after 3 months showed complete resolution of the lesions. Vemurafenib was discontinued after 6 months, with bone marrow biopsy showing no evidence of residual hairy cell leukemia. There have only been limited reports of HCL involvement in the central nervous system in the literature. Due to the rarity of the condition, it is not clear which treatments can be effective for intracranial disease control. Our report shows the successful use of vemurafenib, resulting in complete remission of relapsed HCL with CNS involvement.

KEYWORDS

hairy cell leukemia, vemurafenib, hairy cell, leukemia, hematologic malignancies, brain metastasis

Introduction

Hairy cell leukemia (HCL) is an indolent, mature B-cell lymphoproliferative disorder characterized by distinct clinical and pathological features. With only 600 to 800 new cases in the USA each year, this remains a rare hematologic malignancy. Most reported cases occur in middle-aged men with an average age at diagnosis of approximately 55 and male to female ratio of 4:1. Neoplastic B cells are described morphologically by their "hairy" cytoplasmic projections and accumulate in the bone marrow, spleen, and peripheral blood, with affected individuals presenting most often with symptomatic cytopenias and/or splenomegaly. Although it was first described by Bouroncle et al. in 1958, hairy cell leukemia remained a poorly understood entity, with management primarily consisting of splenectomy, which results in short-term survival (1). Outcomes were significantly improved with the use of purine analogs and anti-CD20 monoclonal antibody therapy, resulting in durable responses and remissions (2). Relapsed or refractory disease remained a treatment challenge until the identification of *BRAF* V600E mutations as the causal genetic abnormality, offering a targeted therapy for this pretreated population (3). Classic HCL (HCLc) and HCL variant (HCLv) have unique immunophenotypic and molecular differences with an overwhelming majority of HCLc harboring a *BRAF* V600E mutation and following an indolent course. *BRAF* V600E mutation is absent in HCLv, has an aggressive clinical course, and is less responsive to standard therapies. CNS involvement with either subtype of HCL has rarely been described in the literature. Treatment remains unclear in this situation and is often adopted from case reports. We describe a case of relapsed *BRAF*-mutated HCLc presenting with hyperlymphocytosis and intracranial involvement that was successfully treated with the oral BRAF inhibitor, vemurafenib.

Case description

An 80-year-old white man with a history of HCL presented with complaints of fatigue, dizziness, shortness of breath, blurring of vision, and headache. He also had a history of diabetes, hypertension, and sleep apnea. HCL was initially diagnosed 9 years prior and treated with cladribine with partial response. He relapsed 3 years later after first-line therapy and was treated with pentostatin and rituximab. Follow-up evaluation with PET/CT and bone marrow biopsy showed no signs of residual disease. Following disease relapse 5 years later when he presented with lymphocytosis and splenomegaly, molecular testing was positive for *BRAF* V600E mutation. He was treated with cladribine and rituximab but was incompletely treated due to complications of neutropenic fever and an admission for intracranial hemorrhage.

Physical examination revealed multiple petechiae and bruising in the upper and lower extremities. He had marked abdominal distension with a spleen tip palpable beyond the umbilicus. Neurologic examination showed no focal deficits. Axillary and inguinal lymph nodes were palpable. Labs showed a marked leukocytosis of 371,700 $\times$ 10^9/L (normal: 3,500–13,000 $\times$ 10^9/L) with 82% atypical lymphocytes, 4% segmented neutrophils, 3% lymphocytes, and 3% monocytes; hemoglobin of 6.4 g/dl (normal: 11–17 g/dl); and platelet count of 99,000 $\times$ 10^9/L (normal: 135,000–450,000 $\times$ 10^9/L). The patient was hospitalized with these acute findings. A peripheral blood smear showed significant lymphocytosis with oval to slightly irregular nuclei, homogenous ground-glass chromatin, and abundant pale blue cytoplasmic hairy projections, normocytic anemia with anisopoikilocytosis, and marked thrombocytopenia (Figure 1). A computerized tomography (CT) scan of the chest, abdomen, and pelvis showed splenomegaly of 22 cm, ground-glass opacities in

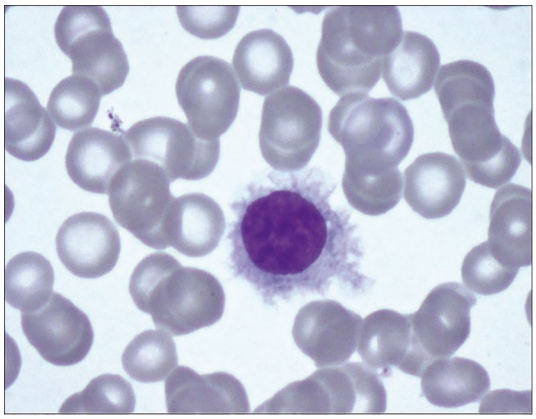

FIGURE 1
Peripheral blood smear with Wright-Giemsa staining showing hairy cell with abundant pale blue cytoplasm, slightly irregular nucleus with ground glass chromatin and hairy cell projections.

bilateral upper lung fields, and small pleural effusions bilaterally. With worsening shortness of breath, increasing oxygen requirement, and the CT findings concerning leukostasis (Figure 2), he was started on hydroxyurea 2 g daily and underwent three sessions of leukapheresis over a period of a week with significant cytoreduction. He reported improvement in respiratory symptoms with an objective reduction in white blood count (WBC) to 89,000 × 10^9/L. Flow cytometry on peripheral blood returned a kappa light chain monoclonal B-cell population expressing CD11c, partially dim CD10, CD103, and aberrant CD5, but without CD25 expression, consistent with relapsed HCL.

To identify the etiology of headache and dizziness, a CT scan of the head was done, which revealed foci of minimal hypoattenuation in both cerebellar hemispheres and periventricular white matter. This was followed by a magnetic resonance imaging (MRI) of the head with and without contrast, which showed multiple soft tissue masses in the supratentorial and infratentorial regions involving the cerebellar lobes, the left frontal and bilateral temporal lobes, with the largest lesion seen in the left cerebellum (14 × 12mm) (Figure 3A). A biopsy was not pursued due to the risk of the procedure and medical frailty. Extensive infectious disease evaluation was pursued with negative serology for HIV, hepatitis B and C, syphilis, toxoplasma, and fungal organisms including *Aspergillus*, *Blastomyces*, coccidiosis, histoplasma, and quantiferon TB. We initiated therapy with ibrutinib at 420 mg daily, but this was discontinued due to thrombocytopenia, epistaxis, and retinal hemorrhage after 7 days of treatment. Therapy was changed to BRAF inhibitor vemurafenib at 240 mg twice daily. Because he tolerated the treatment well and his symptoms improved, the dose was increased to 480 mg twice daily and he was discharged home.

He reported that his neurologic symptoms had resolved completely 1 month later. Labs showed a WBC of 28,400 × 10^9/L, hemoglobin of 13.7 g/dl, and platelet count of 44,000 × 10^9/L. An MRI of the brain, 3 months after initiation of vemurafenib, showed complete resolution of the intracranial lesions (Figure 3B), and abdominal imaging revealed a marked decrease in spleen size. Follow-up ophthalmologic evaluation showed resolution of leukemic retinopathy. He is planning to continue vemurafenib, with a goal to discontinue treatment once a bone marrow biopsy confirms morphologic remission

Discussion

Historically speaking, HCLc follows a more indolent course, often not requiring treatment for extended periods of time. Once there is a treatment indication based on constitutional symptoms of fatigue and weight loss, symptomatic cytopenias, and or discomfort associated with organomegaly, first-line therapy with purine analogs results in durable remissions. With subsequent courses, however, there is the risk of toxicity and decreased efficacy. Although the central nervous involvement of HCL has been cited in the literature, it is an extremely rare entity and is often thought to be associated with a more atypical or aggressive course.

Our patient had an atypical presentation with extreme leukocytosis (371,700 × 10^9/L) resulting in leukostasis, massive

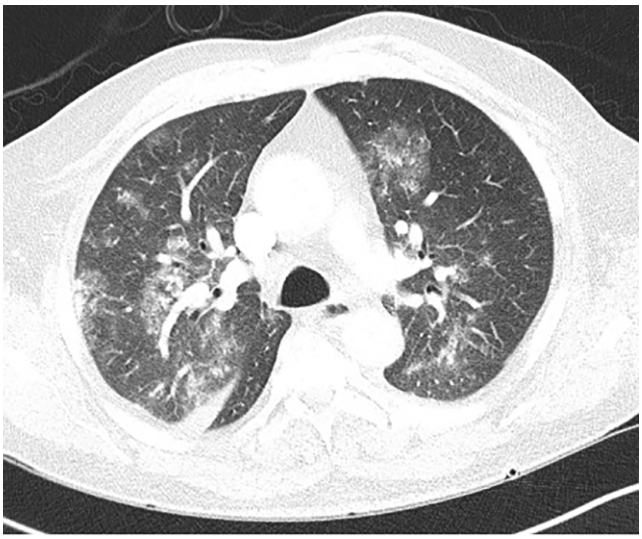

FIGURE 2
CT chest (axial) showing diffuse ground glass opacities in bilateral lung parenchyma and no radiologic evidence of pulmonary hemorrhage.

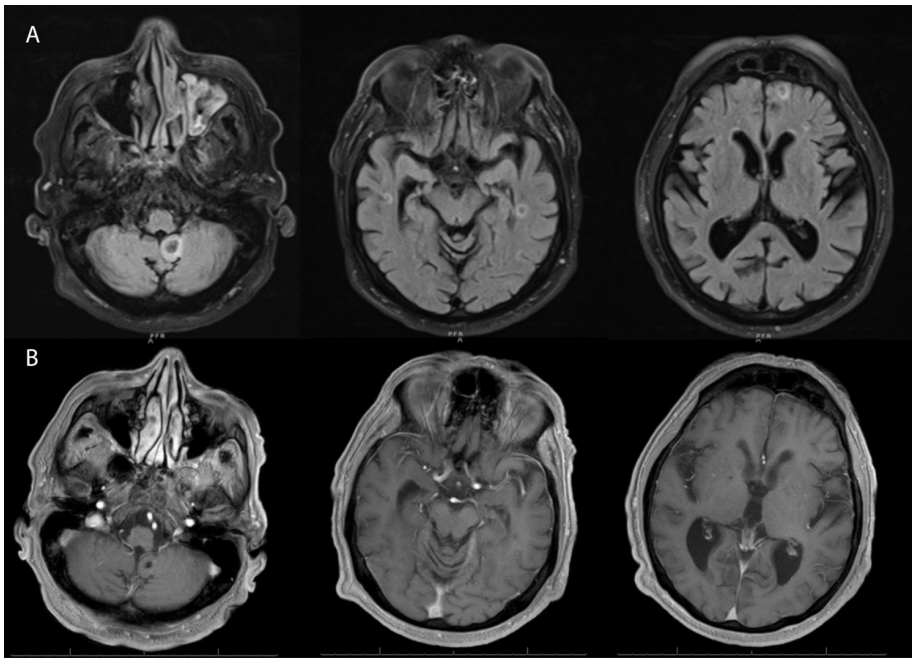

FIGURE 3
(A) Magnetic resonance imaging (axial section) of brain at recurrence showing numerous non-enhancing lesions (only showing index lesions) in the supratentorial and infratentorial brain with susceptibility artifact and subtle restricted diffusion of the margins and T2 hyperintense signals surrounding them, with the largest lesion in the left cerebellar vermis (14x12mm). **(B)** Follow up MRI after 4 months showing resolution of the non-enhancing lesions and only a small foci of low signal intensity noted within the posterior fossa representing chronic hemorrhage.

splenomegaly, and CNS involvement concerning for HCLv. Results of his flow cytometry and *BRAF* V600E mutation were most consistent with HCLc, although there was a lack of CD25 expression, which has often been associated with a more aggressive course. Given his symptoms associated with leukostasis, he was treated with cytoreductive therapy and underwent multiple sessions of leukapheresis with a brief improvement in his shortness of breath. He was started on ibrutinib based on data by Rogers et al. (4), yet this was held by our team after 1 week due to rapidly worsening thrombocytopenia and bleeding complications. Moxetumomab, an anti-CD22 immunotoxin, although a therapeutic option for relapsed and refractory HCLc, was not chosen in this case due to the availability of the drug and a lack of data in CNS disease. Based on evidence supporting oral BRAF inhibitors in relapsed or refractory BRAF-mutated HCL, he was started on vemurafenib at 240 mg twice a day, the lowest dose due to age and expected toxicity (5. He had a significant response with improvement in WBC (39,000 × 10^9/L) and platelet count (89,500 × 10^9/L) within 1 week of treatment. Although anti-CD20 monoclonal antibody therapy is suggested with BRAF inhibitor in the relapsed setting, we did not include this due to the high disease burden and risk of tumor lysis syndrome. Our case demonstrates the importance of evaluating any neurological symptoms in patients with HCL with imaging. A limitation in our case is that the intracranial lesions were not biopsy-proven to be involved in HCL. Due to the patient's medical frailty and tenuous respiratory status, a brain biopsy and lumbar puncture were felt to represent significant potential harm and were therefore not pursued. An extensive infectious workup was negative, and the treatment response confirms the diagnosis.

There have been a few other case reports of CNS involvement with HCL. A reported patient from 1985 presented with CNS involvement of hairy cells in the cerebrospinal fluid (CSF) and was treated with intrathecal methotrexate with neurological improvement but had complications of *Cryptococcus neoformans* meningitis. Further treatment with alpha interferon helped in disease control (6). Another case from 1984 involved a patient who presented with leukemic meningitis, which was confirmed by morphologic exam of leukemia cells in his CSF and bone marrow. He was treated with whole brain radiation and intrathecal chemotherapy, with a resolution of his symptoms (7). More recently, a patient presented with CNS involvement and was treated with high-dose methotrexate, cladribine for 7 days, and high-dose steroids. Unfortunately, he died from gastrointestinal bleeding and sepsis (8). Another case

of newly diagnosed BRAF-mutated HCLc presented with biopsy-proven multifocal CNS involvement and lymphocytosis (35.4 × 10^9/L). He was treated successfully with cladribine and rituximab, resulting in the resolution of intracranial lesions. This patient eventually relapsed and was treated with vemurafenib, achieving a complete response (9). There is only one other case of relapsed *BRAF* V600E-mutated HCL presenting with pancytopenia and CNS involvement, initially thought to be mantle cells. This patient was treated with high-dose cytarabine, intrathecal methotrexate, and rituximab, achieving a partial response. He had immediate progression of his disease and was again treated with rituximab and intrathecal methotrexate, which stabilized the disease. At subsequent progression, he was successfully treated with vemurafenib at 960 mg twice daily, which resulted in the resolution of intracranial lesions (10).

This case demonstrates that vemurafenib can be effective at lower doses than originally suggested and without the addition of anti-CD20 monoclonal antibody therapy. Our patient was treated with vemurafenib at 480 mg twice a day; however, based on the trajectory of his response, we suspect the dose likely would have been effective at 240 mg twice a day. Additionally, there has been previous concern and speculation that vemurafenib may not be effective in treating CNS disease due to its molecular weight and inability to effectively pass the blood–brain barrier although recent literature has supported its effectiveness (11–13). This case clearly demonstrates the efficacy of vemurafenib in the setting of central nervous system disease.

Patients receiving therapy should be counseled on potential side effects such as fatigue, alopecia, rash and photosensitivity, nausea, and arthralgias. The optimal duration of oral vemurafenib is thought to be approximately 16 to 18 weeks based on prior research, with a median time to response of 8 to 12 weeks. A longer course of therapy has not been shown to improve the duration of response, with highly effective response rates and some complete remissions observed within the recommended course of treatment (14).

Data availability statement

The original contributions presented in the study are included in the article/supplementary material. Further inquiries can be directed to the corresponding authors.

Ethics statement

Written informed consent was obtained from the individual for the publication of any potentially identifiable images or data included in this article.

Author contributions

AJo, AR, AJa and GH were involved in conceptualization, manuscript preparation, editing and review of the manuscript. All authors agree to be accountable for the content of the work. All authors contributed to the article and approved the submitted version.

Conflict of interest

The authors declare that the research was conducted in the absence of any commercial or financial relationships that could be construed as a potential conflict of interest.

Publisher's note

References

1. Bouroncle BA, Wiseman BK, Doan CA. Leukemic reticuloendotheliosis. *Blood* (1958) 13(7):609–30. doi: 10.1182/blood.V13.7.609.609

2. Saven A, Burian C, Koziol JA, Piro LD. Long-term follow-up of patients with hairy cell leukemia after cladribine treatment. *Blood* (1998) 92(6):1918–26. doi: 10.1182/blood.V92.6.1918

3. Tiacci E, Trifonov V, Schiavoni G, Holmes A, Kern W, Martelli MP, et al. BRAF mutations in hairy-cell leukemia. *N Engl J Med* (2011) 364(24):2305–15. doi: 10.1056/NEJMoa1014209

4. Rogers KA, Andritsos LA, Wei L, McLaughlin EM, Ruppert AS, Anghelina M, et al. Phase 2 study of ibrutinib in classic and variant hairy cell leukemia. *Blood* (2021) 137(25):3473–83. doi: 10.1182/blood.2020009688

5. Tiacci E, De Carolis L, Simonetti E, Capponi M, Ambrosetti A, Lucia E, et al. Vemurafenib plus rituximab in refractory or relapsed hairy-cell leukemia. *N Engl J Med* (2021) 384(19):1810–23. doi: 10.1056/NEJMoa2031298

6. Knecht H, Budmiger H, Groscurth P, Streuli RA. Central nervous system involvement in hairy cell leukemia. *Klin Wochenschr* (1985) 63(9):423–7. doi: 10.1007/BF01733668

7. Wolfe DW, Scopelliti JA, Boselli BD. Leukemic meningitis in a patient with hairy cell leukemia. a case report. *Cancer* (1984) 54(6):1085–7. doi: 10.1002/1097-0142(19840915)54:61085::aid-cncr28205406263.0.co;2-s

8. Chandana SR, Kotecha R, Al-Janadi A, Chang HT, Conley BA. Rare case of hairy cell leukemia with brain parenchymal involvement: a diagnostic dilemma. *J Clin Oncol* (2013) 31(11):e186–8. doi: 10.1200/JCO.2012.44.8787

9. Perry AM, Matsuda K, Wadhwa V, Hewitt D, Almiski M, Johnston JB, et al. Multifocal brain involvement in a patient with hairy cell leukemia successfully treated with rituximab and cladribine. *Blood Adv* (2017) 1(14):899–902. doi: 10.1182/bloodadvances

10. McDowell MM, Zhu X, Agarwal N, Nikiforova MN, Lieberman FS, Drappatz J, et al. Response of relapsed central nervous system hairy cell leukemia to vemurafenib. *Leuk Lymphoma* (2016) 57(12):2952–54. doi: 10.1080/10428194.2016.1177773

11. Gampa G, Vaidhyanathan S, Resman BW, Parrish KE, Markovic SN, Sarkaria JN, et al. Challenges in the delivery of therapies to melanoma brain metastases. *Curr Pharmacol Rep* (2016) 2(6):309–25. doi: 10.1007/s40495-016-0072-z

12. Dummer R, Goldinger SM, Turtschi CP, Eggmann NB, Michielin O, Mitchell L, et al. Vemurafenib in patients with BRAF(V600) mutation-positive melanoma with symptomatic brain metastases: final results of an open-label pilot study. *Eur J Cancer* (2014) 50(3):611–21. doi: 10.1016/j.ejca.2013.11.002

13. McArthur GA, Maio M, Arance A, Nathan P, Blank C, Avril MF, et al. Vemurafenib in metastatic melanoma patients with brain metastases: an open-label, single-arm, phase 2, multicentre study. *Ann Oncol* (2017) 28(3):634–41. doi: 10.1093/annonc/mdw641

14. Tiacci E, Park JH, De Carolis L, Chung SS, Broccoli A, Scott S, et al. Targeting mutant BRAF in relapsed or refractory hairy-cell leukemia. *N Engl J Med* (2015) 373(18):1733–47. doi: 10.1056/NEJMoa1506583

frontiers | Frontiers in Oncology

TYPE Case Report
PUBLISHED 18 January 2023
DOI 10.3389/fonc.2022.1079890

OPEN ACCESS

EDITED BY
Osamu Imataki,
Kagawa University, Japan

REVIEWED BY
Valentina Giudice,
University of Salerno, Italy
Jayant Goda,
Tata Memorial Hospital, India

*CORRESPONDENCE
Zengjun Li
zengjunli@163.com

SPECIALTY SECTION
This article was submitted to Hematologic Malignancies, a section of the journal Frontiers in Oncology

RECEIVED 25 October 2022
ACCEPTED 28 December 2022
PUBLISHED 18 January 2023

CITATION
Xing L, Wang H, Liu D, He Q and Li Z (2023) Case report: Successful management of a refractory double-expressor diffuse large B-cell lymphoma patient under the guidance of *in vitro* high-throughput drug sensitivity test. *Front. Oncol.* 12:1079890. doi: 10.3389/fonc.2022.1079890

Case report: Successful management of a refractory double-expressor diffuse large B-cell lymphoma patient under the guidance of *in vitro* high-throughput drug sensitivity test

Lijie Xing, Hui Wang, Dan Liu, Qiang He and Zengjun Li*

Department of Hematology, Shandong Cancer Hospital and Institute, Shandong First Medical University and Shandong Academy of Medical Sciences, Jinan, China

Introduction: Double-expressor diffuse large B-cell lymphoma (DEL), harboring double expression of MYC and BCL2, has an inferior prognosis following standard first-line therapy with rituximab, cyclophosphamide, doxorubicin, vincristine, and prednisolone (R-CHOP). We initiated a clinical trial to treat newly diagnosed DEL with R-CHOP plus Bruton's tyrosine kinase (BTK) inhibitor (BTKi) zanubrutinib (ZR-CHOP) and achieved a high complete response (CR) rate while four patients progressed during therapy, one of them carrying ATM and CD58 mutations. We applied an *in vitro* high-throughput drug sensitivity test for the prediction of clinical responses to different drugs in this patient.

Case presentation: We report a 30-year-old female patient diagnosed with stage III (DEL), with ATM and CD58 mutations. The patient achieved partial response (PR) after two cycles of ZR-CHOP and remained PR after four cycles of ZR-CHOP, while the disease progressed after six cycles of ZR-CHOP. High-throughput drug screening using a panel of 117 compounds identified a range of therapies with efficacy for this patient. The primary tumor cells showed moderate sensitivity to bortezomib, thalidomide, and gemcitabine as a single agent and bortezomib, thalidomide, and dexamethasone (VTD) as a combined regimen. The patient was treated with two cycles of VTD regimen (bortezomib 1.3 mg/m^2, d1, 4, 8, 11; thalidomide 100 mg, d1-21; dexamethasone 20 mg, d1, 2, 4, 5, 8, 9) and achieved PR with only a small lesion left. Another two cycles of VTD plus gemcitabine were then administered, and the patient achieved CR. Stem cells were mobilized, and autologous hematopoietic stem cell transplantation was carried out afterward. The patient remained CR for more than 3 months after transplantation.

Conclusion: In this article, we present a first-line chemoresistant DEL patient with ATM and CD58 mutations who was treated successfully with VTD plus gemcitabine under the guidance of *in vitro* high-throughput drug sensitivity test.

KEYWORDS

DE-DLBCL, ATM, CD58, VTD, drug sensitivity screening

Introduction

Diffuse large B-cell lymphoma (DLBCL) is the most common subtype of non-Hodgkin's lymphoma (NHL) with high heterogeneity. Approximately 30%~40% of DLBCL patients will develop relapsed or refractory disease, which is the major cause of mortality due to limited therapeutic options (1). Double-expressor DLBCL (DEL), harboring double expression of MYC and BCL2, represents nearly 1/3 of all DLBCL patients and shows a much poorer prognosis to rituximab plus cyclophosphamide, doxorubicin, vincristine, and prednisone (R-CHOP) treatment. The 5-year overall survival (OS) of DEL patients is only around 30%~40% with the standard regimen of R-CHOP (2), indicating there is an urgent clinical need for optimal treatment of these disease entities. We initiated a clinical trial to treat newly diagnosed DEL with R-CHOP plus Bruton's tyrosine kinase (BTK) inhibitor (BTKi) zanubrutinib (ZR-CHOP) and obtained a promising complete response (CR) rate of 85.7% after six cycles of therapy (3), while four patients progressed during therapy, one of whom was carrying ATM and CD58 mutations, as reported here. We used extraordinary agents as the second line of therapy under the guidance of an *in vitro* high-throughput drug sensitivity test. The patient achieved a complete response, and consequently, autologous hematopoietic stem cell transplantation was completed.

Case presentation

A 30-year-old female patient visited our hospital in May 2021, complaining of a nontender anterior neck mass rapidly increasing in size over the last month. The patient had no fever, night sweats, or weight loss. She lived a regular life and had no family history of malignant tumors. Physical examination revealed multiple swollen lymph nodes on the neck, which were firm, fixed, and nontender.

18F-FDG-PET showed the presence of fluorodeoxyglucose avid uptake in multiple parts, including several lymph nodes around the right carotid sheath with a maximum diameter of 3.4 cm and the standard uptake volume (SUVmax) of 33.3; an enlarged right tonsil with a SUVmax of 17.5; and a nodule in the soft tissue of upper segment of the left thigh with a length of 1.3 cm and a SUVmax of 6.3. No bone marrow infiltration was found by cytology, flow cytometry, and bone marrow biopsy.

The pathologic biopsy and immunohistochemistry (IHC) of neck lymph nodes revealed DLBCL, a nongerminal center B-cell-like (non-GCB) subtype, and overexpression of MYC (50%) and BCL2 (50%). The MYC, BCL2, and BCL6 rearrangements detected by fluorescence *in situ* hybridization (FISH) of the tumor tissue were negative.

Secondary gene detection was performed, and mutation analysis of the *DLBCL-43* gene was performed using capture-based next-generation sequencing (NGS) testing: ATM exon 27 p. C1366* missense mutation, abundance 38.1%; and CD58 exon p.I185fs frameshift mutation, abundance 16.4%. No mutations were detected in TP53.

Diagnosis of DLBCL (non-GCB subtype) was made based on her clinical presentation, morphology, and immunohistochemistry evaluation of lymph node specimens. She was in stage III, according to the Ann Arbor system. DLBCL (non-GCB subtype, DEL, stage III, group A, aaIPI 1) was confirmed by a multidisciplinary team composed of a pathologist, a radiologist, and an oncologist. The study was approved by the Institutional Review Board and carried out in accordance with the principles of the Declaration of Helsinki. Our study was approved by the Ethics Committee of the Shandong Cancer Hospital and Institute (Ethics No.: 2020-129-02). Informed consent was obtained from this patient.

The patient achieved a partial response (PR) after two cycles of ZR-CHOP (rituximab 375 mg/m^2, d1; cyclophosphamide 750 mg/m^2, d2; doxorubicin 50 mg/m^2, d2; vincristine 1.4 mg/m^2, d2 (to a maximum of 2 mg total dose); prednisolone 100 mg, d2-6; and zanubrutinib 160 mg, bid, d1-21). The patient remained PR after four cycles of ZR-CHOP, while the disease progressed after six cycles of ZR-CHOP. 18F-FDG-PET imaging demonstrated enlarged lymph nodes in the right neck area and an enlarged right tonsil with much higher FDG uptake (SUV_{max} = 32.6) compared to the liver (SUV_{max} = 3.0). A repeated biopsy of neck lymph nodes was performed and diagnosed with DLBCL, still with overexpression of MYC (50%~70%) and BCL2 (80%). The IHC showed CD20 (−), CD79a (little+), CD19 (−), PAX5 (+), CD3 (−), CD10 (+), MUM-1 (+), P53 (+, 80%, wild type), CD30 (−), CD5 (−), CyclinD1 (−), CD21 (−), Ki-67 (+, 80%), and EBER (−).

Due to the clinical situation and unfavorable prognosis, all therapeutic options were discussed with the patient. In addition to the current standard of second-line treatment options and clinical trials, the possibility of individual healing under the guidance of an *in vitro* high-throughput drug sensitivity test (DST) was discussed. The patient was informed in detail about the experimental nature of such treatment as well as the possible risks, and she actively agreed to receive the treatment under the guidance of DST.

In vitro high-throughput drug sensitivity testing is a method for determining the sensitivity of tumor-fresh viable cells to agents (as many as several hundred) (4). This patient's biopsy specimen of neck lymph nodes was used for DST. Primary cancer cells were obtained and amplified *in vitro*. Live cells were seeded and cultured in 384-well plates with drugs. Except for platinum drugs (oxaliplatin, cisplatin, carboplatin), all drugs were dissolved and diluted using dimethyl sulfoxide (DMSO). The concentrations were those used in clinical practice, which met the international drug standard. The control group was treated with DMSO. A dose (0.1 μl/well) was performed using a JANUS automated workstation. After incubation, cell viability was measured by the CellCounting-Lite 2.0 Luminescent Cell Viability Assay. The sensitivity of each treatment is listed in Supplementary Table 1. The primary tumor cells showed moderate sensitivity to bortezomib, thalidomide, gemcitabine as a single agent, and bortezomib, thalidomide, and dexamethasone (VTD) as a combined regimen. Gemcitabine is one of the routine drugs for relapsed/refractory DLBCL, while VTD is rarely reported for lymphoma treatment. The patient was treated with a VTD regimen, as that used in myeloma (bortezomib 1.3 mg/m^2, d1, 4, 8, 11; thalidomide 100 mg, d1-21; dexamethasone 20 mg, d1, 2, 4, 5, 8, 9, 11, and 12). After two cycles of therapy, PR was obtained with only a small lesion left. Another two cycles of VTD plus gemcitabine were then administered, and the patient achieved a complete response

(CR). No adverse events, such as peripheral neuropathy, pneumonia, liver and kidney function damage, and digestive tract discomfort, were detected during treatment. Stem cells were mobilized, and autologous hematopoietic stem cell transplantation was carried out afterward. The patients remained CR for more than 5 months after transplantation (Figure 1).

Discussion

DLBCL is the most common non-Hodgkin lymphoma and accounts for about 40% of all NHL. R-CHOP is the standard regimen and cures about 60% of all patients, while the rest of the 40% are either refractory or relapsed after R-CHOP treatment. Throughout the past decades, the focus has been on how to improve the outcomes of DLBCL patients. However, few studies achieved positive results compared to those of R-CHOP. Given the high heterogeneity of DLBCL, accurately predicting outcomes and providing risk stratification or even personalized therapy can be one of the strategies.

DEL takes about 30% of DLBCL, and the 5-year PFS is only about 27% when treated with R-CHOP. However, studies of DEL are rare. In the CAVALLI study, seven out of eight (87.5%) double-hit DLBCL patients achieved CR, while no benefit for DEL patients compared with historical control (5). A phase II study of chidamide combined with an R-CHOP regimen in the treatment of elderly high-risk DLBCL patients showed that 100% of DE patients achieved CR, and the 2-year PFS rate and OS rate were 83% and 91%, respectively (6).

The BCR signaling pathway is highly activated in DEL patients, implying that a BTK inhibitor may be effective for DEL. In the Phoenix study, R-CHOP plus ibrutinib (IR-CHOP) had no benefit compared with R-CHOP plus placebo. Subgroup analysis showed IR-CHOP improved both PFS and OS markedly for younger patients (<60 years) with the double expression of c-MYC and BCL2. The benefit was counteracted in older patients due mainly to the issue of safety when combined with ibrutinib. Zanubrutinib is a more selective BTK inhibitor than ibrutinib. ZR-CHOP was initiated as a clinical study regimen in our center for DEL patients. A total of 89.3% patients (25/28) obtained CR after ZR-CHOP treatment, and only three progressed during therapy and follow-up (one patient was proved to be a false positive by PET-CT in the EHA report P1201, 85.7% CRR was reported). The case reported here is one of the three patients who progressed shortly after six cycles of ZR-CHOP.

Due to the high heterogeneity of DLBCL, it is difficult to accurately predict outcomes and provide individualized salvage therapies, both of which are essential for individualized cancer therapy (ICT). High-throughput DST is a personalized functional precision oncology approach that offers an assessment of additional possible treatments and combinations to identify effective therapeutic strategies for patients (4). For this patient, the primary tumor cells showed moderate sensitivity to bortezomib, thalidomide, and gemcitabine as a single agent, and VTD as a combined regimen. The result was confirmed by the clinical response to the treatment. Here, we will discuss the potential mechanisms underlying the efficacy, especially the effect of proteasome inhibitor (PI) on the tumor cells with ATM and CD58 mutations.

ATM is a protein kinase enzyme with a crucial role in the DNA repair system, acting as an intracellular sensor in response to DNA double-strand break (DSB) and then phosphorylating downstream proteins such as p53, chk2, and chk1, to initiate a cell-cycle arrest, apoptosis, and DNA repair (7). ATM alterations with putative pathogenic effects have been found in 13%–20% of DLBCL patients. The mutations of ATM were related to inferior PFS in localized DLBCL as well as GCB-DLBCL patients (8, 9).

ATM deficiency increases genomic instability by impairing DNA DSB repair as well as enhancing the dependence of cancer cells on other DNA repair mechanisms. Poly (ADP-ribose) polymerase-1

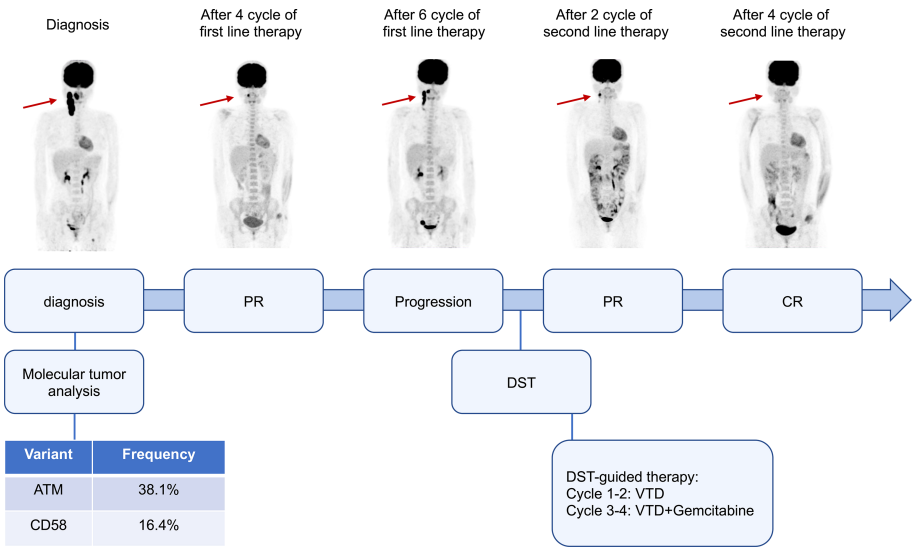

FIGURE 1
Clinical course and response images of the patient. PR, partial response; CR, complete response; DST, drug sensitivity test; VTD, bortezomib, thalidomide, and dexamethasone.

(PARP1) is another protein involved in DNA repair. PARP inhibitors have shown promising results in tumor cells defective in DNA damage repair (DDR) (10). In some studies, ATM loss showed that PARP inhibition was synthetically lethal, which is dependent on the tumor's genetic background (11). Bortezomib (BTZ) was reported to impair the DNA homology-dependent repair (HDR), which is critical for the recovery of DNA DSB (12). In this patient, both DST and clinical results showed tumor cells were sensitive to BTZ treatment. As we know, when the amount of DNA damage exceeds the repair capacity, the damaged cells will be cleared through apoptosis. Therefore, we speculate that the DNA damage triggered by BTZ exceeds the repair capacity in ATM-deficient cells. Further preclinical studies are needed to reveal the new synthetic lethal effect of BTZ in the ATM mutation DLBCL. Indeed, inhibitors targeting other proteins in the DNA damage response are being developed for ATM-mutation cancers.

CD58 is the receptor for CD2, which is expressed on T cells and natural killer (NK) cells and is necessary for T-cell- and NK-cell-mediated cytotoxicity. CD58 mutations or loss occur in 21% of DLBCL patients, while the expression is deregulated in approximately 67% of DLBCL patients (12). BTZ can trigger specific antitumor immunity *via* immunogenic cell death (ICD), in which endogenous tumor cell proteins are recognized as damage-associated molecular patterns (DAMP) and activate cancer-specific immune responses (13). No studies show BTZ is effective in DLBCL with abnormal CD58. Further studies are needed to explore whether BTZ can overcome the immunodeficiency of patients with abnormal CD58 by inducing an ICD response.

This patient progressed after six cycles of ZR-CHOP chemotherapy, which may be related to ATM and CD58 mutations in addition to the poor response of patients with DEL. Proteasome inhibitors, such as bortezomib or carfilzomib, have shown encouraging efficacy in DLBCL but showed no benefit on PFS in the phase 3 study (14). However, in this case, the patient showed a good response to BTZ, which may be due to BTZ-induced DNA damage mutations leading to cell death in patients with ATM; BTZ overcomes the immunodeficiency of DLBCL caused by CD58 mutation by triggering the ICD response.

Conclusion

Although gene mutations of ATM and CD58 increase molecular heterogeneity, they can be the potential therapeutic targets implicated in cancer therapy and clinical outcomes. To our knowledge, this case is the first chemoresistant DEL patient with ATM and CD58 mutations treated successfully with VTD plus gemcitabine, which provides new insights into the management of DLBCL. Prospective clinical trials are necessary to draw firm conclusions. Although there is still a long way to go in terms of curing DLBCL, optimal combinations of novel and traditional drugs will promote precision medicine in patients with DLBCL under the guidance of detailed genetic information.

Data availability statement

The original contributions presented in the study are included in the article/Supplementary Material. Further inquiries can be directed to the corresponding author.

Ethics statement

The studies involving human participants were reviewed and approved by Medical Ethical Committee of Shandong Cancer Hospital and Institute. The patients/participants provided their written informed consent to participate in this study. Written informed consent was obtained from the individual(s) for the publication of any potentially identifiable images or data included in this article.

Author contributions

LX and ZL designed the study, performed treatments, collected and analyzed data, and wrote the manuscript. HW, DL, and QH collected data on clinical follow-up. All authors contributed to the article and approved the submitted version.

Funding

This work was funded by the National Natural Science Foundation of China (82200224 to LX) and the Natural Science Foundation of Shandong Province (ZR2021MH072 to LX).

Conflict of interest

The authors declare that the research was conducted in the absence of any commercial or financial relationships that could be construed as a potential conflict of interest.

Publisher's note

Supplementary material

The Supplementary Material for this article can be found online at: https://www.frontiersin.org/articles/10.3389/fonc.2022.1079890/full#supplementary-material

References

1. Sehn LH, Salles G. Diffuse Large b-cell lymphoma. *New Engl J Med* (2021) 384 (9):842–58. doi: 10.1056/NEJMra2027612

2. Green TM, Young KH, Visco C, Xu-Monette ZY, Orazi A, Go RS, et al. Immunohistochemical double-hit score is a strong predictor of outcome in patients with diffuse large b-cell lymphoma treated with rituximab plus cyclophosphamide, doxorubicin, vincristine, and prednisone. *J Clin Oncol* (2012) 30(28):3460–7. doi: 10.1200/JCO.2011.41.4342

3. He Q, Xie L, Zhao RR, Ma J, Wang H, Li J, et al. P1201: Zanubrutinib plus Rchop (Zr-chop) regimen achieves high complete response rate in the treatment of newly-diagnosed double-expression diffuse Large b cell lymphoma. *Hemasphere* (2022) 6 (Suppl):1087–8. doi: 10.1097/01.HS9.0000847668.08542.45

4. Popova AA, Levkin PA. Precision medicine in oncology: In vitro drug sensitivity and resistance test (DSRT) for selection of personalized anticancer therapy. *Advanced Ther* (2020) 3(2):1900100. doi: 10.1002/adtp.201900100

5. Zelenetz AD, Salles G, Mason KD, Casulo C, Gouill SL, Sehn LH, et al. Venetoclax plus r- or G-CHOP in non-Hodgkin lymphoma: Results from the CAVALLI phase 1b trial. *Blood* (2019) 133(18):1964–76. doi: 10.1182/blood-2018-11-880526

6. Zhang MC, Fang Y, Wang L, Cheng S, Fu D, He Y, et al. Clinical efficacy and molecular biomarkers in a phase II study of tucidinostat plus r-CHOP in elderly patients with newly diagnosed diffuse large b-cell lymphoma. *Clin Epigenet* (2020) 12(1):160. doi: 10.1186/s13148-020-00948-9

7. Armstrong SA, Schultz CW, Azimi-Sadjadi A, Brody JR, Pishvaian MJ. ATM Dysfunction in pancreatic adenocarcinoma and associated therapeutic implications. *Mol Cancer Ther*. (2019) 18(11):1899–908. doi: 10.1158/1535-7163.MCT-19-0208

8. Qin W, Fi D, Shi Q, Dong L, Yi HM, Huang HY, et al. Molecular heterogeneity in localized diffuse Large b-cell lymphoma. *Front Oncol* (2021) 11:638757–7. doi: 10.3389/fonc.2021.638757

9. Juskevicius D, Jucker D, Klingbiel D, Mamot C, Dirnhofer S, Tzankov A. Mutations of CREBBP and SOCS1 are independent prognostic factors in diffuse large b cell lymphoma: mutational analysis of the SAKK 38/07 prospective clinical trial cohort. *J Hematol Oncol* (2017) 10(1):1–10. doi: 10.1186/s13045-017-0438-7

10. Dias MP, Moser SC, Ganesan S, Jonkers J. Understanding and overcoming resistance to PARP inhibitors in cancer therapy. *Nat Rev Clin Oncol* (2021) 18 (12):773–91. doi: 10.1038/s41571-021-00532-x

11. Mak JPY, Ma HT, Poon RYC. Synergism between ATM and PARP1 inhibition involves DNA damage and abrogating the G(2) DNA damage checkpoint. *Mol Cancer Ther* (2020) 19(1):123–34. doi: 10.1158/1535-7163.MCT-19-0474

12. Neri P, Ren L, Gratton K, Stebner E, Johnson J, Klimowicz A, et al. Bortezomib-induced "BRCAness" sensitizes multiple myeloma cells to PARP inhibitors. *Blood* (2011) 118(24):6368–79. doi: 10.1182/blood-2011-06-363911

13. Gulla A, Morelli E, Samur MK, Botta C, Hideshima T, Bianchi G, et al. Bortezomib induces anti-multiple myeloma immune response mediated by cGAS/STING pathway activation. *Blood Cancer Discov* (2021) 2(5):468–83. doi: 10.1158/2643-3230.BCD-21-0047

14. Davies A, Cummin TE, Barrans S, Maishman T, Mamot C, Novak U, et al. Gene-expression profiling of bortezomib added to standard chemoimmunotherapy for diffuse large b-cell lymphoma (REMoDL-b): an open-label, randomised, phase 3 trial. *Lancet Oncol* (2019) 20(5):649–62. doi: 10.1016/S1470-2045(18)30935-5

frontiers | Frontiers in Oncology

TYPE Case Report
PUBLISHED 20 January 2023
DOI 10.3389/fonc.2023.1036455

OPEN ACCESS

EDITED BY
Ahmad Antar,
Almoosa Specialist Hospital, Saudi Arabia

REVIEWED BY
Monica Makiya,
Italian Hospital of Buenos Aires, Argentina
Guangsheng He,
Nanjing Medical University, China

*CORRESPONDENCE
Eugenia Accorsi Buttini
eugenia.accorsi@gmail.com

SPECIALTY SECTION
This article was submitted to Hematologic Malignancies, a section of the journal Frontiers in Oncology

RECEIVED 04 September 2022
ACCEPTED 02 January 2023
PUBLISHED 20 January 2023

CITATION
Accorsi Buttini E, Farina M, Lorenzi L, Polverelli N, Radici V, Morello E, Colnaghi F, Almici C, Ferrari E, Bianchetti A, Leoni A, Re F, Bosio K, Bernardi S, Malagola M, Re A and Russo D (2023) High risk-myelodysplastic syndrome following CAR T-cell therapy in a patient with relapsed diffuse large B cell lymphoma: A case report and literature review. *Front. Oncol.* 13:1036455. doi: 10.3389/fonc.2023.1036455

High risk-myelodysplastic syndrome following CAR T-cell therapy in a patient with relapsed diffuse large B cell lymphoma: A case report and literature review

Eugenia Accorsi Buttini[1]*, Mirko Farina[1], Luisa Lorenzi[2], Nicola Polverelli[1], Vera Radici[1], Enrico Morello[1], Federica Colnaghi[1], Camillo Almici[3], Emilio Ferrari[3], Andrea Bianchetti[3], Alessandro Leoni[1,4], Federica Re[1,4], Katia Bosio[1,4], Simona Bernardi[1,4], Michele Malagola[1], Alessandro Re[5] and Domenico Russo[1]

[1]Unit of Blood Diseases and Bone Marrow Transplantation, Cell Therapies and Hematology Research Program, Department of Clinical and Experimental Science, University of Brescia, ASST Spedali Civili di Brescia, Brescia, Italy, [2]Department of Molecular and Translational Medicine, Section of Pathology, University of Brescia, ASST Spedali Civili di Brescia, Brescia, Italy, [3]Stem Cell Laboratory, Section of Hematology and Blood Coagulation, Clinical Chemistry Laboratory, Diagnostics Department, ASST Spedali Civili di Brescia, Brescia, Italy, [4]Research Center Ail (CREA), Chair of Hematology Department of Clinical and Experimental Science, University of Brescia, ASST Spedali Civili di Brescia, Brescia, Italy, [5]Hematology Unit, ASST Spedali Civili di Brescia, Brescia, Italy

Background: Chimeric antigen receptor (CAR) T-cell therapy represents the most advanced immunotherapy against relapsed/refractory B cell malignancies. While cytokine release syndrome and immune effector cell-associated neurotoxicity syndrome are distinctive, known CAR T-cell acute adverse events, hematological toxicity has been increasingly reported. Cytopenia following CAR T-cell treatment is attributed in most cases to lymphodepletion regimens, bridging chemotherapy, or radiotherapy. However, when cytopenia becomes prolonged, the development of myelodysplastic syndrome (MDS) should be considered.

Case presentation: We report a case of high risk (HR)-MDS following CAR T-cell therapy in a patient with relapsed diffuse large B cell lymphoma. Eight months after CAR T-cell infusion, the blood count showed progressive, worsening cytopenia and the bone marrow biopsy revealed multilineage dysplasia without excess of blasts associated with chromosome 7 deletion and *RUNX1* mutation. Next generation sequencing analysis, retrospectively performed on stored samples, showed a germ line *CSF3R* mutation, *CEBPA* clonal hematopoiesis, but no *RUNX1* lesion.

Conclusion: We describe a case of HR-MDS, with deletion of chromosome 7 and acquisition of *RUNX1* mutation, developing after CAR T-cell therapy in a patient with clonal hematopoiesis (CH). Previous chemotherapy favored MDS onset; however, we could not exclude the fact that the impairment of immunosurveillance related to either lymphodepletion or CAR T-cell infusion may play a role in MDS development. Thus, we designed a multicenter

10.3389/fonc.2023.1036455

prospective study (ClonHema-CAR-T-Study) to investigate if cytopenia after CAR T-cell treatment may be due to underling CH as well as the presence of secondary myeloid malignancies.

KEYWORDS

CAR T-cell therapy, myelodysplastic syndrome, diffuse large B cell lymphoma, next generation sequencing, clonal hematopoiesis

Introduction

Chimeric antigen receptor (CAR) T-cell therapy has shown impressive efficacy in treating relapsed and refractory B-cell malignancies (1, 2). CAR T-cell therapy is frequently complicated by cytokine release syndrome (CRS) and immune effector cell-associated neurotoxicity syndrome (ICANS) (3). Besides these distinctive acute adverse events, hematological toxicity is emerging as the most relevant long term side effect (4). Cytopenias after CAR T therapy most likely have a multifactorial etiology due to active inflammation milieu, together with the impact of previous and lymphodepleting chemotherapy. Among the possible causes of persistent cytopenia, the development of secondary myeloid malignancies should be considered due to the previous history of chemo and/or radiation therapy and the significant impairment of immunosurveillance related to disease and CAR-T treatment (5). To the best of our knowledge, secondary myelodysplastic syndrome (MDS) clearly related to CAR T-cell treatment has not been described to date. We report the first case of high risk (HR)-MDS with chromosome 7 deletion and *RUNX1* mutation, which developed after CAR T-cell therapy in a patient with relapsed diffuse large B cell lymphoma (DLBCL).

Case presentation

In August 2019, a 57-year-old woman with a previous history of diabetes mellitus and obesity was diagnosed with germinal-center DLBCL, Ann-Arbor stage IVs-A. At diagnosis, the patient presented cervical lymphadenopathies and spleen involvement. A bone marrow (BM) biopsy revealed the presence of 25% infiltrate of lymphocytes in the context of normal hematopoiesis. She was classified with age-adjusted International Prognostic Index (IPI) (score 3) and central nervous system (CNS-IPI) (score 4) high risk score. The patient was treated with four cycles of rituximab, cyclophosphamide, adriamycin, vincristine, and prednisolone (R-CHOP), achieving a computed tomography complete response (CR). Subsequently, she received one course of consolidation chemotherapy with rituximab, mitoxantrone, cytarabine, and dexamethasone (R-MAD), and one course of high dose cytarabine with stem cell collection showing a metabolic CR according to the Lugano criteria. In April 2020, autologous stem cell transplantation (ASCT) was performed using FEAM (fotemustine, etoposide, cytarabine, and melphalan) as a conditioning regimen. Unfortunately, in December 2020 the patient relapsed with enlarged retroperitoneal lymph-nodes, a hypodense liver, and uterine lesions. A BM biopsy was performed, and no signs of lymphoma infiltration or dysplasia were found. She was considered eligible for CAR T-cell treatment and underwent lymphocytes apheresis followed by two bridging courses of R-ESHAP (etoposide, cisplatin, cytarabine, and methylprednisolone). On the first day of standard lymphodepletion, the blood count showed grade II anemia, leukopenia, and grade I thrombocytopenia according to the Common Terminology Criteria of Adverse Events. The patient did not develop either CRS or ICANS, only an episode of fever occurred caused by *Staphilococcus haemolyticus*. Two months after CAR T-cell treatment, the patient was in CR and a BM biopsy presented normal cellularity, without dysplastic features or cytogenetic alterations. In the following months, the blood count showed a progressive normalization of leukocytes values, with hemoglobin ranging between 8.5 and 10.4 g/dl and platelets between 20 and 40 x10 (6)/L (Figure 1). Seven months later, the cytopenia worsened (grade III anemia, grade IV thrombocytopenia, grade III leukopenia), requiring recombinant human G-CSF and erythrocyte and platelet support. In December 2022, a BM biopsy ruled out lymphoma infiltration but revealed multilineage dysplasia without excess of blasts (Figure 2), associated with chromosome 7 deletion. A diagnosis of HR revised-IPSS MDS was made, and the patient was treated with azacitidine followed by allogeneic hematopoietic stem cell transplantation (allo-HCT).

Discussion

Uni- or multi-lineage cytopenias are increasingly recognized as a side effect associated with CAR T-cell therapy. In the ZUMA trial, 17% of the patients treated with axicabtagene ciloleucel (axi-cel) presented with grade 3 or higher cytopenia at 3 month or later. Four patients developed MDS after CART-cell infusion, which was considered to be related to previous treatment (1). In the JULIET study, grade 3/4 thrombocytopenia persisted in 38% of patients 3 months after CAR T-cell treatment, while no case of grade 3/4 neutropenia was reported (2). Recently, Cordeiro et al. reported late adverse events after CAR T-cell treatment in patients who survived at least one year after therapy. Three of the 19 patients with ongoing CR had prolonged cytopenia without evidence of MDS after receiving CAR-T cells (5). Subsequent MDS occurred in four patients, and notably, two of these had cytogenetics abnormalities prior to CAR-T cell therapy. Apart from clinical trials, a multicenter analysis on 258 patients receiving axi-cel and tisa-cel showed prolonged neutropenia in 64% of patients (6). In addition, a case of BM aplasia after axi-cel treatment for DLBCL was submitted to allo-HCT (7) and a case of

10.3389/fonc.2023.1036455

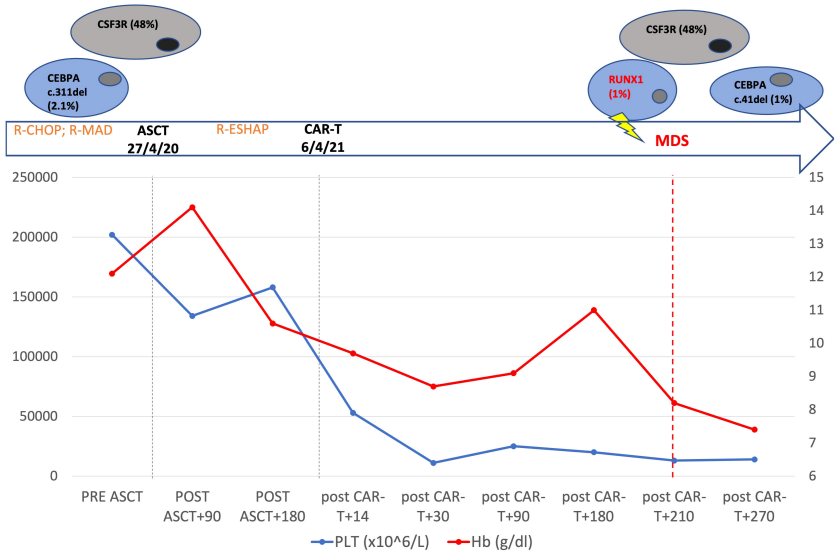

FIGURE 1
Patient's timeline. Top: mutational profile detected by next generation sequencing. Middle: the main patient treatments. Changes of hemoglobin and platelets from the beginning of patient therapy to 9 months after CAR T cell-therapy are shown.

sustained myelosuppression after BCMA-CART therapy for relapsed myeloma was successfully treated with backup of autologous stem cells (8). While early cytopenia after CAR T infusion seems to be related to the myelotoxic effect of lymphodepletion, the development of late cytopenia likely has a multifactorial origin and it remains poorly understood (9). Some authors have shown that baseline cytopenia and elevated baseline levels of C-reactive protein (CRP) and ferritin were correlated with the duration of neutropenia after CAR T-cell therapy (6). Thus, the low marrow stem cell reserve, resulting from previous chemotherapy and the high levels of inflammation, were most likely correlated to hematologic toxicity. Based on this result, a CAR-HEMATOTOX score, capable to identify patients who are at high risk of developing significant cytopenia, was developed. In our patient, the CAR HEMATOTOX score was low, determined only by a high level of ferritin (1,016 ng/mL). Therefore, in order to explain the worsening of cytopenia 7 months after CAR T-cell treatment, we performed a BM biopsy and a diagnosis of HR-MDS was made. Notably, she developed a deletion of chromosome 7, which is considered one of the hallmark features of therapy related MDS (t-MDS). Secondary MDS following ASCT has an incidence estimated between 5 and 20%, and two main types of t-MDS have been described. The first is associated with previous exposure to topoisomerase II inhibitors, usually occurs 2–3 years after therapy, and translocations involving 11q23 or 21q22 are frequently associated. The second is related to alkylating agents, usually occurs 5–7 years after exposure, and loss or deletion of chromosomes 5 or 7 are the most common cytogenetic abnormalities described (10). Our patient was treated with both alkylating agents and topoisomerase II inhibitors before undergoing CAR T-cell therapy; therefore, she was at increased risk to developing MDS related to the mutagenic effect of previous chemotherapy. At the same time, we cannot exclude the fact that the CAR T-cell treatment may play a role in the development of the MDS. Recently, a case of diagnosis of acute myeloid leukemia (AML), which developed two months after CAR T-cell treatment for DLBCL was described by Falini at al (11). On top of AML diagnosis, next generation sequencing (NGS) detected mutations of the following genes: *DNMT3A* V626Gfs Ter4 (VAF: 46.2%), *RUNX1* splicing-site mutation (VAF: 16.8%), missense mutation N136K (VAF: 9.2%), and *PPM1D* S453 (VAF: 1.4%). Targeted sequencing of stored DNA from a BM sample taken before CAR T-cell treatment was also performed, which already showed the *DNMT3A* and the *PPM1D* mutations, but not *RUNX1*. Therefore, the patient had clonal hematopoiesis (CH) driven by *DNMT3A*, already present at the time of the DLBCL diagnosis, and the acquisition of *RUNX1* mutations 2 months after CAR T-cell infusion likely promoted the evolution to AML, most likely through cooperation with the deletion of chromosome 7.

In our case, NGS performed on a medullary sample using the commercial Myeloid Solution produced by SOPHiA GENETICS

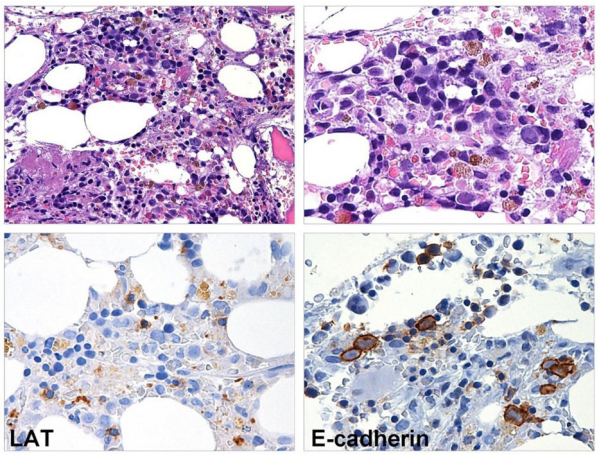

FIGURE 2
BM biopsy performed eight months after CAR T-cell infusion. Myeloid maturation is shifted to the left, granulocytes are rare and hyposegmented. The megakaryopoiesis is hypoplastic (LAT stain) and erythroid precursors show megaloblastoid features (E-caherin stain).

(SOPHiA GENETICS, Saint-Sulpice, Switzerland) 8 months after CAR T-cell treatment identified mutations of the following genes: *CSF3R* c.1319G>A; p.R440Q (VAF: 48%), *CEBPA* c.41del; p.P14R (VAF: 1%), and *RUNX1* c.508-2T>C (VAF: 1%). When we retrospectively performed the NGS analysis on a cryopreserved sample collected during the harvest of peripheral blood stem cells before ASCT, *CSF3R* c.1319G>A;p.R440Q (VAF: 48%) and *CEBPA* c.311_313del;p.G104del (VAF: 2.1%) were detected. *CSF3R* gene lesions are uncommon in MDS, occurring at a rate of 3%, and they are an age-independent and mostly IPSS-R independent risk factor for leukemia-free survival (12). In the setting of AML, *CSF3R* mutations are frequently associated with abnormalities of *RUNX1*, *CBFB*, *CEBPA*, and *NPM1 (13)*. Conversely, *RUNX1* mutations occur in 8–23% of MDS, most commonly in the setting of therapy-related MDS, and are frequently detected in patients who develop AML, with a negative impact on survival (14).

In our case, the patient had a dominant clone with *CSF3R* mutation and a subclone with a *CEBPA* lesion before being submitted to ASCT. Considering the consistent variant allele fraction, without fluctuations over time, *CSF3R* mutation is likely to be of germ line origin, while we can consider the *CEBPA* lesion belonging to CH. Eight months after tisa-cel infusion, the cytopenia worsened dramatically and BM assessment revealed monosomy of 7 and the onset of *RUNX1* mutation (Figure 1). Thus, the patient most likely presented with a germ line *CSF3R* mutation and *CEBPA* CH before ASCT. Subsequently, the acquisition of chromosome 7 deletion and *RUNX1* mutation promoted the development of MDS. Currently, the patient has been submitted to allo-HCT from a haploidentical donor, and she is in CR after two months.

Conclusion

This is the first case report of HR-MDS developing after CAR T-cell treatment and, in addition to the case described by Falini et al, the second in which deletion of chromosome 7 and acquisition of *RUNX1* are reported. The coincidental recurrence of these genomic alterations could be occasional, and this would certainly appear to be a limitation of our case report; however they may reveal a peculiar stepwise leukemogenic evolution starting from the presence of a pre-CAR T-cell CH trait.

The role of genotoxic damage related to previous chemotherapy and ASCT in patients with DLCBL is well-known. Conversely, the impairment of immunosurveillance, related either to the lymphoma or to T/B-cells aplasia (15) induced by lymphodepletion and CAR T-cell therapy, remain to be clarified and new studies are needed to investigate the impact of CAR T-cell therapy on risk of secondary hematological malignancies. The observation of these two first cases strongly suggest that a NGS genomic profile study for investigating the presence of CH before CAR-T-cell therapy should be performed. For these reasons, we have designed an Italian multicentric study, the ClonHema-CAR-T study, with the aim to evaluate CH before CAR T and monitor its clonal evolution after CAR T-cell infusion in the case of persistent cytopenia.

Data availability statement

The original contributions presented in the study are included in the article/supplementary materials. Further inquiries can be directed to the corresponding author.

Ethics statement

The studies involving human participants were reviewed and approved by Comitato etico di Brescia. The patients/participants provided their written informed consent to participate in this study. Written informed consent was obtained from the individual(s) for the publication of any potentially identifiable images or data included in this article.

Author contributions

Manuscript writing: EAB. Review and editing: MF, LL, NP, VR, AT, EM, FC, CA, EF, AB, AL, FR, KB, SB, MM, AR, and DR. Figures: LL and MF. All authors contributed to the article and approved the submitted version.

Conflict of interest

The authors declare that the research was conducted in the absence of any commercial or financial relationships that could be construed as a potential conflict of interest.

Publisher's note

All claims expressed in this article are solely those of the authors and do not necessarily represent those of their affiliated organizations, or those of the publisher, the editors and the reviewers. Any product that may be evaluated in this article, or claim that may be made by its manufacturer, is not guaranteed or endorsed by the publisher.

References

1. Locke FL, Ghobadi A, Jacobson CA, Miklos DB, Lekakis LJ, Oluwole OO, et al. Long-term safety and activity of axicabtagene ciloleucel in refractory large b-cell lymphoma (ZUMA-1): a single-arm, multicentre, phase 1-2 trial. *Lancet Oncol* (2019) 20(1):31–42. doi: 10.1016/S1470-2045(18)30864-7

2. Schuster SJ, Bishop MR, Tam CS, Waller EK, Borchmann P, McGuirk JP, et al. Tisagenlecleucel in adult relapsed or refractory diffuse Large b-cell lymphoma. *N Engl J Med* (2019) 380(1):45–56. doi: 10.1056/NEJMoa1804980

3. Lee DW, Santomasso BD, Locke FL, Ghobadi A, Turtle CJ, Brudno JN, et al. ASTCT consensus grading for cytokine release syndrome and neurologic toxicity associated with immune effector cells. *Biol Blood Mar- row Transplant* (2019) 25(4):625–38. doi: 10.1016/j.bbmt.2018.12.758

4. Fried S, Avigdor A, Bielorai B, Meir A, Besser MJ, Schachter J, et al. Early and late hematologic toxicity following CD19 CAR-T cells. *Bone Marrow Transplant* (2019) 54 (10):1643–50. doi: 10.1038/s41409-019-0487-3

5. Cordeiro A, Bezerra ED, Hirayama AV, Hill JA, Wu QV, Voutsinas J, et al. Late events after treatment with CD19-tar- geted chimeric antigen receptor modified T cells. *Biol Blood Marrow Transplant* (2020) 26(1):26–33. doi: 10.1016/j.bbmt.2019.08.003

6. Rejeski K, Perez A, Sesques P, Hoster E, Berger C, Jentzsch L, et al. CAR-HEMATOTOX: a model for CAR T-cell-related hematologic toxicity in relapsed/refractory large b-cell lym- phoma. *Blood* (2021) 138(24):2499–513. doi: 10.1182/blood.2020010543

7. Qasrawi A, Arora R, Ramlal R, Munker R, Hildebrandt GC. Allogenic hematopoietic stem cell transplantation for pro- longed bone marrow aplasia after chimeric antigen receptor (CAR) T-cell therapy for relapsed diffuse large b-cell lymphoma. *Am J Hematol* (2020) 95(4):E89–91. doi: 10.1002/ajh.25725

8. Lin Q, Liu X, Han L, Liu L, Fang B, Gao Q, et al. Autologous hematopoietic stem cell infusion for sustained mye- losuppression after BCMA-CAR-T therapy in patient with relapsed myeloma. *Bone Marrow Transplant* (2020) 55(6):1203–5. doi: 10.1038/s41409-019-0674-2

9. Mo G, Wang HW, Talleur AC, Shahani SA, Yates B, Shalabi H, et al. Diagnostic approach to the evaluation of myeloid ma- lignancies following CAR T-cell therapy in b-cell acute lymphoblastic leukemia. *J Immunother Cancer* (2020) 8(2):e001563. doi: 10.1136/jitc-2020-001563

10. Vaxman I, Ram R, Gafter-Gvili A, Vidal L, Yeshurun M, Lahav M, et al. Secondary ma- lignancies following high dose therapy and autologous hematopoietic cell transplantation-sys- tematic review and meta-analysis. *Bone Marrow Transplant* (2015) 50(5):706–14. doi: 10.1038/bmt.2014.325

11. Falini L, Venanzi A, Tini V, Innocente A, Ballanti S, Saldi S, et al. Acute myeloid leukemia development soon after anti-CD19 chimeric antigen receptor T-cell infusion in a patient with refractory diffuse large B-cell lymphoma and pre-existing clonal hematopoiesis. *Haematologica* (2022) 108(1):290–4. doi: 10.3324/haematol.2022.281351

12. Tefferi A, Lasho TL, Patnaik MM, Saeed L, Mudireddy M, Idossa D, et al. Targeted next-generation sequencing in myelodysplastic syndromes and prognostic interaction between mutations and IPSS-r. *Am J Hematol* (2017) 92(12):1311–7. doi: 10.1002/ajh.24901

13. Zhang Y, Wang F, Chen X, Zhang Y, Wang M, Liu H, et al. CSF3R mutations are fre- quently associated with abnormalities of RUNX1, CBFB, CEBPA, and NPM1 genes in acute myeloid leukemia. *Cancer* (2018) 124(16):3329–38. doi: 10.1002/cncr.31586

14. Cook MR, Karp JE, Lai C. The spectrum of genetic mutations in myelodysplastic syndrome: Should we update prognostication? *EJHaem* (2021) 3(1):301–13. doi: 10.1002/jha2.317

15. Farina M, Bernardi S, Gandolfi L, Zanaglio C, Morello E, Turra A, et al. Case report: Late onset of myelodysplastic syndrome from donor progenitor cells after allogeneic stem cell transplantation. which lessons can we draw from the reported case? *Front Oncol* (2020) 10:564521. doi: 10.3389/fonc.2020.564521

frontiers | Frontiers in Oncology

TYPE Case Report
PUBLISHED 30 January 2023
DOI 10.3389/fonc.2023.1091074

OPEN ACCESS

EDITED BY
Arpad Szallasi,
Semmelweis University, Hungary

REVIEWED BY
Breno Moreno De Gusmão,
Beneficência Portuguesa de São Paulo, Brazil
Na Wang,
Huazhong University of Science and Technology, China

*CORRESPONDENCE
Mingxia Shi
shmxia2002@sina.com

†These authors have contributed equally to this work and share first authorship

SPECIALTY SECTION
This article was submitted to Hematologic Malignancies, a section of the journal Frontiers in Oncology

RECEIVED 06 November 2022
ACCEPTED 13 January 2023
PUBLISHED 30 January 2023

CITATION
Yang Y, Li Z, Li Y, Zhao Y and Shi M (2023) Relapsed/refractory diffuse large B cell lymphoma with cardiac involvement: A case report and literature review. *Front. Oncol.* 13:1091074. doi: 10.3389/fonc.2023.1091074

Relapsed/refractory diffuse large B cell lymphoma with cardiac involvement: A case report and literature review

Yuanyuan Yang[1,2†], Zixuan Li[1,2†], Yuntao Li[1,2], Yue Zhao[3] and Mingxia Shi[1,2*]

[1]Department of Hematology, the First Affiliated Hospital of Kunming Medical University, Kunming, China, [2]Hematology Research Center of Yunnan Province, Kunming, China, [3]Department of Cardiology, the First Affiliated Hospital of Kunming Medical University, Kunming, China

Background: Hematological malignancies of the heart (CHMs) are extremely rare, and include leukemia, lymphoma infiltration, and multiple myeloma with extramedullary manifestations. Cardiac lymphoma can be divided into primary cardiac lymphoma (PCL) and secondary cardiac lymphoma (SCL). Compared to PCL, SCL is relatively more common. Histologically, the most frequent SCL is diffuse large B-cell lymphoma (DLBCL). The prognosis of lymphoma in patients with cardiac involvement is extremely poor. CAR T-cell immunotherapy has been recently become a highly effective treatment for relapsed or refractory diffuse large B-cell lymphoma. To date, there are no guidelines that provide a clear consensus on the management of patients with secondary heart or pericardial involvement. We report a case of relapsed/refractory DLBCL that secondarily affected the heart.

Case presentation: A male patient was diagnosed with double-expressor DLBCL based on biopsies of mediastinal and peripancreatic masses and fluorescence *in situ* hybridization. The patient received first-line chemotherapy and anti-CD19 CAR T cell immunotherapy, but developed heart metastases after 12 months. Considering his physical condition and economic situation of the patient, two cycles of multiline chemotherapies were administered, followed by CAR-NK cell immunotherapy and allogeneic hematopoietic stem cell transplantation (allo-HSCT) at another hospital. After achieving a six-month survival, the patient died of severe pneumonia.

Conclusion: The response of our patient emphasizes the importance of early diagnosis and timely treatment to improve the prognosis of SCL and serves as an important reference for SCL treatment strategies.

KEYWORDS

cardiac hematological malignancy, secondary cardiac lymphoma, B-cell lymphoma, CAR T-cell immunotherapy, case report

Introduction

Secondary cardiac lymphoma (SCL) is a relatively uncommon cancer that affects the heart and/or pericardium, with mortality rates of approximately 8.5% to 25% (1). It is most common in men, especially in immunosuppressed patients, with a median age of 60 years (2, 3). Among cardiac lymphomas, diffuse large B-cell lymphoma (DLBCL) is the most prevalent histology (80%); other histological subtypes are less common (1, 3, 4). The clinical signs and symptoms of SCL tend to be nonspecific, including the superior vena cava (SVC), dyspnea, constitutional complaints, chest pain and B-symptoms (i.e., weight loss, fatigue, night sweats) and so on, resulting in frequently missed diagnoses (1, 2, 4). As secondary cardiac lymphoma is a rare disease, treatment recommendations are largely derived from retrospective studies and case reports (2, 4). Therapies for cardiac lymphoma include mainly chemotherapy, often combined with radiotherapy, surgery, autologous stem cell transplantation, and T cell therapy with the chimeric antigen receptor (CAR) (1, 5, 6). Chemotherapy with cyclophosphamide, vincristine, doxorubicin, and prednisolone (CHOP) is widely used as first-line treatment, but its overall survival rate (OS) is only 18 months, while patients treated with BACOP (bleomycin + doxorubicin + cyclophosphamide + vincristine + prednisone) have a survival of 49 months. Patients receiving surgical resection have a survival of more than 18 months and those with radiotherapy achieve a survival of 15 months (7). The addition of a monoclonal CD20 antibody (rituximab) to the CHOP protocol has shown potential to increase OS rate (1, 8, 9). Despite the fact that these therapies are associated with the greatest improvement in survival, not every patient receives complete multimodal treatment due to individual factors. Therefore, more effective treatment strategies should be developed to improve the outcomes of patients with cardiac involvement. Here, we report a case of relapsed/refractory DLBCL that secondarily affected the heart and was novelly treated with CAR-NK and allo-HSCT.

Case report

A 59-year-old man came to our hospital on 10 November 2020, complaining of persistent pitting edema of the face and neck that had been occurring for one month, along with night sweats and backaches, with no weight loss, low fever, dyspnea, cough, pitting edema of the lower extremities, and other symptoms. Laboratory test results are as follows: hemoglobin 114 g/L, platelet count 454×10^9/L, LDH 519 IU/L, serum β_2 microglobulin 2.59 mg/L. Chest computed tomography (CT) revealed multiple space-occupying lesions in the middle and upper mediastinum. Positron emission tomography CT (PET-CT) revealed abnormally increased fluorodeoxyglucose (FDG) uptake in the middle and upper mediastinum lymph nodes with a maximum lymph node size of 6.3 × 4.3 cm and the maximum standard uptake value (SUV_{max}) was 13.8, the boundary between cardiovascular vessels and masses was not clear (Figures 1A-C, E, F).

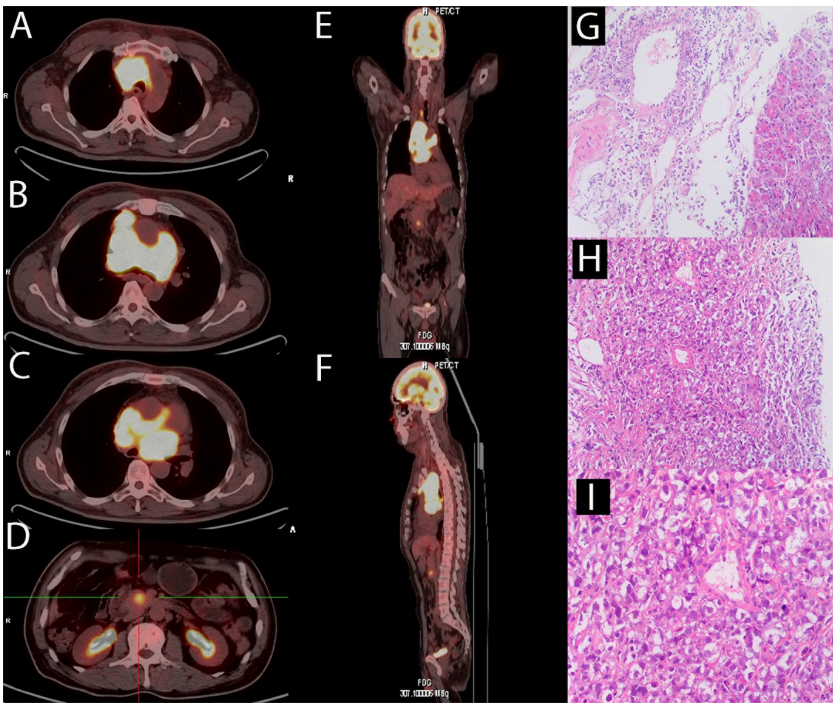

FIGURE 1
At diagnosis of lymphoma, a PET-CT scan and a biopsy were performed. **(A-C)** PET/CT revealed multiple enlarged lymph nodes in the middle and upper mediastinum and the maximum plane size was approximately 6.3 cm x 4.3 cm. There were masses showing infiltration around the ascending aorta and pulmonary artery. The SUVmax was 13.8. **(D)** PET/CT revealed the uncinate process of pancreas infiltration, with a diameter of about 2 cm and the SUVmax was 5.7. **(E, F)** Overall, there is no significant abnormal radiation uptake outside of the pancreas and mediastinal lymph nodes. **(G)**The hematoxylin-eosin staining revealed medium to large cells with irregular nucleus in the pancreas (original magnification 10 x). **(H, I)** The hematoxylin-eosin staining revealed medium to large cells with irregular nucleus in the mediastinum (H:original magnification 10 x; G:original magnification 20 x).

The pancreatic uncinate showed a round focus with high FDG uptake of approximately 2.0 cm in diameter, the SUV_{max} was 5.7 (Figures 1D-F). On 18 November 2020, a CT-guided percutaneous pancreas and mediastinum biopsy was performed. Hematoxylin-eosin staining of pancreatic mases (Figure 1G) and mediastinum (Figures 1H, I) showed medium to large abnormal lymphocytes with irregular nucleus. Immunohistochemical staining revealed that tumor cells were positive for CD19 (>95%), CD3, CD20, CD30, BCL-6, PAX-5, c-Myc, Ki-67 (90%+), and was negative for Syn, CgA, CK, CA199, CK20, CK7, CD56, and BCL-2. Both bone marrow cytology and biopsy results revealed no aberrant lymphocyte infiltration. In summary, the patient was diagnosed with DLBCL at stage IVB. The IPI score was 3 and the ECOG performance status was 1. The immunohistochemistry results revealed a non-germinal center B-cell-like lymphoma (non-GCB) subtype. The patient had no family history of hematological malignancies.

The patient was started on induction chemotherapy with one course of R-CHOP (rituximab 375 mg/m^2 on day 0, doxorubicin 30 mg/m^2 and cyclophosphamide 750 mg/m^2 on day 1, vincristine 2 mg on day 1, and prednisolone 60 mg/m^2 on days 1–5) and three courses of R^2-CHOP (rituximab 375 mg/m^2 on day 0, doxorubicin 30 mg/m^2, cyclophosphamide 750 mg/m^2, and vincristine 2 mg on day 1, prednisolone 60 mg/m^2 on days 1–5, and lenalidomide 25 mg on days 1–21), he achieved partial remission by PET-CT. The patient then received two separate apheresis procedures, including granulocyte colony-stimulating factor (G-CSF)-stimulated autologous hematopoietic stem cell (HSC) collection ($CD34^+$ 4.35×10^6/kg). Followed by three more courses of R^2-CHOP. Unfortunately, although the patient had no obvious symptoms, PET-CT showed progressive disease. To prevent the progression of the disease, he was transferred to another institution for CAR T cell therapy. The patient was given a standard dose of FC (Fludarabine 25mg/m^2 on days -7 to -5, cyclophosphamide 250 mg/m^2 on days -7 to -5) as conditioning regimen one week before CAR-T cell therapy. On 6 September 2021 (day 0), CD19-targeted CAR-T cells (CAR19) ($2.0x10^7$ cells/kg) were infused into the patient. One month after CAR-T cell therapy, a second contrast-enhanced chest CT during follow-up showed that lymph nodes in the middle and upper mediastinum were larger than before. Shortness of breath, palpitations, hypoxemia, and fever ensued. Combined with the history of the disease and PET-CT, he was considered to have a progressive disease. On PET-CT, the largest lymph node was approximately 8.3 cm and the SUV_{max} was 13, the masses fused in the pulmonary gaps and their boundaries were unclear, the Deauville score was 5. He had pneumonia and refractory bilateral pleural effusion; bilateral drainage was performed as a salvage procedure. Cytology, biochemistry, and flow cytometric analysis of the pleural fluid did not show any infiltration of abnormal lymphocytes. As a result of antibiotic therapy, pleural chest drainage, and supportive therapies, the patient's symptoms improved. R-GemOx (gemcitabine 1000 mg/m^2 and oxaliplatin100 mg/m^2 on day 1, and rituximab 375mg/m^2 on day 0) was initiated on 13 November 2021. Three weeks later, the patient's symptoms began to worsen, and the pleural fluid was sent for a circulating tumor DNA (ctDNA) test, which revealed somatic hypermutation (MYC, SOCS1, IGLL5, BTG1, DTX1, PIM1) and high-frequency mutation (TET2, IL4R, ACTG1, B2M, SGK1, HIST1H1E), indicating malignant pleural effusion. Transthoracic echocardiography left ventricular contrast echocardiography (LVO) and myocardial contrast echocardiography (MCE) detected heart metastases (Figures 2A-F). All clinical evidence indicated that the patient's dyspnea and refractory bilateral pleural effusion were due to cardiac metastases; the possibility of thrombi was excluded. The patient was then treated with one cycle of PD-1+BR (sintilimab 200 mg on day 0, rituximab 375 mg/m^2 on day 1, bendamustine 90 mg/m^2 on days 2–3). After that, he was eager to undergo a CAR-T clinical trial for the second time. Unfortunately, at this time his T cell counts were very low. He was then treated with CAR-NK immunotherapy. He was administered the FCM regimen (fludarabine 30 mg/m^2 on days -5, -4, -3, cyclophosphamide 300 mg/m^2 on day -5, melphalan100 mg/m^2 on day -4) regimen five days before CAR-NK. On 31 January 2021 (day 0), CAR-NK cells ($5.6x10^6$ cells/kg) were infused into the patient. On+7d he experienced grade 2 cytokine release syndrome (CRS) and was treated with tocilizumab 8 mg/kg, after which his symptoms improved. One month after CAR-NK immunotherapy, patient white blood cells and lymphocytes did not graft and the copy numbers of the CAR-NK transgene decreased. He experienced a transient reduction in pleural effusion and relief of dyspnea, chest CT showed that the cardiac mass was smaller than before which indicated stable disease. We then informed the patient and his family about his condition and treatment plan, and both signed consent forms for allogeneic hematopoietic stem cell transplantation. He received FBM (fludarabine 30mg/m^2 on days -7 to -2d, busulfan 3.2 mg/kg on days -7, -6, and melphalan100 mg/m^2 on day -2). Graft-versus-host disease (GVHD) prophylaxis consisted of anti-thymocyte globulin 2 mg/kg on day -1, cyclophosphamide 30 mg/kg on days +3 and +4, dexamethasone 40 mg/kg on days +3 and +4, ruxolitinib 5 mg twice a day from on days -1 to +50, 2.5 mg twice a day on days +51 to +100, and 2.5 mg once a day on days +101 to +180, myfortic 720 mg twice a day on days +5 to +34, ciclosporin 15 mg/kg/d (adjusted according to blood concentration), methotrexate 5 mg/m^2 on days +3 and +6d. On 31 March 2022 (day 0), the patient underwent haploid allogeneic hematopoietic stem cell transplantation ($CD34^+$ 6.35×10^6/kg), the donor was his son. Leukocytes and platelet engraftment occurred on day +16. After allo-HSCT, the patient's condition continued to remain stable. 100% donor chimerism was achieved. On 30 April 2022, chest CT showed no new lesions and his pleural effusion decreased significantly. The timeline of clinical treatment and the state of the disease are shown in Figure 3A. However, during this period, he experienced severe fungal pneumonia. Despite multiple antifungal, antibacterial, and antiviral treatments, the patient eventually died from septic shock on 18 June 2022.

Discussion

Cardiac hematological malignancies (CHM), which comprise leukemic, lymphoma infiltration, and extramedullary manifestations of multiple myeloma, are rarer than any other malignant cardiac tumors (3). Primary and secondary cardiac lymphomas are of two varieties (10). Primary cardiac lymphomas, which comprise approximately 0.5% of all lymphomas and approximately 1.3% of

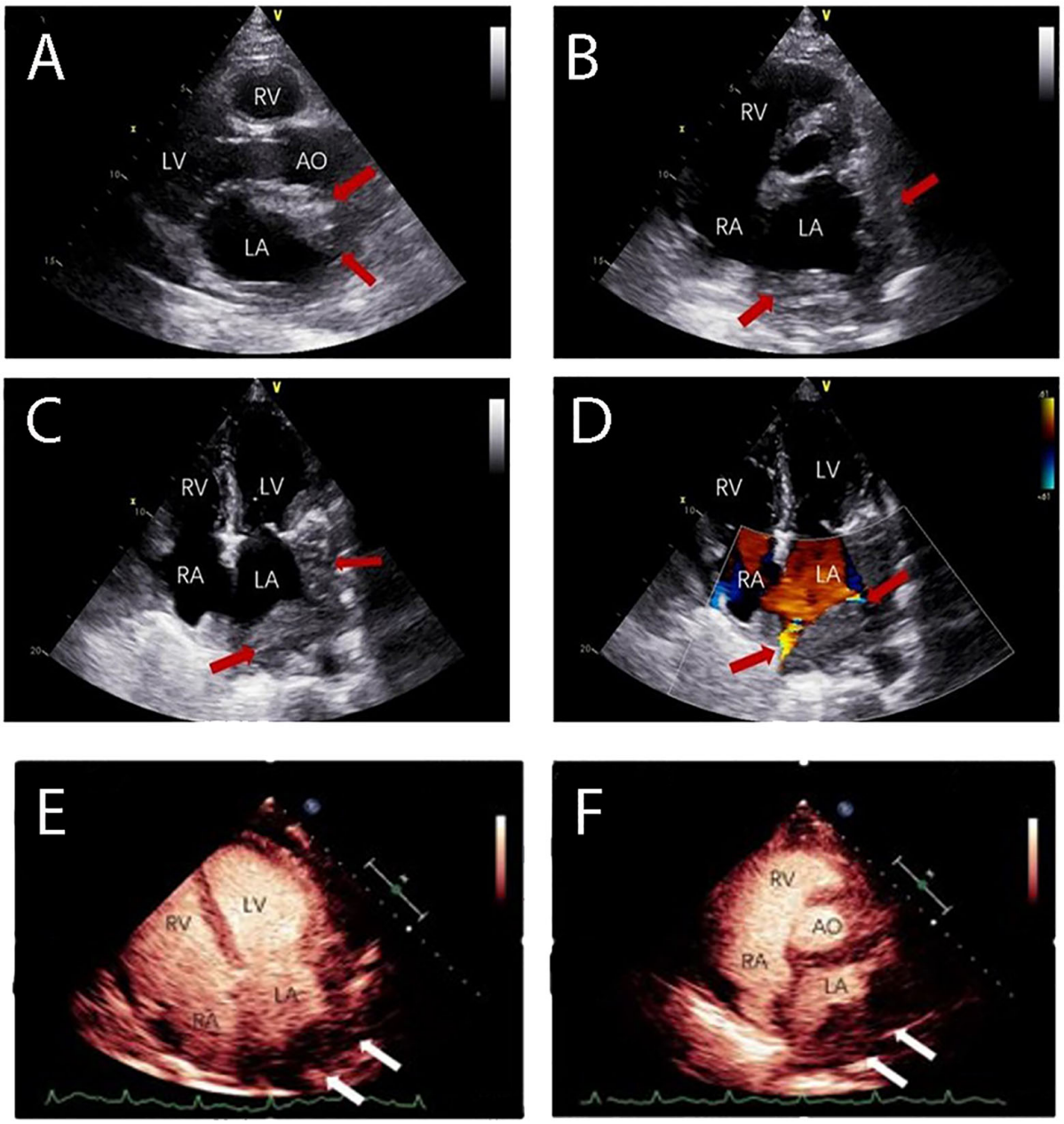

FIGURE 2
The patient experienced dyspnea and had a refractory bilateral pleural effusion after receiving multi-line chemotherapy. Transthoracic echocardiography showed the heart infiltrated by lymphoma. **(A)** Long axis section of left ventricle showing a slight hypoechoic mass in the anterior wall of the left atrium. **(B)** Lateral wall of left atrium and left atrial appendage were infiltrated. **(C, D)** Four-chamber view showed pulmonary vein infiltration. Cardiac ventricular opacification (CVO): **(E, F)** An irregular mass was present at the entrance of pulmonary veins in the left atrium with rapid irregular perfusion and complete enhancement. (LV: Left Ventricle; RA: Right Atrium; RV: Right Ventricle; LA: Left Atrium).

all primary cardiac malignancies, are lymphomas that primarily affect the heart and/or pericardium (49). Secondary cardiac lymphomas, which are 20–40 times more prevalent than initial cardiac lymphomas, account for approximately 5%–20% of disseminated diseases (1, 50). Approximately all cardiac lymphomas have B-cell origins, and DLBCL are the most common type (80%) (1). In a retrospective investigation, DLBCL (58%), T-cell lymphoma (16%), Burkitt lymphoma (9%), and small lymphocytic lymphoma (6%) were the most prevalent histologic subtypes of NHL with biopsy-proven cardiac involvement (4). Here, we reviewed 44 patients with secondary cardiac lymphoma published on PubMed and CNKI between 1976 and 2022 (Table 1). Patients with SCL had an average age of 55 years. SCL is more common in men than in women (64.3% vs 35.7%). DLBCL was the most prevalent NHL subtype in patients with morphologic evidence of cardiac involvement (Figure 3B), accounting for 59.09% of cases, followed by T-cell lymphoma (16%) and Burkitt's lymphoma (2.27%). There is a chance of direct, lymphatic, or hematogenous heart metastases (51).

Since cardiac lymphoma often does not present symptoms or abnormal behavior, its diagnosis is often delayed (51, 52). Depending

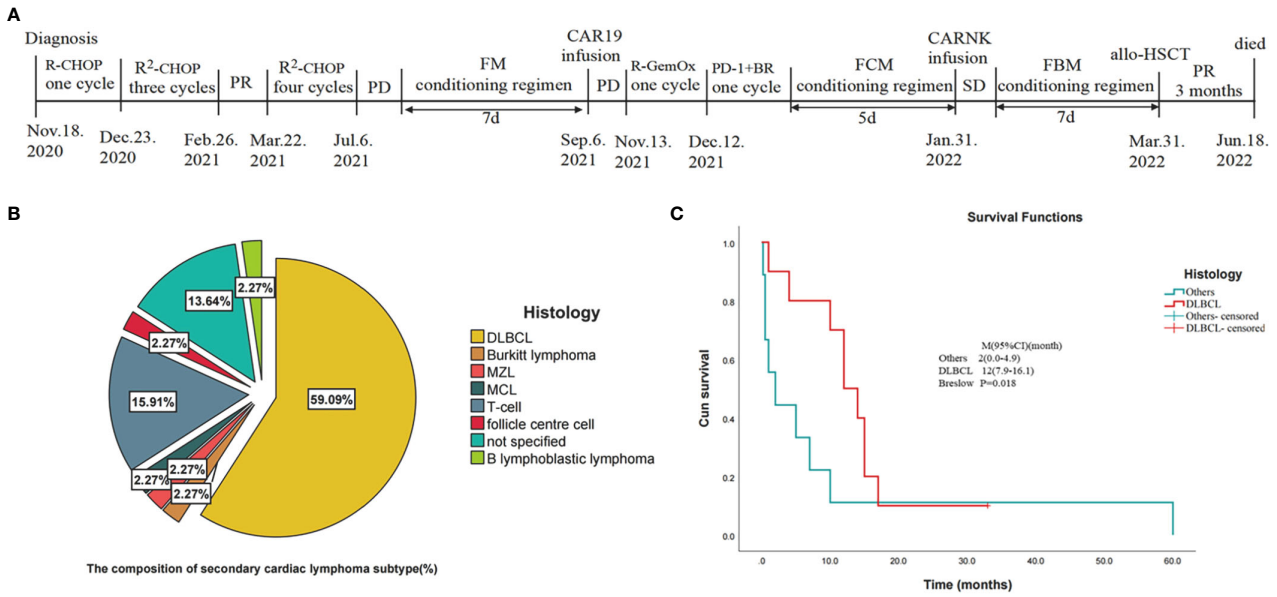

FIGURE 3
Statistical analysis of the data in the literature review (10–48) and the timeline of disease status and corresponding treatment regimens of our patient. **(A)** Timeline of disease status and corresponding treatment regimens. **(B)** Pie chart of tissue type composition of secondary cardiac lymphoma. (DLBCL, diffuse large B-cell lymphoma; MZL, marginal zone lymphoma; MCL, mantle cell lymphoma; T-cell: T cell lymphoma). **(C)** Kaplan-Meier survival curves for secondary cardiac lymphomas comparing DLBCL with other cancers included in the statistics. (CI, confidence interval).

on the location, size, growth rate, degree of invasion, and friability of the tumor, patients with cardiac involvement present with a variety of symptoms (10, 53). Based on our review of the literature, 44 cases of secondary cardiac lymphoma were located (Table 1). More specifically, in decreasing order of frequency, the right atrium, right ventricle, left atrium, and left ventricle were affected more frequently. The patient may have symptoms of right heart failure or superior vena cava syndrome (SVC) if a tumor is found in the right atrium or right ventricle (10). However, shortness of breath is often seen if a large mass occurs in the left atrial or left ventricular region (10). The most common clinical symptom described is dyspnea (64%), followed by constitutional problems (26%) and chest pain (24%) (11, 54). In our review (Table 1), the results are the same. In this case, our patient presented dyspnea, left facial swelling, and tachycardia. This was associated with lymphoma that affected the superior vena cava (SVC) and the pulmonary vein, causing limited venous inflow, which is called SVC syndrome (5–8%) (1). As a result, he was diagnosed with secondary cardiac lymphoma.

When regard to detecting cardiac involvement, ECG and chest radiographs are generally insensitive or nonspecific (51, 55, 56). A transthoracic echocardiogram is the first non-invasive method used to examine the heart and pericardium; however, the small acoustic window of this technology remains a major drawback (53). A study that included PCL patients found that transesophageal echocardiography (TEE) had higher sensitivity than transthoracic echocardiogram (TTE) for the diagnosis of lymphomatous involvement (97% vs 75.9%) (51, 57). With a high degree of spatial and temporal resolution, cardiac masses can be diagnosed by computed tomography (CT) based on their distribution, shape, and size (1). Early detection and treatment of cardiac abnormalities, as well as tracking of chemotherapy response, are now possible thanks to PET/CT (1, 51). The optimum imaging technique to determine whether the malignancy has affected the heart is CMRI (1, 51). Cardiovascular tumors show hypointense in T1-weighted sequences, while appearing hyperintense in T2-weighted sequences (11, 51). If there is a possibility of cardiac involvement, magnetic resonance imaging should be chosen despite the fact that these various imaging modalities should be considered complementary rather than competitive (53, 54).

The prognosis for cardiac lymphoma tends to be extremely poor (1). These neoplasms are often not recognized until postmortem due to their nonspecific symptoms (1). Gordon et al. found that patients with primary cardiac B-cell NHL had better outcomes than those with secondary cardiac involvement (2 months versus 6 months) (4). We found that DLBCL secondary cardiac lymphomas had a better median survival time (MST) compared to non-DLBCL secondary cardiac lymphomas (12 vs 2 months) (Figure 3C). It is important to note that patients who are immunocompromised, have extracardiac disease, left ventricular involvement, and do not have an arrhythmia are the most important adverse prognostic factors (58). Treatment guidelines are not available (58); thus, the treatment of cardiac lymphoma is varied. The medical literature presents a variety of treatment options, including chemotherapy, radiotherapy, surgery, and even autologous stem cell transplantation (1). However, it should be noted that chemotherapy is the most effective treatment and, in many cases, is used only for palliative purposes (2). The main chemotherapeutic regimen for cardiac lymphoma is CHOP (1). Adding the monoclonal CD20 antibody rituximab and other monoclonal therapies has been shown to increase overall survival rates (1). Cardiac lymphoma is also sensitive to radiotherapy (59). Radiation is, however, restricted to cardiac masses that progress despite chemotherapy due to cardiovascular side effects (2). Yang et al. suggested that the overall response rate to secondary cardiac lymphoma was 63.2% and the median survival time was 18 months. Petrich et al. reported that the overall response rate of primary cardiac

TABLE 1 Clinical characteristics of patients with cardiac lymphoma reported to date (10–48).

Characteristics	
Age, n (%)	
16-60	21 (47.7)
>60	23 (52.3)
Male sex, n (%)	27(64.3)
Lymphoma type, n (%)	
B cell	31(70.4)
T cell Not specified	8(18.2) 5 (11.4)
Previous HIV/AIDS, n (%)	
Yes	17(38.6)
No	7 (15.9)
Unknown	20(45.5)
Clinical symptoms, n (%)	
Dyspnea	23(63.9)
Fatigue	5 (13.9)
Abdominal pain	4(11.1)
Fever	4(11.1)
Cough	3(8.3)
Chest tightness	3(8.3)
Palpitation	3(8.3)
Dysphagia	2(5.6)
Weight loss	2(5.6)
Night sweat	2(5.6)
Others	7(15.6)
Mass localization in the heart, n (%)	
Left atrium	6(14.3)
Left ventricle	7(16.7)
Right atrium	17(40.5)
Right ventricle	7(16.7)
Tricuspid valve	3(7.14)
Epicardium	1(2.3)
Pericardium	2(4.8)
Atrial septum	3(7.14)
Endomyocardium	1(2.3)
Septal myocardium	1(2.3)
Right myocardial wall	1(2.3)

lymphoma to chemotherapy was 79% and complete remission was 59% (57). Similar results have been reported for secondary lymphoma (57). The management of patients with R/R DLBCL has improved significantly in the last year (60). Various novel antibodies, ADCs, specific small-molecule inhibitors, as well as CAR-T cells, have been approved for the treatment of affected patients (61, 62). The outlook for cardiac lymphoma remains poor (1).

Conclusion

Lymphoma metastases to the heart are rare and are associated with a poor prognosis. We report a case of secondary cardiac lymphoma and analyze published case reports. Unfortunately, our patient was unable to undergo an endomyocardial biopsy due to his poor physical condition. Despite the rapid changes in currently available treatment options, the prognosis for cardiac lymphoma remains poor. Various treatments appeared to have improved our patient, but he unfortunately died of severe pneumonia in the end. Therefore, early diagnosis and timely treatment are still significant for improving survival. And our experience has shown that early allo-HSCT has an irreplaceable role in the survival benefit of patients. When an individual has a history of recurrent pleural effusions, dyspnea, and lymphoma, cardiac infiltration should be considered. To improve patient survival, additional treatment options should be explored.

Patient perspective

Despite the death outcome, the encouragement and optimism of the patient's family (particularly his son) inspired him to confront the disease. Throughout the treatment procedure, he showed a determined will to survive. He was willing to attempt a variety of treatments that may have been more effective but also riskier. With regard to the disease and treatment, he and his family expressed gratitude to our hospital and doctors.

Data availability statement

The original contributions presented in the study are included in the article/supplementary material. Further inquiries can be directed to the corresponding author.

Ethics statement

Written informed consent was obtained from the individual(s) for the publication of any potentially identifiable images or data included in this article.

Author contributions

YY wrote the manuscript and analyzed the data. MS, YY, and ZL revised the manuscript and processed images. YL, MS, YY, and ZL diagnosed and treated the patient. YZ operated cardiac ultrasound and elaborated the picture of cardiac ultrasound. MS funded the research. All authors contributed to the article and approved the submitted version.

Funding

The present study was supported by the National Natural Science Foundation of China (No. 81760035).

Acknowledgments

The authors would like to acknowledge all who contributed to case diagnosis, therapy, and decision-making. Acknowledgment is given to the hospital of First Affiliated Hospital of Kunming Medical University, Kunming, China and especially for the department of Hematology and cardiology.

Conflict of interest

The authors declare that the research was conducted in the absence of any commercial or financial relationships that could be construed as a potential conflict of interest.

Publisher's note

All claims expressed in this article are solely those of the authors and do not necessarily represent those of their affiliated organizations, or those of the publisher, the editors and the reviewers. Any product that may be evaluated in this article, or claim that may be made by its manufacturer, is not guaranteed or endorsed by the publisher.

References

1. Jeudy J, Burke AP, Frazier AA. Cardiac lymphoma. *Radiol Clin North Am* (2016) 54 (4):689–710. doi: 10.1016/j.rcl.2016.03.006

2. Bonelli A, Paris S, Bisegna S, Milesi G, Gavazzi E, Giubbini R, et al. Cardiac lymphoma with early response to chemotherapy: A case report and review of the literature. *J Nucl Cardiol* (2021) 29(6):3044–56. doi: 10.1007/s12350-021-02570-5

3. Voigt P, Wienbeck S, Weber M-A, Oyama-Manabe N, Beimler M, Schob S, et al. Cardiac hematological malignancies: Typical growth patterns, imaging features, and clinical outcome. *Angiology* (2018) 69(2):170–6. doi: 10.1177/0003319717713581

4. Gordon MJ, Danilova O, Spurgeon S, Danilov AV. Cardiac non-hodgkin's lymphoma: Clinical characteristics and trends in survival. *Eur J Haematol* (2016) 97 (5):445–52. doi: 10.1111/ejh.12751

5. Ikeda H, Nakamura S, Nishimaki H, Masuda K, Takeo T, Kasai K, et al. Primary lymphoma of the heart: Case report and literature review. *Pathol Int* (2004) 54(3):187–95. doi: 10.1111/j.1440-1827.2003.01606.x

6. Miller DV, Firchau DJ, McClure RF, Kurtin PJ, Feldman AL. Epstein-Barr Virus-associated diffuse Large b-cell lymphoma arising on cardiac prostheses. *Am J Surg Pathol* (2010) 34(3):377–84. doi: 10.1097/PAS.0b013e3181ce9128

7. Hsueh S-C, Chung M-T, Fang R, Hsiung M-C, Young M-S, Lu H-F. Primary cardiac lymphoma. *J Chin Med Assoc* (2006) 69(4):169–74. doi: 10.1016/S1726-4901(09)70200-X

8. Morillas P, Quiles J, Nuñez D, Senent C, Martínez S, Fernández JA, et al. Complete regression of cardiac non-Hodgkin lymphoma. *Int J Cardiol* (2006) 106(3):426–7. doi: 10.1016/j.ijcard.2005.01.020

9. Takenaka S, Mitsudo K, Inoue K, Goto T, Kadota K, Fujii S, et al. Successful treatment of primary cardiac lymphoma with atrioventricular nodal block. *Int Heart J* (2005) 46(5):927–31. doi: 10.1536/ihj.46.927

10. Kondo S, Osanai H, Sakamoto Y, Uno H, Tagahara K, Hosono H, et al. Secondary cardiac lymphoma presenting as sick sinus syndrome and atrial fibrillation which required leadless pacemaker implantation. *Intern Med* (2021) 60(3):431–4. doi: 10.2169/internalmedicine.5573-20

11. Lucchini E, Merlo M, Ballerini M, Porcari A, Sinagra G, Pagnan L, et al. Case report: Cardiac involvement by lymphoma: Rare but heterogeneous condition with challenging behaviors. *Front Oncol* (2021) 11:665736. doi: 10.3389/fonc.2021.665736

12. Opherk JP, Lotz J, Galanski M. [Cardiac infiltration as complication of cutaneous T-lymphoblastic non-hodgkin's lymphoma]. *Rofo* (2007) 179(2):175–6. doi: 10.1055/s-2006-927233

13. Khalid K, Faza N, Lakkis NM, Tabbaa R. Cardiac involvement by burkitt lymphoma in a 49-Year-Old man. *Tex Heart Inst J* (2020) 47(3):210–2. doi: 10.14503/THIJ-17-6448

14. Baek Y-S, Shin S-H, Yi H-G, Kim D-H, Woo S-I, Park K-S, et al. Cardiac involvement in Cd56 negative primary pancreatic extranodal Nk/T-cell lymphoma, nasal type, presenting with ventricular tachycardia during the early stages of chemotherapy. *Intern Med* (2014) 53(20):2333–6. doi: 10.2169/internalmedicine.53.2764

15. Sanna P, Bertoni F, Zucca E, Roggero E, Passega Sidler E, Fiori G, et al. Cardiac involvement in hiv-related non-hodgkin's lymphoma: A case report and short review of the literature. *Ann Hematol* (1998) 77(1-2):75–8. doi: 10.1007/s002770050416

16. Magagnoli M, Nozza A, Romano Lutman F, Santoro A. Cardiac involvement in non-hodgkin's lymphoma. *Br J Haematol* (2002) 119(4):887. doi: 10.1046/j.1365-2141.2002.03868.x

17. Khan NUA, Ahmed S, Wagner P, Rumley RL, Movahed A. Cardiac involvement in non-hodgkin's lymphoma: With and without hiv infection. *Int J Cardiovasc Imaging* (2004) 20(6):477–81. doi: 10.1007/s10554-004-2783-1

18. Nagayama H, Sueyoshi E, Hayashida T, Sakamoto I, Taguchi J, Kudo T, et al. Cardiac involvement of adult T-cell Leukemia/Lymphoma. *Can J Cardiol* (2012) 28 (4):516.e9–516.e10. doi: 10.1016/j.cjca.2011.11.013

19. Baeßler B, Rudolph V, Friedrichs N, Maintz D, Bunck AC. Case of myocardial relapse of a T-cell lymphoma after hematopoietic stem cell transplantation demonstrated by cardiovascular magnetic resonance and endomyocardial biopsy. *Circulation* (2014) 130 (6):e44–e7. doi: 10.1161/CIRCULATIONAHA.114.010065

20. Kawasaki H, Shigeno K, Ohnishi K, Tsuchida T, Miura K, Kato T, et al. A case of primary cutaneous natural Killer/T-cell lymphoma, nasal type, directly invading to the heart. *Leuk Lymphoma* (2008) 49(5):1008–11. doi: 10.1080/10428190801947518

21. Wiernik PH, Sutherland JC, Stechmiller BK, Wolff J. Clinically significant cardiac infiltration in acute leukemia, lymphocytic lymphoma, and plasma cell myeloma. *Med Pediatr Oncol* (1976) 2(1):75–85. doi: 10.1002/mpo.2950020109

22. Liang R, Yu CM, Au WY, Choy CK, Kwong YL. Diagnosis in oncology. case 2: Secondary lymphoma of the heart manifesting as intracavitary masses. *J Clin Oncol* (2000) 18(9):1998–9.

23. Ban-Hoefen M, Zeglin MA, Bisognano JD. Diffuse Large b cell lymphoma presenting as a cardiac mass and odynophagia. *Cardiol J* (2008) 15(5):471–4.

24. Gurunathan S, Ahmed A, Aqel N, Vamvakidou A, Karogiannis N, Senior R. Giant lymphomatous cardiac mass: *In vivo* imaging and histological findings. *Int J Cardiol* (2016) 202:81–3. doi: 10.1016/j.ijcard.2015.08.151

25. Lal KS, Tariq RZ, Okwuosa T. Haemodynamic instability secondary to cardiac involvement by lymphoma. *BMJ Case Rep* (2016) 2016:bcr2016215775. doi: 10.1136/bcr-2016-215775

26. Rogowitz E, Babiker HM, Krishnadasan R, Jokerst C, Miller TP, Bookman M. Heart of lymphoma: Primary mediastinal Large b-cell lymphoma with endomyocardial involvement. *Case Rep Oncol Med* (2013) 2013:814291. doi: 10.1155/2013/814291

27. Tsubokura M, Asada N, Odawara J, Aoki T, Yamakura M, Takeuchi M, et al. Identification of cardiac metastasis of primary gastric diffuse Large b-cell lymphoma. *Br J Haematol* (2007) 137(3):179. doi: 10.1111/j.1365-2141.2007.06511.x

28. Sibbing D, Barthel P, Abbrederis K, Dennig K, Gaa J. Intracardiac right ventricular metastatic tumor of malignant T-cell lymphoma. *Int J Cardiol* (2007) 117(2):e84–e5. doi: 10.1016/j.ijcard.2006.11.191

29. Cohen Y, Ne D, Libster D, Gillonb D, Polliack A. Large B-cell lymphoma manifesting as an invasive cardiac mass: Sustained local remission after combination of methotrexate and rituximab. *Leuk Lymphoma* (2002) 43(7):1485–7. doi: 10.1080/1042819022386699

30. Hafeez I, Alai MS, Iqbal K, Aslam K, Lone A, Bhat IA, et al. Lymphoma presenting as severe left ventricular systolic dysfunction: A case report. *Oman Med J* (2014) 29 (3):223–5. doi: 10.5001/omj.2014.55

31. Kanesvaran R, Tao M, Huat ITB, Weng DTS, Eng DNC, Thye LS. Malignant arrhythmia: A case report of nasal Nk/T-cell lymphoma with cardiac involvement. *Acta Oncol* (2009) 48(4):637–9. doi: 10.1080/02841860902740923

32. Morgan R, Murdock R, Leng P. A man in his 50s presenting with rapid-onset dyspnea and obstructive shock. *Chest* (2018) 154(6):e153–e6. doi: 10.1016/j.chest.2018.07.048

33. Kumar A, Puvvada S. Mantle cell lymphoma presenting as cardiac tamponade. *Blood* (2015) 126(10):1255. doi: 10.1182/blood-2015-03-626051

34. Harris S, Waddell J. Non-hodgkin's lymphoma: An unusual cause of myocardial infarction and hypercalcaemia. *Clin Oncol (R Coll Radiol)* (1993) 5(3):189–90. doi: 10.1016/S0936-6555(05)80328-0

35. Weijs LE, Arsos G, Baarslag HJ, Wittebol S, de Klerk JM. Pericardial involvement in a non-Hodgkin lymphoma patient: Coregistered fdg-pet and ct imaging. *Eur Heart J* (2007) 28(22):2698. doi: 10.1093/eurheartj/ehm218

36. Manabe M, Yoshii Y, Mukai S, Sakamoto E, Kanashima H, Nakao T, et al. Precursor b-lymphoblastic lymphoma involving an intracardiac mass and myocardial infiltration: A case report. *Intern Med* (2012) 51(3):315–9. doi: 10.2169/internalmedicine.51.6075

37. Yamamoto E, Tomita N, Ishigatsubo Y. Primary diffuse Large b-cell lymphoma of the testis relapsing in the right atrium. *Br J Haematol* (2015) 168(4):469. doi: 10.1111/bjh.13212

38. Zlotchenko G, Futuri S, Dillon E, Machnicki S. A rare case of lymphoma involving the tricuspid valve. *J Cardiovasc Comput Tomogr* (2013) 7(3):207–9. doi: 10.1016/j.jcct.2013.05.007

39. Panareo S, Urso L, Santi I, Rigolin GM, Cuneo A, Cittanti C, et al. Right atrium mass assessed with 18f-fdg Pet/Ct scan turns out to be an uncommon relapse of testicular diffuse Large b-cell lymphoma: A case report. *Diagn (Basel)* (2020) 10(11):987. doi: 10.3390/diagnostics10110987

40. Johnston ID, Popple AW. Right ventricular outflow tract obstruction secondary to small intestinal lymphoma. *Br Heart J* (1980) 43(5):593–6. doi: 10.1136/hrt.43.5.593

41. Donnelly MS, Weinberg DS, Skarin AT, Levine HD. Sick sinus syndrome with seroconstrictive pericarditis in malignant lymphoma involving the heart: A case report. *Med Pediatr Oncol* (1981) 9(3):273–7. doi: 10.1002/mpo.2950090311

42. Cove M, Johnston R, Cowan R, Haji-Michael P. Symptomatic, obstructive cardiac metastasis can respond to chemotherapy. *Am J Med* (2009) 122(5):e5–6. doi: 10.1016/j.amjmed.2008.12.013

43. Yoshihara M, Itamura H, Fukushima N, Itoh M, Furukawa K, Nagatomo D, et al. Therapeutic management in cardiac lymphoma. *Leuk Lymphoma* (2014) 55(5):1215–7. doi: 10.3109/10428194.2013.828355

44. Lin Y-S, Chu P-H, Kuo M-C, Jung S-M, Lim K-E, Kuo C-T, et al. Use of a b-type natriuretic peptide in evaluating the treatment response of a relapsed lymphoma with cardiac involvement. *Int J Hematol* (2006) 83(1):44–6. doi: 10.1532/IJH97.A10502

45. Takaya T, Takeuchi Y, Nakajima H, Nishiki-Kosaka S, Hata K, Kijima Y, et al. Usefulness of transesophageal echocardiographic observation during chemotherapy for cardiac metastasis of non-Hodgkin lymphoma complicated with left ventricular diastolic collapse. *J Cardiol* (2009) 53(3):447–52. doi: 10.1016/j.jjcc.2008.08.009

46. Chemello D, Raupp-da-Rosa P, Teló G, Clausell N. Ventricular tachycardia associated with non-hodgkin's lymphoma. *Arq Bras Cardiol* (2011) 97(6):e132–e4. doi: 10.1590/S0066-782X2011001500017

47. Sen Z, Yunxiang C, Guihua Y, Wenhao D. Echocardiographic follow-up of a case of secondary atrial septal lymphoma during chemotherapy. *Chin J Misdiagn* (2019) 14 (05):232–3.

48. Liqun W, Yaqi M, Jie L, Lu S, Xin S, Aitao G. Clinicopathological analysis of 4 cases of cardiac lymphoma. *Chin J Diagn Pathol* (2019) 26(12):793–6.

49. Travis WD, Brambilla E, Burke AP, Marx A, Nicholson AG. Introduction to the 2015 world health organization classification of tumors of the lung, pleura, thymus, and heart. *J Thorac Oncol* (2015) 10(9):1240–2. doi: 10.1097/JTO.0000000000000663

50. Yang C-C, Tsai H-W, Lai S-T, Wu HC, Lo C-Y, Chang Y. Mediastinal diffuse Large b-cell lymphoma invading the left atrium mimicking coronary artery disease with a mural thrombus. *J Chin Med Assoc* (2012) 75(11):606–9. doi: 10.1016/j.jcma.2012.08.009

51. Al-Mehisen R, Al-Mohaissen M, Yousef H. Cardiac involvement in disseminated diffuse Large b-cell lymphoma, successful management with chemotherapy dose reduction guided by cardiac imaging: A case report and review of literature. *World J Clin cases* (2019) 7(2):191–202. doi: 10.12998/wjcc.v7.i2.191

52. Poterucha TJ, Kochav J, O'Connor DS, Rosner GF. Cardiac tumors: Clinical presentation, diagnosis, and management. *Curr Treat Options Oncol* (2019) 20(8):66. doi: 10.1007/s11864-019-0662-1

53. Ito K, Nishimura Y, Tanaka H, Tejima T. Epicardial pacemaker implantation for sick sinus syndrome in a patient with supra vena cava obstructed by a primary cardiac lymphoma. *J Cardiol cases* (2020) 21(6):234–7. doi: 10.1016/j.jccase.2020.03.007

54. Ryu SJ, Choi BW, Choe KO. Ct and Mr findings of primary cardiac lymphoma: Report upon 2 cases and review. *Yonsei Med J* (2001) 42(4):451–6. doi: 10.3349/ymj.2001.42.4.451

55. Faganello G, Belham M, Thaman R, Blundell J, Eller T, Wilde P. A case of primary cardiac lymphoma: Analysis of the role of echocardiography in early diagnosis. *Echocardiography* (2007) 24(8):889–92. doi: 10.1111/j.1540-8175.2007.00472.x

56. McDonnell PJ, Mann RB, Bulkley BH. Involvement of the heart by malignant lymphoma: A clinicopathologic study. *Cancer* (1982) 49(5):944–51. doi: 10.1002/1097-0142(19820301)49:5<944::AID-CNCR2820490519>3.0.CO;2-C

57. Petrich A, Cho SI, Billett H. Primary cardiac lymphoma: An analysis of presentation, treatment, and outcome patterns. *Cancer* (2011) 117(3):581–9. doi: 10.1002/cncr.25444

58. O'Mahony D, Peikarz RL, Bandettini WP, Arai AE, Wilson WH, Bates SE. Cardiac involvement with lymphoma: A review of the literature. *Clin Lymphoma Myeloma* (2008) 8(4):249–52. doi: 10.3816/CLM.2008.n.034

59. Reynen K, Köckeritz U, Strasser RH. Metastases to the heart. *Ann Oncol* (2004) 15 (3):375–81. doi: 10.1093/annonc/mdh086

60. Qian Y, Wen T, Li Z. Clinical analysis of 65 patients with secondary lymphoma of heart. *Cancer Res On Prev Treat* (2004) 031(007):424–425,432. Huaihua, China.

61. Sehn LH, Salles G. Diffuse Large b-cell lymphoma. *N Engl J Med* (2021) 384 (9):842–58. doi: 10.1056/NEJMra2027612

62. Vic S, Lemoine J, Armand P, Lemonnier F, Houot R. Transplant-ineligible but chimeric antigen receptor T-cells eligible: A real and relevant population. *Eur J Cancer* (2022) 175:246–53. doi: 10.1016/j.ejca.2022.08.019

frontiers | Frontiers in Oncology

TYPE Case Report
PUBLISHED 31 January 2023
DOI 10.3389/fonc.2022.1018250

OPEN ACCESS

EDITED BY
Arpad Szallasi,
Semmelweis University, Hungary

REVIEWED BY
Ting Niu,
Sichuan University, China
Fen Zhou,
Huazhong University of Science and Technology, China

*CORRESPONDENCE
Liangchun Hao
shengjing_wrn@126.com

†These authors have contributed equally to this work and share first authorship

SPECIALTY SECTION
This article was submitted to Hematologic Malignancies, a section of the journal Frontiers in Oncology

RECEIVED 17 August 2022
ACCEPTED 17 November 2022
PUBLISHED 31 January 2023

CITATION
Wang R, Wang W, Liu X, Wang H, Zhang B, Li S, Zhang H, Yang J, Zhao J, He Q, Zhang J, Liu D and Hao L (2023) Treatment for a B-cell acute lymphoblastic leukemia patient carrying a rare *TP53* c.C275T mutation: A case report. *Front. Oncol.* 12:1018250. doi: 10.3389/fonc.2022.1018250

Treatment for a B-cell acute lymphoblastic leukemia patient carrying a rare *TP53* c.C275T mutation: A case report

Runan Wang[1†], Wenliang Wang[2†], Xuan Liu[3], Huan Wang[1], Bin Zhang[1], Shuang Li[1], Haining Zhang[1], Jiawei Yang[1], Jishun Zhao[1], Qiuying He[1], Jihong Zhang[3], Danping Liu[2] and Liangchun Hao[1*]

[1]Department of Pediatrics, Shengjing Hospital of China Medical University, Shengyang, Liangning, China, [2]Precision Targeted Therapy Discovery Center, Institute of Technology Innovation, Hefei Institutes of Physical Science, Chinese Academy of Sciences, Hefei, Anhui, China, [3]Hematology Laboratory, Shengjing Hospital of China Medical University, Shengyang, Liangning, China

TP53 mutations are associated with poor prognosis in the vast majority of cancers. In this study, we present a pediatric B-cell acute lymphoblastic leukemia (B-ALL) patient carrying a rare *TP53* c.C275T mutation. This extremely rare mutation affects an amino acid residue located between the TAD domain and the DNA-binding domain of p53. The patient was resistant to most conventional chemotherapy regimens and remained minimal residual disease (MRD)-positive after five rounds of such regimens. We tested the sensitivity of the patient's leukemic cells to 21 anti-cancer drugs by performing *in vitro* drug sensitivity assays. The results showed that bortezomib had a very strong killing effect on the patient's leukemic cells. Therefore, we subsequently treated the patient with bortezomib combined with vindesine, cytarabine, and fludarabine. After one course of treatment, the patient became MRD-negative, and there was no recurrence during a 9-month follow-up. In conclusion, our report suggests that the *TP53* c.C275T mutation is associated with poor prognosis in B-ALL. Fortunately, bortezomib combined with chemotherapy could achieve a better therapeutic effect than conventional regimens in this type of ALL.

KEYWORDS

B-cell acute lymphoblastic leukemia, TP53 c.C275T mutation, bortezomib, MRD, children

Introduction

B-cell acute lymphoblastic leukemia (B-ALL) is a type of ALL caused by malignant transformation and cloning of B-cell precursors in the bone marrow and thymus (1–3). Patients with B-ALL usually present with symptoms such as infection, anemia, hemorrhage, and tissue infiltration, which arise owing to the destruction of normal hematopoietic function and the accumulation of tumor cells (4–6).

B-ALL is the most common type of ALL in children, and nearly 20% of B-ALL patients relapse and die from the disease (7, 8). Children with relapsed B-ALL have poor prognosis, with overall survival rates as low as 35% to 40% even after intensive chemotherapy or stem cell transplantation (9, 10). Minimal residual disease (MRD) is an important factor leading to chemotherapy resistance and tumor recurrence in B-ALL. Targeted treatment has shown improved efficacy in MRD-positive pediatric B-ALL patients (11, 12).

Genetic alterations affecting genes involved in cell proliferation, cell differentiation, and apoptosis have been implicated in ALL. These genetic alterations include chromosomal rearrangements, chromosomal gains or losses, deletions, and point mutations (13, 14). Only 6% to 8% of *TP53* genetic alterations have been identified in ALL patients (15). These *TP53* mutations were mainly identified in relapsed lesions of pediatric ALL patients and were associated with poor therapy responses. Common mutations in *TP53* include R175H, H179R, H193R, V216M, G245S, and R273C. Although the roles of these common mutations in tumors have been extensively studied and reported (16–19), the role of rare *TP53* mutations in ALL has not been thoroughly investigated.

Herein, we present a case report of a pediatric B-ALL patient carrying a rare *TP53* c.C275T mutation. We summarize the clinical features of this patient and the efficacy of our treatment regimens, thereby providing a reference for the diagnosis and management of pediatric B-ALL patients carrying this mutation.

Case presentation

A 2-year-old girl was admitted to our hospital on July 28, 2020, owing to persistent lymph node enlargement for 3 months. She had no family history of genetic disorders. Laboratory evaluation demonstrated a white blood cell count of 5.39×10^9/L, a hemoglobin level of 92 g/L, a platelet count of 90×10^9/L, a neutrophil ratio of 0.8%, and a lymphocyte ratio of 89.6%. Notably, immature cells accounted for 85% of peripheral blood cells. Bone marrow aspiration was performed and revealed hypercellularity with predominant blasts, which was in accordance with the bone marrow findings of L2-type ALL (Figure 1A). Flow cytometry showed that the blasts were mainly positive for CD45min, CD34, CD10, CD19, CD9, CD56, CD22, CD58, CD81, cCD79a, and HLA-DR, partially positive for CD79b and cTdT, and negative for CD7, CD117, CD33, CD13, CD20, CD15, CD38, cIgM, and MPO, indicating a diagnosis of early-stage B-ALL (Figure 1B). Karyotyping analysis of the peripheral blood illustrated that the patient had normal karyotype (Figure 1C). Reverse transcription PCR covering the 72 commonly detected fusion genes in leukemia was performed on the bone marrow sample and detected no gene fusion (Supplementary Table 1). Next-generation sequencing covering the 236 commonly mutated genes in ALL was performed and identified a *KDM6B* (NM_001080424) mutation: exon 22: c.C5042A (p.S1681X) (48.31%) and a *TP53* (NM_000546) mutation: exon 4: c.C275T (p.P92L) (50.46%) (Supplementary Table 2).

Chemotherapy schemes received by the patient are shown in Figure 1D. On day 30 after the first induction, there were still 39.6% blasts in the bone marrow as revealed by flow cytometry, suggesting resistance to routine chemotherapy. For economic reasons, family members refused bone marrow transplantation and CAR-T therapy and insisted on chemotherapy despite persistent MRD positivity. Then, we modified the induction chemotherapy regimen. At the same time, a second course of induction therapy was given to the patient. However, by day 30 after the second induction, the patient had still failed to achieve complete remission (CR), with 5.7% blasts in the bone marrow. Afterwards, the patient received three additional rounds of induction therapy but was still MRD-positive, as detailed in Figure 1F. Overall, the patient was failed to achieve CR after five rounds of induction therapy. Then, leukemic cells were obtained from bone marrow aspirates of the patient by Ficoll density gradient centrifugation and cultured in ALL complete medium (Precedo, Hefei, China) for drug sensitivity analysis of a panel of 21 anti-cancer drugs, including targeted therapy drugs, and antibody drugs (the 21 anti-cancer drugs are listed in Supplementary Table 3). The drug concentrations in the *in vitro* experiment were converted according to the dose and Css data from clinical trials. The results showed that the patient's leukemic cells were resistant to most of the drugs commonly used in ALL treatment, which was consistent with our *in vivo* results (Supplementary Table 3). Drugs with an inhibition rate greater than 50% are shown in Figure 1E. Finally, the patient received the scheme vincristine 1.5 mg/m^2 day 1 + cytarabine 2000 mg/m^2 days 1-3 + bortezomib 1 mg/m^2 days 1 and 5, + fludarabine 25 mg/m^2 days 1 -5, and achieved CR and became MRD-negative. Then, two cycles of the same scheme were given as consolidation chemotherapies. Owing to personal reasons, the patient did not receive a subsequent bone marrow transplantation and was discharged from the hospital for maintenance treatment (vincristine 1.5 mg/m^2 day 1 + dexamethasone 8 mg/m^2 days 1 - 5 + methotrexate 25 mg/m^2 days 8, 15 and 22 + mercaptopurine 50 mg/m^2 days 8-28) and was followed up regularly every 1-2 months. The patient

10.3389/fonc.2022.1018250

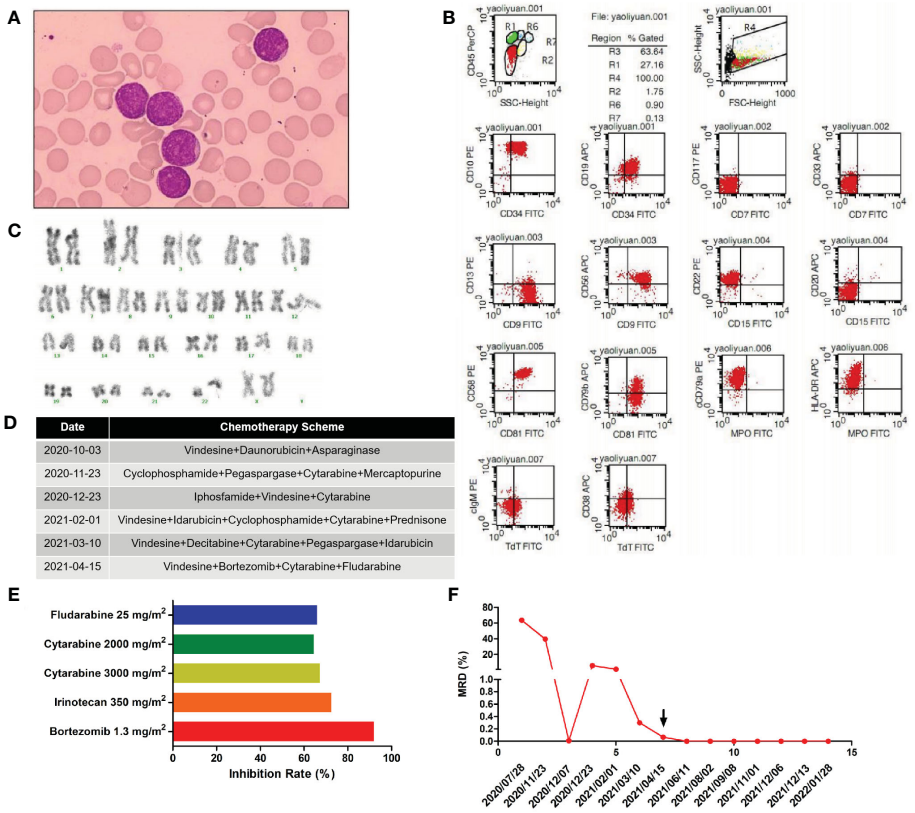

FIGURE 1
(A) Morphology of the patient's lymphoblasts (scale: 10×). **(B)** Results of our flow cytometry analysis. **(C)** Karyotype analysis for this patient. **(D)** Treatment flow chart. **(E)** Sensitivity of the patient's leukemic cells to 21 drugs tested. Drugs with a relative inhibition rate higher than 50% are listed. **(F)** MRD values during the treatment period.

remained leukemia-free and MRD-negative at 9-month follow-up and was lost to follow-up thereafter.

Discussion

ALL is the most common type of childhood cancer worldwide and chemotherapy is the main treatment for this malignancy. Although the current 5-year survival rate of children with ALL is as high as 80%-90%, 15%-20% of children with ALL will experience relapse (20, 21). After recurrence, the 5-year survival rate is only 30%-40%. Drug resistance-associated recurrence is an important cause of treatment failure in pediatric ALL (22–24). Deciphering the mechanisms of drug resistance and relapse in pediatric ALL and optimizing the current treatment plans have become the focus of research in this field.

TP53 has long been a "star" gene in the field of cancer research. About half of malignant tumor types are associated with *TP53* mutations (25). There are various types of *TP53* gene mutations, including deletions, insertions, and missense point mutations. Among them, missense point mutations account for up to 80% of all mutations. There are two mechanisms by which point mutations affect the interaction between p53 and DNA. One is that certain p53 mutations, such as those affecting residues Arg248 and Arg273, impede the contact between p53 and DNA. The other is that some mutations (such as those affecting Arg175, Gly245, Arg249, and Arg282 residues) of p53 prevent the protein from folding properly and binding tightly to DNA, thereby destroying the protein's tumor suppressor ability. p53 mutants not only lose their tumor-suppressing activity but also have disrupted the function of wild-type p53 proteins, which further promotes the progression of tumors (26–28). For example, myelodysplastic syndrome and acute myeloid leukemia patients with *TP53* mutations were found to have poor chemotherapy response and short remission period, especially those with biallelic mutations of *TP53* and those with complex karyotypes, who were more prone to relapse even after bone marrow transplantation (29, 30).

In ALL, *TP53* is altered at a frequency of 19% and mutated at a frequency of only 8% (15). In relapsed ALL, however, the *TP53*

mutation frequency rises to about 10% and represents a strong and independent predictor of treatment failure. Around 80% of *TP53* point mutations affect the DNA-binding domain of the protein. In this study, we identified a c.C275T mutation in *TP53*. This mutation converts Pro 92, an amino acid residue located between the TAD domain and the DNA-binding domain of p53, into leucine. Although we did not investigate the effect of this mutation on the function of the p53 protein, we found that our B-ALL patient with this mutation had severe disease and had failed to fully respond to most clinical treatments. So far, there are two reports in the literature of *TP53* c.C275T mutation. The first report describes a study of actinic keratosis. The researchers identified *TP53* c.C275T mutation in a patient with actinic keratosis (31). The other report describes a study of chronic lymphocytic leukemia (CLL). The researchers found that the frequency of *TP53* mutations was significantly higher in CLL patients in Taiwan than in the West. The *TP53* c.C275T mutation was detected in one patient. However, the role of *TP53* c.C275T mutation in disease initiation and progression has not been investigated (32). We also found that our patient carried a *KDM6B* c.C5042A mutation, although this was a stop-gain mutation. However, compared with the wild-type KDM6B, the mutant protein had only lost two amino acids at the end of the C-terminus. Protein secondary structure prediction analysis showed no known functional motif at the extreme C-terminal end, thus, it is unlikely that this mutation affects the overall protein conformation and function. Therefore, we speculate that *TP53* c.C275T mutations in this patient are predominantly.

Bortezomib is a reversible inhibitor of the chymotrypsin-like activity of the 26S proteasome in mammalian cells. *In vitro* tests have demonstrated that bortezomib is toxic to various types of cancer cells. *In vivo* studies in preclinical tumor models have demonstrated that bortezomib delays the growth of tumors of various types, including multiple myeloma (33, 34). Bortezomib has been approved as a single agent for the treatment of previously untreated multiple myeloma patients who are not suitable for high-dose chemotherapy and myelosuppression or who have relapsed after at least one course of treatment (35–37). Owing to its excellent therapeutic effect against multiple myeloma, the use of bortezomib has been actively expanded into the treatment of other cancers. A number of clinical studies of bortezomib in ALL are currently underway. One study found that bortezomib monotherapy was not an ideal treatment for ALL because no significant clinical response was observed (38). On the other hand, bortezomib combined with other chemotherapy regimens exhibited a significantly improved treatment effect in ALL patients. A phase II clinical trial found that 73.6% of patients with relapsed ALL achieved CR after receiving bortezomib combined with chemotherapy (39). Another study showed that 88.9% of patients with relapsed or refractory ALL achieved CR after receiving bortezomib combined with chemotherapy (40). A study conducted by Bertaina et al. demonstrated that combination of bortezomib with chemotherapy achieved a remarkable effect in relapsed/refractory ALL of childhood. Twenty-seven patients (72.9%) achieved CR or CR with incomplete platelet recovery (CRp). Twenty-two of 30 BCP-ALL patients (73.3%) and five of seven patients (71%) with T-cell ALL achieved CR/CRp (41). Hasegawa et al. reported that CR was achieved in all three patients with a combination of bortezomib and chemotherapy (42). A phase III clinical trial (AALL1231) conducted by Teachey et al. demonstrated that outcomes for SR and IR T-ALL patients treated with bortezomib were excellent despite elimination of prophylactic CRT (43).

In our study, the B-ALL patient with a *TP53* c.C275T mutation remained MRD-positive after multiple rounds of conventional chemotherapy. Subsequently, we found *via* high-throughput drug sensitivity tests that bortezomib had a strong killing effect on the patient's leukemic cells. Therefore, we treated the patient with bortezomib combined with chemotherapy and found that the patient became MRD-negative after one round of the treatment. In addition, no recurrence was observed during the subsequent 9-month follow-up. It has been reported that bortezomib could induce apoptosis by activating caspase-3 activity in p53-deficient cells (44). Therefore, we speculated that bortezomib may have inhibited ALL cells with *TP53* c.C275T mutation through a similar mechanism.

In conclusion, our study suggests that the *TP53* c.C275TC mutation is indicative of poor prognosis in ALL. Fortunately, bortezomib combined with chemotherapy achieved a good therapeutic effect in our patient. This study is expected to provide new ideas for the treatment of ALL patients with the *TP53* c.C275T mutation.

Data availability statement

The datasets presented in this article are not readily available because of ethical/privacy restrictions. Requests to access the datasets should be directed to the corresponding author.

Ethics statement

Ethical approval was not provided for this study on human participants because Ethical review and approval was not required for this study in accordance with the local legislation and institutional requirements. Written informed consent to participate in this study was provided by the participants' legal guardian/next of kin. Written informed consent was obtained from the individual(s), and minor(s)' legal guardian/next of kin,

for the publication of any potentially identifiable images or data included in this article.

Author contributions

Funding acquisition: RW, Investigation: RW, XL, JZhao, Resources: HW, QH, Data curation: BZ, SL, HZ, JY, JZhang, DL, Formal analysis: WW, Project administration: LH, Writing-review & editing: WW, Supervision: LH, RW, WW.

Funding

This study was supported by grants from Key R&D Guidance Plan Projects of Liaoning Province (2020JH1/10300001).

Acknowledgments

The authors would like to thank Hefei PreceDo Pharmaceuticals Co., Ltd for their work on drug sensitivity test.

Conflict of interest

The authors declare that the research was conducted in the absence of any commercial or financial relationships that could be construed as a potential conflict of interest.

Publisher's note

Supplementary material

The Supplementary Material for this article can be found online at: https://www.frontiersin.org/articles/10.3389/fonc.2022.1018250/full#supplementary-material

References

1. Baruchel A, Schaison G. Recent advances in b cell acute lymphoblastic leukemia (Burkitt leukemia) therapy in childhood. *Nouv Rev Fr Hematol* (1993) 35(1):106–8. doi: 10.1017/cbo9780511977633.016

2. Rosanda C, Cantù-Rajnoldi A, Invernizzi R, Castagni M, Cataldo A, Fenu S, et al. B-cell acute lymphoblastic leukemia (B-ALL): a report of 17 pediatric cases. *Haematologica* (1992) 77(2):151–5. doi: 10.1007/978-981-15-0548-5_15

3. Lalit S, Rajesh K, Sunil G, Bhargava M. B-cell acute lymphoblastic leukemia in a child with ataxia telangiectasia. *Pediatr Hematol Oncol* (2008) 25(5):473–6. doi: 10.1080/08880010802106614

4. Lowichik A, Bernini J, Tonk V, Ansari M, Rollins N, Winick N, et al. Relapse of precursor b-cell acute lymphoblastic leukemia as an isolated central nervous system mass lesion 9 years after initial diagnosis. *Med Pediatr Oncol* (1996) 26 (2):129–34. doi: 10.1200/jco.1985.3.5.622

5. Wang J, Huang F, Chi C, Chou G, Chang T. Skull mass as a heralding sign of precursor b-cell acute lymphoblastic leukemia in a toddler. *J Pediatr* (2006) 149 (4):577. doi: 10.1016/j.jpeds.2006.05.049

6. Salaverria I, Siebert R. The gray zone between burkitt's lymphoma and diffuse large b-cell lymphoma from a genetics perspective. *J Clin Oncol* (2011) 29 (14):1835–43. doi: 10.1200/JCO.2010.32.8385

7. Fujita N, Kobayashi R, Atsuta Y, Iwasaki F, Suzumiya J, Sasahara Y, et al. Hematopoietic stem cell transplantation in children and adolescents with relapsed or refractory b-cell non-Hodgkin lymphoma. *Int J Hematol* (2019) 109(4):483–90. doi: 10.1007/s12185-019-02608-y

8. Jeffrey W, Konrad MA, Ge Y, Naber JM, Scott JS, Matherly LH, et al. High frequency of leukemic clones in newborn screening blood samples of children with b-precursor acute lymphoblastic leukemia. *Blood* (2002) 99(8):2992–6. doi: 10.1182/blood.v99.8.2992

9. Shukla N, Sulis ML. Blinatumomab for treatment of children with high-risk relapsed b-cell acute lymphoblastic leukemia. *JAMA* (2021) 325(9):830–2. doi: 10.1001/jama.2021.1395

10. Asare JM, Rabik CA, Muller B, Brown PA, Cooper S. Investigational treatment options in phase I and phase II trials for relapsed or refractory acute lymphoblastic leukemia in pediatric patients. *Expert Opin Investig Drugs* (2021) 30 (6):611–20. doi: 10.1080/13543784.2021.1916466

11. Kruse A, Abdel-Azim N, Kim HN, Ruan Y, Phan V, Ogana H, et al. Minimal residual disease detection in acute lymphoblastic leukemia. *Int J Mol Sci* (2020) 21 (3):1054. doi: 10.3390/ijms21031054

12. Medinger M, Heim D, Lengerke C, Halter J, Passweg J. Acute lymphoblastic leukemia diagnosis and therapy. *Ther Umsch* (2019) 76(9):510–5. doi: 10.1024/0040-5930/a001127

13. Inaba H, Mullighan C. Pediatric acute lymphoblastic leukemia. *Haematologica* (2020) 105(11):2524–39. doi: 10.3324/haematol.2020.247031

14. Terwilliger T, Abdul-Ha M. Acute lymphoblastic leukemia: a comprehensive review and 2017 update. *Blood Cancer J* (2017) 7(6):e577. doi: 10.1038/bcj.2017.53

15. Salmoiraghi S, Rambaldi A, Spinelli O. TP53 in adult acute lymphoblastic leukemia. *Leuk Lymphoma* (2018) 59(4):778–89. doi: 10.1080/10428194.2017.1344839

16. Comeaux E, Mullighan C. TP53 mutations in hypodiploid acute lymphoblastic leukemia. *Cold Spring Harb Perspect Med* (2017) 7(3):a026286. doi: 10.1101/cshperspect.a026286

17. Yu C, Chang W, Jou S, Lin T, Chang Y, Lin C, et al. TP53 alterations in relapsed childhood acute lymphoblastic leukemia. *Cancer Sci* (2020) 111(1):229–38. doi: 10.1111/cas.14238

18. Ueno H, Yoshida K, Shiozawa Y, Nannya Y, Iijima-Yamashita Y, Kiyokawa N, et al. Landscape of driver mutations and their clinical impacts in pediatric b-cell precursor acute lymphoblastic leukemia. *Blood Adv* (2020) 4(20):5165–73. doi: 10.1182/bloodadvances.2019001307

19. Demir S, Boldrin E, Sun Q, Hampp S, Tausch E, Eckert C, et al. Therapeutic targeting of mutant p53 in pediatric acute lymphoblastic leukemia. *Haematologica* (2020) 105(1):170–81. doi: 10.3324/haematol.2018.199364

20. Inaba H, Pui C. Immunotherapy in pediatric acute lymphoblastic leukemia. *Cancer Metastasis Rev* (2019) 38(4):595–610. doi: 10.1007/s10555-019-09834-0

21. Abdelmabood S, Fouda A, Boujettif F, Mansour A. Treatment outcomes of children with acute lymphoblastic leukemia in a middle-income developing country: high mortalities, early relapses, and poor survival. *J Pediatr (Rio J)* (2020) 96(1):108–16. doi: 10.1016/j.jped.2018.07.013

22. Ma J, Chen Y, Yu L. Research progress on drug-resistance of acute lymphoblastic leukemia–review. *Zhongguo Shi Yan Xue Ye Xue Za Zhi* (2016) 24 (1):261–5. doi: 10.20517/cdr.2019.11

23. Chen S. Asparaginase therapy in pediatric acute lymphoblastic leukemia: A focus on the mode of drug resistance. *Pediatr Neonatol* (2015) 56(5):287–93. doi: 10.1016/j.pedneo.2014.10.006

24. Pogorzala M, Kubicka M, Rafinska B, Wysocki M, Styczynski J. Drug-resistance profile in multiple-relapsed childhood acute lymphoblastic leukemia. *Anticancer Res* (2015) 35(10):5667–70. doi: 10.1007/978-3-319-39708-5_11

25. Aubrey B, Strasser A, Kelly G. Tumor-suppressor functions of the TP53 pathway. *Cold Spring Harb Perspect Med* (2016) 6(5):a026062. doi: 10.1385/1-59259-328-3:117

26. Petitjean A, Mathe E, Kato S, Ishioka C, Tavtigian S, Hainaut P, et al. Impact of mutant p53 functional properties on TP53 mutation patterns and tumor phenotype: lessons from recent developments in the IARC TP53 database. *Hum Mutat* (2007) 28(6):622–9. doi: 10.1002/humu.20495

27. Bykov V, Eriksson S, Bianchi J, Wiman K. Targeting mutant p53 for efficient cancer therapy. *Nat Rev Cancer* (2018) 18(2):89–102. doi: 10.1038/nrc.2017.109

28. Li L, Li M, Wang X. Cancer type-dependent correlations between TP53 mutations and antitumor immunity. *DNA Repair (Amst)* (2020) 88:102785. doi: 10.1016/j.dnarep.2020.102785

29. Sallman D, DeZern A, Garcia-Manero G, Steensma D, Roboz G, Sekeres M, et al. Eprenetapopt (APR-246) and azacitidine in TP53-mutant myelodysplastic syndromes. *J Clin Oncol* (2021) 39(14):1584–94. doi: 10.1200/JCO.20.02341

30. Niparuck P, Police P, Noikongdee P, Siriputtanapong K, Limsuwanachot N, RerkamnuaychokeB, et al. TP53 mutation in newly diagnosed acute myeloid leukemia and myelodysplastic syndrome. . *Diagn Pathol* (2021) 16(1):100. doi: 10.1186/s13000-021-01162-8

31. Ziegler A, Jonason AS, Leffell DJ, Simon JA, Sharma WH, Kimmelman J, et al. Sunburn and p53 in the onset of skin cancer. *Nature* (1994) 372(6508):773–6. doi: 10.1038/372773a0

32. Wu SJ, Lin CT, Agathangelidis A, Lin LL, Kuo YY, Tien HF, et al. Distinct molecular genetics of chronic lymphocytic leukemia in Taiwan: clinical and pathogenetic implications. *Haematologica* (2017) 102(6):1085–90. doi: 10.3324/haematol.2016.157552

33. Scott K, Hayden P, Will A, Wheatley K, Coyne K. Bortezomib for the treatment of multiple myeloma. *Cochrane Database Syst Rev* (2016) 4:CD010816. doi: 10.1007/978-3-7643-8948-2_4

34. Robak P, Robak T. Bortezomib for the treatment of hematologic malignancies: 15 years later. *Drugs R D* (2019) 19(2):73–92. doi: 10.1007/s40268-019-0269-9

35. Breitkreutz I, Raab M, Goldschmidt H. First-line treatment of multiple myeloma. *Internist (Berl)* (2019) 60(1):23–33. doi: 10.1007/s00108-018-0527-x

36. Kropff M, Bisping G, Schuck E, Liebisch P, Lang N, Hentrich M, et al. Bortezomib in combination with intermediate-dose dexamethasone and continuous low-dose oral cyclophosphamide for relapsed multiple myeloma. *Br J Haematol* (2007) 138(3):330–7. doi: 10.1111/j.1365-2141.2007.06656.x

37. Wang Y, Ding S, Wu F, Wang Z, Wang Q. Safety and efficacy of subcutaneous administration of bortezomib in the treatment of multiple myeloma. *Sichuan Da Xue Xue Bao Yi Xue Ban* (2014) 45(3):529–32. doi: 10.47939/mh.v2i11.402

38. Cortes J, Thomas D, Koller C. Phase I study of bortezomib in refractory or relapsed acute leukemias. *Clin Cancer Res* (2004) 10(10):3371–6. doi: 10.1158/1078-0432.ccr-10-22-corb

39. Messinger YH, Gaynon PS, Sposto R. Bortezomib with chemotherapy is highly active in advanced b-precursor acute lymphoblastic leukemia: Therapeutic advances in childhood. *Leukemia Lymphoma (TACL) Study. Blood* (2012) 120 (2):285–90. doi: 10.3410/f.717957011.793461504

40. Zhao J, Wang C, Song Y, Liu Y, Fang B. Treatment of refractory/relapsed adult acute lymphoblastic leukemia with bortezomibbased chemotherapy. *Int J Gen Med* (2015) 8:211–4. doi: 10.2147/ijgm.s59537

41. Bertaina A, Vinti L, Strocchio L, Gaspari S, Caruso R, Algeri M, et al. The combination of bortezomib with chemotherapy to treat relapsed/refractory acute lymphoblastic leukaemia of childhood. *Br J Haematol* (2017) 176(4):629–36. doi: 10.1111/bjh.14505

42. Hasegawa D, Yoshimoto Y, Kimura S, Kumamoto T, Maeda N, Hara J, et al. Bortezomib-containing therapy in Japanese children with relapsed acute lymphoblastic leukemia. *Int J Hematol* (2019) 110(5):627–34. doi: 10.1007/s12185-019-02714-x

43. Wu SJ, Lin CT, Agathangelidis A, Lin LI, Kuo YY, Tien HF, et al. Distinct molecular genetics of chronic lymphocytic leukemia in Taiwan: clinical and pathogenetic implications. *J Clin Oncol* (2022) 40(19):2106–18. doi: 10.1200/JCO.21.02678

44. Yerlikaya A, Okur E, Ulukaya E. The p53-independent induction of apoptosis in breast cancer cells in response to proteasome inhibitor bortezomib. *Tumour Biol* (2012) 33(5):1385–92. doi: 10.1007/s13277-012-0386-3

frontiers | Frontiers in Oncology

TYPE Case Report
PUBLISHED 02 March 2023
DOI 10.3389/fonc.2023.1054175

OPEN ACCESS

EDITED BY
Ahmad Antar,
Almoosa Specialist Hospital, Saudi Arabia

REVIEWED BY
Sabrin Albeituni,
St. Jude Children's Research Hospital, United States
Ryan Wilcox,
University of Michigan, United States
Rui Zhang,
Beijing Children's Hospital, Capital Medical University, China

*CORRESPONDENCE
Lin Zhao
sg1520@shutcm.edu.cn

†These authors have contributed equally to the work

SPECIALTY SECTION
This article was submitted to Hematologic Malignancies, a section of the journal Frontiers in Oncology

RECEIVED 28 September 2022
ACCEPTED 17 February 2023
PUBLISHED 02 March 2023

CITATION
Zhao L, Yang H, Qu W-y, Lu Y-j and Feng Z (2023) Case report: Ruxolitinib plus dexamethasone as first-line therapy in haemophagocytic lymphohistiocytosis. *Front. Oncol.* 13:1054175. doi: 10.3389/fonc.2023.1054175

Case report: Ruxolitinib plus dexamethasone as first-line therapy in haemophagocytic lymphohistiocytosis

Lin Zhao[1*†], Hui Yang[2†], Wei-ying Qu[1], Ying-jia Lu[1] and Zhou Feng[1]

[1]Department of Haematology, Shuguang Hospital Affiliated to Shanghai University of Traditional Chinese Medicine, Shanghai, China, [2]Department of Clinical Laboratory, Shuguang Hospital Affiliated to Shanghai University of Traditional Chinese Medicine, Shanghai, China

Haemophagocytic lymphohistiocytosis (HLH) is a cytokine-driven inflammatory syndrome caused by uncontrolled hypersecretion of inflammatory cytokines. Conventional first-line treatment for HLH included HLH-94 and HLH-2004 regimens. However, quite a few patients do not respond to treatment or cannot tolerate intensive chemotherapy. We reported two cases of HLH, one caused by natural killer (NK)/T-cell lymphoma and another associated with missense variants in the *perforin 1* gene. They both received the ruxolitinib plus dexamethasone protocol and had a rapid response to treatment without obvious adverse effects. Our report indicates that treatment with ruxolitinib plus dexamethasone might be a potential option for HLH, and clinical trials warrant further investigation. In addition, the detection of HLH-related genes is necessary for the identification of late-onset familial HLH in certain settings.

KEYWORDS

haemophagocytic lymphohistiocytosis, ruxolitinib, dexamethasone, first-line, therapy

Introduction

Haemophagocytic lymphohistiocytosis (HLH) is a rare, life-threatening, and rapidly progressive syndrome characterized by hyperinflammation caused by inherited or acquired immune dysregulation. Primary HLH often refers to patients with clear familial inheritance or genetic causes. Autosomal recessive inheritance is a common mode of inheritance of this disease [also known as familial hemophagocytic lymphohistiocytosis (FHL)]. Secondary HLH (sHLH) is typically triggered by malignant, infectious, or autoimmune/autoinflammatory stimuli, often without known HLH pathogenic genetic disorders and family history (1). Due to its rapid progression and high mortality, timely initiation of appropriate treatment is critical to improving prognosis.

The treatment of HLH is generally divided into two stages. First, induction regimens mainly target the excessive inflammatory state to control the progression of HLH. Then, aetiologic therapy focuses on correcting the underlying immune deficiency and controlling

the primary disease to prevent HLH recurrence. The etoposide-based HLH-94 and HLH-2004 regimens remain widely accepted as the standard treatment for HLH. Nevertheless, quite a few patients do not respond to treatment or are unable to tolerate intensive chemotherapy (2, 3). The Janus kinase (JAK) 1/2 inhibitor ruxolitinib (RUX) is a promising option for the treatment of HLH (4–6), and combined glucocorticoid therapy might further improve the efficacy. As of September 2022, eighteen human studies have been reported evaluating RUX in patients with HLH. Sixteen of these studies used RUX in sHLH as a first-line or salvage setting, with a dozen case reports each consisting of a single patient. However, reports using RUX as a first-line therapy among patients with active malignancy or primary HLH are scarce (7). Herein, we report 2 cases of HLH (1 case of sHLH associated with natural killer (NK)/T-cell lymphoma, and 1 case of primary HLH with missense variants in the *perforin gene* (*PRF1*), highlighting the contribution of RUX plus dexamethasone (DXM) in controlling hyperinflammation in sHLH or primary HLH.

Case presentation

Case 1

A previously healthy 27-year-old man presented with skin ulceration and exudation in January 2022. He received antibiotics. Three months later, fever, generalized body swelling, and fatigue were experienced by the patient. The laboratory data revealed abnormal liver functions, with an alanine aminotransferase (ALT) level of 92 units/L (normal: 7-40 units/L), aspartate aminotransferase (AST) level of 181.3 units/L (normal: 13-35 units/L), and total bilirubin (TBil) level of 73 μmol/L (normal: 0-23 μmol/L). The laboratory data also revealed thrombocytopenia with a platelet (PLT) count of 24×10^9/L (Figure 1A). The level of haemoglobin (HGB) was 74 g/L. His ferritin level was 13504 ng/ml (normal: 23.9-336.2 ng/ml), and triglyceride (TG) level was 3.61 mmol/L (normal: 0-1.7 mmol/L) (Figure 1C, D). He had severe hypoalbuminemia (20 g/L). Epstein-Barr virus (EBV)-DNA in blood plasma was 3.46×10^3 copies/ml (normal: < 400 copies/ml). The level of soluble CD25 (sCD25) was 12062 pg/ml (normal: ≤ 6000 pg/ml) (Figure 1C). The patient tested negative for human immunodeficiency virus (HIV). He denied a personal and family history of haematological pathologies, specifically HLH.

The patient's symptoms worsened, as evidenced by deteriorated coagulopathy with a prothrombin time (PT) of 25.5 s (normal: 10.4-12.7 s) and an active thromboplastin time (APTT) of 102 s (normal: 22.3-32.5 s) (Figure 1B). The fibrinogen level was only 0.41 g/L (normal: 1.8-3.5 g/L) (Figure 1D). Bone marrow aspiration and biopsy demonstrated inflammatory changes and an increase in the number of macrophages and histiocytes with intense haemophagocytosis. Therefore, the patient fulfilled 7 of 8 diagnostic criteria for HLH (Table 1). NK-cell activity was not analysed due to the lack of availability in Shanghai during the pandemic.

The patient experienced extreme fatigue, severe oedema, persistent high fever, and large skin ulcerations with exudation. He became expressionless and unresponsive. We decided to start with RUX 15 mg twice daily plus dexamethasone (DXM) 10 mg/m^2/day per HLH-94 dosing, not only because of his poor performance status (PS) and progressive deterioration of liver function but also because of the short supply of blood products, including red blood cells and platelets, at specific periods in Shanghai. Fourteen days later, DXM was reduced to 5 mg/m^2/day. Broad-spectrum antibiotics, fibrinogen, prothrombin complex, and immunoglobulin were also given. The patient had no fever on Day 3 (Day 0 corresponds to RUX initiation). Eighty percent of skin ulcers were healed on Day 7. Oedema and fatigue symptoms were significantly relieved. The TBil level dropped to 58 μmol/L. After two weeks of therapy, the PLT count recovered to 136×10^9/L (Figure 1A). The fibrinogen level, PT, and APTT improved (Figure 1B, D). The sCD25 level decreased to 7238 pg/ml (Figure 1C). The patient achieved a partial response (PR) according to the response criterion described in previous studies (9, 10). He underwent two skin biopsies and a cervical lymph node biopsy by a core needle, but all were negative for lymphoma. The histopathology of the excised right inguinal lymph node indicated an NK/T-cell lymphoma on Day 22. The pegaspargase + Gemox regimen was started on Day 23. He developed a fever again on Day 28. The levels of C-reactive protein (CRP, 97 mg/L) and ferritin (10532 ng/ml) were all elevated (Figure 1A, C). The values of PLT (31×10^9/L) and fibrinogen (0.80 g/L) were reduced again (Figure 1A, D). The pulmonary computed tomography (CT) scan suggested pneumonia. The result of alveolar lavage fluid culture was *Pseudomonas aeruginosa*. Although broad-spectrum antibiotics were administered according to the drug susceptibility, the patient died on Day 33 with incomplete induction chemotherapy.

Case 2

A 33-year-old female with a history of encephalomyelitis treated with high-dose methylprednisolone in 2018 presented with neutropenia and mild anaemia in November 2021. A month later, she developed a high fever, fatigue, headache, and pancytopenia with an absolute neutrophil count (ANC) of 0.3×10^9/L, HGB of 93 g/L, and PLT of 37×10^9/L (Figure 1E, H). The CRP level was 131 mg/L (normal: 0-8 mg/L) (Figure 1E). She was admitted to our hospital. Bone marrow aspiration and biopsy demonstrated haemophagocytosis. Flow cytometric (FC) analysis of bone marrow showed no clonal abnormalities, and chromosome karyotype analysis was normal. The laboratory data revealed abnormal liver function with an ALT of 70 units/L, AST of 182 units/L, and TBil of 24 μmol/L. Coagulation detection showed a decreased level of fibrinogen (0.25 g/L) and prolonged APTT (75.4 s) (Figure 1F, H). Her ferritin level was 12459 μg/L and the TG level (7.04 mmol/L) was four times higher than normal (Figure 1G). EBV-DNA in blood plasma was 896.68 copies/ml (normal: <400 copies/ml). EBV nuclear antigen IgG (EBNA-IgG) and EBV capsid antigen IgG (EBCA-IgG) antibody titers were 235 U/ml (normal: < 5 U/ml) and 218 U/ml (normal: < 20 U/ml), respectively. Abdominal CT showed splenomegaly. The patient denied that she had repeatedly developed HLH and denied a

10.3389/fonc.2023.1054175

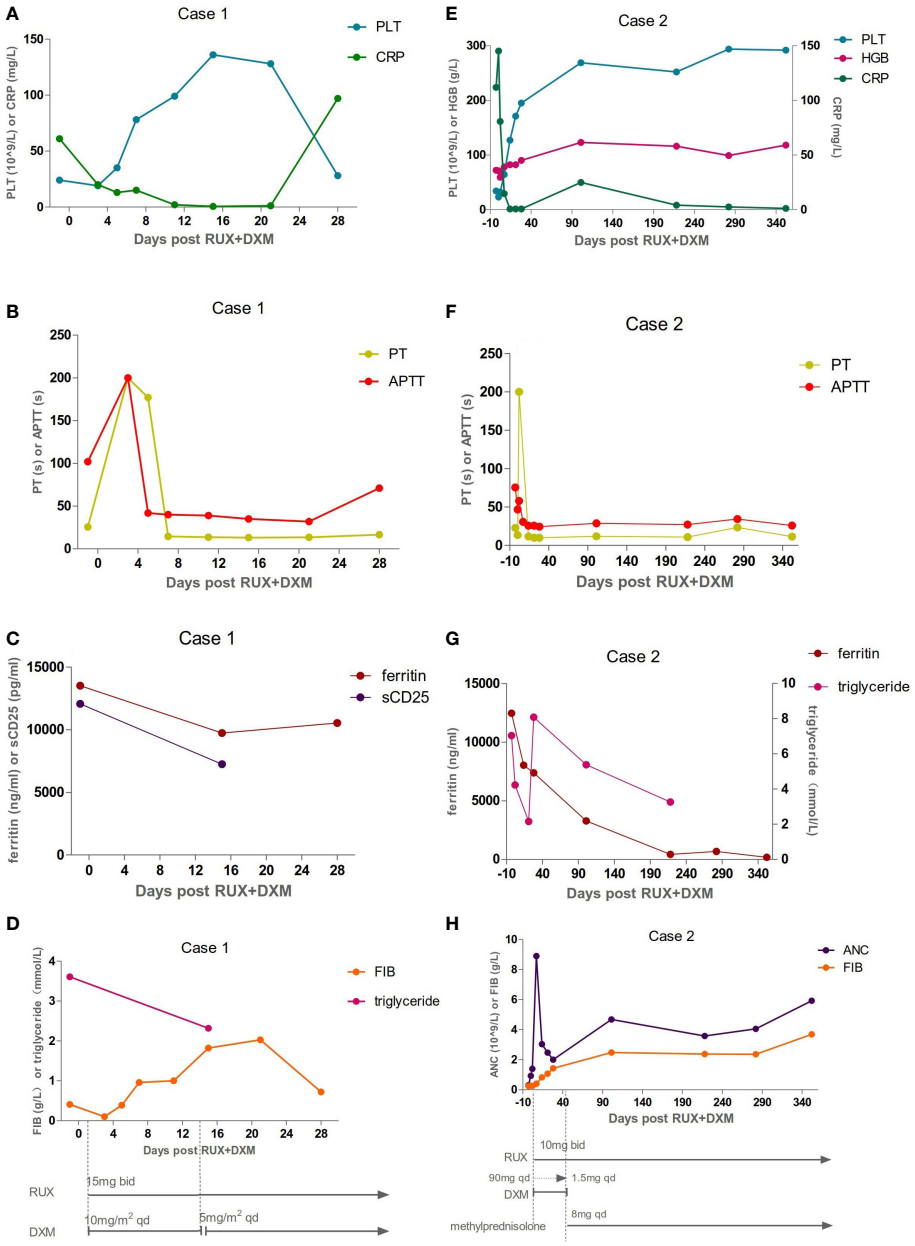

FIGURE 1
Inflammatory, coagulation function, and hematologic responses to HLH therapies: Day 0 corresponds to ruxolitinib (RUX) initiation. Treatment schedules, lines, and bars represent continuous therapy and individual doses of drugs with intermittent schedules. Arrows indicate that treatment was continued. **(A–D)** The laboratory assessments of Case 1. The levels of platelet (PLT), prothrombin time (PT), active thromboplastin time (APTT), C-reactive protein (CRP), fibrinogen (FIB), ferritin, soluble CD25 (sCD25), and triglyceride were abnormal before Day 0 and gradually improved after therapy. But he developed a fever again on Day 28. The levels of ferritin and CRP were all elevated. The values of FIB and PLT were reduced again. **(E–H)** The laboratory assessments of Case 2. The dexamethasone (DXM) dose was reduced by half every three days, finally reaching a reduced dose of 1.5 mg on Day 42. It was replaced by methylprednisolone on Day 43. Inflammatory, coagulation function, and hematologic parameters were abnormal before Day 0, and gradually improved after therapy.

family history of HLH. According to her clinical manifestations and laboratory parameters, she was diagnosed with HLH (Table 1).

Magnetic resonance imaging (MRI) showed multiple inflammatory demyelinating lesions in the bilateral paraventricular area, bilateral radiation crown area, and bilateral frontoparietal temporal cortex. Cerebrospinal fluid pressure was high, protein content was normal, and no tumour cell infiltrations were found. The recurrence of encephalomyelitis was considered. No clear malignant, autoimmune, or infectious triggers for HLH were identified. EBV infection was suspected as a potential trigger for her HLH. The level of sCD25 and NK-cell activity were unavailable during this time in Shanghai.

The patient was given 90 mg DXM a day for 3 days. At the same time, RUX 10 mg was administered orally twice a day. The DXM

10.3389/fonc.2023.1054175

TABLE 1 Clinical and laboratory parameters measured in both patients at diagnosis and Day 14 post-ruxolitinib (post-RUX).

Parameter	Proposed HLH diagnostic criteria (requires 5/8) (8)	Data of Case 1		Data of Case 1	
		at diagnosis	Day 14 post-RUX	at diagnosis	Day 14 post-RUX
Fever	≥38.5°	Present	No	No	No
Spleen	Splenomegaly	Present	No	Present	No
Bicytopenia	HGB <90 g/L, and/or PLT <100× 10^9/L, and/or ANC< 1.0× 10^9/L	74 g/L 24 × 10^9/L 2.1× 10^9/L	87 g/L 136 × 10^9/L 3.6× 10^9/L	93 g/L 37 × 10^9/L 0.3 × 10^9/L	82 g/L 127 × 10^9/L 3.04 × 10^9/L
Hypertriglyceridemia and/or hypofibrinogenemia	>3 mmol/L < 1.5 g/L	3.61 mmol/L 0.41 g/L	2.32 mmol/L 1.82 g/L	7.04 mmol/L 0.25 g/L	4.23 mmol/L 0.83 g/L
Hyperferritinemia	≥500 μg/L	13504 μg/L	9728 μg/L	12459 μg/L	8034 μg/L
Soluble CD25	Elevated	Yes (12062 pg/ml)	Yes (7238 pg/ml)	Not tested	Not tested
NK Cell Activity	Absent or Low	Not tested	Not tested	Not tested	Not tested
Haemophagocytosis	Observed in BM, LN, spleen, or liver	Observed in BM	Not valued	Observed in BM	Not observed in BM
Alternatively:					
Genetics	Homozygosity or compound heterozygosity for HLH-associated mutations in an appropriate clinical setting	Not tested		*PRF1* and *LYST*	

HLH, Haemophagocytic lymphohistiocytosis; HGB, Haemoglobin; PLT, Platelet; ANC, Absolute neutrophil count; BM, Bone marrow; LN, Lymph node; *PRF1*, The perforin gene; *LYST*, Lysosomal trafficking regulator.

dose was reduced by half every three days, finally reaching a reduced dose of 10 mg. After that, the dose was adjusted every two weeks to 1.5 mg according to the patient's laboratory examination results. Then, DXM was replaced with 8 mg methylprednisolone for maintenance treatment. Her fever was controlled on Day 2. The PLT and ANC counts had normalized on Day 7 (Figure 1E, H). The ferritin, fibrinogen, and TG level improved on Day 14 (Figure 1G, H). She achieved PR according to the response criterion on Day 14 (9, 10).

Treatment with RUX and a low dose of methylprednisolone were continuous. Plasma EBV-DNA load was 423 copies/ml on Day 265. EBNA-IgG and EBCA-IgG antibody titers were 185 U/ml and > 750 U/ml on Day 273, respectively. Two antibodies were still positive with high avidity. The onset of primary HLH in adults may lead clinicians to ignore or even misdiagnose the disease. To further clarify the aetiology of HLH in Case 2, the next-generation sequencing (NGS) of HLH-related genes was performed on Day 275. A mutation of the *PRF1* gene, c.1349C > T (p. T450M) was reported. Two mutations of the lysosomal trafficking regulator (*LYST*) were also detected: c.1183C > T (p. R395C) and c.2183G > T (p. S938I). All of them were heterozygous missense mutations. The NGS results are shown in Table 2. Unlike *PRF1* mutations, which are known pathogenic variants responsible for FHL, the clinical significance of the two *LYST* gene variants is unclear. FC analysis revealed the decreased expression of PRF1 in NK cells (Figure 2A). NK cells stimulation test showed severe dysregulation of immune response (Figure 2B) on Day 352. The final diagnosis of the patient was FHL type 2 from homozygous c.1349C > T (p. T450M) missense variants in the *PRF1* gene. The patient's parents were reluctant to test HLH-related genes for financial stress, so it was impossible to determine the location of these variants. She remained well without neurological symptoms at the monthly follow-up. The brain MRI on Day 329 showed stable disease without any new lesions. The ferritin level, liver function, coagulation, and hematologic parameters were normal at the last follow-up on Day 353 (Figure 1E, F, G, H). The patient is currently enjoying excellent PS.

TABLE 2 Genetic test* results of Case 2.

	Chromosome position	Transcript mutation position	Nucleotide change	Amino acid change	Homozygous/heterozygous	Disease/ phenotype	Genetic mode
PRF1	chr10: 72358128	NM_001083116 Exon3	c.1349C >T	p. T450M	Heterozygous	FHL2	AR
LYST	chr1: 235972935	NM_00008.4 Exon5	c.1183C > T	p. R395C	Heterozygous	CHS	AR
LYST	chr1: 235969623	NM_00008.4 Exon6	c.2813G >T	p. S938I	Heterozygous	CHS	AR

PRF1, The perforin gene; *LYST*, Lysosomal trafficking regulator; AR, Autosomal recessive inheritance; FHL2, Familial haemophagocytic lymphohistiocytosis 2; CHS, Chediak-Higashi.
* HLH-related genes were detected using high-throughput sequencing (sequencing type, targeted sequencing; average sequencing depth, 115X; mutation types, SNV, Indel, CNV).

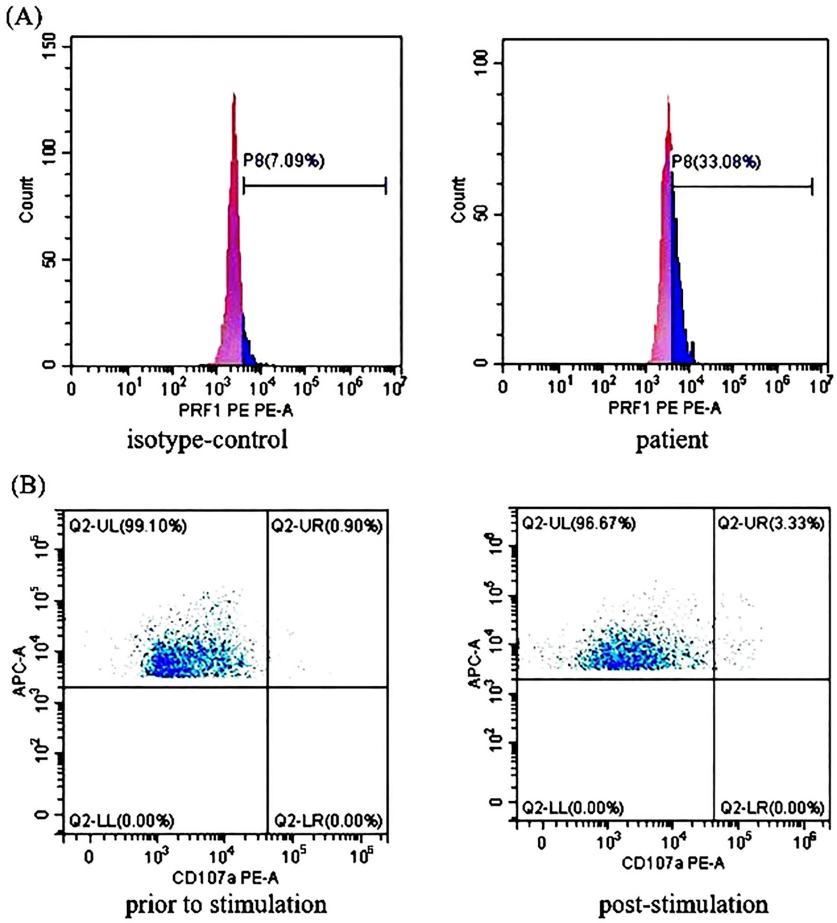

FIGURE 2
The perforin protein (PRF1) expression and ΔCD107a in natural killer (NK) cells of Case 2: **(A)** Flow cytometry analysis revealed the decreased expression rates of PRF1 in NK cells of Case 2. The expression rates of PRF1 were 7.09% of the negative control and 33.08% of the patient sample. The negative control was treated with isotype-control antibodies to eliminate the false positive interference caused by the non-specific binding of antibodies to the cells. Thus, the actual expression rates of PRF1 were 25.99% (i.e., 33.08% - 7.09% = 25.99%, normal: ≥81%). **(B)** The NK cells stimulation test showed severe dysregulation of the immune response. The expression rates of CD107a in the NK cells of Case 2 were 0.90% (before stimulation) and 3.33% (post-stimulation). Thus, ΔCD107a was 2.43% (ΔCD107a >10% indicates normal degranulation function).

Discussion

HLH-94 and HLH-2004 are the recommended first-line treatment protocols for HLH, but they are all based on clinical studies of children with HLH. There is no consensus on HLH in adults, especially for patients with severe cytopenia or poor PS. Less toxic treatment for HLH has emerged as a subject of intense interest and study (11).

RUX, an inhibitor of JAK 1 and JAK 2, blocks cytokine signaling through JAK/STAT and inhibits the action of proinflammatory cytokines. In murine models, treatment with RUX significantly lessened the clinical and laboratory manifestations of primary HLH and sHLH (12). Since Broglie L et al. first reported the use of RUX in a refractory HLH paediatric case of unknown aetiology (13), there has been an increasing number of publications describing the use of this drug in patients with HLH. Zhang et al. presented the largest prospective study reported to date, enrolling fifty-two newly diagnosed paediatric patients, demonstrating the clinical benefit of RUX as a first-line targeted therapy. RUX has a rapid efficacy for paediatric HLH with few attributable serious adverse events (6).

For HLH secondary to aggressive lymphoma, controlling HLH with fewer side effects as soon as possible could create conditions for lymphoma chemotherapy (14). Although the outcome of Case 1 was disappointing, HLH was controlled and the induction therapy was initiated. The cause of failure may be rapid tumour progression or infection caused by intensive chemotherapy and/or RUX plus DXM. Therefore, for highly suspected aggressive lymphoma, it is important to clarify the diagnosis and initiate aetiologic treatment as soon as possible.

Allogeneic haematopoietic stem cell transplantation (allo-HSCT) is the only available curative treatment for FHL at present. The success of HSCT is dependent on complete control of the disease prior to transplantation (15). Case 2 describes a patient with FHL successfully treated in first intention by a

combination of RUX and DXM. Our observation suggests that this less toxic and effective treatment regimen could be used as a first-line therapy for FHL and help bridge eligible patients to HSCT even if Case 2 abandoned HSCT for personal reasons.

The management of HLH often requires adjustment of guideline-directed therapies due to treatment-related toxicity or the complexities of managing the underlying trigger and resultant hyperinflammation simultaneously. Our two cases had poor PS and could not tolerate the standard protocol containing chemotherapy. In this setting, the application of RUX was a good option. Both patients had a prompt response to RUX plus DXM. The initial manifestation of the treatment response was rapid control of fever, followed by improvement of abnormal coagulation and PLT counts. Consistent with other reports, they both appeared to be well-tolerated (16, 17).

RUX combined with glucocorticoids or conventional chemotherapy may further improve efficacy. However, there is no conclusion as to which combination therapy is better. RUX plus glucocorticoids are frequently used. There is no definitive conclusion on whether glucocorticoids, methylprednisolone, or DXM should be used when initiating RUX therapy. In addition, the optimal dose and schedule of glucocorticoid administration remain to be determined. A minimum of 10 cases were arbitrarily chosen to identify larger studies. At the time of writing this report, 3 independent larger studies describing 122 unique patients have been published. In one retrospective study, 36 patients with lymphoma-associated haemophagocytic syndrome were treated with RUX combined with doxorubicin, etoposide, and dexamethasone (DEP) (18). In two single-centre prospective studies, 34 refractory/relapsed HLH patients and 52 paediatric HLH patients were enrolled (5, 6). According to the protocols of these prospective studies, glucocorticoids could be continued if the patient was receiving them before enrolment. In Case 1, we initiated treatment with RUX at a dose of 15 mg twice daily. Because the cause of HLH was not clear, DXM 10 mg/m^2/day per HLH-94 dosing was used. In Case 2, we used high-dose DXM because the patient's presentation was complicated with recurrent encephalomyelitis. Similar to HLH, glucocorticoids have been the mainstay of treatment in encephalomyelitis.

In both cases, abnormal elevation of EBV-DNA was detected. During the follow-up of Case 2, persistent slight abnormalities of serum EBV-DNA were revealed even though the patient's clinical symptoms improved significantly. EBV infection may play an important role in the occurrence of haemophagocytosis in Case 2. EBV may be involved in malignancy-related HLH, rheumatic immune disease-related HLH, or primary HLH with known genetic defects. For somewhat unclear reasons, EBV is highly associated with HLH in Asia. In one report, it was observed to be associated with nearly 3/4 of HLH patients (19). Sustained primary EBV infection can trigger this immediately fatal disorder, especially in patients with unknown congenital or acquired immunodeficiencies (20, 21). In addition, EBV-DNA copies in whole blood and plasma of EBV-HLH patients before and after RUX treatment did not change, indicating that RUX improves inflammation without affecting the underlying primary cause of HLH (5).

Malignancy, particularly lymphoma-associated HLH, was a prominent adverse prognostic marker correlating with poorer survival in several studies (22–24). Patients with T-cell lymphoma generally had worse outcomes than those with B-cell lymphoma (25). Case 1 died despite prompt treatment for the primary disease after diagnosis.

There is an increasingly recognized overlap between primary HLH and sHLH as new cases are described and genetic discoveries are better understood. At present, it is believed that sHLH also has a genetic background, such as heterozygous changes and polymorphisms of primary HLH-related genes, and exhibits HLH pathogenesis after suffering the "second hit" of external trigger factors (such as a virus infection). sHLH is much more commonly described than primary HLH in adults; therefore, adults are rarely tested for genetic abnormalities, which leads to the misdiagnosis of late-onset cases. Gene sequencing is recommended for patients with HLH whose aetiology is unknown and/or who have recurrent episodes to identify the rare late-onset case of primary HLH. Patients who have not been detected the currently known pathogenic genes of HLH and cannot be determined the secondary aetiology needs to be continuously sought in subsequent treatment and follow-up.

In Case 2, NGS revealed c.1349C > T (p. T450M) heterozygous missense variations in the coding sequence of exon 3 of the *PRF1* gene. The oldest individual ever documented to be diagnosed with FHL Type 2 from homozygous c.1349C > T (p. T450M) missense variants in the *PRF1* gene was a 33-year-old Indian man of a similar age to Case 2 (26). Perforin is encoded by the *PRF1* gene and forms pores in target cell membranes in a process highly dependent upon its C2 domain, allowing granzyme to enter and initiate caspase-mediated apoptosis of the target cell (27). Functional studies showed that the mutant perforin c.1349C > T (p. T450M) heterozygous missense variant was completely inactivated at 37°C. The scale-invariant feature transform (SIFT) predicted value was -4.921, which was considered a harmful variant. According to the 2017 publication of the American College of Medical Genetics (ACMG) and Genomics guidelines (28, 29), it is inferred that the c.1349C > T mutation is a pathogenic mutation. The delayed onset of FHL Type 2 may be related to the mutation type (30), triggering factors (31), and pathogenic variation pattern of *PRF1* (32). A possible explanation for the delayed onset of HLH is that these patients carry heterozygous missense mutations, which encode some *PRF1* activities. Two missense mutations of *LYST* genes were also found in Case 2. The relevant literature on the mutation was not reported in the Human Gene Mutation Database (HGMD) database. According to the ACMG guidelines, the clinical significance of this mutation is uncertain.

In conclusion, RUX is effective and less toxic in both primary HLH and sHLH. However, there are still several additional questions of RUX that warrant further study, including dosing, duration, and combinations. Moreover, genetic screening is

recommended to exclude adult-onset FHL to reduce patient mortality, especially for patients with unexplained recurrence of disease.

Data availability statement

The original contributions presented in the study are included in the article/supplementary material. Further inquiries can be directed to the corresponding author.

Ethics statement

Ethical review and approval was not required for the study on human participants in accordance with the local legislation and institutional requirements. The patients/participants provided their written informed consent to participate in this study.

Author contributions

LZ gathered the clinical information and drafted the manuscript. LZ and HY approved the final diagnosis and formulated the therapeutic strategies. W-YQ, Y-JL, and ZF reviewed multiple drafts of the manuscript. W-YQ made the chart and picture. All authors listed have made a substantial, direct, and intellectual contribution to the work and approved it for publication.

Acknowledgments

We thank the pathologists, clinicians, nurses, and administrative employers who have provided support for the study.

Conflict of interest

The authors declare that the research was conducted in the absence of any commercial or financial relationships that could be construed as a potential conflict of interest.

Publisher's note

References

1. Knaak C, Schuster FS, Nyvlt P, Spies C, Feinkohl I, Beutel G, et al. Treatment and mortality of hemophagocytic lymphohistiocytosis in adult critically ill patients: a systematic review with pooled analysis. *Crit Care Med* (2020) 11:e1137–46. doi: 10.1097/CCM.0000000000004581

2. Trottestam H, Horne A, Aricó M, Egeler RM, Filipovich AH, Gadner H, et al. Chemoimmunotherapy for hemophagocytic lymphohistiocytosis: Long-term results of the HLH - 94 treatment protocol. *Blood* (2011) 17:4577–4584. doi: 10.1182/blood-2011-06-356261

3. Bergsten E, Horne A, Aricó M, Astigarraga I, Egeler RM, Filipovich AH, et al. Confirmed efficacy of etoposide and dexamethasone in HLH treatment: Long - term results of the cooperative HLH - 2004 study. *Blood* (2017) 25:2728–2738. doi: 10.1182/blood-2017-06-788349

4. Ahmed A, Merrill SA, Alsawah F, Bockenstedt P, Campagnaro E, Devata S, et al. Ruxolitinib in adult patients with secondary haemophagocytic lymphohistiocytosis: An open-label, single-centre, pilot trial. *Lancet Haematol* (2019) 12:e630–7. doi: 10.1016/S2352-3026(19)30156-5

5. Wang J, Wang Y, Wu L, Wang X, Jin Z, Gao Z, et al. Ruxolitinib for refractory/relapsed hemophagocytic lymphohistiocytosis. *Haematologica* (2020) 5:e210–2. doi: 10.3324/haematol.2019.222471

6. Zhang Q, Zhao YZ, Ma HH, Wang D, Cui L, Li WJ, et al. A study of ruxolitinib response-based stratified treatment for pediatric hemophagocytic lymphohistiocytosis. *Blood* (2022) 24:3493–3504. doi: 10.1182/blood.2021014860

7. Summerlin J, Wells DA, Anderson MK, Halford Z. A review of current and emerging therapeutic options for hemophagocytic lymphohistiocytosis. *Ann Pharmacother* (2022) 9:10600280221134719. doi: 10.1177/10600280221134719

8. Henter JI, Horne A, Aricó M, Egeler RM, Filipovich AH, Imashuku S, et al. HLH2004: Diagnostic and therapeutic guidelines for hemophagocytic lymphohistiocytosis. *Pediatr Blood Cancer* (2007) 2:124–131. doi: 10.1002/pbc.21039

9. Marsh RA, Allen CE, McClain KL, Weinstein JL, Kanter J, Skiles J, et al. Salvage therapy of refractory hemophagocytic lymphohistiocytosis with alemtuzumab. *Pediat Blood Cancer* (2013) 1:101–109. doi: 10.1002/pbc.24188

10. Locatelli F, Jordan MB, Allen C, Cesaro S, Rizzari C, Rao A, et al. Emapalumab in children with primary hemophagocytic lymphohistiocytosis. *N Engl J Med* (2020) 19:1811–1822. doi: 10.1056/NEJMoa1911326

11. Keenan C, Nichols KE, Albeituni S. Use of the JAK inhibitor ruxolitinib in the treatment of hemophagocytic lymphohistiocytosis. *Front Immunol* (2021) 12:614704. doi: 10.3389/fimmu.2021.614704

12. Das R, Guan P, Sprague L, Verbist K, Tedrick P, An QA, et al. Janus kinase inhibition lessens inflammation and ameliorates disease in murine models of hemophagocytic lymphohistiocytosis. *Blood* (2016) 13:1666–75. doi: 10.1182/blood-2015-12-684399

13. Broglie L, Pommert L, Rao S, Thakar M, Phelan R, Margolis D, et al. Ruxolitinib for treatment of refractory hemophagocytic lymphohistiocytosis. *Blood Adv* (2017) 19:1533–1536. doi: 10.1182/bloodadvances.2017007526

14. Wang H, Gu Liang X, Mao X, Wang ZQ, Huang W. Low dose ruxolitinib plus HLH-94 protocol: A potential choice for secondary HLH. *Semin Hematol* (2020) 1:26–30. doi: 10.1053/j.seminhematol.2018.07.006

15. Marsh RA, Haddad E. How I treat primary haemophagocytic lymphohistiocytosis. *Br J Haematol* (2018) 2:185–99. doi: 10.1111/bjh.15274

16. Goldsmith SR, Saif Ur Rehman S, Shirai CL, Vij K, DiPersio JF. Resolution of secondary hemophagocytic lymphohistiocytosis after treatment with the JAK1/2 inhibitor ruxolitinib. *Blood Adv* (2019) 23:4131–4135. doi: 10.1182/bloodadvances.2019000898

17. Sin JH, Zangardi ML. Ruxolitinib for secondary hemophagocytic lymphohistiocytosis: First case report. *Hematol Oncol Stem Cell Ther* (2019) 3:166–170. doi: 10.1016/j.hemonc.2017.07.002

18. Zhou LL, Liu YN, Wen ZZ, Yang SM, Li MJ, Zhu QH, et al. Ruxolitinib combined with doxorubicin, etoposide, and dexamethasone for the treatment of the lymphoma-associated hemophagocytic syndrome. *J Cancer Res Clin Oncol* (2020) 11:3063–3074. doi: 10.1007/s00432-020-03301-y

19. Xu XJ, Wang HS, Ju XL, Xiao PF, Xiao Y, Xue HM, et al. Clinical presentation and outcome of pediatric patients with hemophagocytic lymphohistiocytosis in China: a retrospective multicenter study. *Pediatr Blood Cancer* (2017) 4:1–6. doi: 10.1002/pbc.26264

20. Marsh RA. Epstein-Barr Virus and hemophagocytic lymphohistiocytosis. *Front Immunol* (2018) 8:1902. doi: 10.3389/fimmu.2017.01902

21. Dunmire SK, Verghese PS, Balfour HHJr. Primary Epstein - Barr virus infection. *J Clin Virol* (2018) 102:84–92. doi: 10.1016/j.jcv.2018.03.001

22. Arca M, Fardet L, Galicier L, Riviere S, Marzac C, Aumont C, et al. Prognostic factors of early death in a cohort of 162 adult haemophagocytic syndrome: Impact of triggering disease and early treatment with etoposide. *Br J Haematol* (2015) 1:63 – 8. doi: 10.1111/bjh.13102

23. Riviere S, Galicier L, Coppo P, Marzac C, Aumont C, Lambotte O, et al. Reactive hemophagocytic syndrome in adults: A retrospective analysis of 162 patients. *Am J Med* (2014) 11:1118 – 25. doi: 10.1016/j.amjmed.2014.04.034

24. Hayden A, Park S, Giustini D, Lee AYY, Chen LYC. Hemophagocytic syndromes (HPSs) including hemophagocytic lymphohistiocytosis (HLH) in adults: A systematic scoping review. *Blood Rev* (2016) 6:411–420. doi: 10.1016/j.blre.2016.05.001

25. Li F, Li P, Zhang RY, Yang GP, Ji DX, Huang XB, et al. Identification of clinical features of lymphoma-associated hemophagocytic syndrome (LAHS): an analysis of 69 patients with hemophagocytic syndrome from a single-center in central region of China. *Med Oncol* (2014) 4:902. doi: 10.1007/s12032-014-0902-y

26. Godby RC, Kraemer RR, May J, Soni S, Reddy V, Thomas JV, et al. Lymphohistiocytosis type 2 and chronic active Epstein-Barr virus in adulthood. *Am J Med Sci* (2021) 3:388–93. doi: 10.1016/j.amjms.2020.10.004

27. Yagi H, Conroy PJ, Leung EWW, Law RHP, Trapani JA, Voskoboinik I, et al. Structural basis for Ca2+ - mediated interaction of the perforin C2 domain with lipid membranes. *J Biol Chem* (2015) 42:25213–25226. doi: 10.1074/jbc.M115.668384

28. Richards S, Aziz N, Bale S, Bick D, Das S, Gastier-Foster J, et al. ACMG laboratory quality assurance committee. standards and guidelines for the interpretation of sequence variants: A joint consensus recommendation of the American college of medical genetics and genomics and the association for molecular pathology. *Genet Med* (2015) 17:405–424. doi: 10.1038/gim.2015.30

29. Abou Tayoun AN, Pesaran T, DiStefano MT, Oza A, Rehm HL, Biesecker LG, et al. ClinGen sequence variant interpretation working group (ClinGen SVI). recommendations for interpreting the loss of function PVS1 ACMG/AMP variant criterion. *Hum Mutat* (2018) 39:1517–1524. doi: 10.1002/humu.23626

30. Feng WX, Yang XY, Li JW, Gong S, Wu Y, Zhang WH, et al. Neurologic manifestations as initial clinical presentation of familial hemophagocytic lymphohistiocytosis Type2 due to PRF1 mutation in Chinese pediatric patients. *Front Genet* (2020) 11:126. doi: 10.3389/fgene.2020.00126

31. Birndt S, Schenk T, Heinevetter B, Brunkhorst FM, Maschmeyer G, Rothmann M, et al. Hemophagocytic lymphohistiocytosis in adults: Collaborative analysis of 137 cases of a nationwide German registry. *J Cancer Res Clin Oncol* (2020) 146:1065–1077. doi: 10.1007/s00432-020-03139-4

32. Zhang K, Chandrakasan S, Chapman H, Valencia CA, Husami A, Kissell D, et al. Synergistic defects of different molecules in the cytotoxic pathway leads to clinical familial hemophagocytic lymphohistiocytosis. *Blood* (2014) 124:1331–1334. doi: 10.1182/blood-2014-05-573105

frontiers | Frontiers in Oncology

TYPE Case Report
PUBLISHED 15 March 2023
DOI 10.3389/fonc.2023.1017230

OPEN ACCESS

EDITED BY
Ahmad Antar,
Almoosa Specialist Hospital, Saudi Arabia

REVIEWED BY
Shinsuke Takagi,
Toranomon Hospital, Japan
Govind Babu Kanakasetty,
HCG Cancer Hospital, India

*CORRESPONDENCE
Haitham Abdelhakim
habdelhakim@kumc.edu

SPECIALTY SECTION
This article was submitted to Hematologic Malignancies, a section of the journal Frontiers in Oncology

RECEIVED 17 August 2022
ACCEPTED 01 March 2023
PUBLISHED 15 March 2023

CITATION
Tabak C, Hyter S, Yacoub A, Byrd K, McGuirk J, Godwin AK and Abdelhakim H (2023) Case report: Invasive fungal infection in a patient with a rare CVID-causing gene (*TNFRSF13B*) mutation undergoing AML treatment. *Front. Oncol.* 13:1017230. doi: 10.3389/fonc.2023.1017230

Case report: Invasive fungal infection in a patient with a rare CVID-causing gene (*TNFRSF13B*) mutation undergoing AML treatment

Carine Tabak, Stephen Hyter, Abdulraheem Yacoub, Kenneth Byrd, Joseph McGuirk, Andrew K. Godwin and Haitham Abdelhakim*

Division of Hematologic Malignancies and Cellular Therapeutics, University of Kansas School of Medicine, Kansas City, MO, United States

Acute myeloid leukemia (AML) is a complex diagnosis that puts patients at a higher risk for developing infections, particularly invasive fungal infections (IFI). Mutations in *TNFRSF13B* have been shown to cause dysfunction in B-cell homeostasis and differentiation, making it a risk factor for developing immunodeficiency syndromes. In this case, a male patient in his 40s presented to our emergency department (ED) with symptoms leading to a diagnosis of AML with concurrent mucormycosis of the lungs and sinuses. Targeted next generation sequencing (NGS) of the patient's bone marrow showed, among other variants, a loss of function mutation in the *TNFRSF13B* gene. While most patients present with fungal infections after prolonged periods of neutropenia associated with AML treatment, this case presented with IFI at diagnosis without neutropenia suggesting an immunodeficiency syndrome. The concurrent IFI and AML diagnoses create a delicate balance between treatment of the infection and the malignancy. This case highlights the risk of infection in patients receiving chemotherapy, especially those with unrecognized immunodeficiency syndromes, and emphasizes the importance of NGS for prognosis and treatment.

KEYWORDS

acute myeloid leukemia, invasive fungal infections, *TNFRSF13B*, CVID, NGS

Background

Acute myeloid leukemia (AML) is a hematological malignancy that is characterized by abnormal proliferation and infiltration of the blood and bone marrow by cells of the hematopoietic lineage (1). Over the past few decades, advanced therapies and a better understanding of the pathology of AML have turned the fatal disease into a treatable

condition. However, many comorbidities can still make AML management aggressive and complex. Due to the hematological nature of the cancer, AML patients often present with a weakened immune system, making them more likely to develop opportunistic infections.

An AML diagnosis puts patients at a high risk for developing infections in general and invasive fungal infections (IFI) in particular. IFI is a major cause for mortality in patients with leukemia (2). The incidence of IFI in patients with AML has been reported to be as high as 12% (3). Due to the limited efficacy of most antifungal agents against IFIs, a risk-adapted strategy with an emphasis on prophylactic treatment is often implemented with an AML diagnosis (4). Candidemia and aspergillosis pathogens are the most common cause of fungal infections. However, the spectrum of fungal infections has shifted dramatically to include more fluconazole-resistant non-*Aspergillus* and non-*Candida albicans* species over the last few decades (5). The infection can become disseminated and can affect various organ systems depending on the pathogen, most prevalent are infections of the lungs, sinuses and of the bloodstream (2). Patients have a probability of 11.1% of developing IFI infections within 100 days of an AML diagnosis and experience a 35% cause-specific mortality due to the infection (6, 7). Furthermore, the diagnosis leads to substantial increases in health expenditure and hospital stay length (8). The regular use of anti-fungal prophylaxis has improved the outcomes of patients with AML (9, 10). However, breakthrough infections are not uncommon (11, 12).

Various genetic mutations could put patients, including patients with AML, at a higher risk for developing opportunistic infections. Mutations in *TNFRSF13B* have been noted as a possible risk factor to developing immunodeficiency syndromes, specifically CVID-like (common variable immune deficiency) manifestations (13). CVID is characterized by an inability to mount a full antibody immune response, and is associated with recurrent bacterial infections, autoimmunity, and lymphoproliferative disorders (14).

TNFSF13B encodes for B cell-activating factor (BAFF), which binds three TNF receptors expressed on B cells known as BAFFR (BAFF receptor, encoded by *TNFRS13C*), BCMA (B cell maturation protein A, encoded by *TNFRSF17*), and TACI (transmembrane activator and CAML interactor, encoded by *TNFRSF13B*) (13). Of the three sequence variants, mutations in TACI (encoded by *TNFRSF13B*) are of note due to their association with immunodeficiency syndromes. TACI loss of function mutations have been reported in 7-10% of patients diagnosed with CVID and have also been reported in IgA deficiency (14). TACI is a tumor necrosis factor receptor superfamily member that is expressed on peripheral B-cells, with the highest grade of expression on CD27+ B-cell subset 3. TACI binds two ligands that influence cell proliferation: a proliferation inducing ligand (APRIL) and B-cell activating factor (BAFF) (15). APRIL has been tied to impaired class switching to IgA7 in mice models and T-cell independent class switch recombination in functional studies (13). Therefore, variants in *TNFRSF13B* gene can lead to critical dysfunction in B-cell homeostasis, class-switch recombination, antibody secretion and plasma cell differentiation (16, 17). Due to this association with immune dysfunction, variants in *TNFRSF13B* would potentially place patients with AML at higher risk for developing opportunistic infections, such as invasive fungal infections. This study was IRB approved.

Clinical course

A male patient in his 40s presented to the ED with fever, malaise and mouth lesions after a recent dental procedure. The patient had a past medical history of depression and recurrent upper respiratory tract infections, not requiring hospitalization, and no personal history of malignancy or autoimmune disease. His surgical history includes appendectomy and cholecystectomy. Family history was positive for diabetes in his father and brother, and negative for any history of malignancy. Upon ED laboratory evaluation, the patient was found to have hyperleukocytosis with suspicion for acute leukemia. The patient was found to be hypoxic on admission and needed supplemental oxygen. CT scan of the lungs showed evidence of bilateral infiltration suggestive of fungal pneumonia but could not rule out leukemic infiltration. Lung CT scan also showed bronchial dilatation and wall thickenings (Figure 1A). Respiratory viral panel including RSV, COVID and flu testing were negative. Due to hyperleukocytosis and spontaneous tumor lysis syndrome, the patient was started on hydroxyurea for cytoreduction. Treatment with broad coverage with antibiotics and posaconzaole was initiated. He underwent bronchoscopy with bronchoalveolar lavage which was inconclusive with persistent negative cultures.

The bone marrow biopsy confirmed AML diagnosis with core binding factor. FISH studies showed results consistent with acute myeloid leukemia with 46,XY, inv(16)(p13.1.q22). NGS was performed using a 141 myeloid-focused gene panel and showed a pathogenic *NRAS* mutation. These prognostic markers put the patient in the favorable risk group. The patient was started on daunorubicin/cytarabine (standard 7 + 3 regimen) + gemtuzumab after improvement in tumor lysis parameters with hydroxyurea cytoreduction. The patient's clinical picture deteriorated with persistent fever, sinus pain, development of hypoxic respiratory failure after one week. Repeat CT chest showed progression of nodular multifocal pneumonia suggestive fungal pneumonia. Sinus MRI confirmed acute invasive fungal sinusitis with right orbital spread. The patient was started on liposomal amphotericin, isavuconazole and micafungin. To debulk and identify the infection, the patient underwent debridement with septoplasty, right maxillary antrostomy, right total ethmoidectomy and sphenoidectomy with tissue debridement. Two days later, the patient underwent nasal endoscopy with debridement, endoscopic orbital decompression and debridement. Bronchoscopy was repeated with bronchoalveolar lavage and transbronchial biopsy. Both the sinus and respiratory specimens confirmed angioinvasive fungal infection, histologically most consistent with Mucorales species, but with negative cultures. Triple anti-fungal therapy was continued. Bone marrow biopsy showed persistent AML disease and patient opted not to receive chemotherapy treatment and was discharged home.

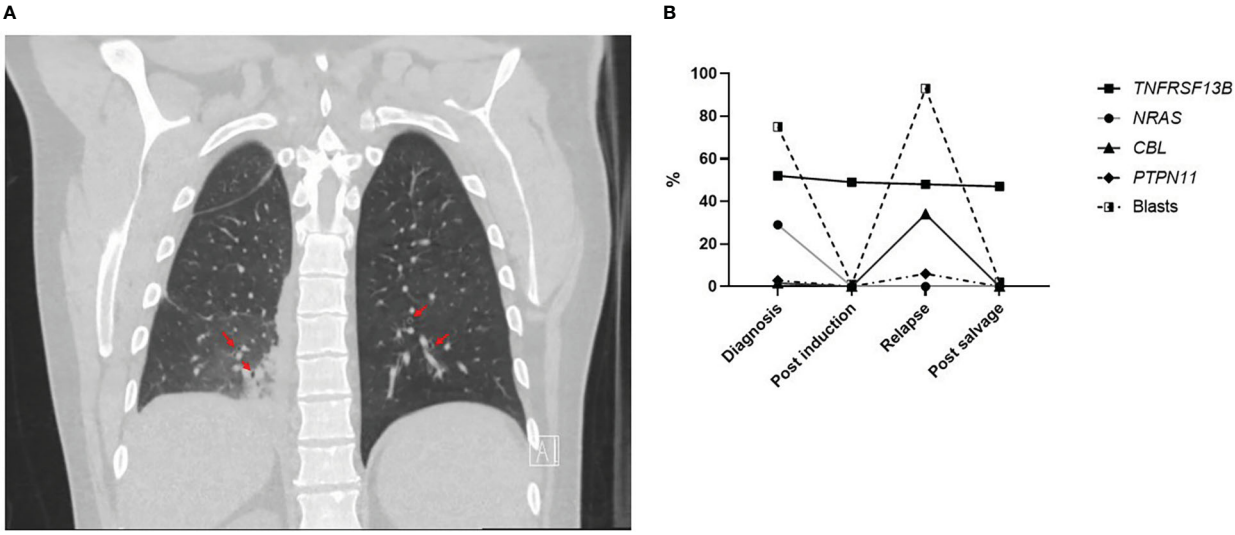

FIGURE 1
(A) Coronal section of lung CT scan showing bronchiectasis (red arrows). **(B)** Percentage of different gene variants detected on NGS and percentage of AML blasts on morphology from bone marrow samples evaluated at different timepoints during the treatment course.

After 2 months, the patient had significant clinical improvement, He re-established care with the leukemia clinic. CT showed improvement in multifocal pneumonia, with mild residual opacities possibly from scarring and/or recurrent infection. Further follow-up showed remission of AML and recovery of blood counts. Fungal infection was persistent on nasal endoscopy and biopsy. He opted to delay chemotherapy and continue anti-fungal treatments with close follow up. AML relapsed 8 months from the original diagnosis but is back in remission after reinduction chemotherapy with mitoxantrone, etoposide and cytarabine (MEC). Patient stayed on antifungal therapy, and he tolerated the treatment without a flare of the IFI. He proceeded with allogeneic stem cell transplant with reduced intensity conditioning from a full matched sibling 11 month after the initial diagnosis. Patient achieved 98%, 100% donor chimerism at D60,100 post-transplant respectively. However, he had AML relapse 6 months after transplant.

The presence of invasive fungal infection at AML diagnosis before starting treatment without indication of prior prolonged neutropenia prompted assessment of immunoglobulins levels. The patient had low IgG levels when checked after complete recovery from chemotherapy at multiple visits (610-628 mg/dl). IgA was low normal (41 mg/dl) and IgM was within normal limits at this time (157 mg/dl). Absolute neutrophil, monocyte and lymphocyte counts were within normal level when AML was in remission (3400-5900/µL, 500-1100/µL,900-2200/µL, respectively). Furthermore, NGS results at initial diagnosis showed a likely pathogenic loss-of-function variant in the *TNFRSF13B* gene (c.311G>A/p.C104Y) at a variant allelic fraction (VAF) of 52%. Although germline testing was not performed, this particular lesion involves the same codon as the well-known C104R familial variant linked to CVID, suggesting the patient had unrecognized CVID prior to AML diagnosis (13, 18). Additional evidence for the non-somatic nature of this *TNFRSF13B* variant is the VAF stability seen during remission and relapse stages of this patient's disease in comparison to other pathogenic variants associated with AML (Figure 1B). In addition to hypogammaglobulinemia, patients had mild supraclavicular, mediastinal, abdominal lymphadenopathy with slightly large spleen (10.5 cm) at diagnosis that remained unchanged during AML remission. All lymph nodes were subcentimeteric so further diagnostic intervention was not pursued. Lymphoproliferation with mild splenomegaly and lymphadenopathy is predominant in CVID patients (14). Interestingly, repeat CT scan 6 months post-allogeneic stem cell transplant showed resolution of all lymphadenopathy and splenomegaly. Moreover, IgG level normalized (894 mg/dl) which coincided with the presence of full donor lymphoid chimerism concurrently with drop in donor myeloid chimerism and AML relapse. This highlights that hypogammaglobulinemia and lymphoproliferation are likely unrelated to the AML diagnosis and likely associated with CVID that was cured after hematopoietic stem transplant and replacement of the patient's *TNFRSF13B* mutated lymphoid system.

Discussion

Several scientific advancements over the last decade have improved our understanding of the genetic diversity of AML and have led to the development of new therapies (19). The goal of induction chemotherapy treatment in patients with AML is achieving remission and is associated with severe neutropenia and immunosuppression. This puts patients with AML at higher risk for IFI, which usually develops after a prolonged neutropenic period (3). Nevertheless, the patient in this case presented with IFI at diagnosis with no prior prolonged neutropenic period. This presentation raised the question of an immunodeficiency syndrome that would make him susceptible to infections and his risk for infections further surged with development of AML. While we cannot prove that the *TNFRSF13B* mutation caused the infection, the diagnosis of the IFI in the presence of preexisting bronchiectasis, hypogammaglobulinemia and the lack

history of prior neutropenia make it highly likely that the mutation played a role at least in the development of this life-threatening infection.

Various immune deficiency syndromes, such as CVID, can further increase the risk of infections in patients receiving chemotherapy. Loss of function mutations in *TNFRSF13B*, specifically, have been linked to immune deficiency and dysfunction due to dysregulation of B-cell homeostasis, differentiation, and antibody secretion (14). Yet, it is uncommon for an individual to present with AML and concurrently be diagnosed with an immunodeficient mutation, as with the presented case.

Immunodeficiency adds an additional challenge to treating invasive fungal infections in patients with an AML diagnosis. Both the nature of the disease and the associated treatments induce an immunocompromised state in patients that leaves them more vulnerable for infections. On the other hand, patients diagnosed with IFI may be forced to delay chemotherapy for their AML to complete treatment for the infection in order to avoid a prolonged period of neutropenia. Without proper induction and consolidation therapy, patients are extremely unlikely to reach complete remission of their malignancy. This creates a delicate balance between the risk and benefit of treating the malignancy and controlling the fungal infection.

This case highlights the high risk of infection in patients with AML receiving intensive chemotherapy, especially in the rare instance of a concurrent immunodeficiency syndrome. Moreover, it highlights the role of NGS as a powerful tool not only for delineating prognosis of patients with AML but also capturing germline mutations with potential implications of infectious complications during treatment.

Data availability statement

The original contributions presented in the study are included in the article/supplementary material. Further inquiries can be directed to the corresponding author.

Ethics statement

The studies involving human participants were reviewed and approved by University of Kansas Medical Center. Written informed consent for participation was not required for this study in accordance with the national legislation and the institutional requirements.

Author contributions

CT and HA designed the study and wrote the manuscript. AG, JM and SH provided data, and interpretation and contributed to writing and reviewing the manuscript. AY and KB provided data and interpretation and reviewed the manuscript. All authors contributed to the article and approved the submitted version.

Conflict of interest

The authors declare that the research was conducted in the absence of any commercial or financial relationships that could be construed as a potential conflict of interest.

Publisher's note

References

1. Dohner H, Weisdorf DJ, Bloomfield CD. Acute myeloid leukemia. *N Engl J Med* (2015) 373(12):1136–52. doi: 10.1056/NEJMra1406184

2. Bhatt VR, Viola GM, Ferrajoli A. Invasive fungal infections in acute leukemia. *Ther Adv Hematol* (2011) 2(4):231–47. doi: 10.1177/2040620711410098

3. Pagano L, Caira M, Candoni A, Offidani M, Fianchi L, Martino B, et al. The epidemiology of fungal infections in patients with hematologic malignancies: The seifem-2004 study. *Haematologica* (2006) 91(8):1068–75.

4. Nucci M, Anaissie E. How we treat invasive fungal diseases in patients with acute leukemia: The importance of an individualized approach. *Blood* (2014) 124(26):3858–69. doi: 10.1182/blood-2014-04-516211

5. Singh N. Trends in the epidemiology of opportunistic fungal infections: Predisposing factors and the impact of antimicrobial use practices. *Clin Infect Dis* (2001) 33(10):1692–6. doi: 10.1086/323895

6. Hammond SP, Marty FM, Bryar JM, DeAngelo DJ, Baden LR. Invasive fungal disease in patients treated for newly diagnosed acute leukemia. *Am J Hematol* (2010) 85 (9):695–9. doi: 10.1002/ajh.21776

7. Auberger J, Lass-Florl C, Ulmer H, Nogler-Semenitz E, Clausen J, Gunsilius E, et al. Significant alterations in the epidemiology and treatment outcome of invasive fungal infections in patients with hematological malignancies. *Int J Hematol* (2008) 88 (5):508–15. doi: 10.1007/s12185-008-0184-2

8. Morgan J, Meltzer MI, Plikaytis BD, Sofair AN, Huie-White S, Wilcox S, et al. Excess mortality, hospital stay, and cost due to candidemia: A case-control study using data from population-based candidemia surveillance. *Infect Control Hosp Epidemiol* (2005) 26(6):540–7. doi: 10.1086/502581

9. Cornely OA, Maertens J, Winston DJ, Perfect J, Ullmann AJ, Walsh TJ, et al. Posaconazole vs. fluconazole or itraconazole prophylaxis in patients with neutropenia. *New Engl J Med* (2007) 356(4):348–59. doi: 10.1056/NEJMoa061094

10. Halpern AB, Lyman GH, Walsh TJ, Kontoyiannis DP, Walter RB. Primary antifungal prophylaxis during curative-intent therapy for acute myeloid leukemia. *Blood* (2015) 126(26):2790–7. doi: 10.1182/blood-2015-07-627323

11. Shuman K, Hunt RG, Hibino M, Stone T, Dralle S, Manuel M, et al. Incidence of breakthrough fungal infections in acute myeloid leukemia patients receiving low intensity therapy in the upfront and Relapsed/Refractory setting. *Blood* (2021) 138:3372. doi: 10.1182/blood-2021-146620

12. Wasylyshyn A, Linder KA, Castillo CG, Zhou S, Kauffman CA, Miceli MH. Breakthrough invasive fungal infections in patients with acute myeloid leukemia. *Mycopathologia* (2020) 185(2):299–306. doi: 10.1007/s11046-019-00418-8

13. Salzer U, Chapel HM, Webster AD, Pan-Hammarstrom Q, Schmitt-Graeff A, Schlesier M, et al. Mutations in Tnfrsf13b encoding taci are associated with common variable immunodeficiency in humans. *Nat Genet* (2005) 37(8):820–8. doi: 10.1038/ng1600

14. Pulvirenti F, Zuntini R, Milito C, Specchia F, Spadaro G, Danieli MG, et al. Clinical associations of biallelic and monoallelic Tnfrsf13b variants in Italian primary antibody deficiency syndromes. *J Immunol Res* (2016) 2016:8390356. doi: 10.1155/2016/8390356

15. Wu Y, Bressette D, Carrell JA, Kaufman T, Feng P, Taylor K, et al. Tumor necrosis factor (Tnf) receptor superfamily member taci is a high affinity receptor for tnf family members April and blys. *J Biol Chem* (2000) 275(45):35478–85. doi: 10.1074/jbc.M005224200

16. Castigli E, Wilson SA, Scott S, Dedeoglu F, Xu S, Lam KP, et al. Taci and baff-r mediate isotype switching in b cells. *J Exp Med* (2005) 201(1):35–9. doi: 10.1084/jem.20032000

17. Romberg N, Virdee M, Chamberlain N, Oe T, Schickel JN, Perkins T, et al. Tnf receptor superfamily member 13b (Tnfrsf13b) hemizygosity reveals transmembrane activator and caml interactor haploinsufficiency at later stages of b-cell development. *J Allergy Clin Immunol* (2015) 136(5):1315–25. doi: 10.1016/j.jaci.2015.05.012

18. Poodt AE, Driessen GJ, de Klein A, van Dongen JJ, van der Burg M, de Vries E. Taci mutations and disease susceptibility in patients with common variable immunodeficiency. *Clin Exp Immunol* (2009) 156(1):35–9. doi: 10.1111/j.1365-2249.2008.03863.x

19. Yeoh ZH, Bajel A, Wei AH. New drugs bringing new challenges to aml: A brief review. *J Pers Med* (2021) 11(10). doi: 10.3390/jpm11101003

frontiers | Frontiers in Oncology

TYPE Case Report
PUBLISHED 16 March 2023
DOI 10.3389/fonc.2023.1100559

OPEN ACCESS

EDITED BY
Osamu Imataki,
Kagawa University, Japan

REVIEWED BY
Alexander Klein,
LMU Munich University Hospital, Germany
Hong Duan,
Sichuan University, China
Xiang Fang,
Sichuan University, Chengdu, China,
in collaboration with reviewer HD

*CORRESPONDENCE
Kirill A. Lyapichev
kilyapic@utmb.edu

SPECIALTY SECTION
This article was submitted to Hematologic Malignancies, a section of the journal Frontiers in Oncology

RECEIVED 21 November 2022
ACCEPTED 27 February 2023
PUBLISHED 16 March 2023

CITATION
Bhakta P, Hunzeker ZE, Garcia JD, Youssef A, Grant BJ, Alfattal R, Weaver D, Bhargava P, Rischall A, Musunuru T, Muthukumarana PV, Mallick J and Lyapichev KA (2023) Pathological fracture due to primary bone lymphoma in a patient with a history of prostate cancer: A case report and review of literature. *Front. Oncol.* 13:1100559. doi: 10.3389/fonc.2023.1100559

Pathological fracture due to primary bone lymphoma in a patient with a history of prostate cancer: A case report and review of literature

Pooja Bhakta[1], Zachary E. Hunzeker[2], Juan D. Garcia[3], Ayman Youssef[2], Bradley J. Grant[3], Rasha Alfattal[3], Dylan Weaver[4], Peeyush Bhargava[4], Ariel Rischall[5], Tejo Musunuru[5], Palawinnage V. Muthukumarana[3], Jayati Mallick[3] and Kirill A. Lyapichev[3]*

[1]Department of Internal Medicine, John Sealy School of Medicine, University of Texas Medical Branch at Galveston, Galveston, TX, United States, [2]John Sealy School of Medicine, University of Texas Medical Branch at Galveston, Galveston, TX, United States, [3]Department of Pathology, John Sealy School of Medicine, University of Texas Medical Branch at Galveston, Galveston, TX, United States, [4]Department of Radiology, John Sealy School of Medicine, University of Texas Medical Branch at Galveston, Galveston, TX, United States, [5]Division of Hematology and Oncology, Department of Internal Medicine, John Sealy School of Medicine, University of Texas Medical Branch at Galveston, Galveston, TX, United States

Primary bone lymphoma (PBL) is a rare extranodal presentation within lymphomas and primary bone malignancies. Pathologic fracture (PF) is a common complication of metastatic bone disease but is, rarely, the presentation of a primary bone tumor. We report a case of an 83-year-old man with a history of untreated prostate cancer, presenting with atraumatic fracture of his left femur after months of intermittent pains and weight loss. Radiographic workup revealed a lytic lesion suspicious for PF secondary to metastatic prostate cancer; however, initial core biopsy results were inconclusive for malignancy. A complete blood count with differential and complete metabolic panel was within normal limits. During surgical fixation and nailing of the femur, a reaming biopsy was performed as a repeat measure and revealed diffuse large B-cell lymphoma. Staging with positron emission tomography and computed tomography found no evidence of lymphatic or visceral involvement and chemotherapy was promptly initiated. This case highlights the diagnostic workup challenges for PF secondary to PBL, especially in the setting of concurrent malignancy. Because of the non-specific presentation of a lytic lesion on imaging associated with atraumatic fracture, we highlight PBL as an important diagnostic consideration.

KEYWORDS

primary bone lymphoma, diffuse large B cell lymphoma (DLBCL), femur, diaphyseal fracture, pathological fracture, rituximab, CHOP

Introduction

The 2020 World Health Organization classification of tumors of bone classifies primary non-Hodgkin lymphoma of the bone as a neoplasm of malignant lymphoid cells in the bone with no lymph node involvement or other extranodal involvement (1). Originally termed "reticulum sarcoma of the bone" nearly a century ago, primary bone lymphoma (PBL) began to officially be histologically and cytologically recognized in the 1970s (2). However, PBL accounts for less than 1% of all lymphomas and less than 5% of all primary bone tumors (3, 4). Given its rarity, it has been difficult to employ a consistent definition and to fully understand the clinical and pathologic characteristics of this unique entity (5). On the basis of the available data, the average age of diagnosis is 45–60 years old with a slight predominance toward male patients (4).

Approximately 95% of diagnosed PBL is pathologically characterized as diffuse large B-cell lymphoma (PB-DLBCL) (4, 6, 7). Most cases present with localized pain, and nearly half of all cases are associated with localized swelling (8). Unlike other symptoms, pathological fracture (PF) is an unusual PBL complication (8). Commonly involved sites include the spine, lower extremity bones, and pelvis, with a predisposition toward the long bones at the site of the metaphysis and/or diaphysis (8, 9). Because of the non-specific features of this entity, the diagnostic process utilized in PBL contains many challenges. However, prompt treatment with rituximab and cyclophosphamide, doxorubicin, vincristine, and prednisone (CHOP)–based therapy in cases of PB-DLBCL has been shown to demonstrate favorable 5-year overall survival (OS) and progression-free survival (PFS) rates (7, 8).

Herein, we present an unusual presentation of PB-DLBCL as a PF in a patient with concurrent untreated prostate cancer. This case highlights the importance of considering PBL in the differential diagnosis for patients with a PF.

Case presentation

An 83-year-old male Caucasian prison inmate with a past medical history of untreated prostate cancer presented to the prison hospital after spontaneous development of pain and weight-bearing limitation in the left leg. Over the previous 2 months, the patient reported intermittent sharp shooting pains in his left thigh and 10 pounds of unintentional weight loss. He denied experiencing any episodes of fever, chills, or night sweats, and the only other positive symptoms upon a review of systems included occasional constipation and diarrhea. Family and social histories were, otherwise, felt to be non-contributory. The physical exam was significant for tenderness to the left lower extremity at the superior femur with warmth but no bruising. Dorsalis pedis and posterior tibial pulses were palpable bilaterally. On musculoskeletal exam, the patient was able to move his toes and ankle without pain bilaterally but exhibited pain during left knee and hip range of motion tests. The range of motion at the left hip was completely inhibited by pain. He had a full painless range of motion in his right lower extremity. Complete blood count showed a decreased hemoglobin level of 10.5 g/dl with no other abnormalities; basic metabolic panel was notable for hypocalcemia to 7.9 mg/dl with all other electrolytes and creatinine within normal limits. Prostate specific antigen was 5.08 ng/ml. Left lower extremity x-ray showed an irregular 2.5-mm displaced left femur shaft fracture with a "moth-eaten" appearance consistent with PF (Figure 1A).

Computed tomography (CT) scan of the left lower extremity showed a comminuted fracture of the mid-femoral diaphysis with permeative appearance of the cortex at the level of the fracture. A large heterogeneous surrounding soft tissue enhancement was noted, representing a possible soft tissue lesion *vs.* hematoma (Figures 1B–D). Ultrasound-guided core needle biopsy did not reveal evidence of malignancy. Additional CT imaging of the chest/abdomen/pelvis was inconclusive.

Magnetic resonance imaging (MRI) was planned for the left leg, but the patient first underwent intramedullary nail fixation and reduction, during which a repeat and conclusive intraoperative left femur reaming biopsy was taken (Figures 1E, F). Histological and immunohistochemical (IHC) evaluation identified a focally necrotic, atypical lymphoid population positive for CD10 (>30%), CD20, CD45, PAX-5, Bcl-2 (>50%), and Bcl-6 (>30%) (Figure 2). Assessment *via* Ki-67 indicated a high proliferation rate at approximately 80%–90% in the viable areas. *In situ* hybridization was negative for Epstein–Barr virus. This established a diagnosis of DLBCL. Because of the presence of a solitary osseous lesion without extraosseous evidence of disease, the tumor was further classified as PB-DLBCL. The diagnostic assistance of MRI was no longer needed, so attention was turned toward treatment and staging.

Initial treatment was delayed because of the necessary post-operative recovery. A positron emission tomography (PET) and CT scan was performed, which revealed hypermetabolic activity of the mid-femoral bone at the site of the bone lesion (Figures 1D–F). Fluorodeoxyglucose (FDG) uptake of gastrointestinal sites prompted evaluation by esophagogastroduodenoscopy and colonoscopy, which showed no evidence of malignancy. The patient was consequently classified as having stage - 1E PB-DLBCL (10).

The patient completed five of six planned cycles of R-miniCHOP chemotherapy, consisting of 3-week intervals of rituximab (375 mg/m^2), cyclophosphamide (400 mg/m^2), doxorubicin (25 mg/m^2), and vincristine (1 mg) all given intravenously on day 1 of each cycle (C) and oral prednisolone (40 mg/m^2) on days 1–5. During this time, he noted a steady progression in his ambulatory status ultimately using a walker in his prison unit. Of note, vincristine was dropped after C2 from the regimen due to development of constipation, neuropathy, and palpitations. Pancytopenia was noted after C5 but resolved. Radiation therapy was planned with pending CT simulation, set to begin after completing chemotherapy. However, prior to his appointment for C6, the patient had a fall in his unit resulting in fracture of his right femur. He underwent subsequent right hip hemiarthroplasty which delayed C6. CT Simulation scan of the left hip was still done, which found incomplete response to chemotherapy. Repeat PET-CT was planned to re-stage, but the patient unfortunately developed septic shock secondary to right lower lobe pneumonia and died before any further diagnostic or treatment methods were employed.

10.3389/fonc.2023.1100559

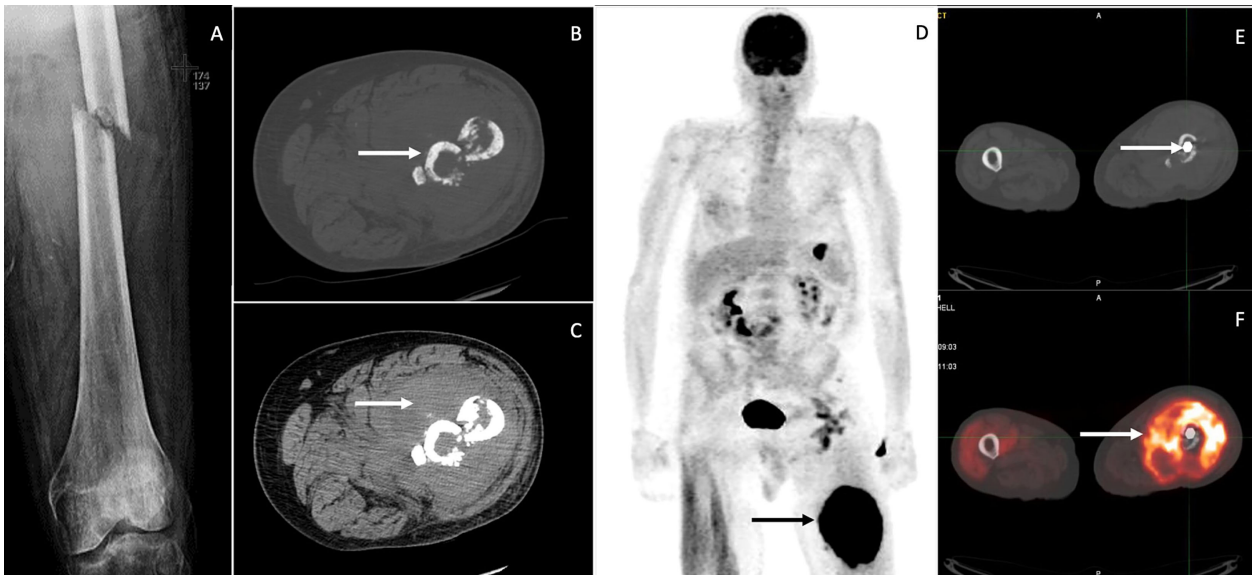

FIGURE 1
X-ray demonstrates displaced mid femoral pathologic fracture through a permeative lesion with improved alignment and diffuse osteopenia **(A)**. Axial images from CT of the left lower extremity showing a pathologic fracture involving the left proximal femur with sclerotic and fragmented bones (arrow in **(B)**, and a large heterogeneous soft tissue density mass surrounding the bone fragments (arrow in **(C)**. Whole-body image from the FDG PET/CT scan **(D)** shows intense hypermetabolism in the left thigh mass, consistent with neoplastic involvement. Other foci of increased uptake were thought to be non-neoplastic. The pathologic fracture has been internally fixed with an intramedullary nail (arrow in **(E)**, and the axial fused PET/CT image shows intense hypermetabolism in the mass surrounding the proximal femur (arrow in **(F)**.

Discussion

PBL presents similarly compared to other bone malignancies. More than 90% of primary bone tumors are sarcomas including osteosarcoma, chondrosarcoma, and Ewing sarcomas (11). Unfortunately, both PBL and the sarcomas, as well as bone metastases, all typically feature pain and less frequently swelling, neurologic symptoms, and pathologic fracture (PF) (11–13). Thus, diagnosis requires radiographic characterization and pathology results. However, a primary bone tumor with no other concurrent tumors may entail a different diagnostic management plan than a new lesion in the setting of known metastatic disease. In our case, we were caught between these in the uncommon scenario where one solitary bone lesion of unknown etiology is found in the setting of a known primary, particularly one with a strong predisposition toward bony metastasis.

This case highlights the diagnostic challenge in delineating between primary and secondary bone malignancy in a patient with pre-existing prostate cancer and a newfound bone lesion, in this case presenting with PF. Pathological fractures are often indicative of advanced malignancy that has metastasized to the bone—namely, breast, prostate, lung, thyroid, and kidney cancers (14). Metastatic cancer spread involving bone results in PF in 20% of all cases of skeletal-related events (15). Metastatic prostate cancer was initially suspected in our patient, as most patients develop bone metastasis over the disease course (16), and most PFs are due to metastatic rather than primary bone cancer (17). Even within the scope of primary bone malignancy, PBL makes up less than 5% of cases (18). Hence, suspicion for PBL was exceedingly low at the onset of this case, but maintaining the adage that "a bone lesion with unknown etiology is a primary bone tumor until proven otherwise" provides an appropriate framework for approaching such a presentation (19). The diagnostic workup for PFs with unknown etiology outlined by Willeumier et al. suggests that, in the setting of a known pre-existing malignancy with no prior metastases, biopsy of the new unknown solitary lesion should be considered (19).

The most crucial diagnostic component in the evaluation of PF is the histologic assessment from biopsy (20). For initial biopsy of bone and soft tissue tumors, core needle biopsy is the standard alongside the incisional biopsy as compared to fine needle aspiration (FNA) (21). Percutaneous imaging–guided biopsy for pathologic bone lesions is especially difficult in the setting of PF (21). The well-known risks of an open procedure biopsy include infection, hematoma, and seeding of tumor cells among others (21). Moreover, a study by Afinowi et al. showed that 51% of reaming biopsies provided a positive diagnosis, whereas another 45% of cases of reportedly adequate samples resulted in false-negative results most commonly from samples associated with crushed artifacts or non-viable bone ($P = 0.015$) (22). The presence of crushed artifact and necrosis on biopsy samples from PBL lesions is well described in the literature and poses a serious challenge in obtaining diagnostic biopsy tissue samples (23). The usage of FNA to then perform flow cytometry has been discussed as an important diagnostic tool that may alleviate the issue of crushed artifact and necrosis associated with PBL (24, 25). In our case, without conclusive results from the initial biopsy, we decided to perform reaming biopsy during the intramedullary nailing (IMN)

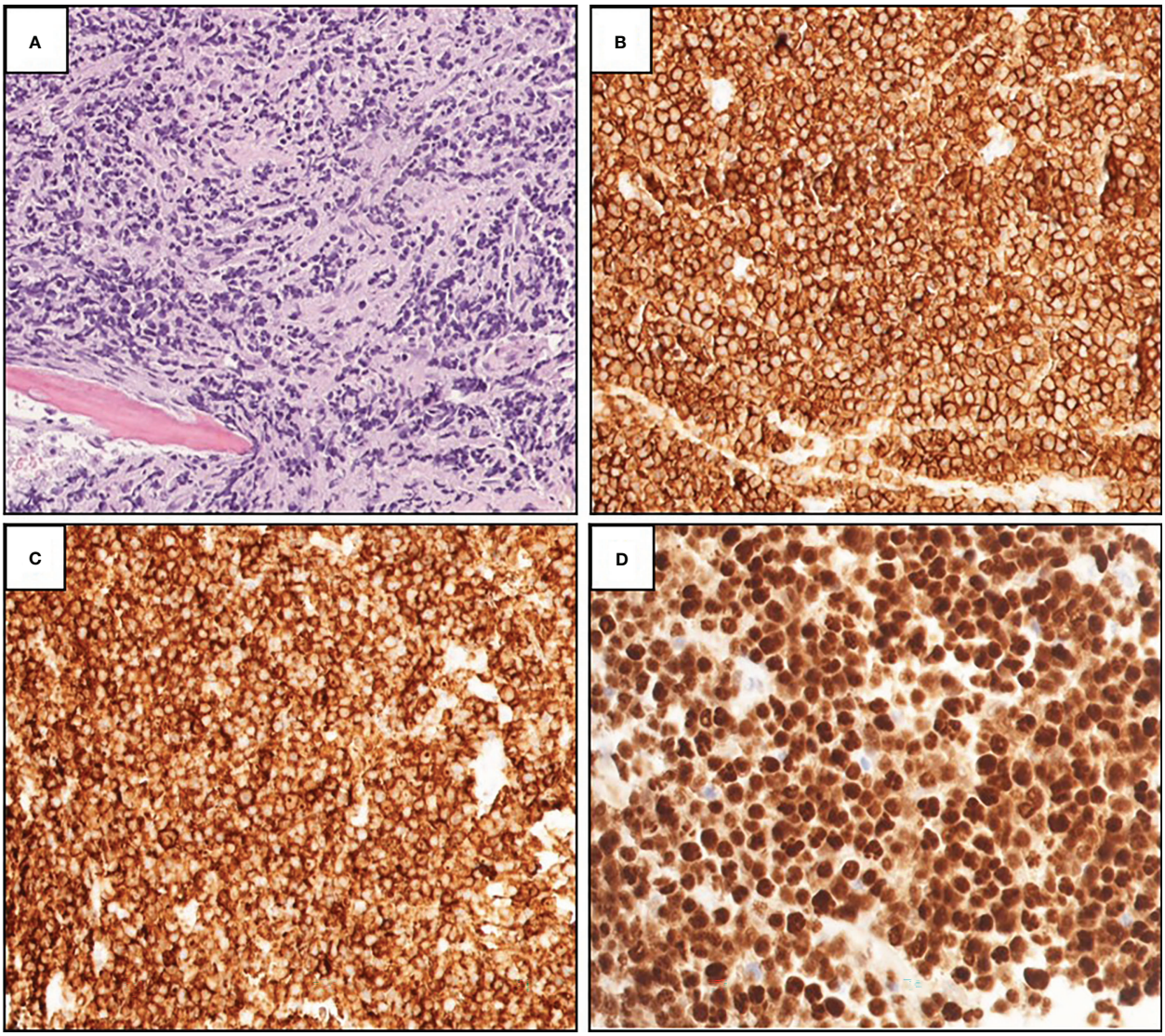

FIGURE 2
(A) Histopathological examination of showed focally necrotic and fibrotic diffuse lymphoid infiltrate surrounding bone trabecular (H&E, 200×). Immunohistochemistry showing strongly positive staining for CD20 **(B)**, 200×), CD10 **(C)**, 200×), and PAX-5 **(D)**, 200×).

fixation and reduction procedure. Although Gusho et al. pushed against a role for reaming biopsies during IMN fixation and reduction in known metastatic bone disease patients due to frequent inadequacy of samples and little impact on clinical management, this dual diagnostic/therapeutic management step is poorly described in patients with a known primary and solitary new lesion but no prior metastases (26). In such patients, this case demonstrates that performing a reaming biopsy during IMN fixation may help get additional information regarding new mutations.

This case also illustrates multiple similarities between prostatic metastasis and PBL, particularly on imaging. Metastatic prostate cancer and PBL both frequently present in the vertebral column, most commonly in the lumbar spine (6, 27). The rates of long bone involvement in PBL and metastatic prostate cancer are also significant, at 23% and 15%, respectively (6, 28). Up to 22% of metastatic prostate cancer in bone results with PF (29). However, PF in PBL is less common and has accounted for approximately 10%–15% of presentations in previous studies (30–32).

The typical radiographic and CT characteristics that indicate pathologic rather than stress fractures include aggressive (rather than benign) periosteal reaction, a lytic or permeative marrow pattern, and the presence of a soft-tissue mass (33). Although we were unable to use MRI, it is a more suitable imaging modality for this purpose, with characteristic findings for PF including homogenous T1-hypointense signal abnormality at the site of fracture due, in part, to the tumor itself and potentially, in part, to edema and bleeding at the site (33). Whereas prostatic metastases are typically osteosclerotic or osteoblastic in appearance on plain film radiography, PBL and the sarcomas predominantly exhibit an

osteolytic pattern with soft tissue extension (34–36). Moreover, PBL and Ewing Sarcoma are known to cause periosteal reactions (35, 36). However, prostatic bony metastases were found in one study to present as osteolytic themselves 16.4% of the time (37). Likewise, mixed blastic-lytic lesions are a possible radiological presentation of both prostatic metastases and PBL (34, 35). Last, one significant finding on CT was the surrounding soft tissue enhancement. With a hallmark of PF appearance on CT, soft tissue enhancement can represent extraosseous or soft tissue extension of a bony tumor. However, although this phenomenon is noteworthy for PBL, it has also been found in up to a third of prostatic metastases (35, 38). Thus, osteolytic appearance on plain film radiography may be of more clinical utility than soft tissue extension in distinguishing between these two entities.

Although MRI is an excellent diagnostic tool in the workup of unknown bone malignancy, it was ultimately not needed upon diagnosis with histopathology and staging *via* PET. PET-CT scanning is quickly gaining interest as a tool for initial characterization, staging, biopsy selection, evaluation of treatment response, and surveillance of tumor recurrence (39, 40). This is largely due to the high sensitivity of PET-CT imaging in the detection of PBL lesions, with a sensitivity of 90%–100% (4, 39, 40). PET-CT imaging can be particularly valuable in the staging of PBL due to its ability to evaluate for the presence of whole-body disease involvement, as opposed to nuclear MRI or CT imaging (41). Furthermore, repeat post-treatment imaging with a PET-CT scan can evaluate the response to treatment through the measurement of metabolic activity using standard uptake value quantification (39, 40).

IHC evaluation of diagnostic material was positive for DLBCL Germinal Center B-cell (GCB), which has a better prognosis and is commonly found in PB-DLBCL (7, 8). A study by de Groen et al. evaluated different OS/PFS rates in patients with PB-DLBCL, NO-DLBCL, polyostotic-DLBCL, and disseminated-DLBCL using histologic, IHC, FISH, gene expression profiling, and targeted next-generation sequencing (5). Their study revealed that 68% of stage I/II PB-DLBCL tumors had at least one mutation in B2M, EZH2, IRF8, and TNFRSF14 compared with fewer mutations in stage I/II NO-DLBCL tumors (5). Furthermore, PB-DLBCL had significant differences in immune surveillance gene expression compared with NO-DLBCL (5). Their study also revealed that stage I/II PB-DLBCL had a statistically significant greater difference in OS/PFS versus stage I/II NO-DLBCL (5). These distinct differences in gene expression and outcomes between these two classifications of DLBCL provide additional evidence that PB-DLBCL should be treated as a unique entity and may be useful in the differentiation of PB-DLBCL and NO-DLBCL with osseous involvement.

Although surgery plays an important role in bone stabilization and resolution of fracture, PBL treatment typically consists of anti-CD20 (rituximab) and CHOP based therapies, with the possible addition of radiotherapy (RT) if necessary (8). Compared with NO-DLBCL, patients with PB-DLBCL have favorable 5-year OS rates, ranging from 60% to 95% (mean OS, 82%) (7, 8). A study by Li et al. demonstrated that 90% of PB-DLBCL has a GCB-like immunophenotype that is associated with better prognosis compared with non-GCB–like immunophenotype (7). However, despite better OS and PFS in PB-DLBCL, pre-treatment characteristics and events such as PF are associated with worse prognostic outcomes (8, 9). A multicenter study by Govi et al. demonstrated that initial treatment of PF with RT in patients with DLBCL experienced worse OS compared with patients treated initially with chemotherapy (5-year OS: 22 ± 14% versus 64 ± 9%, P = 0.007) (9). Nevertheless, studies evaluating the role of RT in PB-DLBCL have produced mixed results.

One severe limitation in our approach to this case was poor access to MRI, normally an essential aid to diagnosis of any bone lesion suspicious for cancer. Likewise, our initial ultrasound-guided core needle biopsy was unhelpful, the inconclusive results of which may be insufficient amount of diagnostic material. However, we were able to obtain an adequate sample to establish our diagnosis from the reaming biopsies. Furthermore, lack of interim or routine surveill

63ance PET-CT (i.e., every two cycles as recommended by Zhang et al.) hindered our treatment plan, as the patient was ultimately not showing much response to the r-mini CHOP regimen (42). However, this result may have been further complicated by having to stop vincristine due to adverse effects.

Conclusion

Here, we summarize our experience with managing PB-DLBCL presenting with PF in a patient with a synchronous untreated prostate cancer and provide a comprehensive review of literature on this topic, with emphasis on the diagnostic challenges and use of reaming biopsy during fracture stabilization to make the diagnosis. Although PBL rarely presents with PF and even more rarely is synchronous with another primary tumor, it should be considered as a possible primary bone tumor in the differential diagnosis for PF.

Data availability statement

The original contributions presented in the study are included in the article/supplementary material. Further inquiries can be directed to the corresponding author.

Ethics statement

Written informed consent was obtained from the individual(s) for the publication of any potentially identifiable images or data included in this article.

Author contributions

Study conception and design: PoB, AY, and KL. Manuscript preparation/drafting: PoB, ZH, AY, BG, RA, DW, PeB, AR, TM,

PM, JM, and KL. Expert review: KL. All authors contributed to the article and approved the submitted version.

Conflict of interest

The authors declare no conflicts of interest for this work and that there are no conflicts of interest regarding the publication of this article.

Publisher's note

References

1. Board WCoTE. *Soft tissue and bone tumours*. Lyon: International Agency for Research on Cancer (2020).

2. Boston HCJr., Dahlin DC, Ivins JC, Cupps RE. Malignant lymphoma (so-called reticulum cell sarcoma) of bone. *Cancer* (1974) 34(4):1131–7. doi: 10.1002/1097-0142(197410)34:4<1131::AID-CNCR2820340424>3.0.CO;2-X

3. Sharma A, Ahmed R, Agrawal N, Kapoor J, Sharma A, Khushoo V, et al. Primary bone lymphoma: A 13 year retrospective institutional analysis in the chemo-immunotherapy era. *Indian J Hematol Blood Transfus* (2021) 37(2):240–8. doi: 10.1007/s12288-020-01327-3

4. Bindal P, Desai A, Delasos L, Mulay S, Vredenburgh J. Primary bone lymphoma: A case series and review of literature. *Case Rep Hematol* (2020) 2020:4254803. doi: 10.1155/2020/4254803

5. de Groen RAL, van Eijk R, Bohringer S, van Wezel T, Raghoo R, Ruano D, et al. Frequent mutated B2M, EZH2, IRF8, and TNFRSF14 in primary bone diffuse large b-cell lymphoma reflect a GCB phenotype. *Blood Adv* (2021) 5(19):3760–75. doi: 10.1182/bloodadvances.2021005215

6. Liu CX, Xu TQ, Xu L, Wang PP, Cao C, Gao GX, et al. Primary lymphoma of bone: A population-based study of 2558 patients. *Ther Adv Hematol* (2020) 11:2040620720958538. doi: 10.1177/2040620720958538

7. Li X, Xu-Monette ZY, Yi S, Dabaja BS, Manyam GC, Westin J, et al. Primary bone lymphoma exhibits a favorable prognosis and distinct gene expression signatures resembling diffuse Large b-cell lymphoma derived from centrocytes in the germinal center. *Am J Surg Pathol* (2017) 41(10):1309–21. doi: 10.1097/PAS.0000000000000923

8. Messina C, Christie D, Zucca E, Gospodarowicz M, Ferreri AJ. Primary and secondary bone lymphomas. *Cancer Treat Rev* (2015) 41(3):235–46. doi: 10.1016/j.ctrv.2015.02.001

9. Govi S, Christie D, Messina C, Bruno Ventre M, Gracia Medina EA, Porter D, et al. The clinical features, management and prognostic effects of pathological fractures in a multicenter series of 373 patients with diffuse large b-cell lymphoma of the bone. *Ann Oncol* (2014) 25(1):176–81. doi: 10.1093/annonc/mdt482

10. Cheson BD, Fisher RI, Barrington SF, Cavalli F, Schwartz LH, Zucca E, et al. Recommendations for initial evaluation, staging, and response assessment of Hodgkin and non-Hodgkin lymphoma: the lugano classification. *J Clin Oncol* (2014) 32(27):3059–68. doi: 10.1200/JCO.2013.54.8800

11. Palmerini E, Righi A, Staals EL. Rare primary malignant bone sarcomas. *Cancers (Basel)* (2020) 12(11). doi: 10.3390/cancers12113092

12. Ibrahim T, Mercatali L, Amadori D. Bone and cancer: The osteoncology. *Clin cases Miner Bone Metab* (2013) 10(2):121–3.

13. Evola FR, Costarella L, Pavone V, Caff G, Cannavo L, Sessa A, et al. Biomarkers of osteosarcoma, chondrosarcoma, and Ewing sarcoma. *Front Pharmacol* (2017) 8:150. doi: 10.3389/fphar.2017.00150

14. Coleman RE. Skeletal complications of malignancy. *Cancer* (1997) 80(8 Suppl):1588–94. doi: 10.1002/(SICI)1097-0142(19971015)80:8+<1588::AID-CNCR9>3.0.CO;2-G

15. Rizzoli R, Body JJ, Brandi ML, Cannata-Andia J, Chappard D, El Maghraoui A, et al. Cancer-associated bone disease. *Osteoporos Int* (2013) 24(12):2929–53. doi: 10.1007/s00198-013-2530-3

16. Coleman RE. Clinical features of metastatic bone disease and risk of skeletal morbidity. *Clin Cancer Res* (2006) 12(20 Pt 2):6243s–9s. doi: 10.1158/1078-0432.CCR-06-0931

17. Maurer F, Ambacher T, Volkmann R, Weller S. [Pathologic fractures: diagnostic and therapeutic considerations and results of treatment]. *Langenbecks Arch Chir* (1995) 380(4):207–17.

18. Mulligan ME, McRae GA, Murphey MD. Imaging features of primary lymphoma of bone. *AJR Am J Roentgenol* (1999) 173(6):1691–7. doi: 10.2214/ajr.173.6.10584821

19. Willeumier JJ, van der Linden YM, van de Sande MAJ, Dijkstra PDS. Treatment of pathological fractures of the long bones. *EFORT Open Rev* (2016) 1(5):136–45. doi: 10.1302/2058-5241.1.000008

20. Macedo F, Ladeira K, Pinho F, Saraiva N, Bonito N, Pinto L, et al. Bone metastases: An overview. *Oncol Rev* (2017) 11(1):321.

21. Datir A, Pechon P, Saifuddin A. Imaging-guided percutaneous biopsy of pathologic fractures: a retrospective analysis of 129 cases. *AJR Am J Roentgenol* (2009) 193(2):504–8. doi: 10.2214/AJR.08.1823

22. Afinowi RA, Chaturvedi A, Cattermole HR. Diagnostic use of intramedullary reaming biopsy in metastatic long bone disease. *Ann R Coll Surg Engl* (2017) 99(6):452–5. doi: 10.1308/rcsann.2017.0049

23. Kitsoulis P, Vlychou M, Papoudou-Bai A, Karatzias G, Charchanti A, Agnantis NJ, et al. Primary lymphomas of bone. *Anticancer Res* (2006) 26(1A):325–37.

24. Bonar SF. Lymphoma of bone. In: Santini-Araujo E, Kalil RK, Bertoni F, Park Y-K, editors. *Tumors and tumor-like lesions of bone: For surgical pathologists, orthopedic surgeons and radiologists*. London: Springer London (2015). p. 385–411.

25. Bhakta P, Youssef A, Bigham L, Mallick J, Bhargava P, Rawas F, et al. Proposal of diagnostic approach of periodontal primary non Hodgkin lymphoma of bone with flow cytometry as an essential diagnostic component. *Head Neck Pathol* (2022) 16(4):1091–102. doi: 10.1007/s12105-022-01469-y

26. Gusho CA, Blank AT. Is there a role for intramedullary tissue sampling during internal fixation of metastatic disease in long bones? A systematic review and an institutional experience. *Iowa Orthop J* (2021) 41(1):77–82.

27. Wang C, Shen Y. Study on the distribution features of bone metastases in prostate cancer. *Nucl Med Commun* (2012) 33(4):379–83. doi: 10.1097/MNM.0b013e3283504528

28. Bubendorf L, Schopfer A, Wagner U, Sauter G, Moch H, Willi N, et al. Metastatic patterns of prostate cancer: An autopsy study of 1,589 patients. *Hum Pathol* (2000) 31(5):578–83. doi: 10.1053/hp.2000.6698

29. Saad F, Gleason DM, Murray R, Tchekmedyian S, Venner P, Lacombe L, et al. A randomized, placebo-controlled trial of zoledronic acid in patients with hormone-refractory metastatic prostate carcinoma. *J Natl Cancer Inst* (2002) 94(19):1458–68. doi: 10.1093/jnci/94.19.1458

30. Ramadan KM, Shenkier T, Sehn LH, Gascoyne RD, Connors JM. A clinicopathological retrospective study of 131 patients with primary bone lymphoma: a population-based study of successively treated cohorts from the British Columbia cancer agency. *Ann Oncol* (2007) 18(1):129–35. doi: 10.1093/annonc/mdl329

31. Horsman JM, Thomas J, Hough R, Hancock BW. Primary bone lymphoma: a retrospective analysis. *Int J Oncol* (2006) 28(6):1571–5. doi: 10.3892/ijo.28.6.1571

32. Jamshidi K, Jabalameli M, Hoseini MG, Bagherifard A. Stage IE primary bone Lymphoma:Limb salvage for local recurrence. *Arch Bone Jt Surg* (2015) 3(1):39–44.

33. Marshall RA, Mandell JC, Weaver MJ, Ferrone M, Sodickson A, Khurana B. Imaging features and management of stress, atypical, and pathologic fractures. *Radiographics* (2018) 38(7):2173–92. doi: 10.1148/rg.2018180073

34. Dotan ZA. Bone imaging in prostate cancer. *Nat Clin Pract Urol* (2008) 5(8):434–44. doi: 10.1038/ncpuro1190

35. Krishnan A, Shirkhoda A, Tehranzadeh J, Armin AR, Irwin R, Les K. Primary bone lymphoma: radiographic-MR imaging correlation. *Radiographics* (2003) 23(6):1371–83. doi: 10.1148/rg.236025056

36. Igrec J, Fuchsjager MH. Imaging of bone sarcomas and soft-tissue sarcomas. *Rofo* (2021) 193(10):1171–82.

37. Cheville JC, Tindall D, Boelter C, Jenkins R, Lohse CM, Pankratz VS, et al. Metastatic prostate carcinoma to bone: clinical and pathologic features associated with cancer-specific survival. *Cancer* (2002) 95(5):1028–36. doi: 10.1002/cncr.10788

38. Kawaguchi M, Kato H, Nakano M, Goshima S, Matsuo M. Clinical features of bone metastasis with extraosseous soft-tissue mass in prostate cancer patients. *BJR|Open* (2019) 1(1):20180042. doi: 10.1259/bjro.20180042

39. Liu Y. The role of 18F-FDG PET/CT in staging and restaging primary bone lymphoma. *Nucl Med Commun* (2017) 38(4):319–24. doi: 10.1097/MNM.0000000000000652

40. Behzadi AH, Raza SI, Carrino JA, Kosmas C, Gholamrezanezhad A, Basques K, et al. Applications of PET/CT and PET/MR imaging in primary bone malignancies. *PET Clin* (2018) 13(4):623–34. doi: 10.1016/j.cpet.2018.05.012

41. O'Connor AR, Birchall JD, O'Connor SR, Bessell E. The value of 99mTc-MDP bone scintigraphy in staging primary lymphoma of bone. *Nucl Med Commun* (2007) 28 (7):529–31. doi: 10.1097/MNM.0b013e3281e2c861

42. Zhang X, Fan W, Xia ZJ, Hu YY, Lin XP, Zhang YR, et al. Use of subsequent PET/CT in diffuse large b-cell lymphoma patients in complete remission following primary therapy. *Chin J Cancer* (2015) 34(2):70–8. doi: 10.5732/cjc.014.10124

Frontiers in Oncology

Advances knowledge of carcinogenesis and tumor progression for better treatment and management

The third most-cited oncology journal, which highlights research in carcinogenesis and tumor progression, bridging the gap between basic research and applications to imrpove diagnosis, therapeutics and management strategies.

Discover the latest Research Topics

See more →

Frontiers

Avenue du Tribunal-Fédéral 34
1005 Lausanne, Switzerland
frontiersin.org

Contact us

+41 (0)21 510 17 00
frontiersin.org/about/contact